University College London

Desert and Sonic Hedgehog Signalling in T cell Differentiation

by

AMAL ALSHAMMARY

A thesis submitted to University College London for the Degree of Doctor of Philosophy

June 2015

UCL Institute of Child Health
Faculty of Population Health Sciences
University College London

This is a declaration that all work presented in this thesis is my own unless otherwise clearly stated

Amal Alshammary

June 2015

Abstract

T cells develop in the thymus. The thymus provides a unique microenvironment with all the cytokines, cell surface ligands and extra-cellular matrix components necessary for thymocytes to develop. The cellular programme of this development is well characterized, whereby $CD4^{-}CD8^{-}$ double negative (DN) cells require pre-TCR induced signals to give rise to the $CD4^{+}CD8^{+}$ double positive (DP) cells. The DP population undergoes selection to form self-MHC restricted and self-tolerant $CD4^{+}$ or $CD8^{+}$ single positive (SP) T cells. The Hedgehog (Hh) family of secreted intracellular signalling molecules plays a major role in many patterning processes and organogenesis during embryonic development and are involved in the homeostasis and renewal of adult tissues. This thesis focuses on studying the functions of hedgehog-pathway components in the thymus by detecting differences in T cell differentiation and transition from one developmental stage to the next.

The Hh family member, Sonic Hedgehog (Shh) has been previously found to influence T cell development and transition at the double negative stage (DN). We have utilized T cell receptor transgenic mice models (TCR-transgenics) to investigate the role of Shh in T cell development and repertoire selection. Our data from thymic organ cultures (FTOCs) have shown that Shh influences T cell selection and maturation during the later stages of T cell development in their transition from DP to SP cell population. Another Hh family member, Dhh has been previously found to negatively regulate multiple stages of erythrocyte differentiation. Using Dhh-wild type and Dhh-knockout mice models, our data have shown that Dhh also play a negative regulatory role in T cell production in

the thymus and peripheral lymphoid organs. Furthermore, we investigated the impact of Hh morphogene by utilizing Hh mutant mice and setting up different crosses to analyse transgenic repertoire selection in different mouse mutants, our data have shown that Hh-signalling regulate T cell development by attenuating gene transcription of various genes.

In loving memory of King Abdullah, whose vision in creating a new scholarship program, which allowed me and many other female students to pursue a higher education abroad, marked the history of female education in Saudi Arabia.

August 1924 – January 2015

Acknowledgments

First and foremost I offer my sincerest gratitude and appreciation to my remarkable supervisor, Prof. Tessa Crompton. You have supported me through the development of my thesis, from the very first day when you welcomed me into your group until the final moments of my thesis submission. I attribute the level of my PhD degree to you, as your guidance and encouragement afforded me the space to work and expand in my own way. Without you, this thesis would not have been completed or even written. Over the past four years, my passion for immunology has grown as your enthusiasm and immense knowledge firmly implanted my feet into the world of immunology, and I became very fond of this field and was driven to become a bright scientist as you are. Your guidance exceeded the boundaries of academia as you supported me emotionally along the rough road to finish this thesis. One simply could not ask for a better supervisor—you are truly the best, and I am honoured and fortunate that life has led me to meet you.

This work would have been immensely more difficult had I not had the critical support, encouragement, and insightful comments of Anna, Jose and Baby Sue. I would like to express my appreciation and gratitude to you, as you helped tutor me regarding all the methods necessary to conduct my project. I also would like to thank Hemant and Rain: thank you for your help and scientific support from the early years of my study to the end. Special thanks go out to Alessandro, Costas, Anisha, Sonia and Diana for all the stimulating discussions and for all the fun we have had over the past four years.

The support of my family, in which the most basic source of life and happiness resides, has been unconditional, as they have cherished every great moment with me and supported me whenever I needed it. Dad, I owe you my eternal gratitude for believing in me and for encouraging me to aim high and achieve my dreams. I value your sacrifice and your complete trust; without you I would not be where I am now. You are my hero, my inspiration and my true north. Mum, thank you for supporting me spiritually throughout my life; you are my solid earth and my shinning sun. As for my sisters, I have been blessed with five angels protecting and guiding me throughout my life. Rania, my guardian angel, Faten, my spiritual angel, Haifa, my joyful angel, Amna, my angel of wisdom, and Heba, my sweet angel of laughter—thank you all for always supporting me and for brightening my soul with laughter and pure happiness.

My sincerest thanks goes to Dr Mohammed Al Ahdal: you enlightened me with my first glimpse into the world of research and offered me my first summer internship opportunity, which led me to work with diverse, exciting projects. You have taught me, both consciously and unconsciously, how good experimental immunology is conducted; your insights shaped my future, and I am forever grateful for your encouragement, motivation and support.

Last but not least, I would like to thank my dearest friends and sisters in life, Hanan and Hadeel: you have always been there to cheer me up, and you have stood by me through the good and the bad. Words cannot express how grateful I am to have you in my life. Your friendship has sustained me thus far.

Table of Contents

List of Tables

List of Figures

Abbreviations

−/−	Knockout
+/+	Wild type
+/−	Heterozygote
µg	Microgram
µl	Microlitre
AIRE	Autoimmune regulator
APC	Antigen presenting cell
APS1	Autoimmune disease polyglandular syndrome type 1
BCC	Basal cell carcinoma
BMP	Bone morphogenetic protein
BMPR	BMP receptor
Boc	Brother of Cdo
bp	Base pair
CCL	Chemokine ligand
CCR	Chemokine receptor
CD	Clusters of differentiation
CD40L	CD40 ligand
cDNA	Complementary DNA
CI	Cubitus Interruptus
CKI	Casein kinase I
Cos2	Costal2
Co-Smad	Common-mediator Smads
DC	Dentdritic cell
dH2O	Distilled water
Dhh	Desert Hedgehog
DN	Double negative
DNA	Deoxyribonucleic acid
dNTPs	Deoxynucleotide triphosphates
DP	Double positive
E	Embryonic day
EDTA	Ethylenediaminetetraacetic acid
ERK	Extra-cellular signal related kinase

ETP	Early thymocyte progenitor
FACS	Fluorescence activated cell sorter
FCS	Fetal calf serum
FITC	Fluorscein Isothiocyanate
FSC/SSC	Forward scatter/ Side scatter
FTOC	Foetal thymic organ culture
Fu	Fused
GATA3	GATA binding protein 3
Gli	Glioma associated oncogene
Gnb4	Guanine nucleotide binding protein beta-4 subunit
GSK3	Glycogen synthase kinase 3
HC	Hyrocortisone
Hh	Hedgehog family
Hhip	Hedgehog-interacting protein
Hh-N	Hh precursor N-terminal
Hh-C	Hh precursor C-terminal
HhSC	Hedgehog signalling complex
Ihh	Indian Hedgehog
HPRT	Hypoxanthine Guanine Phosphoribosyl Transferase
HSC	Haematopoietic Stem Cell
HSA	Heat-stable antigen
IC	Intra-cellular
IFN	Interferon
Ig	Immunoglobulin
IL	Interleukin
ISP	CD8+ Immature single-positive cell
ITAMs	Immunoreceptor tyrosine-based activation motifs
kb	Kilo base
kD	Kilo Dalton
KO	Knockout
LAT	Linker for activation of T cells
Lck	Lymphocyte protein tyrosine kinase
LEF	Lymphoid enhancer factor

LN	Lymph node
LSK	Lin^{-} $Sca\text{-}1^{+}$ $c\text{-}kit^{+}$
MAP	Mitogen activated protein
mAB	Monoclonal antibody
mg	Milligram
MHC	Major histocompatibility complex
mL	Milliliter
mm	Millimeter
NF-κB	Nuclear factor-κB
ng	Nanogram
NK	Natural killer cell
P	Platelet
p	p-value
PBS	Phosphate buffered saline
PCR	Polymerase chain reaction
PE	Phycoerythrin
PI	Propidium iodide
PMA	Phorbol myristate acetate
PKC	Protein kinase C
PM	Plasma membrane
pMHC	Peptide-Major Histocompatibility Complex
Pre-TCR	Pre-T cell receptor complex
PSGL	Platelet-selectin glycoprotein ligand
pTα	Pre-T alpha chain
Ptch	Patched
qRT-PCR	Quantitative reverse transcriptase polymerase chain reaction
RAG	Recombinase activating gene
Ras	Rat Sarcoma
RSS	Recombination signal sequence
rShh	Recombinant Shh
rmShh	Recombinant mouse Shh
RT-PCR	Reverse transcriptase polymerase chain reaction
RNA	Ribonucleic acid

S1P1	Sphingosine-1-Phosphate receptor 1
SCID	Severe combined immunodeficiency
SD	Standard deviation
SE	Standard error
SEM	Standard error of mean
Shh	Sonic hedgehog
Shh-N	Shh N-terminal
siRNA	Silencing ribonucleic acid
Smo	Smoothened
SP	Single positive
Su(Fu)	Suppressor of fused
TCF	T cell factor
TCR	T cell receptor
TCRα	T cell receptor alpha chain
TCRβ	T cell receptor beta chain
TEC	Thymic epithelial cells
TFBS	Transcription factor binding site
TGF	Transforming growth factor
Th1	T helper type 1 cell
Th2	T helper type 2 cell
Th-POK	T-helper-inducing POK/Kruppel like factor
TNF	Tumour necrosis factor
V(D)J	Variable(Diversity)Joining
WT	Wild type
αβ T cell	T cell with alpha beta TCR
γδ T cell	T cell with gamma delta TCR

Chapter 1

Chapter One: Introduction

The mature mammalian blood system is made up of an array of functionally and morphologically diverse and distinct cell types, including erythrocytes (red blood cells), leukocytes (white blood cells) and thrombocytes (platelets). As diverse as these circulating blood cells are, they all originate from a common self-renewing multi-potent haematopoietic stem cell (HSC) (Rossi et al. 2012; Kondo et al. 2003).

1.1 Haematopoiesis

Haematopoiesis is the process by which haematopoietic stem cells (HSCs) develop and differentiate, giving rise to all lineages of mature blood cells throughout the lifetime of an organism (Kondo et al. 2003; Clements & Traver 2013). As the life-span of many haematopoietic cells is short, pool size of HSC is regulated through establishing a delicate balance between differentiation and self-renewal to fulfil the continuous and enormous daily supply of blood cells in an adult human (reaching approximately $1x10^{12}$ cells per day to maintain homeostatic blood levels) (Weissman 2000; Kanji et al. 2011; Vaziri et al. 1994; Cheshier et al. 1999; Doulatov et al. 2012). This is possible as the multipotency of HSCs is conserved through continuous cell divisions, while their progeny are directed towards lineage differentiation (Wilson & Trumpp 2006; Mikkola & Orkin 2006).

1.1.1 Ontogeny of HSCs

The pool of HSCs is formed during embryogenesis in a complex coherent process that involves several factors and multiple anatomical sites such as the yolk sac, the dorsal aorta (DA), placenta, foetal liver and eventually, after birth, the bone marrow (Kanji et al. 2011; Mikkola & Orkin 2006). During embryonic development the anatomy of the embryo changes resulting in a continuous site shift of haematopoiesis to multiple different anatomical locations that follows the embryo's anatomical development and organogenesis (Kanji et al. 2011; Golub & Cumano 2013; Costa et al. 2012). The existence of multiple foetal haematopoietic sites is a common feature in many non-vertebrate and vertebrate animals, such as, flies, amphibians, fish, birds, rodents and humans (Ciau-Uitz et al. 2000; Traver & Zon 2002; Kanji et al. 2011). Murine HSC development is well characterized and serves as a model for human haematopoiesis (Tavian & Péault 2005b; Tavian & Péault 2005a).

It has been established that during murine embryonic development, haematopoiesis is characterized by at least three sequential waves (Medvinsky et al. 2011; Ciau-Uitz et al. 2014). The first wave takes place in the yolk sac blood islands at embryonic day-7 (E7) (Golub & Cumano 2013; Ciau-Uitz et al. 2014). This wave produces progenitor cells that give rise to a primitive population of myeloid cells and a transient population of erythrocytes (Palis et al. 1999; Tober et al. 2007; Moore & Metcalf 1970; Ferkowicz & Yoder 2005). Subsequently, the second wave also occurs in the yolk sac but in the haemogenic endothelium embedded in the wall of functional blood vessels. This wave produces multipotent progenitor cells which migrate to the foetal liver and differentiate to give rise to primitive myeloid and lymphoid lineages (Ciau-Uitz et al. 2014).

Shortly after this, the third wave initiates in the haemogenic endothelium localized in the ventral wall of the dorsal aorta (DA) between embryonic days-10 and 11 (E10-11) (Medvinsky et al. 1993; de Bruijn et al. 2000; Medvinsky & Dzierzak 1996) producing functional HSCs that migrate to the placenta and foetal liver and are responsible for haematopoiesis in the late foetus until birth (Kumaravelu et al. 2002; Mikkola et al. 2005).

Finally, after birth, haematopoiesis relocates permanently to the bone marrow (BM) throughout adult murine life. HSCs produced in the bone marrow generate all of the haematopoietic progenitors that proliferate and differentiate into committed haematopoietic lineages (Yoder 2004; Fleischman et al. 1982; Muller et al. 1994; Orkin & Zon 1997).

1.1.2 Lineage commitment of HSCs

The earliest most primitive haematopoietic progenitors in the mouse bone marrow are known as LSK cells (Spangrude et al. 1988; Ikuta & Weissman 1992; Bhandoola et al. 2007). LSK cells lack lineage specific markers found on differentiated cells (Lin^-) but possess self-renewal capacity and express stem cell marker antigen-1 (Sca-1) and c-Kit, which is the cytokine receptor for stem cell factor (SCF) (Adolfsson et al. 2005; Igarashi et al. 2002). The LSK cell population is heterogeneous and it has been further subdivided based on the expression of the cytokine receptor FMS-like tyrosine kinase-3 (FLT3) and other markers such as CD150 and CD48 (Kiel et al. 2005; Love & Bhandoola 2011). The $FLT3^-$ $CD150^+$ subset of LSK contains long-term self-renewing haematopoietic stem cells (HSCs). Furthermore, $FLT3^{LOW}$ $CD150^-$ cells

downstream of HSCs are cells which have reduced self-renewal capacity but have the ability to differentiate into all blood cell types, these cells are known as multipotent progenitors (MPPs) (Christensen & Weissman 2001; Morrison & Weissman 1994; Love & Bhandoola 2011).

MPPs are a heterogeneous population of cells, which upon differentiation give rise to two oligopotent progenitors, the common myeloid erythroid progenitors (CMPs) and common lymphoid progenitors (CLPs) (Kondo et al. 1997; Serwold et al. 2009). CMPs give rise to all myeloid and erythroid cells, including erythrocyte, megakaryocyte, granulocyte and monocyte lineages (Pronk et al. 2007; Nakorn et al. 2002; Kanji et al. 2011; Chen et al. 2005). CLPs mostly produce all T and B lymphocytes and natural killer cells (NK) (Bell & Bhandoola 2008; Kondo et al. 1997) (Figure 1.1). However, recent studies have shown that CLPs are a heterogeneous population of cells and only those which express recombination activating genes, *Rag1* and *Rag2* are lymphoid primed (Adolfsson et al. 2005; Igarashi et al. 2002).

Studies in foetal haematopoiesis have suggested a conceptual change in building the hierarchical progeny of HSCs in regards to lineage commitment and cell fate. The classical original model proposes that the first HSC branch-point produces one or two distinct haematopoietic progenitors, the myeloid-erythroid lineage and lymphoid lineage. This model was strongly supported as progenitors with distinct cell surface phenotypes that qualify as CMP or CLPs have been identified. However, the segregation of myeloid and lymphoid lineages might not be clear as previously thought and another model of divergence has been proposed where the myeloid lineage is considered the default lineage. This model is based on the identification of foetal-liver-derived progenitors capable of producing myeloid

and lymphoid cells suggesting a deviation from the classical model (Kawamoto 2006; Kawamoto et al. 1997; Adolfsson et al. 2005; Kawamoto et al. 1999). In regards to recent research findings, lineage commitment is not absolute as discrepancies regarding HCS hierarchy and lineage commitment still exist (Bell & Bhandoola 2008; Wada et al. 2008; Montecino-Rodriguez et al. 2001).

1.1.3 T cell progenitors and lineage commitment

Adult T cell progenitors originate in the bone marrow and seed the thymus where they differentiate to become T cell lineage committed progenitors (Wu 2006; Rodewald 1995; Schwarz & Bhandoola 2004). The molecular characteristics and degree of lineage specificity of the bone marrow-derived progenitor cells colonizing the thymus from the blood is still unclear. However, although many progenitor cells have been shown to possess T lineage commitment potentiality, only a very small number of progenitors are able to migrate and settle in the thymus (Basch & Kadish 1977; Spangrude & Scollay 1990). Given this observation, it has been proposed that regardless of their cellular origin, thymus seeding progenitors (TSPs) upon encountering the thymic microenvironment generate T cell progenitors, known as the early thymocyte progenitors (ETPs) (Allman et al. 2003; Porritt et al. 2004; Benz et al. 2008; Hosoya et al. 2010).

ETPs are the earliest known intra-thymic T cell progenitors characterized. Shortly after entering the thymus, ETPs differentiate to become specified to the T cell lineage and lose their B cell potential (Sambandam et al. 2005; Tan et al. 2005). The greatest T cell developmental potential is found among a rare subset of ETPs expressing c-kit^{hi} Lin^{-} (Tan et al. 2005; Porritt et al. 2004; Matsuzaki et al. 1993;

Allman et al. 2003). This subset comprises approximately 0.01% of total thymocytes but can expand extensively and ultimately generate mature T cells (Allman et al. 2003).

1.2 The role of the thymus in T cell development

T cells or T lymphocytes belong to a group of white blood cells and play a major role in mediating the acquired immune response. They derive their name from their site of maturation, the thymus, where the majority of T cells develop.

The basis of immune tolerance and adaptive immunity is associated with the ability of the immune system to orchestrate a series of developmental steps that take the undifferentiated stem cells to finally become mature thymocytes. T cell development takes place within the unique micro-environment of the thymus. Through a complex well orchestrated network of signals within the thymus, developing thymocytes acquire all necessary cell surface ligands, cytokines and extra-cellular matrix components to develop and mature, producing a repertoire of diverse and functional non-self reactive T cells (Boyd et al. 1993).

1.2.1 Thymus structure

The thymus is the primary lymphoid organ. Immediately after birth, the thymus grows considerably until it reaches its maximum size by sexual maturity then gradually involutes (Pearse 2006). In mammals, it is situated in the upper anterior thorax, just above the heart and consists of two identical lobes each surrounded by a capsule of thin connective tissue which extends into the parenchyma of the

organ forming trabeculae (or connective tissue wall) dividing the organ lobes into numerous lobules. Histological morphology divide each lobule into distinct regions of outer cortex (peripheral), inner medulla (central), separated by a cortico-medullary region (Haley 2003). The structure of the thymus is histologically consistent across species (Haley 2003).

The unique functions of the thymus reside in a network of supporting framework composed of epithelial-reticular cells, known as the thymic stroma or thymic epithelial cells (TEC), which arise early during embryonic development from endoderm-derived structures known as the third pharyngeal pouch and the third branchial cleft (van Ewijk 1991; van Ewijk 1988; Boyd et al. 1993). Together, these structures form the rudimentary thymus which becomes colonized by bone marrow-derived progenitor cells which develop within the unique micro-environment the thymus provides, and give rise to a large number of cells committed to T cell lineage (Cordier & Haumont 1980; Boyd et al. 1993; Von Gaudecker et al. 1997).

1.2.2 TEC and thymocyte crosstalk

Development of T cells in the thymus requires the dynamic migration of developing thymocytes through the thymus. Thymus architectural stroma and travelling thymocytes have to communicate with each other both in close proximity and remotely. This crosstalk or communication is pivotal, providing bidirectional signals at different stages between thymic stroma and developing thymocytes, essential for the maturation of both parties (Zinkernagel et al. 1978;

van Ewijk et al. 1994; Scollay et al. 1980; Shortman et al. 1991; Goldrath & Bevan 1999).

Such crosstalk signals come in the form of chemokines, morphogens and cell adhesion molecules produced by thymic stromal cells guiding the direction of migrating thymocytes within the different compartments of the thymus. In contrast, developing thymocytes find their way by sequentially expressing different cell surface receptors to accomplish maturation, proliferation and selection during their constant motion.

Early thymocyte progenitors (ETPs) migrate into the thymus, and depending on the stage of embryogenesis, they can come from two different origins. During the early stages of embryogenesis, before vascularisation of the thymus, the seeding of the thymus comes from the foetal liver. At this stage ETPs enter the thymus not through the bloodstream, but through the mesenchynal layer which later forms the capsule of the adult thymus (Wilkinson et al. 1999; Suniara et al. 1999). In contrast, during the later stages of embryogenesis and postnatally after vascularisation, ETPs travel from the bone marrow through the bloodstream (Bleul & Boehm 2000; Takahama 2006). Thymic seeding begins as early as embryonic day 11.5 (E11.5) in mice, and around the eighth week of gestation in humans (Owen & Ritter 1969; Haynes & Heinly 1995) and continues in adulthood (Foss et al. 2001; Le Douarin & Jotereau 1975; Havran & Allison 1988).

During the early stages of embryogenesis, chemokine ligand-21 (CCL21) and chemokine ligand-25 (CCL25) among several other chemokines are expressed by foetal thymus primordium providing a chemotactic attraction to colonize the thymus for lymphoid progenitors expressing chemokine receptor-7 (CCR7), the

receptor for CCL21, and chemokine receptor-9 (CCR9), the receptor for CCL25 (Liu et al. 2005; Wurbel et al. 2001; Bleul & Boehm 2000). Mutant mice with deficiency in CCL21 or its receptor (CCR7) exhibit a partial but significant decrease in total thymocytes number until they reach E14.5 compared to normal mice (Liu et al. 2005). Furthermore, mice deficient in CCR9 or its receptor CCL25 show a three-fold decrease in total thymocyte number until E17.5 compared to normal mice (Wurbel et al. 2001). However, it is unclear whether the combination of ligands, CCL21 and CCL25 or their receptors, CCR7 and CCR9, is sufficient for foetal thymus progenitor colonization or if other chemokines are involved in this process. In contrast, the chemokine ligand-12 (CXC12) and its receptor, chemokine receptor-4 (CXCR4) have been found not to be involved in the colonization process by progenitors during the early stages of embryogenesis (Ara et al. 2003).

The role of chemokines in seeding the postnatal thymus is as yet unclear, however, it has been reported that the adhesive interaction between platelet (P)-selectin expressed by the adult thymic endothelium, and the P-selectin glycoprotein ligand-1 (PSGL1) expressed by circulating lymphoid progenitor cells guide the transmigration of lymphoid progenitors from blood to the thymus parenchyma (Takahama 2006; Rossi et al. 2005). It has been reported that mice deficient in either of these molecules exhibit severe inhibition of thymic seeding by progenitors (Takahama 2006; Rossi et al. 2005; Ladi et al. 2006).

Following their entry into the thymus, T cell progenitors begin their maturation and development into T cells, a process accomplished by expression of different chemokine receptors to enable them to dynamically relocate between the distinct compartments of the thymus (Carpenter & Bosselut 2010). The specific roles of

chemokines and their receptors in guiding the thymic progenitors and developing thymocytes on their way to maturation are not yet fully understood (Koch & Radtke 2011). The main reason behind this is due to the fact that T cell maturation requires them to migrate in a continuous circular motion inward and outward within the thymus compartments including, the cortico-medullary junction (CMJ), the cortex, the subcapsular zone (SCZ) and medulla. This motion results in a continuous upregulation and downregulation of chemokines and their ligands to guide their migration and subsequently their development within the thymus.

It has been postulated that several chemokines including, CXCR4, CCR7 and CCR9 may influence the survival of T cells during selection and mediate thymocyte development (Plotkin et al. 2003; Benz et al. 2004; Misslitz et al. 2004). CXCR4-deficient thymocytes fail to migrate outward from the cortico-medullary junction (CMJ) towards the cortex resulting in a defect in differentiation of T cells during their early stages of development (Plotkin et al. 2003). CCR7-deficient thymocytes are arrested at the cortico-medullary junction (CMJ) and are blocked from progressing to further developmental stages (Misslitz et al. 2004). CCR9-deficient mice exhibit normally distributed thymocytes within the cortex but that they are inefficient at accumulating in the sub-capsular zone (SCZ) (Benz et al. 2004). Furthermore, it has been found that the sphingosin-1-phosphate receptor-1 (S1P1) facilitates T cell exit from the thymus after maturation. S1P1 deficient thymocytes are unable to exit and are retained inside the thymus (Chaffin & Perlmutter 1991; Matloubian et al. 2004; Allende et al. 2004).

1.3 T cell development

In order for the immune system to be capable of anticipating all manner of pathogenic entities, immature thymocytes must undergo several critical developmental stages followed by fastidious tests to select those cells amongst the immature thymocytes that express antigen receptor (T-cell receptor (TCR)) restricted to and tolerant of self-peptides presented by the major histocompatibilty complexes (MHC-I, MHC-II). The result of this crucial selection is a repertoire of mature T cells that under healthy conditions, does not attack or destroy host tissues, but reacts efficiently against the unlimited range of foreign antigens.

1.3.1 T cell selection and maturation

In postnatal thymus, the first site of entry of ETPs from blood is around the highly vascularised cortico-medullary junction (CMJ) (Lind et al. 2001) where progenitors commit to the T cell lineage and undergo subsequent developmental stages marked by changes in the rearrangement status of T cell receptor genes and in the expression of T cell surface receptors as they migrate towards the sub-capsular zone (Porritt et al. 2003; Benz et al. 2008). These surface changes reflect the functional maturation of T cells and are used as markers of different stages of maturation (Shortman & Wu 1996).

The earliest T cell subset is identified by lack of the expression of CD4 and CD8 surface receptors, these cells are known as double-negative cells (DN) (Pearse et al. 1989; Shinkai et al. 1992). The DN cell population is heterogeneous and is further subdivided into four large fractions (DN1 to DN4) based on the differential expression of CD25, CD44 and CD117 (c-kit). DN1 cells reside in the

cortico-medulary junction and express cell surface markers $CD25^{-}$ $CD44^{+}$ $CD117^{+}$ (Porritt et al. 2003; Prockop & Petrie 2000) In these cells, the genes encoding the T cell receptor (TCR) α and β chains are in the germline configuration. As they mature, they leave the cortico-medullary junction and migrate deeper toward the sub-capsular zone where they acquire the expression of CD25 and become DN2, expressing $CD25^{+}$ $CD44^{+}$ $CD117^{+}$ surface markers (Shortman & Wu 1996). Rearrangement of TCRγ, TCRδ and TCRβ gene loci are initiated at the DN2 stage, a process that is completed later on at the DN3 stage (Capone et al. 1998; Livák et al. 1999; Petrie & Zúñiga-Pflücker 2007; Godfrey et al. 1993; MacDonald et al. 2001).

Maturation of the DN2 population proceeds within the sub-capsular zone and requires the loss of CD44 and CD117 expression where they become DN3, expressing the surface markers, $CD25^{+}$ $CD44^{-}$ $CD117^{-}$. When thymocytes reach the DN3 stage, they continue to rearrange their DNA at the β, γ and δ loci to express functional TCR chains. Lineage specification occurs at this stage when α β versus γδ T cell fate is specified. The expression of recombination-activating genes 1 and 2 (RAG1 and RAG2), is required for successful recombination. γδ T cells require production of a complex composed of TCRδγ and CD3. In contrast, recombination of TCRβ chain and an invariant pre-TCR receptor α chain called (pTα) produces the pre-TCR complex composed of TCRβ, pre-TCRα chain (pTα) and CD3. The formation of this complex causes signals that lead to αβ T cell lineage commitment and takes the thymocytes into an important check point known as the β-selection, which requires that pTα and β chains to signal through a functional pre-TCR (Burtrum et al. 1996; von Boehmer 2005; Mallick et al. 1993).

The β-selection check point at the DN3 stage requires the expression of a consistency functional pre-TCR for further development. This check point is critical as it ceases further recombination of the TCRβ chain loci and promotes differentiation of thymocytes into the DN4 stage (Marrella et al. 2012). However, unsuccessful rearrangement of the TCRβ chain forces developing thymocytes to undergo apoptosis (Wilson et al. 1996; Dudley et al. 1995).

DN3 thymocytes expressing pre-TCR receptor develop into DN4 cells when they lose the expression of both surface markers and become $CD25^{-}$ $CD44^{-}$. DN4 thymocytes begin to migrate from the sub-capsular zone toward the medulla. During this migration within the cortex, they acquire the expression of CD4 and CD8 and become double-positive (DP) (Porritt et al. 2003; Koch & Radtke 2011). DP thymocytes express both co-receptors, CD4 and CD8 via a rapidly cycling immature intermediate single positive thymocyte population expressing CD8 (ISP) (MacDonald et al. 1988).

Within the cortex, the DP thymocytes begin rearrangement of their α chain and RAG genes are expressed. DP thymocytes expressing correctly assembled αβ TCR, undergo a critical survival and differentiation checkpoint determined by the specificity and binding strength of a functional TCR to major histocompatibilty complex (MHC). This crucial step is known as positive-selection, which ultimately produces single-positive thymocytes (SP) committed to either CD4 or CD8 T cell lineages, with self-MHC-restricted TCRs. DP thymocytes interacting with intermediate avidity to MHC class I, are selected to become SP8 thymocytes, where they lose the expression of CD4 surface marker. DP thymocytes interacting with intermediate avidity to MHC class II, are selected to become SP4 thymocytes, where they lose the expression of CD8 surface marker. Thymocytes

successfully completing the positive-selection stage travel towards the medulla where they express either, CD4 or CD8 surface markers. DP thymocytes which fail to react with any of the two MHC molecules undergo apoptosis (Klein et al. 2009).

In the medulla, SP thymocytes undergo another critical developmental stage known as negative-selection to eliminate thymocytes that are self-reactive. SP4 and SP8 thymocytes with high affinity TCRs reacting strongly against self-antigens undergo apoptosis. Mature thymocytes which successfully pass the negative-selection stage egress from the thymus and migrate toward the peripheral lymphoid organs through the blood stream (Figure 1.2) (Klein et al. 2009; Koch & Radtke 2011).

1.3.2 The pre TCR and β-selection

Thymocytes must pass through a major developmental checkpoint known as, the β-selection, to progress from DN to DP. At the DN3 stage of thymocyte development, rearrangement of the gene loci of TCRβ chain and the surrogate non-polymorphic pre T cell receptor α chain (pTα) produce a multi-subunit receptor complex expressed on the surface of developing thymocytes known as pre-TCR (Boehmer & Fehling 1997; Malissen & Malissen 1996). The Pre-TCRα chain is unique and differs in its structure from the TCRα chain, in the position of the cysteine residue which promotes pairing with TCRβ. Furthermore, TCRα chain is not interchangeable with pre-TCRα chain during thymocyte development. Several studies conducted on mutant mice have shown that the differences

between the pre-TCR and TCR reside in their α chain (Fehling et al. 1995; Saint-Ruf et al. 1998).

Successful rearrangement and production of the TCRβ chain and signalling through the pre-TCR complex suppresses the rearrangement of other TCRβ genes (allelic exclusion) and promotes thymocytes to continue their development and maturation by upregulating CD4 and CD8 cell surface expression and TCRα gene rearrangement (Malissen & Malissen 1996; Wilson et al. 1994; Uematsu et al. 1988; Levin et al. 1993; Boehmer & Fehling 1997).

The signalling mechanism is very similar in both the pre-TCR and TCR complexes, as they both rely on the CD3 chains to transmit signals from the surface of T cells to the nucleus. However, pre-TCR signal transduction does not require ligand binding but at a lower threshold allows cell-autonomous signalling, whereas the mature TCR require ligand engagement with MHC molecules and peptides to transmit signals (Michie & Zúñiga-Pflücker 2002; Irving et al. 1998).

Several factors have been found to play a role in regulating the early stages of thymocyte development and maturation in the thymus. Lymphoid-specific recombinase proteins (Rag1 and Rag2) are critical in regulating thymocyte development through controlling the process of TCR chain rearrangement. Mice lacking Rag1 and Rag2 show defects in the thymocytes maturation and thymocytes are arrested at the DN3 stage (Shinkai et al. 1992; Mombaerts et al. 1992; Oettinger et al. 1990). Furthermore, the thymocyte arrest at the DN3 stage observed in these mice is rescued by anti-CD3 antibody treatment. This observation highlights the importance of CD3 cross-linking in pre-TCR signal transduction (Shinkai & Alt 1994). Other studies also support this view as it has

been shown that the pre-Tα amino acid charged extracellular domain induces spontaneous oligomerization attracting CD3 subunits to close proximity to promote pre-TCR signal transduction (Yamasaki et al. 2006; Pang et al. 2010).

The tyrosine kinase receptor proteins, Lck and Fyn play a crucial role in regulating T cell development during their early stages. Lck and Fyn double deficient mice show completely arrested development at the DN stage (van Oers et al. 1996). However, mice deficient in Fyn show normal thymocyte development, while Lck-deficient mice show partial arrest of thymocytes at the DN stage (Molina et al. 1992), suggesting a functional redundancy between Fyn and Lck in pre-TCR signal transduction.

Recent studies have shown the role of several other signalling molecules in pre-TCR signal transduction. Activation of Zap-70/Syk causes phosphorylation of LAT and SLP-76 which in turn leads to activation of Ras-MAPK signalling pathway and mobilization of Ca^{2+} resulting in the activation of the Nuclear factor of activated T cells (NFAT), in addition to the Nuclear factor-kb (NF-κb) (von Boehmer 2005; Crompton et al. 1996; Molina et al. 1992; Mombaerts et al. 1994; Pivniouk et al. 1998).

The basic loop helix E-protein (E2A and HEB) has been found to play a key role in regulating β-selection of thymocytes. Mice deficient in both proteins exhibit reduced pre-Tα expression and thymocyte proliferation is blocked (Wojciechowski et al. 2007).

1.3.3 T cell receptor (TCR) and gene rearrangement

The development of T cells in the thymus is tightly regulated and only about 3% of mature T cells are selected to leave the thymus and egress to the peripheral lymphoid organs, such as the spleen and lymph nodes (Egerton et al. 1990). Their immunological response is mediated by a potent cell surface structure, the T cell receptor (TCR).

The TCR is a disulfide-linked membrane-anchored heterodimer of α and β chains expressed as a complex structure in conjunction with the invariant CD3 molecules. Both α and β chains contains two extracellular domains, the constant (C) and variable (V) region. The amino terminal domain in the V region of α and β chains harbour sequence variations, whereas, the C-terminal domains have a constant sequence (Sherman et al. 2013).

The development and maturation of T cells requires them to undergo TCR gene rearrangement which is essential for numerous cell lineage and fate decisions (Kanji et al. 2011). The somatic rearrangement of the four TCR genes (*Tcrα, Tcrβ, Tcrγ, Tcrδ*) generate a diverse repertoire of T cells. TCR genes are assembled through the recombination of the variable (V), diversity (D) and joining (J) gene segments in a sequential manner of events analogous to the immunoglobulin rearrangement. These events are directed by a site specific recombination process of the Rag proteins and ubiquitously expressed DNA repair proteins (Bassing et al. 2002). In mouse, the TCRα locus is organized in 100 (V), 50 (J) and (C) gene segments, while the TCRβ locus is organized in 25 (V), 2 (D) and 12 (J) and (C) gene segments (Fugmann et al. 2000). Rag (Rag1) and (Rag2) proteins recognize recombination signal sequences (RSS) and flank V, D, and J

segments by creating double strand breaks resulting in random continuous non-homologous end joining (Krangel 2009; Fugmann et al. 2000). The combinational joining of the many TCR gene segments allows for great diversity among the TCR repertoire of cells. Furthermore, the imprecise joining (junctional flexibility) and base insertion between the segments create further diversity of T cell repertoire (Nikolich-Zugich et al. 2004).

Thymocyte lineage commitment to either αβ, or γδ is controlled by the outcome of TCR gene recombination events (Bassing et al. 2002; Hayday & Pennington 2007). At the DN2/DN3 stage D-J rearrangement takes place first at both alleles of TCRβ locus followed by V-DJ rearrangement at different alleles (Capone et al. 1998; Livák et al. 1999). The two gene clusters of the β-chain locus allow thymocytes to increase their chances of a productive rearrangement of the gene by attempting a second rearrangement. TCRα gene rearrangements occur at the DP stage and are initiated at the V-J gene segment following pre-TCR signal transduction (Capone et al. 1998).

1.3.4 T cell positive and negative selection

Immune tolerance is provided by the ability of T cells to distinguish between self and non-self antigens. This is done through the engagement of TCR with peptide-associate MHC (pMHC) complex. This interaction is crucial for elimination of self reactive T cells. TCR repertoire tuning is ensured by undergoing two consecutive key selection events, positive and negative selection. The basis of this selection is the specificity and affinity of TCR interaction with pMHC molecules.

Positive selection ultimately produces SP cells committed to either CD4 or CD8 T cell lineages whereas negative selection eliminates self-reactive SP thymocyts.

Historically, the first evidence for repertoire selection was presented using thymectomized (AXB)H-$2^{a/b}$ F1 mice grafted with strain B-thymus and reconstituted with (AXB) bone marrow cells (Zinkernagel et al. 1978). These mice were infected with lymphocytic choriommenegitis (LCM) virus and probed in vitro for ability of cytotoxic T cells to eliminate LCM-infected strain-A or strain-B. This study showed that only those thymocytes bearing the TCRs that are able to recognize the virus in the context of strain B MHC were selected in the thymus for maturation (Zinkernagel et al. 1978; Doherty & Zinkernagel 1975).

Evidence for deletion of self-reactive cells was demonstrated using the elegant HY-TCR transgenic mouse model. The TCR of these transgenic mice recognizes the male specific HY peptide (derived from the Smy gene) presented by the MHC-I molecule H-$2D^b$ (Kisielow et al. 1988; Markiewicz et al. 1998). It was found that all transgenic cells expressing CD8 (including DP cells) were deleted in male HY-TCR-transgenic mice. While in female HY-TCR-transgenic mice, CD8 expressing cells survived as the male specific HY-peptide is not present (Kisielow et al. 1988; Markiewicz et al. 1998). These observations suggest that auto-reactive thymocytes were "negatively" selected for deletion at the DP stage of thymocyte development (Kisielow et al. 1988).

Another study used the 2B4-TCR transgenic mouse model where the transgenic TCR recognizes moth cytochrome c presented by the MHC-II associated I-E^k. 2B4-TCR transgenic mice expressing I-E^k molecules on H-2^k background, showed a higher proportion of CD4SP cells compared to mice not expressing I-E^k

molecules on H-2^b background. Furthermore, mice with restricted-epithelial expression of I-E^k in the cortical or medullary compartments strongly suggested that DP cells undergo positive selection before reaching the medulla (Berg et al. 1989).

It is clear from the extensive research on thymic-selection that positive and negative selection mechanisms involve the interaction of TCR with pMHC complexes. Binding of the TCR complex to its ligand suggested a later divergence in signals downstream of the initial interaction that determine whether a cell is positively or negatively selected (Gil et al. 2005).

Two hypotheses were postulated to explain the mechanism of thymic-selection after the initial engagement of TCR with pMHC (Moran & Hogquist 2012). First is a quantitative model which explains the events of selection by measuring the differential strength or avidity of TCR interactions. Thymocytes with TCRs able to weakly bind a diverse collection pMHC molecules, are selected for survival. While thymocytes with TCRs that are unable to react with pMHC molecules are selected to die, and those with strong interaction with deleted.

The avidity model is supported by experiments applied using TCR transgenic mice deficient in Tap-1 peptide transporter, which is essential in the transportation of antigens from the cytoplasm to the endoplasmic reticulum to become associated with MHC-I molecules. Foetal thymic organ cultures (FTOCs) experiments showed that the number of SP CD8 T cells increased rapidly when a low concentration of the peptide specific for the transgenic TCR is added. However, adding higher concentration of the same peptide reduced the number of SP CD8 T cells (Abele & Tampé 2004).

The second model is qualitative based on measuring the differential signalling of TCR interactions with pMHC. This model postulate that pMHC molecules either deliver a partly or complete activating signal which decides the fate of selected thymocytes. pMHC delivering a partly activating signal leads to positive selection, while the delivery of a complete activating signal results in negative selection (Hogquist et al. 1994).

Thymic expression and presentation of self-peptides to developing thymocytes is the key requirement for a successful deletion of self-reactive T cells. The autoimmune regulator (Aire) transcription factor has been found to regulate expression of several ectopic peripheral proteins (Anderson et al. 2002). Aire transcription factors are expressed in medullary thymic epithelial cells and monocyte populations which play an essential role in presenting self-peptides to developing thymocytes (Anderson et al. 2002; Kogawa et al. 2002; Liston et al. 2003).

Experiments on Aire deficient mice show that the negative selection of thymocytes is defective as T cells which are normally deleted were allowed to escape selection in the thymus (Liston et al. 2003). Mutations in Aire gene have been linked to autoimmune polyglandular syndrome type 1 (APS1) (Nagamine et al. 1997), suggesting that Aire controls the mechanism of screening of thymocytes for auto-reactivity to antigens they encounter before leaving the thymus (Nagamine et al. 1997).

Other factors have been postulated to play a role in regulating thymocyte selection in the thymus. One study showed that the disruption of the extracellular-regulate-kinase (Erk) activation influenced positive selection (Neilson et al. 2004).

However, another study showed that phosphorylation of p53 disrupted T cell signalling by influencing its ability to undergo negative selection (Gong et al. 2001). The Ikaros transcription factor is essential in positive and negative selection of thymocytes. Deficiency of Ikaros has been shown to cause defects in TCR selection and lineage decision (Urban & Winandy 2004; Tinsley et al. 2013).

1.3.5 T cell lineage commitment

DP thymocytes express both co-receptors CD4 and CD8 on their cell surface, and will eventually downregulate the expression of either CD4 or CD8 and continue their lineage commitment as CD4SP or CD8SP T cells. Cells expressing TCRs restricted by MHC-II become CD4SP cells, and cells expressing TCRs restricted by MHC-I become CD8SP cells (Teh et al. 1988). Several models have been put forward to explain lineage commitment (Singer et al. 2008). The stochastic selection model, postulates that the transcription of one of the two co-receptors is terminated stochastically, independent of TCR specification, following their interaction with MHC molecules and thereafter the newly generated SP cells must express TCRs and either one of the co-receptors CD4 or CD8, with matching specificities with MHC molecules or otherwise, they will be induced to die (Chan et al. 1993; Davis et al. 1993; Itano et al. 1994; Leung et al. 2001). However, experimentally, this model has not been found to be completely true (Keefe et al. 1999; Sarafova et al. 2005).

The instructive model is based on the signal strength of the interaction between DP thymocytes co-receptor and their TCRs with MHC molecules. The differential signals expressed by MHC-I or MHC-II restricted TCRs promote DP thymocytes

to terminate expression of their mismatching co-receptor molecules (Itano et al. 1996). It has been shown that CD4 generates stronger signals upon its engagement than CD8, as CD4 have been found to bind more lymphocyte-specific protein kinase (Lck) on its intracellular cytoplasmic tail than CD8 (Itano et al. 1996). Another study used chimeric co-receptor transgenes, where a CD8 molecule was constructed expressing the cytoplasmic tail of CD4 (Shaw et al. 1989). The chimeric CD8 expressing cells developed into MHC-II restricted 'CD4' cells suggesting that quantitative signalling differences between CD4 and CD8 coreceptors lead to lineage determination and commitment (Wiest et al. 1993). However, research conducted on the basis of changing TCR-signalling strength by manipulating several kinase activities to influence lineage commitment, failed to support this model influence TCR (Broussard et al. 2006; Fischer et al. 2005; Hernández-Hoyos et al. 2000; Schmedt & Tarakhovsky 2001; Sohn et al. 2001). Furthermore, ITAM deficient mice revealed results contradicting the basis of the instructive model (Holst et al. 2008).

The third model is instructional based on TCR signal duration, known as the duration-of-signal model. This model postulate that during positive selection, longer TCR signals terminate CD8 transcription, while shorter TCR signals terminate CD4 transcription (Yasutomo et al. 2000). This model promotes the idea that during positive selection, DP thymocytes on TCR-mediated signalling undergo cell surface complex changes, the result of this is a disruption in the MHC-I restricted TCR signalling (but not MHC-II) which in turn lead to a reduction in CD8 expression. However, it is unclear why DP thymocytes express the asymmetric phenotype $CD4^{+}CD8^{low}$, but it is strongly believed that these cells

are CD4SP and CD8SP precursors not committed to either lineages (Lundberg et al. 1995; Suzuki et al. 1995).

These collective experimental observations led to the formulation of non-classical model based on the classical kinetic signalling model where lineage commitment is mediated by TCR signal duration (Singer et al. 2008). It suggests that regardless of TCR specificities, DP thymocytes terminate CD8 gene transcription and convert to $CD4^{+}CD8^{-}$ transcription which appear phenotypically as $CD4^{+}CD8^{low}$ cells. Cells of this phenotype are thought to be responsible for thymocyte SP lineage decision (Singer et al. 2008). The non-classical model is based on the signal duration controlled by the common cytokine receptor γ chain signalling cascade which in turn is induced by interlukin-7 (IL-7) (Brugnera et al. 2000; Singer et al. 2008). IL-7 influences co-receptor reversal by the enhancement of CD4 gene silencing and re-initiates CD8 transcription (Yu et al. 2003).

It has been found that IL-7 mediated signalling events are blocked by persistent TCR signalling resulting in the formation of CD4SP cells. On the contrary, disruption of TCR signalling enables continuous IL-7 signalling which results in the formation of CD8SP cells (Singer et al. 2008). Furthermore, experiments based on modulation of the interleukin-7 receptor (IL-7R) signals by using specific antibodies against γc receptors and blocking the expression of negative regulators, (Gfi-1), resulted in a decrease and an increase of CD8SP and CD4SP cells respectively. These findings support the idea of TCR and cytokine-receptor cross-talk playing a role during T cell development (Yu et al. 2003; Yücel et al. 2003). It has also been shown that in DP cells, CD8 enhancer activity is suppressed by prolonged TCR signalling (Sarafova et al. 2005), while IL-7R signalling can enhance the activity of the CD8 enhancer through a signal

transducer and activator of transcription-5 (Stat-5) mediated process (Park et al. 2007). Further support for the non-classical model comes from the Zap-70 deficient mice where, Zap-70 signalling activity is blocked in cells expressing $CD4^{+}CD8^{low}$ leading to rapid TCR signal disruption. As a result, thymocytes become CD8SP including MHC-II restricted cells (Liu & Bosselut 2004).

In addition to the four models discussed, an ordinary differential model has been put to explain the 4:1 bias in CD4SP over CD8SP expression in total thymocytes. One study revealed that DP $TCR^{int}CD5^{hi}$ cell population exhibits asymmetry in death rates, as a result of higher apoptosis among MHC-I restricted cells compared to MHC-II restricted cells, regardless of the fact that their initial counts were similar (Sinclair et al. 2013).

The identification of several transcription factors has subsequently advanced our understanding of SP lineage determination and commitment. Research studies identified The–helper-inducing POK/Kruppel like factor (Th-POK) as essential in determining CD4 lineage choice, as it is expressed by CD4SP cells but not CD8SP cells (He et al. 2005; Sun et al. 2005). Positive selection was directed to CD4 lineage under forced expression of Th-POK, while in Th-POK knockout mice, the thymus lacks CD4SP cells despite the equivalent total number of SP cells. Furthermore, it has been shown that Th-POK suppresses the enhancer activity of CD8 and at the same time maintains the transcription of CD4 by preventing the run-related-transcription-factor-3 (Runx3), from silencing CD4 (Jenkinson et al. 2007). Runx3 is upregulated in $CD4^{+}CD8^{low}$ thymocytes, and it has been shown to bind the enhancer of CD8 in addition to the silencer element of CD4, mediating co-receptor reversal (Sato et al. 2005; Taniuchi et al. 2002; Grueter et al. 2005). Experimental evidence have shown that Runx3 binds *Zbtb7b*

gene which codes for Th-POK and blocks its expression. This interaction plays a central role in mediating CD4/CD8 transcription and lineage determination (Setoguchi et al. 2008).

Another key transcription factor is the Gata binding protein-3 (Gata3) which upon binding to *Zbtb7b* gene can regulate Th-POK activity. Gata3 deficient mice exhibit DP cells which did not express Th-POK and had markedly decreased CD4 differentiation (Pai et al. 2003; Wang et al. 2008). However, Gata3 does not induce MHC-I restricted thymocytes to commit to CD4SP, which suggest a more complicated role for this protein in thymocyte development (Hernández-Hoyos et al. 2003). Furthermore, the thymus high mobility group box protein (Tox) has been found to play a similar role to Gata3 protein in T cell development. DP thymocytes deficient in Tox protein, fail to produce CD4SP thymocytes and lack the expression of Th-POK. During positive selection Tox have been found to be upregulated and may influence the activity of Th-POK in a Gata3-dependent manner (Wilkinson et al. 2002; Aliahmad & Kaye 2008; Aliahmad et al. 2004).

1.3.6 T cell activation

Mature CD4SP and CD8SP thymocytes egress from the thymus after completing their development and migrate to the secondary lymphoid organs such as the lymph node and spleen. These un-primed T cells are in the G_0 resting phase of cell cycle and require the engagement with their cognate antigen for further maturation, as the initial engagement of their TCRs and co-receptors CD4 and CD8 with pMHC molecules during development, is not sufficient to stimulate signals necessary for clonal expansion. The co-stimulatory signals from antigen

presenting cells (APCs) result in the initiation of multiple signalling pathways necessary for proliferation, survival and effector functions of T cells.

The interaction of CD28 expressed on the surface of T cells with the B7 co-stimulatory molecules, glycoproteins CD80 and CD86 on APCs is essential for T cell maturation and clonal expansion. In the absence of this co-stimulation during TCR engagement anergic T cells are produced (Chen & Flies 2013). Treatment with anti-CD3 and anti-CD28 antibodies can mimic T cell clonal expansion in vitro. Co-stimulatory signals promote *IL-2* RNA stabilization and increase the synthesis of IL-2 by activated T cells (Hombach et al. 2001). IL-2 production supports T cell survival and proliferation. The CD40 molecule expressed on the surface of APCs interacts with CD40 ligand (CD40L) expressed on T cells leading to upregulation of CD80 and CD86 molecules expressed on the surface of APCs, thus stimulating T cell proliferation. The activation process slowly upregulates the CD28-like molecule, CTLA-4 (CD125) on T cells, which interacts with B7 glycoproteins with a higher avidity but at the same time, in an antagonistic manner (Linsley et al. 1991; Azuma et al. 1993; Hathcock et al. 1993). CTLA-4 can be detected after 24 hours of stimulation but reaches its peak expression only after 2 to 3 days.

A diverse range of molecules are regulated upon the activation of T cells including CD69 and CD25 (IL2-α). Activated CD8 T cells express tumour necrosis factor (TNF-α) and secrete interferon γ (IFNγ) (Zhang & Bevan 2011). On the other hand, CD4 activation subsequently results in the differentiation of CD4 into several types of effector cells, including T-helper-1 (Th1) and T-helper-2 (Th2) (Luckheeram et al. 2012). Th1 differentiation is promoted by IL-27, IL-12 and IFNγ produced by APCs and regulated by the transcription factor Tbx21 (or

Tbet) (Owaki et al. 2005; Trinchieri et al. 2003; Afkarian et al. 2002; Lugo-Villarino et al. 2003). Th2 cells produce IL4 and play an essential role in mediating the acquired immune response by coordinating the antibody response. Th2 cells are regulated by the cytokine signals of IL-4 and Gata3 expression. Th2 cells produce cytokines including IL-4 and IL-13 which are involved in the defence mechanism against extracellular pathogens and in allergic reactions, In addition, there are other Th populations, including Th17 cells (Kaplan et al. 1996; Glimcher & Murphy 2000).

1.3.7 Peripheral T cell tolerance

In the thymus, thymocytes are educated during their selection to achieve central tolerance, however, this selection process is not sufficient to induce tolerance to all peripheral antigens and T cells must undergo further maturation in the periphery to ensure their tolerance to self-antigens, and their activation on encountering non-self antigens (Kuklina 2013).

Peripheral tolerance of T cells occurs at various levels. Immunological ignorance of T cells means that they never have been exposed to a range of additional antigens because of their anatomical isolation, such as, the eye lens. Immunological ignorance also occurs when the processed peptide on the cell surface exists in concentrations which are not sufficient to activate auto-reactive T cells. Furthermore, peripheral tolerance can occur when T cells recognize pMHC in the absence of the co-stimulatory molecule CD28 making them anergic so that they become impossible to activate (Jenkins & Schwartz 1987; Boussiotis et al.

1993; Wells et al. 2000; Quill & Schwartz 1987; Jenkins et al. 1990; Macián et al. 2004).

Regulatory T cells (Tregs) are involved in the mechanism of peripheral tolerance and this population of cells is categorized as two subsets of cells. $CD4^{+}CD25^{+}$ natural T regulatory cells (nTregs) develop in the thymus following strong self-MHC-II recognition during TCR repertoire selection. The adaptive regulatory cells (aTregs) develop in the periphery as a result of activation, and specific cytokines, such as, IL-10 and transforming growth factor β (TGFβ) (Maggi et al. 2005; Bensinger et al. 2001). Furthermore, expression of The Forkhead/winged helix transcription factor (Foxp3) plays a key role in determining the fate of naive T cell by converting them into Tregs (Hori et al. 2003).

1.3.8 Notch and T cell lineage commitment

The Notch signalling pathway in vertebrates regulates many developmental processes and plays an essential role in thymocyte development and maturation, by inducing T cell lineage commitment (Guidos 2006; Jenkinson et al. 2007; Artavanis-Tsakonas 1999). There are four mammalian Notch receptors identified, (Notch1-4) and five Notch ligands (Delta1,3,4 and Jagged1,2) which have been found to be expressed on thymocytes and thymic epithelial cells (Felli et al. 1999). Ligand binding of Notch results in cleavage of the intracellular domain of the Notch receptor allowing its translocation into the nucleus and interaction with Cbf1/Rbp-jk cofactor, and mastermind-like (Maml) coactivator, to form a transcriptional complex, which eventually activates Notch target genes (Mumm & Kopan 2000; Nam et al. 2003; Struhl & Adachi 1998).

Hes proteins 1 and 5 have been found to be important effectors of the Notch signalling pathway in haematopoietic cells (Kawamata et al. 2002; Tomita et al. 1999). The removal of Notch signalling by a conditional deletion of Notch1, or inhibition of the Notch signalling pathway by receptor-ligand binding interference in haematopoietic progenitors led to the development of B cells in the thymus rather than T cells (Radtke et al. 1999; Koch et al. 2001; Wilson et al. 2001; Tanigaki et al. 2004; Maillard et al. 2004). Furthermore, overexpression of Notch1 can lead to the generation of T cells in the bone marrow where they overshadow B cell production (Radtke et al. 1999; Koch et al. 2001; Wilson et al. 2001; Maillard et al. 2004; Tanigaki et al. 2004). These observations showed that Notch signalling plays a key role in influencing progenitor cells in the thymus to commit to become T cells. However, other studies have suggested that the role of Notch signalling is to support T cell development in the thymus (Schwarz et al. 2007; Masuda et al. 2005).

Notch signalling plays a crucial role in the survival of early DN thymocytes and until the DN3 stage where Notch activation is required for induction of pre-TCR expression through co-operation with E2A protein (Michie et al. 2007; Wolfer et al. 2002). Notch signalling is downregulated during β-selection as Id3 protein rapidly increases as a result of the signal transduction of pre-TCR, and E2A-mediated Notch expression is suppressed (Yashiro-Ohtani et al. 2009). Notch is involved in determining CD4:CD8 cell ratio as a result of the differential expression of Notch receptors and ligands during foetal and adult development (Jiménez et al. 2001).

1.4 Morphogens influence thymocytes development

Many protein families first identified as developmental regulators of *Drosophila* have been found to influence thymocyte development and T cell lineage commitment. Among these are the Wnt family (Wnt), Bone morphogenic protein 2 and 4 (BMP2/4), and Hedgehog family of proteins (Hh) (Outram et al. 2000; Staal & Clevers 2003; Varas et al. 2003). While Wnt signalling promotes thymocyte development, the Bmp2/4 and Hh molecules promote and negatively regulate thymocyte development in the thymus (Crompton et al. 2007; Varas et al. 2003).

The secreted signalling molecules of the Wnt family are required for normal thymocyte development (Varas et al. 2003). It has been shown that Wnt signalling is necessary for normal thymic cellularity, and it promotes thymocyte survival and regulates their proliferation at the DN stage (Hsu et al. 2001; Mulroy et al. 2002; Staal et al. 2001). Wnt family signalling molecules transduce their signal into developing thymocytes through the Frizzled family of serpentine receptors and the low-density lipoprotein receptor-related proteins in addition to the Wnt/Ca^{2+} pathway (Tamai et al. 2000; Yang-Snyder et al. 1996; Bhanot et al. 1996; Liang et al. 2007). Wnt signalling results in the stabilization and nuclear translocation of β-catenin which acts via the lymphoid enhancer factor 1 (Lef1) and T cell factors 1 and 3 (Tcf1 and Tcf3), which leads to the activation of target genes including, those encoding Gata3 and Bcl11b, which are important for thymocyte development (Schilham et al. 1998; Hinck et al. 1994; Moon et al. 2002). In the absence of Wnt signalling, β-catenin is degraded causing an arrest in thymocyte development at the pro-T cell stage due to the absence of Lef1 and Tcf1 and overexpression of an inhibitor of the Wnt co-receptor, mDkk-1 (Weber et al.

2011; Weerkamp et al. 2006; Hinck et al. 1994; Moon et al. 2002; Okamura et al. 1998). The induction of the non-canonical pathway Wnt5a/C^{2+} through Wnt5a over-expression, increased apoptosis in foetal thymocytes (Liang et al. 2007).

The Bone morphogenic proteins 2 and 4 (Bmp2/4), regulate the development of many tissues and are secreted by thymic epithelium and their receptors are expressed by both the thymic stroma and thymocytes (Winnier et al. 1995; Zhang & Evans 1996; Outram et al. 2000; Graf et al. 2002; Hager-Theodorides et al. 2002; Hager-Theodorides et al. 2014). It has been shown that Bmp4 inhibits thymocyte proliferation and survival. Treatment of FTOCs with Bmp4 arrested thymocyte differentiation at the DN stage before T cell lineage commitment, and during the transition from DN to DP (Hager-Theodorides et al. 2014; Hager-Theodorides et al. 2002; Graf et al. 2002). Bmp2 and Bmp4 are members of the transforming growth factor-β (TGF β) family of secreted proteins. They transduce their signal through the ligation and hetero-dimerization of type I and type II serine-theronine kinase receptors, which phosphorylate R-smads (Smad-1, Smad-5, and Smad-8) (Wall & Hogan 1994; Miyazono et al. 2001). The phosphorylation of Smads, recruit Co-Smad/Smad4 and translocate to the nucleus forming complexes with several transcription factors to eventually activate Bmp target genes. The extracellular inhibitors of Bmp, Nogin, Cordin and Twisted gastrulation (Tsg) help regulate its signalling (Gazzerro & Canalis 2006). Tsg is expressed by the thymic epithelium and thymocytes and is upregulated after pre-TCR signalling after TCR signalling during the transition from DP to SP (Graf et al. 2002). It has been suggested that Bmp4's negative regulation of thymocyte development helps to control thymocyte numbers and maintain a pluripotent precursor population (Sacedón et al. 2003).

1.4.1 The discovery of Hedgehog

The Hedgehog (Hh) family of secreted proteins are found in all bilaterians and are key mediators of embryonic development and are implicated as essential regulators in many fundamental processes such as, growth, patterning and morphogenesis during animal development (Ingham et al. 2011).

The hedgehog (Hh) gene was first identified by Nusslein-Volhard and Wieschaus in 1980 by a large scale phenotype-driven screen for mutations that impair or change the development of the *Drosophila melanogaster* (fruit fly) larval body plan, which led to them to win the Nobel prize in 1995 (Nüsslein-Volhard & Wieschaus 1980). Hh mutant larvae appear to have ventral cuticle that has little segmental patterning compared to wild type and each segment is entirely covered with denticles. This appearance of a spiky larva inspired the name 'hedgehog' (Nüsslein-Volhard & Wieschaus 1980). Shortly after hh discovery in Drosophila, multiple homologues from invertebrates and vertebrates were identified, including Leech, sea-urchins, mouse, rat, chick, zebra, and human (Echelard et al. 1993; Roelink et al. 1994; Marigo et al. 1995; Chang et al. 1994; Riddle et al. 1993; Krauss et al. 1993).

The molecular mechanisms of Hh signal transduction have been characterized primarily using Drosophila genetics. In contrast, mammalian Hh signalling pathway is incompletely understood and harbours some differences and additional pathway components compared with Drosophila. However, most of the key events in the Hh signalling pathway are conserved between vertebrates and invertebrates (Varjosalo & Taipale 2008).

1.4.2 Hedgehog proteins

The Hh family of secreted intracellular signalling molecules play a major role in many patterning processes and organogenesis during embryonic development (Ingham & McMahon 2001) and are involved in the homeostasis and renewal of adult tissues, including skin, lung, gut, blood and thymus (Bhardwaj et al. 2001; Taipale & Beachy 2001; Sacedón et al. 2003; Outram et al. 2000). Hh proteins can function in both short and long-range signalling and also in a dose dependent manner, inducing cell fate and regulating cell survival and proliferation within a target field (Ingham & McMahon 2001; Duman-Scheel et al. 2002; Roy & Ingham 2002).

Philip Ingham, Andrew McMahon and Clifford Tabin identified three mammalian Hh proteins, Sonic Hedgehog (Shh), Desert Hedgehog (Dhh), and Indian Hedgehog (Ihh) (Krauss et al. 1993; Echelard et al. 1993; Riddle et al. 1993; Hammerschmidt et al. 1997). All three Hh proteins share 90% homology to each other and function as morphogens controlling multiple developmental processes, where they play essential non-redundant roles due to their diverse pattern of expression (Ingham & McMahon 2001; McMahon et al. 2003; Shimeld 1999; Pasca di Magliano & Hebrok 2003). A molecular evolutionary study found that the mammalian Hedgehog gene family arose by two gene duplications from an original single gene, the first gave rise to *DHH*, whereas the second produced the *IHH* and *SHH* (Kumar et al. 1996). As a result, *SHH* and *IHH* has been found to be more closely related to each other than to *DHH*. Furthermore, based on sequence similarity, *DHH* was found to be the closest vertebrate to the Drosophila *hh* gene (Varjosalo & Taipale 2008), whereas upon ectopic expression, Shh has

been shown to mimic embryonic Drosophila *hh* (Chang et al. 1994; Krauss et al. 1993).

1.4.2 (1) Sonic Hedgehog

Multiple homologues of *SHH* have been found in >104 organisms, and Zebrafish contain duplicated copies of Shh (Shha and Shhb) (Krauss et al. 1993; Ekker et al. 1995; Concordet et al. 1996; Koudijs et al. 2008). Shh homologues are highly conserved in vertebrates, with highest conservation found to be in the amino-terminal half (Echelard et al. 1993; Krauss et al. 1993; Riddle et al. 1993). Human *SHH* is 92.4% identical to its mouse homologue, whereas mouse and chicken are 84% identical, and mouse and zebrafish are 68% identical (Marigo et al. 1995). Human *SHH* consists of 3 exons and spans 9410 bps of the long arm (q) of chromosome 7 at position 36 (Marigo et al. 1995). Whereas the mouse *Shh* gene consists of 5 exons and spans 10262 bps of chromosome 5 in a region showing homology to human chromosome 7 (Marigo et al. 1995).

Amongst the three Hh proteins, Shh is the most broadly expressed Hh protein in mammals controlling development from embryo to adult. Its expression starts shortly after the onset of gastrulation in the presumptive midline mesoderm, from the node, throughout the notochord, the floorplate of the neural tube, the early gut endoderm, and the posterior of the limb buds (Ekker et al. 1995; Krauss et al. 1993; Chang et al. 1994; Echelard et al. 1993; Roelink et al. 1994; Hammerschmidt et al. 1997; Riddle et al. 1993; Johnson et al. 1994). During vertebrate embryogenesis, it is involved in many developmental processes, including left-right axis asymmetry (Dale et al. 1997; Logan et al. 1998), anterior-posterior polarity of the limbs and patterning of the brain and spinal cord (Riddle

et al. 1993; Roelink et al. 1995). Throughout embryonic development and in adults, Shh is mainly expressed in epithelial tissues and affects the development of a wide range of organs and tissues including, spinal cord, brain, heart, lung, gut, kidney, pancreas, pituitary gland, ovary, prostate, bone, thymus, cartilage, muscle, sensory organs, tooth and hair follicles (Ingham & McMahon 2001).

Shh plays a critical role as a morphogen controlling patterning during embryogenesis. The expression of Shh in the midline tissues, including the node, notochord and floorplate, controls left-right and dorsal-ventral asymmetry by regulating patterning of both, the left-right axes and dorso-ventral axes (Dale et al. 1997; Logan et al. 1998; Schilling et al. 1999; Watanabe & Nakamura 2000; Meyer & Roelink 2003). Blocking Shh expression leads to various biological defects, including cyclopia, ventral neural tube defects, somite and foregut patterning defects (Chiang et al. 1996; Varjosalo & Taipale 2008). Failure of patterning during embryogenesis affects the organogenesis of many systems resulting in various defects including, absence of the vertebrate and ribs, lung branching defects and sever distal limb malformation (Pepicelli et al. 1998; Litingtung et al. 1998; Varjosalo & Taipale 2008). Shh knockout in mice is embryonically lethal; they appear much smaller than their littermates and exhibit major craniofacial, limb and neural defects (Chiang et al. 1996).

The development of the central nervous system (CNS) is promoted by the expression of Shh through establishing a gradient expression emanating from the notochord and floorplate that is responsible for inducing the ventral-neuroepithelium into generating distinct neural subtypes of neural progenitor domains (Jessell 2000). Ectopic expresstion of Shh in-vivo and in-vitro, revealed that Shh induces the formation of the floorplate and regulates the differentiation of

the ventral motor neurons (Martí, Bumcrot, et al. 1995; Ericson et al. 1996). Blocking the expression of Shh produced in the notochord demonstrated that it is an essential regulator of notochord-mediated induction of motor neuron fates, and Shh mutants lack neuron induction and exhibit no floorplate and ventral spinal cord characteristics (Hammerschmidt et al. 1997; Martí, Takada, et al. 1995; Chiang et al. 1996).

Studies of Shh expression levels have shown that increasing the concentration levels of Shh induce the development of the ventral neuron fates (Dessaud et al. 2007; Ericson et al. 1997; Stamataki et al. 2005; Hammerschmidt et al. 1997; Martí, Takada, et al. 1995). It has been found that the lower concentration of Shh produced by the notochord and floorplate, induces motor-neurons at more distant regions (Yamada et al. 1993). Furthermore, the duration of Shh expression has been implicated in the regulation of neural-subtype identity as more ventral-neural identities require longer durations of Shh expression (Dessaud et al. 2007; Dessaud et al. 2010).

In the development and patterning of the vertebrate limb buds, the expression of Shh by a subset of posterior mesenchymal cells known as the ‘zone of polarizing activity (ZPA)’ located in the posterior limb bud region, regulates patterning of the distal elements of the limbs, including the anterior-posterior digit identity (Riddle et al. 1993; Chang et al. 1994; Johnson et al. 1994; Martí, Takada, et al. 1995; Hammerschmidt et al. 1997). A mirror-image duplication of limb digits has been generated through ectopic expression of Shh (Chang et al. 1994; Riddle et al. 1993; López-Martínez et al. 1995). Digit identity has been found to be primarily dependent on Shh concentration. It has been found that reducing Shh expression in the ZPA resulted in the loss of the ulna and posterior digits (Miller & Sassoon

1998). In addition to the anterior-posterior regulation of the limbs, Shh has been implicated in the regulation of the proximal and distal outgrowth of the limbs by inducing the expression of fibroblast growth factor 4 (FGF-4) in the posterior apical ectodermal ridge (AER) (Laufer et al. 1994; Niswander et al. 1994). Shh mutants lack distal limb structures as a consequence of the loss of FGF-4 expression in the dorsal ectoderm region (Chiang et al. 1996).

Shh has also been found to regulate vertebrate paraxial regions, the somites in the trunk, and the head mesenchyme rostral of the somites (Fan et al. 1995; Hammerschmidt et al. 1996; Johnson et al. 1994; Weinberg et al. 1996). Research conducted in chick and mouse found that Shh induces the expression of sclerotome-specific markers, including *Pax1* and *Twist* (Hammerschmidt et al. 1997; Fan & Tessier-Lavigne 1994).

Shh has also been implicated in the development of the brain as ectopic expression of Shh lead to ventralization of the mid- and hind- regions of the brain in mouse (Goodrich et al. 1996; Echelard et al. 1993). A study revealed that Shh controls patterning from a distance during brain development as the size, shape and orientation of the cell population produced depends on Shh source of signalling (Agarwala et al. 2001).

In the animal visual system, Shh has also been found to be expressed in the first retinal neurons as it induces neuronal differentiation across the retina (Neumann & Nuesslein-Volhard 2000). In the early tooth development, Shh plays a role positional signalling necessary for tooth growth (Thesleff 2003; Hardcastle et al. 1998).

Shh's role in cancer has also been studied. Shh signalling promotes lung development and plays a role in the regeneration and carcinogenesis of airway epithelium. During the repair of acute airway injury, extensive activation of Hh expression has been found characterized by induced signalling of Shh within epithelial compartment leading to neuroendocrine differentiation (Watkins et al. 2003). Furthermore, inhibition of Shh signalling induced chemoresistance in human cancer cell lines by increasing drug-efflux in an ABC transporter-dependent manner. It has been shown that Shh regulates ABC transporters ABCB1 and ABCG2 as targeted knockdown of these two transporters reversed Shh-induced chemoresistance (Sims-Mourtada et al. 2007).

1.4.2 (2) Desert Hedgehog

Multiple homologues of *DHH* have been found in 101 organisms. To determine the evolutionary relationship of these homologues to mammalian *DHH,* a phylogenetic tree constructed using complete sequences of all three Hh genes showed that non-mammalian "*DHH"* do not cluster with mammalian *DHH*, suggesting an independent evolutionary origin (O'Hara et al. 2011; Lewis & Eisen 2001). Several organisms have been identified to share putative homologs of human *DHH* gene, including cattle, dog, rat, mouse and western clawed frog. Human *DHH* spans 5398 bps of the long arm (q) of chromosome 12 at position 13.1 (Echelard et al. 1993; Kamisago et al. 1999; Marigo et al. 1995; Tate et al. 2000). The mouse Dhh gene spans 5510 bps of chromosome 15 in a region showing homology to human chromosome 12 (Tate et al. 2000; Kamisago et al. 1999; Marigo et al. 1995).

In the murine embryo, Dhh was found to be expressed by several tissues, including the heart, blood vessels, epithelium, peripheral nerve tissues, foetal liver, testis and ovaries (Bitgood & McMahon 1995; Bitgood et al. 1996; Parmantier et al. 1999; Ren et al. 2012). In adults, Dhh expression is restricted to the thymus, spleen, bone marrow, testis, ovaries and peripheral nerves (Bajestan et al. 2006; Spicer et al. 2009; Szczepny et al. 2006; Sacedón et al. 2003; Perry et al. 2009; Lau et al. 2012). The distinct expression pattern of Dhh during embryogenesis indicates a wide range of functions during the early stages of embryonic development. In contrast, the restricted pattern of expression in adults may indicate maintenance and regulatory functions restricted to Dhh-expressed tissues and their interacting cells and molecules.

Dhh has been found to play a role in gonadal development and gametogenesis**.** Dhh is expressed in the presumptive testis in mouse from E11.5 through to the adult stages and it has been found to be a key molecule in male germ line proliferation and spermatogenesis (Szczepny et al. 2006; Bitgood et al. 1996; O'Hara et al. 2011). Dhh-knockout male mice are infertile and have small gonads, devoid of sperm as a result of a deficiency in the production of male steroid hormone accompanied by a dramatic decrease in Leydig cell numbers (Bitgood & McMahon 1995; Bitgood et al. 1996). However, over-expression of Dhh in somatic cells can induce Leydig cell development indicating its role as an important regulator of Leydig cell development (Yao et al. 2002). In contrast, in females, Dhh expression has been detected in the granulose cells of pre-antral and antral follicles, however, Dhh-knockout female mice do not show disrupted ovarian phenotype and are fertile (Bitgood et al. 1996; Yao et al. 2002; Barsoum et al. 2009; Wijgerde et al. 2005).

In Human, *DHH* mutations have been identified in a small number of people with swyer syndrome also known as 46,XY complete or pure gondal dysgenesis (PGD). Homozygous Dhh mutations in 46,XY male patients impair the process of male sexual differentiation by causing a range of phenotypic spectrums, including complete pure gonadal dysgenesis (PGD), bilateral streak gonads, normally developed Mullerian ducts and female external genitalia (Canto et al. 2004; O'Hara et al. 2011). These patients develop a female appearance despite having the male chromosome pattern. In contrast, patients with a heterozygous mutation of *DHH* exhibit partial PGD and exhibit ambiguous genitals which do not appear clearly as male or female (Umehara et al. 2000; Canto et al. 2004).

Dhh is important for development of the nervous system as it is expressed in Schwann cells and signals to the connective tissues surrounding peripheral neurons to form a collagenous sheath around peripheral nerves. In Dhh-knockout mice the perineurial sheaths surrounding the nerve fascicles were abnormally thin as extensive minifascicles consisting of perineurial-like cells were found to be formed within the endoneurium (Bitgood et al. 1996). It has also been found that Dhh may play a key role in the maintenance of the adult nervous system and is responsible for its degeneration and regeneration after injury through nerve-schwan cell interactions (Parmantier et al. 1999; Mirsky et al. 1999; Bitgood & McMahon 1995). Induced sciatic nerve injury revealed a severe degeneration of the myelinated fibres in Dhh-knockout mice compared to WT. Furthermore, minifascicular formation in regenerated nerves was more severe compared to intact nerves in Dhh-knockout mice. Additionally, Dhh expression was down regulated in WT mice post-injury during nerve degeneration and upregulated following nerve regeneration (Bajestan et al. 2006).

Neuro-psychiatric and behavioural abnormalities are linked to Dhh gene mutation. Genome wide association studies (GWAS) have implicated it in risk for psychiatric disorders. A GWAS analysis on 1218 bipolar individuals and 2913 controls identified genetic variations in four genes including *DHH*, suggesting a link between Dhh as a causative agent in bipolar disorder (Green et al. 2013). In Autism, a study performed on 57 autistic individuals and 27 controls, found that serum levels of Dhh in autistic individuals are lower than those of controls (Bashir et al. 2014).

Behavioural abnormalities linked to the low testosterone levels and abnormal development in the testes are found in Dhh-knockout mice. Motor, sensory, learning, memory functions and mood fluctuations has been examined in Dhh-knockout mice. In a forced swimming test, Dhh-knockout male mice exhibited a prolonged immobility time indicating a depressive and anxiety-like behaviour compared to WT male mice. In contrast, Dhh-knockout female mice did not show any significant behavioural abnormalities (Umehara et al. 2006).

Dhh has been implicated in prostate cancer as the expression of Dhh is upregulated in androgen-deprived and castration-resistant prostate cancer (CRPC) (Ibuki et al. 2013). Childhood Acute Myeloid Leukemia (AML) has also been linked to Dhh. A recent study performed a whole-transcriptome sequencing of 237 cases of cytogenetically normal paediatric AML identified Dhh as a recurrent fusion transcript in the worse survival outcome group of AML. Furthermore, gene expression analysis carried on these patients also revealed over-expression of Dhh (Masetti et al. 2013).

In mouse erythropoiesis, our laboratory showed that Dhh is involved in murine erythropoiesis by negatively regulating multiple stages of erythrocyte differentiation. Bone marrow analysis of Dhh-knockout mice revealed an increase in the common myeloid progenitor (CMP) population. However, CMP differentiation to granulocyte/macrophage progenitors was decreased, and there was a decreased granulocyte population compared to WT. In contrast, CMP differentiation to megakaryocyte/erythrocyte progenitors was found to be increased in Dhh-knockout compared to WT. The same study revealed that Dhh negatively regulated erythroblast differentiation and erythroblasts were Dhh-responsive in-vitro and and ex-vivo (Lau et al. 2012). Under stress-induced erythropoiesis, erythrocyte differentiation was increased in both bone marrow and spleen of Dhh-knockout mice compared to WT (Lau et al. 2012).

1.4.2 (3) Indian Hedgehog

Multiple homologues of *IHH* have been found in about 119 organisms. Several organisms have been identified to share putative homologs to human *IHH*, including chimpanzee, rhesus monkey, cattle, dog, mouse, rat, chicken, western clawed frog and zebrafish. Two extra Ihh homologs have been found in zebrafish, echidna hedgehog (Ehh) and Qiqihar hedgehog (Qhh) (Currie & Ingham 1996; Ingham & McMahon 2001). Human *IHH* consists of 3 exons and spans 6097 bps of the long arm (q) of chromosome 2 between positions 33 and 35 (Marigo et al. 1995; Leek et al. 1997). The mouse *Ihh* gene consists of 3 exons and spans 6358 bps of chromosome 1 (Marigo et al. 1995).

Ihh is expressed by epithelial cells in a restricted number of tissues, including the primitive endoderm, gut, pre-hypertrophic chondrocytes in the growth plates of bones, kidney, liver and in the thymus (St-Jacques et al. 1999; Outram et al. 2000; Dyer et al. 2001; van den Brink 2007; Marigo et al. 1995). The expression of Ihh starts from the early somite stages and is mainly involved in bone morphogenesis, gastrointestinal development and uterine-embryo implantation (Bitgood & McMahon 1995; Echelard et al. 1993).

Several studies found that Ihh is important in endochondrial bone development through regulating chondrocyte and perichondrial differentiation. Ihh is expressed in the prehypertrophic chondrocytes of cartilage elements regulating the rate of hypertrophic differentiation (Vortkamp et al. 1996). Disruption of Ihh expression prevents chondrocytes undergoing proliferation from imitating the hypertrophic differentiation process resulting in abnormal limb development (Lai & Mitchell 2005; St-Jacques et al. 1999).

Ihh knockout in mice is embryonically lethal as all embryos die during embryogenesis, or at birth due to respiratory failure as a result of restrictive under-development of the rib cage (Varjosalo & Taipale 2008; St-Jacques et al. 1999). Surviving embryos do not have gross visible abnormalities, however, they exhibit shortened limbs compared to WT littermates as a result of cortical bone defects and aberrant chondrocyte development in the long bones (St-Jacques et al. 1999; Colnot et al. 2005). Shh and Ihh double mutant embryos die much earlier than the single knockouts, indicating that overlapping functions and redundancies exist between Shh and Ihh proteins (Zhang et al. 2001; Pathi et al. 2001). In post natal mouse, Ihh has been found to be reduced as osteoblasts matured, and performing selective upregulation of Ihh resulted in sever osteopenia characterized by

increased bone formation and excessive bone resorption (Mak et al. 2008). Furthermore, inhibiting Ihh signalling in mature osteoblasts increase bone mass and protection from bone loss in older mice (Mak et al. 2008).

In human, homozygous hypomorphic mutations of *IHH* has been linked to two congenital conditions, brachydactyly type A-1 characterized by shortness of the fingers and toes, and acrocapitofemoral dysplasia characterized by exhibiting bone defects with short stature (Hellemans et al. 2003; Gao et al. 2001).

Ihh has also been found to regulate the development of mammalian gastrointestinal tract and is involved in human gastrointestinal malformations (Ramalho-Santos et al. 2000). Ihh mutant mice show reduced epithelial stem cell proliferation and differentiation accompanied by reduced smooth muscle, gut malrotation and annular pancreas (Ramalho-Santos et al. 2000; Hebrok et al. 2000). On the contrary, a wide range of digestive tract tumors have been linked to Ihh ligand expression, including oesophagus, stomach, biliary tract, colon and pancreas suggesting a role in Ihh essential for tumor growth (Berman et al. 2003).

Research has also found that Ihh is a key mediator of progesterone signalling in the mouse uterus. Uterine epithelial tissues express Ihh under the control of the steroid hormone, progesterone. The role of Ihh has been found important in regulating progesterone action in the uterus and mediating uterine-epithelium communication with stroma essential for embryo implantation (Lee et al. 2006).

1.4.3 Hedgehog proteins synthesis and modification

Hh proteins, Shh, Dhh and Ihh are synthesized as a pro-protein of 45KDa which contains all functions necessary for signalling. The N-terminal (N-Hh) contains signal activity sequence and a conserved "hedge" domain, the C-terminal (C-Hh) contains auto-proteolysis activity sequences and a conserved "Hog" domain (Lee et al. 1994). The C-Hh peptide cleaves Hh precursor through nucleo-philic attack catalysed by auto-proteolysis. This reaction releases the 19KDa N-Hh peptide from the precursor, which immediately undergoes lipid modifications by the addition of cholesterol at its C-termini (C-termini of N-Hh peptide) via covalent coupling, followed by palmitoylation of the cystein residue closest to its N-terminal (N-terminal of N-Hh peptide) by acyl-transferase, Hhat (Figure 1.3) (Porter et al. 1996; Pepinsky et al. 1998).

These lipid modifications promote Hh signalling by helping secretion of the proteins and enable a longer range of action by the formation of a freely diffusible multimeric complexes (Zeng et al. 2001; Peters et al. 2004). Both domains, the "hedge" and "hog" have been linked to a wide variety of ancient organisms by several independent pre-existing proteins. It has been suggested that both domains first appeared together as hedgehog in the common ancestor of Cnidarians and bilateria about 650 million years ago (Ingham et al. 2011).

1.4.4 The Hedgehog signalling mechanism

All three mammalian Hh proteins trigger a common signalling pathway. The secretion of Hh intracellular proteins from Hh producing cells initiates a signalling cascade by modulating gene transcription upon Hh proteins binding

with their receptor patched (Ptc1), a 12-span transmembrane protein on the surface of Hh responsive cells. In the absence of Hh, Ptc represses the functions of Smoothened (Smo), a 7-span transmembrane protein that acts as the central transducer for Hh signalling (Figure 1.4) (McMahon et al. 2003; Hooper & Scott 2005; Alcedo et al. 1996). Two mammalian homologues of Ptc has been identified, Ptc1 and Ptc2, which all bind to Hh proteins (Goodrich et al. 1996; Stone et al. 1996; Motoyama et al. 1998). Ptc1 is expressed close to Shh and Ihh expressing cells, whereas Ptc2, is expressed in Shh expressing cells.

Ptc mutations in fly and mouse reveal that Ptc suppress Hh target genes suggesting that Hh proteins act by antagonising the activity of Ptc (Goodrich et al. 1997; Ingham et al. 1991). Mutation and biochemical studies revealed that Ptc directly binds to Hh through its first transmembrane domain and two extra cellular loops, following their binding, both proteins become internalised inside the cell and to intra-cellular vesicles or lysosomes (Marigo & Tabin 1996; Stone et al. 1996; Philip W. Ingham & McMahon 2001; Mullor & Guerrero 2000; Incardona et al. 2000; Mastronardi et al. 2000).

Binding of Hh with its receptor Ptc releases Smo from inhibition and activates members of the gliomma-associated oncogene transcription factors (Gli1-Gli3) (P W Ingham & McMahon 2001; Lum & Beachy 2004; Hooper & Scott 2005; Rowbotham et al. 2007). The molecular basis of Ptc mediated Smo inhibition is not fully understood. However, there is consensus agreement that it is not a direct one to one interaction, as Ptc at sub-stoichiometric ratios can inhibit Smo (Taipale & Beachy 2001). Several studies have shown that the activation of the Hedgehog pathway induces opposite effects on the localization of Ptc and Smo inside the cell (Denef et al. 2000; Incardona et al. 2002). Additionally, approximately 50

molecules of Smo are inhibited as a result of only one Ptc molecule, suggesting that Ptc regulates Smo via unidentified intermediates.

Recent studies have shown that Ptc mediates inhibition through the synthesis of phosphotidylinsositol-4-phosphate (Yavari et al. 2010). It has been shown that Ptc has a sterol-sensing domain which shares structural similarities with other proteins involved in cellular tracking (Nakano et al. 1989; Scott & Ioannou 2004; Carstea et al. 1997). It has been suggested that Ptc may act as a transporter by trafficking hydrophobic molecules that regulate Smo activity (Huangfu & Anderson 2006). Furthermore, it has been found that Ptc has dual actions on Smo, by inhibiting Smo activation and also limiting its expression on the plasma membrane (PM) through the transportation of an unidentified small-molecule inhibitor which alter the localization of Smo upon binding with Ptc (Denef et al. 2000; Incardona et al. 2002; Taipale et al. 2002).

Downstream of Hh signalling are the Glioma-associated oncogene family of transcription factors (Gli) which play a critical role as principal regulators or effectors of Hh signalling (Sasaki et al. 1999). There are three mammalian members of Gli (Gli1-3). However, *Drosophila* has one downstream transcriptional mediator, coded by cubitus interruptus (Ci) gene (Medvinsky & Dzierzak 1996). Gli1 was the first to be discovered and was initially identified as an amplified gene and a potential oncogene in a human glioma line (Kinzler et al. 1987; Kinzler et al. 1988).

Upon activation of Hh signalling, Gli proteins are transported to the nucleus to promote target gene transcription. In the absence of Hh signalling, Gli2 and Gli3 undergo modification by phosphorylation and truncation of their transactivation

domain and are transported to the nucleus where they function as repressors of target gene transcription (Matise & Joyner 1999; Koebernick & Pieler 2002; Crompton et al. 2007; Aza-Blanc et al. 2000; Sasaki et al. 1999). The phosphorylation of Gli proteins is induced through kinase recognition motifs near the C-terminal of Gli proteins by protein kinase-A (PKA), casein kinase-1 (CKI) and glycogen synthase kinase-3 (GSK3), followed by ubiquitylation catalysed by Btrcp protein resulting in protesome degradation of the C-terminal (Wang et al. 2000; Pan et al. 2009; Price & Kalderon 2002; Tempé et al. 2006; Jia et al. 2005).

Several studies have shown that the fruit-fly motor protein, Costal2 (Cos2) is essential in the recruitment of Ci, PKA, CKI, and GSK3 to form a Hh signalling complex (HhSc) (Stegman et al. 2000; Forbes et al. 1993). Following Hh binding to Ptc, the activity of Ptc is blocked allowing the translocation of Smo to the PM, where it undergoes phosphorylation by PKA, CKI and GSK3. This binding leads to a conformational change enhancing its interactions with Cos resulting in the phosphorylation of Cos by another serine/threonine kinasse, Fused (Fu) (Park et al. 2007) and eventually, Ci is released from the HhSc. Fu-dependent phosphorylation of the kinase suppressor of Fused (Su(fu)) ensures the disassociation and translocation of the full length form of Ci into the nucleus (Lum et al. 2003; Ruel et al. 2003). The full length form of Ci is mildly activated and promotes transcription activation of Hh genes by undergoing further processing into a more activating form Ci-A (Ruel et al. 2003; Lum et al. 2003; Sisson et al. 1997; Robbins et al. 1997).

In mice, Hh signal transduction is similar with Kif7, the mouse orthologue of Cos2, controling the processing of Gli proteins by regulating their intracellular localization (Robbins et al. 1997; Sisson et al. 1997). Furthermore, non-

haematopoietic murine cells rely on the primary cilium to transduce Hh signalling. In these cells, high exposure to Hh localizes Smo to the axoneme of the cilium followed by Sufu-Gli accumulation at the tip which aids the dissociation of the complex in response to Smo activity by a yet unknown mechanism (Goetz & Anderson 2010).

Other co-receptors have also been identified in mice, including, Cdo (brother of Cdo (Boc)) and Gas1, which upon binding with Hh, result in enhanced signal transduction by either facilitating ligand presentation to Ptc or counteracting the effects of the feedback mediated sequestration (Kang et al. 2007; Tenzen et al. 2006). Mice deficient in any of these co-receptors develop holoprocencephaly. The cell surface receptor Hedgehog-interacting protein (Hhip), has also been identified in vertebrates. However, it has been found to have no role in signal transduction but exclusively sequesters Hh ligands unlike Ptc, Boc, Cdo and Gas (Allen et al. 2011; Beachy et al. 2010).

In vertebrates, Gli2 and Gli3 have dual functions, as transcriptional activators or transcriptional repressors (Sasaki et al. 1999; Aza-Blanc et al. 2000). Gli1 can only act as a transcriptional activator and it is not required to initiate the Hh signalling cascade (Park et al. 2000). However, Gli1 itself is a target gene of Hh signalling and measurement of its transcription can indicate Hh signalling in a population of cells (Crompton et al. 2007). Mim/Beg4, the transcriptional target of Hh, has been shown to bind and upregulate the transcription activity of both, Gli1 and Gli2 (Callahan et al. 2004; Gonzalez-Quevedo et al. 2005). It has been also shown that the Yak-1 related kinase Drk-1, maintains Gli1 in the nucleolus and enhances its activity (Mao et al. 2002).

Studies on mutant mice have shown that the three Gli proteins exhibit individual or partially overlapping functions. Gli2 and Gli3 knockouts are embryonically lethal, while the homozygous mutants of Gli1 are viable (Mo et al. 1997; Park et al. 2000; Hui & Joyner 1993). Gli2 knockout embryos are small in size and have defects in their palate, and exhibit flattened head and carniofacial abnormalities. Gli3 knockout embryos have polysyndactyly (extra toes), and suffer from skeletal defects. These defects become very severe in mice bearing double knockouts of Gli1 and Gli2, or Gli2 and Gli3, suggesting functional redundancies. This role is observed in a study showing a rescue from Gli2 knockout defects on the expression of Gli1, under control of the Gli2 promoter (Bai & Joyner 2001).

1.4.5 Hedgehog target genes and associated conditions

Members of the Gli family of proteins are characterized as large transcription factors which bind to a specific DNA consensus sequences through the last three fingers of their five-zinc finger domain (Hui et al. 1994). Gli1 and Gli3 recognize the DNA sequence GACCACCCA, and Gli2 recognizes a similar DNA sequence GAAACCACCCA (Tanimura et al. 1998; Vortkamp et al. 1995). Ptc and Hhip1 cell surface molecules were found to be upregulated by Hh signalling and are considered as an important negative feedback mechanism for Hh (Marigo & Tabin 1996; Chuang et al. 2003; Lipinski et al. 2006). Boc, Cdo and Gas1 co-receptors have also been found to be targets of Hh signalling (Tenzen et al. 2006).

Mutation in these co-receptors or Shh result in sever developmental abnormalities including, cyclopia in human and are embryonically lethal causing stillborn abnormalities. In humans, loss of Gli3 function leads to lung and skeletal

abnormalities including, Greig's cephalopolysyndactyly (Hui & Joyner 1993; Vortkamp et al. 1991). Gli2 mutations cause cranio-facial abnormalities including a cleft-palate (Mo et al. 1997).

Hh plays an essential role in regulating the development of a wide range of tissues and organs regulating genes involved in cell structure, proliferation and survival. Several studies have shown that Ccnd2 (Cyclin d2) and E2f1 genes to be involved in the G1 to S transition contain Gli binding sites, and are upregulated directly by Gli1 (Yoon et al. 2002; Brooks et al. 1996). Hh signals have also been shown to upregulate Bcl2, the anti-apoptotic gene, in addition to the growth factors, H19 and Igf2 genes through Gli1 and Gli2, and downregulate the pro-apoptotic gene Tsc22 (TGF-β stimulated clone gene) (Bigelow et al. 2004). In epithelial and mesenchyme cells, Gli has been found to upregulate Snail factor involved in the metastasis, and increase Osteopontin and also decrease Embgin and Plakoglobin levels to promote reduced cell adhesion (Karhadkar et al. 2004).

Many research studies have implicated Hh signalling in cancer. Ptc mutations in humans have been linked in the aetiology of several childhood cancers including, medulloblastoma, and rhabdomyosarcoma, and are the main cause of Gorlin syndrome which increases predisposition to Basal Cell Carcinoma (BCC) (Gorlin 1995; Peters et al. 2004; Hahn et al. 1998). Most cases with BCC exhibit abnormal Gli1 and Gli2 increases (Dahmane et al. 1997; Regl et al. 2002). Many malignant tumours have been linked with abnormal Hh signalling including, stomach, prostate and pancreatic cancers. Unlike BCC, these tumours are dependent on Hh ligands where Hh neutralization can block them in both in-vivo and in-vitro (Thayer et al. 2003; Karhadkar et al. 2004; Chi et al. 2006).

1.4.6 Hedgehog signalling during T cell development

Recent studies have shown that Hh signalling is essential in the human and mouse immune systems, especially in T cell development (Gutiérrez-Frías et al. 2004; Outram et al. 2000; Sacedón et al. 2003; Shah et al. 2004; El Andaloussi et al. 2006). Our laboratory was first to report the expression and function of Hh signalling components in adult and foetal thymus and found that Hh signalling regulates thymocyte development during the transition from DN to DP stage (Outram et al. 2000).

Reverse transcriptase polymerase chain reaction (RT-PCR) and immune-histochemical studies revealed the presence of all three Hh proteins, Shh, Dhh and Ihh in the whole thymus (Sacedón et al. 2003). The thymus epithelial cells in the medulla, sub-capsular region and the cortico-medullary express Hh proteins, while the source of Ihh is mainly the DP thymocytes (Outram et al. 2000; Virts et al. 2006; Outram et al. 2009). However, the nature and strength of Hh signal to developing thymocytes depends on their position within the thymus.

RT-PCR analysis of different thymocyte populations in mice revealed that Smo expression is highest in the DN cells, especially at the DN2 stage. It has also revealed that Smo expression is down-regulated in DP and SP thymocytes, while Ptc could be detected in the DN, DP, and CD8SP cells (Shah et al. 2004; Outram et al. 2000; El Andaloussi et al. 2006; Crompton et al. 2007). Furthermore, the foetal expression pattern of the Gli proteins reveals some activity of Gli2 and Gli3 at the DN1 stage of thymocyte development followed by a rise in the expression of Gli2 at the DN2 stage in conjunction with a peak expression of Gli1 and a dip in that of Gli3. The expression of Gli2 then starts to dip before the formation of

the pre-TCR complex and then rises upon pre-TCR signal transduction. Interestingly, in adult thymus, the expression of Gli3 seems to be in the thymic stroma and not in developing thymocytes (Rowbotham et al. 2009; Rowbotham, Hager-Theodorides, Cebecauer, et al. 2007). In adult human whole thymuses, the expression of Hh pathway member proteins including, Shh, Dhh, Ihh, Smo, Ptc and Gli1-3 have been detected with Shh to be restricted to the medulla and subcapsular regions (Sacedón et al. 2003).

Analysis of murine foetal thymocyte development in Shh-deficient embryos has shown that Shh is essential for the differentiation, proliferation and transition of thymocytes from the DN1 to DN2 stage. Thymi from Shh-knockout mice contained approximately 10 times fewer thymocytes with a partial arrest in the development of thymocytes at the DN1 stage compared to WT of the same litter (Shah et al. 2004; Crompton et al. 2007). These findings also revealed that Shh as a negative regulator of differentiation at the transition from DN3 to DP stage (Outram et al. 2000; Rowbotham et al. 2009). Human thymus reaggregation cultures revealed that the differentiation of $CD34^{+}$ human precursors to DP cells was accelerated with treatment with a neutralizing anti-Shh antibody, and arrested with recombinant Shh (Gutiérrez-Frías et al. 2004). These findings suggest that the removal of the Shh signal accelerated the development of DP thymocytes and that Shh is a negative regulator during this transition. However, ex-vivo analysis of Shh knockout embryos revealed a smaller number and proportion of DP thymocytes compared to wild types (Shah et al. 2004). Furthermore, conditional Smo knockout mice have been reported to exhibit reduced thymic cell numbers and increased cellular apoptosis at the DN stage. These findings suggest that Shh is essential in promoting differentiation of thymocytes from the DN to the DP

stage (El Andaloussi et al. 2006). Studies on mutant mice embryos reveal that Hh signalling plays an essential role in regulating the homeostasis of DN progenitors during the transition from the DN1 to DN2 stage, as this process is hindered in mice lacking Shh or Gli3 (Outram et al. 2009; Shah et al. 2004; Gutiérrez-Frías et al. 2004; Hager-Theodorides et al. 2005).

These collective findings suggest that Shh is a positive regulator during the transition of thymocytes from DN1 to DN2 stage, and negative regulator during the transition of thymocytes from DN3 to DP stage. Our laboratory have shown through using mouse models that Shh driven-negative regulation at the transition from DN3 to DP stage is Gli-dependent (Rowbotham et al. 2009). However, the mechanism of this arrest is still not known.

Studies on Ihh have also shown a similar non-redundant dual role, suggesting that Ihh regulates T cell development prior pre-TCR signalling, and inhibits the development after pre-TCR signalling (Outram et al. 2009). Furthermore, Shh has been shown to reduce TCR signal strength during the later stage of T cell development, by attenuating TCR repertoire selection, T cell CD4SP/CD8SP lineage commitment and Th effector reponses in the periphery (Hager-Theodorides et al. 2009; Rowbotham, Hager-Theodorides, Cebecauer, et al. 2007; Drakopoulou et al. 2010; Rowbotham, Hager-Theodorides, Furmanski, et al. 2007; Lowrey et al. 2002; Stewart et al. 2002; Furmanski et al. 2012; Furmanski et al. 2013).

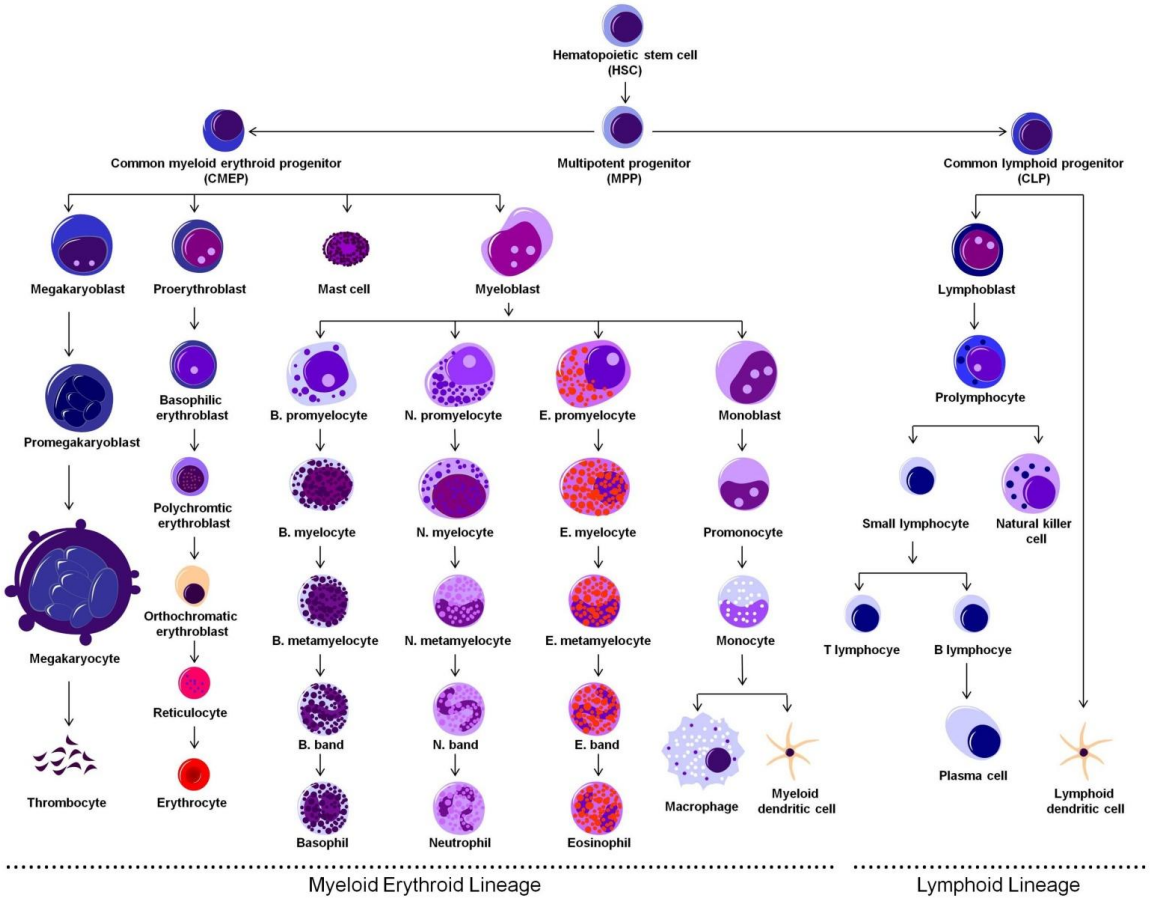

Figure 1.1

Haematopoietic cell development. Haematopoietic cell development from HSC to mature blood cells. HSCs give rise to MPPs which differentiate into either CMPs or CLPs. CMP lineage gives rise to mature erythrocytes, platelets, basophil, neutrophil, eosinophil, macrophage and myeloid dendritic cells. CLP lineage gives rise to T lymphocytes, B lymphocytes, natural killer cells and lymphoid dendritic cells. **HSC;** Heamatopoietic stem cell. **MPP;** Multipotent progenitor. **CMP;** Common myeloid progenitor. **CLP;** Common lymphoid progenitor. **Myeloblast lineage;** (**B;** Basophil. **N;** Neutrophil. **E;** Eosinophil). **Lymphocyte lineage;** (**T;** T cells. **B:** B cells). Figure elements modified from (motifolio.com).

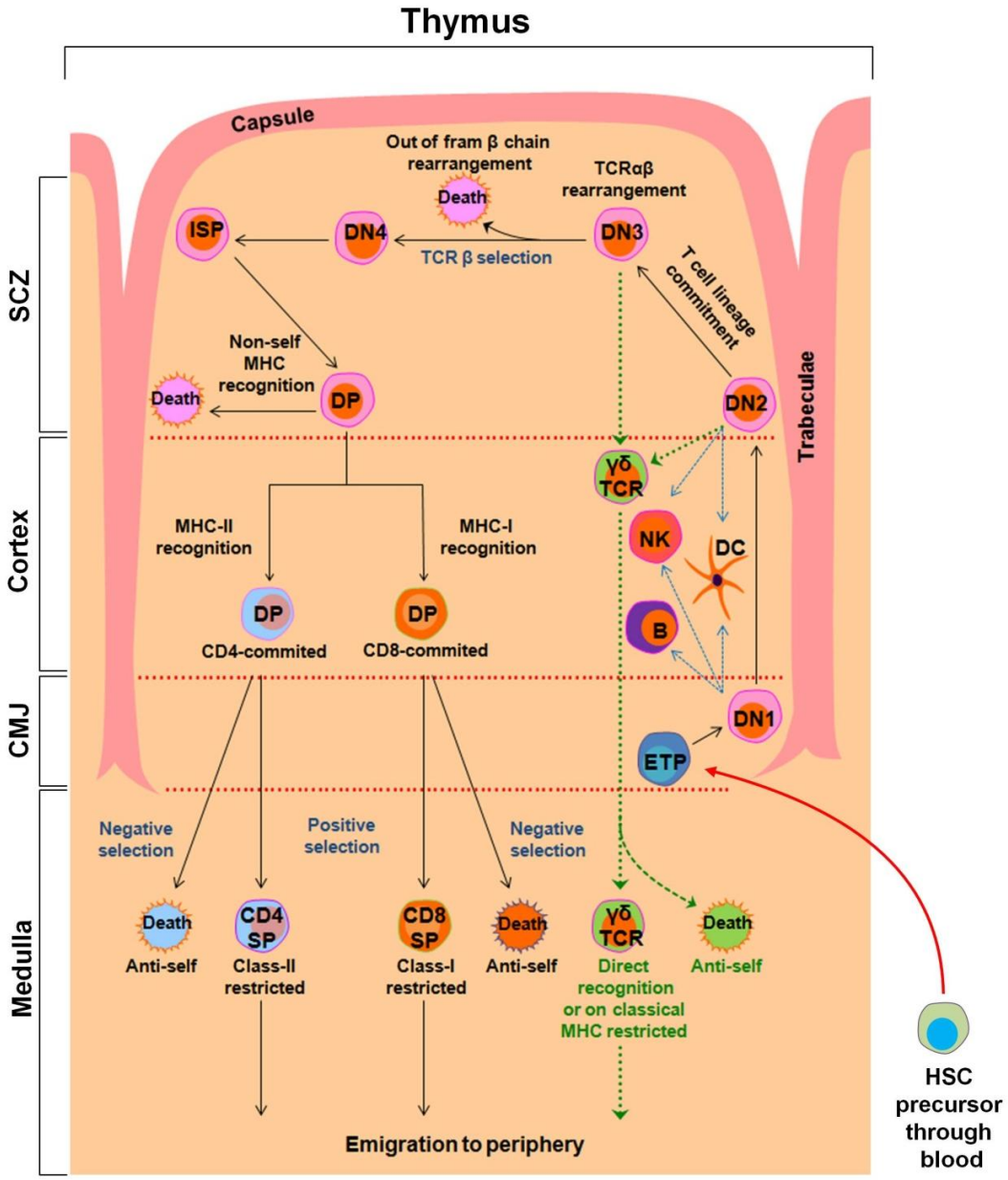

Figure 1.2

Overall scheme of T cell development in the thymus. Early thymocyte progenitors (ETPs) upon entry to the thymus give rise to double negative (DN) thymocytes. As cells progress through the DN2 to the DN4 stages, they express the pre-TCR. Successful pre-TCR expression leads to cell proliferation during the DN4 promoting thymocyte transition to the double positive (DP) stage. The DP thymocytes interact with cortical epithelial cells expressing high density of MHC class-I and class-II molecules associated with self-peptides. Low signalling results in delayed apoptosis (death by neglect), whereas high signalling promote acute apoptosis (negative selection). The expression of an intermediate level TCR signalling, initiate effective maturation (positive selection). Thymocytes that express TCRs that bind self-peptide (MHC class-I) ligands become $CD8^+$ T cells, whereas hymocytes expressing TCRs that bind self-peptide (MHC class-II) ligands become $CD4^+$ T cells. Figure adapted from (Germain 2002). **SCZ;** Subcapsular zone. **CMJ;** Cortico-medullary junction.

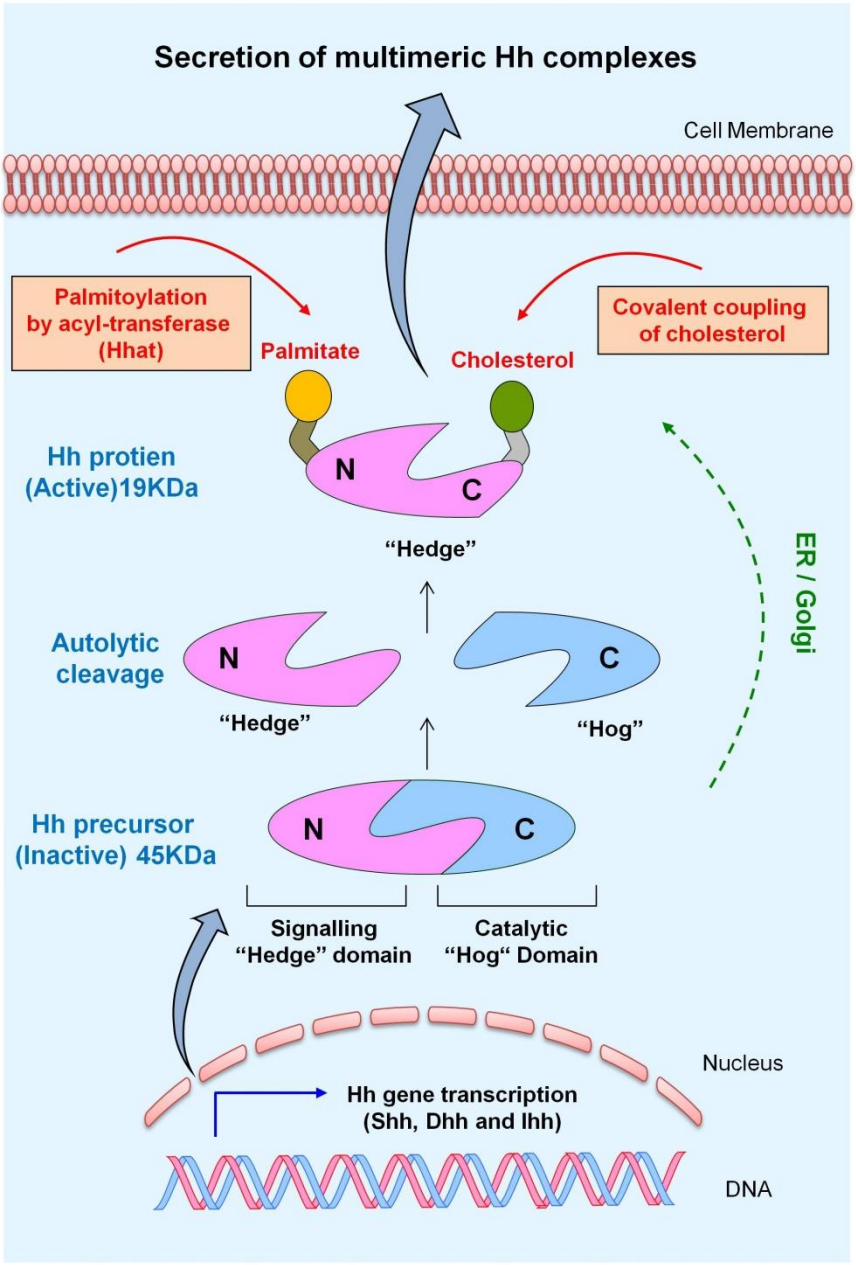

Figure 1.3

Hedgehog proteins synthesis and modification. Hh proteins are synthesized as a pro-peptide of 45KDa. The N-terminal (N-Hh) contains signal activity sequence and a conserved "hedge" domain, the C-terminal (C-Hh) contains auto-proteolysis activity sequences and a conserved "Hog" domain. The C-Hh peptide cleaves Hh precursor through nucleo-philic attack catalysed by auto-proteolysis. This reaction releases the 19KDa N-Hh peptide from the precursor, which immediately undergoes lipid modifications by the addition of cholesterol at its C-termini (C-termini of N-Hh peptide) via covalent coupling, followed by palmitoylation of the cystein residue closest to its N-terminal (N-terminal of N-Hh peptide) by acyl-transferase, Hhat. These lipid modifications promote Hh signalling by helping secretion of the proteins and enable a longer range of action by the formation of a freely diffusible multimeric complexes.

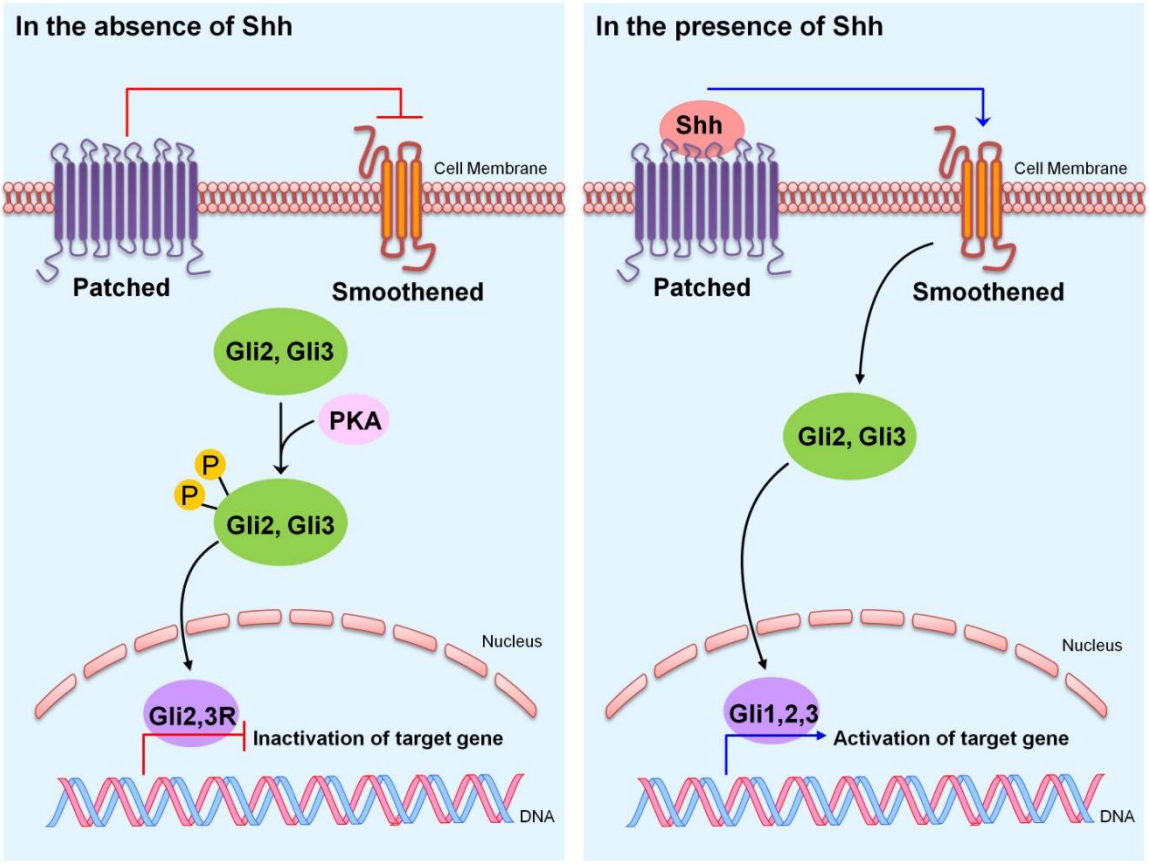

Figure 1.4

Shh signalling mechanism. Patched (Ptc1) inhibits smoothened (SMO) activity in the absence of Shh, allowing the phosphorylation and truncation of Gli2 and Gli3 by the activity of protein kinase A (PKA). Gli2rep and Gli3rep are transported to the nucleus where they negatively regulate gene transcription. In the presence of Shh protein, the interaction of Shh with Ptc1 relives SMO from inhibition. Activated SMO protects Gli proteins from PKA-mediated modification and activates them. Gli1-act and Gli3-act are then translocated to the nucleus where they activate target gene transcription. Figure adapted from (Crompton et al. 2007).

1.5 Thesis Objectives

Herein, we hypothesised that the Hedgehog family of secreted proteins play a central role in T cell development and maturation in the thymus. Their role in the periphery remains less understood.

Specific aims of this thesis are:

1. To determine the effect of Hedgehog signalling on thymocyte development and maturation by utilising mouse models that use genetically active/suppressor of Hh signalling.
2. To determine the effect of Desert Hedgehog (Dhh) on T cell development and maturation in the periphery by utilizing mouse models where the physiological expression of Dhh is either suppressed or activated.
3. To determine the effect of Hh-signalling on T cell repertoire selection by utilizing mouse models bearing rearranged αβ TCRs where lineage choice is biased by the specificity of their transgenic TCR.
4. To determine the effect of Sonic Hedgehog (Shh) on T cell development and lineage choice by performing Shh-treated thymic organ cultures taken from mouse models bearing rearranged αβ TCRs.

Despite extensive work, the function(s) of hedgehog-pathway components in the thymus as well as in the periphery, is still not fully understood. To improve our understanding of this family of ligands, various knock-out murine models were employed. Differences in differentiation and transition from one developmental stage to the next in mouse models where Hh-signalling was either suppressed or activated was investigated. In addition, similar analysis was performed where T

cell selection was biased by expressing transgenic TCRs expressing rearranged TCR αβ chains.

The consequence of intrinsic Hh signalling in thymocytes during development (in models bearing an *in-vivo* reporter of Hh signalling where the physiological expression of Hh in T cells was either suppressed or over-activated) was recorded by measuring the impact of hh signalling on thymocyte gene expression. Whole genome microarray analysis was performed on sorted double-positive (DP) thymocytes and compared between various systems (Chapter 3).

The role of Desert Hedgehog (Dhh) in T cell development and maturation is yet unexplored. I will investigate the role of physiological Dhh signalling on T cell development by using Dhh wild-type, heterogeneous and knockout mice. A direct observation of T cell populations in the thymus, spleen and lymph node will reveal whether or not Dhh is signalling positively or negatively to T cells during their development and maturation (Chapter 4).

I will investigate the role of physiological Hedgehog signalling on T cell development and lineage selection by using two TCR transgenic mice in which T cell repertoire selection is biased by expressing rearranged transgenic TCR αβ chains, in conjunction with the presence or absence of Hh-signalling components. This model will provide information as to whether or not Hh signalling plays a role in T cell selection and lineage choice (Chapter 5).

To further examine the functions of Sonic Hedgehog (Shh) in the thymus during selection, I will investigate the differences in differentiation and transition from one developmental stage to the next on Shh-treatment. This is done using an in-vitro system of foetal thymus cultures (FTOCs) taken from two TCR transgenic

mice in which T cell repertoire selection is biased by expressing rearranged transgenic TCR αβ chains (Chapter 6).

Chapter 2

Chapter Two: Material and Methods

2.1 Mice

HY-TCR transgenic mice were as described (Kisielow et al. 1988; Teh et al. 1988). Marilyn-TCR transgenic mice were as described (Lantz et al. 2000). $Dhh^{+/-}$ mice were a kind gift from Dr Andrew McMahon (Harvard University, Cambridge, MA) (Bitgood et al. 1996). GBS-GFP mice were as described (Balaskas et al. 2012). Gli2 transgenic mice, *Lck*-Gli2ΔN2 (N2, GliA) and *Lck*-Gli2ΔC2 (C2, Gli2R) were as described (Rowbotham et al. 2008; Rowbotham, Hager-Theodorides, Cebecauer, et al. 2007). HY-Dhh and Marilyn-Gli2ΔC2 transgenic mice were generated during the course of this PhD, in addition to GBS-GFP/Gli2ΔC2 transgenic mice. Timed mates were performed by mating male with two females and monitoring the females for plugs. The day the plug was found was counted as embryonic day 0.5 (E0.5). All adult mice used were between 4-8 weeks old. The genotypes of adult and embryonic mice were determined by PCR (Polymerase Chain Reaction) from genomic DNA as described in Section (2.2). Mice were bred and maintained at Institute of Child Health, University College London (ICH, UCL, UK) under UK home office regulations.

2.2 DNA extraction and genotyping

DNA from mice was extracted from 2mm ear biopsies by digesting tissue in 100µL lysis buffer; 50mM KCI, 1.5 Mm $MgCl_2$, 10Mm Tris-HCI (pH 8.5), 0.01% gelatine, 0.45% Nonident P-40, 0.45% Tween 20, and 0.5 µg/ml proteinase K

(Sigma-Aldrich, USA) in ultra-pure water (Life Technologies, USA). Samples were incubated at 500rpm at 56^0C overnight for digestion. Samples were then spun at 13000rpm in a micro-centrifuge for 5 minutes and 1μL supernatant containing the DNA (~1μg) was used as template. Genotypes of mice were determined by polymerase chain reaction (PCR) of genomic DNA as described in section (2.3). For sex determination of embryo and neonate mice, DNA was amplified by PCR for YMT_2 / B sequence (a member of the Ssty family present on the long arm of Y-chromosome).

2.3 Polymerase chain reaction (PCR)

Primers used for amplifying the PCR products are listed in table (2.1). Each PCR reaction consisted of a 20μL mix composed of 50% GreenTaq DNA Polymerase (Sigma-Aldrich, USA) and 1μM of each relevant primer made in ultra pure water (Life Technologies, USA). PCR was carried out on a Stratagene Robocycler (Stratagene, USA) as follows: 5 minutes at 94^0C, 38 cycles for 1:30 minute at 94^0C, 1 minute at 58^0C, 1:20 minute at 72^0C and 10 minutes at 72^0C.

2.4 Gel Electrophoresis

PCR products were resolved on a 2% agarose gel (Sigma-Aldrich, USA), 1x Tris-Borate-EDTA (Life Technologies, USA), stained with GelRed (Biotium, US). A 1kb marker (Life Technologies, USA) was loaded to estimate band sizes. The visualization of the gel was done using ultra-violet light by Herolab gel

documentation system (Herolab, Germany), and a photograph taken using Sony UP-D897 Digital B/W Printer (A6) (Sony, UK).

2.5 Foetal thymic organ cultures (FTOCs)

Foetal thymi were cultured on 0.8μm Millipore filters (Millipore, Bedford, MA) on 1ml AIM-V serum free medium (Life Technologies, USA) in 24-well plates and incubated with 0.05μg/ml recombinant mouse sonic hedgehog protein (rmshh) (R&D Systems, UK). Cultures were incubated at 37^0C and 5% CO_2. Analysis by flow cytometry was carried out after 7 days.

2.6 Cell suspension and cell counts

Single cell suspension were obtained by crushing the organ between two pieces of ground glass and passing through 70 μm cell strainer (BD Falcon, USA) in AIM-V medium (Life Technologies, USA). Cell suspensions were then diluted in 1:1 ratio using same media. Using haemocytometer all viable cells in the specified field (25 boxes) were counted and doubled to allow for the AIM-V media dilution. This is equal to the number of cells by a factor of 10^4/mL. Cells were then adjusted to 0.5-1x10^6 cells/mL in FACS buffer; phosphate buffered saline, PBS (Sigma-Aldrich, UK), 2% foetal calf serum FCS, .01% sodium azide (Severn Biotech, UK).

2.7 Antibodies and flow cytometry

2.7.1 Cell surface staining

Cell suspensions were stained using combinations of the following directly conjugated antibodies supplied by BD Pharminogen (San Diego, CA) and E Biosciences (San Diego, USA): anti-CD44$_{FITC}$, anti-CD44$_{PE}$, anti-CD25$_{FITC}$, anti-CD25$_{PE}$, anti-CD45$_{CYCHROME}$, anti-CD4$_{FITC}$, anti-CD4$_{PE}$, antiCD4$_{CYCHROME}$, anti-CD4$_{APC}$, anti-CD8$_{FITC}$, anti-CD8$_{PE}$, anti-CD8$_{CYCHROME}$, anti-CD8$_{APC}$, anti-CD2$_{FITC}$, anti-CD2$_{PE}$, anti-CD3$_{FITC}$, anti-CD3$_{PE}$, anti-CD5$_{FITC}$, anti-CD5$_{PE}$, anti-CD69$_{FITC}$, anti-CD69$_{PE}$, anti-CD62L$_{FITC}$, anti-Qa2 $_{FITC}$, anti-CD24$_{PE}$, anti-CD197, anti-vβ6$_{PE}$, anti-T3.7$_{FITC}$, anti-T3.7$_{APC}$.

Suspensions were stained for 30 minutes on ice in 50μL PBS (Sigma-Aldrich, USA) supplemented with 2% FCS and 0.01% sodium azide. Cells were washed in this medium between incubations prior to analysis by Accuri C6 (BD Biosciences), FACScan and FACSCalibur (BD Biosciences). Minimum events of (10^4) was acquired in list mode using CellQuest (BD Biosciences, USA) and analyzed using Flowjo 7.6.4 (Tree Star, USA).

2.7.2 Intracellular staining of Gata3 and Foxp3

Intracellular staining of Gata3 and Foxp3 was performed using the PE anti-mouse Gata3 Staining Set and PE anti-mouse Foxp3 Staining Set (eBiosciences, San Diego, CA). Cell surface staining was performed using isolated cell suspensions. After washing with PBS, cells were incubated with Fixation/Permeabilization working solution for 30 minutes in the dark. Following this, cells were washed

twice with permeabilization buffer then stained with anti-Gata3 antibody or anti-Foxp3 antibody in permeabilization buffer for 30 minutes. After incubation, cells were washed twice with permeabilization buffer followed by washing with FACS buffer. Samples were analyzed using flow cytometry.

2.7.3 Intracellular staining for Cytokines

Splenocytes were isolated and cultured in AIM-V medium (Life Technologies, USA) supplemented with 50ng/ml PMA (phorbol myristate acetate) (Sigma-Aldrich, USA), 500ng/ml Ionomycin (Sigma-Aldrich, US) and 3μg/ml Brefeldin A (eBiosciences, USA) (Sigma-Aldrich, USA) at a concentration of $5x10^6$ cells/ml in 12 well plates (Nunc) (Thermo Scientific, USA) at 37^0C and 5% CO_2. Activation was carried out using 0.01μg/ml of anti-CD3 and anti-CD28 (BD Pharmingen, USA). Cells were harvested at 4 hours and stained with anti-CD4 and anti-CD8. Cells were then fixed and permeabilized (Fix and Perm cell permeabilization kit, Caltag Laboratories, UK) and stained for intracellular IFN-γ, IL-2, IL-4 and IL-17 expression.

2.8 Activation cultures

Fresh splenocyte suspensions were cultured in AIM-V serum-free medium (Life Technologies, USA) at a concentration of $5x10^6$ cells/ml in 12-well plates (Nunc) (Thermo Scientific, USA) at 37^0C and 5% CO_2. Activation was induced by addition of anti-CD3Ɛ (BD Pharmingen, USA) and anti-CD28 (BD Pharmingen, USA) monoclonal antibodies at 0.01μg/ml each. IL-2 was added to some wells at

20IU/ml. Cells were harvested at 4 hours for CD69 analysis and 20 hours for CD25 analysis using flow cytometry.

2.9 RNA extraction and cDNA synthesis

Cell suspensions were pelleted and re-suspended in appropriate amounts of lysis buffer and β-mercaptoethanol (Stratagene, USA). RNA was extracted using Strataprep® total RNA miniprep kit (Stratagene, USA) as per manufacturer's protocol. RNA concentration was measured using Nanodrop 1000 (Thermo Scientific, USA). cDNA was synthesized from this RNA using High Capacity cDNA Reverse Transcription kit (Applied Biosystems, USA). The reaction mix was made up as follows in 13µl HPLC grade water (Life Technologies, USA) and incubated at 65^0C for 5 minutes to denature RNA; 50-100ng RNA, 800µM dNTPs (Promega), 500ng random primers (Promega). RNA was placed on ice for 1 minute, spun briefly and then the following were added; 20% first strand buffer (Invitrogen, USA), 10mM DTT (Invitrogen, USA), 200 units superscript III reverse transcriptase (Invitrogen, USA). The volume was made to 20µL and incubated at 25^0C for 10 minutes to allow primer binding. Further it was placed sequentially at 42^0C for 50 minutes to allow elongation then at 70^0C for 15 minutes to terminate the reaction. RNA was stored at -80^0C and cDNA was stored at -20^0C.

2.10 Cell sorting and microarray

Thymocytes from adult mice (6-8 weeks) were sorted utilizing ICH/GOSH Flow Cytometry Core Facility using a Modular Flow Cytometer (MoFlo XDP; Bechman Coulter). Staining with anti-$CD4_{FITC}$, anti-$CD8_{PE}$ and anti $CD-45_{CYCHROME}$ allowed sorting of the DP thymic populations. All cells collected fell within the forward scatter/side scatter (FCS/SSC) live gate. RNA extracted from DP thymocyte populations were sent to UCL Genomics, UCL. GeneChip® Mouse Genome MOE430.2 array (Affymetrix, USA) was used for analysis.

2.11 Quantitative reverse transcribed-polymerase chain reaction (qRT-PCR)

QRT-PCR was carried out by analysis of cDNA sample in triplicate on an iCycler (Bio-Rad) using the iQ™SYBR® Green supermix (Bio-Rad, UK) according to manufacturer's instructions. The housekeeping gene hypoxanthin-guanine phosphoribosyltransferase (HPRT) was used to allow quantification of template and normalisation for each gene. Amplification of HPRT and Gnb4 (Guanine nucleotide-binding protein subunit β-4) was quantitated using a dilution series of cDNA prepared from embryo head RNA. Pre-validated primers were used (Qiagen QuantiTec® Primer Assay, UK). Primers were selected that span exon-exon boundaries to prevent the amplification of genomic DNA. Each reaction mixture contained the following: approximate 10ng cDNA, 0.3M forward primer, 0.3M reverse primer, 10µl SYBR Green 2x supermix (containing 100mM KCI, 40Mm Tris-HCI, PH8.4, 0.4mM of each dNTP (dATP, dCTP, dGTP, dTTP) iTaq™ DNA polymerase (50 units/ml), 6mM $MgCl_2$, SYBR Green 1, 20Nm

Fuoresein and stabilizers) made up to 20µl with HPLC grade water. RT-PCR was performed under the following conditions: for HPRT and Gnb4; 180 minutes at 95^0C, then 40 cycles of 30 seconds at 95^0C followed by 30 seconds. A melt curve was also carried out as per the manufacturer's programme to check the melting temperature of the products produced to ensure the product was the size expected and not the result of primer-dimers.

2.12 Data analysis

Statistical analysis using at least three independent experiment was performed using Microsoft Excel 2007 (Microsoft Inc, USA) and GraphPad Prism (GraphPad Inc, USA). An unpaired two tailed student's t test was used to test the significance of differences observed in WT, Het and KO littermates, unless stated otherwise. The microarray data was analyzed by Hemant Sahni using the tools and packages available in R and Bioconductor (Bioconductor.org).

Table 2.1 Primers used for genotyping of mice by PCR

Transcript	Primer Direction	Oligonucleotide Sequence (5'>3')	Product Size (bp)
YMT_2/B sequence (Y-chromosome)	Forward	CTGGAGCTCTACAGTGATGA	350
	Reverse	CAGTTACCAATCAACACATCAC	
HY transgene	Forward	CACATGGAGGCTGCAGTCAC	300
	Reverse	GTTTCTGCACTGTTATCACC	
Marilyn transgene	Forward	GCAGAGGAACCTGGGAGCTGT	350
	Reverse	TGCTGTCTGTACCACCAGAAATAC	
Dhh wild type gene	Forward	ATCCACGTATCGGTCAAAGC	442
	Reverse	GGTCCAGGAAGAGCAGCAC	
Dhh mutated gene	Forward	GGCATGCTGGGGATGCGGTG	110
	Reverse	GGTCCAGGAAGAGCAGCAC	
Gli2ΔC2 transgene	Forward	AGAACCTGAAGACCACCTGCG	850
	Reverse	AGAACCTGAAGACACACCTGCG	
Gli2ΔN2 transgene	Forward	AAACAAAGCTCCTGTCACG	600
	Reverse	ATGCCTGCTCTTTACTGAAG	
Rag2 wild type gene	Forward	TTAATTCAACCAGGCTTCTCACTT	973
	Reverse	GCCTGCTTATTGTCTCCTCCTGGTATG	
Rag2 mutated gene	Forward	CCAACGCTATGTCCTGATAGCGGT	1107
	Reverse	GCCTGCTTATTGTCTCCTCCTGGTATG	
eGFP transgene	Forward	TGCAGTGCTTCAGCCGCTAC	172
	Reverse	CCAGCAGGACCATGTGATCG	

Table 2.2 Primers used for Real-time PCR

Transcript	Primer Direction	Oligonucleotide Sequence (5'>3')	Product Size (bp)
HPRT	Forward	TGATTATGGACAGGACTGAAAG	55
	Reverse	GGTCAGCAAAGAACTTATAGCC	
Gnb4	Forward	Proprietary Qiagen QuantiTec Primer Assay	300
	Reverse		

Chapter 3

Chapter Three: Hh activation in thymocytes and T cells

3.1 Introduction

3.1.1 Hh signalling in thymocytes and T cells

Hedgehog proteins have been found to be essential for differentiation, survival and proliferation of thymocyte progenitors, and during the later stages of thymocyte development. Thymocyte intrinsic Hh mediated transcription has been also found to play a regulatory role in T cell development, suggesting that Hh proteins expressed by the epithelial tissue within the thymus signal directly to developing thymocytes.

Our lab has shown that repression of intrinsic Hh-mediated transcription in thymocytes increased T cell differentiation and activation from DP to SP thymocytes. Our lab has also shown that the DP thymocytes are Hh-responsive and that thymocyte-intrinsic Hh-mediated transcription plays a role in modulating the production of SP4 and SP8, whereas repression of physiological Hh-mediated transcription in thymocytes altered the proportions of DP and SP4 thymocytes (Crompton et al. 2007; Rowbotham, Hager-Theodorides, Furmanski, et al. 2007; Furmanski et al. 2012).

3.1.2 Chapter objectives

The purpose of this chapter is to investigate the role of Hh signalling directly to thymocytes. For these experiments, two mouse models bearing an in-vivo reporter

of Hh signalling (GBS(Gli)-GFP) were used; (1) *Lck*-driven Gli2ΔC2 (Gli2ΔC2) (C2, Gli2R) transgenic mice which express a truncated form of Gli2 which acts as a repressor of Hh-dependent transcription. (2) The reciprocal *Lck*-Gli2ΔN2 (Gli2ΔN2) (non-TCR-transgenic-Gli2ΔN2) (N2, Gli2A) transgenic mice which express a transgene encodes a truncated form of Gli2 that leads to constitutive activation of Gli2-dependent transcription in T-lineage cells (Hager-Theodorides et al. 2009). Both transgene constructs are otherwise identical in sequence, sharing DNA-binding domains.

Furthermore, we have crossed *Lck*-Gli2ΔN2 and *Lck*-Gli2ΔC2 with GBS-GFP transgenic mouse. The GBS-GFP transgenic mouse model has eight binding sites for Gli transcription factors which regulate GFP expression and serve as a reporter for active Hh-induced Gli activity in-vivo (Balaskas et al. 2012). A direct observation of T cell populations in the thymus, spleen and lymph node will allow us to measure Hh signalling in T cell selection and maturation.

In addition, to further investigate the consequence of Hh signalling in thymocytes on gene expression, Mouse whole genome microarray analysis was performed on sorted DP thymocytes extracted from *Lck*-Gli2ΔC2 and WT mice for comparison.

3.2 Results

3.2.1 Genotyping GBS-GFP/Gli2ΔN2 and GBS-GFP/Gli2ΔC2 littermates

Two strains of mice were generated; the first is GBS-GFP/Gli2ΔN2**,** created by crossing GBS-GFP transgenic mice with Gli2ΔN2 transgenic mice. The result of this crossing resulted in two genotypes of mice, the first bearing GBS-GFP transgene (GBS-GFP/WT). The second bearing GBS-GFP and Gli2ΔN2 transgenes (GBS-GFP/Gli2ΔN2^{+}). The second strain used is GBS-GFP/Gli2ΔC2 mice, created by crossing GBS-GFP transgenic mice with Gli2ΔC2 transgenic mice. The result of this crossing resulted in two genotypes of mice, the first bearing GBS-GFP transgene (GBS-GFP/WT). The second bearing GBS-GFP and Gli2ΔC2 transgenes (GBS-GFP/Gli2ΔC2^{+}).

Littermates were genotyped for eGFP, Gli2ΔN2 and Gli2ΔC2 transgenes. PCR analysis using genomic DNA from ear biopsies was performed in order to identify the genotype of littermates, using three sets of primers specific for eGFP, Gli2ΔN2 and Gli2ΔC2 transgenes. According to this strategy, eGFP transgene should generate a PCR product of 172bp, Gli2ΔN2 transgene should generate a PCR product of 600bp, and Gli2ΔC2 transgene should generate a PCR product of 850bp.

GBS-GFP/Gli2ΔN2 and GBS-GFP/Gli2ΔC2 mutants were identified according to the PCR results. Mice with a PCR product positive for eGFP transgene and negative for Gli2ΔN2 and Gli2ΔC2 transgenes, were genotyped as (GBS-GFP/WT). Mice with PCR a product positive for eGFP transgene and positive for Gli2ΔN2 transgene, were genotyped as (GBS-GFP/ Gli2ΔN2^{+}). Mice with PCR a

product positive for eGFP transgene and positive for Gli2ΔC2 transgene, were genotyped as (GBS-GFP/ Gli2ΔC2^{+}) (Figure 3.1).

3.2.2 Thymocytes and splenocytes in GBS-GFP/Gli2ΔN2^{+} and GBS-GFP/Gli2ΔC2^{+} littermates

Following anatomical extraction of the thymus and spleen from GBS-GFP/ Gli2ΔN2 and GBS-GFP/Gli2ΔC2 littermates, the thymocytes and splenocytes were collected for analysis. In regards to live cell counts in the thymus, we observed no significant difference in the mean cell numbers in GBS-GFP/ Gli2ΔN2 compared to GBS-GFP/WT control ($p>0.05$, n=3). On the contrary, we observed a significant increase in the mean cell number of thymocytes in GBS-GFP/ Gli2ΔC2 compared to GBS-GFP/WT control ($p\leq0.05$, n=3) consistent with Hh signalling negatively regulating thymocyte numbers (Outram et al. 2000). In regards to live cell counts in the spleen, we observed no significant difference between the two genotypes of mice compared to their GBS-GFP/WT control ($p>0.05$, n=3) and ($p>0.05$, n=3) respectively (Figure 3.2).

3.2.3 Role of Hh signalling in thymocyte development during development in GBS-GFP/Gli2ΔN2^{+} and GBS-GFP/Gli2ΔC2^{+} mice

In order to mesure the proportion of thymocytes transducing Hh signals during their development and selection in the thymus, thymocytes from GBS-GFP/Gli2ΔN2^{+} and GBS-GFP/Gli2ΔC2^{+} and their GBS-GFP/WT littermate mice were analyzed for Gli-GFP, CD8 and CD4 cell surface expression (Figure 3.3) and (Figure 3.4). According to GFP expression, cells were sub-grouped into two main populations, Gli-GFP positive cells (Gli-GFP^{+}) and GFP negative cells (Gli-

GFP^{-}). When we measured GFP expression in the major thymocyte populations of GBS-GFP/WT littermates, we found GFP^{+} cells in DN, DP, CD8SP and CD4SP with highest proportion in the DN population (~9.5%) (Figure 3.3) consistent with the role of Hh signalling in DN thymocyte homeostasis and differentiation (Outram et al. 2000; Shah et al. 2004). We then examined GFP expression in GBS-GFP/Gli2ΔN2 littermates, in which Hh-mediated transcription is activate. The proportions of GFP^{+} cells was increased to 16.6% in the DN population, consistent with the action of the Gli2ΔN2 transgene on differentiation of DN cells (Rowbotham et al. 2009).

Our data show that over-expression of intrinsic Hh signalling (constitutive Hh-mediated transcription) altered the proportions of DN, SP8 and SP4 cells that expressed GFP. Our analysis revealed that the percentage of SP4 cells was significantly increased in the GBS-GFP/Gli2ΔN2^{+} Compared to the GBS-GFP/WT ($p \leq 0.05$, n=3) (Figure 3.3).

Interestingly, our data also revealed that intrinsic suppression of Hh signalling in thymocytes influenced the proportions of DP, and SP cells expressing GFP in the thymus, as our analysis show that the percentage of SP4 cells was significantly increased in the GBS-GFP/Gli2ΔC2^{+} Compared to the GBS-GFP/WT ($p \leq 0.05$, n=3) (Figure 3.4).

3.2.4 Influence of Hh signalling on the expression of CD3 in GBS-GFP/Gli2ΔN2^{+} and GBS-GFP/Gli2ΔC2^{+} thymocytes

In order to assess the potential role of Hh signalling in regulating differentiation and TCR signal transduction of GBS-GFP/Gli2ΔN2 and GBS-GFP/Gli2ΔC2

thymocytes during development and selection, we analyzed the cell surface expression of TCR signalling associated molecule (CD3) in DN, DP, SP8 and SP4 cells in GBS-GFP/Gli2ΔN2^{+} and GBS-GFP/Gli2ΔC2^{+} in comparison with their relative GBS-GFP/WT. Furthermore we compared the mean fluorescence intensity (MFI) of staining for CD3 molecule.

Our data show that active Hh signalling in thymocytes alters the expression of CD3 in developing thymocytes. Our analysis revealed that the percentage of CD3 in SP8 cells was significantly lower in the GBS-GFP/Gli2ΔN2^{+} compared to the GBS-GFP/WT ($p \leq 0.05$, n=3). However, the percentage of CD3 in DN, DP and SP4 was not different between the three genotypes of mice ($p > 0.05$, n=3). Furthermore, CD3 MFI in SP8 and SP4 was significantly increased in the GBS-GFP/Gli2ΔN2^{+} compared to the GBS-GFP/WT ($p \leq 0.05$, n=3) and ($p \leq 0.005$, n=3) respectively ($p > 0.05$, n=3) (Figure 3.5).

Furthermore, our analysis show that suppressing Hh signalling in thymocytes alters the expression of CD3 as our data show that the percentage of CD3 in DN, SP8 and SP4 cells was significantly increased in the GBS-GFP/Gli2ΔC2^{+} compared to the GBS-GFP/WT ($p \leq 0.005$, n=3), ($p \leq 0.05$, n=3) and ($p \leq 0.05$, n=3) respectively. However, the percentage of CD3 in DP was not different between the two genotypes of mice ($p > 0.05$, n=3). Additionally, CD3 MFI in SP8 was significantly increased in GBS-GFP/Gli2ΔC2^{+} compared to GBS-GFP/WT (($p \leq 0.03$, n=3), ($p \leq 0.02$, n=3)) respectively (Figure 3.6).

3.2.5 Role of Hh signalling in Foxp3 expression in thymocytes during development and selection in GBS-GFP/Gli2ΔN2$^+$ and GBS-GFP/Gli2ΔC2$^+$ mice

In order to assess the role of Hh signalling in the expression of Foxp3 during thymocyte development and selection, thymocytes were analyzed for Foxp3 expression within the GFP$^+$ SP4 cells.

Our data show that in Hh active thymocytes, Hh signalling influences the phenotype of SP4 cells by promoting the expression of Foxp3, which is the transcription factor believed to be master regulator of the Treg lineage. Our analysis revealed that the percentage of Foxp3 in SP4 cells was significantly higher in the GBS-GFP/Gli2ΔN2$^+$ Compared to the GBS-GFP/WT ($p \leq 0.05$, n=3) (Figure 3.7).

3.2.6 Role of Hh signalling in thymocyte maturation during development and selection in GBS-GFP/Gli2ΔN2$^+$ and GBS-GFP/Gli2ΔC2$^+$ mice

In order to assess the role of Hh signalling in influencing cell maturation of the single positive populations during thymocyte development and selection, thymocytes from GBS-GFP/Gli2ΔN2$^+$ and GBS-GFP/Gli2ΔC2$^+$ in addition to their relative GBS-GFP/WT were analyzed for HSA expression in DP, SP8 and SP4 cells.

Our data show that over-expression of Hh in thymocytes does not alter the maturation status of developing thymocytes, as our analysis revealed no

difference in the percentage of HSA on GFP^+ thymocytes between the two genotypes of mice ($p>0.05$, $n=3$) (Figure 3.8).

Similarly, our data show that suppressing Hh signalling in thymocytes dose not influence thymocyte maturation in Gli active cells. Our analysis revealed no difference in the percentage of HSA in GFP^+ thymocytes between the two genotypes of mice ($p>0.05$, $n=3$) (Figure 3.9).

3.2.7 Influence of Hh signalling in spleen T cells of GBS-GFP/Gli2ΔN2$^+$ and GBS-GFP/Gli2ΔC2$^+$ mice

In order to visulize Hh signalling ex-vivo in spleen T cells in the periphery, splenocytes from GBS-GFP/Gli2ΔN2$^+$ and GBS-GFP/Gli2ΔC2$^+$ in addition to their relative GBS-GFP/WT littermates were analyzed for Gli-GFP, CD8 and CD4 cell surface expression. According to GFP expression, cells were sub-grouped into two main populations, Gli-GFP positive cells (Gli-GFP^+) and GFP negative cells (Gli-GFP^-). Within the Gli-GFP positive compartment, cells were sub-grouped according to the cell surface expression of CD8 and CD4 into three main populations, the $CD8^-CD4^-$ (DN), $CD8^+CD4^-$ (SP8) and $CD8^-CD4^+$ (SP4).

Our data show that active Hh signalling has no influence on mature splenocytes in the spleen as our analysis revealed that the percentage of splenocytes between the two genotypes of mice was not statistically different ($p>0.05$, $n=3$) (Figure 3.10).

Furthermore, our analysis from the spleen show that suppressing Hh signalling has no influence on mature splnocytes, as our data show that the percentage of

splenocytes between the two genotypes of mice was not statistically different ($p>0.05$, n=3) (Figure 3.11).

3.2.8 Influence of Hh signalling on the expression of CD3 in GBS-GFP/Gli2ΔN2^{+} and GBS-GFP/Gli2ΔC2^{+} splenocytes

In order to assess the potential role of Hh signalling in regulating differentiation and TCR signal transduction in splenocytes, we analyzed the cell surface expression of TCR associated signalling molecule (CD3) in DN, DP, SP8 and SP4 cells in GBS-GFP/Gli2ΔN2^{+} and GBS-GFP/Gli2ΔN2^{+} in addition to their relative GBS-GFP/WT. Furthermore we compared the mean fluorescence intensity (MFI) of staining for CD3 molecule.

Our data show that increased Hh signalling does not alter the expression of CD3 in the spleen as our analysis revealed that the percentage of CD3 in splenocytes was not statistically different between the two genotypes of mice ($p>0.05$, n=3). Similarly, CD3 MFI was not different in splenocytes between the two genotypes of mice ($p>0.05$, n=3) (Figure 3.12).

Furthermore, our analysis from the spleen shows that suppressing Hh signalling in splenocytes alters the expression of CD3. Our data show that the percentage of CD3 in SP8 and SP4 was significantly lower in the GBS-GFP/Gli2ΔC2^{+} compared to the WT (($p>0.05$, n=3), ($p>0.05$, n=3)) respectively. In addition, we measured the CD3 MFI in splenocytes and our analysis reveals that CD3 MFI was not different between the two genotypes of mice ($p>0.05$, n=3) (Figure 3.13).

3.2.9 Role of Hh signalling in Foxp3 expression in splnocytes during development and selection in GBS-GFP/Gli2ΔN2^{+} and GBS-GFP/Gli2ΔC2^{+} mice

In order to assess the role of Hh signalling in the expression of Foxp3 in the spleen, splenocytes were analyzed for Foxp3 expression within the SP4 cells. Foxp3 is the transcription factor believed to be master regulator of the Treg lineage.

Our data from Foxp3 in the spleen confirmed our observation in that increased Hh signalling influence the phenotype of SP4 cells, as our data from the spleen show that the percentage of Foxp3 in SP4 cells was significantly higher in the GBS-GFP/Gli2ΔN2^{+} Compared to the GBS-GFP/WT ($p \leq 0.05$, n=3) (Figure 3.14).

Furthermore, inhibition of Hh signalling in thymoctes had no influence on the expression of Foxp3. Our analysis revealed that the percentage of Foxp3 in SP4 cells was not statistically different in the GBS-GFP/Gli2ΔC2^{+} Compared to the GBS-GFP/WT ($p > 0.05$, n=3) (Figure 3.14).

3.2.10 Influence of Hh signalling in lymph node T cells of GBS-GFP/Gli2ΔN2^{+} and GBS-GFP/Gli2ΔC2^{+} mice

In order to assess the influence of Hh signalling in lymph node T cells in the periphery, cells from GBS-GFP/Gli2ΔN2^{+} and GBS-GFP/Gli2ΔC2^{+} in addition to their relative GBS-GFP/WT were analyzed for Gli-GFP, CD8 and CD4 cell surface expression. According to GFP expression, cells were sub-grouped into two main populations, Gli-GFP positive cells (Gli-GFP^{+}) and GFP negative cells

(Gli-GFP^{-}). Within the Gli positive compartment, cells were sub-grouped according to the cell surface expression of CD8 and CD4 into three main populations, the CD8^{-}CD4^{-} (DN), CD8^{+}CD4^{-} (SP8) and CD8^{-}CD4^{+} (SP4).

Our data analysis from the lymph node show that Hh expression has no influence on T cells in the lymph node. Our data show that the percentage of cells was not different (Figure 3.15). Similarly, Hh suppression in T cells has no influence in the proportion of cells during as our analysis show that the percentage of T cell population was not different between the two genotypes of mice ($p>0.05$, $n=3$) (Figure 3.16).

3.2.11 Influence of Hh signalling on the expression of CD3 in GBS-GFP/Gli2ΔN2^{+} and GBS-GFP/Gli2ΔC2^{+} lymph node T cells

In order to assess the potential role of Hh signalling in regulating differentiation and TCR signal transduction in lymph node T cells, we analyzed the cell surface expression of TCR associated signalling molecule (CD3) in CD8^{-}CD4^{-}, SP8 and SP4 cells in GBS-GFP/Gli2ΔN2^{+} and GBS-GFP/Gli2ΔC2^{+} in addition to their relative GBS-GFP/WT. Furthermore we compared the mean fluorescence intensity (MFI) of staining for CD3 molecule.

As in the thymus, our data revealed that Hh signalling alters the expression of CD3 in T cells, as our analysis revealed that the percentage of CD3 in SP8 was significantly higher in the GBS-GFP/Gli2ΔN2^{+} compared to the GBS-GFP/WT ($p\leq0.005$, $n=3$). Additionally, CD3 MFI was not different in lymph node T cells between the two genotypes of mice ($p>0.05$, $n=3$) (Figure 3.17).

Furthermore, our data from the lymph node revealed that suppression of Hh signalling in T cells influence the expression of CD3. Our analysis show that the percentage of CD3 in $CD4^{-}CD8^{-}$, SP8 and SP4 cells was significantly higher in the GBS-GFP/Gli2ΔC2^{+} compared to the GBS-GFP/WT ($p \leq 0.05$, n=3). Furthermore, CD3 MFI in SP8 and SP4 was significantly decreased in the GBS-GFP/Gli2ΔC2^{+} compared to the GBS-GFP/WT (($p \leq 0.005$, n=3), ($p \leq 0.05$, n=3)) respectively (Figure 3.18).

3.2.12 Role of Hh signalling in Foxp3 expression in lymph node T cells during development and selection in GBS-GFP/Gli2ΔN2^{+} and GBS-GFP/Gli2ΔC2^{+} mice

In order to assess the role of Hh signalling in the expression of Foxp3 in the lymph node, T cells were analyzed for Foxp3 expression within the SP4 cells. Foxp3 is the transcription factor believed to be master regulator of the Treg lineage.

Our data from the lymph node shows that the percentage of Foxp3 in SP4 cells was not significantly different between the two genotypes of mice ($p > 0.05$, n=3) (Figure 3.19). Similarly, our data from Hh-suppressed cells in the lymph node revealed that the percentage of Foxp3 in SP4 cells was not statistically different between the two genotypes of mice ($p > 0.05$, n=3) (Figure 3.19).

3.2.13 Hh signalling and gene expression

To further investigate the consequence of Hh signalling in thymocytes on gene expression, we extracted DP thymocytes for whole genome expression analysis from Hh-suppressed, Hh-activated mouse models and WT mice for comparison. We used Lck-driven Gli2ΔC2 (ΔC2) (C2, Gli2R) transgenic mice which express a truncated form of Gli2 which acts as a repressor of Hh-dependent transcription. The reciprocal Lck- Gli2ΔN2 (ΔN2) (non-TCR-transgenic-Gli2ΔN2) (N2, Gli2A) transgene also encodes a truncated form of Gli2 that leads to constitutive activation of Gli2-dependent transcription in T-lineage cells. Both transgene constructs are otherwise identical in sequence, sharing DNA-binding domains.

Microarray data analysis showed an increase by at least 2-folds in the expression of 35 genes in WT compared to *Lck*-Gli2ΔC2 (Table 3.1). Furthermore, Glioma-associated oncogene (Gli-2), Guanine nucleotide binding protein β-subunit (Gnb4) and chemokine ligand-19 (Ccl-19) showed increased expression by at least 2-folds in *Lck*-Gli2ΔC2 compared to WT (Table 3.2) (Figure 3.20).

Following this observation quantitative qRT-PCR was carried out to study the expression of Gnb4 in DP thymocytes from *Lck*-Gli2ΔN2, *Lck*-Gli2ΔC2 and WT. We showed that Gnb4 was highly expressed in *Lck*-Gli2ΔC2 DP thymocytes with a 2.6-fold change compared to DP thymocytes from *Lck*-Gli2ΔN2 mice ($p \leq 0.05$, n=3) (Figure 3.21).

Genes Higher expression in WT	Description
B930036n10rik	Unclassified gene
9430008c03Rik	LincRNA gene
Wfdc17	Cellular component
Snora2b, Snora3, Snora21, Snora28, Snora33, Snora44 & Snora69	Small nuclear RNA
Rnu3a, Rnu1b1 & Rnu12	Small nuclear RNA
Vaultrc5	Unclassified RNA coding gene
Snord22, Snord33 & Snord118	Small nucleolar RNA
Snhg8	Small nucleolar RNA (non-coding)
Scarna8	Small cajal body-specific RNA
Rny1 & Rny3	RNA, Y small cytoplasmic (associated with Ro protein)
Rn4.5s	rRNA gene
Hist1h2bg, Hist1h2ac, Hist1h3g & Hist2h3c2-ps	Histone cluster
Eif2s3y (Eukaryotic translation initiation factor-2 subunit-3)	Structural gene Y-linked
Top2a (topoisomerase (DNA) II alpha)	Ubiquitously expressed enzymes
Ndufb4 (NADH dehydrogenase (ubiquitin) 1 beta subcomplex-4)	Accessory subunit of the mitochondrial membrane respiratory chain NADH dehydrogenase (Complex-I)
Kdm5d	Lysine (K)-specific demethylase 5D
Vmn2r42 (Vomeronasal 2, receptor 42)	G-protein coupled receptor
Hbb-b1	Haemoglobin, beta adult major chain
Uty	Ubiquitously transcribed tetratricopeptide repeat gene, Y-linked
Ddx3y	Probable ATP-dependent RNA helicase
Srsy	Sex determining region Y

Table 3.1
Gene expression higher in WT

Genes **Higher expression in Lck-Gli2ΔC2**	**Description**
Gli2 (Gliomma-associated oncogene-2)	Transcription activator
Gnb4 (Guanine nucleotide binding protein (G protein) beta-4 subunit)	Modulator or transducer in various transmembrane signalling systems
Ccl19 (Chemokine (C-C motif) ligand-19)	Cellular trafficking and migration

Table 3.2
Gene expression higher in *Lck*-Gli2ΔC2

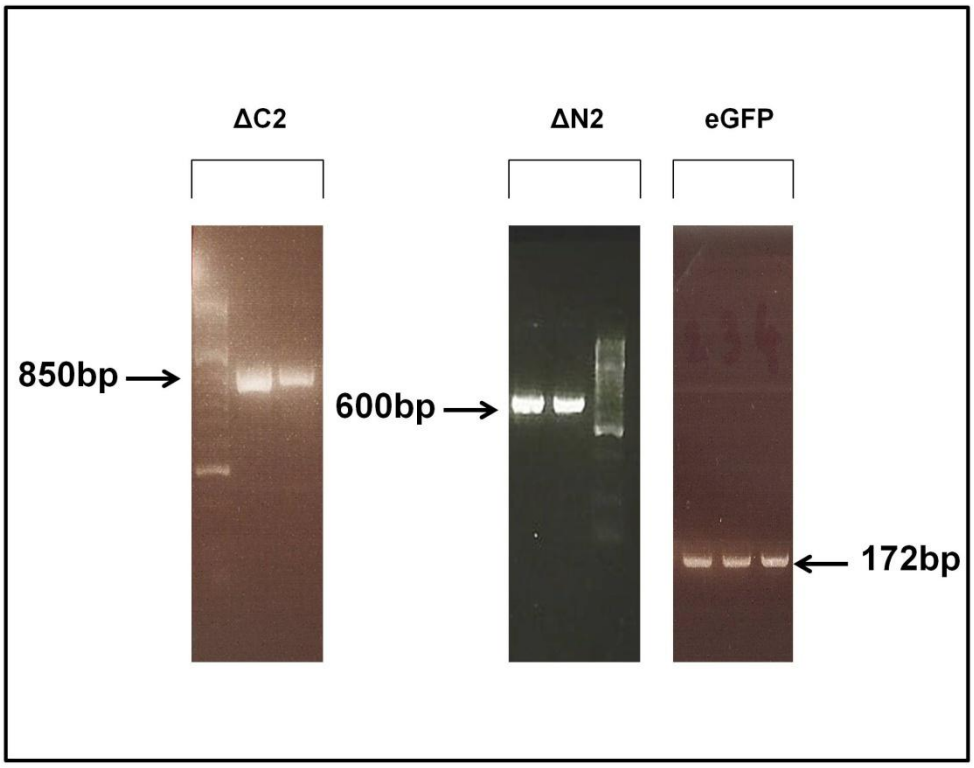

Figure 3.1

Genotyping of GBS-GFP/Gli2ΔN2 and GBS-GFP/Gli2ΔC2 littermates. GBS-GFP/Gli2ΔN2 and GBS-GFP/Gli2ΔC2 mutants were identified according to the PCR results. The presence of the Gli2ΔN2 transgene generated a PCR product of 600bp. The presence of the Gli2ΔC2 transgene generated a PCR product of 850bp. The presence of the eGFP transgene generated a PCR product of 172bp. Mice with PCR a product positive for eGFP transgene and negative for Gli2ΔN2 and Gli2ΔC2 transgene, were genotyped as (GBS-GFP/WT). Mice with PCR a product positive for eGFP transgene and positive for Gli2ΔN2 transgene, were genotyped as (GBS-GFP/Gli2ΔN2^{+}). Mice with PCR a product positive for eGFP transgene and positive for Gli2ΔC2 transgene, were genotyped as (GBS-GFP/ Gli2ΔC2^{+}).

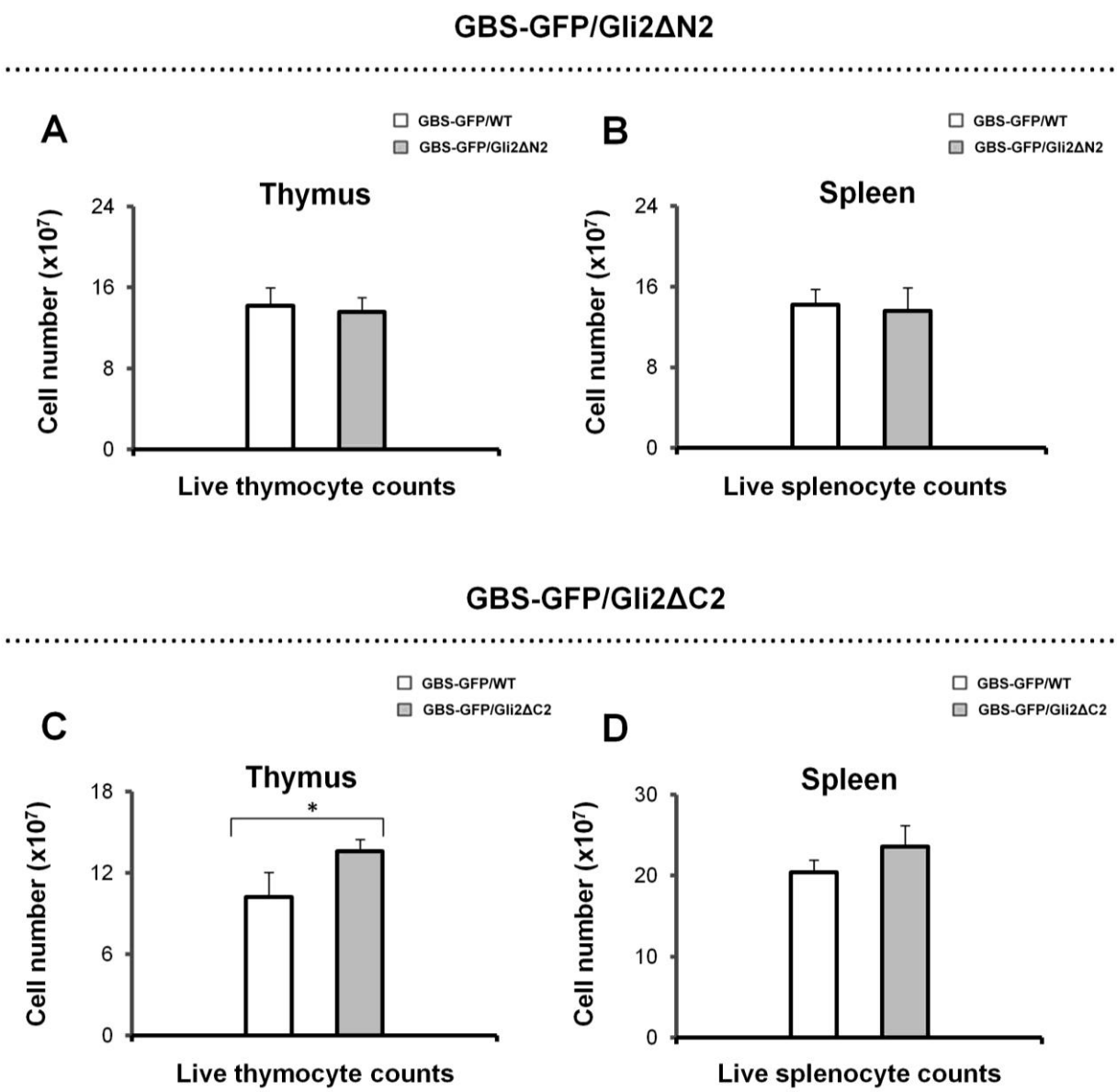

Figure 3.2

Thymus and spleen live cell counts in male GBS-GFP/Gli2ΔN2 and GBS-GFP/Gli2ΔC2 littermates. Thymocyte and splenocyte total counts from adult GBS-GFP/Gli2ΔN2, GBS-GFP/Gli2ΔC2 and GBS-GFP/WT littermates. **(A)** Live thymocyte counts in GBS-GFP/Gli2ΔN2. **(B)** Live splenocyte counts in GBS-GFP/Gli2ΔN2. **(C)** Live thymocyte counts in GBS-GFP/Gli2ΔC2. **(D)** Live splenocyte counts in GBS-GFP/Gli2ΔC2. Mean and standard deviation of each population are given. Bars represent mean ± standard deviations. **Thymocyte counts; GBS-GFP/Gli2ΔN2** (p=0.8, n=3). **GBS-GFP/Gli2ΔC2** (p=0.05, n=3). **Splenocyte counts; GBS-GFP/Gli2ΔN2 splenocytes;** (p=0.3, n=3). **GBS-GFP/Gli2ΔC2 splenocytes;** (p=0.4, n=3). *represents $p \leq 0.05$.

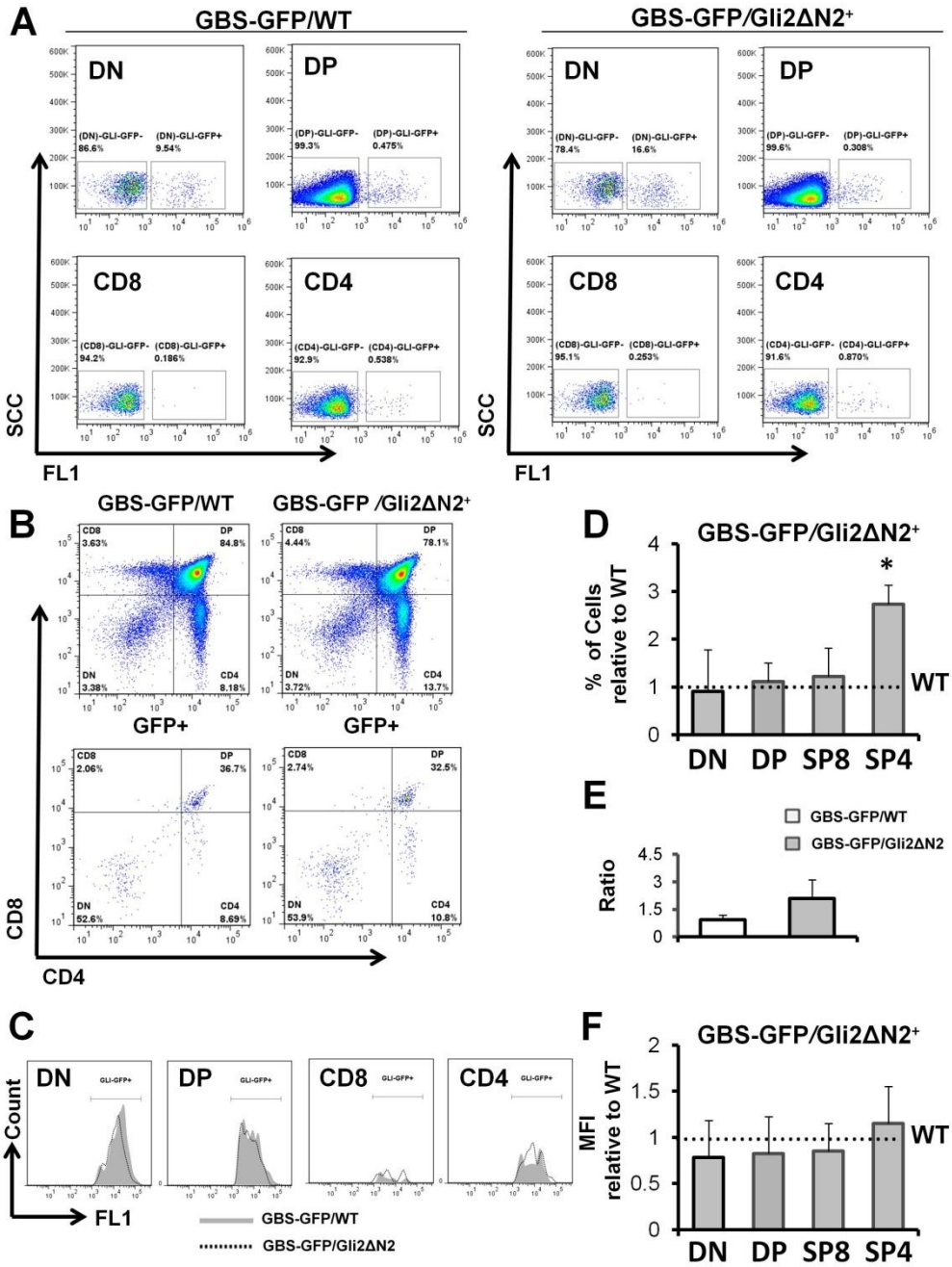

Figure 3.3

Major thymocyte populations in GBS-GFP/Gli2ΔN2. Percentage of thymocyte populations from adult GBS-GFP/Gli2ΔN2 and GBS-GFP/WT littermates. Thymocytes were stained for anti-CD8 and anti-CD4, and analyzed by flow cytometry. Cells were gated on Gli-GFP$^+$ cells. **(A)** Representative dot plot of thymocyte populations gated on GLI-GFP$^+$ and Gli-GFP$^-$ for DN, DP, SP8 and SP4 cells. **(B)** Representative dot plot of thymocyte populations gated on total and GLI-GFP$^+$ cells. **(C)** Representative histogram of GLI-GFP$^+$ DN, DP, SP8 and SP4 cells. **(D)** Representative bar graph of GLI-GFP$^+$ percentages in DN, DP, SP8 and SP4 cells. **(E)** Representative bar graph of CD4:CD8 ratio from GLI-GFP$^+$ cells. **(F)** Representative bar graph of GLI-GFP$^+$ MFI in DN, DP, SP8 and SP4 cells. Figures are representative of 3 independent sets of GBS-GFP/Gli2ΔN2 littermates. Mean and standard deviation of each population are given. Bars represent mean ± standard deviations. **Thymocyte percentages; DN** (p= 0.4, n=3). **DP** (p= 0.5, n=3). **SP8** (p= 0.5, n=3). **SP4** (p=0.04, n=3). **GLI-GFP MFI; DN** (p= 0.3, n=3). **DP** (p= 0.6, n=3). **SP8** (p= 0.6, n=3). **SP4** (p=0.9, n=3). *represents p≤0.05.

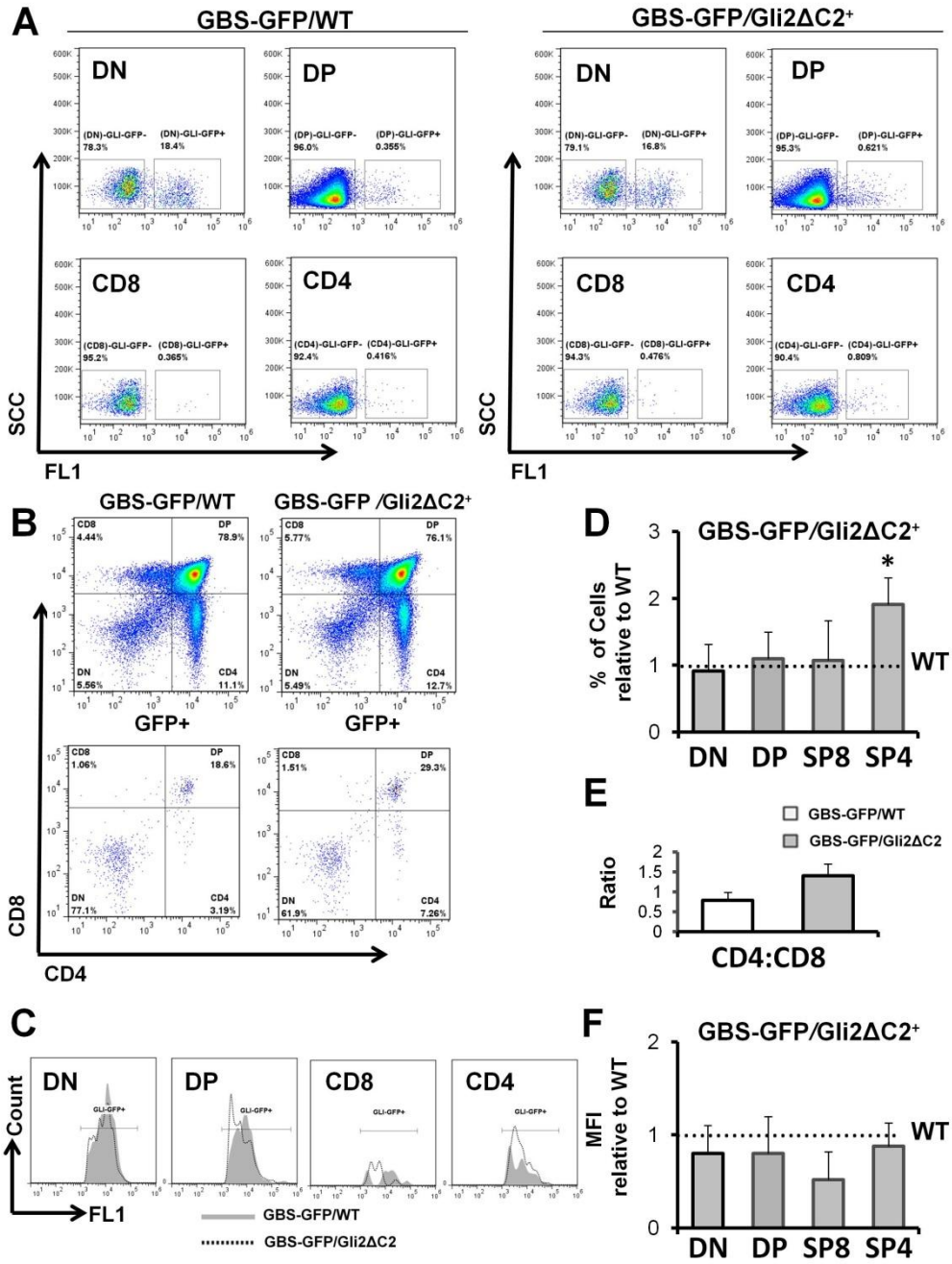

Figure 3.4

Major thymocyte populations in GBS-GFP/Gli2ΔC2. Percentage of thymocyte populations from adult GBS-GFP/Gli2ΔC2 and GBS-GFP/WT littermates. Thymocytes were stained for anti-CD8 and anti-CD4, and analyzed by flow cytometry. Cells were gated on Gli-GFP$^+$ cells. **(A)** Representative dot plot of thymocyte populations gated on GLI-GFP$^+$ and Gli-GFP$^-$ for DN, DP, SP8 and SP4 cells. **(B)** Representative dot plot of thymocyte populations gated on total and GLI-GFP$^+$ cells. **(C)** Representative histogram of GLI-GFP$^+$ DN, DP, SP8 and SP4 cells. **(D)** Representative bar graph of GLI-GFP$^+$ percentages in DN, DP, SP8 and SP4 cells. **(E)** Representative bar graph of CD4:CD8 ratio from GLI-GFP$^+$ cells. **(F)** Representative bar graph of GLI-GFP$^+$ MFI in DN, DP, SP8 and SP4 cells. Figures are representative of 3 independent sets of GBS-GFP/Gli2ΔN2 littermates. Mean and standard deviation of each population are given. Bars represent mean ± standard deviations. **Thymocyte percentages; DN** (p= 0.2, n=3). **DP** (p= 0.1, n=3). **SP8** (p= 0.3, n=3). **SP4** (p=0.01, n=3). **GLI-GFP MFI; DN** (p= 0.4, n=3). **DP** (p= 0.7, n=3). **SP8** (p= 0.3, n=3). **SP4** (p=0.7, n=3). *represents p≤0.05.

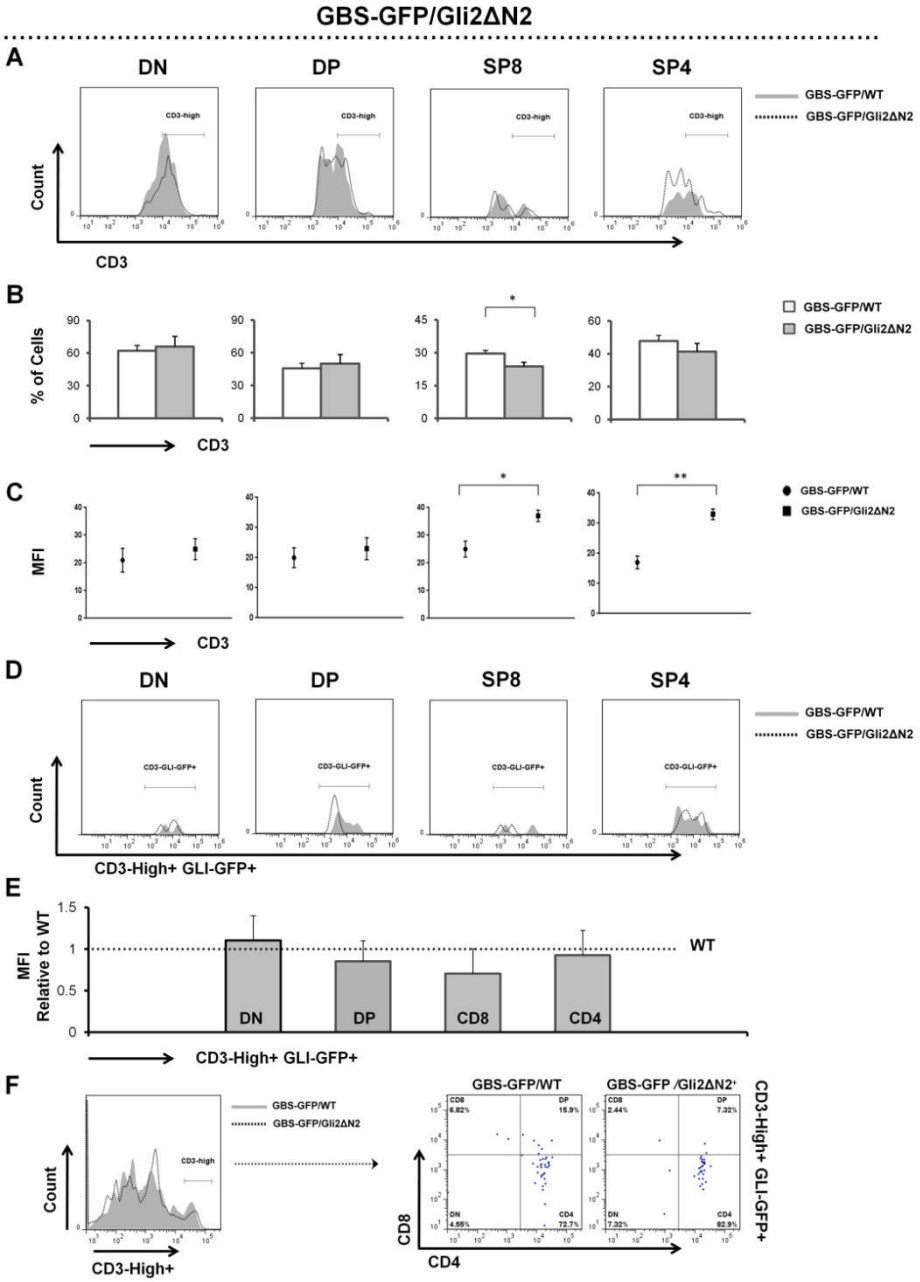

Figure 3.5

Expression of CD3 in GBS-GFP/Gli2ΔN2 thymocytes. Expression of CD3 in DN, DP, SP8 and SP4 cells from adult GBS-GFP/Gli2ΔN2 and GBS-GFP/WT littermates. Thymocytes were stained for anti-CD3, anti-CD8 and anti-CD4, and analyzed by flow cytometry. Cells were gated on Gli-GFP$^+$ cells. **(A)** Representative histogram of CD3 expression in DN, DP, SP8 and SP4 cells. **(B)** Representative bar graph of CD3 percentages in DN, DP, SP8 and SP4 cells. **(C)** Representative scatter plot of CD3 MFI in DN, DP, SP8 and SP4 cells. **(D)** Representative histogram of GLI-GFP in CD3 from DN, DP, SP8 and SP4 cells. **(E)** Representative bar graph of GLI-GFP percentages in CD3 from DN, DP, SP8 and SP4 cells. **(F)** Representative histogram and dot plot of CD3-high expression then gated on CD8 and CD4. Figures are representative of 3 independent sets of GBS-GFP/Gli2ΔN2 littermates. Mean and standard deviation of each population are given. Bars represent mean ± standard deviations. **CD3 percentages; DN** (p= 0.5, n=3). **DP** (p= 0.4, n=3). **SP8** (p= 0.01, n=3). SP4 (p= 0.3, n=3). **CD3 MFI; DN** (p= 0.2, n=3). **DP** (p= 0.8, n=3). **SP8** (p= 0.01, n=3). **SP4** (p= 0.004, n=3). **GLI GFP MFI; DN** (p= 0.5, n=3). **DP** (p= 0.4, n=3). **SP8** (p= 0.2, n=3). **SP4** (p= 0.8, n=3).*represents p≤0.05, **represents p≤0.005.

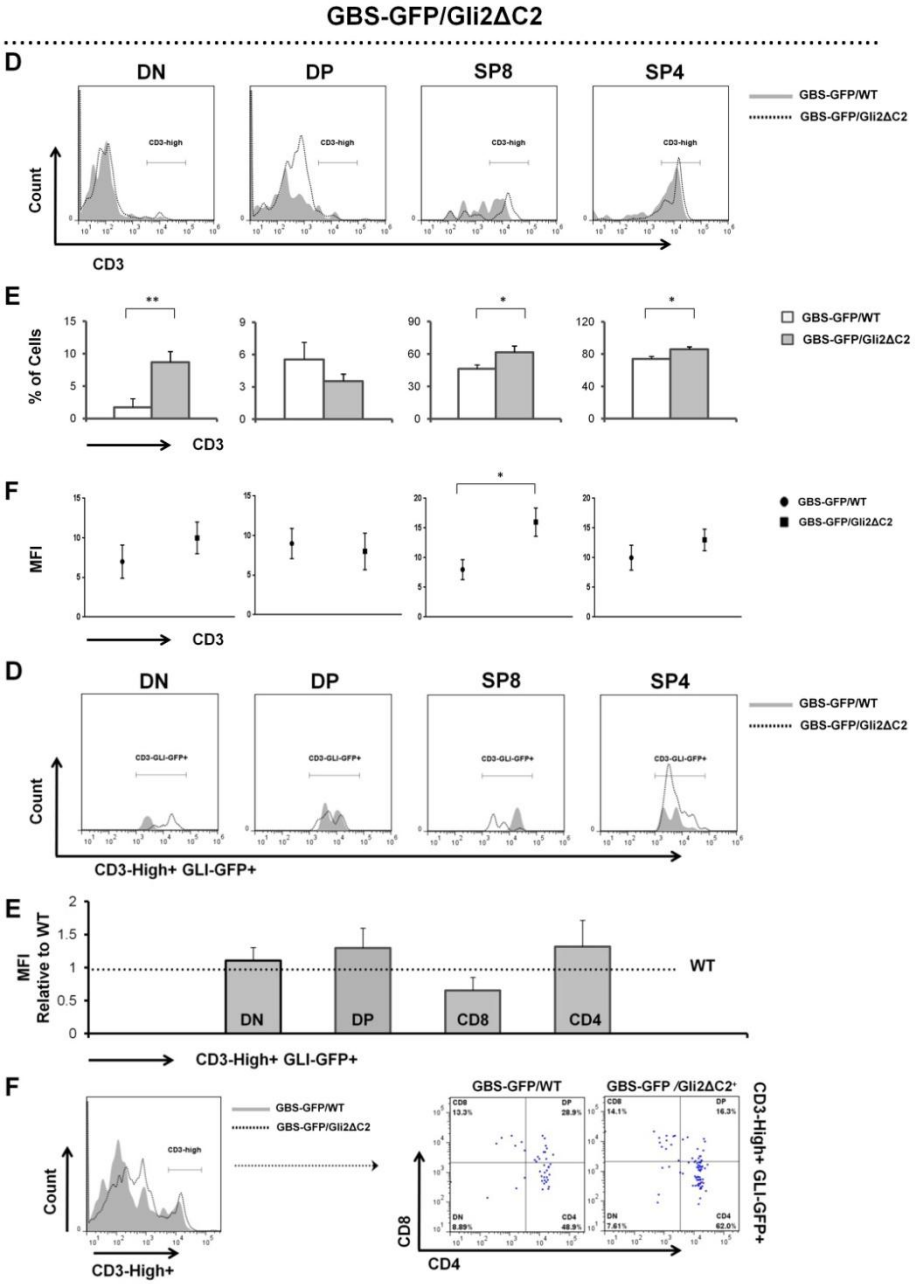

Figure 3.6

Expression of CD3 in GBS-GFP/Gli2ΔC2 thymocytes. Expression of CD3 in DN, DP, SP8 and SP4 cells from adult GBS-GFP/Gli2ΔC2 and GBS-GFP/WT littermates. Thymocytes were stained for anti-CD3, anti-CD8 and anti-CD4, and analyzed by flow cytometry. Cells were gated on Gli-GFP$^+$ cells. **(A)** Representative histogram of CD3 expression in DN, DP, SP8 and SP4 cells. **(B)** Representative bar graph of CD3 percentages in DN, DP, SP8 and SP4 cells. **(C)** Representative scatter plot of CD3 MFI in DN, DP, SP8 and SP4 cells. **(D)** Representative histogram of GLI-GFP in CD3 from DN, DP, SP8 and SP4 cells. **(E)** Representative bar graph of GLI-GFP MFI in CD3 from DN, DP, SP8 and SP4 cells. **(F)** Representative histogram and dot plot of CD3-high expression then gated on CD8 and CD4. Figures are representative of 3 independent sets of GBS-GFP/Gli2ΔC2 littermates. Mean and standard deviation of each population are given. Bars represent mean ± standard deviations. **CD3 percentages; DN** (p= 0.005, n=3). **DP** (p= 0.1, n=3). **SP8** (p= 0.02, n=3). **SP4** (p= 0.008, n=3). **CD3 MFI; DN** (p= 0.3, n=3). **DP** (p= 0.4, n=3). **SP8** (p= 0.04, n=3). **SP4** (p= 0.07, n=3). **GLI-GFP MFI; DN** (p= 0.2, n=3). **DP** (p= 0.6, n=3). **SP8** (p= 0.1, n=3). **SP4** (p= 0.3, n=3).*represents p≤0.05, **represents p≤0.005.

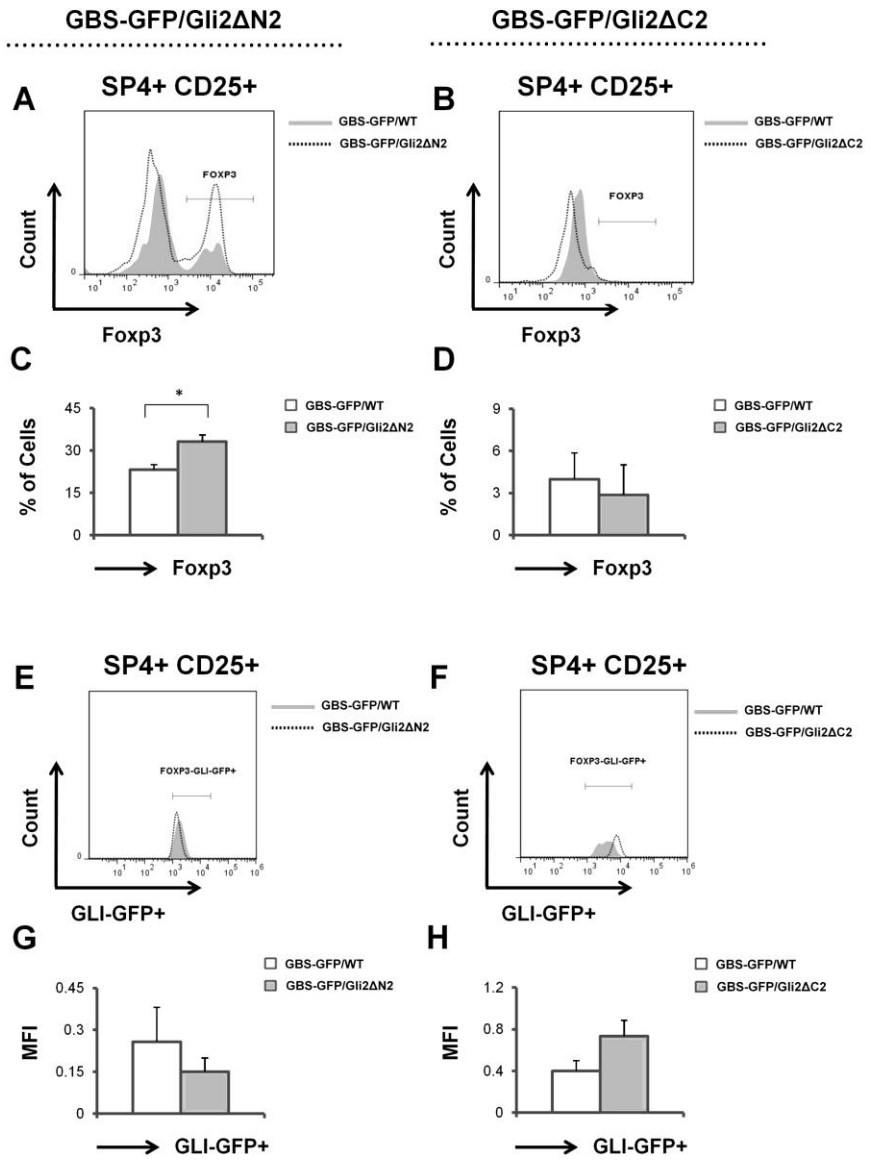

Figure 3.7

Expression of Foxp3 in GBS-GFP/Gli2ΔN2 and GBS-GFP/Gli2ΔC2 SP4 thymocytes. Expression of Foxp3 in SP4 cells from adult GBS-GFP/Gli2ΔN2, GBS-GFP/Gli2ΔC2 and GBS-GFP/WT littermates. Thymocytes were stained for anti-Foxp3, anti-CD25, anti-CD8 and anti-CD4, and analyzed by flow cytometry. Cells were gated on Gli-GFP$^+$ cells. **(A)** Representative histogram of Foxp3 expression in GBS-GFP/Gli2ΔN2 SP4 cells. (**B)** Representative histogram of Foxp3 expression in GBS-GFP/Gli2ΔC2 SP4 cells. **(C)** Representative bar graph of Foxp3 percentages in GBS-GFP/Gli2ΔN2 SP4 cells. **(D)** Representative bar graph of Foxp3 percentages in GBS-GFP/Gli2ΔC2 SP4 cells. **(E)** Representative histogram of GLI-GFP expression in Foxp3 from GBS-GFP/Gli2ΔN2 SP4 cells. **(F)** Representative histogram of GLI-GFP expression in Foxp3 from GBS-GFP/Gli2ΔC2 SP4 cells. **(G)** Representative bar graph of GLI-GFP MFI in Foxp3 from GBS-GFP/Gli2ΔN2 SP4 cells. (**H)** Representative bar graph of GLI-GFP MFI in Foxp3 from GBS-GFP/Gli2ΔC2 SP4 cells. Figures are representative of 3 independent sets of GBS-GFP/Gli2ΔN2 and GBS-GFP/Gli2ΔC2 littermates. Mean and standard deviation of each population are given. Bars represent mean ± standard deviations. **GBS-GFP/Gli2ΔN2 Foxp3 percentage; SP4** (p= 0.006, n=3). **GBS-GFP/Gli2ΔC2 Foxp3 percentage; SP4** (p= 0.1, n=3). **GBS-GFP/Gli2ΔN2 GLI-GFP MFI; SP4** (p= 0.3, n=3). **GBS-GFP/Gli2ΔC2 GLI-GFP MFI; SP4** (p= 0.9, n=3).*represents $p \leq 0.05$.

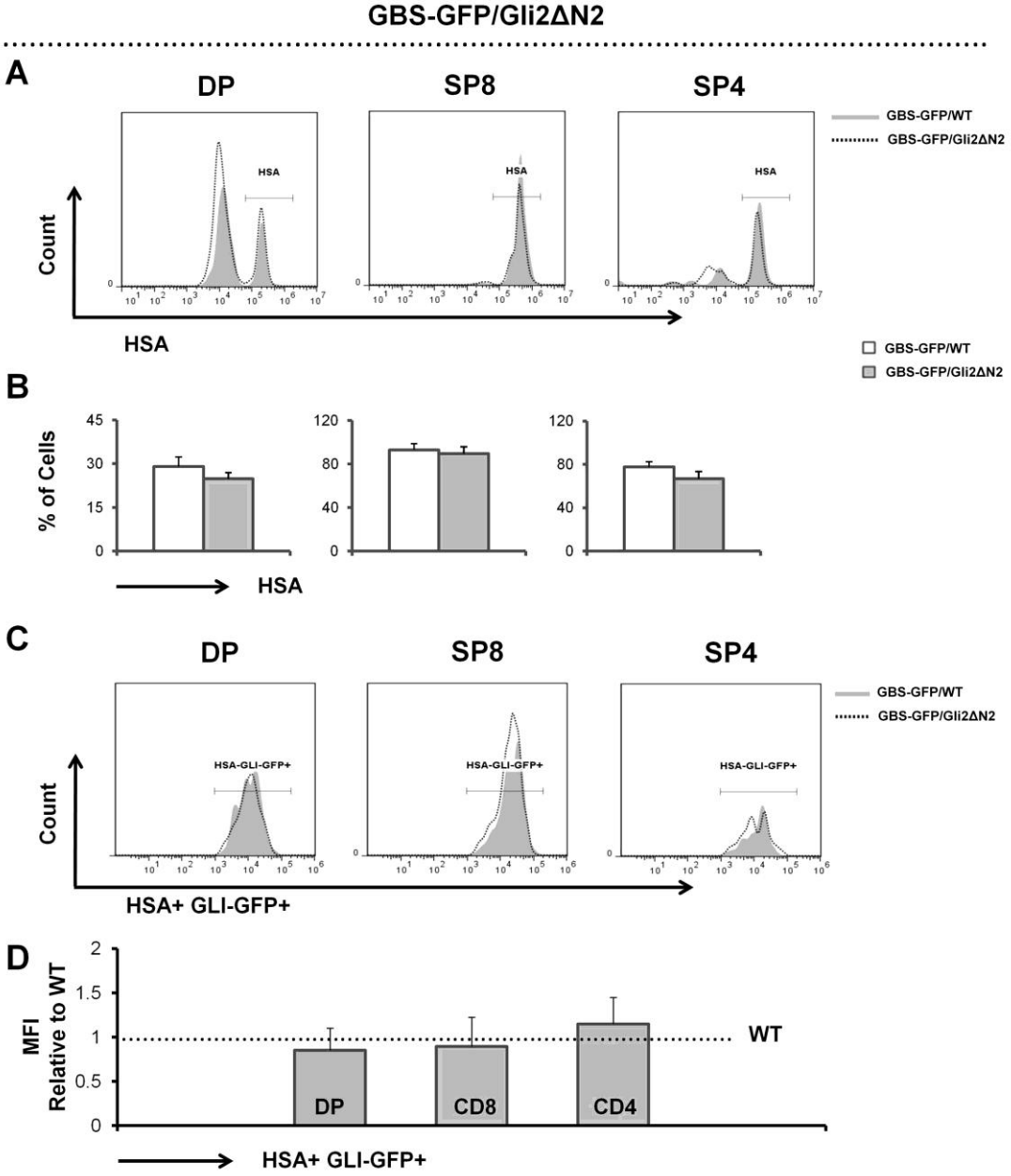

Figure 3.8

Expression of HSA in GBS-GFP/Gli2ΔN2 thymocytes. Expression of HSA in DP, SP8 and SP4 cells from adult GBS-GFP/Gli2ΔN2 and GBS-GFP/WT littermates. Thymocytes were stained for anti-CD24, anti-CD8 and anti-CD4, and analyzed by flow cytometry. Cells were gated on Gli-GFP^{+} cells. **(A)** Representative histogram of HSA expression in DP, SP8 and SP4 cells. **(B)** Representative bar graph of HSA percentages in DP, SP8 and SP4 cells. **(C)** Representative histogram of GLI-GFP expression in HSA for DP, SP8 and SP4 cells. **(D)** Representative bar graph of GLI GFP MFI in HSA from DP, SP8 and SP4 cells. Figures are representative of 3 independent sets of GBS-GFP/Gli2ΔN2 littermates. Mean and standard deviation of each population are given. Bars represent mean ± standard deviations. **HSA percentages; DP** (p= 0.1, n=3). **SP8** (p= 0.5, n=3). **SP4** (p= 0.09, n=3). **GLI-GFP MFI; DP** (p= 0.2, n=3). **SP8** (p= 0.1, n=3). **SP4** (p= 0.4, n=3).

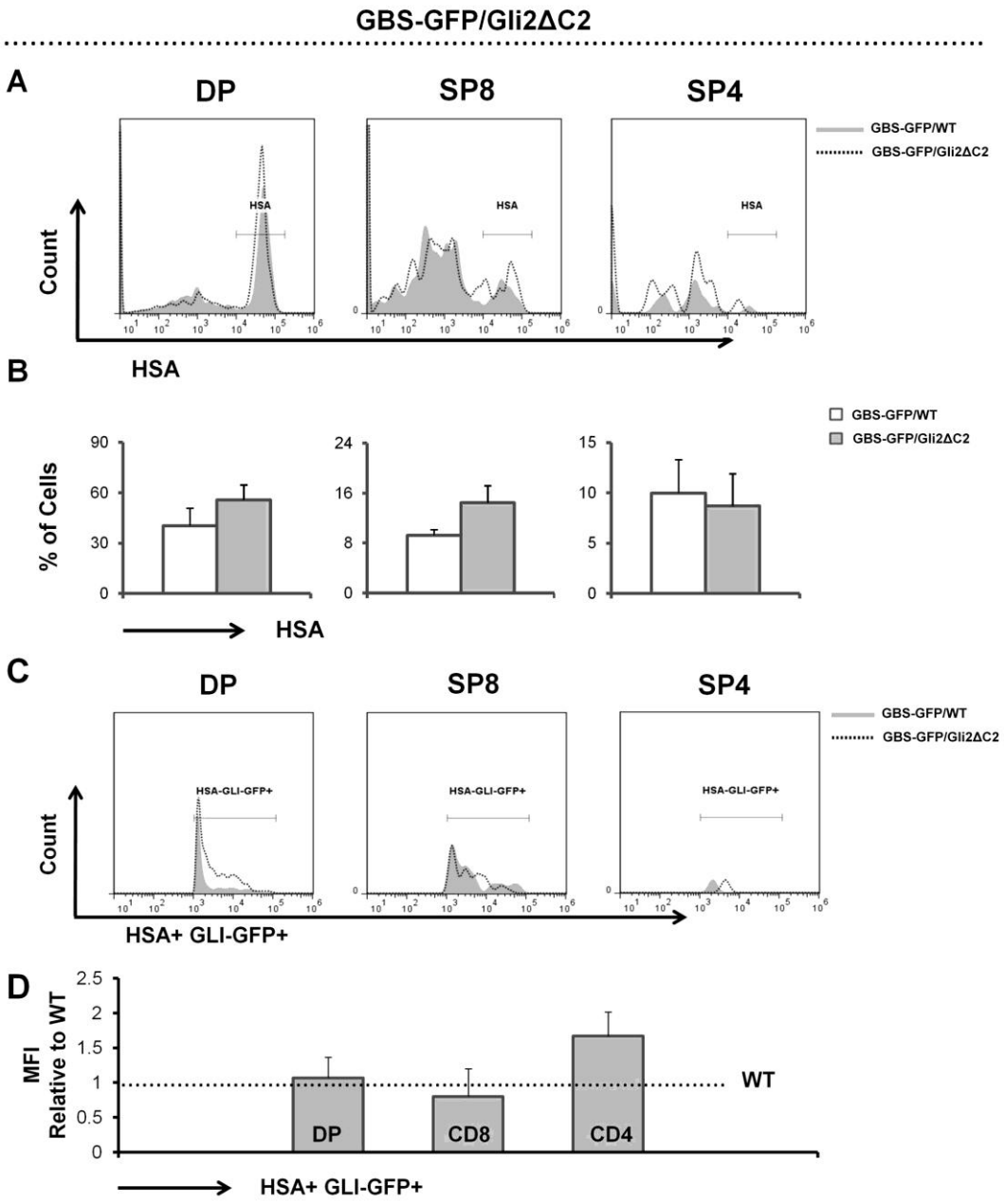

Figure 3.9

Expression of HSA in GBS-GFP/Gli2ΔC2 thymocytes. Expression of HSA in DP, SP8 and SP4 cells from adult GBS-GFP/Gli2ΔC2 and GBS-GFP/WT littermates. Thymocytes were stained for anti-CD24, anti-CD8 and anti-CD4, and analyzed by flow cytometry. Cells were gated on Gli-GFP^{+} cells. **(A)** Representative histogram of HSA expression in DP, SP8 and SP4 cells. **(B)** Representative bar graph of HSA percentages in DP, SP8 and SP4 cells. **(C)** Representative histogram of GLI-GFP expression in HSA from DP, SP8 and SP4 cells. **(D)** Representative bar graph of GLI-GFP MFI in HSA from DP, SP8 and SP4 cells. Figures are representative of 3 independent sets of GBS-GFP/Gli2ΔC2 littermates. Mean and standard deviation of each population are given. Bars represent mean ± standard deviations. **HSA percentages; DP** (p= 0.3, n=3). **SP8** (p= 0.4, n=3). **SP4** (p= 0.2, n=3). **GLI-GFP-MFI;** DP (p= 0.4, n=3). **SP8** (p= 0.1, n=3). **SP4** (p= 0.3, n=3).

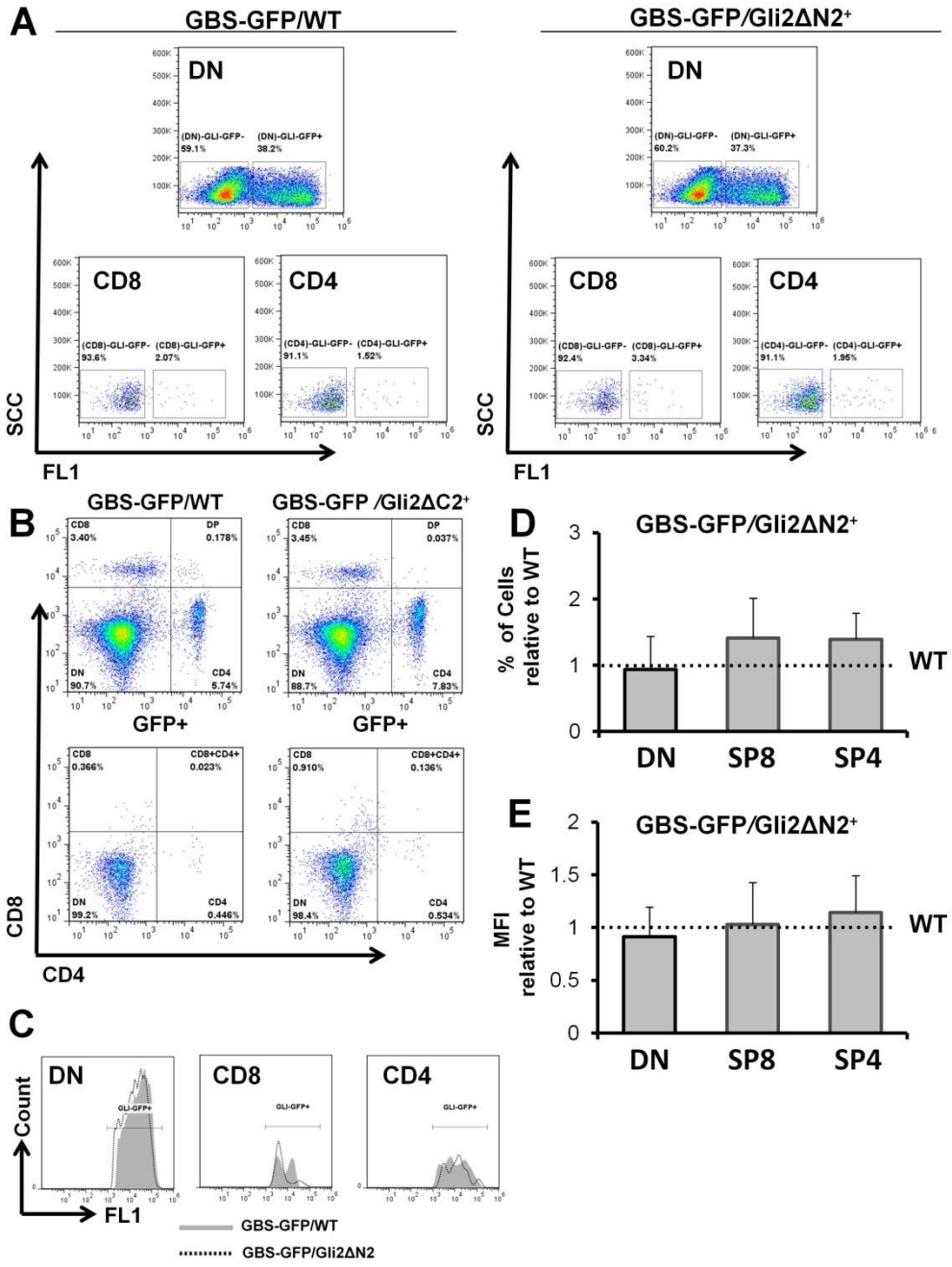

Figure 3.10

Major splenocyte populations in GBS-GFP/Gli2ΔN2 mice. Percentage of splenocyte populations from adult male GBS-GFP/Gli2ΔN2 and GBS-GFP/WT littermates. Splenocytes were stained for anti-CD8 and anti-CD4, and analyzed by flow cytometry. Cells were gated on Gli-GFP$^+$ cells. **(A)** Representative dot plot of splenocyte populations gated on GLI-GFP$^+$ and Gli-GFP$^-$ for CD4$^-$CD8$^-$, SP8 and SP4 cells. **(B)** Representative dot plot of splenocyte populations gated on total and GLI-GFP$^+$ cells. **(C)** Representative histogram of GLI-GFP$^+$ in CD4$^-$CD8$^-$, SP8 and SP4 cells. **(D)** Representative bar graph of GLI-GFP$^+$ percentages in CD4$^-$CD8$^-$, SP8 and SP4 cells. **(E)** Representative bar graph of GLI-GFP$^+$ MFI in CD4$^-$CD8$^-$, SP8 and SP4 cells. Figures are representative of 3 independent sets of GBS-GFP/Gli2ΔN2 littermates. Mean and standard deviation of each population are given. Bars represent mean ± standard deviations. **Splenocyte percentages; CD4$^-$CD8$^-$** (p= 0.5, n=3). **SP8** (p= 0.5, n=3). **SP4** (p= 0.6, n=3). **Gli-GFP MFI percentages; CD4$^-$CD8$^-$** (p= 0.6, n=3). **SP8** (p= 0.7, n=3). **SP4** (p= 0.3, n=3).

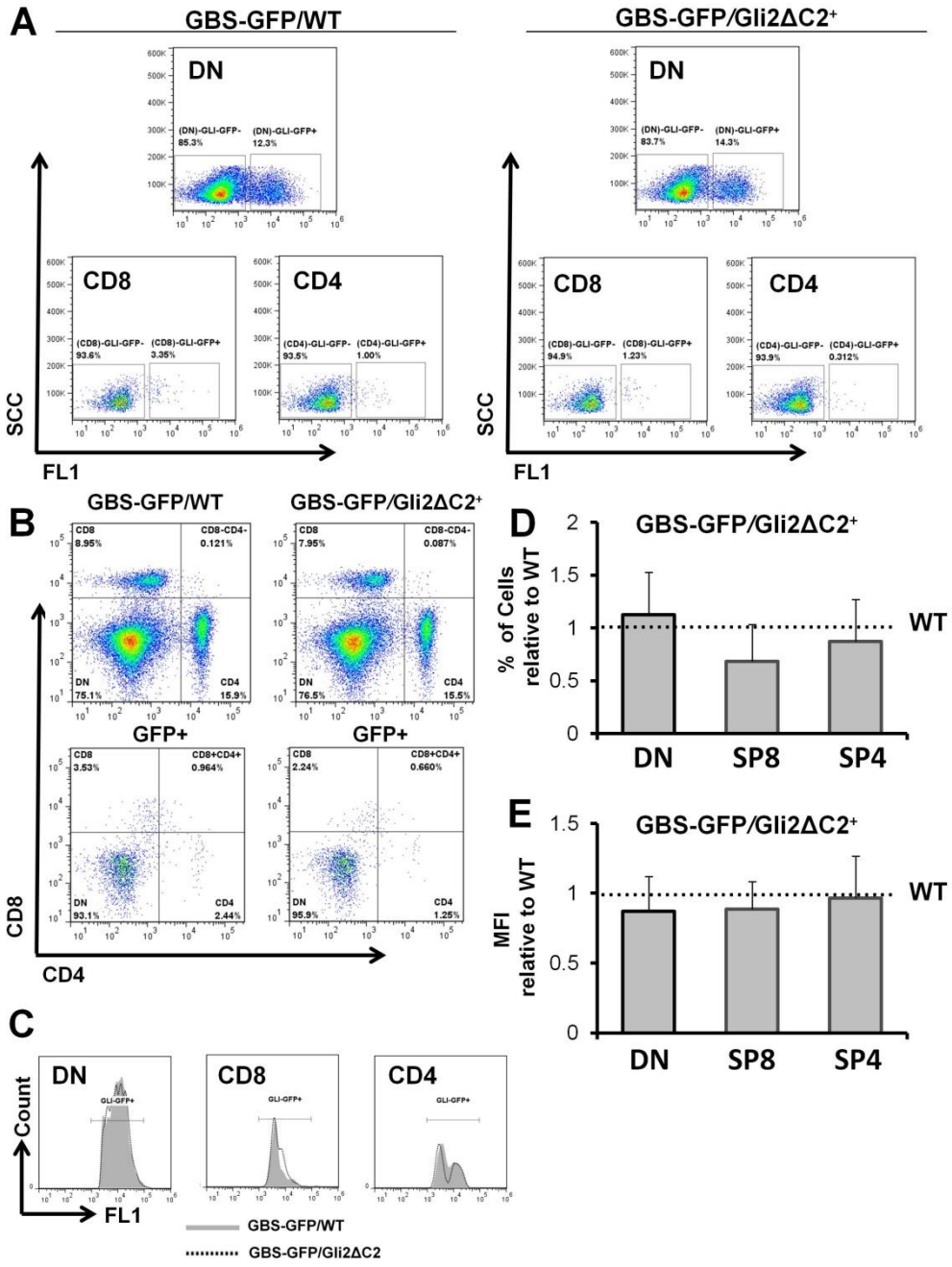

Figure 3.11

Major splenocyte populations in GBS-GFP/Gli2ΔC2 mice. Percentage of splenocyte populations from adult male GBS-GFP/Gli2ΔC2 and GBS-GFP/WT littermates. Splenocytes were stained for anti-CD8 and anti-CD4, and analyzed by flow cytometry. Cells were gated on Gli-GFP$^+$ cells. **(A)** Representative dot plot of splenocyte populations gated on GLI-GFP$^+$ and Gli-GFP$^-$ for CD4$^-$CD8$^-$, SP8 and SP4 cells. **(B)** Representative dot plot of splenocyte populations gated on total and GLI-GFP$^+$ cells. **(C)** Representative histogram of GLI-GFP$^+$ CD4$^-$CD8$^-$, SP8 and SP4 cells. **(D)** Representative bar graph of GLI-GFP$^+$ percentages in CD4$^-$CD8$^-$, SP8 and SP4 cells. **(E)** Representative bar graph of GLI-GFP$^+$ MFI in CD4$^-$CD8$^-$, SP8 and SP4 cells. Figures are representative of 3 independent sets of GBS-GFP/Gli2ΔC2 littermates. Mean and standard deviation of each population are given. Bars represent mean ± standard deviations. **Splenocyte percentages; CD4$^-$CD8$^-$** (p= 0.4, n=3). **SP8** (p= 0.3, n=3). **SP4** (p= 0.1, n=3). **GLI-GFP MFI** (p= 0.3, n=3). **SP8** (p= 0.4, n=3). **SP4** (p= 0.6, n=3).

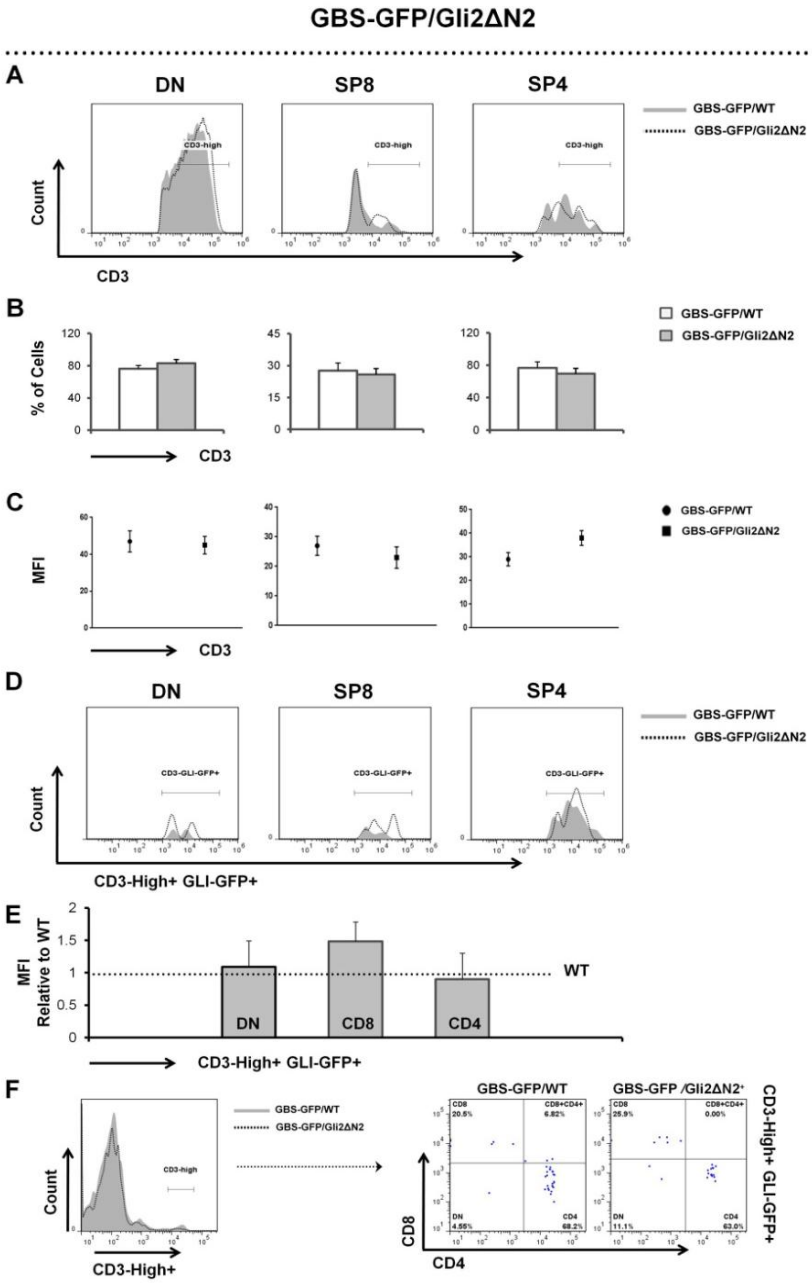

Figure 3.12

Expression of CD3 in GBS-GFP/Gli2ΔN2 splenocytes. Expression of CD3 in CD4$^-$CD8$^-$, SP8 and SP4 cells from adult GBS-GFP/Gli2ΔN2 and GBS-GFP/WT littermates. Splenocytes were stained for anti-CD3, anti-CD8 and anti-CD4, and analyzed by flow cytometry. Cells were gated on Gli-GFP$^+$ cells. **(A)** Representative histogram of CD3 expression in CD4$^-$CD8$^-$, SP8 and SP4 cells. **(B)** Representative bar graph of CD3 percentages in CD4$^-$CD8$^-$, SP8 and SP4 cells. **(C)** Representative scatter plot of CD3 MFI in CD4$^-$CD8$^-$, SP8 and SP4 cells. **(D)** Representative histogram of GLI-GFP expression in CD3 from CD4$^-$CD8$^-$, SP8 and SP4 cells. **(E)** Representative bar graph of GLI-GFP MFI in CD3 from CD4$^-$CD8$^-$, SP8 and SP4 cells. **(F)** Representative histogram and dot plot of CD3-high expression then gated on CD8 and CD4. Figures are representative of 3 independent sets of GBS-GFP/Gli2ΔN2 littermates. Mean and standard deviation of each population are given. Bars represent mean ± standard deviations. **CD3 percentages; CD4$^-$CD8$^-$** (p= 0.1, n=3). **SP8** (p= 0.5, n=3). **SP4** (p= 0.6, n=3). **CD3 MFI; CD4$^-$CD8$^-$** (p= 0.6, n=3). **SP8** (p= 0.2, n=3). **SP4** (p= 0.5, n=3). **GLI-GFP MFI; CD4$^-$CD8$^-$** (p= 0.2, n=3). **SP8** (p= 0.7, n=3). **SP4** (p= 0.4, n=3).

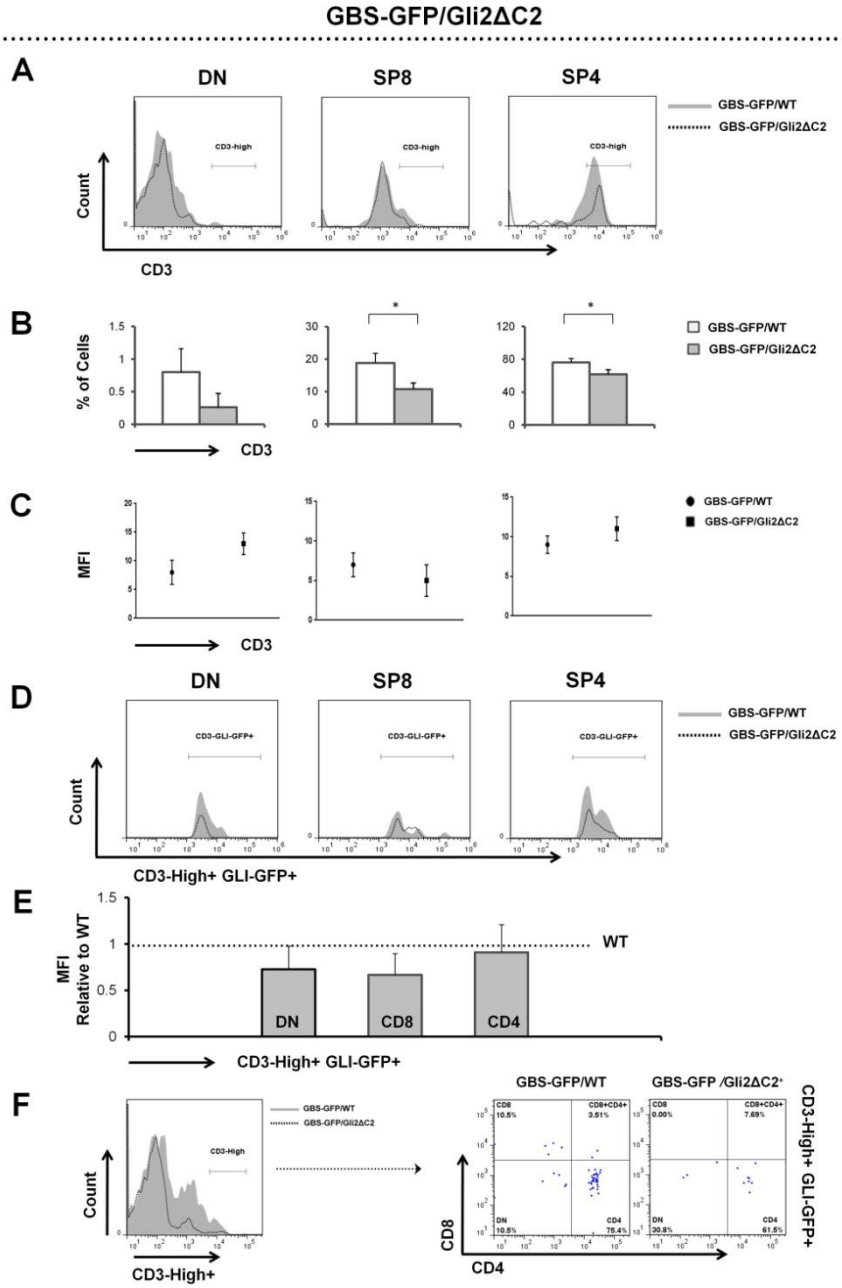

Figure 3.13

Expression of CD3 in GBS-GFP/Gli2ΔC2 splenocytes. Expression of CD3 in CD4$^-$CD8$^-$, SP8 and SP4 cells from adult GBS-GFP/Gli2ΔC2 and GBS-GFP/WT littermates. Splenocytes were stained for anti-CD3, anti-CD8 and anti-CD4, and analyzed by flow cytometry. Cells were gated on Gli-GFP$^+$ cells. **(A)** Representative histogram of CD3 expression in CD4$^-$CD8$^-$, SP8 and SP4 cells. **(B)** Representative bar graph of CD3 percentages in CD4$^-$CD8$^-$, SP8 and SP4 cells. **(C)** Representative scatter plot of CD3 MFI in CD4$^-$CD8$^-$, SP8 and SP4 cells. **(D)** Representative histogram of GLI-GFP expression in CD3 from CD4$^-$CD8$^-$, SP8 and SP4 cells. **(E)** Representative bar graph of GLI-GFP MFI in CD3 from CD4$^-$CD8$^-$, SP8 and SP4 cells. **(F)** Representative histogram and dot plot of CD3-high expression then gated on CD8 and CD4. Figures are representative of 3 independent sets of GBS-GFP/Gli2ΔC2 littermates. Mean and standard deviation of each population are given. Bars represent mean ± standard deviations. **CD3 percentages; CD4$^-$CD8$^-$** (p= 0.1, n=3). **SP8** (p= 0.02, n=3). **SP4** (p= 0.03, n=3). **GLI-GFP MFI; CD4$^-$CD8$^-$** (p= 0.3, n=3). **SP8** (p= 0.4, n=3). **SP4** (p= 0.7, n=3). *represents p≤0.05.

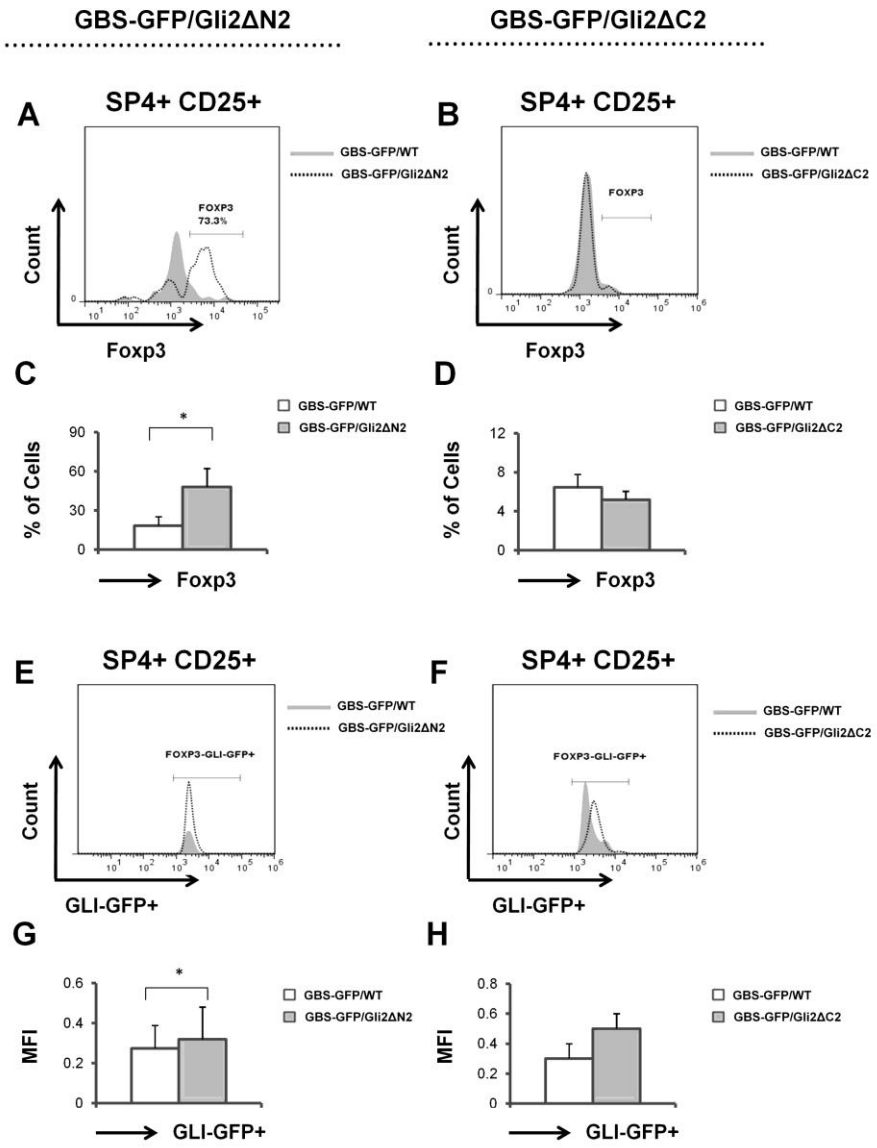

Figure 3.14

Expression of Foxp3 in GBS-GFP/Gli2ΔN2 and GBS-GFP/Gli2ΔC2 SP4 splenocytes. Expression of Foxp3 in SP4 cells from adult GBS-GFP/Gli2ΔN2, GBS-GFP/Gli2ΔC2 and GBS-GFP/WT littermates. Splenocytes were stained for anti-Foxp3, anti-CD25, anti-CD8 and anti-CD4, and analyzed by flow cytometry. Cells were gated on Gli-GFP$^+$ cells. **(A)** Representative histogram of Foxp3 expression in GBS-GFP/Gli2ΔN2 SP4 cells. (**B)** Representative histogram of Foxp3 expression in GBS-GFP/Gli2ΔC2 SP4 cells. **(C)** Representative bar graph of Foxp3 percentages in GBS-GFP/Gli2ΔN2 SP4 cells. **(D)** Representative bar graph of Foxp3 percentages in GBS-GFP/Gli2ΔC2 SP4 cells. **(E)** Representative histogram of GLI-GFP expression in Foxp3 from GBS-GFP/Gli2ΔN2 SP4 cells. **(F)** Representative histogram of GLI-GFP expression in Foxp3 from GBS-GFP/Gli2ΔC2 SP4 cells. **(G)** Representative bar graph of GLI-GFP MFI in Foxp3 from GBS-GFP/Gli2ΔN2 SP4 cells. (**H)** Representative bar graph of GLI-GFP MFI in Foxp3 from GBS-GFP/Gli2ΔC2 SP4 cells. Figures are representative of 3 independent sets of GBS-GFP/Gli2ΔN2 and GBS-GFP/Gli2ΔC2 littermates. Mean and standard deviation of each population are given. Bars represent mean ± standard deviations. **GBS-GFP/Gli2ΔN2 Foxp3 percentage; SP4** (p= 0.02, n=3). **GBS-GFP/Gli2ΔC2 Foxp3 percentage; SP4** (p= 0.08, n=3). **GBS-GFP/Gli2ΔN2 GLI-GFP MFI; SP4** (p= 0.05, n=3). **GBS-GFP/Gli2ΔC2 GLI-GFP MFI; SP4** (p= 0.3, n=3). *represents p≤0.05.

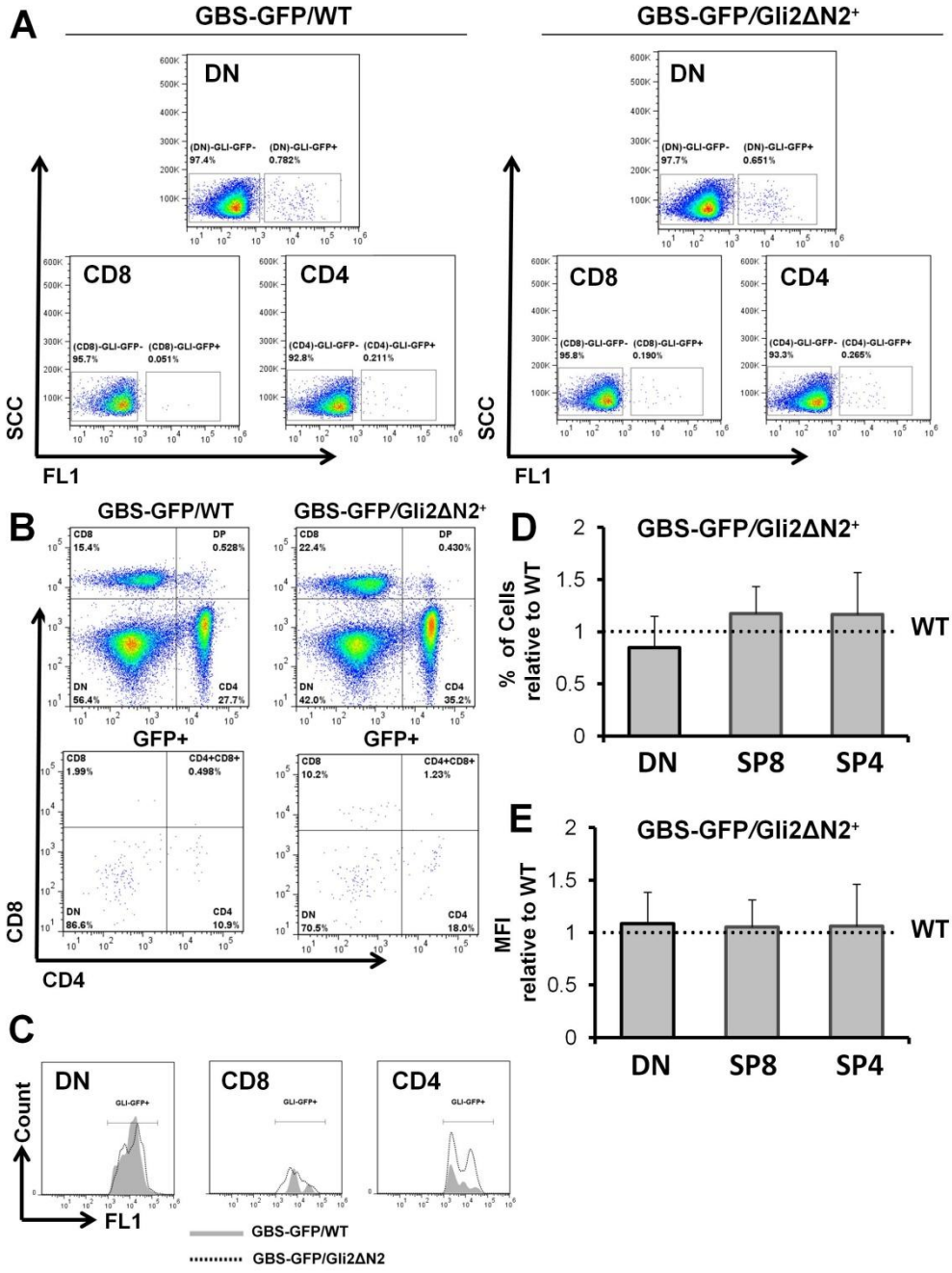

Figure 3.15

Major T cell populations in the lymph node of GBS-GFP/Gli2ΔN2 mice. Percentage of T cell populations from adult GBS-GFP/Gli2ΔN2 and GBS-GFP/WT littermates. Cells were stained for anti-CD8 and anti-CD4, and analyzed by flow cytometry. Cells were gated on Gli-GFP$^+$ cells. **(A)** Representative dot plot of T cell populations gated on GLI-GFP$^+$ and Gli-GFP$^-$ for CD4$^-$CD8$^-$, SP8 and SP4 cells. **(B)** Representative dot plot of T cell populations gated on total and GLI-GFP$^+$ cells. **(C)** Representative histogram of GLI-GFP$^+$ CD4$^-$CD8$^-$, SP8 and SP4 cells. **(D)** Representative bar graph of GLI-GFP$^+$ percentages in CD4$^-$CD8$^-$, SP8 and SP4 cells. **(E)** Representative bar graph of GLI-GFP$^+$ MFI in CD4$^-$CD8$^-$, SP8 and SP4 cells. Figures are representative of 3 independent sets of male Marilyn-Gli2ΔN2 littermates. Mean and standard deviation of each population are given. Bars represent mean ± standard deviations. **T cell percentages; CD4$^-$CD8$^-$** (p= 0.1, n=3). **SP8** (p= 0.2, n=3). **SP4** (p= 0.08, n=3). **GLI-GFP MFI; CD4$^-$CD8$^-$** (p= 0.4, n=3). **SP8** (p= 0.1, n=3). **SP4** (p= 0.3, n=3).

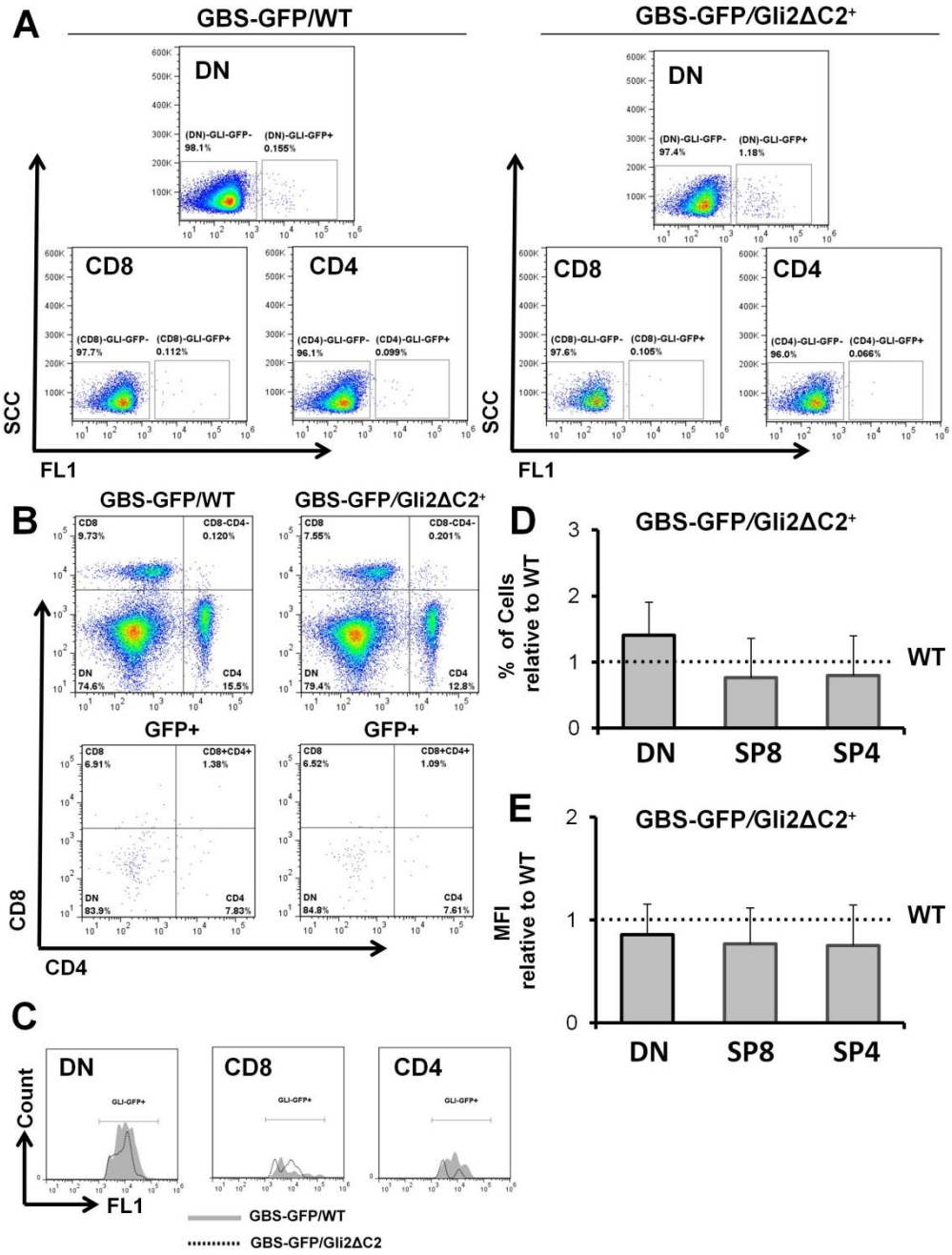

Figure 3.16

Major T cell populations in the lymph node of GBS-GFP/Gli2ΔC2 mice. Percentage of T cell populations from adult GBS-GFP/Gli2ΔC2 and GBS-GFP/WT littermates. Cells were stained for anti-CD8 and anti-CD4, and analyzed by flow cytometry. Cells were gated on Gli-GFP$^+$ cells. **(A)** Representative dot plot of T cell populations gated on GLI-GFP$^+$ and Gli-GFP$^-$ for CD4$^-$CD8$^-$, SP8 and SP4 cells. **(B)** Representative dot plot of T cell populations gated on total and GLI-GFP$^+$ cells. **(C)** Representative histogram of GLI-GFP$^+$ CD4$^-$CD8$^-$, SP8 and SP4 cells. **(D)** Representative bar graph of GLI-GFP$^+$ percentages in CD4$^-$CD8$^-$, SP8 and SP4 cells. **(E)** Representative bar graph of GLI-GFP$^+$ MFI in CD4$^-$CD8$^-$, SP8 and SP4 cells. Figures are representative of 3 independent sets of male GBS-GFP/Gli2ΔC2 littermates. Mean and standard deviation of each population are given. Bars represent mean ± standard deviations. **T cell percentages; CD4$^-$CD8$^-$** (p= 0.3, n=3). **SP8** (p= 0.2, n=3). **SP4** (p= 0.09, n=3). **GLI-GFP MFI; CD4$^-$CD8$^-$** (p= 0.2, n=3). **SP8** (p= 0.1, n=3). **SP4** (p= 0.4, n=3).

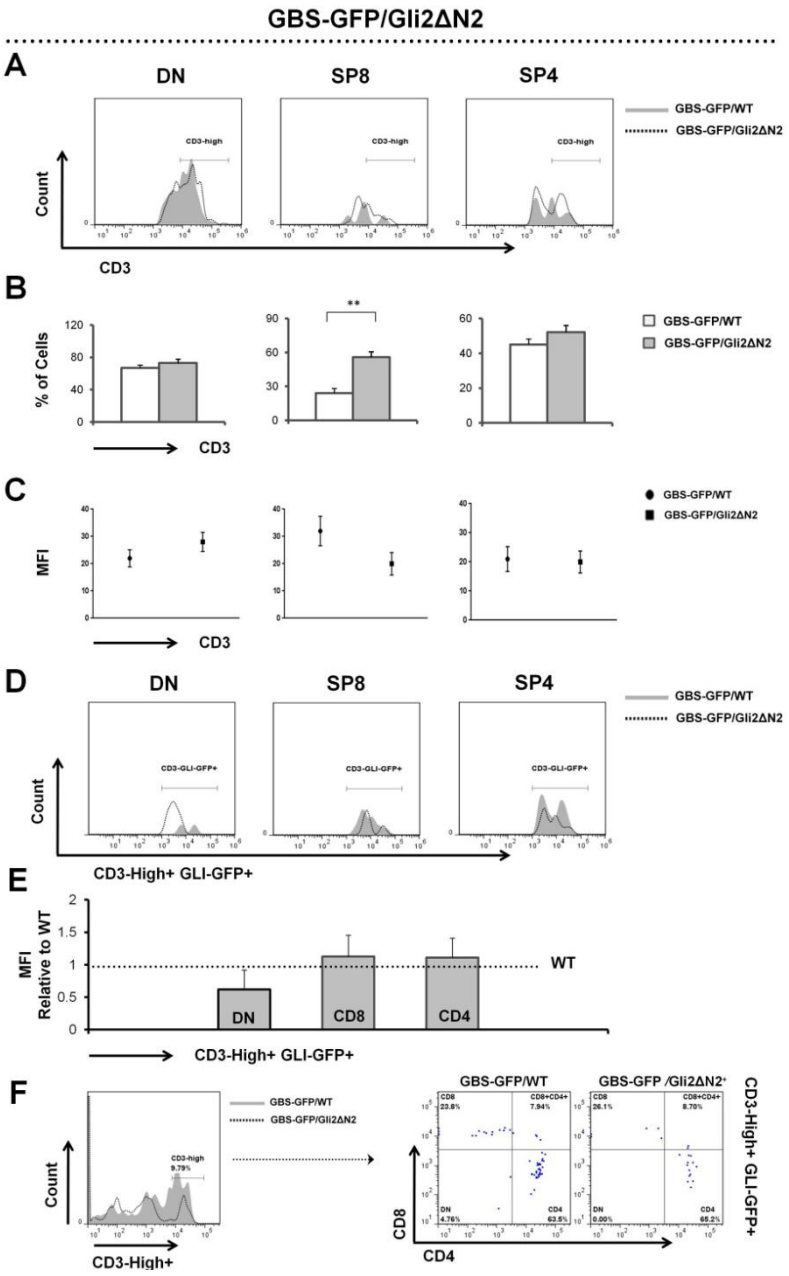

Figure 3.17

Expression of CD3 in GBS-GFP/Gli2ΔN2 lymph node T cells. Expression of CD3 in $CD4^{-}CD8^{-}$, SP8 and SP4 cells from adult GBS-GFP/Gli2ΔN2 and GBS-GFP/WT littermates. Cells were stained for anti-CD3, anti-CD8 and anti-CD4, and analyzed by flow cytometry. Cells were gated on Gli-GFP^{+} cells. **(A)** Representative histogram of CD3 expression in $CD4^{-}CD8^{-}$, SP8 and SP4 cells. **(B)** Representative bar graph of CD3 percentages in $CD4^{-}CD8^{-}$, SP8 and SP4 cells. **(C)** Representative scatter plot of CD3 MFI in $CD4^{-}CD8^{-}$, SP8 and SP4 cells. **(D)** Representative histogram of GLI-GFP expression in CD3 from $CD4^{-}CD8^{-}$, SP8 and SP4 cells. **(E)** Representative bar graph of GLI-GFP MFI in CD3 from $CD4^{-}CD8^{-}$, SP8 and SP4 cells. **(F)** Representative histogram and dot plot of CD3-high expression then gated on CD8 and CD4. Figures are representative of 3 independent sets of male GBS-GFP/Gli2ΔN2 littermates. Mean and standard deviation of each population are given. Bars represent mean ± standard deviations. **CD3 percentages; $CD4^{-}CD8^{-}$** (p= 0.1, n=3). **SP8** (p= 0.001, n=3). **SP4** (p= 0.07, n=3). **GBS-GFP/Gli2ΔN2 CD3 MFI; $CD4^{-}CD8^{-}$** (p= 0.3, n=3). **SP8** (p= 0.4, n=3). **SP4** (p= 0.09, n=5). **GLI-GFP MFI; $CD4^{-}CD8^{-}$** (p= 0.3, n=3). **SP8** (p= 0.4, n=3). **SP4** (p= 0.2, n=3). **represents $p \leq 0.005$.

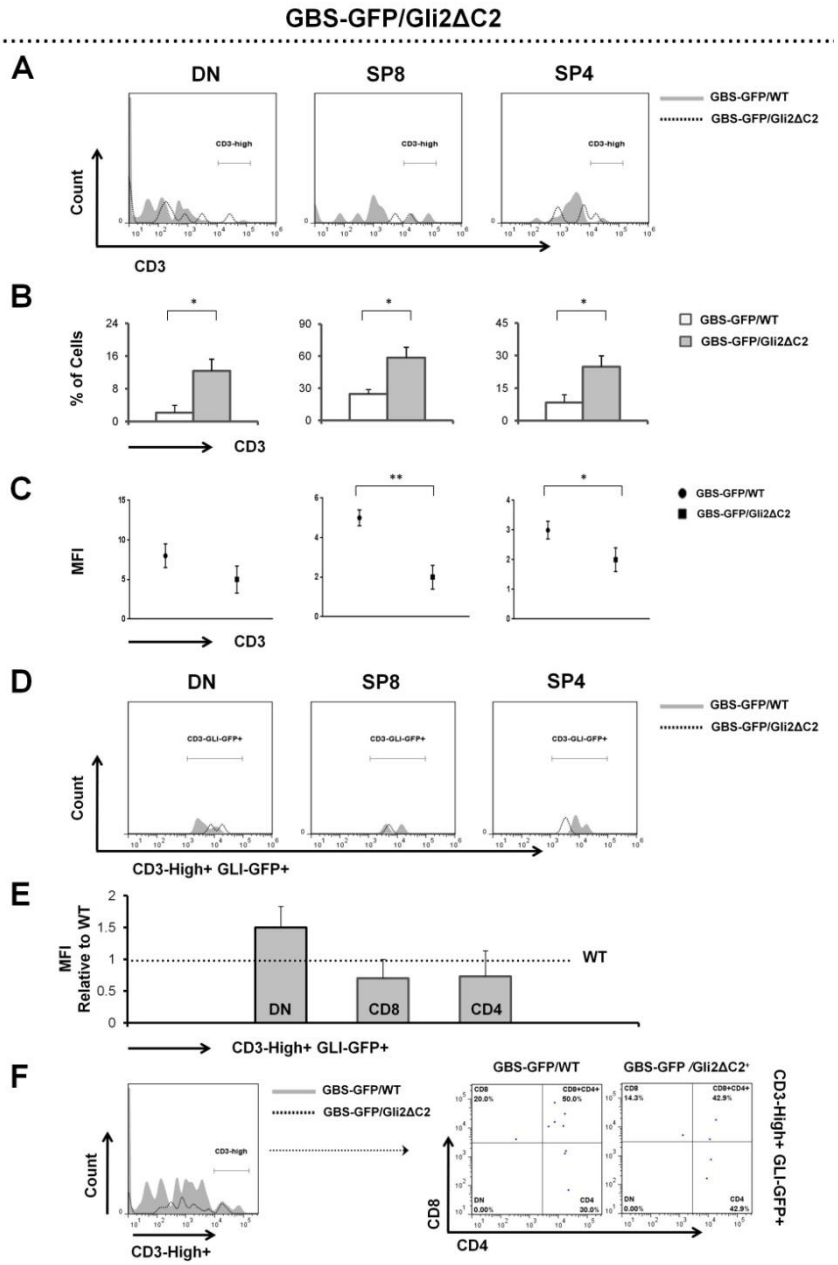

Figure 3.18

Expression of CD3 in GBS-GFP/Gli2ΔC2 lymph node T cells. Expression of CD3 in $CD4^{-}CD8^{-}$, SP8 and SP4 cells from adult GBS-GFP/Gli2ΔC2 and GBS-GFP/WT littermates. Cells were stained for anti-CD3, anti-CD8 and anti-CD4, and analyzed by flow cytometry. Cells were gated on Gli-GFP^{+} cells. **(A)** Representative histogram of CD3 expression in $CD4^{-}CD8^{-}$, SP8 and SP4 cells. **(B)** Representative bar graph of CD3 percentages in $CD4^{-}CD8^{-}$, SP8 and SP4 cells. **(C)** Representative scatter plot of CD3 MFI in $CD4^{-}CD8^{-}$, SP8 and SP4 cells. **(D)** Representative histogram of GLI-GFP expression in CD3 from $CD4^{-}CD8^{-}$, SP8 and SP4 cells. **(E)** Representative bar graph of GLI-GFP MFI in CD3 from $CD4^{-}CD8^{-}$, SP8 and SP4 cells. **(F)** Representative histogram and dot plot of CD3-high expression then gated on CD8 and CD4. Figures are representative of 3 independent sets of male GBS-GFP/Gli2ΔC2 littermates. Mean and standard deviation of each population are given. Bars represent mean ± standard deviations. **CD3 percentages; $CD4^{-}CD8^{-}$** (p= 0.009, n=3). **SP8** (p= 0.01, n=3). **SP4** (p= 0.02, n=3). **CD3 MFI; $CD4^{-}CD8^{-}$** (p= 0.4, n=3). **SP8** (p= 0.003, n=3). **SP4** (p= 0.02, n=5). **GLI-GFP MFI; $CD4^{-}CD8^{-}$** (p= 0.2, n=3). **SP8** (p= 0.3, n=3). **SP4** (p= 0.2, n=5).*represents $p \leq 0.05$, **represents $p \leq 0.005$.

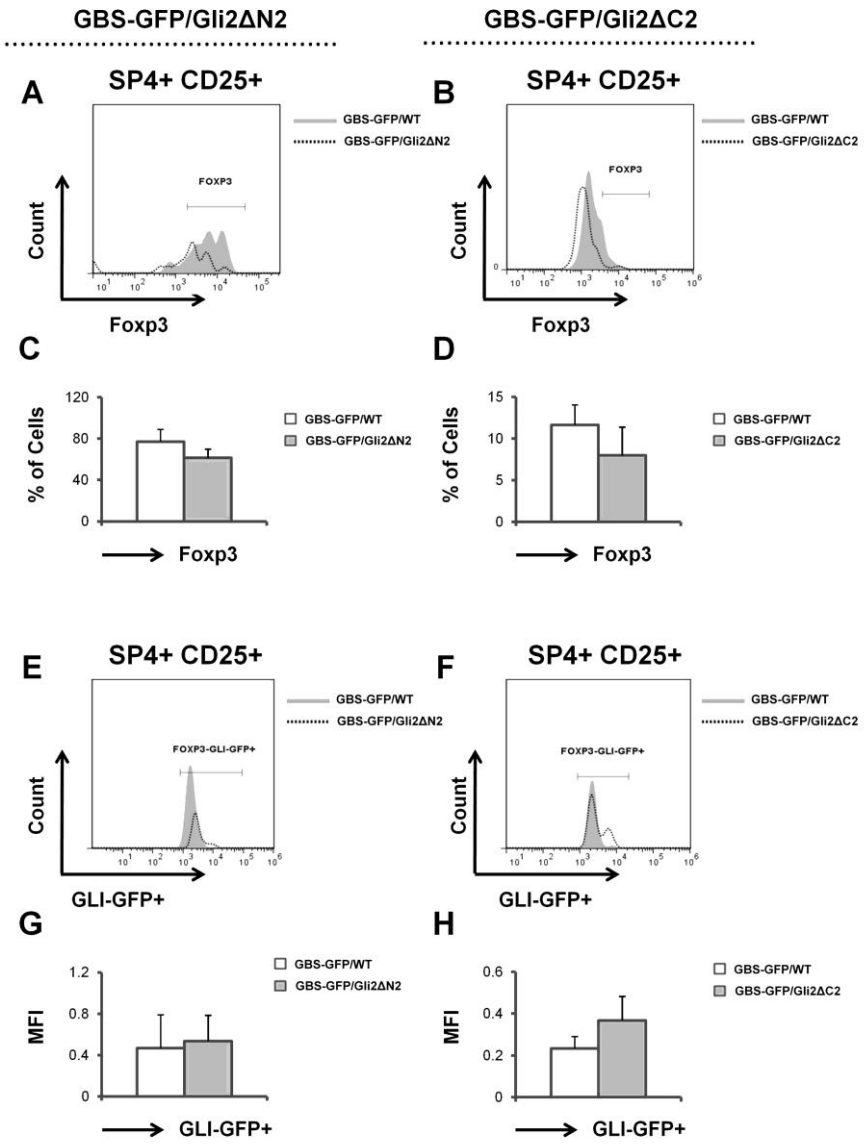

Figure 3.19

Expression of Foxp3 in GBS-GFP/Gli2ΔN2 and GBS-GFP/Gli2ΔC2 SP4 lymph node T cells. Expression of Foxp3 in SP4 cells from adult GBS-GFP/Gli2ΔN2, GBS-GFP/Gli2ΔC2 and GBS-GFP/WT littermates. Cells were stained for anti-Foxp3, anti-CD25, anti-CD8 and anti-CD4, and analyzed by flow cytometry. Cells were gated on Gli-GFP$^+$ cells. **(A)** Representative histogram of Foxp3 expression in GBS-GFP/Gli2ΔN2 SP4 cells. (**B)** Representative histogram of Foxp3 expression in GBS-GFP/Gli2ΔC2 SP4 cells. **(C)** Representative bar graph of Foxp3 percentages in GBS-GFP/Gli2ΔN2 SP4 cells. **(D)** Representative bar graph of Foxp3 percentages in GBS-GFP/Gli2ΔC2 SP4 cells. **(E)** Representative histogram of GLI-GFP expression in Foxp3 from GBS-GFP/Gli2ΔN2 SP4 cells. **(F)** Representative histogram of GLI-GFP expression in Foxp3 from GBS-GFP/Gli2ΔC2 SP4 cells. **(G)** Representative bar graph of GLI-GFP MFI in Foxp3 from GBS-GFP/Gli2ΔN2 SP4 cells. (**H)** Representative bar graph of GLI-GFP MFI in Foxp3 from GBS-GFP/Gli2ΔC2 SP4 cells. Figures are representative of 3 independent sets of GBS-GFP/Gli2ΔN2 and GBS-GFP/Gli2ΔC2 littermates. Mean and standard deviation of each population are given. Bars represent mean ± standard deviations. **GBS-GFP/Gli2ΔN2 Foxp3 percentage; SP4** (p= 0.3, n=3). **GBS-GFP/Gli2ΔC2 Foxp3 percentage; SP4** (p= 0.06, n=3). **GBS-GFP/Gli2ΔN2 GLI-GFP MFI; SP4** (p= 0.2, n=3). **GBS-GFP/Gli2ΔC2 GLI-GFP MFI; SP4** (p= 0.6, n=3).

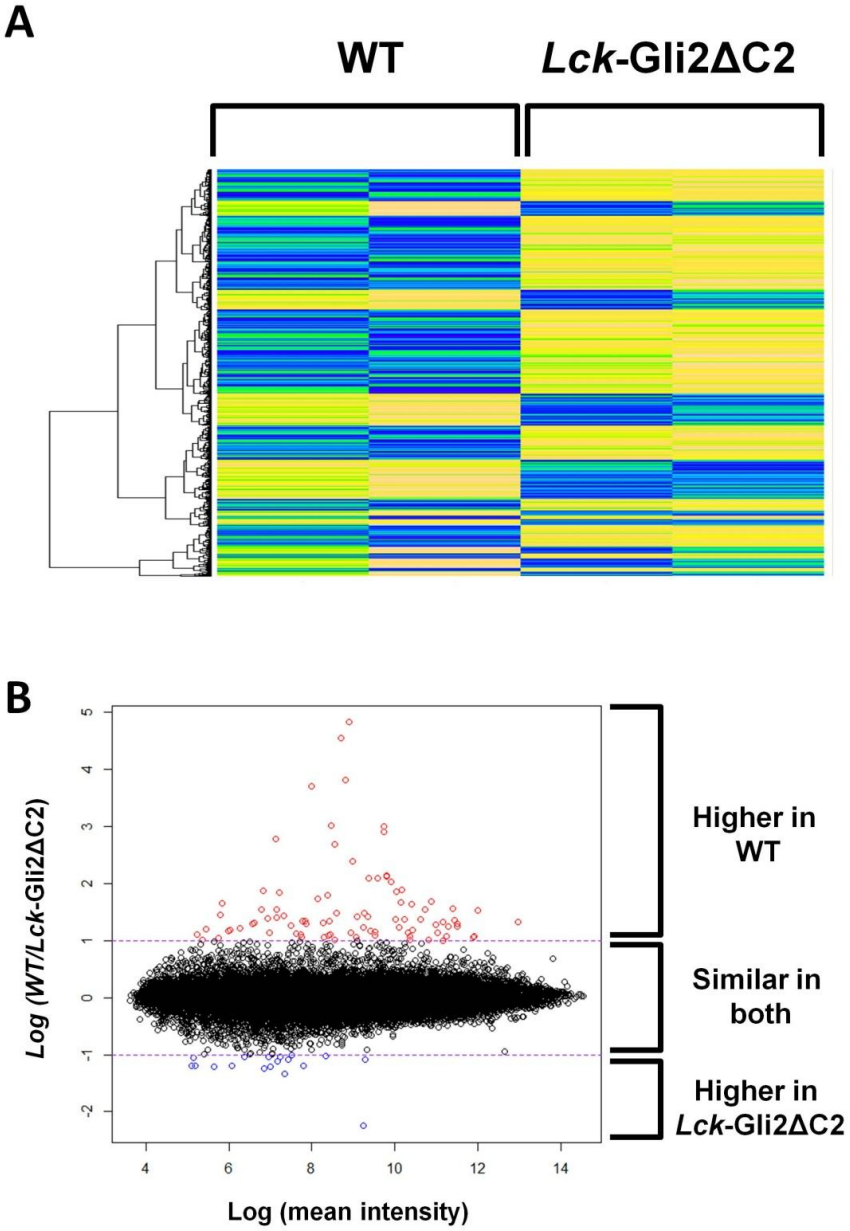

Figure 3.20

Mouse whole genome microarray data. (A) Microarray heat map represent 1000 gene expression clusters in two WT mice and two *Lck*-Gli2ΔC2 mice. Expression values from low, middle and high indicated by colors; blue, green, and yellow respectively. **(B)** Fold change data analysis of mouse whole genome expression performed for 2 *Lck*-Gli2ΔC2 and 2 WT mice. Fold change represent clusters of gene expressions higher or lower in *Lck*-Gli2ΔC2 compared to WT. The middle cluster of gene expressions, represent a similar expression of genes in both sets.

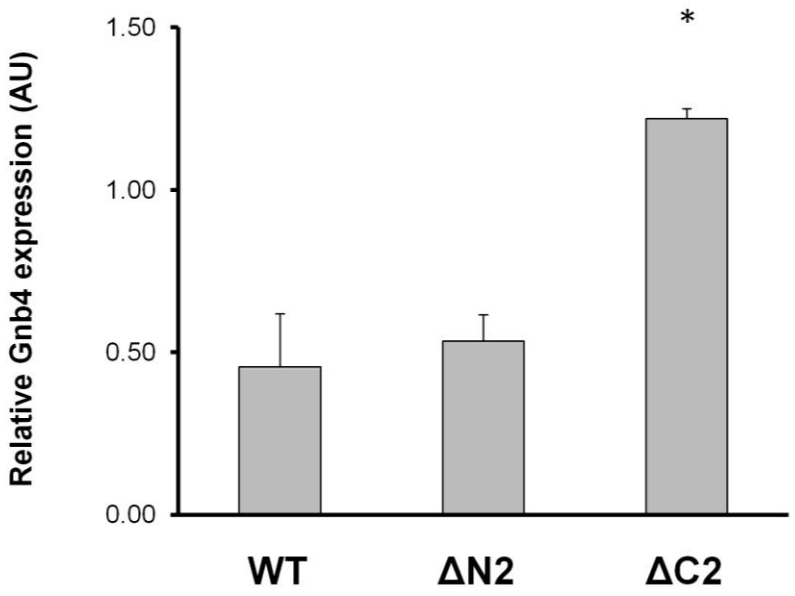

Figure 3.21

Gnb4 expression. Relative mean expression of Gnb4 in DP thymocytes from *Lck*-Gli2 ΔN2, *Lck*-Gli2ΔC2, and WT mice. **GBS-GFP/Gli2ΔC2 expression;** (p= 0.04, n=3). *represents p≤0.05.

3.3 Discussion

Our data revealed that both, intrinsic inhibition and activation of Hh signalling in thymocytes altered the proportions of SP4 cells that express GFP, suggesting a regulatory role of Gli in SP4 thymocytes. Hh signalling promotes target gene transcription through the activation of glioblastoma-associated Gli family of transcription factors, Gli1, Gli2 and Gli3. Both Gli1 and Gli2 are transcription activators dependent on Hh signalling, however, Gli3 functions as a transcriptional regulator independent of Hh signalling (Wang et al. 2000; Pan et al. 2006; Bai et al. 2002). Gli3 has been previously shown to control thymocyte negative selection and TCR signal strength through Hh-dependent and independent mechanisms, moreover, it has been shown that defective Gli3 expression resulted in an inappropriate production of MHC class I-selected CD4 cells (Hager-Theodorides et al. 2009). This is consistent with our finding as the proportions of SP4 cells expressing GFP were increased in both Hh-suppressed and Hh-activated mouse models. Moreover, CD3 expression was reduced in SP cells when Hh-signalling was active and increased when Hh-signalling was inhibited, indicating a regulatory role of Hh in TCR signal transduction through the expression of CD3 molecule.

We have undertaken further characterization of SP4 cells through examining the expression of the master regulator of Treg lineage, Foxp3. Our data have shown that Hh-signalling influences the phenotype of SP4 cells in the thymus and spleen. In contrast, suppression of Hh-signalling in T cells reduced the expression of Foxp3 in SP4 cells suggesting a Hh-dependent regulatory role on these cells.

We investigated Hh-signalling and gene expressions by microarray analysis and our data have shown that Hh-signalling is attenuating gene transcription of various genes that may have a direct effect on T cell development and selection within the thymus. Several genes were found to be differentially expressed in DP thymocytes from mouse model where the physiological Hh-signalling is suppressed. Such a differential expression pattern of these genes in developing thymocytes led us to ask if they play a role in T cell development and maturation within the thymus and the role of Hh signalling in their expression and regulation.

Our data have shown that the expression of Gli2 (glioma-asssociated oncogene-2), was upregulted when Hh-signalling was suppressed by at least 2-folds compared to WT. This increase is probably due to the very design of these mice model, where it expresses a truncated form of Gli2 which acts as a repressor of Hh-dependent transcription, so the microarray is picking up the transgenic transcript.

Our microarray data analysis revealed that Gnb4 (Heterotrimeric Guanine nucleotide binding protein β-4 subunit) was upregulated by 2.6 folds when Hh-signalling was suppressed compared to WT and its expression was validated using qRT-PCR. Gnb4 play a key role in the signal transduction from membrane receptors to intracellular receptors. Activated G-protein coupled receptors result in the activation of many signal transduction cascades via the α-subunit and βγ-dimmers. The effect of βγ -mediated signalling involve the regulation of cell growth and proliferation via Ras activation and it has been found that genetic variations in genes encoding G-protein subunit β4 have been associated with cancer (Riemann et al. 2009; Schwindinger & Robishaw 2001).

Our microarray data also showed an increase in the expression of Ccl-19 (chemokine ligand-19) when Hh is suppressed by at least 2 folds compared to WT. Ccl-19 plays a role in lymphocyte recirculation and homing. It involves in T cell trafficking in the thymus and migration to lymphoid organs. It is possible that Hh-signalling play a role in regulating the expression of Ccl-19 for thymocytes during their development and selection as they constantly travel along the different compartments of the thymus.

3.4 Conclusion

Our data revealed that both, intrinsic inhibition and activation of Hh signalling in thymocytes altered the proportions of SP4 cells that express GFP. Moreover, CD3 expression was reduced in SP cells when Hh-signalling was active and increased when Hh-signalling was inhibited, indicating a regulatory role of Hh in TCR signal transduction through the expression of CD3 molecule. Further characterization of SP4 cells through detecting the expression of the Foxp3 show that Hh-signalling influences the phenotype of SP4 cells in both, the thymus and spleen.

Furthermore, our data have shown that Hh-signalling is attenuating gene transcription of various genes that may have a direct effect on T cell development and selection within the thymus. Such a differential expression pattern of these genes in developing thymocytes suggest a role of Hh signalling directly to T cells during the development and maturation within the thymus.

Chapter 4

Chapter Four: Role of Dhh in T cell development

4.1 Introduction

4.1.1 Dhh in T cell development

The role of Dhh in T cell development and maturation is as yet unexplored. Dhh has been shown to be produced by thymic epithelial cells distributed throughout the thymus indicating a possible role of Dhh in thymocyte development and differentiation (Sacedón et al. 2003). It has been found that thymocytes do not express Dhh, however, their development in the thymus requires a direct interaction with thymic epithelial cells which is essential for their development and maturation (Sacedón et al. 2003).

T cell activation, clonal expansion and peripheral maintenance of tolerance take place in the peripheral lymphoid organs, including the spleen and lymph nodes. Dhh is known to be expressed by stromal tissues in these organs, specifically in the spleen, indicating a possible role of Dhh in peripheral T cell differentiation and maturation (Perry et al. 2009; Lau et al. 2012). Furthermore, as T cell progenitors are liver-derived during embryogenesis and bone marrow-derived postnatally and in adults, it is possible that Dhh may also play a role in signalling to early T cell progenitors, since Dhh is expressed in foetal liver and adult bone marrow (Lau et al. 2012).

4.1.2 Chapter objectives

The purpose of this chapter is to understand the role of Dhh in T cell development in the thymus and its function in the periphery. Studying the functions of Dhh in the Dhh-knockout thymus makes it possible to detect differences in differentiation and transition from one developmental stage to the next. T cell functions in the periphery are also investigated through in-vitro induced activation to assess the role of Dhh in T cell differentiation activation and expansion.

To investigate the role of physiological Dhh signalling on T cell development, I have generated Dhh-KO and Dhh-WT mice from crossing $Dhh^{+/-}$ male and female mice. A direct observation of T cell populations in the thymus, spleen and lymph node will reveal whether or not Dhh is signalling positively or negatively to T cells during their development and maturation.

4.2 Results

4.2.1 Genotyping Dhh littermates

Three genotypes of mice were utilized, the first is wild type (WT) bearing the normal complete Dhh gene. The second is a knockout (Dhh-KO) where the expression of Dhh is completely lost through a mutated gene on both alleles. The third is heterozygous (Dhh-Het) with partial expression of Dhh (one normal allele and one mutated allele). Dhh-KO and Dhh-WT mice were generated from crossing Dhh-Heterozygous male and female mice.

The genotypes of Dhh mice cannot be distinguished visually as Dhh-KO and Dhh-Het mice appear similar to WT. Each littermate was genotyped for both Dhh-WT and Dhh mutant alleles. PCR analysis using genomic DNA from ear biopsies was performed in order to identify the genotype of Dhh littermates. PCR analysis of the three littermates was performed using two sets of primers specific for Dhh-WT and mutant alleles. According to this strategy, WT allele should generate a PCR product of 442bp, while mutant alleles should generate a PCR product of 110bp.

Dhh mutants were identified according to the PCR results. Mice with a PCR product positive for the WT gene and negative for the mutant gene were genotyped as (+/+). Mice with a PCR product negative for WT gene and positive for the mutant gene were genotyped as (−/−). Mice with a PCR product positive for both WT and mutant genes were genotyped as (+/−) (Figure 4.1).

4.2.2 Differences in organ size of Dhh KO and Heterozygous

Thymus and spleen of Dhh-WT, KO and Het were compared following anatomical dissection in order to assess their differences and similarities. All observations were carried out on Dhh littermates. Size comparison was carried out by visual comparison and measuring the horizontal width and vertical length of extracted organs. Thymus extracted from Dhh-KO appeared larger in size compared to both Dhh-WT and Dhh-Het. Thymus extracted from Dhh-Het was also larger than thymus extracted from Dhh-WT but smaller than Dhh-KO (Figure 4.2). The spleen of Dhh-KO was larger compared to Dhh-WT but smaller than Dhh-Het. Surprisingly, the spleen of Dhh-Het appeared larger than both Dhh-WT and Dhh-KO (Figure 4.2).

4.2.3 Thymocytes and splenocytes in Dhh littermates

Following anatomical extraction of the thymus and spleen from Dhh littermates, the thymocytes were collected for analysis. Live cell counts in the thymus was significantly increased in Dhh-KO by at least 6% compared to Dhh-WT ($p \leq 0.05$, n=6), whereas there was no significant difference between Het and WT. Thus, we found that Dhh influences thymocyte numbers (Figure 4.3).

Similarly in the spleen, our data have shown that Dhh also regulates splenocyte numbers (Lau et al. 2012). We observed a significant increase in live splenocyte counts in Dhh-KO of at least 5% compared to Dhh-WT ($p \leq 0.05$, n=6). In Dhh-Het we observed a significant increase of at least 7% compared to Dhh-WT ($p \leq 0.05$, n=6) (Figure 4.3).

4.2.4 Role of Dhh during the early stages of thymocyte development

In order to assess the role of Dhh during the early stages of thymocyte development and differentiation, thymocytes from Dhh-WT, Het and KO were analyzed for CD44 and CD25 and sub-grouped according to their expression into the four main DN populations, the $CD44^{+}CD25^{-}$ (DN1), $CD44^{+}CD25^{+}$ (DN2), $CD44^{-}CD25^{+}$ (DN3) and $CD44^{-}CD25^{-}$ (DN4).

We observed differences in the proportion of DN1, DN3 and DN4 cells indicating a possible role of Dhh in accelerating the transition of immature thymocytes from DN1 through DN3 stage, and eventually arresting cells at the DN4 stage. Surprisingly, Dhh-Het seems to display a different phenotype compared to Dhh-WT. Our data show that the percentage of DN1 cells in Dhh-KO was significantly lower than in the Dhh-WT ($p \leq 0.05$, n=6), and significantly lower than in the Dhh-Het ($p \leq 0.005$, n=6). The percentage of DN3 cells in the Dhh-KO, was significantly lower than in the Dhh-Het ($p \leq 0.05$, n=6). The percentage of DN4 cells in the Dhh-KO was significantly higher than in the Dhh-Het ($p \leq 0.05$, n=6) (Figure 4.4).

These data indicate that Dhh influences the homeostasis and differentiation of DN subsets in a dose-dependent manner. The observation that Dhh and $Dhh^{+/-}$ show opposing phenotype is consistent with Dhh's function as a morphogen, and has previously been observed in the Ihh-mutant thymus (Outram et al. 2009).

4.2.5 Role of Dhh in thymocyte development

In order to assess the role of Dhh in later stages of thymocyte development and differentiation, thymocytes from Dhh-WT, Het and KO were analyzed for CD4 and CD8 cell surface expression and sub-grouped according to their expression into four main populations, the $CD8^{-}CD4^{-}$ (DN), $CD8^{+}CD4^{+}$ (DP), $CD8^{+}CD4^{-}$ (SP8) and $CD8^{-}CD4^{+}$ (SP4). Our data have shown that Dhh negatively regulate DP and SP8 populations during their development in the thymus.

The percentage of DP cells in the Dhh-KO thymus was significantly lower compared to the Dhh-WT ($p \leq 0.05$, n=6). The percentage of SP8 cells in Dhh-KO was significantly higher than in the Dhh-WT ($p \leq 0.05$, n=6) (Figure 4.5). The decrease in DP and increase in SP8 cells we observed in Dhh-mutant mice indicated that Dhh negatively regulates the transition from DP to SP8. Additionally, our data have shown no difference in the proportion of DN and SP4 cells between the three genotypes of Dhh mice ($p > 0.05$, n=6) (Figure 4.5).

4.2.6 Influence of Dhh on expression of CD2, CD3 and CD5 in thymocytes

In order to assess the potential role of Dhh in regulating differentiation and TCR signal transduction during thymocyte development, we analyzed the cell surface expression of molecules associated with TCR signalling (CD2, CD3 and CD5) within the DN, DP, SP8 and SP4 cells in Dhh-WT, Het and KO. Furthermore we compared the mean fluorescence intensity (MFI) of staining for these molecules, as high CD5 expression is associated with high TCR signal strength.

We found that Dhh has no influence on the expression of CD2 in thymocytes during their development in the thymus, as we observed no difference in the expression of CD2 or its MFI in thymocytes between the three genotypes of mice ($p>0.05$, n=6) (Figure 4.6).

The influence of Dhh on CD3 expression in thymocytes seems to be restricted to the SP8 cells, as our data have shown that the percentage of DN, DP and SP4 cells expressing CD3 between the three genotypes was not statistically significant ($p>0.05$, n=6). The percentage of SP8 cells expressing CD3 in the Dhh-KO was found significantly lower than in the Dhh-WT ($p\leq0.05$, n=6). In the Dhh-Het, the percentage of SP8 cells expressing CD3 was also significantly lower than in the Dhh-WT ($p\leq0.05$, n=6). The reduced percentage of CD8SP that express high levels of cell surface CD3 is consistent with an increase in the CD8 ISP population. This ISP CD8 population might account for the increase in CD8SP cells observed in (Figure 4.5). To test if this is the case, we gated on CD3 high cells and examined CD4 and CD8 expression. We also observed no difference in CD3 MFI in thymocyte populations between the three genotypes ($p>0.05$, n=6) (Figure 4.7). In addition, we measured the expression of cell surface CD5 and its MFI. Our data showed no difference between the three genotypes of Dhh littermates ($p>0.05$, n=6) (Figure 4.8).

4.2.7 Role of Dhh in thymocyte interactions

In order to assess further the role of Dhh in influencing thymocyte development, thymocytes from Dhh-WT, Het and KO were analyzed for CD69 expression within the DN, DP, SP8 and SP4 cells (Figure 4.9). CD69 correlates with positive

selection (TCR ligation) in DP and SP populations, and is believed to be associated with cell death in the DN population.

Our data indicated that Dhh negatively regulated the expression of CD69 during the DN and SP4 cells. The percentage of DN cells expressing CD69 in the Dhh-KO was significantly higher than in the Dhh-WT ($p \leq 0.05$, n=4). The differences in the percentage of DP and SP8 cells expressing CD69 between the three genotypes of mice were not statistically significant ($p > 0.05$, n=4). The percentage of SP4 cells expressing CD69 in the Dhh-KO was significantly higher compared to the Dhh-WT ($p \leq 0.05$, n=4) (Figure 4.9). The increase in CD69 expression in the DN compartment in the Dhh-KO is consistent with increased cell death, and suggests that like Shh (Shah et al. 2004), Dhh might provide a survival signal to these cells. The decrease in CD69 expression in the CD4SP population in the Dhh-KO is consistent with a reduction in positive selection to this lineage and increase in differentiation to the CD8SP lineage.

Additionally we measured the expression of CD62L on DN cells and found that Dhh negatively regulates CD62L expression in DN cells. We found that the percentage of DN cells expressing CD62L in the Dhh-KO was significantly higher than in the Dhh-WT ($p \leq 0.05$, n=4) (Figure 4.9). Interestingly, CD62L has recently been shown to be regulated by the Hedgehog signalling pathway in CD4+ T cells from the spleen (Furmanski et al 2015).

4.2.8 Role of Dhh in thymocyte maturation

In order to assess the role of Dhh in influencing SP cell maturation and positive selection during thymocyte development, thymocytes from Dhh-WT, Het and KO

were analyzed for Qa2 and HSA expression within the DP, SP8 and SP4 cells. Expression of Qa2 and HSA allows dissection of the SP compartment by maturity: HSA^+ to HSA^+Qa2^+, to $Qa2^+$.

The percentage of Qa2 in DP cells was significantly increased in the Dhh-KO compared to the Dhh-WT ($p \leq 0.05$, n=3), and significantly higher than in the Dhh-Het ($p \leq 0.05$, n=3). The percentage of $Qa2^+HSA^+$ in DP cells was significantly higher in the Dhh-KO compared to the Dhh-WT ($p \leq 0.05$, n=3), and significantly higher than in the Dhh-Het ($p \leq 0.05$, n=3). The percentage of $Qa2^+HSA^+$ in SP8 cells showed the opposite finding to the DP cells, where the percentage of $Qa2^+HSA^+$ in SP8 cells was significantly lower in the Dhh-KO compared to the Dhh-WT, and significantly lower than in the Dhh-Het ($p \leq 0.05$, n=3). The percentage of HSA in SP4 cells was significantly increased in the Dhh-KO compared to the Dhh-WT, indicating that the CD4SP compartment contains more immature cells in the Dhh-KO than in the WT. Interestingly, in the Dhh-Het we also observed a significant increase in the expression of HSA in SP4 cells compared to the Dhh-WT ($p \leq 0.05$, n=3) (Figure 4.10).

4.2.9 Role of Dhh in spleen T cells

In order to assess the influence of Dhh on spleen T cells in the periphery, splenocytes from Dhh-WT, Het and KO were analyzed for CD4 and CD8 cell surface expression and sub-grouped according to their expression into three main populations, the $CD8^-CD4^-$ (DN), $CD8^+CD4^-$ (SP8) and $CD8^-CD4^+$ (SP4).

Our data show that Dhh regulates SP8 splenocytes, as the percentage of SP8 cells was significantly increased in the Dhh-KO compared to both the Dhh-WT and the

Dhh-Het (($p \leq 0.05$, n=5), ($p \leq 0.005$, n=5)) respectively. In the Dhh-Het we observed no significant difference compared to the Dhh-WT ($p > 0.05$, n=5). As for the DN and SP4 cells, Dhh seemed to have no significant influence between the three genotypes of Dhh littermates (Figure 4.11). The influence of Dhh-deficiency on the $CD8^+$ T cell population in the spleen is consistent with its effect in the thymus.

4.2.10 Influence of Dhh on expression of CD2, CD5 and CD3 in splenocytes

In order to assess the potential influence of Dhh on TCR signal transduction in the periphery, splenocytes from Dhh-WT, Het and KO were analyzed for CD2, CD3, and CD5 expression within the $CD4^-CD8^-$, SP8 and SP4 cells. Furthermore, we calculated the mean fluorescence intensity (MFI) for each of these molecules to estimate TCR signal strength.

Our data show that Dhh has no influence on the expression of CD2 in splenocytes between the three genotypes of Dhh littermates. Similarly, we observed no significant difference in CD2 MFI in splenocytes between the three genotypes of mice (Figure 4.12). We also found that Dhh has no influence on the expression of CD3 in splenocytes, as our data did not show a significant difference between the three genotypes of Dhh littermates. Similarly, our data show no significant difference in CD3 MFI between the three genotypes of mice (Figure 4.13). In addition, our data have shown that Dhh has no influence on the expression of CD5 in splenocytes as we observed no significant difference between the three genotypes of mice. Our data from CD5 MFI also showed no significant difference between the three genotypes of Dhh mice (Figure 4.14).

4.2.11 Further characterization of splenocyte population

In order to assess further the role of Dhh in influencing T cells in the spleen, splenocytes from Dhh-WT, Het and KO were analyzed for CD69 and CD62L expression within the SP8 and SP4 cells. CD69 is an early activation marker, whereas CD62L cell surface expression is late on activation of naïve T cells.

Our data showed that Dhh influenced the expression of CD69 in SP4 splenocytes as we observed a significant decrease in the percentage of CD69 in Dhh-Het compared to Dhh-WT, and Dhh-KO (($p \leq 0.05$, n=4), ($p \leq 0.05$, n=4)) respectively (Figure 4.15). Additionally, we examined the expression of CD62L in splenocytes and our data showed that Dhh regulates its cell surface expression in SP4 cells. Our analysis showed that the percentage of CD62L in SP4 cells was significantly reduced in the Dhh-Het compared to the Dhh-WT ($p \leq 0.05$, n=4) (Figure 4.15). The reduction in cell surface CD62L expression in the Dhh-Het suggested that fewer cells were naïve in those mice.

4.2.12 Influence of Dhh on lymph node T cells

In order to assess the influence of Dhh on T cells in the lymph node, cells from Dhh-WT, Het and KO were analyzed for CD4 and CD8 cell surface expression and sub-grouped according to their expression into three main populations, the $CD8^{-}CD4^{-}$ (DN), $CD8^{+}CD4^{-}$ (SP8) and $CD8^{-}CD4^{+}$ (SP4).

Our data have shown that Dhh influences T cells in the spleen. However, its regulation of SP4 cells in the lymph node is interesting as the difference we observed was between the Dhh-KO and Dhh-Het, suggesting a dual role of Dhh

on T cells in the lymph node. Our analysis show that the percentage of SP4 cells was significantly increased in the Dhh-KO compared to the Dhh-Het ($p \leq 0.05$, n=4). In regards to SP8 cells, we observed no difference between the three genotypes of Dhh littermates ($p > 0.05$, n=4) (Figure 4.16).

4.2.13 Influence of Dhh on expression of CD2, CD5 and CD3 in lymph node T cells

In order to assess the potential influence of Dhh on TCR signal transduction in the lymph node, cells from Dhh WT, Het and KO were analyzed for CD2, CD3, and CD5 expression within the $CD4^{-}CD8^{-}$, SP8 and SP4 cells. Furthermore, we have calculated the mean fluorescence intensity (MFI) for each of these molecules as intensity of CD5 staining correlates with TCR signal strength.

Our data showed that Dhh regulates CD2 expression on SP8 cells, as our analysis show that the percentage SP8 cells expressing CD2 is significantly higher in the Dhh-KO compared to the Dhh-WT ($p \leq 0.05$, n=3), and higher compared to the Dhh-Het, but this increase was not significant ($p > 0.05$, n=3). In the Dhh-Het, the percentage of SP8 cells expressing CD2 was higher compared to the Dhh-WT, but this difference was not significant ($p > 0.05$, n=3). Additionally the percentage of CD2 in $CD4^{-}CD8^{-}$ and SP4 cells was not different between the three genotypes of Dhh mice ($p > 0.05$, n=3). Similarly, CD2 MFI was not different between the three genotypes of Dhh mice ($p > 0.05$, n=3) (Figure 4.17).

In addition, we examined CD3 percentage in T cells in the lymph node, and our data show that Dhh has no influence on its expression. Our analysis show no difference in the expression of CD3 in T cells between the three genotypes of

mice ($p>0.05$, n=4). Similarly CD3 MFI was not different between the three Dhh littermates ($p>0.05$, n=4) (Figure 4.18).

Furthermore, our data show that Dhh has no influence on the expression of CD5 as well, as our analysis show no difference in the percentage of CD5 in T cells between the three genotypes of Dhh mice ($p>0.05$, n=4). Similarly, CD5 MFI was not different between the three genotypes of Dhh littermates ($p>0.05$, n=4) (Figure 4.19).

4.2.14 Influence of Dhh on the phenotype of lymph node SP8 and SP4 cells

In order to assess further the role of Dhh on phenotype of lymph node T cells, cells from Dhh-WT, Het and KO were analyzed for CD69 and CD62L expression within the SP8 and SP4 cells.

Our data show that Dhh has no influence on the expression of CD69 in T cells, as our analysis show that the percentage of CD69 in T cells between the three genotypes of mice was not different ($p>0.05$, n=3) (Figure 4.20). Similarly, our data also show that Dhh has no influence on the expression of CD62L in T cells, as our analysis show no difference in the percentage of CD62L between the three genotypes of Dhh littermates ($p>0.05$, n=3) (Figure 4.20).

4.2.15 Role of Dhh in T cell activation

In order to assess the role of Dhh in T cell activation, splenocytes from Dhh-WT, Het and KO were stimulated with anti-CD3 and anti-CD28 antibodies with or

without the addition of IL-2 in culture, and analyzed by flow cytometry at 4 hours after treatment for cell surface expression of the early activation marker CD69, and at 18 hours after treatment for the expression of the later activation marker CD25.

We examined the expression of CD69 on activation of SP4 and SP8 cells, and our data show that Dhh influence CD69 expression in activated SP8 and SP4 cells. Our analysis show that the percentage of CD69 in both, SP8 and SP4 cells was significantly higher in the Dhh-KO compared to the Dhh-WT (($p \leq 0.05$, n=3), ($p > 0.005$, n=3)) respectively. Additionally, in the Dhh-Het, the percentage of CD69 in activated SP4 was significantly lower than in the Dhh-KO ($p \leq 0.05$, n=3). With IL2 addition, we observed the same difference as our data show that the percentage CD69 in SP8 and SP4 cells was significantly higher in the Dhh-KO compared to the Dhh-WT (($p \leq 0.05$, n=3), ($p > 0.05$, n=3)) respectively (Figure 4.21).

Additionally, our data show that Dhh regulates the expression of CD25 in activated SP8 and SP4 cells, as our analysis show that the percentage of CD25 in both, SP8 and SP4 cells was significantly higher in the Dhh-KO compared to the Dhh-WT (($p \leq 0.05$, n=3), ($p \leq 0.005$, n=3)) respectively. In the Dhh-Het, the percentage of CD25 in activated SP4 was significantly lower than in the Dhh-KO ($p \leq 0.05$, n=3). With IL2 addition, we observed the same difference as our data show that the percentage CD25 in SP8 cells was significantly higher in the Dhh-KO compared to the Dhh-WT ($p \leq 0.05$, n=3). However, our data did not show difference in the expression of CD25 in activated SP4 cells with IL2 addition between the three genotypes of mice ($p \leq 0.05$, n=3) (Figure 4.21).

4.2.16 Intracellular cytokine staining of splenocytes

In order to assess the role of Dhh in influencing production of cytokines by SP8 and SP4 cells, splenocytes from Dhh-WT, Het and KO were cultured with PMA, ionomycin and bredfeldin-A for 4 hours followed by intracellular staining for IFNγ and IL-2 within the SP8 cells, and for IFNγ, IL-2, IL-4 and IL-17 for SP4 cells.

Our data show that Dhh influenced cytokine production in activated SP8 cells. Interestingly, the difference we observed was in the percentage of IL2 in SP8 cells from Dhh-Het. Our analysis show that the percentage of IL2 was significantly increased in the Dhh-Het compared to Dhh-WT ($p \leq 0.05$, n=3), and was higher compared to Dhh-KO, but this difference was not significant ($p > 0.05$, n=3). In the Dhh-KO, the percentage of IL2 was higher compared to the Dhh-WT, but this difference was not significant ($p > 0.05$, n=3). Additionally, we examined the percentage of IFNγ in activated SP8 cells and our data show no difference in its production in SP8 between the three genotypes of Dhh littermates ($p > 0.05$, n=3) (Figure 4.16).

Furthermore, we examined the production of IL2, IL4, IL17 in activated SP4 cells, and our data show no difference between the three genotypes of Dhh mice ($p > 0.05$, n=3). However, the percentage of $IFN\gamma^+$ in SP4 cells was significantly lower in the Dhh-KO compared to the Dhh-WT ($p \leq 0.05$, n=3). In Dhh-Het, the percentage of IFNγ in SP4 was significantly lower compared to the Dhh-WT ($p \leq 0.05$, n=3) (Figure 4.22).

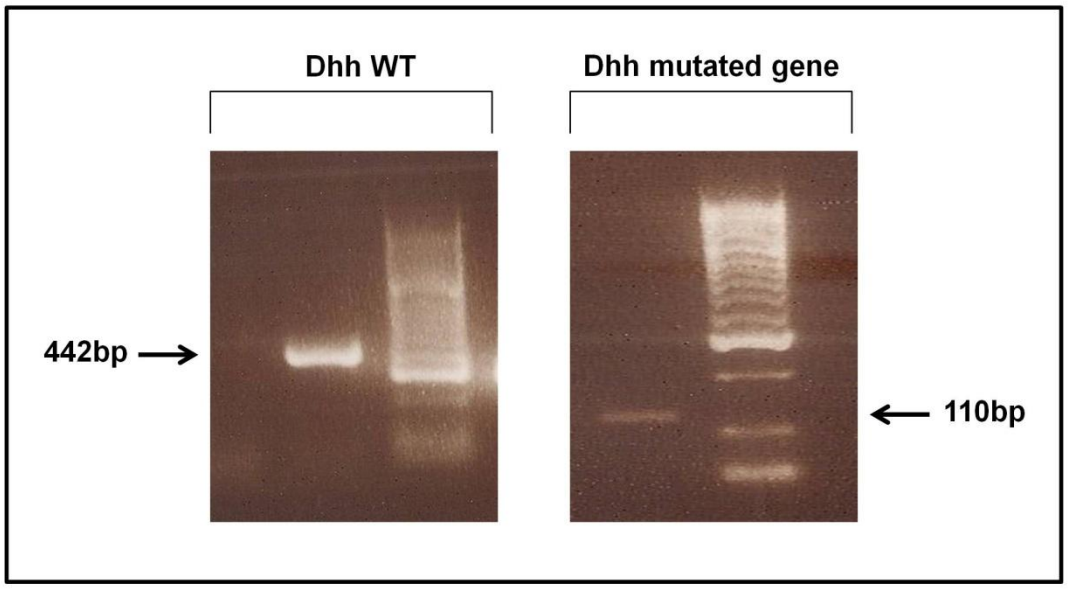

Figure 4.1

Genotyping of Dhh littermates. The genotyping of Dhh littermates by PCR using genomic DNA extracted from ear biopsies. The presence of a wild type (Dhh-WT) allele generated a PCR product of 442bp, while the presence of a mutated allele (Dhh-KO) generated a PCR product of 110bp.

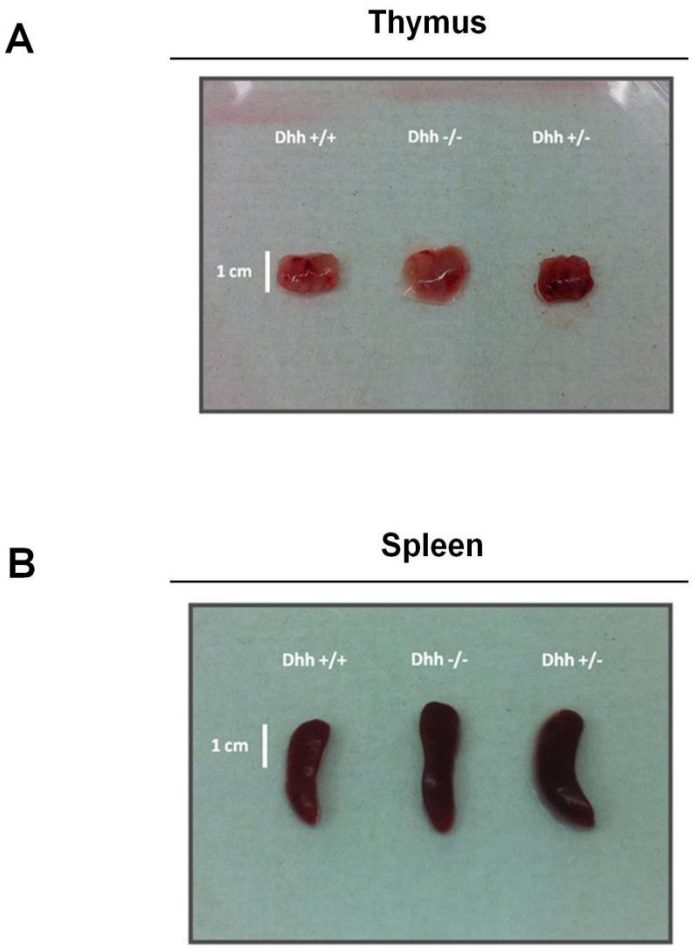

Figure 4.2

Thymus and spleen of Dhh littermates. Freshly isolated **(A)** thymus and **(B)** spleen from 5-weeks old Dhh-WT (left), Dhh-KO (middle) and Dhh-Het (right).

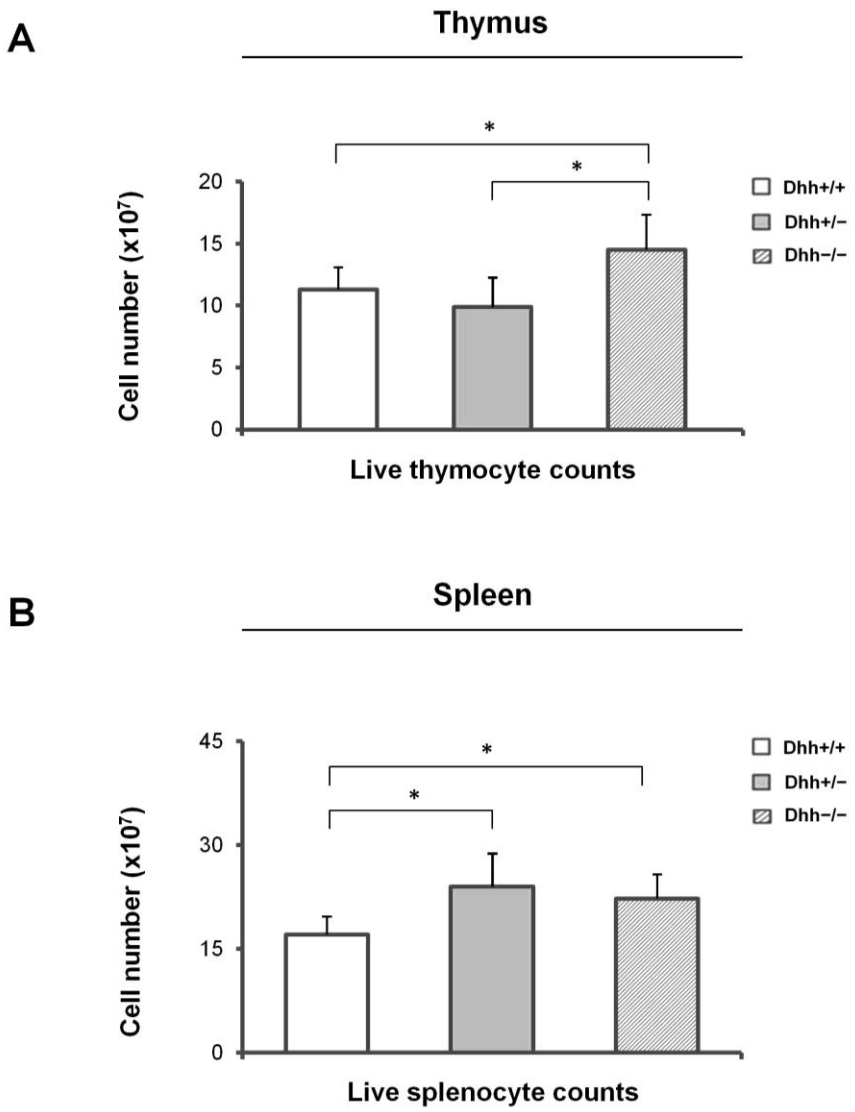

Figure 4.3

Dhh thymus and spleen live cell counts. Thymocyte and splenocyte total counts from adult Dhh-WT, Het and KO littermates. **(A)** Live thymocyte counts. **(B)** Live splenocyte counts. Mean and standard deviation of each population are given. Bars represent mean ± standard deviations. **Thymocytes;** (p=0.06 (WT/Het), 0.04 (WT/KO), 0.01 (Het/KO), n=6). **Splenocytes;** (p=0.01 (WT/Het), 0.02 (WT/KO), 0.2 (Het/KO), n=6). *represents p≤0.05.

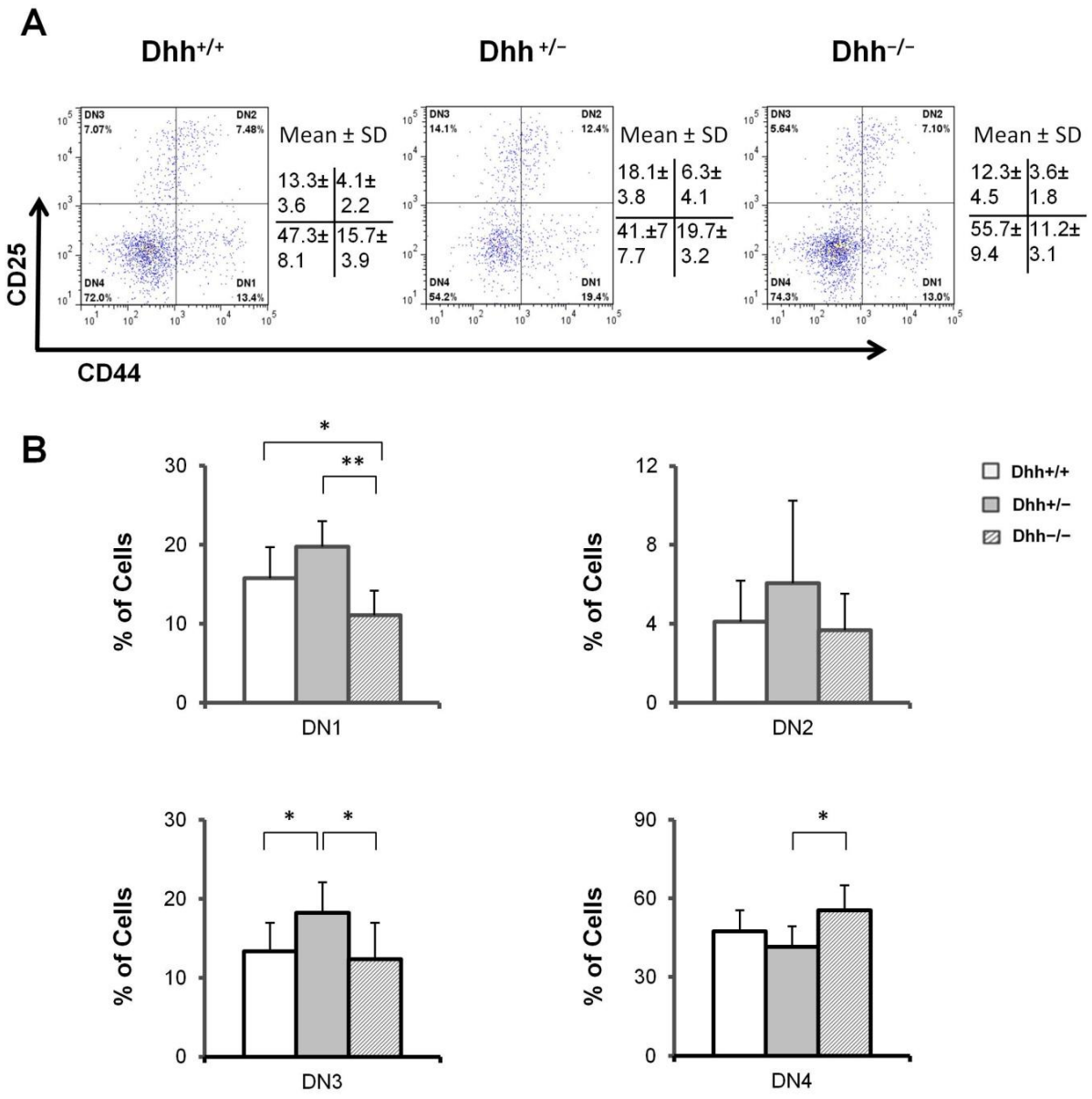

Figure 4.4

Major DN subsets in Dhh littermates. DN thymocyte populations from adult Dhh-WT, Het and KO littermates. Thymocytes were stained for anti-CD44, anti-CD25, anti-CD8, anti-CD4, anti-CD3, anti-B220 and $CD4^+CD8^+CD3^+B220^+$ cells were excluded. Cells were analyzed by flow cytometry. **(A)** Representative dot plot of thymocyte DN populations. **(B)** Representative bar graph of DN1, DN2, DN3 and DN4 percentages. Figures are representative of 6 independent sets of Dhh littermates. Mean and standard deviation of each population are given. Bars represent mean ± standard deviations. **DN1** (p= 0.08 (WT/Het), 0.04 (WT/KO), 0.0007 (Het/KO), n=6). **DN2** (p= 0.3 (WT/Het), 0.7 (WT/KO), 0.2 (Het/KO), n=6). **DN3** (p= 0.04 (WT/Het), 0.6 (WT/KO), 0.03 (Het/KO), n=6). **DN4** (p= 0.2 (WT/Het), 0.1 (WT/KO), 0.01 (Het/KO), n=6). *represents $p \leq 0.05$, **represents $p \leq 0.005$.

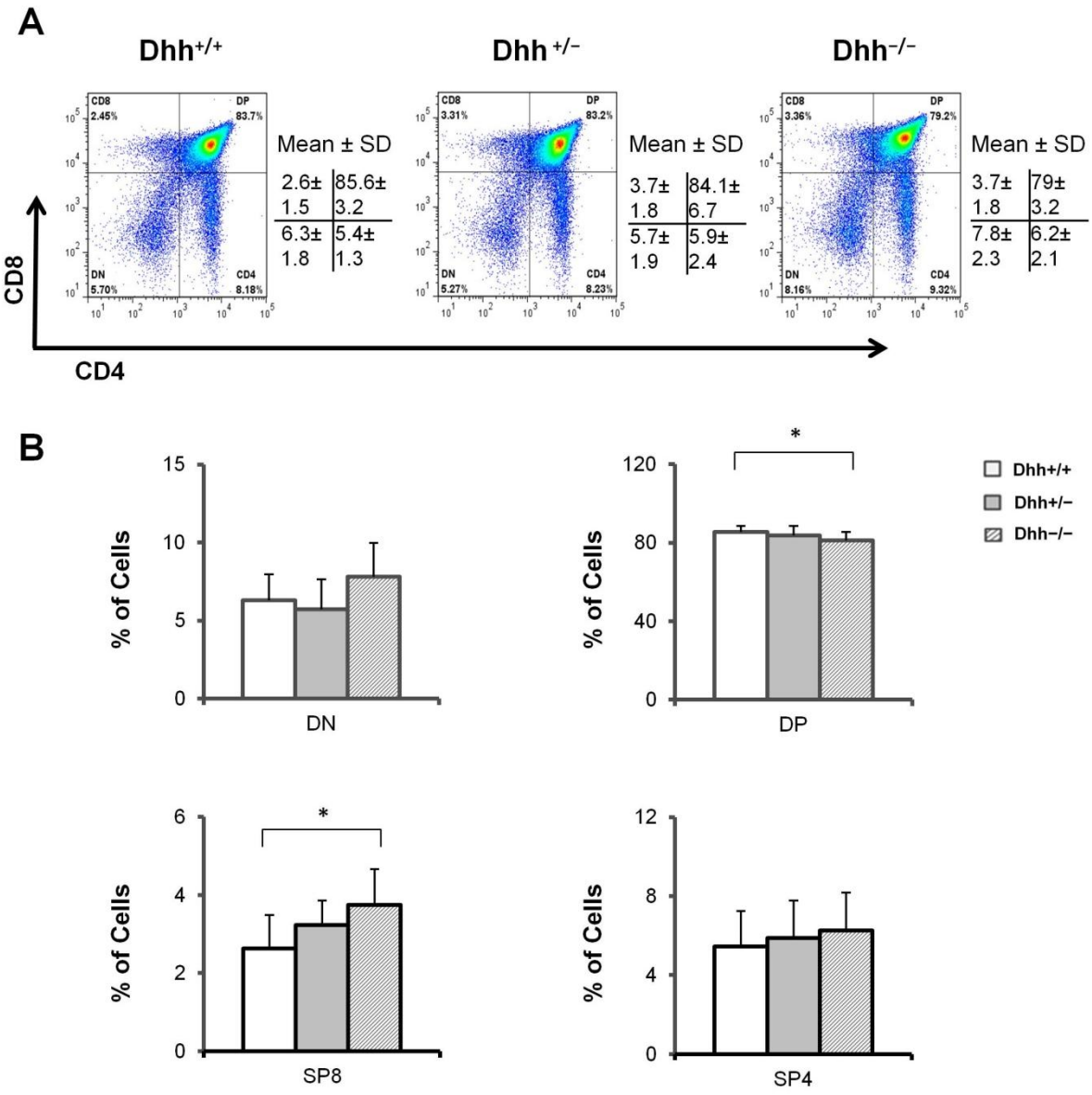

Figure 4.5

Major thymocyte populations in Dhh littermates. Thymocyte populations from adult Dhh-WT, Het and KO littermates. Thymocytes were stained for anti-CD8 and anti-CD4, and analyzed by flow cytometry. **(A)** Representative dot plot of thymocyte populations. **(B)** Representative bar graph of DN, DP, SP8 and SP4 percentages. Figures are representative of 6 independent sets of Dhh littermates. Mean and standard deviation of each population are given. Bars represent mean ± standard deviations. **DN** (p= 0.5 (WT/Het), 0.2 (WT/KO), 0.1 (Het/KO), n=6). **DP** (p= 0.1 (WT/Het), 0.01 (WT/KO), 0.3 (Het/KO), n=6). **SP8** (p= 0.07 (WT/Het), 0.05 (WT/KO), 0.4 (Het/KO), n=6). **SP4** (p= 0.5 (WT/Het), 0.4 (WT/KO), 0.7 (Het/KO), n=6). *represents p≤0.05.

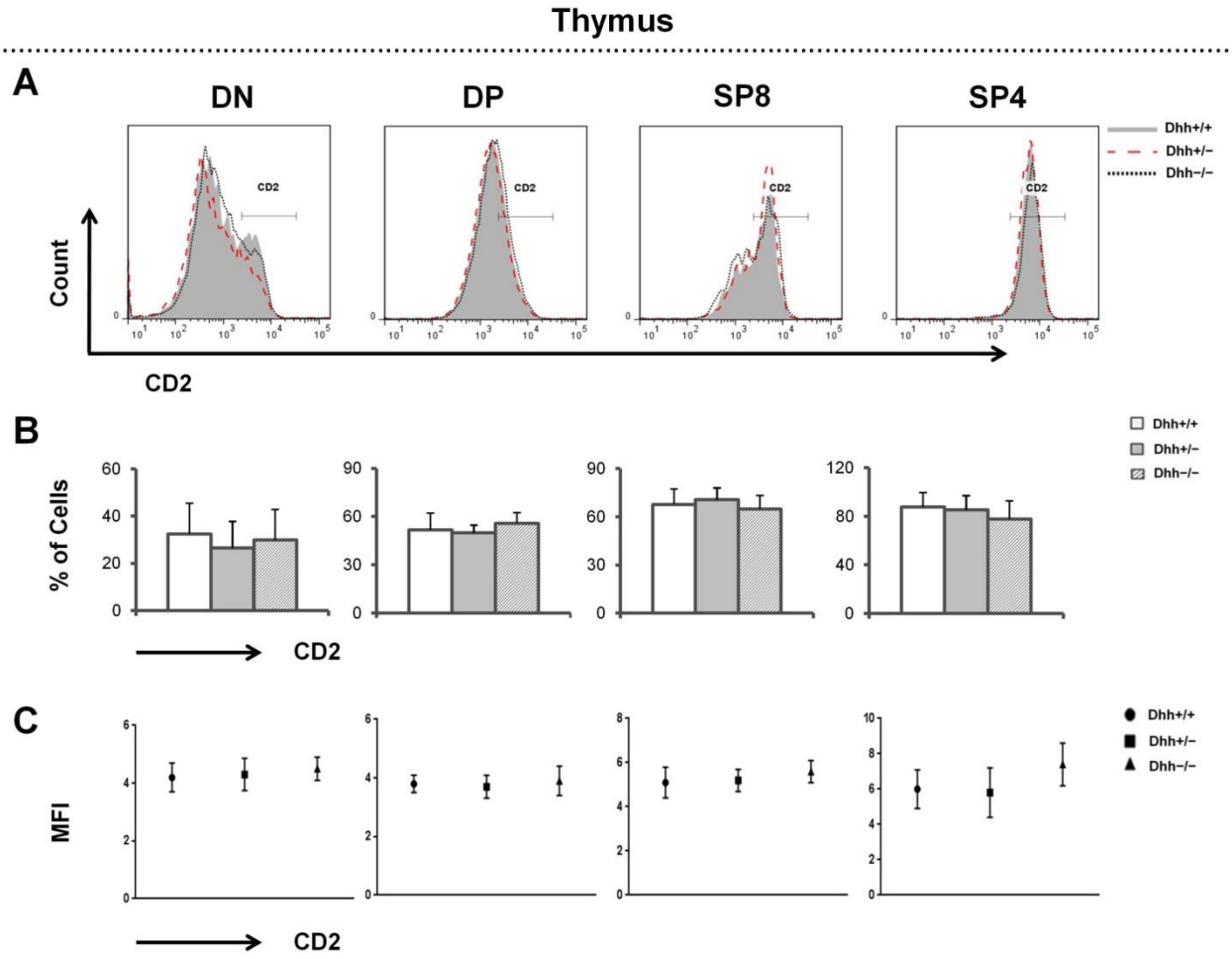

Figure 4.6

Expression of CD2 in Dhh thymocytes. Expression of CD2 in thymocytes from adult Dhh-WT, Het and KO littermates. Thymocytes were stained for anti-CD2, anti-CD8 and anti-CD4, and analyzed by flow cytometry. **(A)** Representative histogram of CD2 expression in DN, DP, SP8 and SP4 cells. **(B)** Representative bar graph of CD2 percentages in DN, DP, SP8 and SP4 cells. **(C)** Representative scatter plot of CD2 MFI in DN, DP, SP8 and SP4 cells. Figures are representative of 6 independent sets of Dhh littermates. Mean and standard deviation of each population are given. Bars represent mean ± standard deviations. **CD2 percentages; DN** (p= 0.4 (WT/Het), 0.6 (WT/KO), 0.7 (Het/KO), n=6). **DP** (p= 0.7 (WT/Het), 0.4 (WT/KO), 0.1 (Het/KO), n=6). **SP8** (p= 0.5 (WT/Het), 0.6 (WT/KO), 0.2 (Het/KO), n=6). **SP4** (p= 0.7 (WT/Het), 0.2 (WT/KO), 0.3 (Het/KO), n=6). **CD2 MFI; DN** (p= 0.07 (WT/Het), 0.08 (WT/KO), 0.06 (Het/KO), n=6). **DP** (p= 0.09 (WT/Het), 0.1 (WT/KO), 0.07 (Het/KO), n=6). **SP8** (p= 0.08 (WT/Het), 0.09 (WT/KO), 0.06 (Het/KO), n=6). **SP4** (p= 0.3 (WT/Het), 0.08 (WT/KO), 0.4 (Het/KO), n=6).

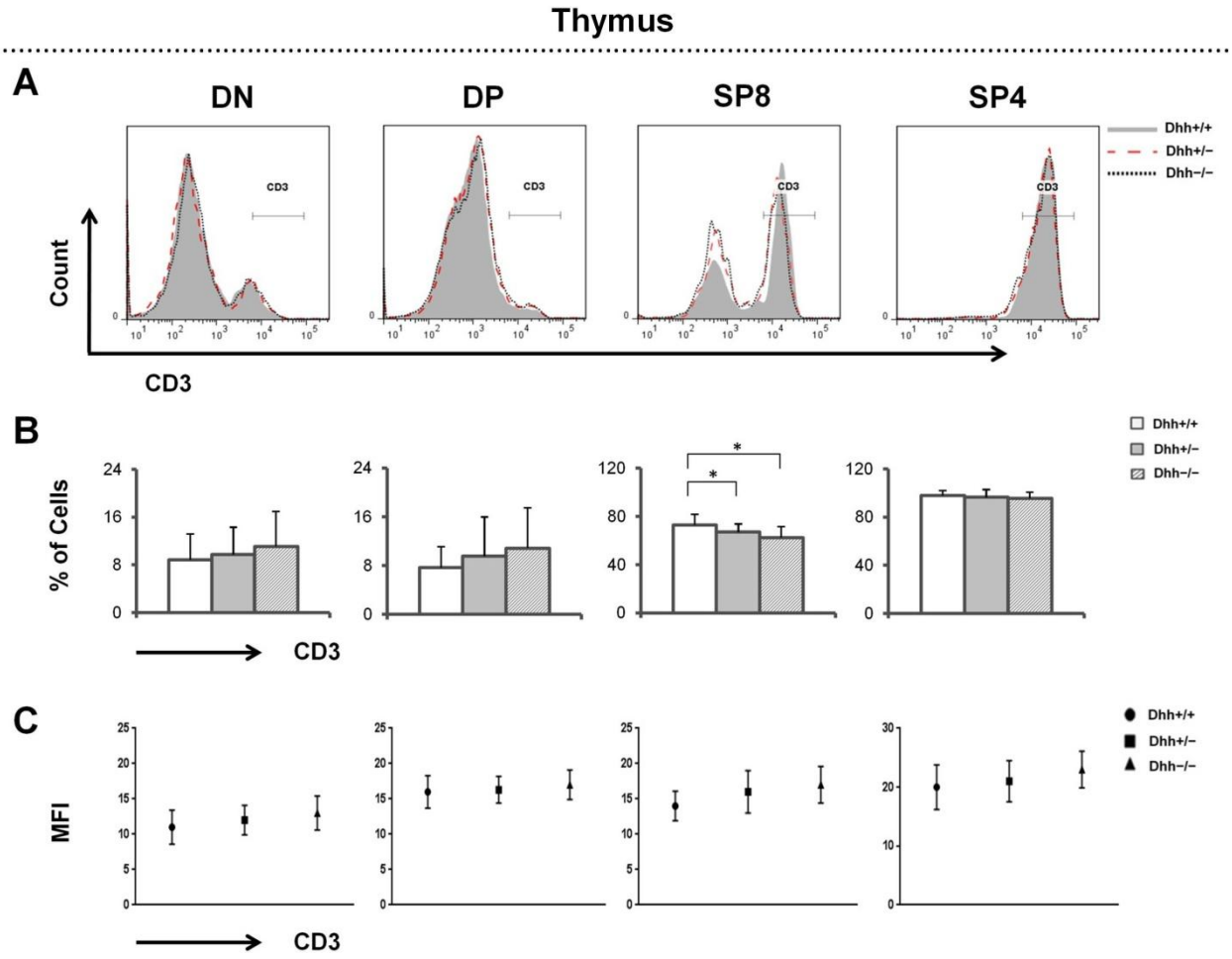

Figure 4.7

Expression of CD3 in Dhh thymocytes. Expression of CD3 in thymocytes from adult Dhh-WT, Het and KO littermates. Thymocytes were stained for anti-CD3, anti-CD8 and anti-CD4, and analyzed by flow cytometry. **(A)** Representative histogram of CD3 expression in DN, DP, SP8 and SP4 cells. **(B)** Representative bar graph of CD3 percentages in DN, DP, SP8 and SP4 cells. **(C)** Representative scatter plot of CD3 MFI in DN, DP, SP8 and SP4 cells. Figures are representative of 6 independent sets of Dhh littermates. Mean and standard deviation of each population are given. Bars represent mean ± standard deviations. **CD3 percentages; DN** (p= 0.7 (WT/Het), 0.4 (WT/KO), 0.6 (Het/KO), n=6). **DP** (p= 0.9 (WT/Het), 0.5 (WT/KO), 0.6 (Het/KO), n=6). **SP8** (p= 0.02 (WT/Het), 0.01 (WT/KO), 0.3 (Het/KO), n=6). **SP4** (p= 0.6 (WT/Het), 0.3 (WT/KO), 0.7 (Het/KO), n=6). **CD3 MFI; DN** (p= 0.9 (WT/Het), 0.08 (WT/KO), 0.3 (Het/KO), n=6). **DP** (p= 0.2 (WT/Het), 0.1 (WT/KO), 0.6 (Het/KO), n=6). **SP8** (p= 0.4 (WT/Het), 0.7 (WT/KO), 0.2 (Het/KO), n=6). **SP4** (p= 0.1 (WT/Het), 0.4 (WT/KO), 0.6 (Het/KO), n=6). *represents $p \leq 0.05$.

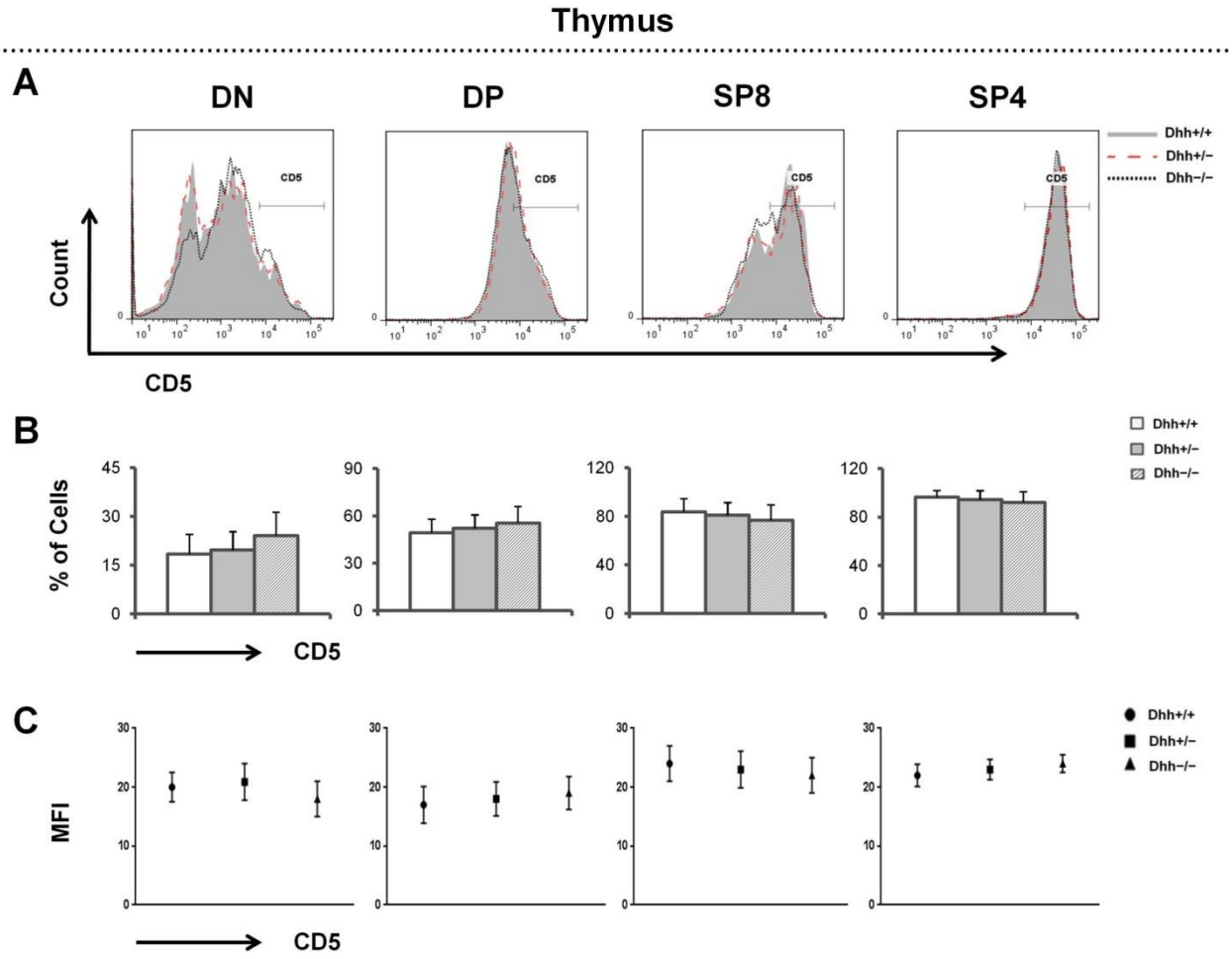

Figure 4.8

Expression of CD5 in Dhh thymocytes. Expression of CD5 in thymocytes from adult Dhh-WT, Het and KO littermates. Thymocytes were stained for anti-CD5, anti-CD8 and anti-CD4, and analyzed by flow cytometry. **(A)** Representative histogram of CD5 expression in DN, DP, SP8 and SP4 cells. **(B)** Representative bar graph of CD5 percentages in DN, DP, SP8 and SP4 cells. **(C)** Representative scatter plot of CD5 MFI in DN, DP, SP8 and SP4 cells. Figures are representative of 6 independent sets of Dhh littermates. Mean and standard deviation of each population are given. Bars represent mean ± standard deviations. **CD5 percentages; DN** (p= 0.6 (WT/Het), 0.1 (WT/KO), 0.2 (Het/KO), n=6). **DP** (p= 0.5 (WT/Het), 0.2 (WT/KO), 0.4 (Het/KO), n=6). **SP8** (p= 0.6 (WT/Het), 0.3 (WT/KO), 0.5 (Het/KO), n=6). **SP4** (p= 0.6 (WT/Het), 0.3 (WT/KO), 0.6 (Het/KO), n=6). **CD5 MFI; DN** (p= 0.06 (WT/Het), 0.8 (WT/KO), 0.9 (Het/KO), n=6). **DP** (p= 0.1 (WT/Het), 0.3 (WT/KO), 0.3 (Het/KO), n=6). **SP8** (p= 0.4 (WT/Het), 0.07 (WT/KO), 0.08 (Het/KO), n=6). **SP4** (p= 0.2 (WT/Het), 0.4 (WT/KO), 0.3 (Het/KO), n=6).

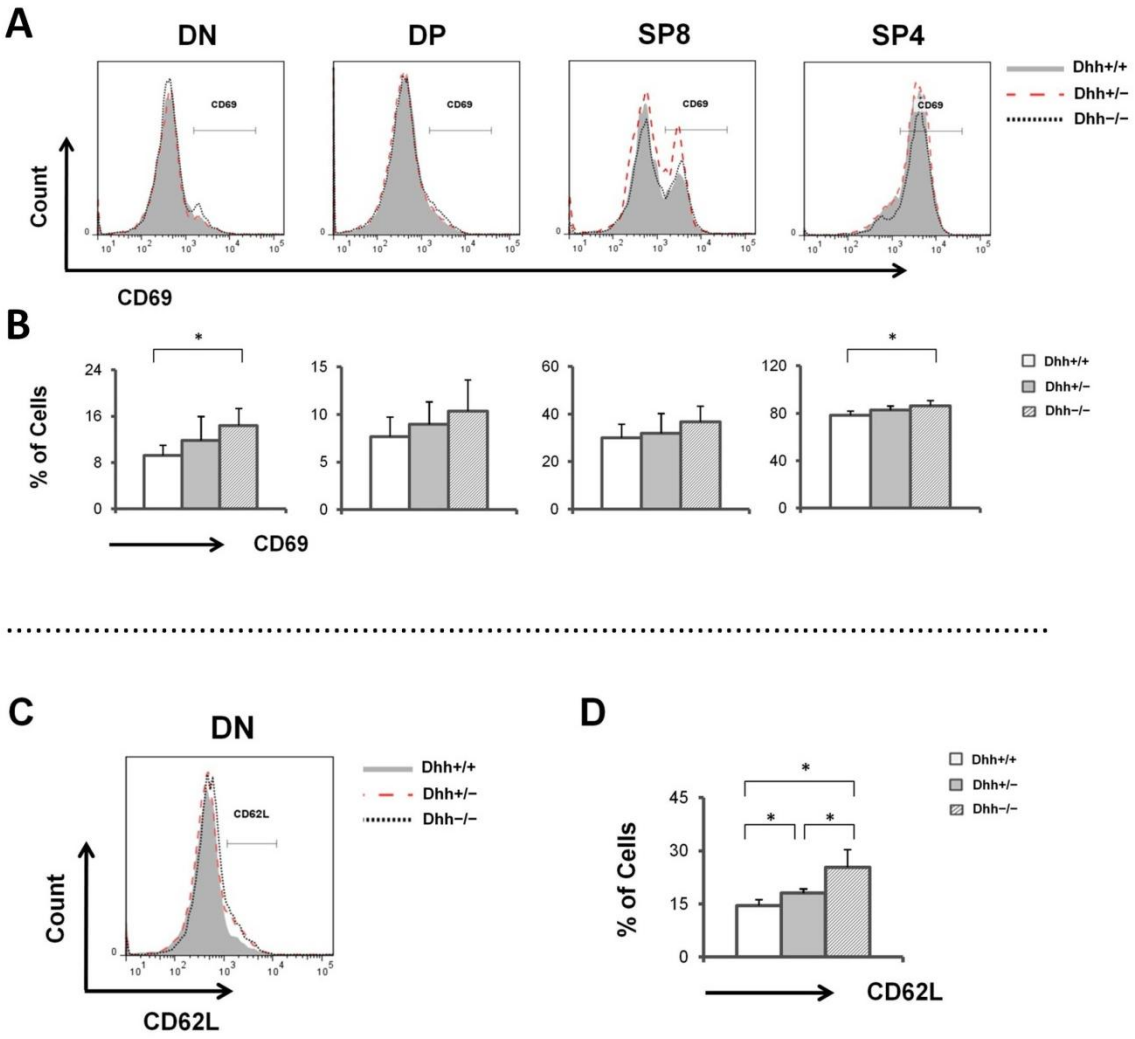

Figure 4.9

Expression of CD69 and CD62L in Dhh thymocytes. Expression of CD69 and CD62L in thymocytes from adult Dhh-WT, Het and KO littermates. Thymocytes were stained for anti-CD69, anti-CD62L, anti-CD8 and anti-CD4, and analyzed by flow cytometry. **(A)** Representative histogram of CD69 expression in DN, DP, SP8 and SP4 cells. **(B)** Representative bar graph of CD69 percentages in DN, DP, SP8 and SP4 cells. **(C)** Representative histogram of CD62L expression in DN cells. **(D)** Representative bar graph of CD62L percentage in DN cells. Figures are representative of 4 and 6 independent sets of Dhh littermates respectively. Mean and standard deviation of each population are given. Bars represent mean ± standard deviations. **CD69 percentages; DN** (p= 0.3 (WT/Het), 0.02 (WT/KO), 0.3 (Het/KO), n=4). **DP** (p= 0.4 (WT/Het), 0.2 (WT/KO), 0.5 (Het/KO), n=4). **SP8** (p= 0.7 (WT/Het), 0.1 (WT/KO), 0.4 (Het/KO), n=6). **SP4** (p= 0.1 (WT/Het), 0.03 (WT/KO), 0.2 (Het/KO), n=6). **CD62L percentage; DN** (p= 0.01 (WT/Het), 0.01 (WT/KO), 0.05 (Het/KO), n=4). *represents $p \leq 0.05$.

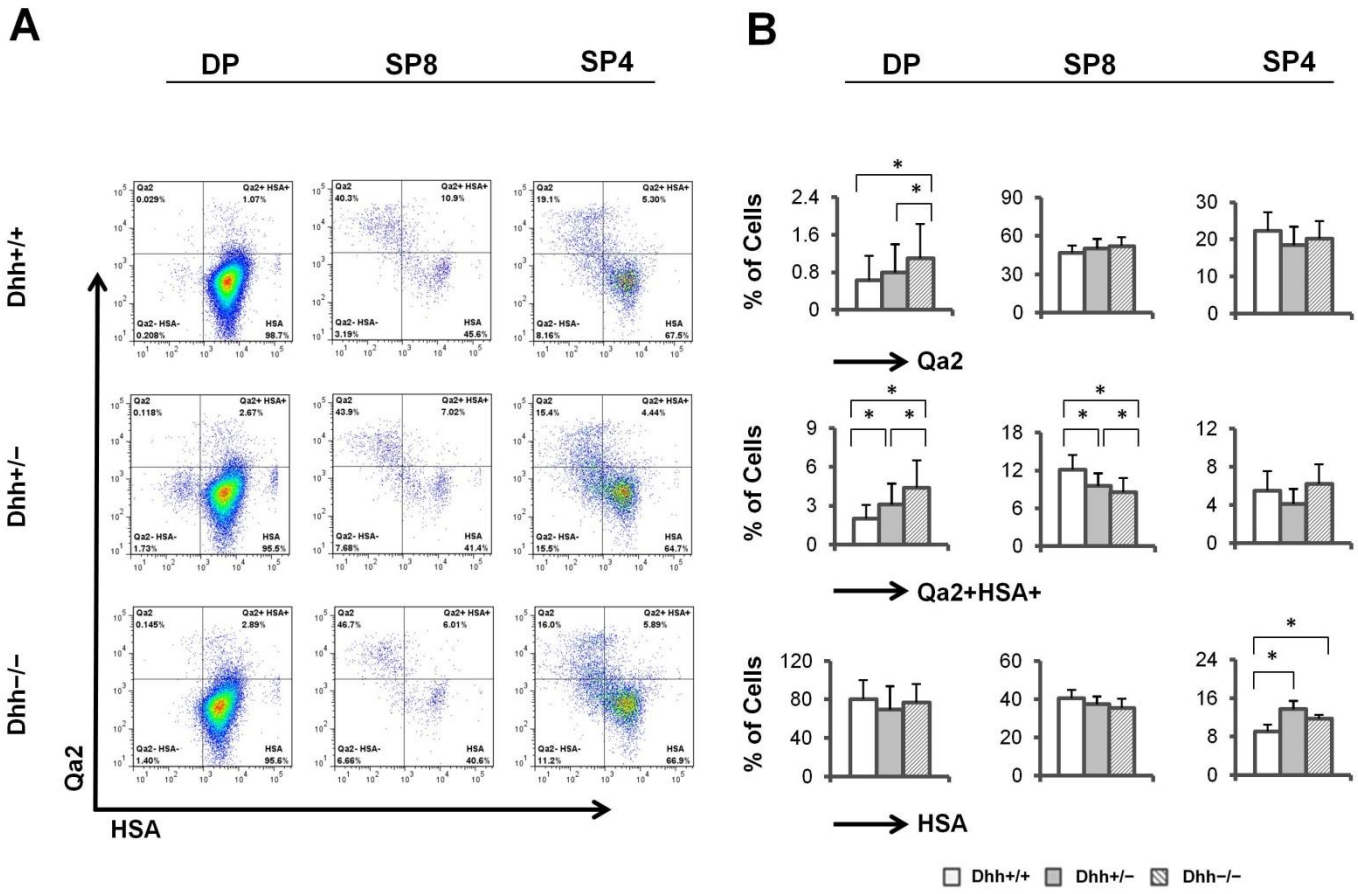

Figure 4.10

Expression of Qa2 and HSA in Dhh thymocytes. Expression of Qa2 and HSA in DP, SP8 and SP4 cells from adult Dhh-WT, Het and KO littermates. Thymocytes were stained for anti-Qa2, anti-CD24, anti-CD8 and anti-CD4, and analyzed by flow cytometry. **(A)** Representative dot plot of Qa2 and HSA expression in DP, SP8 and SP4 cells. **(B)** Representative bar graph of Qa2 and HSA percentages in DP, SP8 and SP4 cells. Figures are representative of 3 independent sets of Dhh littermates. Mean and standard deviation of each population are given. Bars represent mean ± standard deviations. **Qa2 percentages; DP** (p= 0.06 (WT/Het), 0.04 (WT/KO), 0.04 (Het/KO), n=3). **SP8** (p= 0.5 (WT/Het), 0.3 (WT/KO), 0.7 (Het/KO), n=3). **SP4** (p= 0.3 (WT/Het), 0.5 (WT/KO), 0.6 (Het/KO), n=3). **$Qa2^{+}HSA^{+}$ percentages; DP** (p= 0.02 (WT/Het), 0.01 (WT/KO), 0.03 (Het/KO), n=3). **SP8** (p= 0.05 (WT/Het), 0.03 (WT/KO), 0.05 (Het/KO), n=3). **SP4** (p= 0.3 (WT/Het), 0.6 (WT/KO), 0.1 (Het/KO), n=3). **HSA percentages; DP** (p= 0.5 (WT/Het), 0.8 (WT/KO), 0.6 (Het/KO), n=3). **SP8** (p= 0.4 (WT/Het), 0.2 (WT/KO), 0.5 (Het/KO), n=3). **SP4** (p= 0.006 (WT/Het), 0.01 (WT/KO), 0.07 (Het/KO), n=3). *represents $p \leq 0.05$.

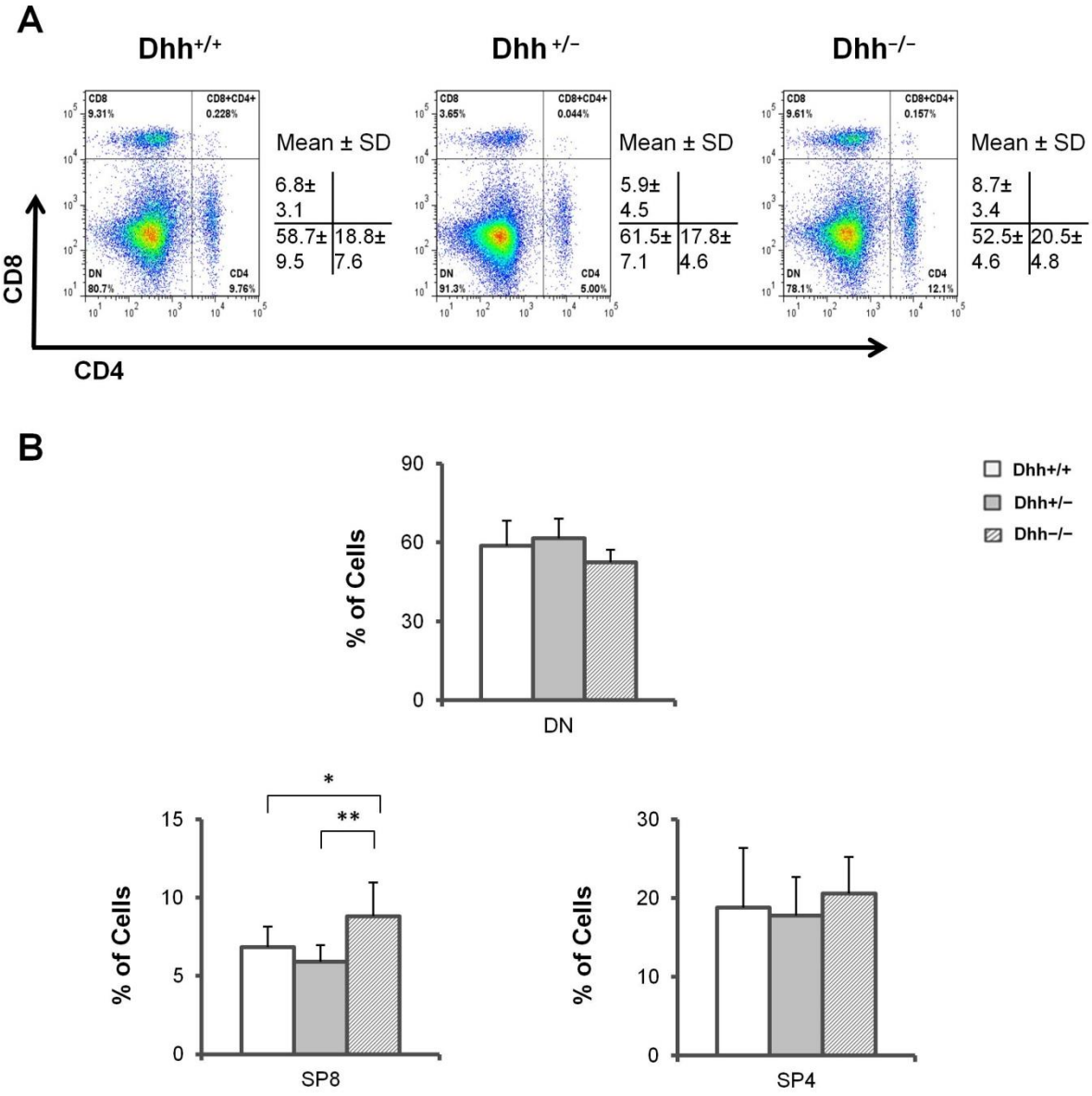

Figure 4.11

Major splenocyte, T cell populations in Dhh littermates. Splenocyte, T cell populations from adult Dhh-WT, Het and KO littermates. Cells were stained for anti-CD8 and anti-CD4, and analyzed by flow cytometry. **(A)** Representative dot plot of splenocyte populations. **(B)** Representative bar graph of $CD4^{-}CD8^{-}$, SP8 and SP4 percentages. Figures are representative of 5 independent sets of Dhh littermates. Mean and standard deviation of each population are given. Bars represent mean ± standard deviations. **$CD4^{-}CD8^{-}$** (p= 0.6 (WT/Het), 0.2 (WT/KO), 0.5 (Het/KO), n=5). **SP8** (p= 0.2 (WT/Het), 0.01 (WT/KO), 0.003 (Het/KO), n=5). **SP4** (p= 0.8 (WT/Het), 0.6 (WT/KO), 0.3 (Het/KO), n=5). *represents $p \leq 0.05$, **represents $p \leq 0.005$.

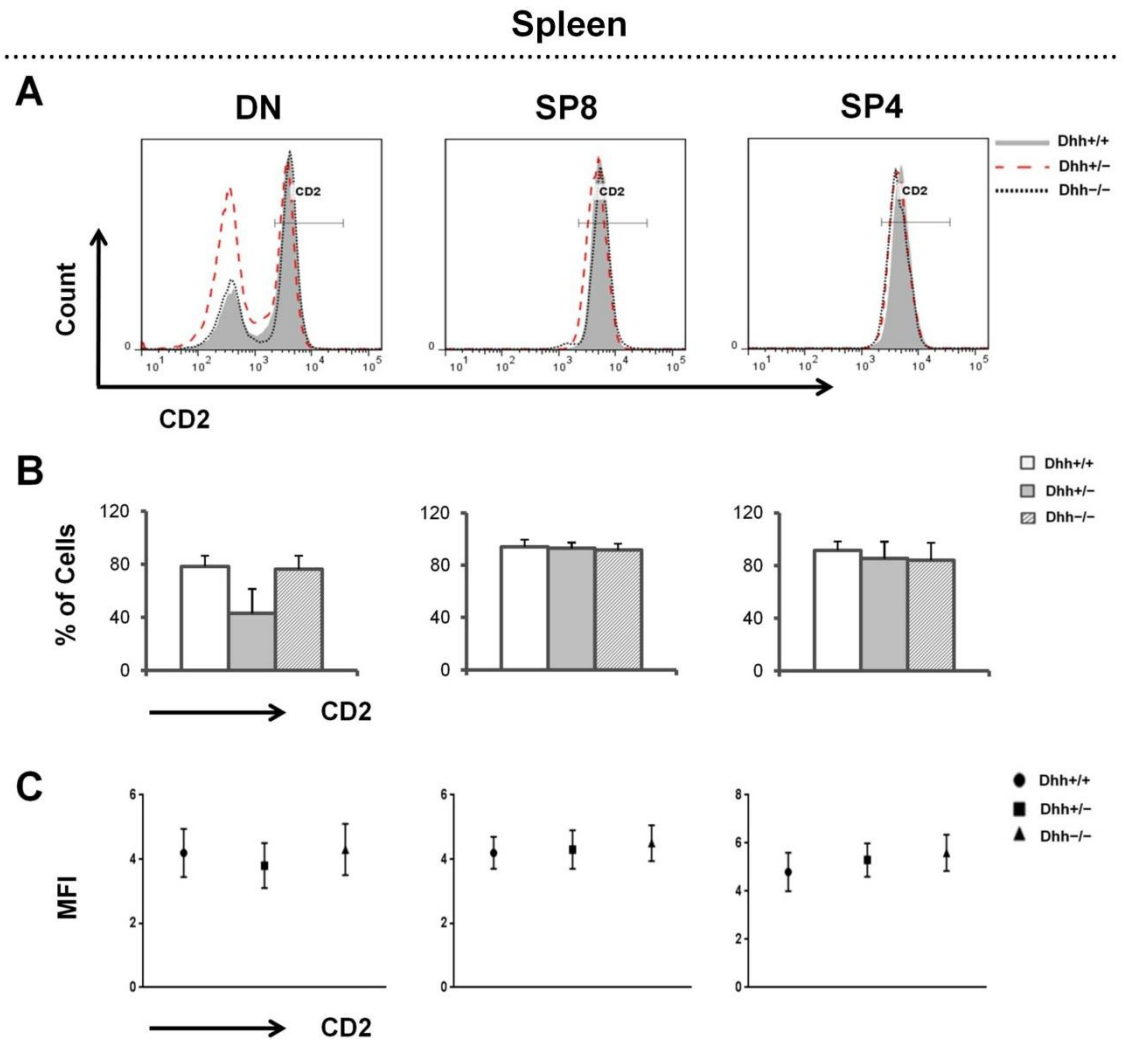

Figure 4.12

Expression of CD2 in Dhh splenocytes. Splenocytes from adult Dhh-WT, Het and KO littermates. Splenocytes were stained for anti-CD2, anti-CD8 and anti-CD4, and analyzed by flow cytometry. **(A)** Representative histogram of CD2 expression in $CD4^{-}CD8^{-}$, SP8 and SP4 cells. **(B)** Representative bar graph of CD2 percentages in $CD4^{-}CD8^{-}$, SP8 and SP4 cells. **(C)** Representative scatter plot of CD2 MFI in $CD4^{-}CD8^{-}$, SP8 and SP4 cells. Figures are representative of 3 independent sets of Dhh littermates. Mean and standard deviation of each population are given. Bars represent mean ± standard deviations. **CD2 percentages; $CD4^{-}CD8^{-}$** (p= 0.06 (WT/Het), 0.7 (WT/KO), 0.06 (Het/KO), n=3). **SP8** (p= 0.7 (WT/Het), 0.5 (WT/KO), 0.6 (Het/KO), n=3). **SP4** (p= 0.5 (WT/Het), 0.4 (WT/KO), 0.9 (Het/KO), n=3). **CD2 MFI; $CD4^{-}CD8^{-}$** (p= 0.7 (WT/Het), 0.6 (WT/KO), 0.4 (Het/KO), n=3). **SP8** (p= 0.5 (WT/Het), 0.7 (WT/KO), 0.8 (Het/KO), n=3). **SP4** (p= 0.5 (WT/Het), 0.6 (WT/KO), 0.9 (Het/KO), n=3).

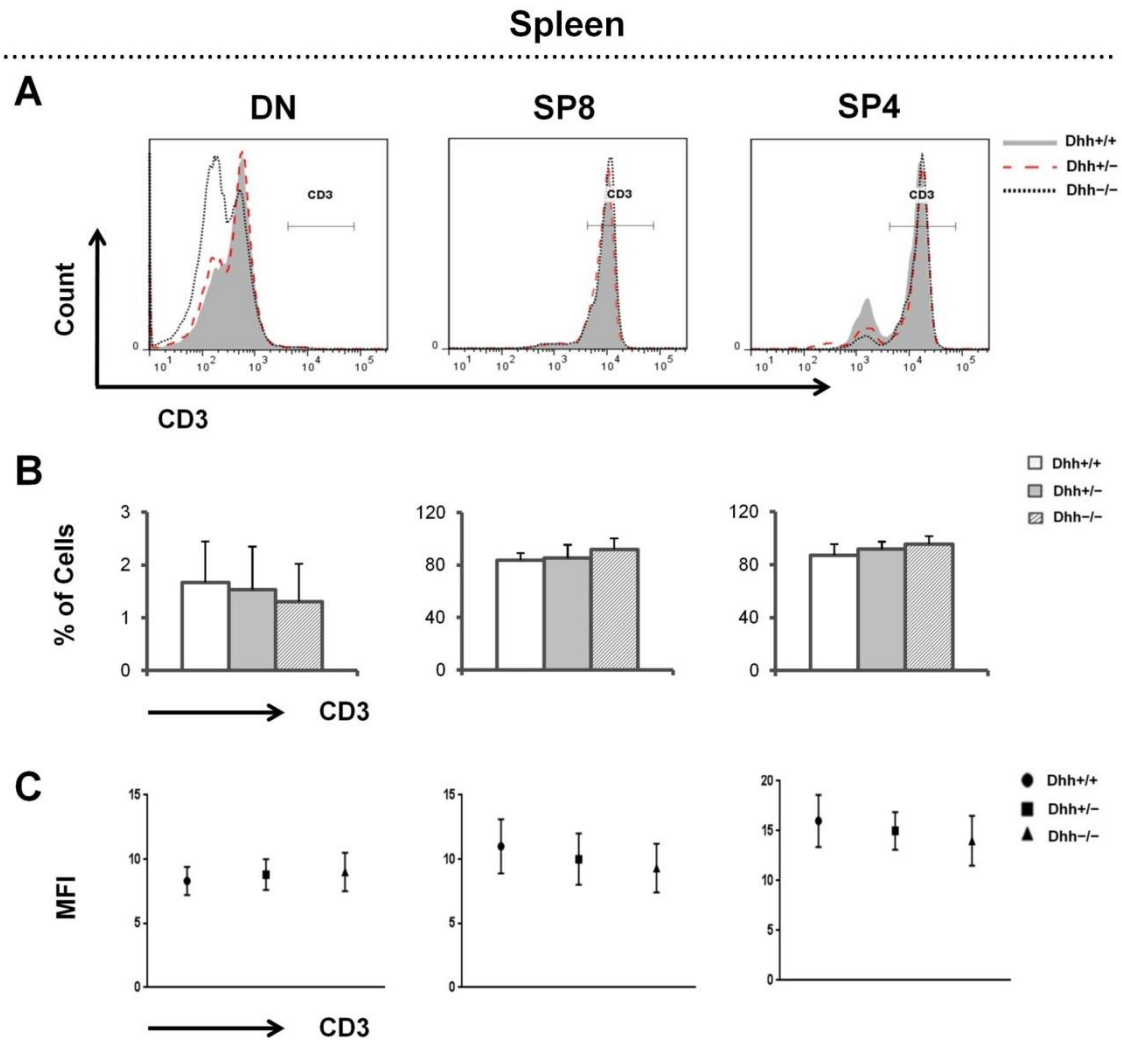

Figure 4.13

Expression of CD3 in Dhh splenocytes. Splenocytes from adult Dhh-WT, Het and KO littermates. Splenocytes were stained for anti-CD3, anti-CD8 and anti-CD4, and analyzed by flow cytometry. **(A)** Representative histogram of CD3 expression in $CD4^{-}CD8^{-}$, SP8 and SP4 cells. **(B)** Representative bar graph of CD3 percentages in $CD4^{-}CD8^{-}$, SP8 and SP4 cells. **(C)** Representative scatter plot of CD3 MFI in $CD4^{-}CD8^{-}$, SP8 and SP4 cells. Figures are representative of 3 independent sets of Dhh littermates. Mean and standard deviation of each population are given. Bars represent mean ± standard deviations. **CD3 percentages; $CD4^{-}CD8^{-}$** (p= 0.8 (WT/Het), 0.5 (WT/KO), 0.7 (Het/KO), n=3). **SP8** (p= 0.7 (WT/Het), 0.1 (WT/KO), 0.3 (Het/KO), n=3). **SP4** (p= 0.5 (WT/Het), 0.2 (WT/KO), 0.5 (Het/KO), n=3). **CD3 MFI; $CD4^{-}CD8^{-}$** (p= 0.3 (WT/Het), 0.7 (WT/KO), 0.7 (Het/KO), n=3). **SP8** (p= 0.3 (WT/Het), 0.4 (WT/KO), 0.8 (Het/KO), n=3). **SP4** (p= 0.4 (WT/Het), 0.7 (WT/KO), 0.09 (Het/KO), n=3).

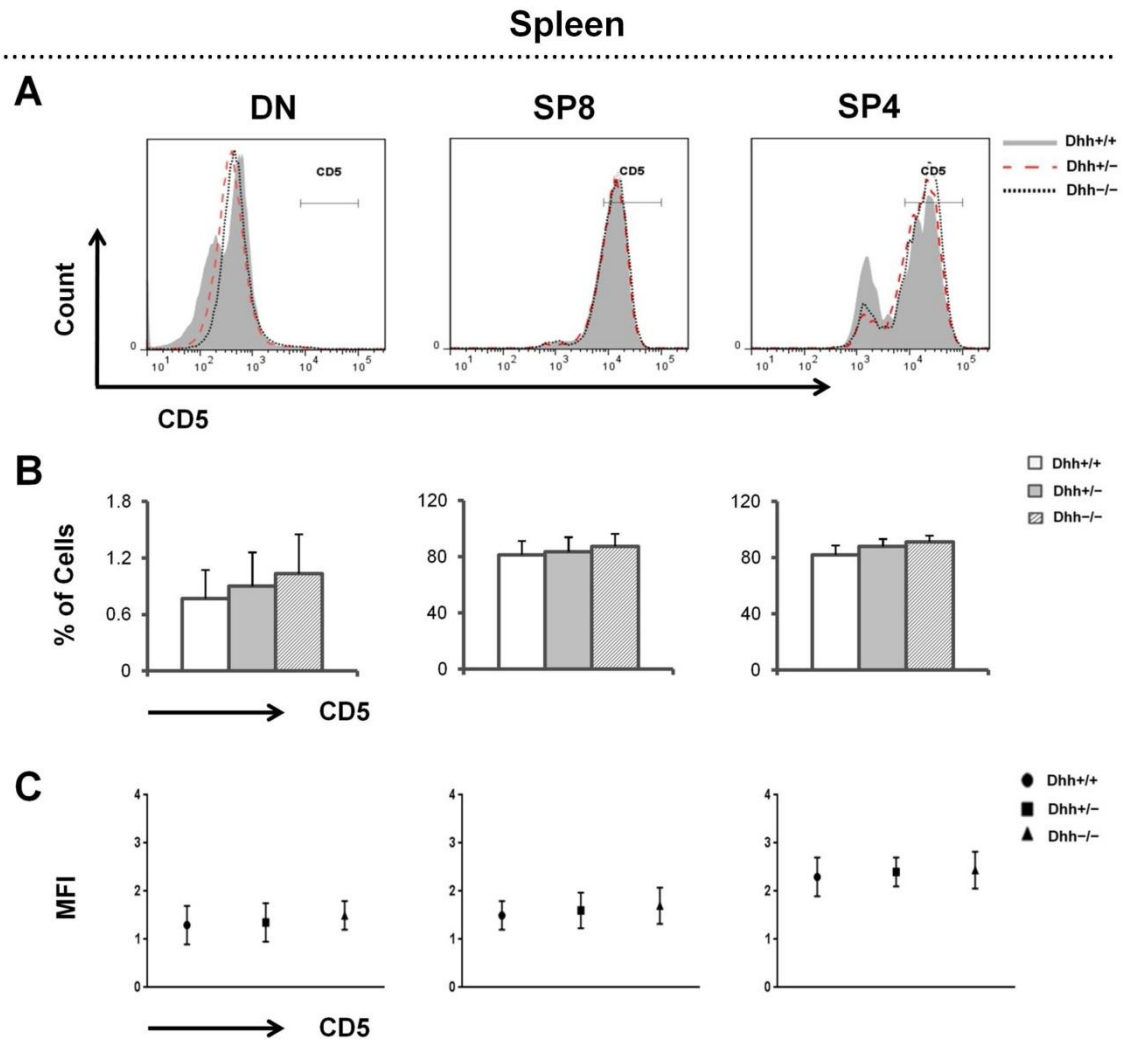

Figure 4.14

Expression of CD5 in Dhh splenocytes. Splenocytes from adult Dhh-WT, Het and KO littermates. Splenocytes were stained for anti-CD5, anti-CD8 and anti-CD4, and analyzed by flow cytometry. **(A)** Representative histogram of CD5 expression in $CD4^{-}CD8^{-}$, SP8 and SP4 cells. **(B)** Representative bar graph of CD5 percentages in $CD4^{-}CD8^{-}$, SP8 and SP4 cells. **(C)** Representative scatter plot of CD5 MFI in $CD4^{-}CD8^{-}$, SP8 and SP4 cells. Figures are representative of 3 independent sets of Dhh littermates. Mean and standard deviation of each population are given. Bars represent mean ± standard deviations. **CD5 percentages; $CD4^{-}CD8^{-}$** (p= 0.6 (WT/Het), 0.4 (WT/KO), 0.6 (Het/KO), n=3). **SP8** (p= 0.7 (WT/Het), 0.4 (WT/KO), 0.6 (Het/KO), n=3). **SP4** (p= 0.2 (WT/Het), 0.4 (WT/KO), 0.1 (Het/KO), n=3). **CD5 MFI; $CD4^{-}CD8^{-}$** (p= 0.5 (WT/Het), 0.8 (WT/KO), 0.2 (Het/KO), n=3). **SP8** (p= 0.07 (WT/Het), 0.3 (WT/KO), 0.1 (Het/KO), n=3). **SP4** (p= 0.3 (WT/Het), 0.7 (WT/KO), 0.4 (Het/KO), n=3).

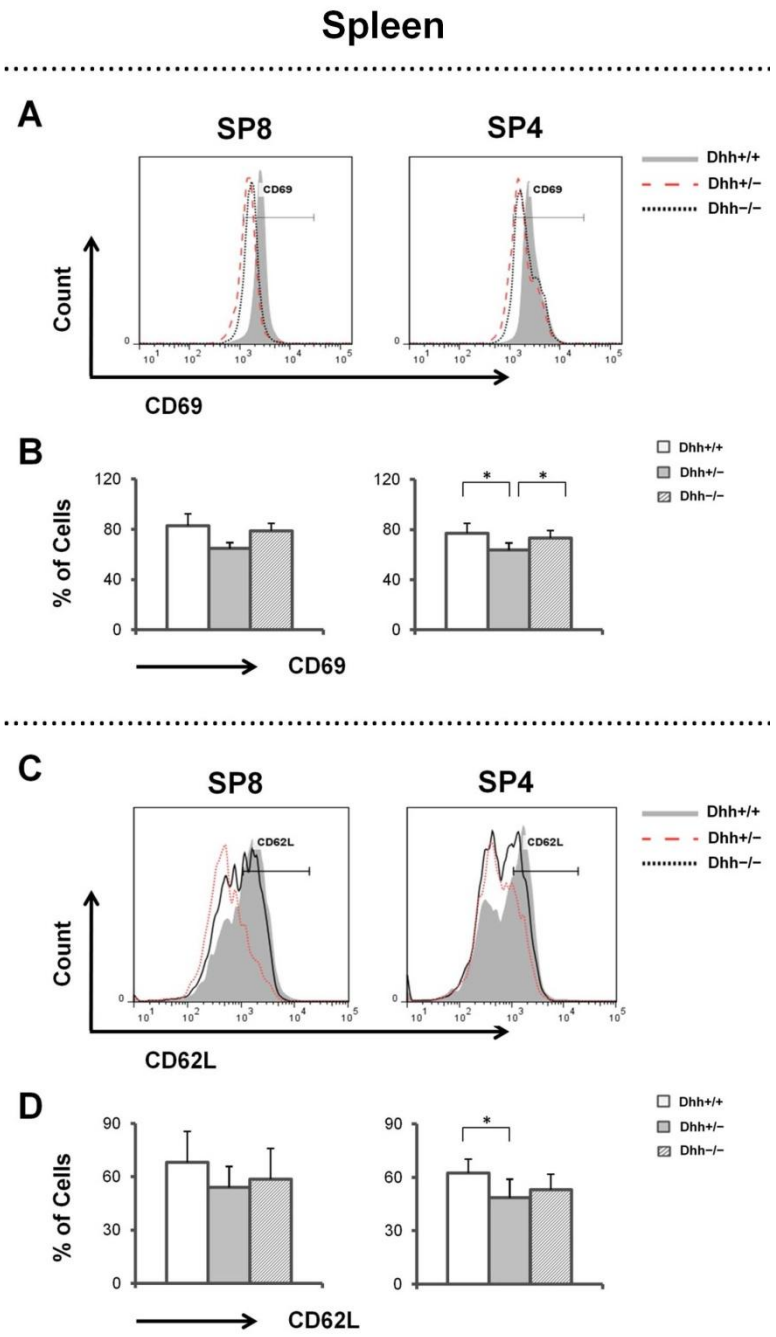

Figure 4.15

Expression of CD69 and CD62L in Dhh splenocytes. Expression of CD69 and CD62L in splenocytes from adult Dhh-WT, Het and KO littermates. Splenocytes were stained for anti-CD69, anti-CD62L, anti-CD8 and anti-CD4, and analyzed by flow cytometry. **(A)** Representative histogram of CD69 expression in SP8 and SP4 cells. **(B)** Representative bar graph of CD69 percentages in SP8 and SP4 cells. **(C)** Representative histogram of CD62L expression in SP8 and SP4 cells. **(D)** Representative bar graph of CD62L percentages in SP8 and SP4 cells. Figures are representative of 4 independent sets of Dhh littermates. Mean and standard deviation of each population are given. Bars represent mean ± standard deviations. **CD69 percentages; SP8** (p= 0.1 (WT/Het), 0.5 (WT/KO), 0.07 (Het/KO), n=4). **SP4** (p= 0.01 (WT/Het), 0.4 (WT/KO), 0.03 (Het/KO), n=4). **CD62L percentages; SP8** (p= 0.3 (WT/Het), 0.5 (WT/KO), 0.7 (Het/KO), n=4). **SP4** (p= 0.04 (WT/Het), 0.1 (WT/KO), 0.4 (Het/KO), n=4). *represents $p \leq 0.05$

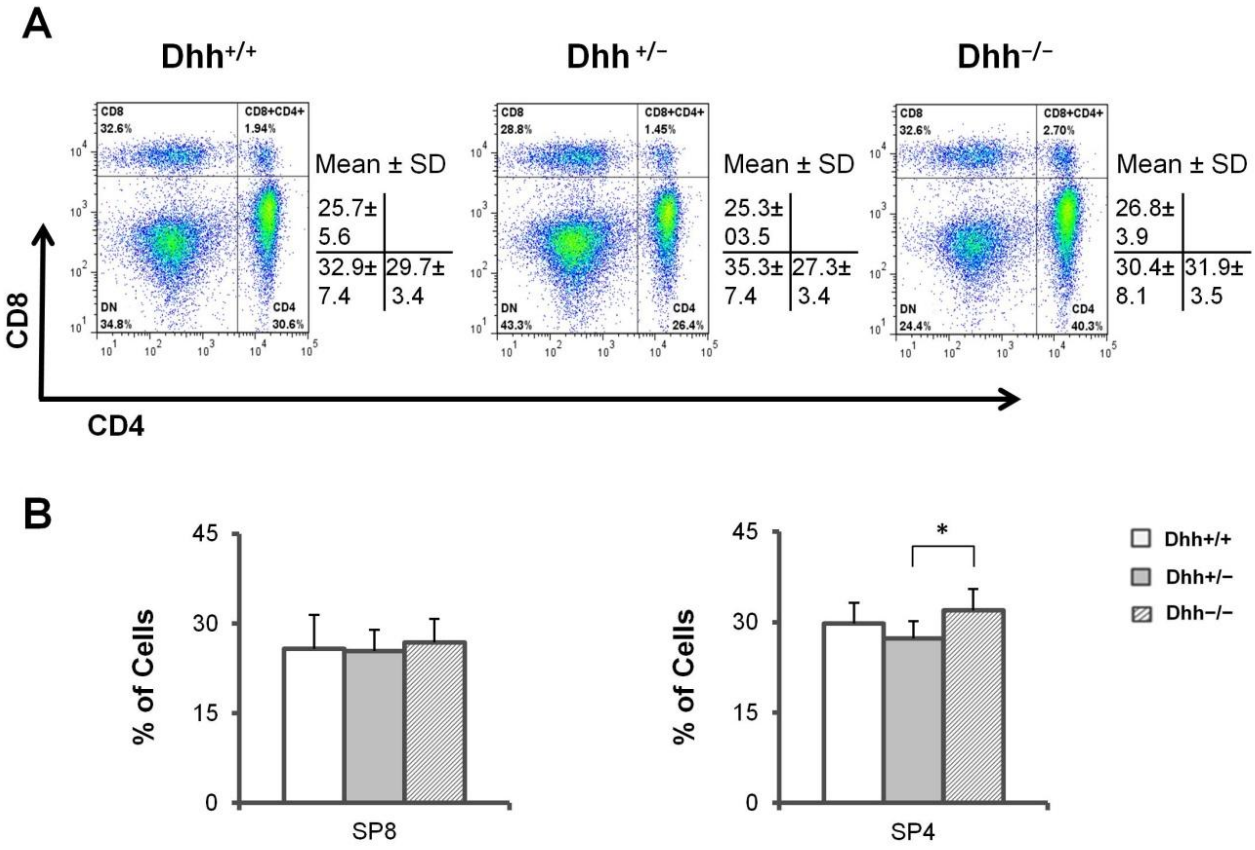

Figure 4.16

Major T cell populations in Dhh littermates. Percentage of lymph node T cell populations from adult Dhh-WT, Het and KO littermates. Cells were stained for anti-CD8 and anti-CD4, and analyzed by flow cytometry. **(A)** Representative dot plot of T cell populations. **(B)** Representative bar graph of $CD4^{-}CD8^{-}$, SP8 and SP4 percentages. Figures are representative of 4 independent sets of Dhh littermates. Mean and standard deviation of each population are given. Bars represent mean ± standard deviations. **SP8** (p= 0.8 (WT/Het), 0.6 (WT/KO), 0.4 (Het/KO), n=4). **SP4** (p= 0.1 (WT/Het), 0.2 (WT/KO), 0.01 (Het/KO), n=4). *represents $p \leq 0.05$.

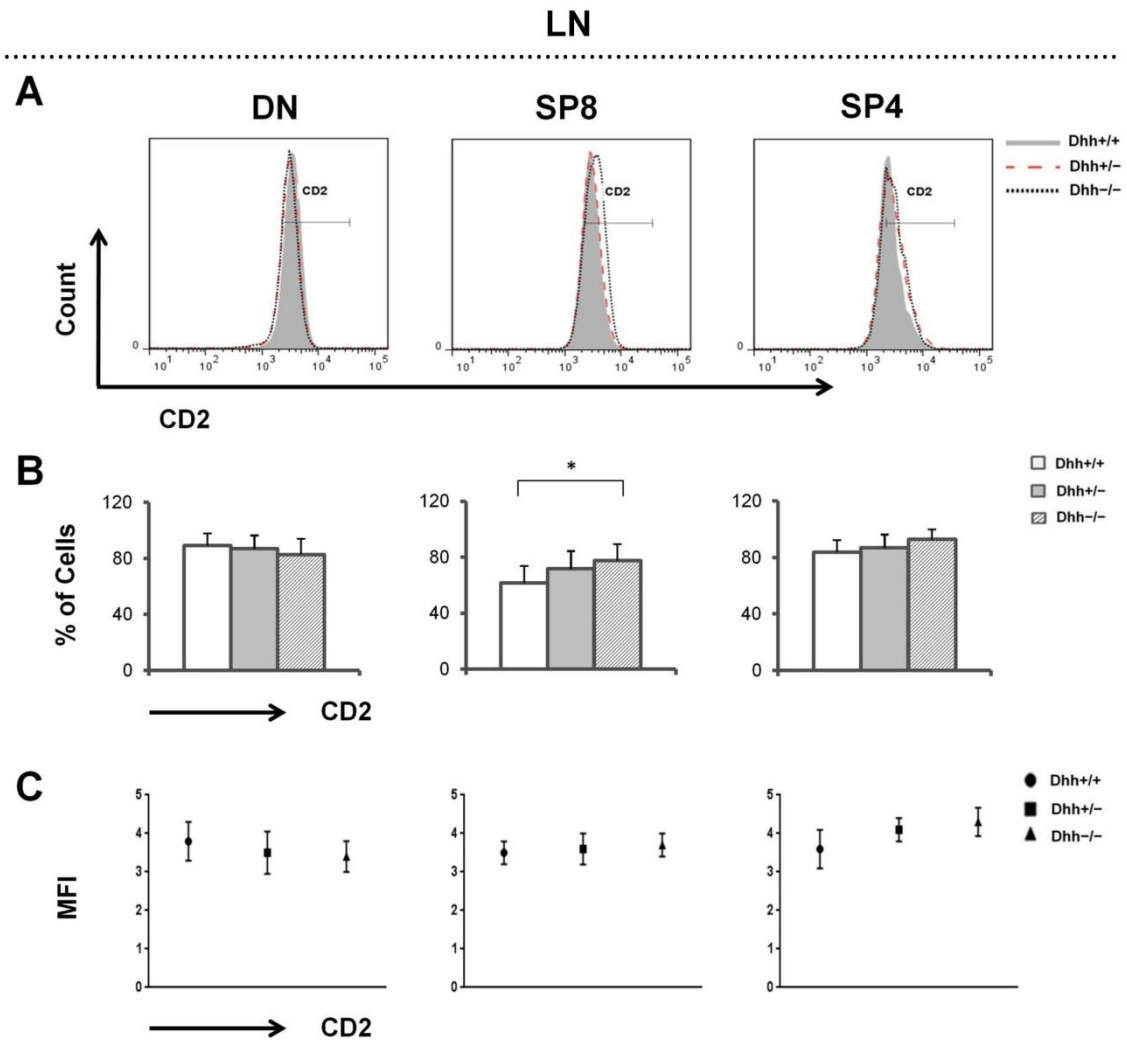

Figure 4.17

Expression of CD2 in Dhh lymph node T cells. Expression of CD2 in lymph node T cells from adult Dhh-WT, Het and KO littermates. Cells were stained for anti-CD2, anti-CD8 and anti-CD4, and analyzed by flow cytometry. **(A)** Representative histogram of CD2 expression in $CD4^{-}CD8^{-}$, SP8 and SP4 cells. **(B)** Representative bar graph of CD2 percentages in $CD4^{-}CD8^{-}$, SP8 and SP4 cells. **(C)** Representative scatter plot of CD2 MFI in $CD4^{-}CD8^{-}$, SP8 and SP4 cells. Figures are representative of 3 independent sets of Dhh littermates. Mean and standard deviation of each population are given. Bars represent mean ± standard deviations. **CD2 percentages; $CD4^{-}CD8^{-}$** (p= 0.7 (WT/Het), 0.4 (WT/KO), 0.7 (Het/KO), n=3). **SP8** (p= 0.1 (WT/Het), 0.04 (WT/KO), 0.4 (Het/KO), n=3). **SP4** (p= 0.6 (WT/Het), 0.1 (WT/KO), 0.3 (Het/KO), n=3). **CD2 MFI; $CD4^{-}CD8^{-}$** (p= 0.2 (WT/Het), 0.6 (WT/KO), 0.7 (Het/KO), n=3). **SP8** (p= 0.07 (WT/Het), 0.4 (WT/KO), 0.8 (Het/KO), n=3). **SP4** (p= 0.09 (WT/Het), 0.3 (WT/KO), 0.6 (Het/KO), n=3). *represents $p \leq 0.05$.

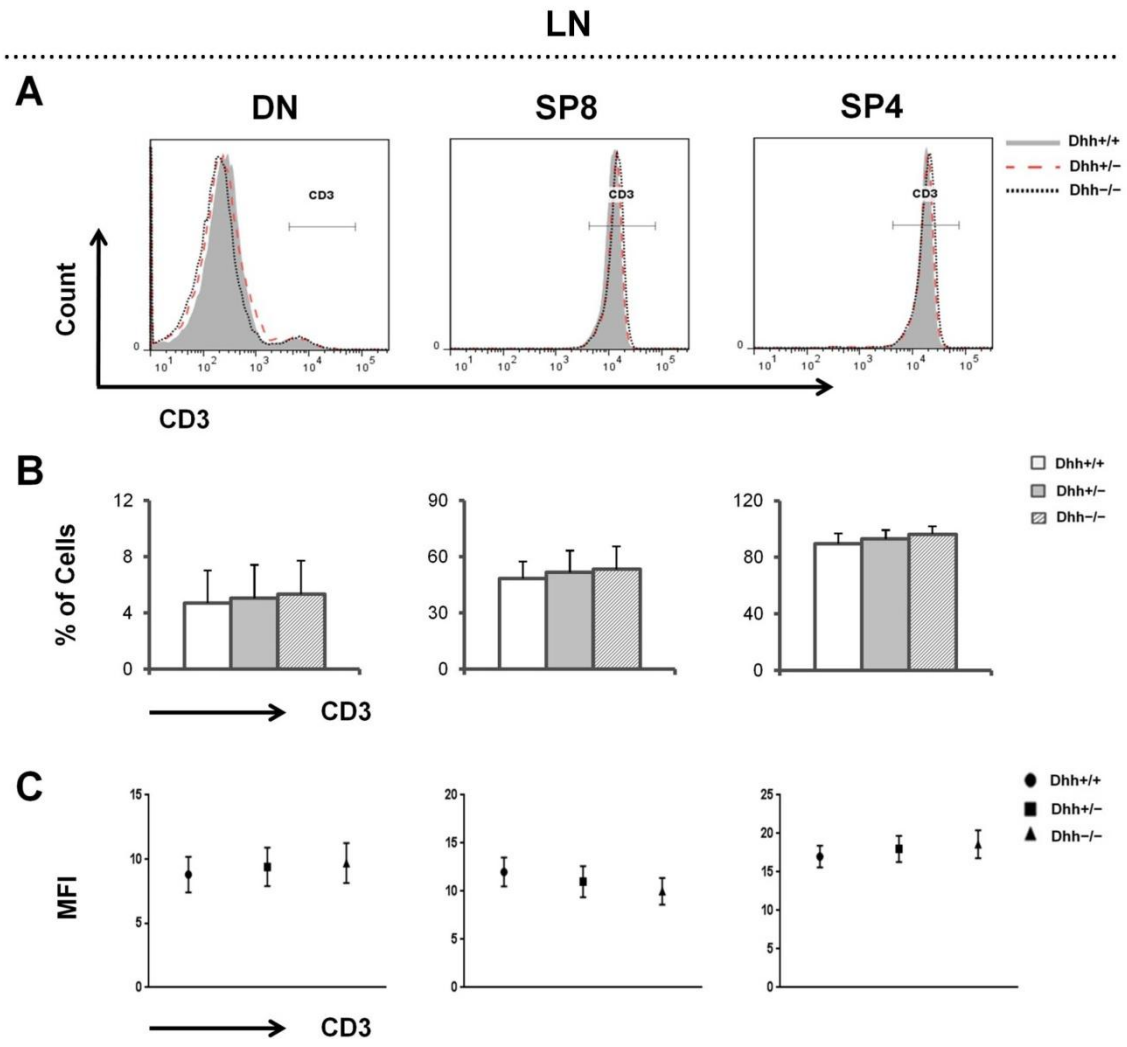

Figure 4.18

Expression of CD3 in Dhh lymph node T cells. Expression of CD3 in lymph node T cells from adult Dhh-WT, Het and KO littermates. Cells were stained for anti-CD3, anti-CD8 and anti-CD4, and analyzed by flow cytometry. **(A)** Representative histogram of CD3 expression in $CD4^{-}CD8^{-}$, SP8 and SP4 cells. **(B)** Representative bar graph of CD3 percentages in $CD4^{-}CD8^{-}$, SP8 and SP4 cells. **(C)** Representative scatter plot of CD3 MFI in $CD4^{-}CD8^{-}$, SP8 and SP4 cells. Figures are representative of 3 independent sets of Dhh littermates. Mean and standard deviation of each population are given. Bars represent mean ± standard deviations. **CD3 percentages; $CD4^{-}CD8^{-}$** (p= 0.8 (WT/Het), 0.7 (WT/KO), 0.8 (Het/KO), n=3). **SP8** (p= 0.5 (WT/Het), 0.3 (WT/KO), 0.7 (Het/KO), n=3). **SP4** (p= 0.5 (WT/Het), 0.1 (WT/KO), 0.4 (Het/KO), n=3). **CD3 MFI; $CD4^{-}CD8^{-}$** (p= 0.4 (WT/Het), 0.3 (WT/KO), 0.4 (Het/KO), n=3). **SP8** (p= 0.4 (WT/Het), 0.8 (WT/KO), 0.2 (Het/KO), n=3). **SP4** (p= 0.7 (WT/Het), 0.5 (WT/KO), 0.8 (Het/KO), n=3).

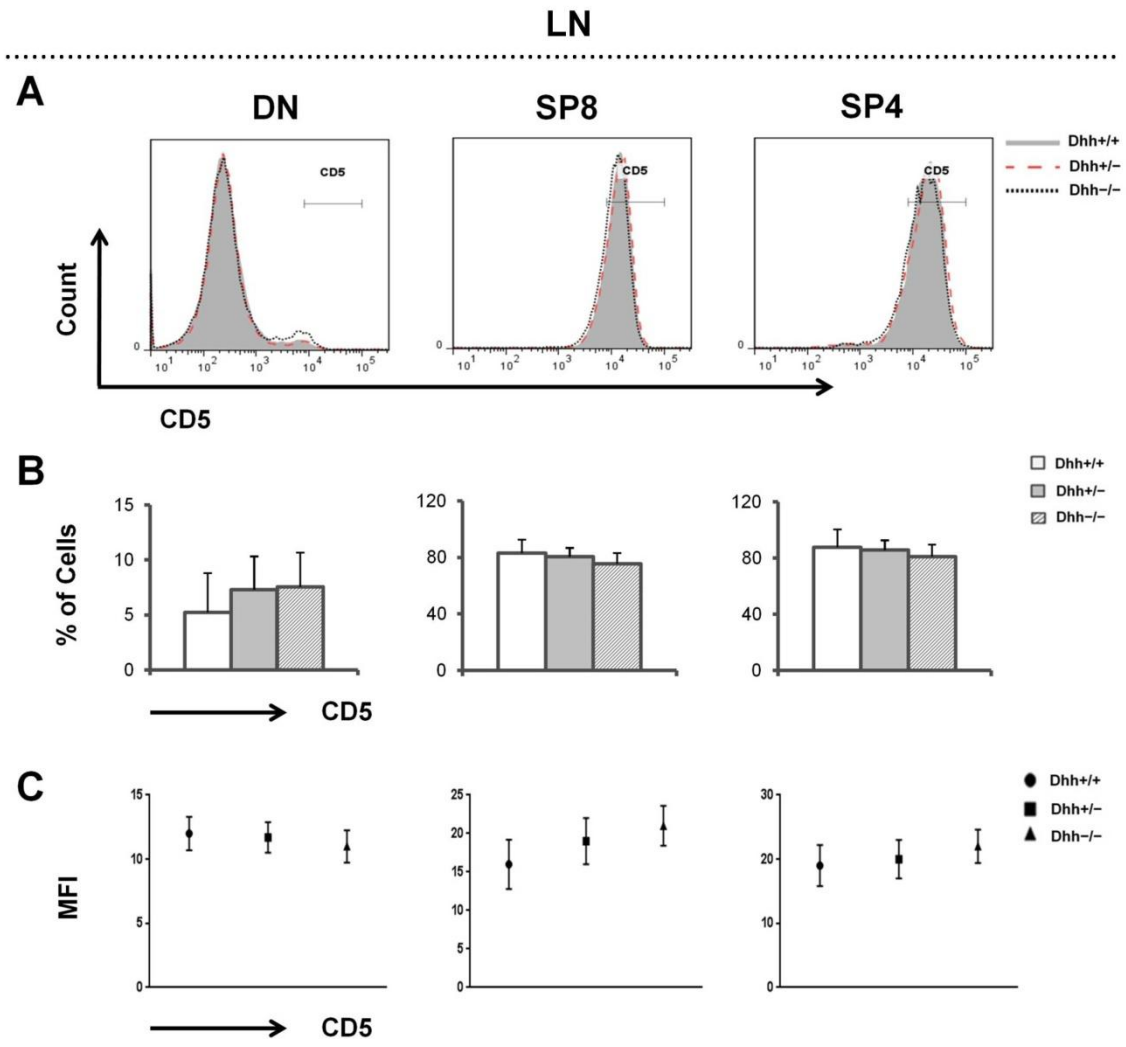

Figure 4.19

Expression of CD5 in Dhh lymph node T cells. Expression of CD5 in lymph node T cells from adult Dhh-WT, Het and KO littermates. Cells were stained for anti-CD5, anti-CD8 and anti-CD4, and analyzed by flow cytometry. **(A)** Representative histogram of CD5 expression in $CD4^{-}CD8^{-}$, SP8 and SP4 cells. **(B)** Representative bar graph of CD5 percentages in $CD4^{-}CD8^{-}$, SP8 and SP4 cells. **(C)** Representative scatter plot of CD5 MFI in $CD4^{-}CD8^{-}$, SP8 and SP4 cells. Figures are representative of 3 independent sets of Dhh littermates. Mean and standard deviation of each population are given. Bars represent mean ± standard deviations. **CD5 percentages; $CD4^{-}CD8^{-}$** (p= 0.1 (WT/Het), 0.4 (WT/KO), 0.3 (Het/KO), n=3). **SP8** (p= 0.9 (WT/Het), 0.5 (WT/KO), 0.09 (Het/KO), n=3). **SP4** (p= 0.8 (WT/Het), 0.4 (WT/KO), 0.3 (Het/KO), n=3). **CD5 MFI; $CD4^{-}CD8^{-}$** (p= 0.4 (WT/Het), 0.07 (WT/KO), 0.4 (Het/KO), n=3). **SP8** (p= 0.3 (WT/Het), 0.6 (WT/KO), 0.08 (Het/KO), n=3). **SP4** (p= 0.2 (WT/Het), 0.6 (WT/KO), 0.4 (Het/KO), n=3).

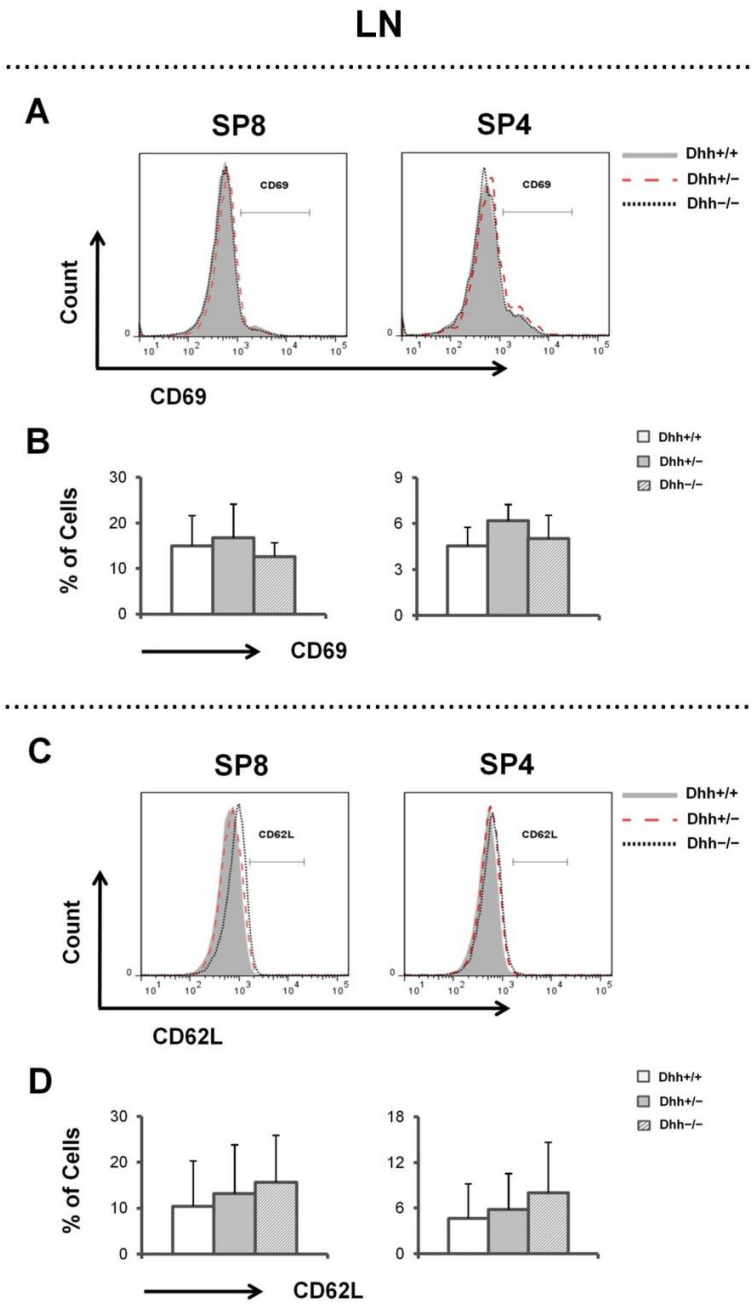

Figure 4.20

Expression of CD69 and CD62L in Dhh lymph node T cells. Expression of CD69 and CD62L in lymph node T cells from adult Dhh-WT, Het and KO littermates. Cells were stained for anti-CD69, anti-CD62L, anti-CD8 and anti-CD4, and analyzed by flow cytometry. **(A)** Representative histogram of CD69 expression SP8 and SP4 cells. **(B)** Representative bar graph of CD69 percentages in SP8 and SP4 cells. **(C)** Representative histogram of CD62L expression in SP8 and SP4 cells. **(D)** Representative bar graph of CD62L percentages in SP8 and SP4 cells. Figures are representative of 3 independent sets of Dhh littermates. Mean and standard deviation of each population are given. Bars represent mean ± standard deviations. **CD69 percentages; SP8** (p= 0.7 (WT/Het), 0.5 (WT/KO), 0.3 (Het/KO), n=3). **SP4** (p= 0.1 (WT/Het), 0.6 (WT/KO), 0.3 (Het/KO), n=3). **CD62L percentages; SP8** (p= 0.7 (WT/Het), 0.4 (WT/KO), 0.7 (Het/KO), n=3). **SP4** (p= 0.7 (WT/Het), 0.5 (WT/KO), 0.6 (Het/KO), n=3).

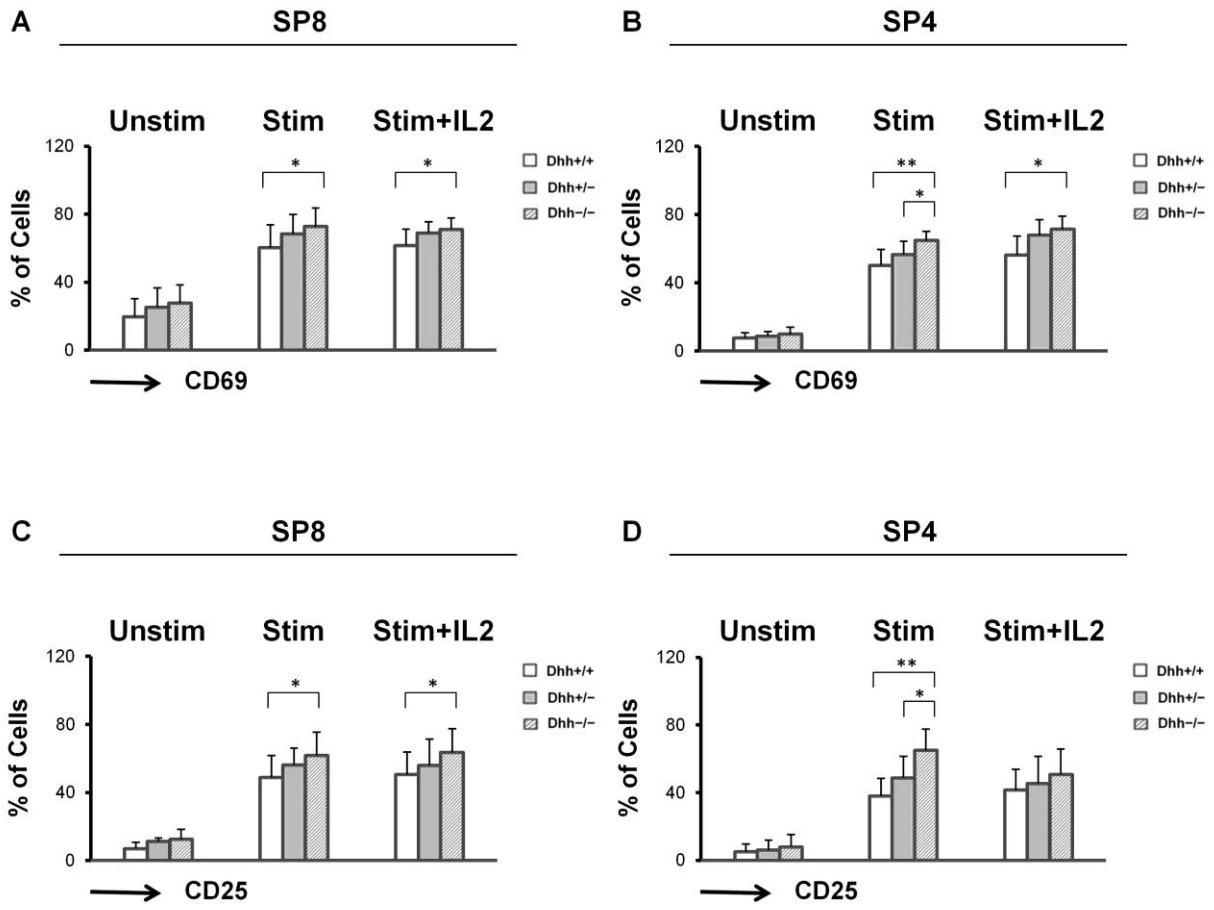

Figure 4.21

Spleen SP8 and SP4 early and late activation. Expression of the early activation marker CD69 and the late activation marker CD25 in spleen SP8 and SP4 cells from adult Dhh-WT, Het and KO littermates. Three culturing conditions were applied, unstimulated cells (condition Unstim), cells stimulated with anti-CD3 and anti-CD28 (condition Stim), and cells stimulated with anti-CD3, anti-CD28 in addition to IL-2 (condition Stim+IL2). Cells were stained for anti-CD69, anti-CD25, anti-CD8 and anti-CD4, and analyzed by flow cytometry. **(A)** Representative bar graph of CD69 percentages in SP8 cells. **(B)** Representative bar graph of CD69 percentages in SP4 cells. **(C)** Representative bar graph of CD25 percentages in SP8 cells. (**D)** Representative bar graph of CD25 percentages in SP4 cells. Figures are representative of 5 independent sets of Dhh littermates. Mean and standard deviation of each population are given. Bars represent mean ± standard deviations. **CD69 percentages; (Unstim); SP8** (p= 0.06 (WT/Het), 0.09 (WT/KO), 0.07 (Het/KO), n=5). **SP4** (p= 0.08 (WT/Het), 0.06 (WT/KO), 0.1 (Het/KO), n=5). **CD69; percentages (Stim); SP8** (p= 0.07 (WT/Het), 0.04 (WT/KO), 0.06 (Het/KO), n=5). **SP4** (p= 0.06 (WT/Het), 0.001 (WT/KO), 0.02 (Het/KO), n=5). **CD69 percentages; (Stim+IL2); SP8** (p= 0.06 (WT/Het), 0.05 (WT/KO), 0.07 (Het/KO), n=5). **SP4** (p= 0.08 (WT/Het), 0.04 (WT/KO), 0.08 (Het/KO), n=5). **CD25 percentages; (Unstim) SP8** (p= 0.09 (WT/Het), 0.1 (WT/KO), 0.2 (Het/KO), n=5). **SP4** (p= 0.2 (WT/Het), 0.09 (WT/KO), 0.1 (Het/KO), n=5). **CD25 percentages; (Stim); SP8** (p= 0.08 (WT/Het), 0.05 (WT/KO), 0.07 (Het/KO), n=5). **SP4** (p= 0.09 (WT/Het), 0.003 (WT/KO), 0.04 (Het/KO), n=5). **CD25 percentages; (Stim+IL2); SP8** (p= 0.09 (WT/Het), 0.05 (WT/KO), 0.08 (Het/KO), n=5). **SP4** (p= 0.07 (WT/Het), 0.06 (WT/KO), 0.06 (Het/KO), n=5). *represents $p \leq 0.05$, **represents $p \leq 0.005$.

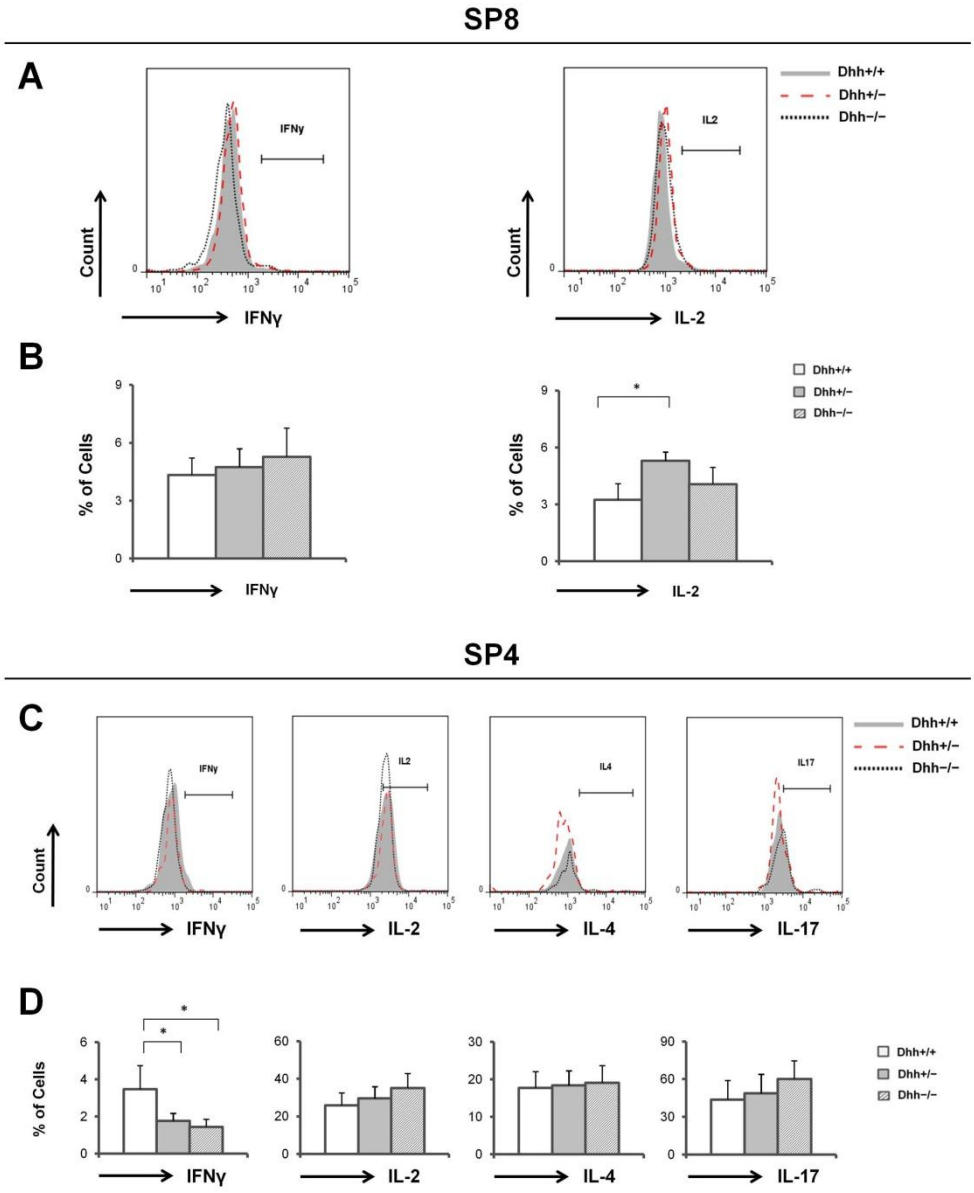

Figure 4.22

Intracellular cytokine staining of spleen SP8 and SP4 cells. Intracellular staining of cytokines (IFNγ and IL-2) in spleen SP8 cells, and Intracellular staining of cytokines (IFNγ, IL-2, IL-4 and IL-17) in spleen SP4 cells from adult Dhh-WT, Het and KO littermates. Cells were cultured with PMA, ionomycin and brefeldin-A for 4 hours followed by intracellular staining with anti-IFNγ, anti-IL-2, anti-IL-4, anti-IL-17, anti-CD8 and anti-CD4. Cells were analyzed by flow cytometry. **(A)** Representative histogram of IFNγ and IL-2 expression in SP8 cells. **(B)** Representative bar graph of IFNγ and IL-2 percentages in SP8 cells. **(C)** Representative histogram of IFNγ, IL-2, IL-4 and IL-17 expression in SP4 cells. **(D)** Representative bar graph of IFNγ, IL-2, IL-4 and IL-17 percentages in SP4 cells. Figures are representative of 3 independent sets of Dhh littermates. Mean and standard deviation of each population are given. Bars represent mean ± standard deviations. **SP8; IFNγ** (p= 0.7 (WT/Het), 0.1 (WT/KO), 0.2 (Het/KO), n=3). **SP8; IL-2** (p= 0.04 (WT/Het), 0.09 (WT/KO), 0.07 (Het/KO), n=3). **SP4; IFNγ** (p= 0.04 (WT/Het), 0.02 (WT/KO), 0.08 (Het/KO), n=3). **SP4; IL-2** (p= 0.4 (WT/Het), 0.2 (WT/KO), 0.1 (Het/KO), n=3). **SP4; IL-4** (p= 0.1 (WT/Het), 0.09 (WT/KO), 0.6 (Het/KO), n=3). **SP4; IL-17** (p= 0.5 (WT/Het), 0.1 (WT/KO), 0.2 (Het/KO), n=3). *represents p≤0.05.

4.3 Discussion

Our data shown that Dhh acts as a negative regulator of T cells during their development and differentiation in the thymus and peripheral lymphoid organs. Analysis of Dhh-WT, Dhh-Het and Dhh-KO mice shows that in the absence of Dhh, the number of thymocytes and splenocytes is increased. However, the phenotype of Dhh-Het is unusual in that, although thymocyte and spleonocyte numbers were increased in Dhh-KO, we observed a decrease in thymocyte numbers and a greater increase in splenocyte numbers in Dhh-Het, suggesting a novel role for Dhh in thymocyte and splenocyte homeostasis.

The influence of Dhh on developing thymocytes starts early in the DN stages, as our data have shown a decrease in the DN1 and DN3 cells, indicating a positive regulatory role of Dhh during early thymocyte differentiation in the thymus, and during pre-TCR complex formation and β selection. Surprisingly, Dhh-Het shows an opposite effect to Dhh-KO, with an increase in the number of thymocytes during the DN1 and DN3 stages.

Dhh also influenced thymocyte populations, as our data have shown that Dhh decreased the number of DP thymocytes and increased the numbers SP8 thymocytes, suggesting that Dhh positively regulate thymocyte development during the formation of the TCR complex, and negatively regulate positive selection of SP8 cells. Furthermore, our data have also shown that Dhh influence TCR associated CD3 molecule on SP8 cells, as partial expression of Dhh decreased the expression of CD3, whereas the complete knockout showed even a greater decrease in CD3 expression. This finding explains the increase of SP8

thymocytes in Dhh-KO which can come as a result of a weak TCR signal transduction defecting negative selection of SP8 thymocytes.

We have also examined the expression of CD69 during thymocyte development and our results shows that CD69 expression is increased in both the DN and SP4 cells, suggesting a negative role of Dhh on CD69 expression in the thymus. CD69 expression in immature thymocytes is believed to be associated with cell death. Additionally, CD69 expression on SP4 correlates with positive selection, our finding thus suggests that Dhh reduced positive selection of SP4 cells. The maturation marker CD62L has also been examined and our data shows that Dhh has a dual function as it negatively regulate CD62L expression in DN, and positively regulate the expression of CD62L in SP4 cells in a dose dependent manner.

During the transition from the DP so the SP, thymocytes undergo maturation through a series of developmental stages before becoming functionally mature cells that exit the thymus. We analyzed the cell surface expression of HSA and Qa2 to measure the maturation status on DP and SP thymocytes. We found that Dhh partially arrested SP4 cell development.

Dhh also continues to regulate mature T cell populations in the spleen, as our data have shown that SP8 splenocytes were increased in Dhh-KO and decreased in the Dhh-Het, suggesting a dual influence of Dhh as a negative regulator and positive regulator of mature SP8 cells. On the contrary, in the lymph node Dhh seems to negatively regulate SP4 cells as our data have shown that SP4 cells were increased in Dhh-KO, suggesting a differential role of Dhh in the periphery between the spleen and lymph node. We have undertaken T cell characterization

in the periphery and our data have shown that Dhh positively regulate the expression of CD62L in SP8 and SP4 splenocytes. Furthermore, we tested whether Dhh-KO mice display changes in splenocytes differentiation and activation, and our data have shown that Dhh negatively regulate the activation of SP splenocytes. Interestingly, IL2 production in SP activated cells were increased in Dhh-Het.

A negative regulatory role for Dhh has been previously described (Lau et al. 2012). In this case, analysis of Dhh mutant mice showed that Dhh negatively regulates multiple stages of erythrocyte differentiation, indicating a negative role of Dhh, we have also found that Dhh is a negative regulator of T cell production. The unusual role of Hh proteins between the heterozygous and knockout has also been reported in Ihh (Outram et al. 2009). In this study, foetal Ihh+/− thymi had increased thymocyte numbers relative to WT, indicating that Ihh also negatively regulates thymocyte development, and our data have shown a similar finding with Dhh as a negative regulator of thymocytes and splenocytes during their development and in the periphery.

A possible explanation might be that Hh signalling provides both a positive and a negative regulatory signal in order to maintain homeostatic control of developing thymocytes and T cells in the periphery. The three Hh proteins are highly conserved in vertebrates and act in the same tissues with overlapping or redundant functions (Kumar et al. 1996). Although Hh overlapping functions have not been well studied, studies on T cell development have shown that the three Hh proteins may have overlapping activities and differential functions in order to regulate T cell differentiation and homeostasis (Crompton et al. 2007; Outram et al. 2009).

4.4 Conclusion

In this chapter, using Dhh-WT, Dhh-Het and Dhh-KO mice models, our data have shown that Dhh play a negative role in T cell production in the thymus as well as in the peripheral lymphoid organs. Moreover, analysis of the thymocyte development showed that Dhh is involved in regulation of thymocytes from the early stages of development in the DN stage through selection and maturation. In addition to the thymus, this regulatory role of Dhh continues in the periphery through altering the proportions of SP T cells and their activation

Chapter 5

Chapter Five: Role of Hh signalling in T cell repertoire selection

5.1 Introduction

5.1.1 Role of Hh proteins in T cell repertoire selection

During their development within the thymus, T cells undergo critical developmental selection to select those cells amongst the immature thymocytes that express T cell receptor (TCR) restricted to and tolerant of self-peptides presented by the major histocompatibilty complexes (MHC-I, MHC-II). The result of this crucial selection is a repertoire of mature T cells that does not attack or destroy host tissues but reacts efficiently against the unlimited range of foreign antigens.

Shh has been shown to modulate TCR signal strength during the later stage of T cell development, attenuating TCR repertoire selection and influencing T cell SP4/SP8 lineage commitment (Hager-Theodorides et al. 2009; Rowbotham, Hager-Theodorides, Cebecauer, et al. 2007; Drakopoulou et al. 2010; Rowbotham, Hager-Theodorides, Furmanski, et al. 2007; Lowrey et al. 2002; Stewart et al. 2002; Furmanski et al. 2012; Furmanski et al. 2013). These findings implicate Hh signalling in regulating the events controlling TCR signal strength and selection within the thymus.

5.1.2 Chapter objectives

The purpose of this chapter is to investigate the role of Hh signalling in T cell selection and lineage choice. To investigate this role, I have generated two mouse models; (1) HY-TCR^{+}/Dhh-WT, HY-TCR^{+}/Dhh-Het and HY-TCR^{+}/Dhh-KO, generated from crossing HY-TCR^{+} transgenic Dhh$^{+/-}$ female mouse with Dhh$^{+/-}$ male mouse. (2) Marilyn-TCR^{+}/*Lck*-Gli2ΔC2^{-} and Marilyn-TCR^{+}/*Lck*-Gli2ΔC2^{+} transgenic mice, generated from back-crossing Marilyn-TCR^{+} Rag2$^{-/-}$ mouse with *Lck*-Gli2ΔC2^{+} mouse (in which Hh-dependent transcription is inhibited). Expression of the *Lck*-Gli2ΔC2 has been previously shown to increase positive and negative selection of a class-I-restricted TCR in the thymus (Furmanski et al. 2012) and to increase TCR activation of peripheral T cells (Rowbotham et al. 2008), by increasing TCR signalling (Furmanski et al. 2015). A direct observation of T cell populations in the thymus, spleen and lymph node will test the hypothesis that Hh signalling plays a role in T cell selection and lineage choice.

5.2 Results

5.2.1 Genotyping HY-Dhh and Marilyn-Gli2ΔC2 littermates

Two strains of mice were generated; the first is HY-Dhh**,** created by back-crossing HY-TCR transgenic male mice with $Dhh^{+/-}$ mice. The result of this crossing resulted in three genotypes of mice, the first bearing MHC class-I restricted TCR in addition to the normal complete Dhh expression gene (HY-$Dhh^{+/+}$). The second bearing MHC class-I restricted TCR in addition to the Dhh mutated gene on both alleles (HY-$Dhh^{-/-}$). The third bearing MHC class-I restricted TCR with a partial expression of Dhh (one normal allele and one mutated allele) (HY-$Dhh^{+/-}$).

The HY-Dhh littermates were genotyped for HY-TCR transgene, Dhh-WT and Dhh mutant alleles. PCR analysis using genomic DNA from ear biopsies was performed in order to identify the genotype of HY-Dhh littermates, using three sets of primers specific for HY-TCR transgene, Dhh-WT and mutant alleles. According to this strategy, HY-TCR transgene should generate a PCR product of 300bp, Dhh-WT allele should generate a PCR product of 442bp, while Dhh-mutant alleles should generate a PCR product of 110bp.

HY-Dhh mutants were identified according to the PCR results. Mice with PCR a product positive for HY-TCR transgene and Dhh-WT gene and negative for the Dhh-mutant gene were genotyped as (HY-$Dhh^{+/+}$). Mice with a PCR product positive for HY-TCR transgene and negative for Dhh-WT gene and positive for the Dhh-mutant gene were genotyped as (HY-$Dhh^{-/-}$). Mice with a PCR product positive for HY-TCR transgene and both, Dhh-WT and Dhh-mutant genes were genotyped as (HY-$Dhh^{+/-}$) (Figure 5.1).

The second strain used is Marilyn-Gli2ΔC2 created from back-crossing Marilyn-TCR transgenic Rag2$^{-/-}$ male mice with Gli2ΔC2 transgenic mice. The result of this crossing resulted in two genotypes of mice, the first bearing MHC class-II restricted TCR without the addition of the Lck-driven Gli2ΔC2 transgene (Marilyn-Gli2ΔC2^{-}). The second bearing MHC class-II restricted TCR in addition to the Lck-driven Gli2ΔC2 transgene (Marilyn-Gli2ΔC2^{+}).

The Marilyn-Gli2ΔC2 littermates were genotyped for Marilyn-TCR, Gli2ΔC2 transgenes and Rag-2 wild-type and mutated genes. PCR analysis using genomic DNA from ear biopsies was performed in order to identify the genotype of Marilyn- Gli2ΔC2 littermates. PCR analysis of the two littermates was performed using four sets of primers specific for Marilyn-TCR, Gli2ΔC2 transgenes and Rag-2 WT and mutated genes. According to this strategy, Marilyn-TCR transgene should generate a PCR product of 350bp, Gli2ΔC2 transgene should generate a PCR product of 850bp, Rag-2 WT gene should generate a PCR product of 973bp, Rag-2 mutant gene should generate a PCR product of 1107bp.

Marilyn-Gli2ΔC2 mutants were identified according to the PCR results. Mice with PCR a product positive for Marilyn-TCR and Gli2ΔC2 transgenes were genotyped as (Marilyn-Gli2ΔC2^{+}). Mice with a PCR product positive for Marilyn-TCR transgene and negative for Gli2ΔC2 transgene were genotyped as (Marilyn-Gli2ΔC2^{-}) (Figure 5.1).

5.2.2 Differences in organ size of HY-Dhh and Marilyn-Gli2ΔC2

Thymus and spleen of HY-Dhh and Marilyn-Gli2ΔC2 mutant mice were compared following anatomical dissection in order to assess their difference and

similarities. All observations were carried out between littermates. Size comparison was carried out by visual comparison and measuring the horizontal width and vertical length of extracted organs. Thymus and spleen extracted from HY-Dhh-mutants appeared normal compared to the original genotype of HY-TCR transgenic mice and Dhh mice. Thymus extracted from the male Marilyn-Gli2ΔC2^{+} was reduced in size as in the Marilyn-TCR transgenic genotype of mice. The spleen of male Marilyn-Gli2ΔC2^{+} appeared reduced in size compared to Marilyn-Gli2ΔC2^{-} (Figure 5.2).

5.2.3 Thymocytes and splenocytes in HY-Dhh littermates

Following anatomical extraction of the thymus and spleen from HY-Dhh littermates, the thymocytes and splenocytes were collected for analysis. In regards to live cell counts in the thymus, we observed no significant difference in the mean cell numbers between the three genotypes of HY-Dhh male and female littermates (($p>0.05$, $n=5$), ($p>0.05$, $n=7$)) respectively. Similarly in regards to live cell counts in the spleen, we observed no significant difference between the three genotypes of HY-Dhh male and female littermates (($p>0.05$, $n=5$), ($p>0.05$, $n=7$) respectively (Figure 5.3)).

5.2.4 Role of Dhh in thymocyte development during Selection in HY-TCR mice

In order to assess the role of Dhh in thymocyte development and differentiation during thymocyte selection, thymocytes from HY/Dhh-WT, HY/Dhh-Het and HY/Dhh-KO male and female mice were analyzed for T3.7, CD8 and CD4 cell

surface expression. According to T3.7 expression, cells were sub-grouped into two main populations, HY-TCR positive cells ($T3.7^{+}$) and HY-TCR negative cells ($T3.7^{-}$). Within the T3.7 positive and negative compartments, cells were sub-grouped according to the cell surface expression of CD8 and CD4 into four main populations, the $CD8^{-}CD4^{-}$ (DN), $CD8^{+}CD4^{+}$ (DP), $CD8^{+}CD4^{-}$ (SP8) and $CD8^{-}CD4^{+}$ (SP4).

Our data indicated that Dhh influences thymocyte selection as we observed significant differences in deletion of self-reactive T cells in Dhh-Het and Dhh-KO in male mice. In female mice, positive selection of SP cells was also increased, indicating a negative role of Dhh during selection. Interestingly, heterozygous expression of Dhh seems to act differently from the complete expression of Dhh as our data from Dhh-Het display opposing phenotype to Dhh-KO.

In male Dhh-HY mice, within the T3.7 positive cells, our data show that the percentage of DN and DP cells was not different between the three genotypes of mice ($p>0.05$, $n=5$). The percentage of SP8 cells was higher in the HY/Dhh-KO than in the HY/Dhh-WT, but this difference was not statistically different ($p>0.05$, $n=5$), and was significantly higher than in the HY/Dhh-Het ($p\leq0.05$, $n=5$). The percentage of SP4 cells was significantly lower in the HY/Dhh-Het than in the HY/Dhh-WT and HY/Dhh-KO (($p\leq0.05$, $n=5$), ($p\leq0.05$, $n=5$)) respectively (Figure 5.4).

In male mice within the T3.7 negative cells, the percentage of DN cells was not different between the three genotypes of mice ($p>0.05$, $n=5$). In addition, the percentage of DP cells was higher in the HY/Dhh-KO compared to the HY/Dhh-WT, but this difference was not statistically different ($p>0.05$, $n=5$), and

significantly higher than in the HY/Dhh-Het ($p \leq 0.05$, n=5). The percentage of SP8 cells was lower in the HY/Dhh-KO compared to the HY/Dhh-WT, but this difference was not significant ($p > 0.05$, n=5), and significantly higher than in the HY/Dhh-Het ($p \leq 0.05$, n=5). Furthermore, the percentage of SP4 cells was decreased in the HY/Dhh-KO compared to the HY/Dhh-WT, but this difference was not significantly different ($p > 0.05$, n=5), and significantly higher than in the HY/Dhh-Het ($p \leq 0.05$, n=5). Interestingly, in the HY/Dhh-Het, the percentage of SP4 was significantly lower than in the HY/Dhh-WT (Figure 5.5).

In female mice within the T3.7 positive cells, the percentage of DN cells between the three genotypes of mice was not significantly different ($p > 0.05$, n=4). The percentage of DP and SP4 cells was significantly higher in the HY/Dhh-KO than in the HY/Dhh-WT (($p \leq 0.05$, n=4), ($p \leq 0.05$, n=4)) respectively. In HY/Dhh-Het, the percentage of DP cells was significantly higher in the HY/Dhh-WT ($p \leq 0.05$, n=4). Furthermore, the percentage of SP8 cells was significantly higher in the HY/Dhh-Het than in the HY/Dhh-WT ($p \leq 0.05$, n=4) (Figure 5.6).

Within the T3.7 negative cells, the percentage of DN, DP and SP8 cells between the three genotypes of mice was not statistically different ($p > 0.05$, n=4). The percentage of SP4 cells in the HY/Dhh-KO was significantly higher compared to the HY/Dhh-Het ($p \leq 0.05$, n=4) (Figure 5.7).

5.2.5 Influence of Dhh on expression of CD3 and CD5 in HY-TCR thymocytes

In order to assess the potential role of Dhh in regulating differentiation and TCR signal transduction of HY-TCR thymocytes during development and selection, we

analyzed the cell surface expression of molecules associated with TCR signalling (CD3 and CD5) within the $T3.7^+$ cells for DN, DP, SP8 and SP4 cells in HY/Dhh-WT, HY/Dhh-Het and HY/Dhh-KO. Furthermore we have compared the mean fluorescence intensity (MFI) of staining for these molecules, as high CD5 expression is associated with high TCR signal strength.

Our data show that Dhh has no influence on the expression of CD3 and CD5 and their MFI in male thymocytes during selection ($p>0.05$, $n=5$) (Figure 5.8) and (Figure 5.9). Similarly, in female mice, the percentage of CD3 and CD5 and their MFI were not different between the three genotypes of mice ($p>0.05$, $n=4$) (Figure 5.10) and (Figure 5.11).

5.2.6 Role of Dhh in thymocyte interactions during development and selection in HY-TCR mice

As CD69 expression correlates with TCR repertoire selection in thymocytes, thymocytes from HY/Dhh-WT, HY/Dhh-Het and HY/Dhh-KO were analyzed for CD69 expression within the $T3.7^+$ cells for DN, DP, SP8 and SP4 cells.

Our data show that Dhh has no influence on the expression of CD69 in thymocytes during selection. We found no significant differences in CD69 expression between the three genotypes of HY-Dhh in male or female mice (Figure 5.12).

5.2.7 Role of Dhh in thymocyte maturation during development and selection in HY-TCR mice

In order to assess the role of Dhh in influencing cell maturation during single positive thymocyte development and selection, thymocytes from HY/Dhh-WT, HY/Dhh-Het and HY/Dhh-KO were analyzed for Qa2 and HSA expression within the $T3.7^{+}$ cells for DP, SP8 and SP4 cells. Our data show that Dhh influence T cell maturation during selection. Interestingly, heterozygous expression of Dhh seems to display a different phenotype from Dhh-WT.

In male mice, the percentage of DP, SP8 and SP4 cells expressing Qa2 between the three genotypes of mice was not statistically significant ($p>0.05$, $n=3$). The percentage of DP and SP4 cells expressing HSA between the three genotypes of mice was not statistically significant ($p>0.05$, $n=3$). The percentage of SP8 cells expressing HSA was significantly lower than in the HY/Dhh-Het compared to the HY/Dhh-WT ($p\leq0.05$, $n=3$) (Figure 5.13).

In female mice, the percentage of DP and SP8 cells expressing Qa2 between the three genotypes of mice was not statistically significant ($p>0.05$, $n=3$). The percentage of Qa2 in SP4 cells was significantly higher in the HY/Dhh-KO compared to the HY/Dhh-WT ($p\leq0.05$, $n=3$). The percentage of DP cells expressing HSA was significantly lower in the HY/Dhh-KO compared to the HY/Dhh-WT ($p\leq0.05$, $n=3$). However, the percentage of SP8 and SP4 cells expressing HSA between the three genotypes of HY-Dhh was not statistically different ($p>0.05$, $n=3$) (Figure 5.14).

5.2.8 Role of Dhh in spleen T cells in HY-TCR mice

In order to assess the role of Dhh in spleen T cells in the periphery in HY-TCR mice, splenocytes from HY/Dhh-WT, HY/Dhh-Het and HY/Dhh-KO were analyzed for T3.7, CD8 and CD4 cell surface expression. According to T3.7 expression, cells were sub-grouped into two main populations, HY-TCR positive cells ($T3.7^{+}$) and HY-TCR negative cells ($T3.7^{-}$). Within the T3.7 positive and negative compartments, cells were sub-grouped according to the cell surface expression of CD8 and CD4 into three main populations, the $CD8^{-}CD4^{-}$ (DN), $CD8^{+}CD4^{-}$ (SP8) and $CD8^{-}CD4^{+}$ (SP4).

Our data from male mice within the T3.7 positive cells showed an interesting finding as the majority of cells were SP8 cells, possibly having escaped deletion during their development in the thymus and eventually migrated to the spleen. However, we found no significance differences in these cells between the three genotypes of mice.

Our analysis of male splenocytes within the T3.7 positive cells show that the percentage of $CD8^{-}CD4^{-}$, SP8 and SP4 cells between the three genotypes of HY-Dhh was not statistically different ($p>0.05$, $n=4$). Similarly within the T3.7 negative cells, the percentage of $CD8^{-}CD4^{-}$, SP8 and SP4 cells between the three genotypes of HY-Dhh was not statistically different ($p>0.05$, $n=4$) (Figure 5.15) and (Figure 5.16).

In female mice, within the T3.7 positive cells, the percentage of $CD8^{-}CD4^{-}$, SP8 and SP4 cells between the three genotypes of HY-Dhh was not statistically different ($p>0.05$, $n=3$). Similarly, within the T3.7 negative cells, the percentage

of $CD8^{-}CD4^{-}$, SP8 and SP4 cells between the three genotypes of HY-Dhh was not different ($p>0.05$, n=3) (Figure 5.17) and (Figure 5.18).

5.2.9 Influence of Dhh on expression of CD3 and CD5 in HY-TCR splenocytes

In order to assess the potential influence of Dhh in TCR signal transduction in the periphery in HY-TCR mice, splenocytes from HY/Dhh-WT, HY/Dhh-Het and HY/Dhh-KO were analyzed for CD3, and CD5 expression within the $T3.7^{+}$ cells for $CD4^{-}CD8^{-}$, SP8 and SP4 cells. Furthermore, we have calculated the mean fluorescence intensity (MFI) for each of these molecules to estimate TCR signal strength.

Our data suggests that Dhh influenced CD3 expression in SP4 cells, as our data show that the expression of CD3 is reduced in these cells. Our analysis of male splenocytes within the T3.7 positive cells, showed that the percentage of $CD4^{-}CD8^{-}$ and SP8 cells expressing CD3 between the three genotypes of HY-Dhh was not different ($p>0.05$, n=4). However, the percentage of SP4 cells expressing CD3 in the HY/Dhh-KO was significantly lower than in the HY/Dhh-WT ($p\leq0.05$, n=4), and lower than in the HY/Dhh-Het, but this difference was not significant ($p>0.05$, n=4). CD3 MFI in $CD4^{-}CD8^{-}$, DP and SP8 cells between the three genotypes was not statistically different ($p>0.05$, n=4) (Figure 5.19).

Additionally, we observed no significant difference in the expression of CD5 or its MFI between the three genotypes of mice ($p>0.05$, n=4) (Figure 5.20). Furthermore, our analysis of female splenocytes within the T3.7 positive and negative cells, show no difference in the expression of CD3 or CD5 and their MFI

in splenocytes between the three genotypes of mice ($p>0.05$, n=3) (Figure 5.21) and (Figure 5.22).

5.2.10 Role of Dhh in splenocyte interactions

In order to assess the role of Dhh in influencing cell-cell interaction in HY-TCR mice, splenocytes from HY/Dhh-WT, HY/Dhh-Het and HY/Dhh-KO were analyzed for CD69 expression within the $T3.7^{+}$ cells for $CD4^{-}CD8^{-}$, SP8 and SP4 cells.

Our data show that Dhh does not alter the expression of CD69 in splenocytes in HY-TCR mice, as our analysis of male and female splenocytes show no difference in the expression of CD69 between the three genotypes of mice (($p>0.05$, n=4), ($p>0.05$, n=3)) respectively (Figure 5.23).

5.2.11 Role of Dhh in lymph node T cells of HY-TCR mice

In order to assess the role of Dhh in lymph node T cells of HY-TCR mice, cells from HY/Dhh-WT, HY/Dhh-Het and HY/Dhh-KO were analyzed for T3.7, CD8 and CD4 cell surface expression. According to T3.7 expression, cells were sub-grouped into two main populations, HY-TCR positive cells ($T3.7^{+}$) and HY-TCR negative cells ($T3.7^{-}$). Within the T3.7 positive and negative compartments, cells were sub-grouped according to the cell surface expression of CD8 and CD4 into three main populations, the $CD8^{-}CD4^{-}$ (DN), $CD8^{+}CD4^{-}$ (SP8) and $CD8^{-}CD4^{+}$ (SP4).

Our data show that Dhh influenced the proportions of SP8 in male mice within the T3.7 positive cells, suggesting its role in mature T cells. Furthermore, our data from female mice within the T3.7 negative cells show that Dhh influenced the proportion of SP4 cells, however, this influence seems to be from partial expression of Dhh.

Our analysis of male T cells within the T3.7 positive cells, show that the percentage of $CD8^{-}CD4^{-}$ and SP4 cells between the three genotypes of mice was not different ($p>0.05$, n=3). The percentage of SP8 cells in the HY/Dhh-KO was significantly higher than in the HY/Dhh-WT ($p\leq0.05$, n=3) (Figure 5.24). Within the T3.7 negative cells, the percentage of $CD8^{-}CD4^{-}$, SP8 and SP4 cells between the three genotypes of mice was not different ($p>0.05$, n=3) (Figure 5.25).

Furthermore, our data from female T cells, within the T3.7 positive cells, shows that the percentage of $CD8^{-}CD4^{-}$and SP8 cells between the three genotypes of mice was not different ($p>0.05$, n=3). The percentage of SP4 cells in HY/Dhh-Het was significantly higher compared to the HY/Dhh-WT ($p\leq0.05$, n=3) (Figure 5.26). Similarly, within the T3.7 negative cells, the percentage of $CD8^{-}CD4^{-}$ and SP8 cells between the three genotypes of mice was not different ($p>0.05$, n=3). However, the percentage of SP4 cells in the HY/Dhh-Het was significantly increased compared to the HY/Dhh-WT ($p\leq0.05$, n=3) (Figure 5.27).

5.2.12 Influence of Dhh on expression of CD3 and CD5 in HY-TCR in the lymph node

In order to assess the potential influence of Dhh in TCR signal transduction in the lymph node of HY-TCR mice, cells from HY/Dhh-WT, HY/Dhh-Het and

HY/Dhh-KO were analyzed for CD3, and CD5 expression within the $T3.7^{+}$ cells for $CD4^{-}CD8^{-}$, SP8 and SP4 cells. Furthermore, we have calculated the mean fluorescence intensity (MFI) for each of these molecules to estimate TCR signal strength.

Our data from male and female mice show that Dhh does not influence the expression of CD3 and CD5. Our analysis of male T cells within the T3.7 positive cells, show that the percentage of $CD4^{-}CD8^{-}$, SP8 and SP4 cells expressing CD3, CD5 and their MFI between the three genotypes of mice was not statistically different ($p>0.05$, n=3) (Figure 5.28) and (Figure 5.29). Furthermore, our analysis of female T cells within the T3.7 positive cells, show that the percentage of $CD4^{-}CD8^{-}$, SP8 and SP4 cells expressing CD3, CD5 and their MFI between the three genotypes of mice was not statistically different ($p>0.05$, n=3) (Figure 5.30) and (Figure 5.31).

5.2.13 Thymocytes and splenocytes in Marilyn-Gli2ΔC2 $Rag2^{-/-}$ littermates

Following anatomical extraction of the thymus and spleen from Marilyn-Gli2ΔC2 $Rag2^{-/-}$ littermates, the thymocytes and splenocytes were collected for analysis. In regards to live cell counts in the thymus, we observed no significant difference in the mean cell numbers between the two genotypes of Marilyn-Gli2ΔC2 male and female littermates (($p>0.05$, n=5), ($p>0.05$, n=5)) respectively. In regards to live cell counts in the spleen, we observed a significant decrease in the male Marilyn-$Gli2\Delta C2^{+}$ compared to the Marilyn-$Gli2\Delta C2^{-}$ ($p\leq0.005$, n=4). Furthermore, in the female spleen, we observed no significant difference between the two genotypes of Marilyn-Gli2ΔC2 littermates ($p>0.05$, n=6) (Figure 5.32).

5.2.14 Role of Hh signalling in thymocyte development during Selection in Marilyn-Gli2ΔC2 Rag2$^{-/-}$ mice

In order to assess the role of Hh signalling in thymocytes during selection, thymocytes from Marilyn-Gli2ΔC2^{-} and Marilyn-Gli2ΔC2^{+} male and female mice were analyzed for Vβ6, CD8 and CD4 cell surface expression. Marilyn-TCR uses Vβ6, and according to the cell surface expression of CD4 and CD8, cells were sub-grouped into four main populations, the CD8^{-}CD4^{-} (DN), CD8^{+}CD4^{+} (DP), CD8^{+}CD4^{-} (SP8) and CD8^{-}CD4^{+} (SP4).

Our data from male and female mice shows that Hh signalling influences selection of thymocytes during their development in the thymus. Our data from male mice, showed that the percentage of DN cells was significantly lower in the Marilyn-Gli2ΔC2^{+} than in the Marilyn-Gli2ΔC2^{-} ($p \leq 0.05$, n=7). In addition, the percentage of DP cells was significantly higher in the Marilyn-Gli2ΔC2^{+} than in the Marilyn-Gli2ΔC2^{-} ($p \leq 0.05$, n=7). The percentage of SP8 cells was decreased in the Marilyn-Gli2ΔC2^{+} compared to Marilyn-Gli2ΔC2^{-}, but this difference was not significant ($p > 0.05$, n=7). The percentage of SP4 cells was significantly higher in the Marilyn-Gli2ΔC2^{+} than in the Marilyn-Gli2ΔC2^{-} ($p \leq 0.005$, n=7) (Figure 5.33).

Furthermore, in female mice, we observed no difference in the percentage of DN cells between the two genotypes of mice ($p > 0.05$, n=6). On the contrary, the percentage of DP was significantly reduced in the Marilyn-Gli2ΔC2^{+} than in the Marilyn-Gli2ΔC2^{-} ($p \leq 0.05$, n=6). The percentage of SP8 and SP4 cells was significantly increased in the Marilyn-Gli2ΔC2^{+} compared to Marilyn-Gli2ΔC2^{-} (($p \leq 0.005$, n=6), ($p \leq 0.05$, n=6)) respectively (Figure 5.34). These data indicate

that inhibition of Hh-dependent transcription by expression of the Gli2ΔC2 transgene increased positive selection of the transgenic TCR, and differentiation from DP to SP cells.

5.2.15 Influence of Hh signalling on the expression of CD3 and CD5 in Marilyn-Gli2ΔC2 thymocytes

In order to assess the potential role of Hh signalling in regulating differentiation and TCR signal transduction of Marilyn-Gli2ΔC2 thymocytes during development and selection, we analyzed the cell surface expression of molecules associated with TCR signalling (CD3 and CD5) in DN, DP, SP8 and SP4 cells in Marilyn-Gli2ΔC2^{-} and Marilyn-Gli2ΔC2^{+}. Furthermore we have compared the mean fluorescence intensity (MFI) of staining for these molecules, as high CD5 expression is associated with high TCR signal strength.

Our analysis of male and female show that inhibition of Hh signalling influenced the expression of CD3 and CD5 and their MFI. Our analysis of male mice show that the percentage of DN, DP and SP8 cells expressing CD3 in the Marilyn-Gli2ΔC2^{+} between the two genotypes of mice was not significant ($p>0.05$, n=6). The percentage of SP4 cells expressing CD3 in the Marilyn-Gli2ΔC2^{+} was significantly higher than in the Marilyn-Gli2ΔC2^{-} ($p\leq0.05$, n=6). Similarly, CD3 MFI in DN, DP and SP8 between the two genotypes of Marilyn-Gli2ΔC2 was statistically not significant ($p>0.05$, n=6). CD3 MFI in SP4 cells was significantly lower in the Marilyn-Gli2ΔC2^{+} compared to the Marilyn-Gli2ΔC2^{-} ($p\leq0.05$, n=6) (Figure 6.35).

Furthermore, we examine the expression of CD5 and our analysis show that the percentage of DN, DP and SP8 cells between the two genotypes of mice was not different ($p>0.05$, n=6). The percentage of SP4 cells expressing high levels of CD5 in the Marilyn-Gli2ΔC2^{+} was significantly higher than in the Marilyn-Gli2ΔC2^{-} ($p\leq0.005$, n=6). Differences in CD5 MFI in DN, DP and SP8 between the two genotypes of mice was statistically not significant ($p>0.05$, n=6), however, CD5 MFI in SP4 cells was significantly higher in the Marilyn-Gli2ΔC2^{+} compared to the Marilyn-Gli2ΔC2^{-} (Figure 5.36). As these mice are Rage$^{-/-}$, the influence on CD5 expression cannot be due to changes in the repertoire of TCRs that have been selected.

In female mice, the percentage of DN, DP, SP8 and SP4 cells expressing CD3 between the two genotypes of Marilyn-Gli2ΔC2 was statistically not significant ($p>0.05$, n=4). Similarly, CD3 MFI in DN, DP, SP8 and SP4 between the two genotypes of mice was not different ($p>0.05$, n=4) (Figure 5.37).

In regards to CD5 expression, our data show that the percentage of DN cells expressing CD5 in the Marilyn-Gli2ΔC2^{+} was not significantly higher than in the Marilyn-Gli2ΔC2^{-} ($p>0.05$, n=4). The percentage of SP4 cells expressing CD5 in the Marilyn-Gli2ΔC2^{+} was not significantly higher than in the Marilyn-Gli2ΔC2^{-} ($p>0.005$, n=4). CD5 MFI in DN and DP cells between the two genotypes of mice was not significantly different ($p>0.05$, n=4). CD5 MFI in SP8 and SP4 cells in the Marilyn-Gli2ΔC2^{+} was not significantly higher than in the Marilyn-Gli2ΔC2^{-} ($p>0.05$, n=4) (Figure 5.38).

5.2.16 Role of Hh signalling in thymocyte interactions during development and selection in Marilyn-Gli2ΔC2 mice

As CD69 expression correlates with positive selection in thymocytes, cells from Marilyn-Gli2ΔC2^{-} and Marilyn-Gli2ΔC2^{+} were analyzed for CD69 expression within the DN, DP, SP8 and SP4 cells.

Our Data show that Hh signalling does not influence the expression of CD69 in developing thymocytes during selection, as our analysis of male and female thymocytes show that the percentage of DN, DP, SP8 and SP4 cells expressing CD69 between the two genotypes of mice was not statistically different (($p>0.05$, $n=3$), ($p>0.05$, $n=3$)) respectively (Figure 5.39).

5.2.17 Influence of Hh signalling on Gata-3 expression in thymocytes during development and selection in Marilyn-Gli2ΔC2 mice

In order to assess the influence of Hh signalling in the expression of Gata-3 during thymocyte development and selection, thymocytes from Marilyn-Gli2ΔC2^{-} and Marilyn-Gli2ΔC2^{+} were analyzed for Gata-3 expression within the DN, DP, SP8 and SP4 cells. Gata-3 is involved in CD4 lineage commitment and stronger TCR signals are believed to lead to higher expression of Gata-3.

Our data show that Hh signalling influences the expression of Gata3 in developing thymocytes. Our analysis of male thymocytes show that the percentage of DN, DP and SP8 cells expressing Gata-3 between the two genotypes of mice was not different ($p>0.05$, $n=3$). Furthermore, the percentage of SP4 cells expressing Gata-3 in the Marilyn-Gli2ΔC2^{+} was significantly lower compared to the Marilyn-

Gli2ΔC2^{-} ($p \leq 0.05$, n=3). In female mice, the percentage of DN, DP, SP8 and SP4 cells expressing Gata-3 between the two genotypes of mice was not statistically different ($p > 0.05$, n=3) (Figure 5.40).

5.2.18 Impact of inhibition of Hh signalling on Foxp3 expression in thymocytes during development and selection in Marilyn-Gli2ΔC2 mice

In order to assess the influence of inhibition of Hh signalling on the expression of Foxp3 during thymocyte development and selection, thymocytes from Marilyn-Gli2ΔC2^{-} and Marilyn-Gli2ΔC2^{+} were analyzed for Foxp3 expression within the SP4 cells. Foxp3 is the transcription factor believed to be master regulator of the Treg lineage.

Our data show that inhibition of Hh signalling influenced the expression of Foxp3 as our analysis of male mice show that the percentage of SP4 cells expressing Foxp3 in the Marilyn-Gli2ΔC2^{+} was significantly higher compared to the Marilyn-Gli2ΔC2^{-} ($p \leq 0.005$, n=3) (Figure 5.41). However, in female mice, the percentage of SP4 cells expressing Foxp3 between the two genotypes of mice was not significantly different ($p > 0.05$, n=3) (Figure 5.41). These increases in Foxp3 expression in the male thymus suggests that inhibition of Hh mediated transcription has increased TCR signal strength in the male to a level where cells which would not have been positively selected are now selected using a very strong signal (in presence of cognate male peptide).

5.2.19 Role of Hh signalling in thymocyte maturation during development and selection in Marilyn-Gli2ΔC2 mice

In order to assess the role of Hh signalling in influencing cell maturation of the single positive populations during thymocyte development and selection, thymocytes from Marilyn-Gli2ΔC2^{-} and Marilyn-Gli2ΔC2^{+} were analyzed for Qa2 and HSA expression in DP, SP8 and SP4 cells.

Our data show that Hh signalling influence maturation of SP cells during their development and maturation within the thymus. Our analysis of male thymocytes show that the differences in the percentage of DP, SP8 and SP4 cells expressing Qa2 or both, Qa2 and HSA, between the two genotypes of mice was not statistically significant ($p>0.05$, n=3). On the contrary, the percentage of DP cells expressing HSA was significantly higher in the Marilyn-Gli2ΔC2^{+} compared to the Marilyn-Gli2ΔC2^{-} ($p\leq0.05$, n=3). Furthermore, the percentage of SP4 cells expressing HSA was significantly higher in the Marilyn-Gli2ΔC2^{+} compared to the Marilyn-Gli2ΔC2^{-} ($p\leq0.05$, n=3) (Figure 5.42). This is consistent with more immature cells getting selected to the CD4 lineage.

In female mice, the percentage of DP and SP4 cells expressing Qa2 and, both Qa2 and HSA between the two genotypes of mice was not statistically significant ($p>0.05$, n=3). The percentage of SP8 cells expressing Qa2 was significantly lower in the Marilyn-Gli2ΔC2^{+} compared to the Marilyn-Gli2ΔC2^{-} ($p\leq0.005$, n=3). On the contrary, the percentage of SP8 cells expressing both Qa2 and HSA was significantly higher in the Marilyn-Gli2ΔC2^{+} compared to the Marilyn-Gli2ΔC2^{-} ($p\leq0.05$, n=3). Furthermore, the percentage of DP, SP8 and SP4 cells expressing HSA was significantly higher in the Marilyn-Gli2ΔC2^{+} compared to

the Marilyn-Gli2ΔC2^{-} (($p \leq 0.005$, n=3), ($p \leq 0.05$, n=3), ($p \leq 0.005$, n=3)) respectively (Figure 5.43). These data are consistent with increased positive selection of more immature cells.

5.2.20 Influence of Hh signalling in spleen T cells of Marilyn-Gli2ΔC2 mice

In order to assess the influence of Hh signalling in spleen T cells in the periphery in Marilyn-Gli2ΔC2 mice, splenocytes from Marilyn-Gli2ΔC2^{-} and Marilyn-Gli2ΔC2^{-} were analyzed for CD8 and CD4 cell surface expression. According to the cell surface expression of CD4 and CD8, cells were sub-grouped into three main populations, the CD8^{-}CD4^{-} (DN), CD8^{+}CD4^{-} (SP8) and CD8^{-}CD4^{+} (SP4).

Our data show that inhibition of Hh signalling also influenced the T cells in the periphery, as our analysis of male mice show that the percentage of SP4 cells in the Marilyn-Gli2ΔC2^{+} was significantly higher compared to the Marilyn-Gli2ΔC2^{-} ($p \leq 0.0005$, n=5). On the contrary, the percentage of SP8 and CD8^{-}CD4^{-} cells between the two genotypes of mice was not different ($p > 0.05$, n=5) and ($p > 0.05$, n=5) respectively (Figure 5.44).

Furthermore, in female mice, the percentage of CD8^{-}CD4^{-} and SP4 cells between the two genotypes of Marilyn-Gli2ΔC2 was not statistically different ($p > 0.05$, n=3). However, the percentage of SP8 cells in the Marilyn-Gli2ΔC2^{+} was significantly higher compared to the Marilyn-Gli2ΔC2^{-} ($p \leq 0.0005$, n=3) (Figure 5.45). Thus, expression of the Gli2ΔC2 transgene allowed the MHC class-II-restricted TCR to be selected to the CD8 lineage, as CD8 T cells were found in the periphery of the female mice.

6.2.21 Influence of Hh signalling on the expression of CD3 and CD5 in Marilyn-Gli2ΔC2 splenocytes

In order to assess the potential role of Hh signalling in regulating differentiation and TCR signal transduction of Marilyn-Gli2ΔC2 splenocytes, we analyzed the cell surface expression of molecules associated with TCR signalling (CD3 and CD5) in DN, DP, SP8 and SP4 cells in Marilyn-Gli2ΔC2^{-} and Marilyn-Gli2ΔC2^{+}. Furthermore we compared the mean fluorescence intensity (MFI) of staining for these molecules, as high CD5 expression is associated with high TCR signal strength.

Our data show that inhibition of Hh signalling influenced the expression of CD3 and CD5 and their MFI in splenocytes. Our analysis of male splenocytes showed that the percentage of CD8^{-}CD4^{-} and SP8 cells expressing CD3 between the two genotypes of mice was not significant ($p>0.05$, n=5). However, the percentage of SP4 cells expressing high levels of CD3 in the Marilyn-Gli2ΔC2^{+} was significantly higher than in the Marilyn-Gli2ΔC2^{-} ($p\leq0.05$, n=5). Differences in CD3 MFI in CD8^{-}CD4^{-} and SP8 cells between the two genotypes of mice were not significant ($p>0.05$, n=5). On the contrary, CD3 MFI in SP4 cells was significantly higher than in the Marilyn-Gli2ΔC2^{-} ($p\leq0.005$, n=5) (Figure 5.46).

In addition, we examined the expression of CD5, and our data show that the percentage of CD8^{-}CD4^{-} and SP4 cells expressing high levels of CD5 between the two genotypes of mice was not significant ($p>0.05$, n=5). However, the percentage of SP8 cells expressing CD5 in the Marilyn-Gli2ΔC2^{+} was significantly higher than in the Marilyn-Gli2ΔC2^{-} ($p\leq0.05$, n=5). Although CD5 MFI in CD8^{-}CD4^{-} and SP8 cells between the two genotypes of mice was not

statistically significant ($p>0.05$, n=5). CD5 MFI in SP4 cells was significantly higher than in the Marilyn-Gli2ΔC2^{-} ($p\leq0.005$, n=5) (Figure 5.47). Cell surface CD5 expression is believed to correlate with TCR signal strength, and so the increase in MFI is consistent with an increase in TCR signal strength.

In female mice, the percentage of CD8^{-}CD4^{-} and SP4 cells expressing CD3 between the two genotypes of mice was statistically not significant ($p>0.05$, n=3). However, the percentage of SP8 cells expressing high levels of CD3 in the Marilyn-Gli2ΔC2^{+} was significantly higher than in the Marilyn-Gli2ΔC2^{-} ($p\leq0.05$, n=4). In regards to CD3 MFI, our data show no statistical difference in CD8^{-}CD4^{-} and SP4 cells between the two genotypes of mice ($p>0.05$, n=4). However, CD3 MFI in SP8 cells was significantly higher in Marilyn-Gli2ΔC2^{+} than in the Marilyn-Gli2ΔC2^{-} ($p\leq0.005$, n=4) (Figure 5.48).

In addition, we examined the expression of CD5 in female mice, and our data showed no difference in the percentage of CD5 expressing CD8^{-}CD4^{-} cells between the two genotypes of mice ($p>0.05$, n=4). On the contrary, the percentage of SP8 cells expressing high levels of cell surface CD5 in the Marilyn-Gli2ΔC2^{+} was significantly higher than in the Marilyn-Gli2ΔC2^{-} ($p\leq0.005$, n=4). The percentage of SP4 cells expressing CD5 in the Marilyn-Gli2ΔC2^{+} was significantly lower than in the Marilyn-Gli2ΔC2^{-} ($p\leq0.05$, n=4). Furthermore, CD5 MFI in CD8^{-}CD4^{-} between the two genotypes of Marilyn-Gli2ΔC2 was not significant ($p>0.05$, n=4). However, CD5 MFI in SP8 and SP4 cells was significantly higher than in the Marilyn-Gli2ΔC2^{-} (($p\leq0.005$, n=4), ($p\leq0.05$, n=4)) (Figure 5.49).

5.2.22 Influence of Hh signalling in splenocyte activation in Marilyn-Gli2ΔC2 mice

In order to assess the influence of Hh signalling on splenocyte activation ex-vivo, splenocytes from Marilyn-Gli2ΔC2^{-} and Marilyn-Gli2ΔC2^{+} were analyzed for CD69 expression within the CD8^{-}CD4^{-}, SP8 and SP4 cells.

Our data show that inhibition of Hh signalling influenced the expression of CD69, as our data from male mice show that the percentage of SP4 cells expressing CD69 in the Marilyn-Gli2ΔC2^{+} was significantly higher compared to the Marilyn-Gli2ΔC2^{-} ($p \leq 0.05$, n=3). On the contrary, the percentage of CD8^{-}CD4^{-}, and SP8 cells expressing CD69 between the two genotypes of mice was not statistically different ($p > 0.05$, n=3) (Figure 5.50).

In female mice, the percentage of CD8^{-}CD4^{-} and SP8 cells expressing CD69 between the two genotypes of mice was not different ($p > 0.05$, n=3). However, the percentage of SP4 cells expressing CD69 was significantly lower in the Marilyn-Gli2ΔC2^{+} compared to the Marilyn-Gli2ΔC2^{-} ($p \leq 0.05$, n=3) (Figure 5.50).

5.2.23 Influence of Hh signalling in lymph node T cells of Marilyn-Gli2ΔC2 mice

In order to assess the effect of inhibition of Hh signalling in lymph node T cells in Marilyn-Gli2ΔC2 mice, cells from Marilyn-Gli2ΔC2^{-} and Marilyn-Gli2ΔC2^{-} were analyzed for CD8 and CD4 cell surface expression.

As in the spleen, our analysis of male mice show that the percentage of SP8 and SP4 cells in the Marilyn-Gli2ΔC2^{+} was significantly higher compared to the

Marilyn-Gli2ΔC2^{-} ($p \leq 0.005$, n=5) (Figure 5.51). However, in female mice, the differences percentage of CD8^{-}CD4^{-}, SP8 and SP4 cells between the two genotypes of mice was not statistically different ($p > 0.05$, n=3) (Figure 5.52).

5.2.24 Influence of inhibition of Hh signalling on the expression of CD3 and CD5 in the lymph node of Marilyn-Gli2ΔC2

We also analyzed the cell surface expression of molecules associated with TCR signalling (CD3 and CD5) in DN, DP, SP8 and SP4 cells in Marilyn-Gli2ΔC2^{-} and Marilyn-Gli2ΔC2^{+}. Furthermore we compared the mean fluorescence intensity (MFI) of staining for these molecules, as high CD5 expression is associated with high TCR signal strength.

Our data from the lymph node confirm our previous finding in the spleen, as we found that inhibition of Hh signalling influenced the expression of CD3 and CD5 in mature cells. Our analysis of male mice show that the percentage of SP8 and SP4 cells expressing high levels of CD3 in the Marilyn-Gli2ΔC2^{+} was significantly higher than in the Marilyn-Gli2ΔC2^{-} (($p \leq 0.005$, n=5), ($p \leq 0.05$, n=4)) respectively. However, CD3 MFI in CD8^{-}CD4^{-}, SP8 and SP4 cells between the two genotypes of mice was not different ($p > 0.05$, n=4) (Figure 5.53).

In regards to CD5 expression, our data show that the percentage of SP8 and SP4 cells expressing high levels of CD5 in the Marilyn-Gli2ΔC2^{+} was significantly higher than in the Marilyn-Gli2ΔC2^{-} (($p \leq 0.05$, n=4), ($p \leq 0.005$, n=4)) respectively. However, CD5 MFI in SP8 cells in the Marilyn-Gli2ΔC2^{+} was significantly lower than in the Marilyn-Gli2ΔC2^{-} ($p \leq 0.05$, n=4). Similarly, CD5 MFI in SP4 cells in

the Marilyn-Gli2ΔC2^{+} was significantly higher than in the Marilyn-Gli2ΔC2^{-} ($p \leq 0.005$, n=4) (Figure 5.54).

In female mice, our data show that the percentage of CD8^{-}CD4^{-}, SP8 and SP4 cells expressing CD3 and CD5 between the two genotypes of mice was statistically not significant ($p > 0.05$, n=3). Similarly, CD3 and CD5 MFI in CD8^{-}CD4^{-}, SP8 and SP4 cells between the two genotypes of mice was not different ($p > 0.05$, n=3) (Figure 5.55) and (Figure 5.56).

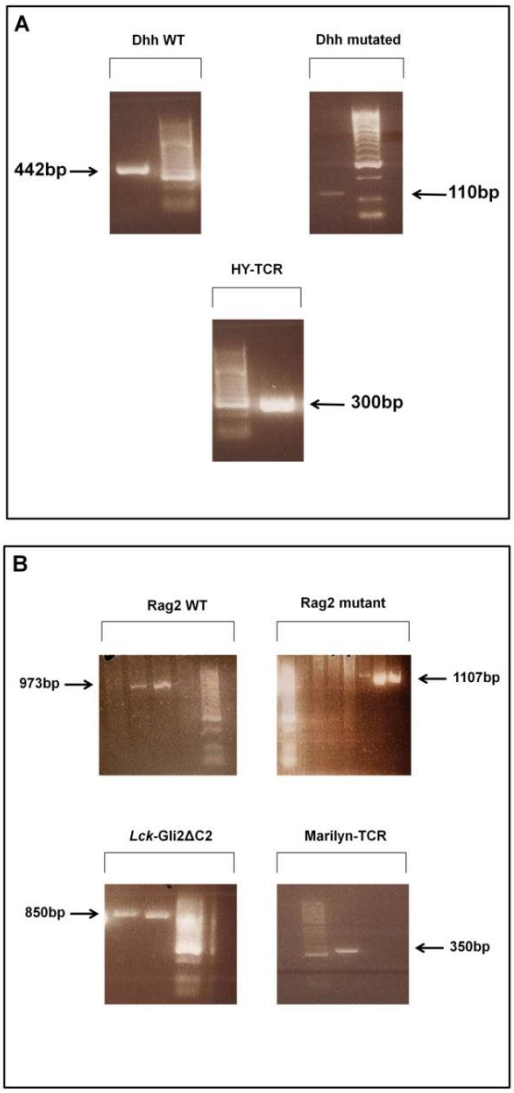

Figure 5.1

Genotyping of HY-Dhh and Marilyn-Gli2ΔC2 littermates. (A) The genotyping of HY-Dhh littermates by PCR using genomic DNA extracted from ear biopsies. The presence of the HY-TCR transgene generated a PCR product of 300bp, the presence of Dhh-wild type (Dhh-WT) allele generated a PCR product of 442bp, while the presence of the Dhh-mutated allele (Dhh-KO) generated a PCR product of 110bp. **(B)** The genotyping of Marilyn-Gli2ΔC2 littermates by PCR using genomic DNA extracted from ear biopsies. The presence of the Marilyn-TCR transgene generated a PCR product of 350bp, the presence of the Gli2ΔC2 transgene generated a PCR product of 850bp, the presence of the Rag-2 WT gene generated a PCR product of 973bp, while the presence of Rag2 mutated gene generated a PCR product of 1107bp.

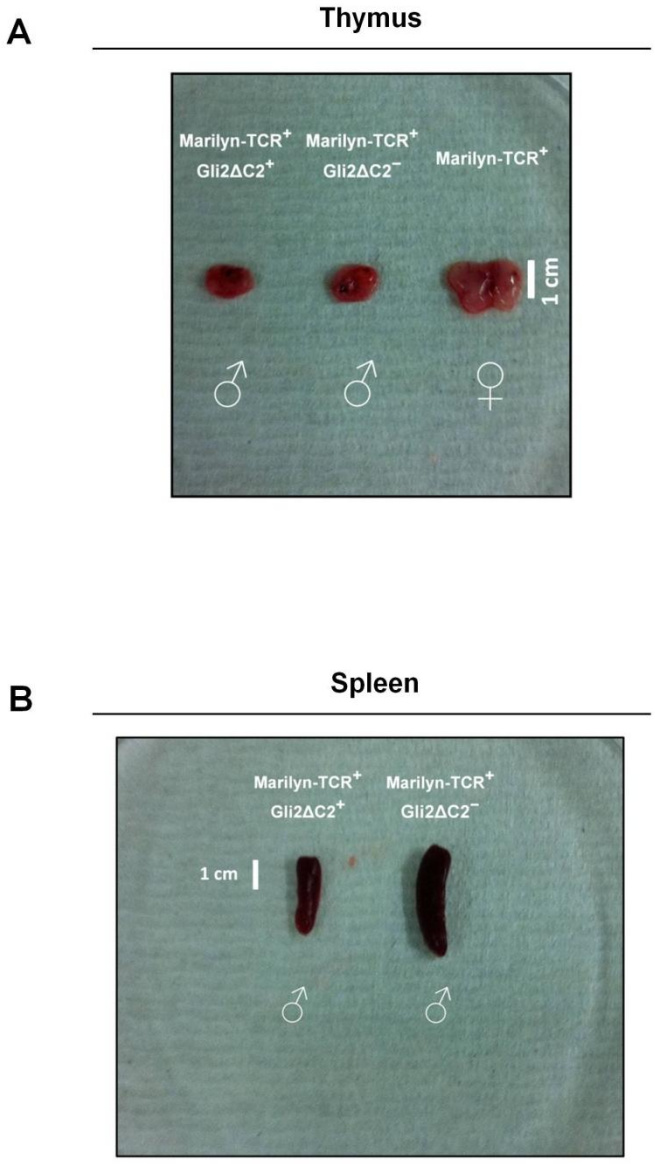

Figure 5.2

Thymus and spleen of male Marilyn-Gli2ΔC2 littermates. Freshly isolated thymus and spleen of 5-weeks old male Marilyn-Gli2ΔC2 littermates. **(A)** Thymus from male Marilyn-Gli2ΔC2^{+} (left), male Marilyn-Gli2ΔC2^{-} (middle) and a female Marilyn-TCR^{+} (right) (the female Marilyn-TCR^{+} thymus was used in this figure for size comparison with male thymus). **(B)** Spleen from male Marilyn-Gli2ΔC2^{+} (left) and male Marilyn-Gli2ΔC2^{-} (right).

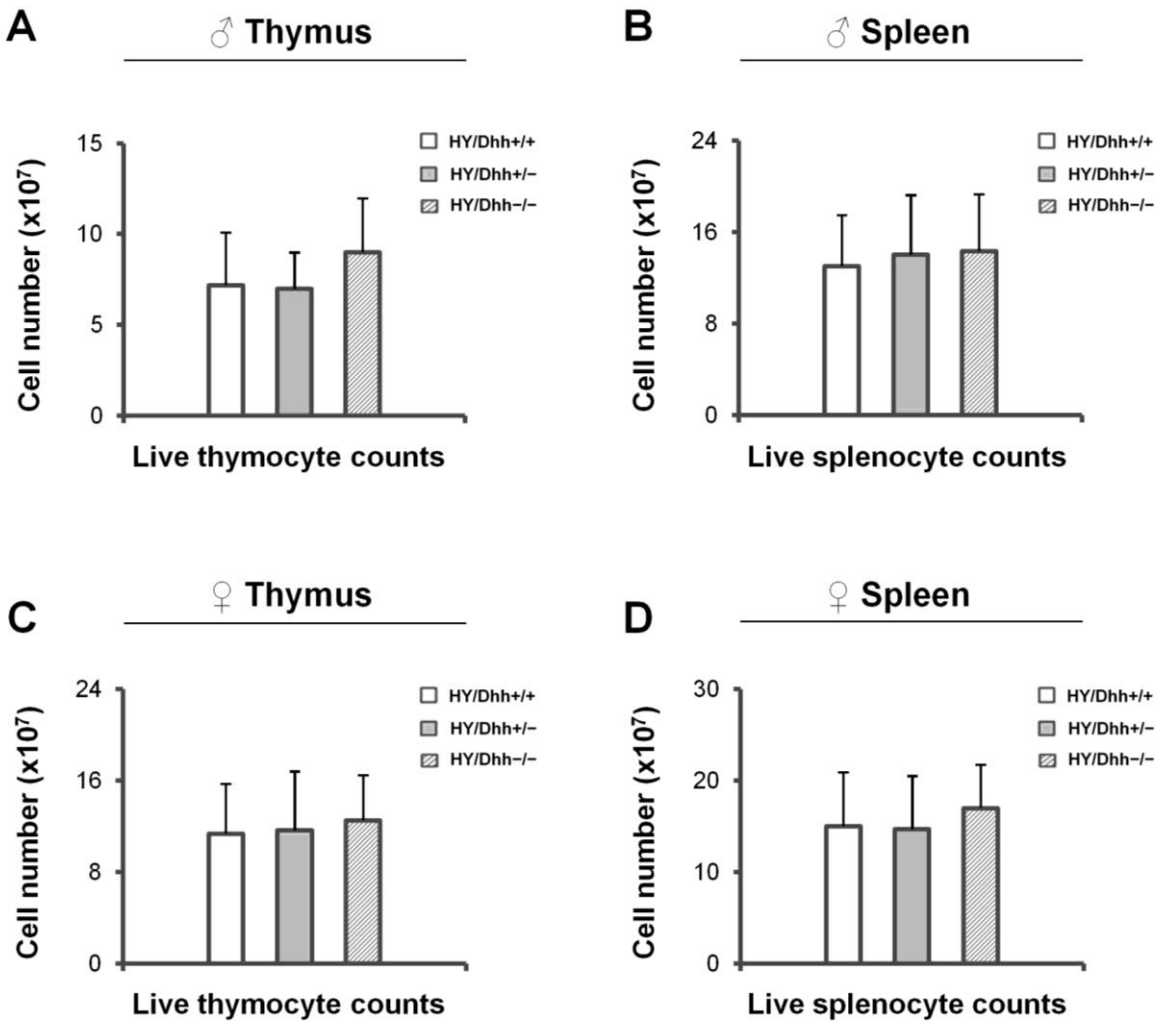

Figure 5.3

Thymus and spleen live cell counts in male and female HY-Dhh littermates. Thymocyte and splenocyte total counts from adult male and female HY/Dhh-WT, HY/Dhh-Het and HY/Dhh-KO littermates. **(A)** Live male thymocyte counts. **(B)** Live male splenocyte counts. **(C)** Live female thymocyte counts. **(D)** Live female splenocyte counts. Mean and standard deviation of each population are given. Bars represent mean ± standard deviations. **Male thymocytes;** (p=0.06 (WT/Het), 0.4 (WT/KO), 0.6 (Het/KO), n=5). **Male splenocytes;** (p=0.1 (WT/Het), 0.3 (WT/KO), 0.2 (Het/KO), n=5). **Female thymocytes;** (p=0.3 (WT/Het), 0.2 (WT/KO), 0.1 (Het/KO), n=7). **Female plenocytes;** (p=0.1 (WT/Het), 0.3 (WT/KO), 0.1 (Het/KO), n=7).

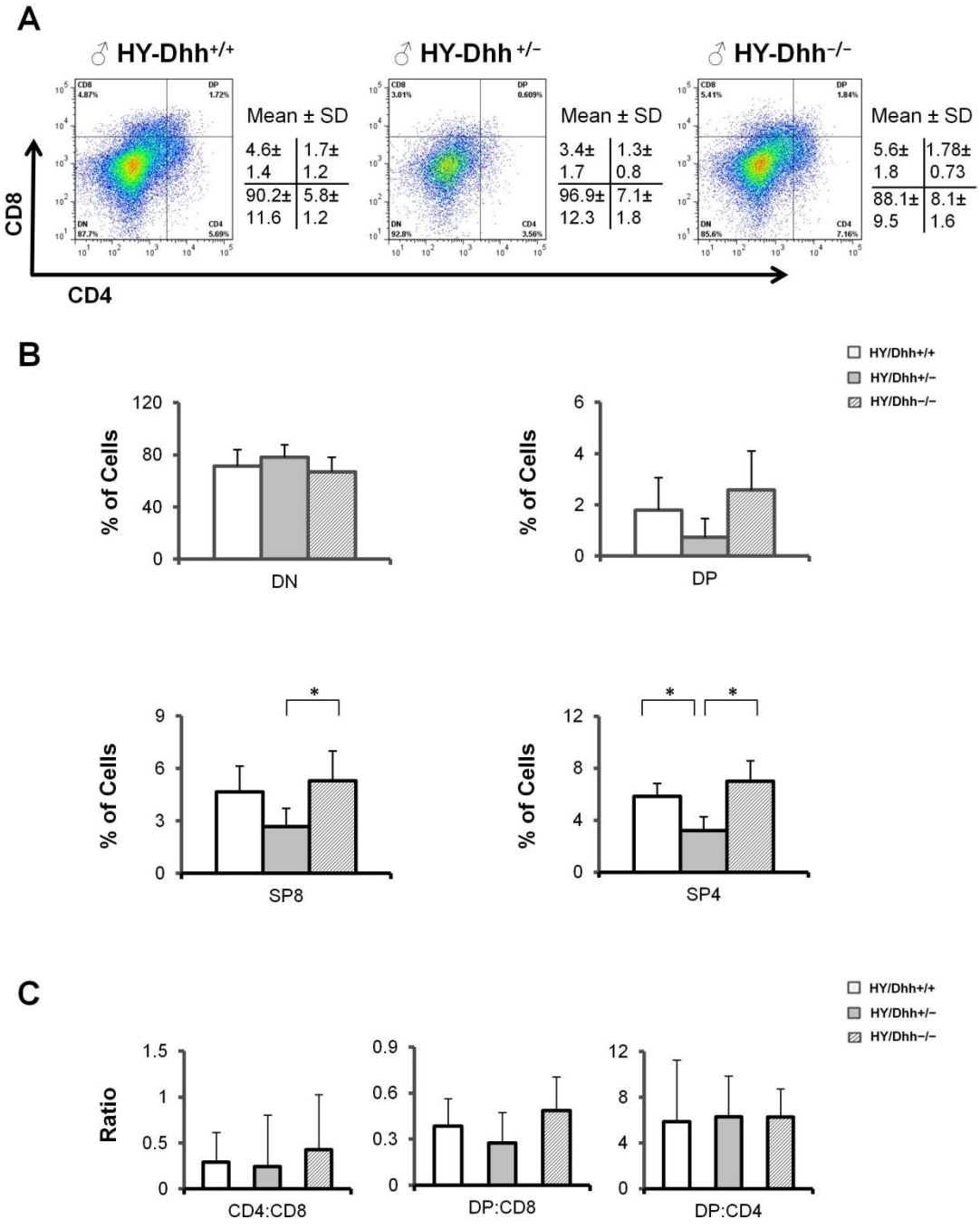

Figure 5.4

Major thymocyte populations in male HY-Dhh within the T3.7 positive cells. Percentage of thymocyte populations from adult male HY/Dhh-WT, HY/Dhh-Het and HY/Dhh-KO littermates. Thymocytes were stained for anti-T3.7, anti-CD8 and anti-CD4, and analyzed by flow cytometry. Thymocyte populations were gated within the $T3.7^{+}$ cells. **(A)** Representative dot plot of thymocyte populations. **(B)** Representative bar graph of DN, DP, SP8 and SP4 percentages. **(C)** Ratios of CD4:C8, DP:CD8 and DP:CD4. Figures are representative of 5 independent sets of male HY-Dhh littermates. Mean and standard deviation of each population are given. Bars represent mean ± standard deviations. **DN** (p= 0.4 (WT/Het), 0.6 (WT/KO), 0.1 (Het/KO), n=5). **DP** (p= 0.2 (WT/Het), 0.4 (WT/KO), 0.9 (Het/KO), n=5). **SP8** (p= 0.07 (WT/Het), 0.5 (WT/KO), 0.04 (Het/KO), n=5). **SP4** (p= 0.01 (WT/Het), 0.2 (WT/KO), 0.009 (Het/KO), n=5). *represents $p \leq 0.05$.

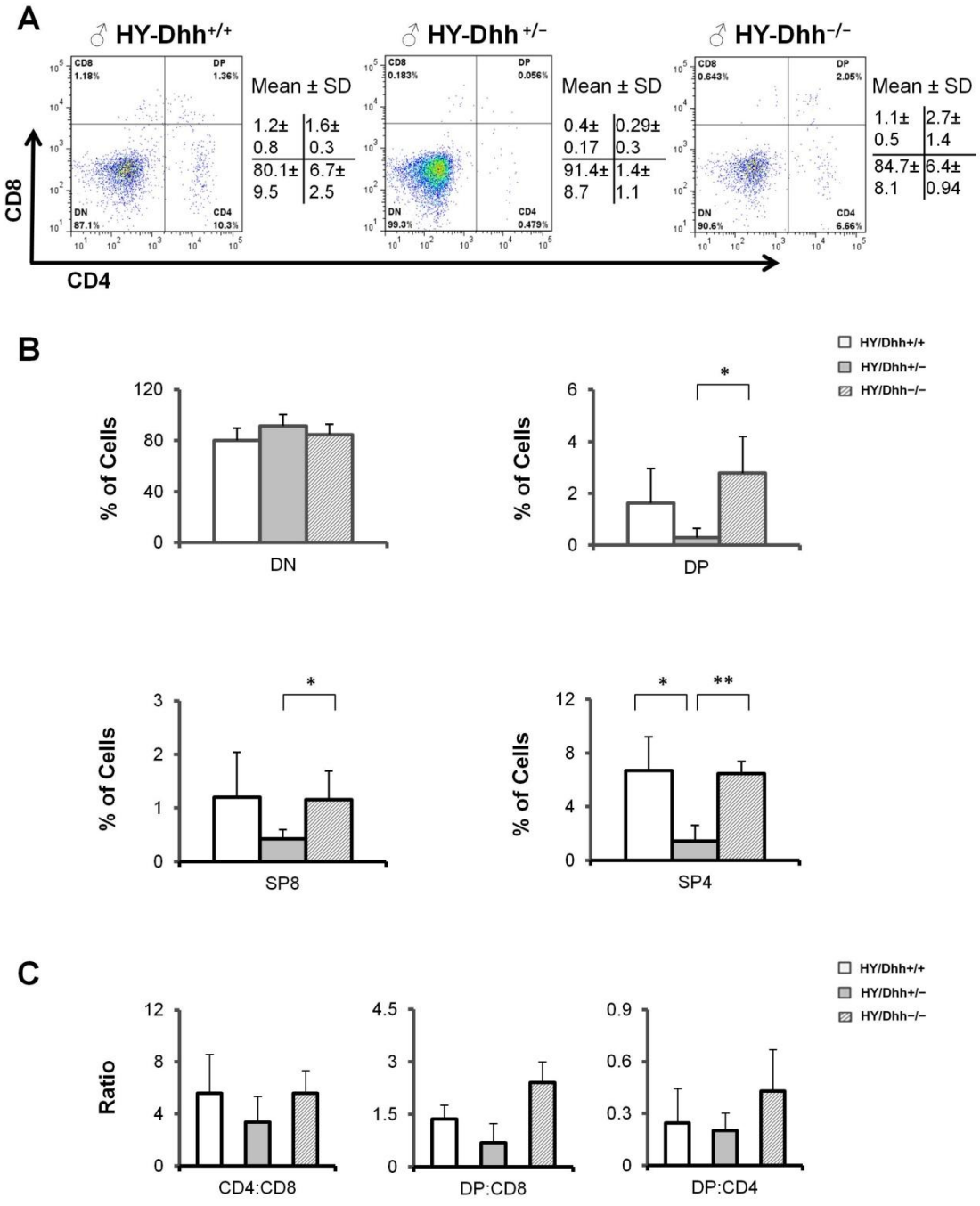

Figure 5.5

Major thymocyte populations in male HY-Dhh within the T3.7 negative cells. Percentage of thymocyte populations from adult male HY/Dhh-WT, HY/Dhh-Het and HY/Dhh-KO littermates. Thymocytes were stained for anti-T3.7, anti-CD8 and anti-CD4, and analyzed by flow cytometry. Thymocyte populations were gated within the $T3.7^{-}$ cells. **(A)** Representative dot plot of thymocyte populations. **(B)** Representative bar graph of DN, DP, SP8 and SP4 percentages. **(C)** Ratios of CD4:C8, DP:CD8 and DP:CD4. Figures are representative of 5 independent sets of male HY-Dhh littermates. Mean and standard deviation of each population are given. Bars represent mean ± standard deviations. **DN** (p= 0.1 (WT/Het), 0.4 (WT/KO), 0.3 (Het/KO), n=5). **DP** (p= 0.1 (WT/Het), 0.2 (WT/KO), 0.03 (Het/KO), n=5). **SP8** (p= 0.1 (WT/Het), 0.9 (WT/KO), 0.05 (Het/KO), n=5). **SP4** (p= 0.01 (WT/Het), 0.8 (WT/KO), 0.0006 (Het/KO), n=5). *represents p≤0.05, **represents p≤0.005.

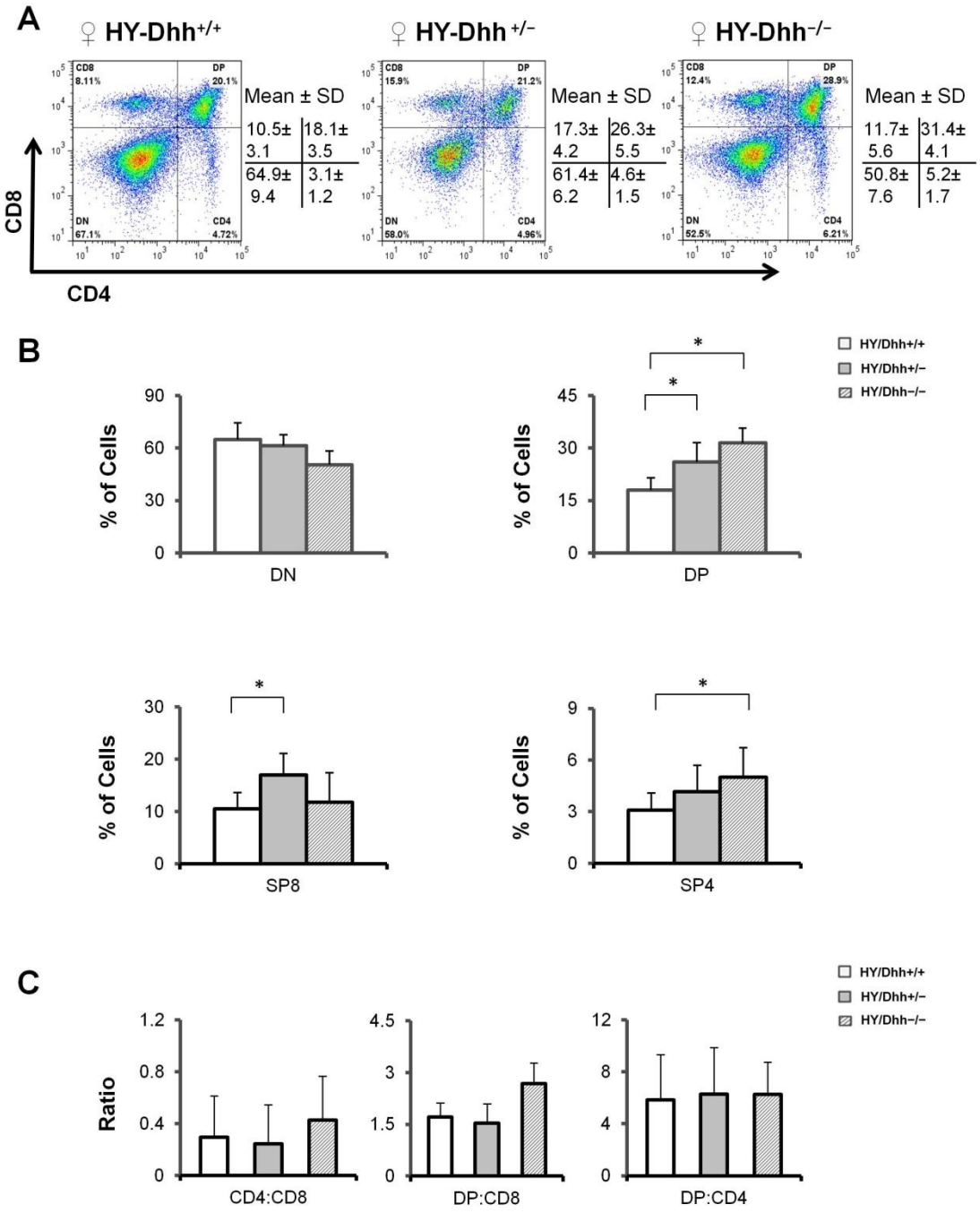

Figure 5.6

Major thymocyte populations in female HY-Dhh within the T3.7 positive cells. Percentage of thymocyte populations from adult female HY/Dhh-WT, HY/Dhh-Het and HY/Dhh-KO littermates. Thymocytes were stained for anti-T3.7, anti-CD8 and anti-CD4, and analyzed by flow cytometry. Thymocyte populations were gated within the $T3.7^{+}$ cells. **(A)** Representative dot plot of thymocyte populations. **(B)** Representative bar graph of DN, DP, SP8 and SP4 percentages. **(C)** Ratios of CD4:C8, DP:CD8 and DP:CD4. Figures are representative of 4 independent sets of female HY-Dhh littermates. Mean and standard deviation of each population are given. Bars represent mean ± standard deviations. **DN** (p= 0.5 (WT/Het), 0.06 (WT/KO), 0.07 (Het/KO), n=4). **DP** (p= 0.05 (WT/Het), 0.02 (WT/KO), 0.1 (Het/KO), n=4). **SP8** (p= 0.04 (WT/Het), 0.7 (WT/KO), 0.1 (Het/KO), n=4). **SP4** (p= 0.2 (WT/Het), 0.05 (WT/KO), 0.4 (Het/KO), n=4). *represents $p \leq 0.05$.

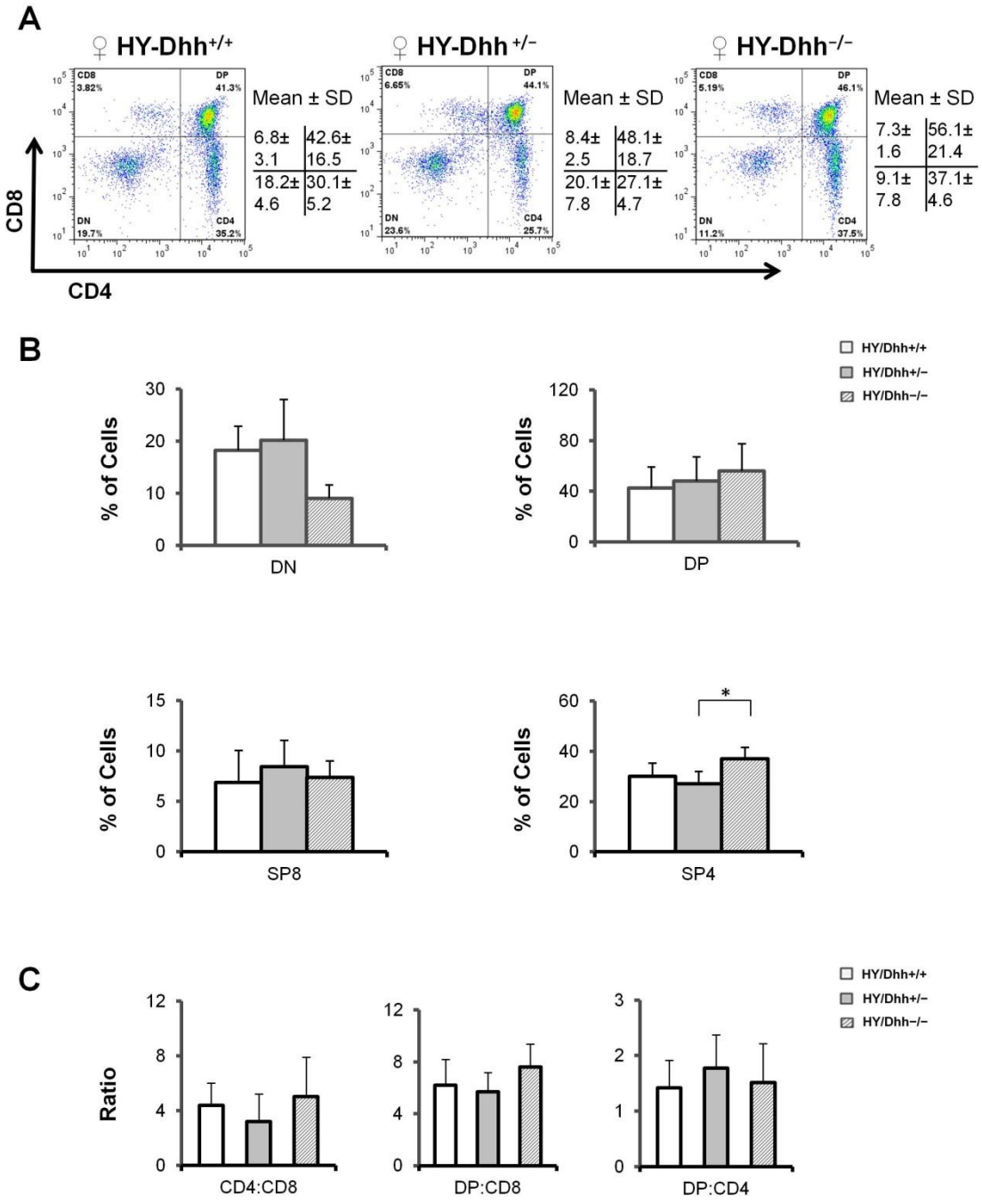

Figure 5.7

Major thymocyte populations in female HY-Dhh within the T3.7 negative cells. Percentage of thymocyte populations from adult female HY/Dhh-WT, HY/Dhh-Het and HY/Dhh-KO littermates. Thymocytes were stained for anti-T3.7, anti-CD8 and anti-CD4, and analyzed by flow cytometry. Thymocyte populations were gated within the T3.7^{-} cells. **(A)** Representative dot plot of thymocyte populations. **(B)** Representative bar graph of DN, DP, SP8 and SP4 percentages. **(C)** Ratios of CD4:C8, DP:CD8 and DP:CD4. Figures are representative of 4 independent sets of female HY-Dhh littermates. Mean and standard deviation of each population are given. Bars represent mean ± standard deviations. **DN** (p= 0.4 (WT/Het), 0.06 (WT/KO), 0.08 (Het/KO), n=4). **DP** (p= 0.6 (WT/Het), 0.3 (WT/KO), 0.6 (Het/KO), n=4). **SP8** (p= 0.4 (WT/Het), 0.7 (WT/KO), 0.5 (Het/KO), n=4). **SP4** (p= 0.4 (WT/Het), 0.09 (WT/KO), 0.02 (Het/KO), n=4). *represents $p \leq 0.05$.

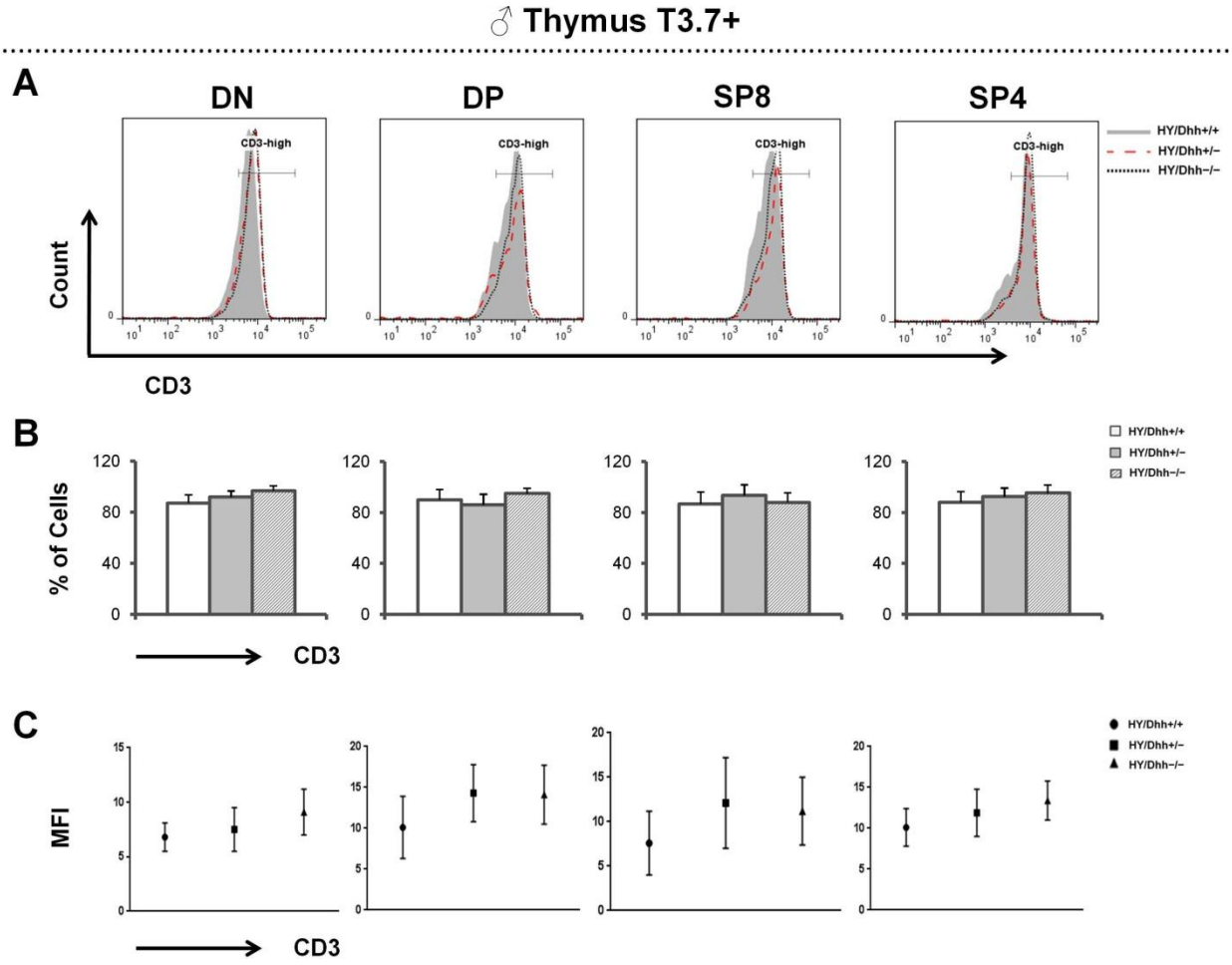

Figure 5.8

Expression of CD3 in male HY-Dhh thymocytes within the T3.7 positive cells. Expression of CD3 in DN, DP, SP8 and SP4 thymocytes from adult male and HY/Dhh-WT, HY/Dhh-Het and HY/Dhh-KO littermates. Thymocytes were stained for anti-T3.7, anti-CD3, anti-CD8 and anti-CD4, and analyzed by flow cytometry. **(A)** Representative histogram of CD3 expression in DN, DP, SP8 and SP4 cells. **(B)** Representative bar graph of CD3 percentages in DN, DP, SP8 and SP4 cells. **(C)** Representative scatter plot of CD3 MFI in DN, DP, SP8 and SP4 cells. Figures are representative of 5 independent sets of male HY-Dhh littermates respectively. Mean and standard deviation of each population are given. Bars represent mean ± standard deviations. **CD3 percentages; DN** (p= 0.7 (WT/Het), 0.1 (WT/KO), 0.2 (Het/KO), n=5). **DP** (p= 0.4 (WT/Het), 0.2 (WT/KO), 0.06 (Het/KO), n=5). **SP8** (p= 0.2 (WT/Het), 0.8 (WT/KO), 0.2 (Het/KO), n=5). **SP4** (p= 0.2 (WT/Het), 0.09 (WT/KO), 0.4 (Het/KO), n=5). **CD3 MFI; DN** (p= 0.4 (WT/Het), 0.7 (WT/KO), 0.9 (Het/KO), n=5). **DP** (p= 0.5 (WT/Het), 0.9 (WT/KO), 0.6 (Het/KO), n=5). **SP8** (p= 0.3 (WT/Het), 0.6 (WT/KO), 0.4 (Het/KO), n=5). **SP4** (p= 0.7 (WT/Het), 0.4 (WT/KO), 0.8 (Het/KO), n=5).

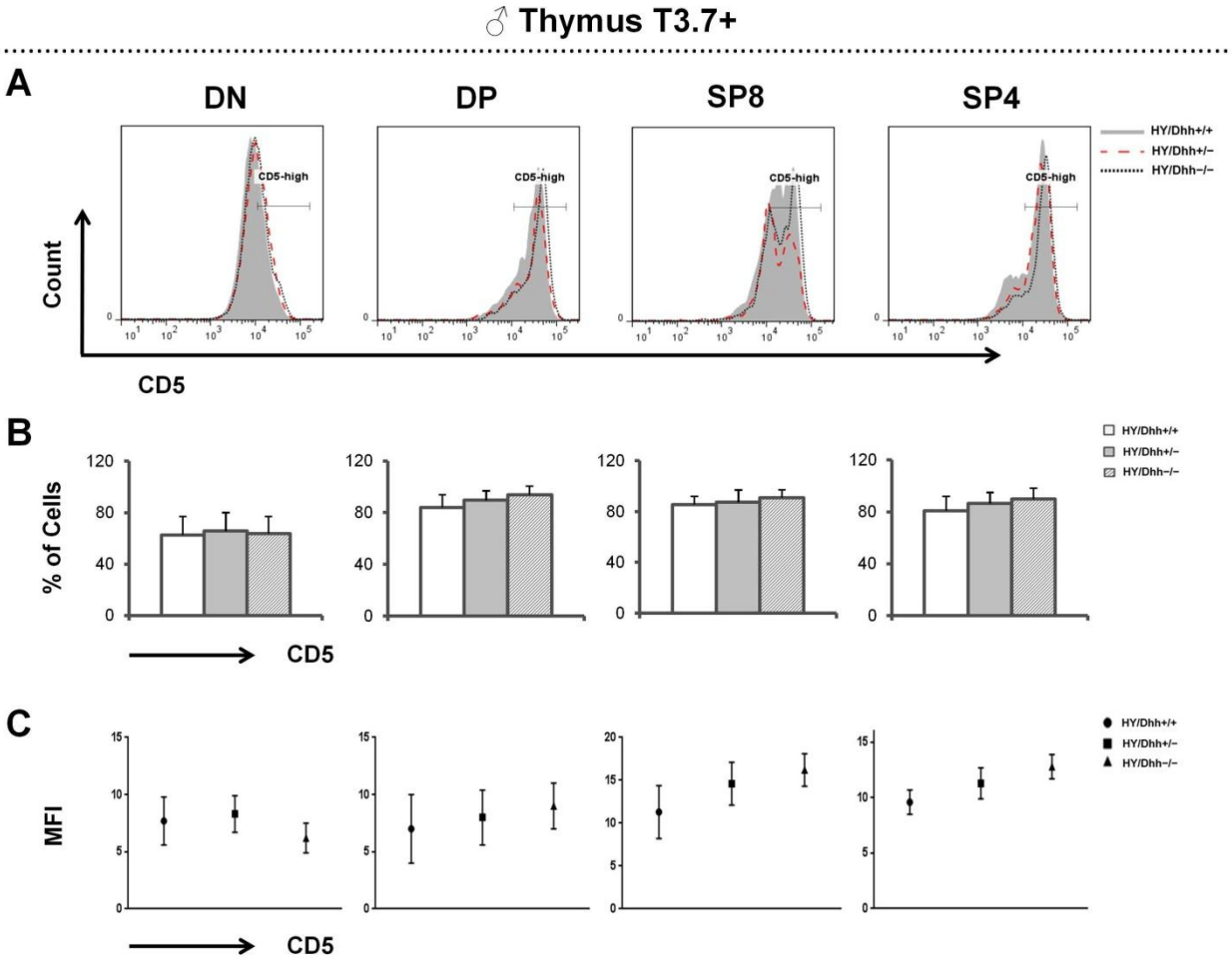

Figure 5.9

Expression of CD5 in male HY-Dhh thymocytes within the T3.7 positive cells. Expression of CD5 in DN, DP, SP8 and SP4 thymocytes from adult male and HY/Dhh-WT, HY/Dhh-Het and HY/Dhh-KO littermates. Thymocytes were stained for anti-T3.7, anti-CD5, anti-CD8 and anti-CD4, and analyzed by flow cytometry. **(A)** Representative histogram of CD5 expression DN, DP, SP8 and SP4 cells. **(B)** Representative bar graph of CD5 percentages in DN, DP, SP8 and SP4 cells. **(C)** Representative scatter plot of CD5 MFI in DN, DP, SP8 and SP4 cells. Figures are representative of 5 independent sets of male HY-Dhh littermates respectively. Mean and standard deviation of each population are given. Bars represent mean ± standard deviations. **CD5 percentages; DN** (p= 0.6 (WT/Het), 0.8 (WT/KO), 0.7 (Het/KO), n=5). **DP** (p= 0.2 (WT/Het), 0.06 (WT/KO), 0.3 (Het/KO), n=5). **SP8** (p= 0.7 (WT/Het), 0.1 (WT/KO), 0.4 (Het/KO), n=5). **SP4** (p= 0.3 (WT/Het), 0.1 (WT/KO), 0.5 (Het/KO), n=5). **CD5 MFI; DN** (p= 0.8 (WT/Het), 0.5 (WT/KO), 0.7 (Het/KO), n=5). **DP** (p= 0.8 (WT/Het), 0.3 (WT/KO), 0.5 (Het/KO), n=5). **SP8** (p= 0.4 (WT/Het), 0.7 (WT/KO), 0.9 (Het/KO), n=5). **SP4** (p= 0.3 (WT/Het), 0.5 (WT/KO), 0.7 (Het/KO), n=5).

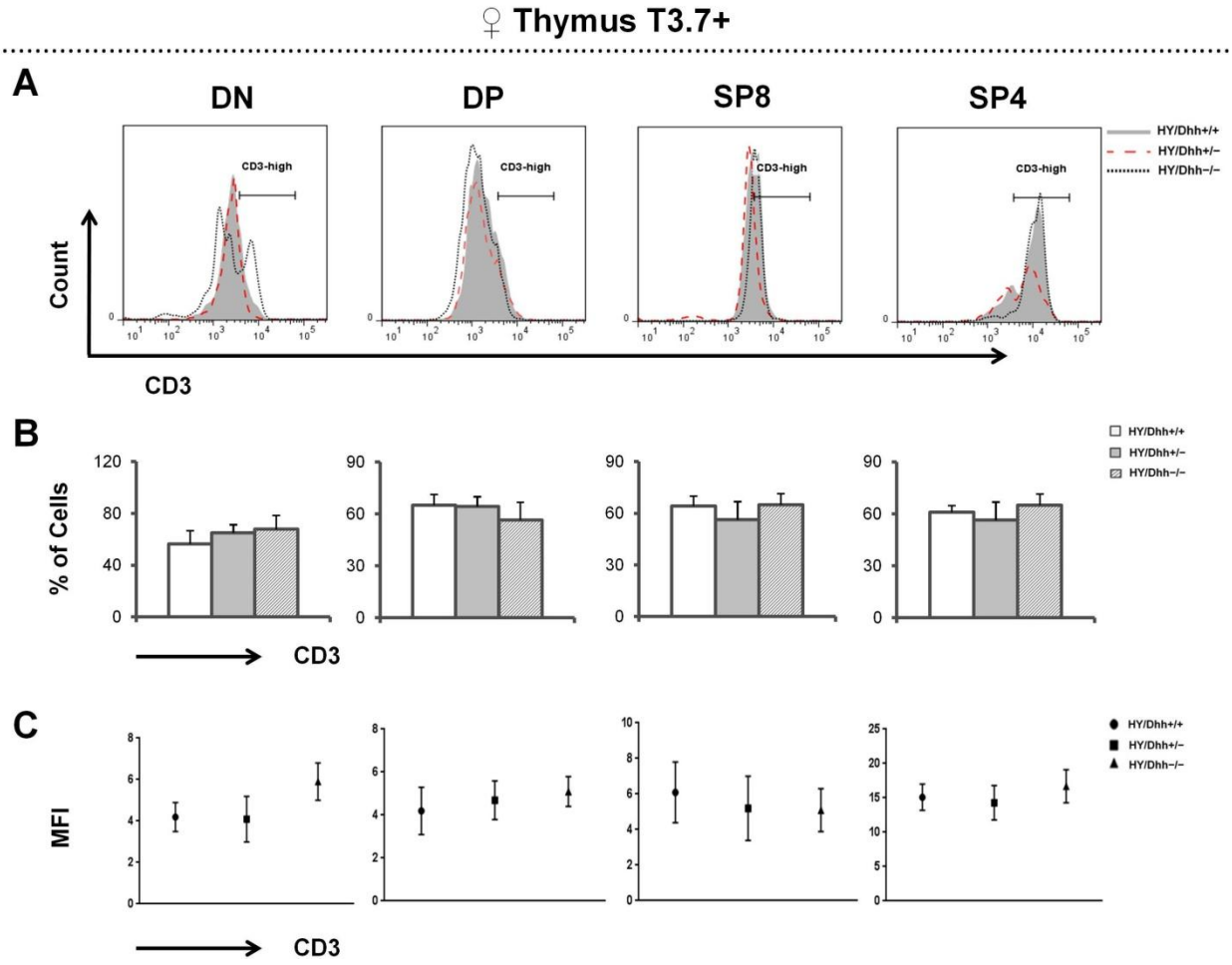

Figure 5.10

Expression of CD3 in female HY-Dhh thymocytes within the T3.7 positive cells. Expression of CD3 in DN, DP, SP8 and SP4 thymocytes from adult female HY/Dhh-WT, HY/Dhh-Het and HY/Dhh-KO littermates. Thymocytes were stained for anti-T3.7, anti-CD3, anti-CD8 and anti-CD4, and analyzed by flow cytometry. **(A)** Representative histogram of CD3 expression in DN, DP, SP8 and SP4 cells. **(B)** Representative bar graph of CD3 percentages in DN, DP, SP8 and SP4 cells. **(C)** Representative scatter plot of CD3 MFI in DN, DP, SP8 and SP4 cells. Figures are representative of 4 independent sets of female HY-Dhh littermates respectively. Mean and standard deviation of each population are given. Bars represent mean ± standard deviations. **CD3 percentages; DN** (p= 0.3 (WT/Het), 0.2 (WT/KO), 0.7 (Het/KO), n=4). **DP** (p= 0.8 (WT/Het), 0.2 (WT/KO), 0.3 (Het/KO), n=4). **SP8** (p= 0.3 (WT/Het), 0.8 (WT/KO), 0.3 (Het/KO), n=4). **SP4** (p= 0.5 (WT/Het), 0.4 (WT/KO), 0.3 (Het/KO), n=4). **CD3 MFI; DN** (p= 0.08 (WT/Het), 0.1 (WT/KO), 0.2 (Het/KO), n=4). **DP** (p= 0.08 (WT/Het), 0.09 (WT/KO), 0.06 (Het/KO), n=4). **SP8** (p= 0.07 (WT/Het), 0.09 (WT/KO), 0.08 (Het/KO), n=4). **SP4** (p= 0.06 (WT/Het), 0.1 (WT/KO), 0.07 (Het/KO), n=4).

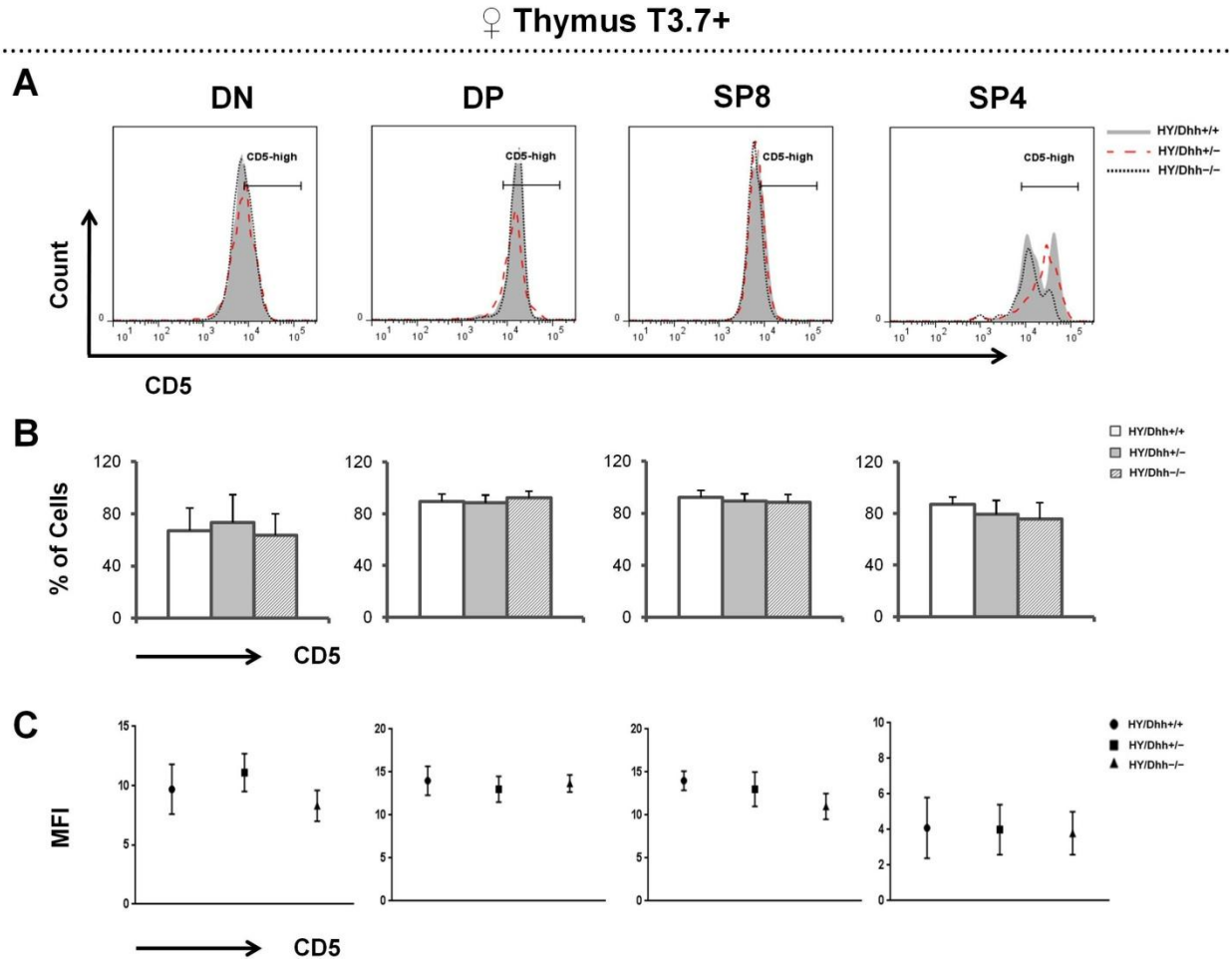

Figure 5.11

Expression of CD5 in female HY-Dhh thymocytes within the T3.7 positive cells. Expression of CD5 in DN, DP, SP8 and SP4 thymocytes from adult female HY/Dhh-WT, HY/Dhh-Het and HY/Dhh-KO littermates. Thymocytes were stained for anti-T3.7, anti-CD5, anti-CD8 and anti-CD4, and analyzed by flow cytometry. **(A)** Representative histogram of CD5 expression in DN, DP, SP8 and SP4 cells. **(B)** Representative bar graph of CD5 percentages in DN, DP, SP8 and SP4 cells. **(C)** Representative scatter plot of CD5 MFI in DN, DP, SP8 and SP4 cells. Figures are representative of 4 independent sets of female HY-Dhh littermates respectively. Mean and standard deviation of each population are given. Bars represent mean ± standard deviations. **CD5 percentages; DN** (p= 0.6 (WT/Het), 0.7 (WT/KO), 0.4 (Het/KO), n=4). **DP** (p= 0.8 (WT/Het), 0.5 (WT/KO), 0.3 (Het/KO), n=4). **SP8** (p= 0.5 (WT/Het), 0.3 (WT/KO), 0.8 (Het/KO), n=4). **SP4** (p= 0.2 (WT/Het), 0.1 (WT/KO), 0.6 (Het/KO), n=4). **CD5 MFI; DN** (p= 0.2 (WT/Het), 0.1 (WT/KO), 0.3 (Het/KO), n=4). **DP** (p= 0.1 (WT/Het), 0.08 (WT/KO), 0.1 (Het/KO), n=4). **SP8** (p= 0.3 (WT/Het), 0.5 (WT/KO), 0.7 (Het/KO), n=4). **SP4** (p= 0.7 (WT/Het), 0.3 (WT/KO), 0.8 (Het/KO), n=4).

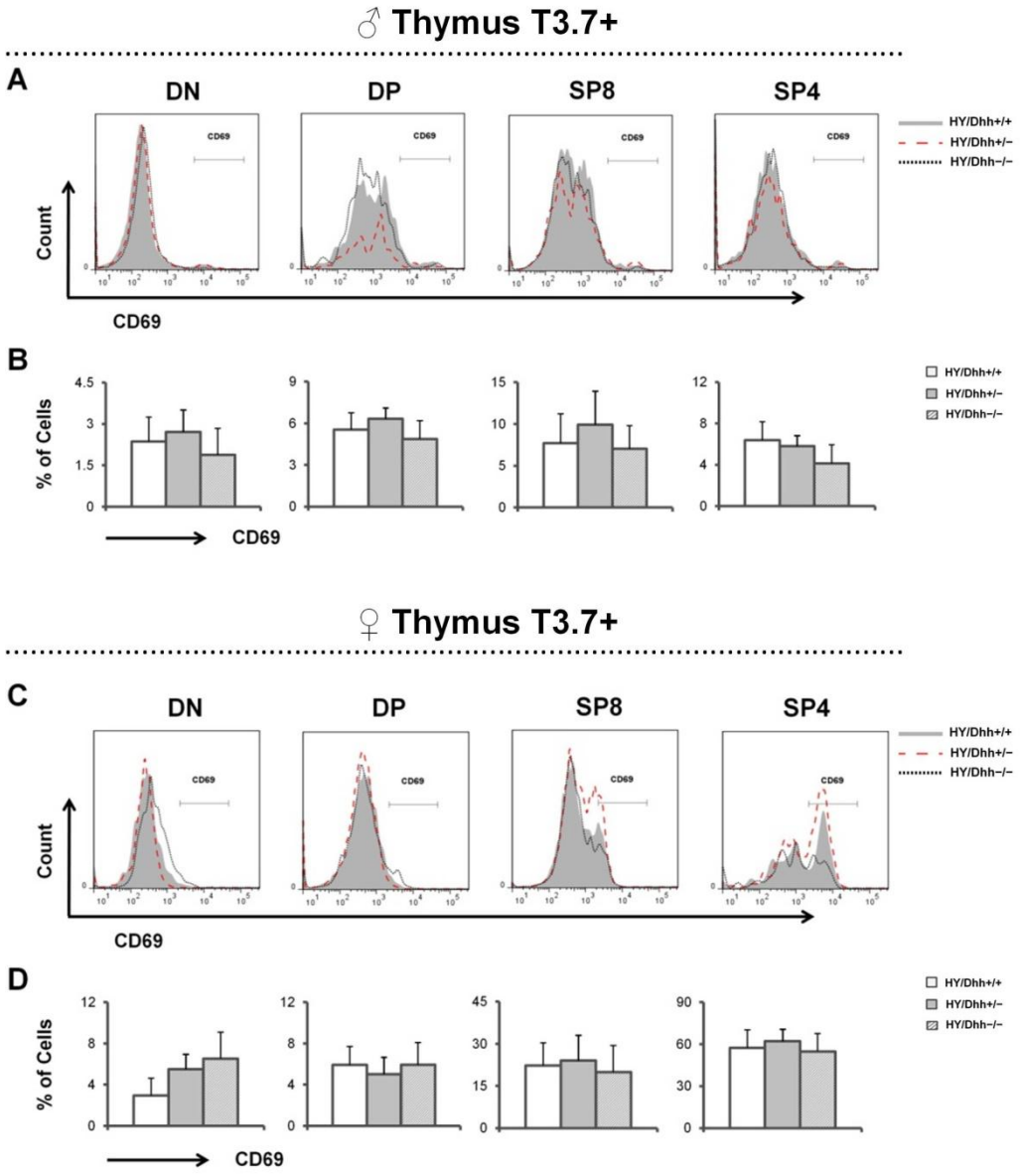

Figure 5.12

Expression of CD69 in male and female HY-Dhh thymocytes within the T3.7 positive cells. Expression of CD69 in DN, DP, SP8 and SP4 thymocytes from adult male and female HY/Dhh-WT, HY/Dhh-Het and HY/Dhh-KO littermates. Thymocytes were stained for anti-T3.7, anti-CD69, anti-CD8 and anti-CD4, and analyzed by flow cytometry. **(A)** Representative histogram of CD69 expression in male DN, DP, SP8 and SP4 cells. **(B)** Representative bar graph of CD69 percentages in male DN, DP, SP8 and SP4 cells. **(C)** Representative histogram of CD69 expression in female DN, DP, SP8 and SP4 cells. **(D)** Representative bar graph of CD69 percentages in female DN, DP, SP8 and SP4 cells. Figures are representative of 4 independent sets of male and female HY-Dhh littermates. Mean and standard deviation of each population are given. Bars represent mean ± standard deviations. **Male CD69 percentages; DN** (p= 0.5 (WT/Het), 0.4 (WT/KO), 0.2 (Het/KO), n=4). **DP** (p= 0.3 (WT/Het), 0.4 (WT/KO), 0.1 (Het/KO), n=4). **SP8** (p= 0.4 (WT/Het), 0.7 (WT/KO), 0.2 (Het/KO), n=6). **SP4** (p= 0.5 (WT/Het), 0.1 (WT/KO), 0.1 (Het/KO), n=6). **Female CD69 percentages; DN** (p= 0.1 (WT/Het), 0.1 (WT/KO), 0.5 (Het/KO), n=4). **DP** (p= 0.5 (WT/Het), 0.9 (WT/KO), 0.5 (Het/KO), n=4). **SP8** (p= 0.8 (WT/Het), 0.7 (WT/KO), 0.6 (Het/KO), n=6). **SP4** (p= 0.6 (WT/Het), 0.8 (WT/KO), 0.4 (Het/KO), n=6).

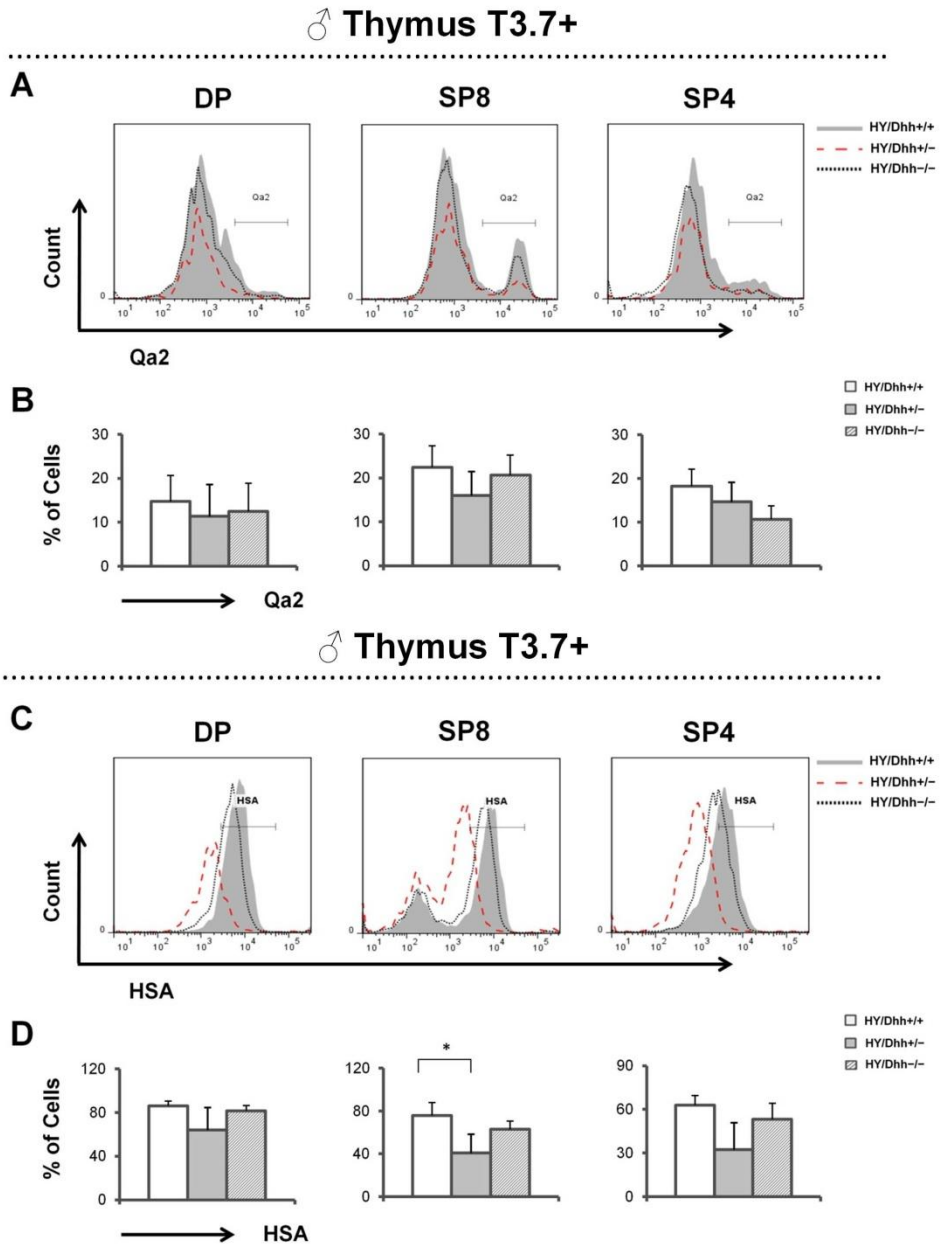

Figure 5.13

Expression of Qa2 and HSA in male HY-Dhh thymocytes within the T3.7 positive cells. Expression of Qa2 and HSA in DP, SP8 and SP4 cells from adult male HY/Dhh-WT, HY/Dhh-Het and HY/Dhh-KO littermates. Thymocytes were stained for anti-Qa2, anti-CD24, anti-CD8 and anti-CD4, and analyzed by flow cytometry. **(A)** Representative histogram of Qa2 expression in DP, SP8 and SP4 cells. **(B)** Representative bar graph of Qa2 percentages in DP, SP8 and SP4 cells. **(C)** Representative histogram of HSA expression in DP, SP8 and SP4 cells. **(D)** Representative bar graph of HSA percentages in DP, SP8 and SP4 cells. Figures are representative of 3 independent sets of male HY-Dhh littermates. Mean and standard deviation of each population are given. Bars represent mean ± standard deviations. **Qa2 percentages; DP** (p= 0.5 (WT/Het), 0.6 (WT/KO), 0.8 (Het/KO), n=3). **SP8** (p= 0.2 (WT/Het), 0.6 (WT/KO), 0.3 (Het/KO), n=3). **SP4** (p= 0.3 (WT/Het), 0.06 (WT/KO), 0.2 (Het/KO), n=3). **HSA percentages; DP** (p= 0.1 (WT/Het), 0.3 (WT/KO), 0.1 (Het/KO), n=3). **SP8** (p= 0.05 (WT/Het), 0.1 (WT/KO), 0.1 (Het/KO), n=3). **SP4** (p= 0.7 (WT/Het), 0.1 (WT/KO), 0.3 (Het/KO), n=3). *represents p≤0.05.

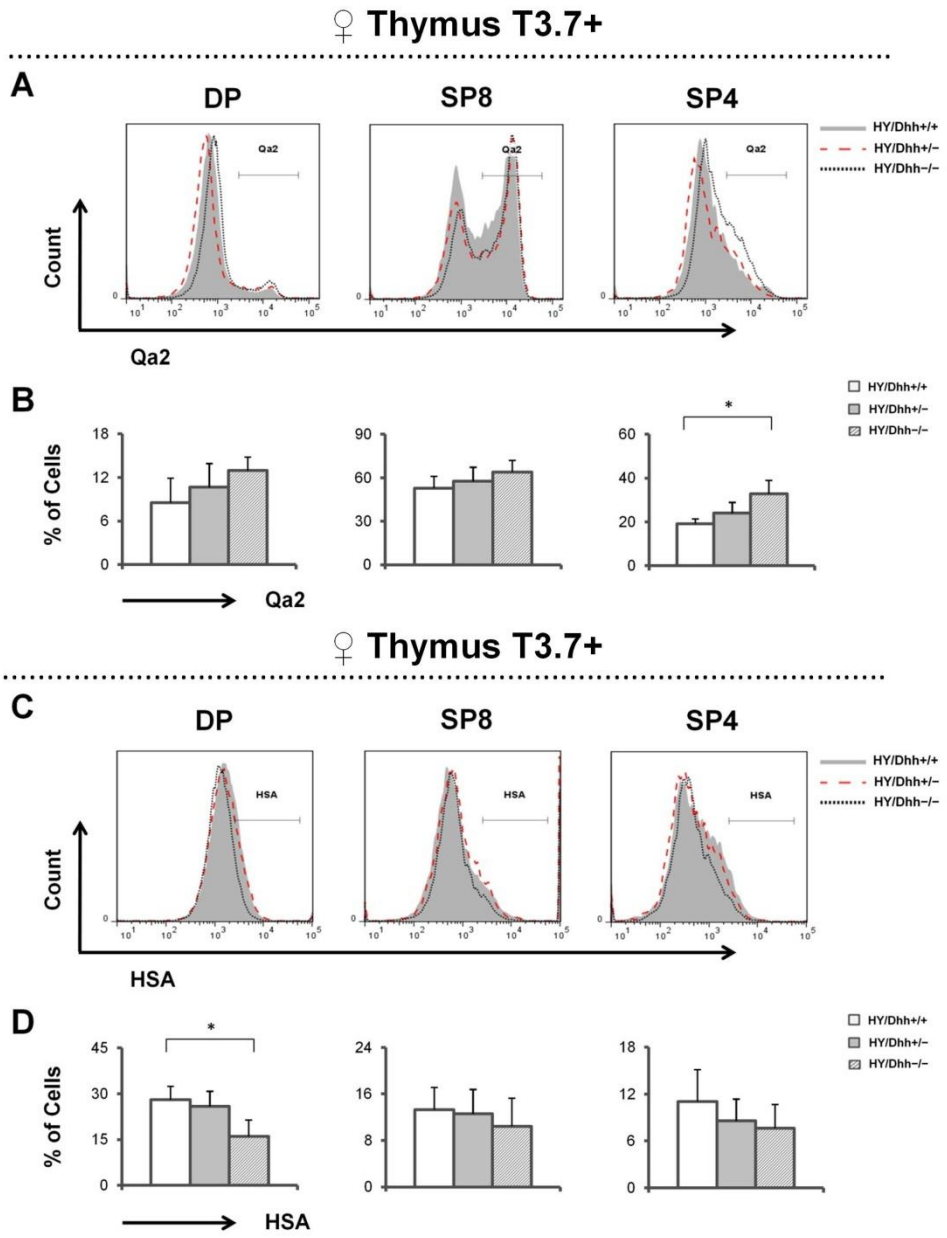

Figure 5.14

Expression of Qa2 and HSA in female HY-Dhh thymocytes within the T3.7 positive cells. Expression of Qa2 and HSA in DP, SP8 and SP4 cells from adult female HY/Dhh-WT, HY/Dhh-Het and HY/Dhh-KO littermates. Thymocytes were stained for anti-Qa2, anti-CD24, anti-CD8 and anti-CD4, and analyzed by flow cytometry. **(A)** Representative histogram of Qa2 expression in DP, SP8 and SP4 cells. **(B)** Representative bar graph of Qa2 percentages in DP, SP8 and SP4 cells. **(C)** Representative histogram of HSA expression in DP, SP8 and SP4 cells. **(D)** Representative bar graph of HSA percentages in DP, SP8 and SP4 cells. Figures are representative of 3 independent sets of female HY-Dhh littermates. Mean and standard deviation of each population are given. Bars represent mean ± standard deviations. **Qa2 percentages; DP** (p= 0.4 (WT/Het), 0.1 (WT/KO), 0.3 (Het/KO), n=3). **SP8** (p= 0.5 (WT/Het), 0.1 (WT/KO), 0.4 (Het/KO), n=3). **SP4** (p= 0.2 (WT/Het), 0.04 (WT/KO), 0.1 (Het/KO), n=3). **HSA percentages; DP** (p= 0.6 (WT/Het), 0.04 (WT/KO), 0.08 (Het/KO), n=3). **SP8** (p= 0.8 (WT/Het), 0.4 (WT/KO), 0.5 (Het/KO), n=3). **SP4** (p= 0.4 (WT/Het), 0.3 (WT/KO), 0.7 (Het/KO), n=3). *represents $p \leq 0.05$.

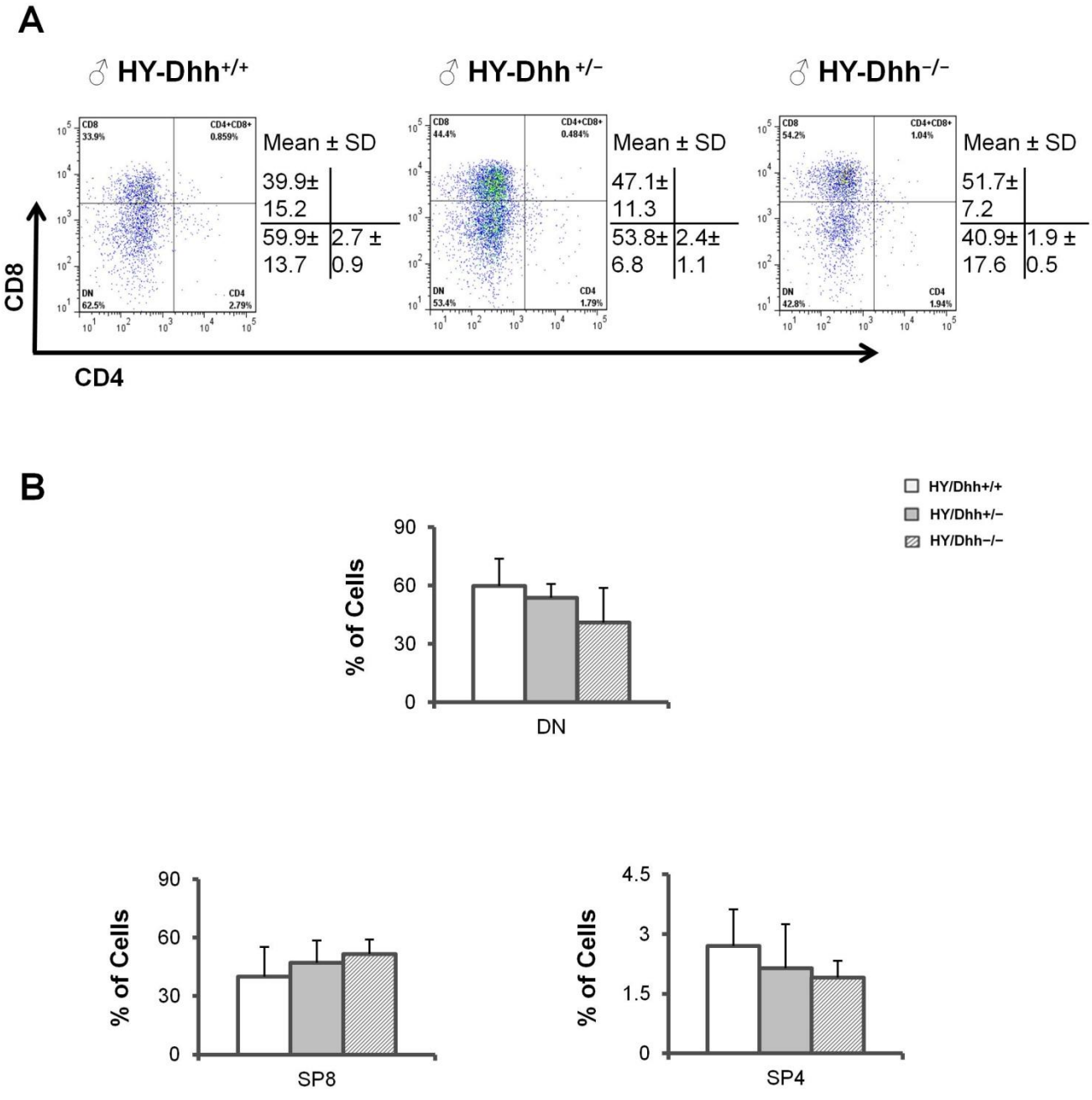

Figure 5.15

Major splenocyte populations in male HY-Dhh within the T3.7 positive cells. Percentage of splenocyte populations from adult male HY/Dhh-WT, HY/Dhh-Het and HY/Dhh-KO littermates. Splenocytes were stained for anti-T3.7, anti-CD8 and anti-CD4, and analyzed by flow cytometry. Splenocyte populations were gated within the $T3.7^+$ cells. **(A)** Representative dot plot of splenocyte populations. **(B)** Representative bar graph of $CD4^-CD8^-$, SP8 and SP4 percentages. Figures are representative of 5 independent sets of male HY-Dhh littermates. Mean and standard deviation of each population are given. Bars represent mean ± standard deviations. **$CD4^-CD8^-$** (p= 0.4 (WT/Het), 0.1 (WT/KO), 0.1 (Het/KO), n=5). **SP8** (p= 0.4 (WT/Het), 0.1 (WT/KO), 0.4 (Het/KO), n=5). **SP4** (p= 0.4 (WT/Het), 0.1 (WT/KO), 0.6 (Het/KO), n=5).

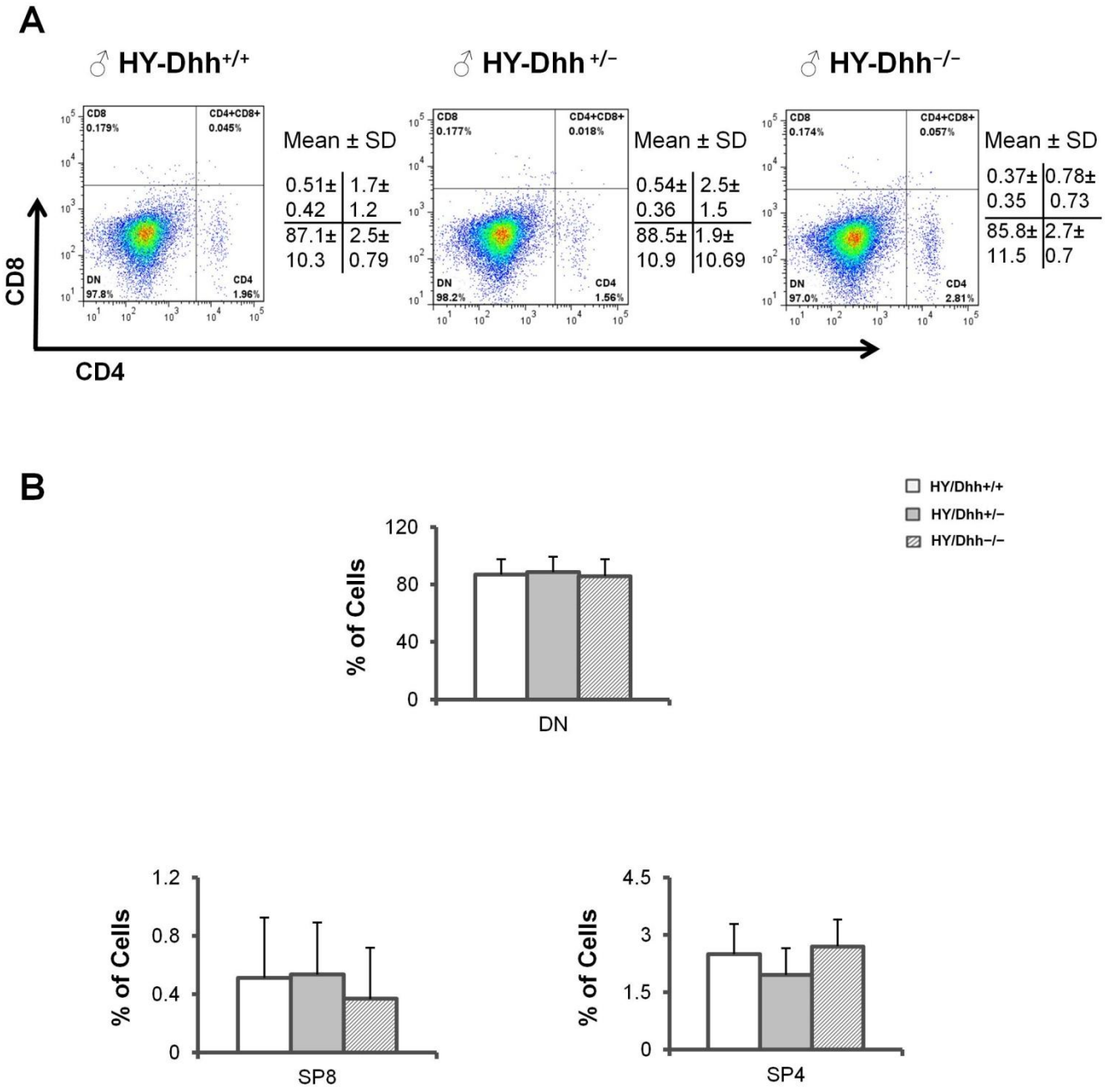

Figure 5.16

Major splenocyte populations in male HY-Dhh within the T3.7 negative cells. Percentage of splenocyte populations from adult male HY/Dhh-WT, HY/Dhh-Het and HY/Dhh-KO littermates. Splenocytes were stained for anti-T3.7, anti-CD8 and anti-CD4, and analyzed by flow cytometry. Splenocyte populations were gated within the $T3.7^{-}$ cells. **(A)** Representative dot plot of splenocyte populations. **(B)** Representative bar graph of $CD4^{-}CD8^{-}$, SP8 and SP4 percentages. Figures are representative of 5 independent sets of male HY-Dhh littermates. Mean and standard deviation of each population are given. Bars represent mean ± standard deviations. **$CD4^{-}CD8^{-}$** (p= 0.8 (WT/Het), 0.8 (WT/KO), 0.7 (Het/KO), n=5). **SP8** (p= 0.9 (WT/Het), 0.5 (WT/KO), 0.7 (Het/KO), n=5). **SP4** (p= 0.2 (WT/Het), 0.6 (WT/KO), 0.1 (Het/KO), n=5).

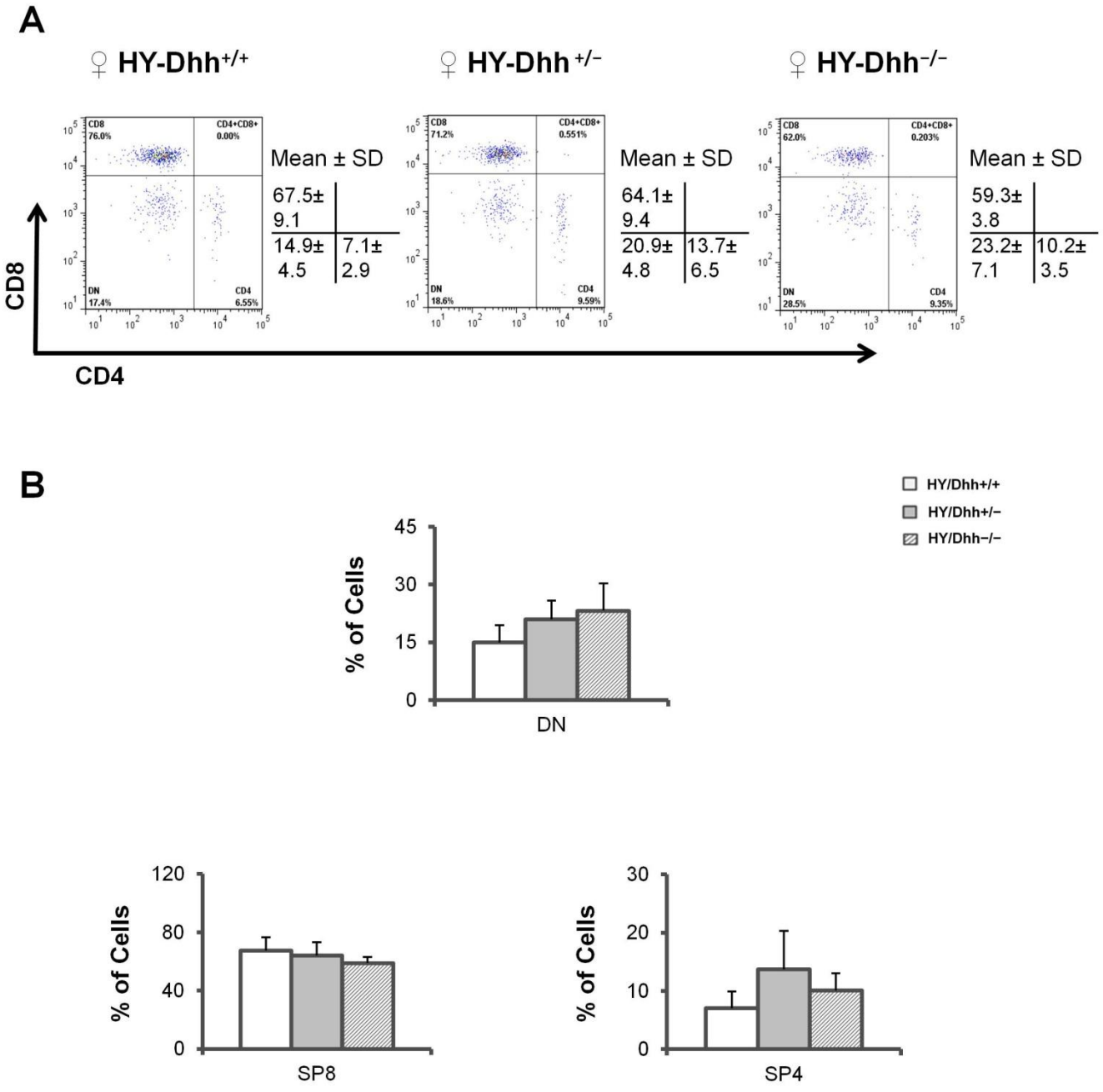

Figure 5.17

Major splenocyte populations in female HY-Dhh within the T3.7 positive cells. Percentage of splenocyte populations from adult female HY/Dhh-WT, HY/Dhh-Het and HY/Dhh-KO littermates. Splenocytes were stained for anti-T3.7, anti-CD8 and anti-CD4, and analyzed by flow cytometry. Splenocyte populations were gated within the $T3.7^+$ cells. **(A)** Representative dot plot of splenocyte populations. **(B)** Representative bar graph of $CD4^-CD8^-$, SP8 and SP4 percentages. Figures are representative of 3 independent sets of female HY-Dhh littermates. Mean and standard deviation of each population are given. Bars represent mean ± standard deviations. **$CD4^-CD8^-$** (p= 0.7 (WT/Het), 0.6 (WT/KO), 0.5 (Het/KO), n=3). **SP8** (p= 0.5 (WT/Het), 0.1 (WT/KO), 0.2 (Het/KO), n=3). **SP4** (p= 0.08 (WT/Het), 0.1 (WT/KO), 0.2 (Het/KO), n=3).

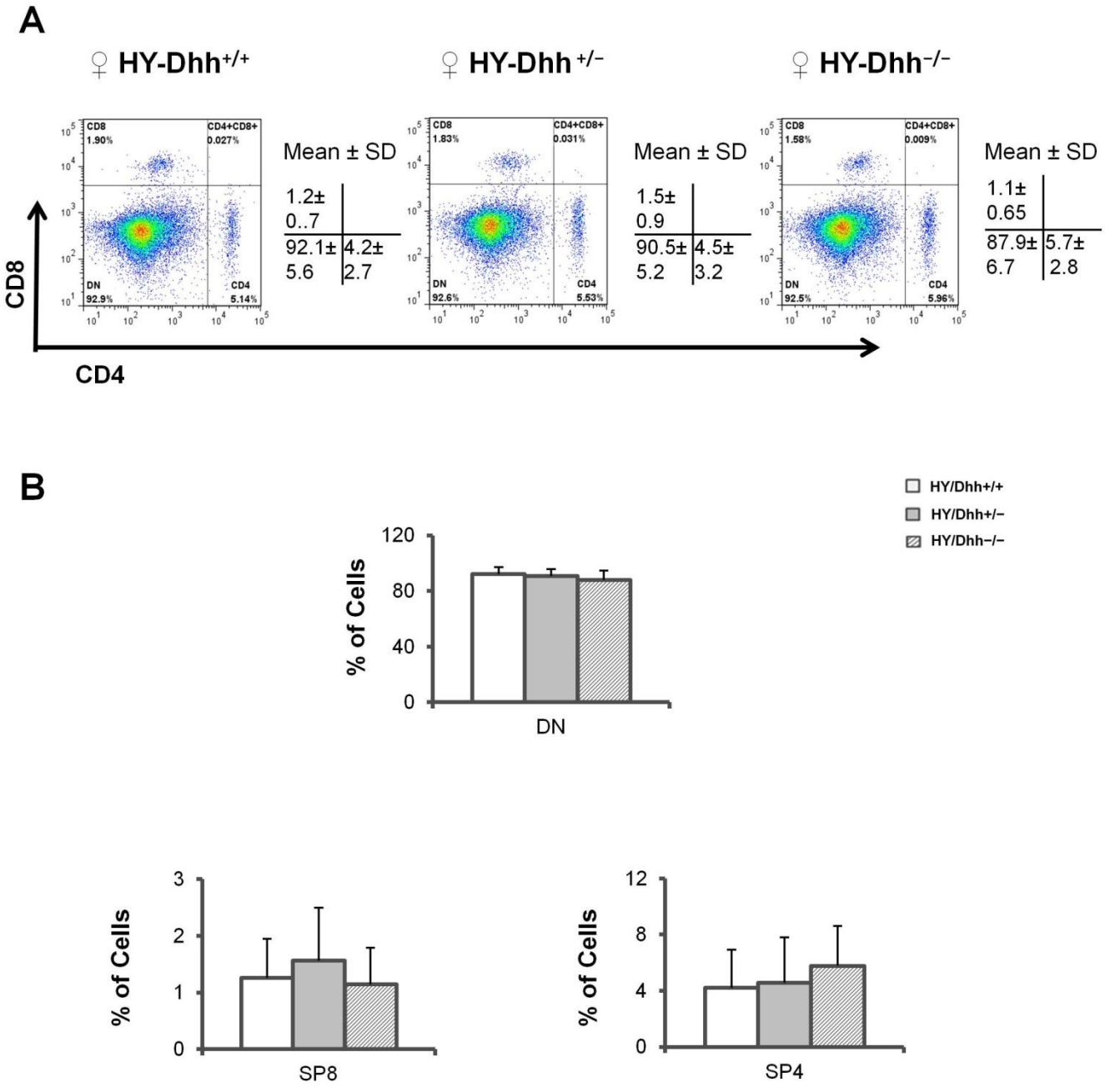

Figure 5.18

Major splenocyte populations in female HY-Dhh within the T3.7 negative cells. Percentage of splenocyte populations from adult female HY/Dhh-WT, HY/Dhh-Het and HY/Dhh-KO littermates. Splenocytes were stained for anti-T3.7, anti-CD8 and anti-CD4, and analyzed by flow cytometry. Splenocyte populations were gated within the $T3.7^+$ cells. **(A)** Representative dot plot of splenocyte populations. **(B)** Representative bar graph of $CD4^-CD8^-$, SP8 and SP4 percentages. Figures are representative of 3 independent experiments sets of female HY-Dhh littermates. Mean and standard deviation of each population are given. Bars represent mean ± standard deviations. **$CD4^-CD8^-$** (p= 0.6 (WT/Het), 0.3 (WT/KO), 0.5 (Het/KO), n=3). **SP8** (p= 0.5 (WT/Het), 0.7 (WT/KO), 0.4 (Het/KO), n=3). **SP4** (p= 0.8 (WT/Het), 0.3 (WT/KO), 0.5 (Het/KO), n=3).

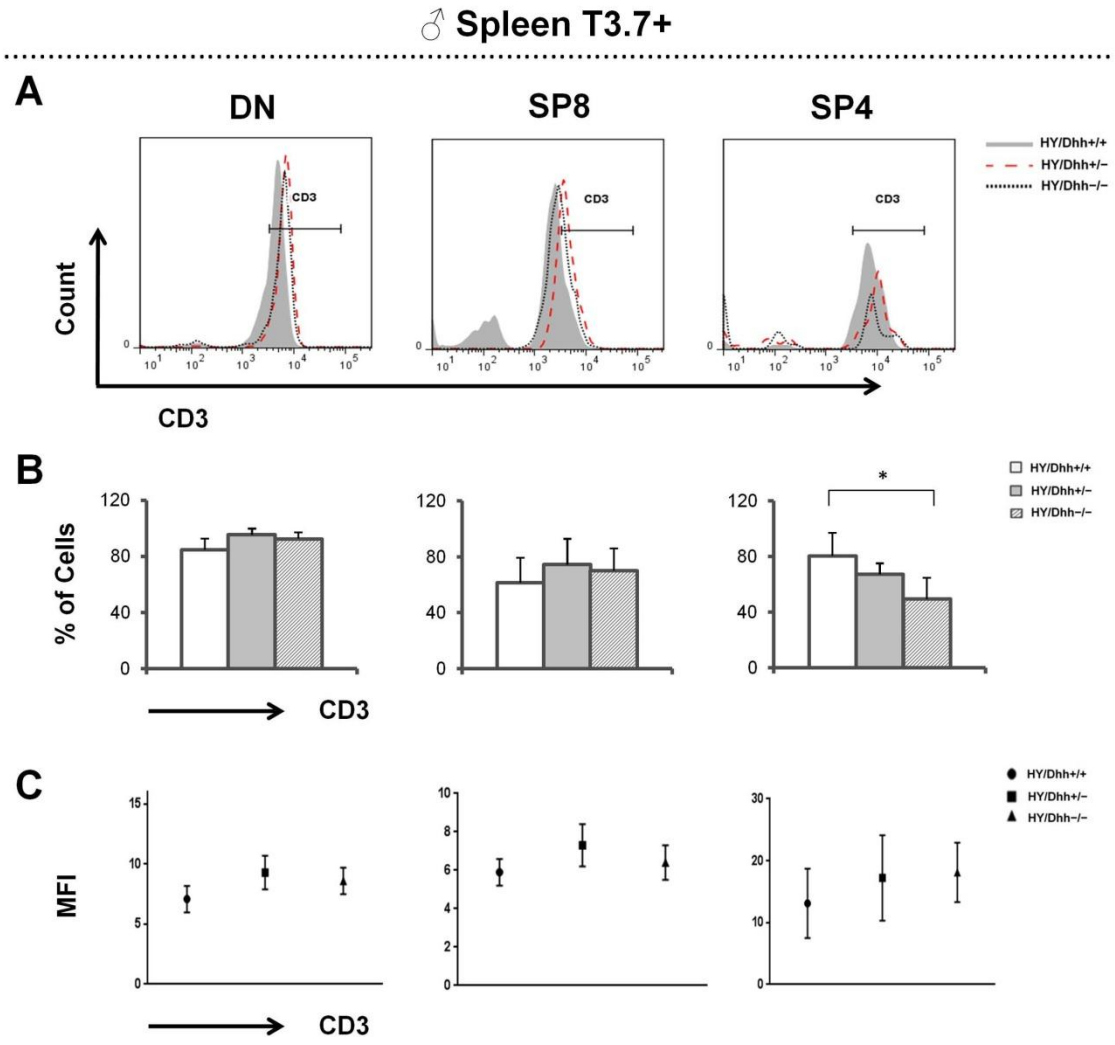

Figure 5.19

Expression of CD3 in male HY-Dhh splenocytes within the T3.7 positive cells. Expression of CD3 in $CD4^{-}CD8^{-}$**,** SP8 and SP4 cells from adult male HY/Dhh-WT, HY/Dhh-Het and HY/Dhh-KO littermates. Splenocytes were stained for anti-T3.7, anti-CD3, anti-CD8 and anti-CD4, and analyzed by flow cytometry. **(A)** Representative histogram of CD3 expression in male $CD4^{-}CD8^{-}$, SP8 and SP4 cells. **(B)** Representative bar graph of CD3 percentages in male $CD4^{-}CD8^{-}$, SP8 and SP4 cells. **(C)** Representative scatter plot of CD3 MFI in male $CD4^{-}CD8^{-}$, SP8 and SP4 cells. Figures are representative of 4 independent sets of male HY-Dhh littermates respectively. Mean and standard deviation of each population are given. Bars represent mean ± standard deviations. **CD3 percentages; $CD4^{-}CD8^{-}$** (p= 0.3 (WT/Het), 0.09 (WT/KO), 0.3 (Het/KO), n=4). **SP8** (p= 0.2 (WT/Het), 0.4 (WT/KO), 0.6 (Het/KO), n=4). **SP4** (p= 0.2 (WT/Het), 0.03 (WT/KO), 0.8 (Het/KO), n=4). **CD3 MFI; $CD4^{-}CD8^{-}$** (p= 0.1 (WT/Het), 0.4 (WT/KO), 0.5 (Het/KO), n=4). **SP8** (p= 0.7 (WT/Het), 0.9 (WT/KO), 0.1 (Het/KO), n=4). **SP4** (p= 0.2 (WT/Het), 0.5 (WT/KO), 0.4 (Het/KO), n=4). *represents $p \leq 0.05$.

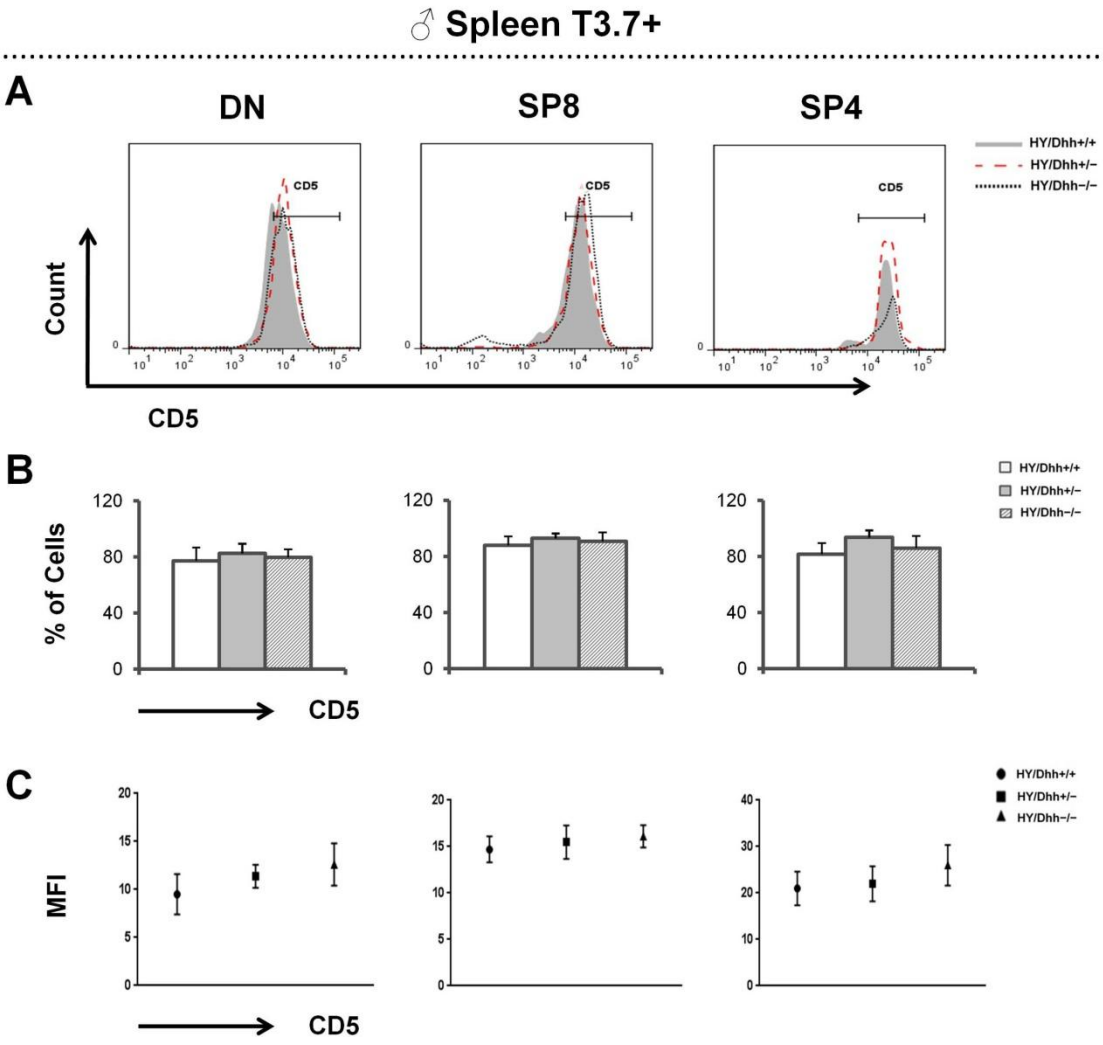

Figure 5.20

Expression of CD5 in male HY-Dhh splenocytes within the T3.7 positive cells. Expression of CD5 in $CD4^{-}CD8^{-}$**,** SP8 and SP4 cells from adult male HY/Dhh-WT, HY/Dhh-Het and HY/Dhh-KO littermates. Splenocytes were stained for anti-T3.7, anti-CD5, anti-CD8 and anti-CD4, and analyzed by flow cytometry. **(A)** Representative histogram of CD5 expression in male $CD4^{-}CD8^{-}$, SP8 and SP4 cells. **(B)** Representative bar graph of CD5 percentages in male $CD4^{-}CD8^{-}$, SP8 and SP4 cells. **(C)** Representative scatter plot of CD5 MFI in male $CD4^{-}CD8^{-}$, SP8 and SP4 cells. Figures are representative of 4 independent sets of male HY-Dhh littermates respectively. Mean and standard deviation of each population are given. Bars represent mean ± standard deviations. **CD5 percentages; $CD4^{-}CD8^{-}$** (p= 0.3 (WT/Het), 0.6 (WT/KO), 0.5 (Het/KO), n=4). SP8 (p= 0.2 (WT/Het), 0.5 (WT/KO), 0.5 (Het/KO), n=4). SP4 (p= 0.4 (WT/Het), 0.5 (WT/KO), 0.1 (Het/KO), n=4). **CD3 MFI; $CD4^{-}CD8^{-}$** (p= 0.3 (WT/Het), 0.4 (WT/KO), 0.1 (Het/KO), n=4). **SP8** (p= 0.2 (WT/Het), 0.6 (WT/KO), 0.4 (Het/KO), n=4). **SP4** (p= 0.8 (WT/Het), 0.2 (WT/KO), 0.6 (Het/KO), n=4).

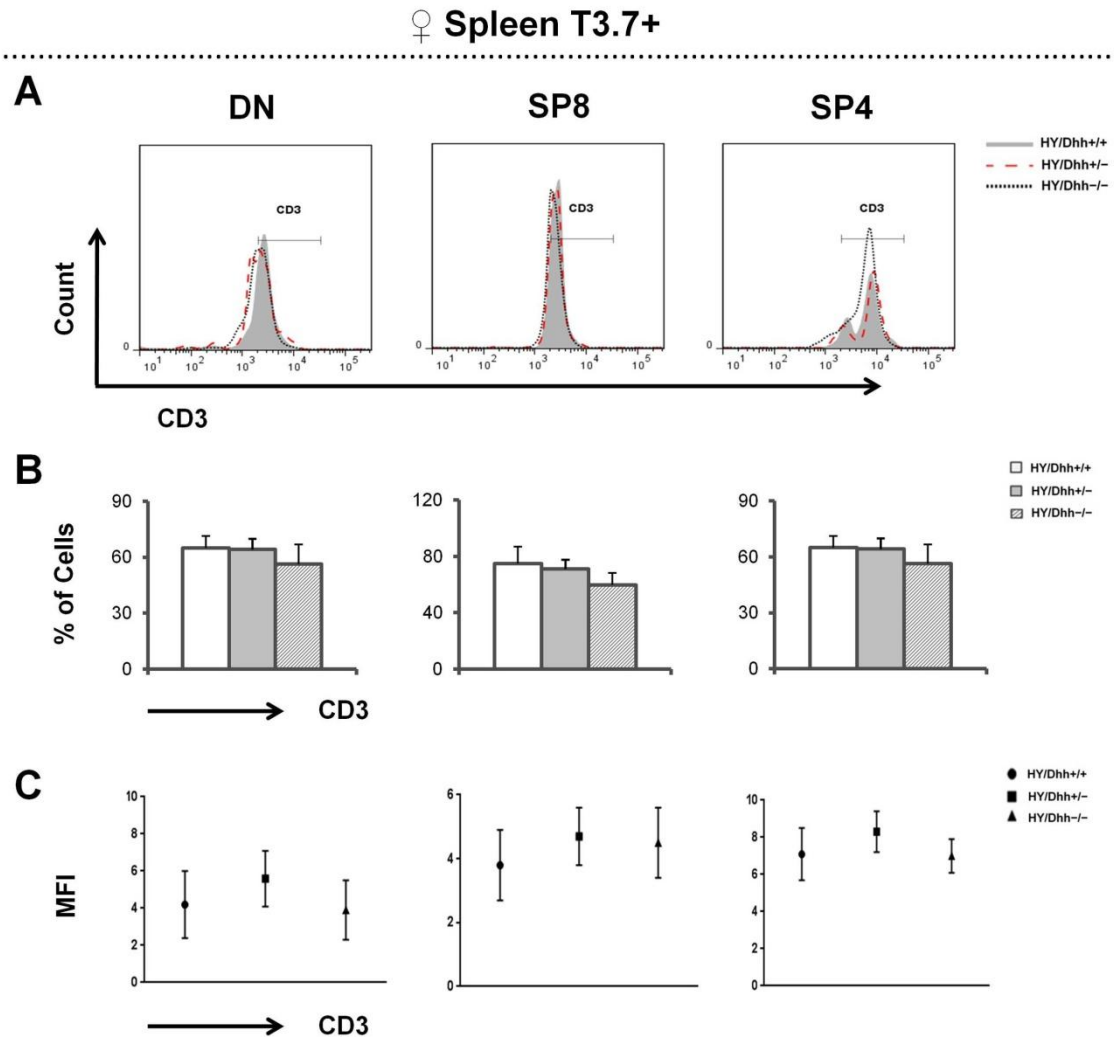

Figure 5.21

Expression of CD3 in female HY-Dhh splenocytes within the T3.7 positive cells. Expression of CD3 in $CD4^{-}CD8^{-}$**,** SP8 and SP4 cells from adult female HY/Dhh-WT, HY/Dhh-Het and HY/Dhh-KO littermates. Splenocytes were stained for anti-T3.7, anti-CD3, anti-CD8 and anti-CD4, and analyzed by flow cytometry. **(A)** Representative histogram of CD3 expression in female $CD4^{-}CD8^{-}$, SP8 and SP4 cells. **(B)** Representative bar graph of CD3 percentages in female $CD4^{-}CD8^{-}$, SP8 and SP4 cells. **(C)** Representative scatter plot of CD3 MFI in female $CD4^{-}CD8^{-}$, SP8 and SP4 cells. Figures are representative of 3 independent sets of female HY-Dhh littermates respectively. Mean and standard deviation of each population are given. Bars represent mean ± standard deviations. **CD3 percentages; $CD4^{-}CD8^{-}$** (p= 0.8 (WT/Het), 0.3 (WT/KO), 0.3 (Het/KO), n=3). **SP8** (p= 0.6 (WT/Het), 0.1 (WT/KO), 0.1 (Het/KO), n=3). **SP4** (p= 0.8 (WT/Het), 0.3 (WT/KO), 0.3 (Het/KO), n=3). **CD3 MFI; $CD4^{-}CD8^{-}$** (p= 0.7 (WT/Het), 0.3 (WT/KO), 0.3 (Het/KO), n=3). **SP8** (p= 0.4 (WT/Het), 0.9 (WT/KO), 0.4 (Het/KO), n=3). **SP4** (p= 0.1 (WT/Het), 0.3 (WT/KO), 0.6 (Het/KO), n=3).

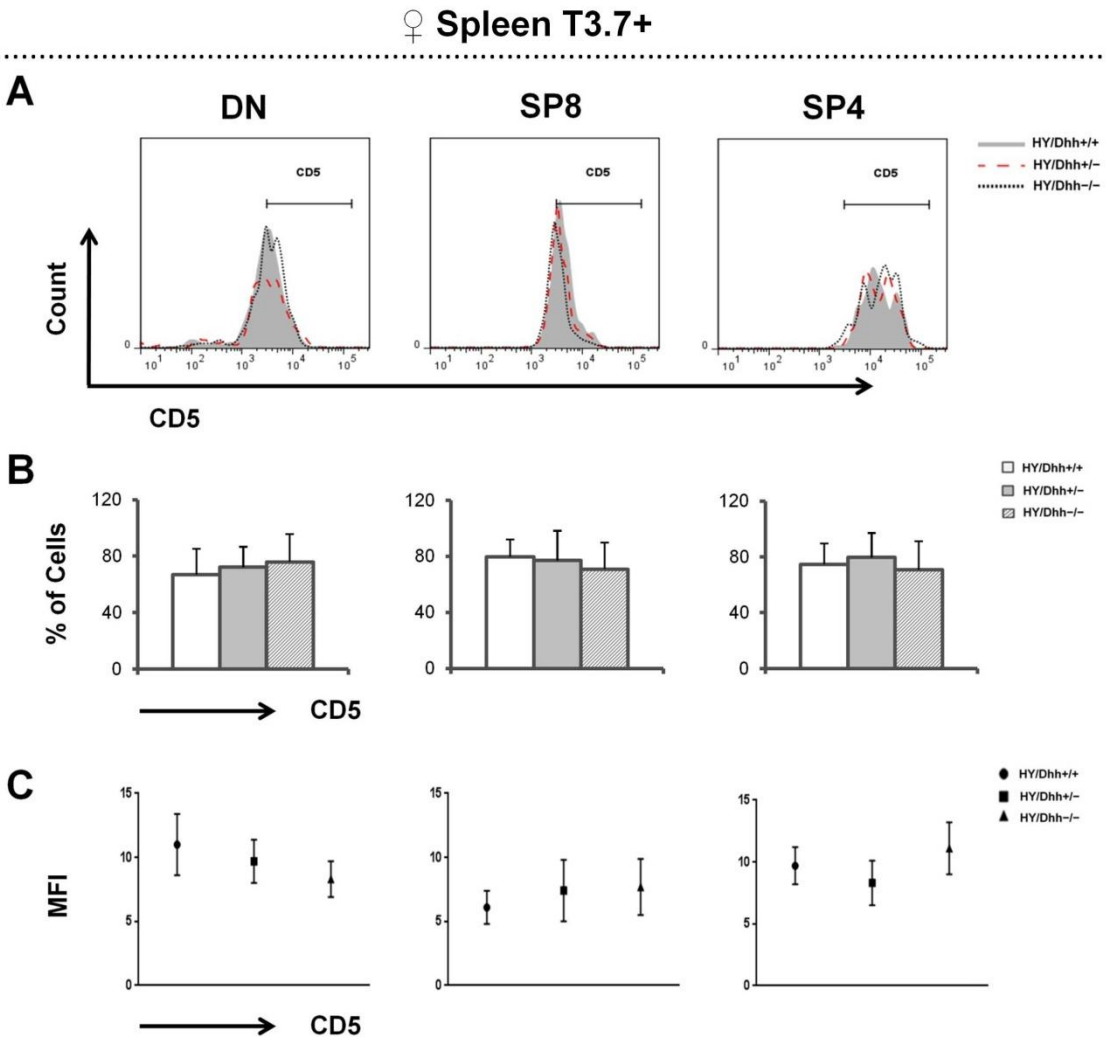

Figure 5.22

Expression of CD5 in female HY-Dhh splenocytes within the T3.7 positive cells. Expression of CD5 in $CD4^{-}CD8^{-}$**,** SP8 and SP4 cells from adult female HY/Dhh-WT, HY/Dhh-Het and HY/Dhh-KO littermates. Splenocytes were stained for anti-T3.7, anti-CD5, anti-CD8 and anti-CD4, and analyzed by flow cytometry. **(A)** Representative histogram of CD5 expression in female $CD4^{-}CD8^{-}$, SP8 and SP4 cells. **(B)** Representative bar graph of CD5 percentages in female $CD4^{-}CD8^{-}$, SP8 and SP4 cells. **(C)** Representative scatter plot of CD5 MFI in female $CD4^{-}CD8^{-}$, SP8 and SP4 cells. Figures are representative of 3 independent sets of female HY-Dhh littermates respectively. Mean and standard deviation of each population are given. Bars represent mean ± standard deviations. **CD5 percentages; $CD4^{-}CD8^{-}$** (p= 0.6 (WT/Het), 0.5 (WT/KO), 0.7 (Het/KO), n=3). **SP8** (p= 0.8 (WT/Het), 0.4 (WT/KO), 0.6 (Het/KO), n=3). **SP4** (p= 0.6 (WT/Het), 0.7 (WT/KO), 0.5 (Het/KO), n=3). **CD5 MFI; $CD4^{-}CD8^{-}$** (p= 0.8 (WT/Het), 0.4 (WT/KO), 0.4 (Het/KO), n=3). **SP8** (p= 0.2 (WT/Het), 0.6 (WT/KO), 0.8 (Het/KO), n=3). **SP4** (p= 0.6 (WT/Het), 0.3 (WT/KO), 0.7 (Het/KO), n=3).

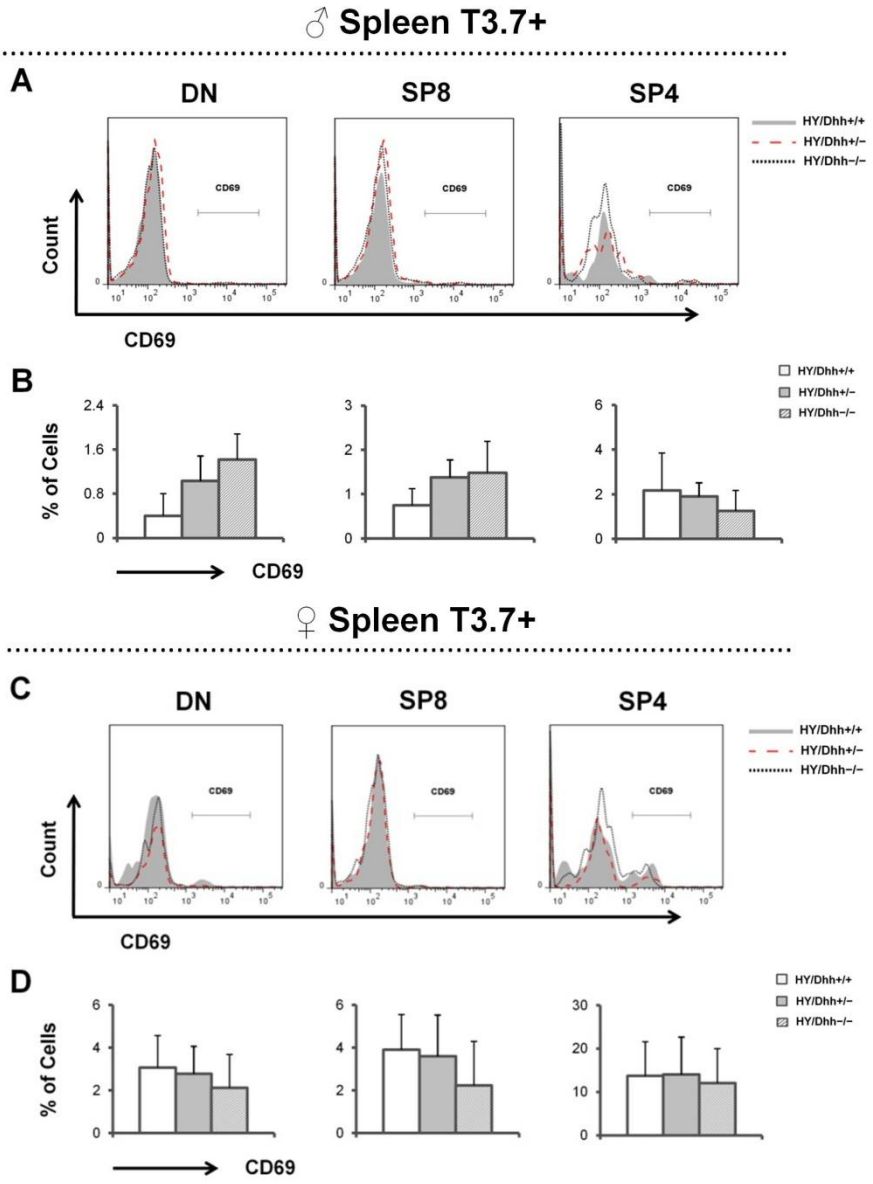

Figure 5.23

Expression of CD69 in male and female HY-Dhh splenocytes within the T3.7 positive cells. Expression of CD69 in $CD4^{-}CD8^{-}$, SP8 and SP4 cells from adult male and female HY/Dhh-WT, HY/Dhh-Het and HY/Dhh-KO littermates. Splenocytes were stained for anti-T3.7, anti-CD69, anti-CD8 and anti-CD4, and analyzed by flow cytometry. **(A)** Representative histogram of CD69 expression in male $CD4^{-}CD8^{-}$, SP8 and SP4 cells. **(B)** Representative bar graph of CD69 percentages in male $CD4^{-}CD8^{-}$, DP, SP8 and SP4 cells. **(C)** Representative histogram of CD69 expression in female $CD4^{-}CD8^{-}$, SP8 and SP4 cells. **(D)** Representative bar graph of CD69 percentages in female $CD4^{-}CD8^{-}$, DP, SP8 and SP4 cells. Figures are representative of 4 and 3 independent sets of male and female HY-Dhh littermates respectively. Mean and standard deviation of each population are given. Bars represent mean ± standard deviations. **Male CD69 percentages; $CD4^{-}CD8^{-}$** (p= 0.1 (WT/Het), 0.4 (WT/KO), 0.3 (Het/KO), n=3). **SP8** (p= 0.1 (WT/Het), 0.2 (WT/KO), 0.8 (Het/KO), n=3). **SP4** (p= 0.8 (WT/Het), 0.4 (WT/KO), 0.3 (Het/KO), n=3). **Female CD69 percentages; $CD4^{-}CD8^{-}$** (p= 0.8 (WT/Het), 0.4 (WT/KO), 0.6 (Het/KO), n=3). **SP8** (p= 0.8 (WT/Het), 0.3 (WT/KO), 0.4 (Het/KO), n=3). **SP4** (p= 0.9 (WT/Het), 0.8 (WT/KO), 0.7 (Het/KO), n=3).

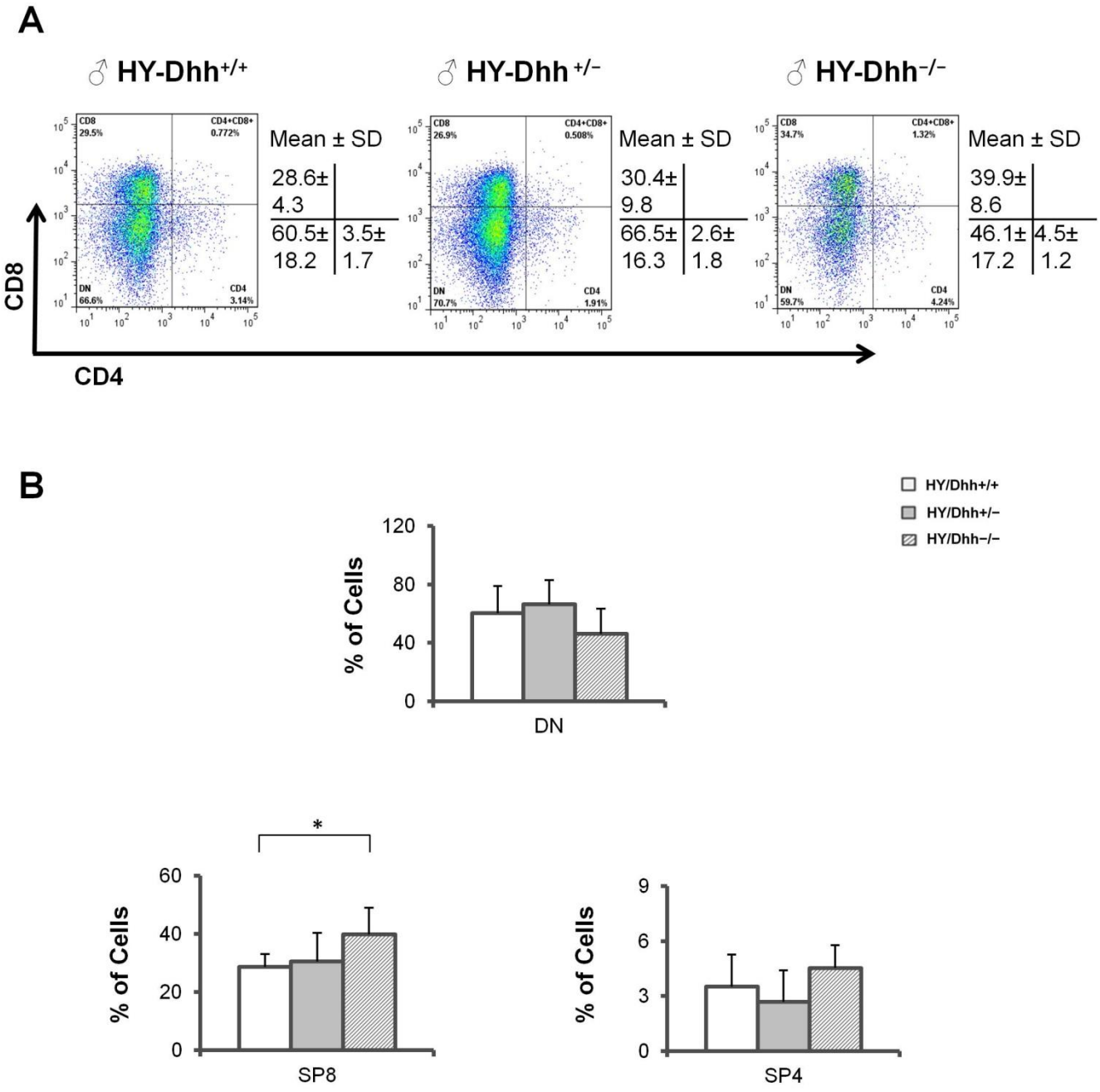

Figure 5.24

Major lymph node T cell populations in male HY-Dhh within the T3.7 positive cells. Percentage of T cell populations in the lymph node from adult male HY/Dhh-WT, HY/Dhh-Het and HY/Dhh-KO littermates. Cells were stained for anti-T3.7, anti-CD8 and anti-CD4, and analyzed by flow cytometry. Cell populations were gated within the $T3.7^+$ cells. **(A)** Representative dot plot of lymph node T cell populations. **(B)** Representative bar graph of $CD4^-CD8^-$, SP8 and SP4 percentages. Figures are representative of 3 independent sets of male HY-Dhh littermates. Mean and standard deviation of each population are given. Bars represent mean ± standard deviations. **$CD4^-CD8^-$** (p= 0.5 (WT/Het), 0.2 (WT/KO), 0.08 (Het/KO), n=3). **SP8** (p= 0.7 (WT/Het), 0.04 (WT/KO), 0.1 (Het/KO), n=3). **SP4** (p= 0.4 (WT/Het), 0.3 (WT/KO), 0.8 (Het/KO), n=3). *represents $p \leq 0.05$.

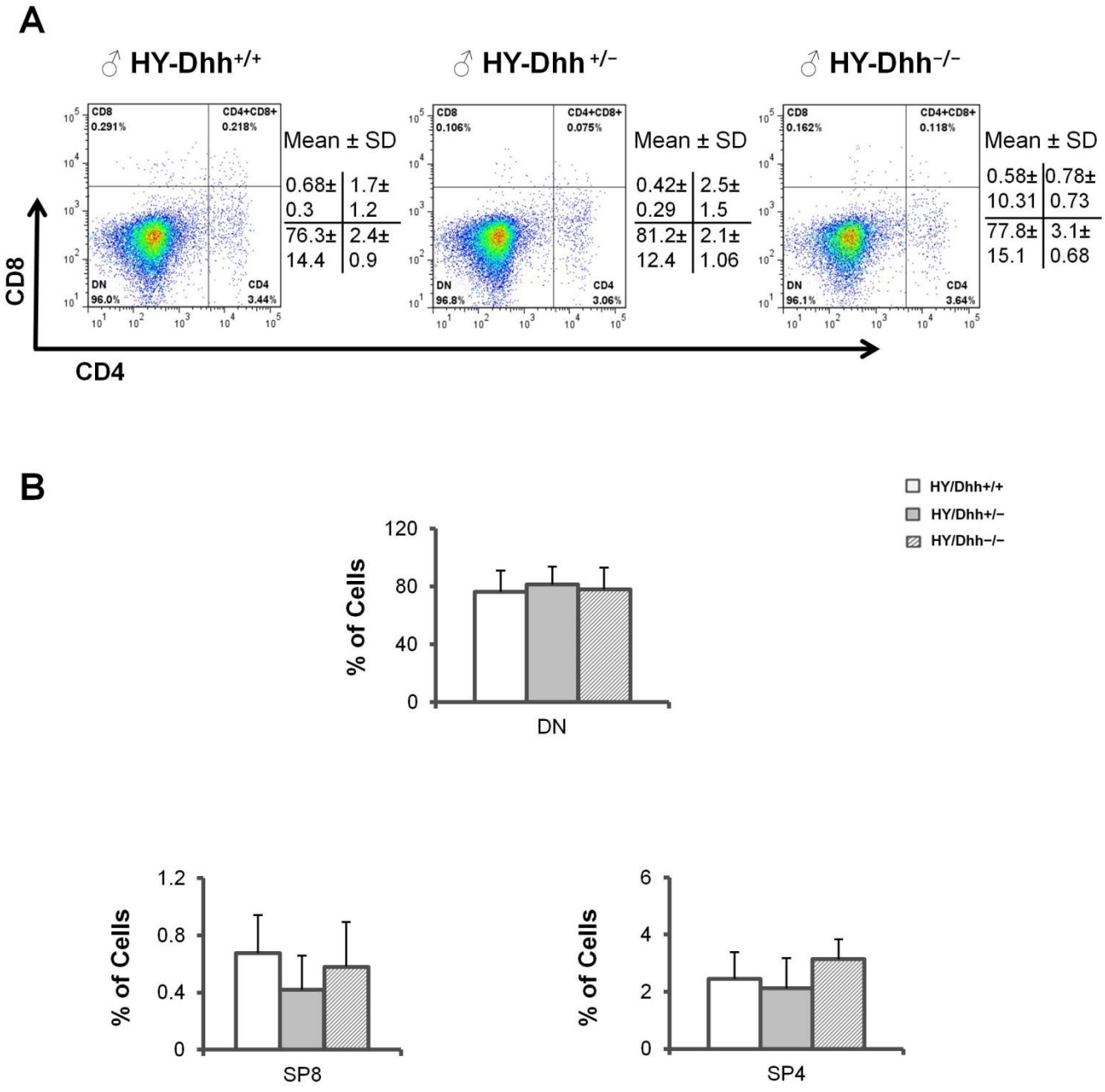

Figure 5.25

Major lymph node T cell populations in male HY-Dhh within the T3.7 negative cells. Percentage of T cell populations in the lymph node from adult male HY/Dhh-WT, HY/Dhh-Het and HY/Dhh-KO littermates. Cells were stained for anti-T3.7, anti-CD8 and anti-CD4, and analyzed by flow cytometry. Cell populations were gated within the $T3.7^{-}$ cells. **(A)** Representative dot plot of lymph node T cell populations. **(B)** Representative bar graph of $CD4^{-}CD8^{-}$, SP8 and SP4 percentages. Figures are representative of 3 independent sets of male HY-Dhh littermates. Mean and standard deviation of each population are given. Bars represent mean ± standard deviations. **$CD4^{-}CD8^{-}$** (p= 0.5 (WT/Het), 0.8 (WT/KO), 0.7 (Het/KO), n=3). **SP8** (p= 0.1 (WT/Het), 0.6 (WT/KO), 0.3 (Het/KO), n=3). **SP4** (p= 0.6 (WT/Het), 0.2 (WT/KO), 0.1 (Het/KO), n=3).

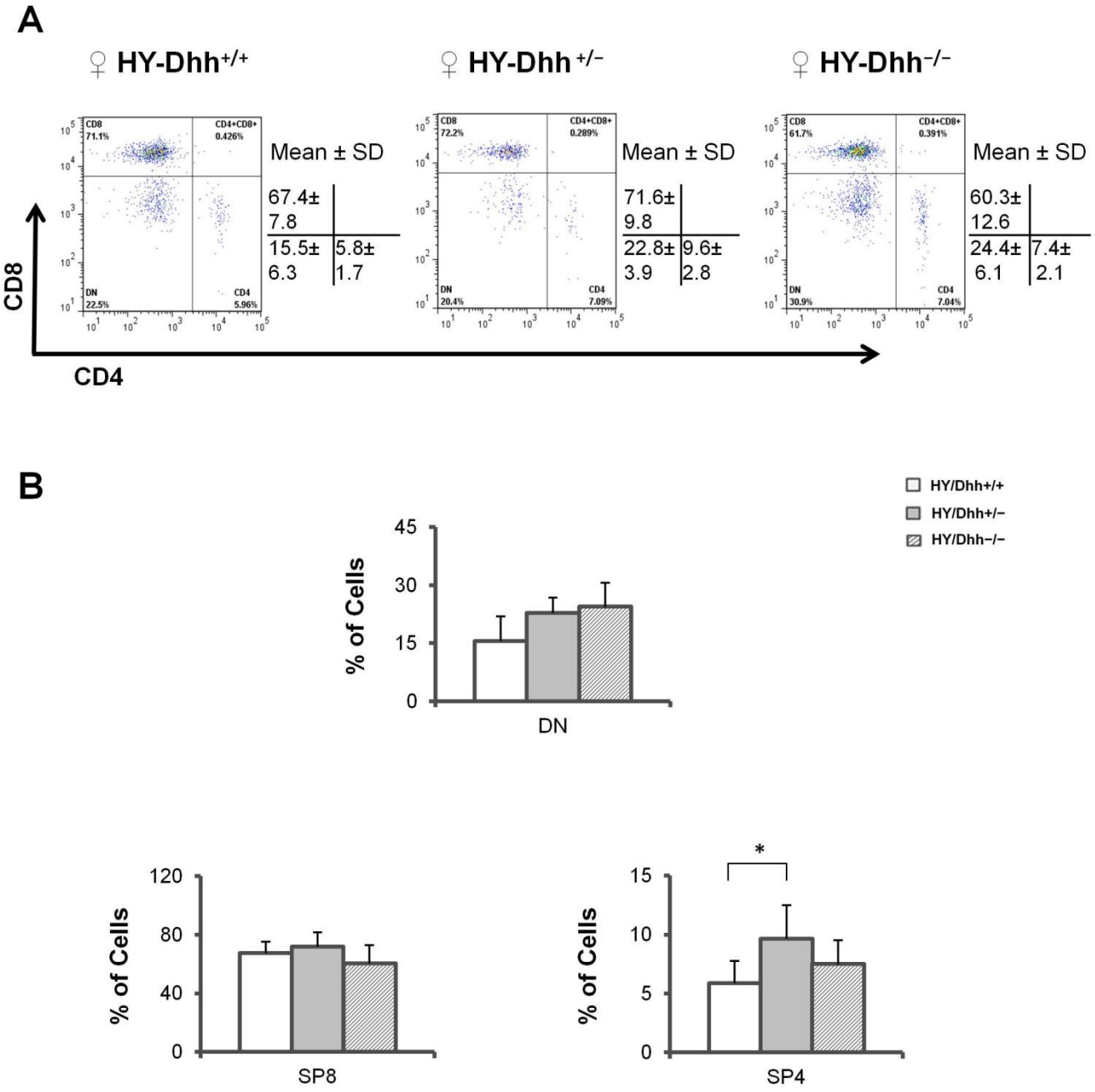

Figure 5.26

Major lymph node T cell populations in female HY-Dhh within the T3.7 positive cells. Percentage of T cell populations in the lymph node from adult female HY/Dhh-WT, HY/Dhh-Het and HY/Dhh-KO littermates. Cells were stained for anti-T3.7, anti-CD8 and anti-CD4, and analyzed by flow cytometry. Cell populations were gated within the $T3.7^+$ cells. **(A)** Representative dot plot of lymph node T cell populations. **(B)** Representative bar graph of $CD4^-CD8^-$, SP8 and SP4 percentages. Figures are representative of 3 independent sets of female HY-Dhh littermates. Mean and standard deviation of each population are given. Bars represent mean ± standard deviations. **$CD4^-CD8^-$** (p= 0.06 (WT/Het), 0.5 (WT/KO), 0.6 (Het/KO), n=3). **SP8** (p= 0.4 (WT/Het), 0.3 (WT/KO), 0.1 (Het/KO), n=3). **SP4** (p= 0.04 (WT/Het), 0.2 (WT/KO), 0.2 (Het/KO), n=3). *represents $p \leq 0.05$.

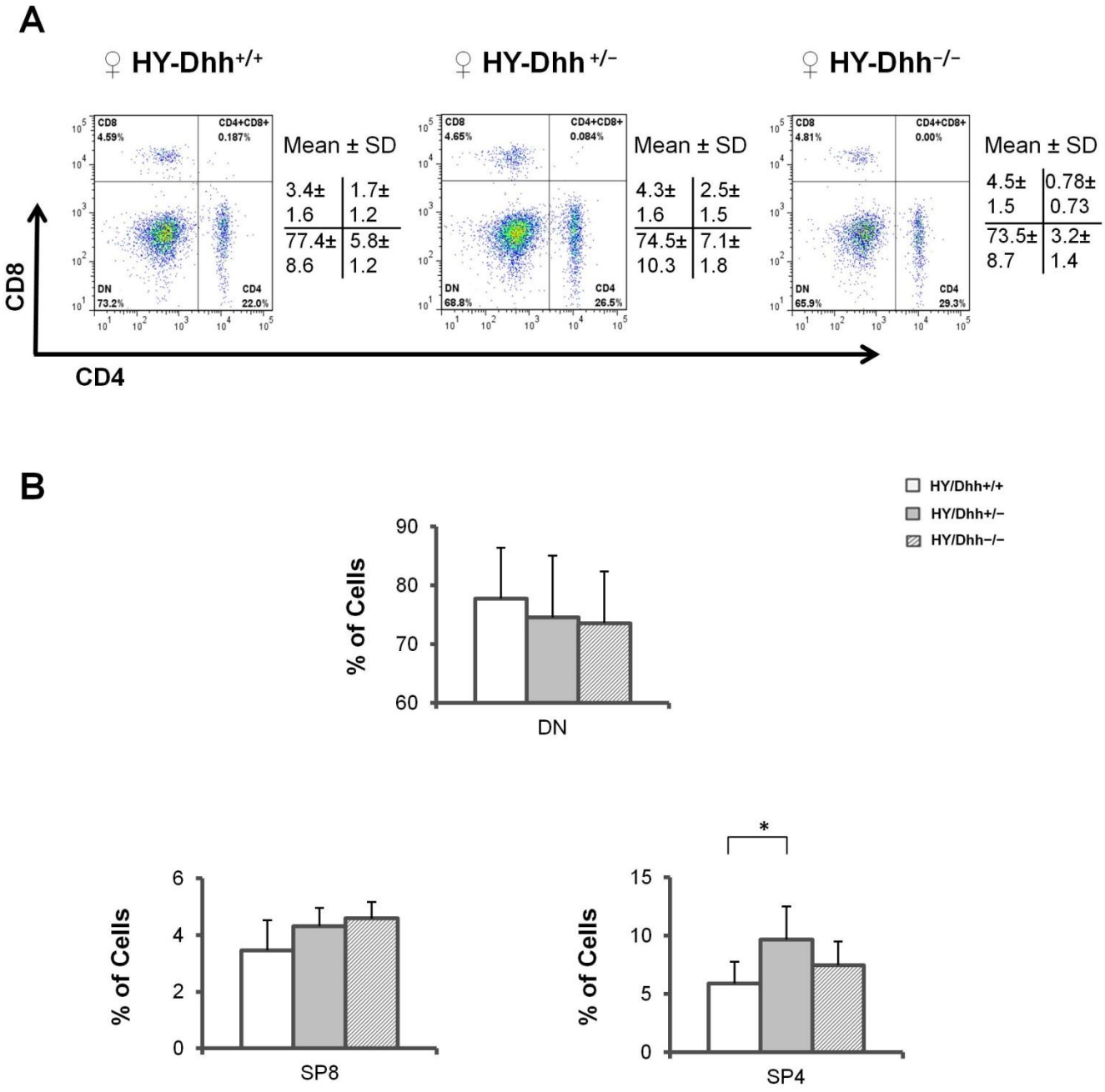

Figure 5.27

Major lymph node T cell populations in female HY-Dhh within the T3.7 negative cells. Percentage of T cell populations in the lymph node from adult female HY/Dhh-WT, HY/Dhh-Het and HY/Dhh-KO littermates. Cells were stained for anti-T3.7, anti-CD8 and anti-CD4, and analyzed by flow cytometry. Cell populations were gated within the $T3.7^-$ cells. **(A)** Representative dot plot of lymph node T cell populations. **(B)** Representative bar graph of $CD4^-CD8^-$, SP8 and SP4 percentages. Figures are representative of 3 independent sets of female HY-Dhh littermates. Mean and standard deviation of each population are given. Bars represent mean ± standard deviations. **$CD4^-CD8^-$** (p= 0.6 (WT/Het), 0.4 (WT/KO), 0.8 (Het/KO), n=3). **SP8** (p= 0.1 (WT/Het), 0.08 (WT/KO), 0.5 (Het/KO), n=3). **SP4** (p= 0.04 (WT/Het), 0.2 (WT/KO), 0.2 (Het/KO), n=3). *represents $p \leq 0.05$.

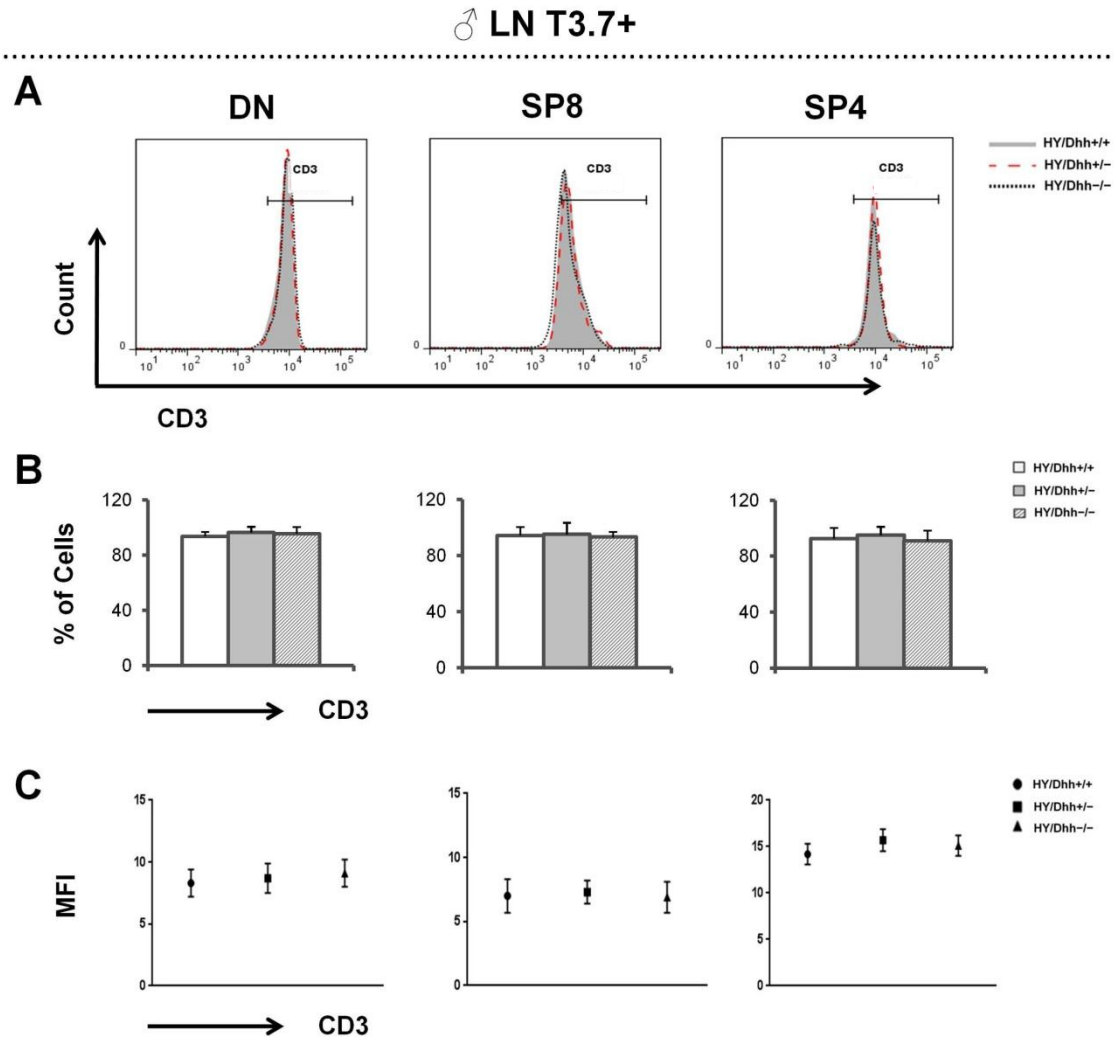

Figure 5.28

Expression of CD3 in male HY-Dhh lymph node T cells within the T3.7 positive cells. Expression of CD3 in $CD4^{-}CD8^{-}$, SP8 and SP4 cells from adult male HY/Dhh-WT, HY/Dhh-Het and HY/Dhh-KO littermates. Cells were stained for anti-T3.7, anti-CD3, anti-CD8 and anti-CD4, and analyzed by flow cytometry. **(A)** Representative histogram of CD3 expression in $CD4^{-}CD8^{-}$, SP8 and SP4 cells. **(B)** Representative bar graph of CD3 percentages in $CD4^{-}CD8^{-}$, SP8 and SP4 cells. **(C)** Representative scatter plot of CD3 MFI in $CD4^{-}CD8^{-}$, SP8 and SP4 cells. Figures are representative of 3 independent sets of male HY-Dhh littermates. Mean and standard deviation of each population are given. Bars represent mean ± standard deviations. **CD3 percentages; $CD4^{-}CD8^{-}$** (p= 0.2 (WT/Het), 0.5 (WT/KO), 0.7 (Het/KO), n=3). **SP8** (p= 0.08 (WT/Het), 0.7 (WT/KO), 0.6 (Het/KO), n=3). **SP4** (p= 0.6 (WT/Het), 0.8 (WT/KO), 0.4 (Het/KO), n=3). **CD3 MFI; $CD4^{-}CD8^{-}$** (p= 0.3 (WT/Het), 0.6 (WT/KO), 0.8 (Het/KO), n=3). **SP8** (p= 0.2 (WT/Het), 0.4 (WT/KO), 0.7 (Het/KO), n=3). **SP4** (p= 0.4 (WT/Het), 0.8 (WT/KO), 0.4 (Het/KO), n=3).

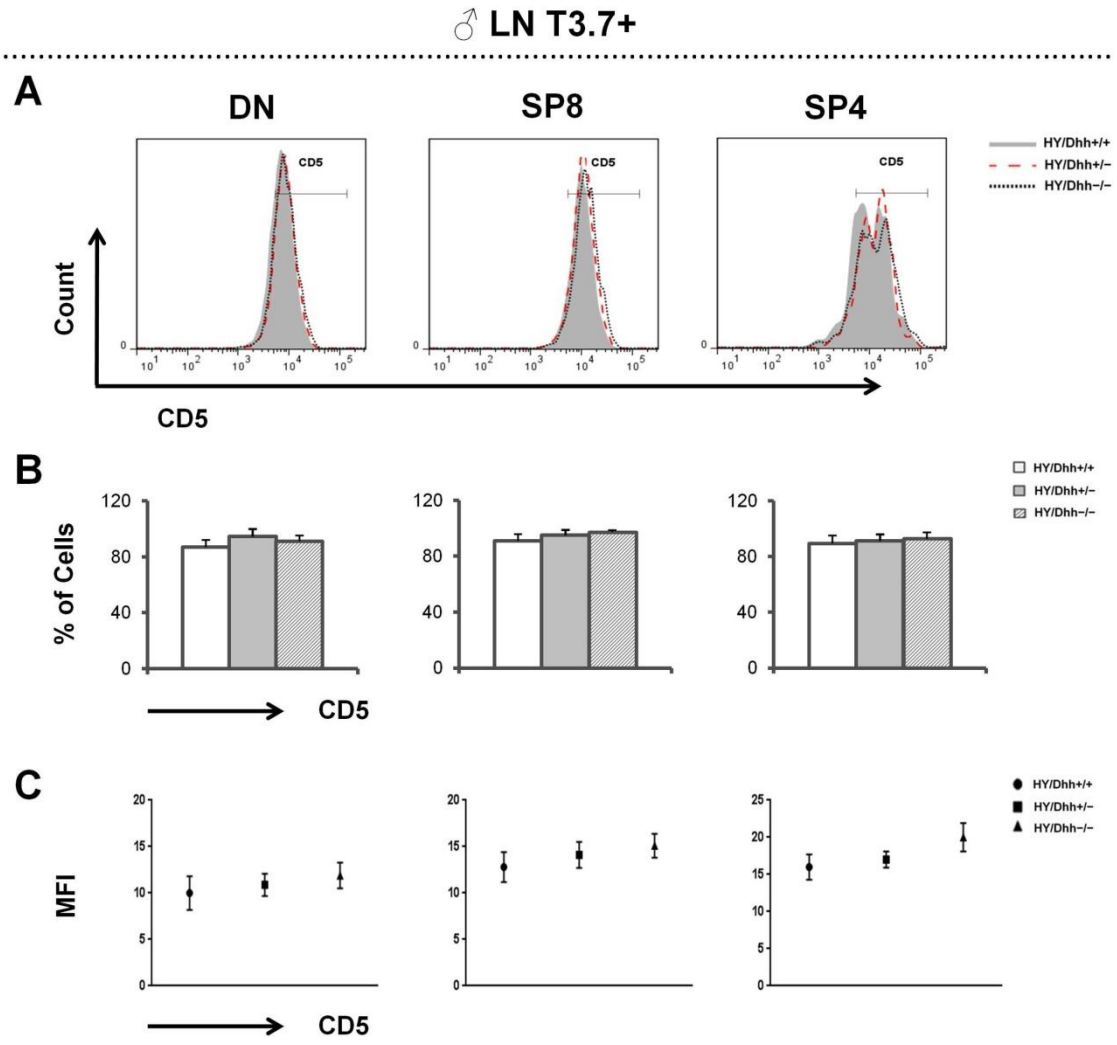

Figure 5.29

Expression of CD5 in male HY-Dhh lymph node T cells within the T3.7 positive cells. Expression of CD5 in $CD4^{-}CD8^{-}$**,** SP8 and SP4 cells from adult male HY/Dhh-WT, HY/Dhh-Het and HY/Dhh-KO littermates. Cells were stained for anti-T3.7, anti-CD5, anti-CD8 and anti-CD4, and analyzed by flow cytometry. **(A)** Representative histogram of CD5 expression in $CD4^{-}CD8^{-}$, SP8 and SP4 cells. **(B)** Representative bar graph of CD5 percentages in $CD4^{-}CD8^{-}$, SP8 and SP4 cells. **(C)** Representative scatter plot of CD5 MFI in $CD4^{-}CD8^{-}$, SP8 and SP4 cells. Figures are representative of 3 independent sets of male HY-Dhh littermates. Mean and standard deviation of each population are given. Bars represent mean ± standard deviations. **CD5 percentages; $CD4^{-}CD8^{-}$** (p= 0.08 (WT/Het), 0.2 (WT/KO), 0.3 (Het/KO), n=3). **SP8** (p= 0.2 (WT/Het), 0.07 (WT/KO), 0.3 (Het/KO), n=3). **SP4** (p= 0.6 (WT/Het), 0.4 (WT/KO), 0.6 (Het/KO), n=3). **CD5 MFI; $CD4^{-}CD8^{-}$** (p= 0.2 (WT/Het), 0.4 (WT/KO), 0.8 (Het/KO), n=3). **SP8** (p= 0.7 (WT/Het), 0.5 (WT/KO), 0.2 (Het/KO), n=3). **SP4** (p= 0.7 (WT/Het), 0.1 (WT/KO), 0.4 (Het/KO), n=3).

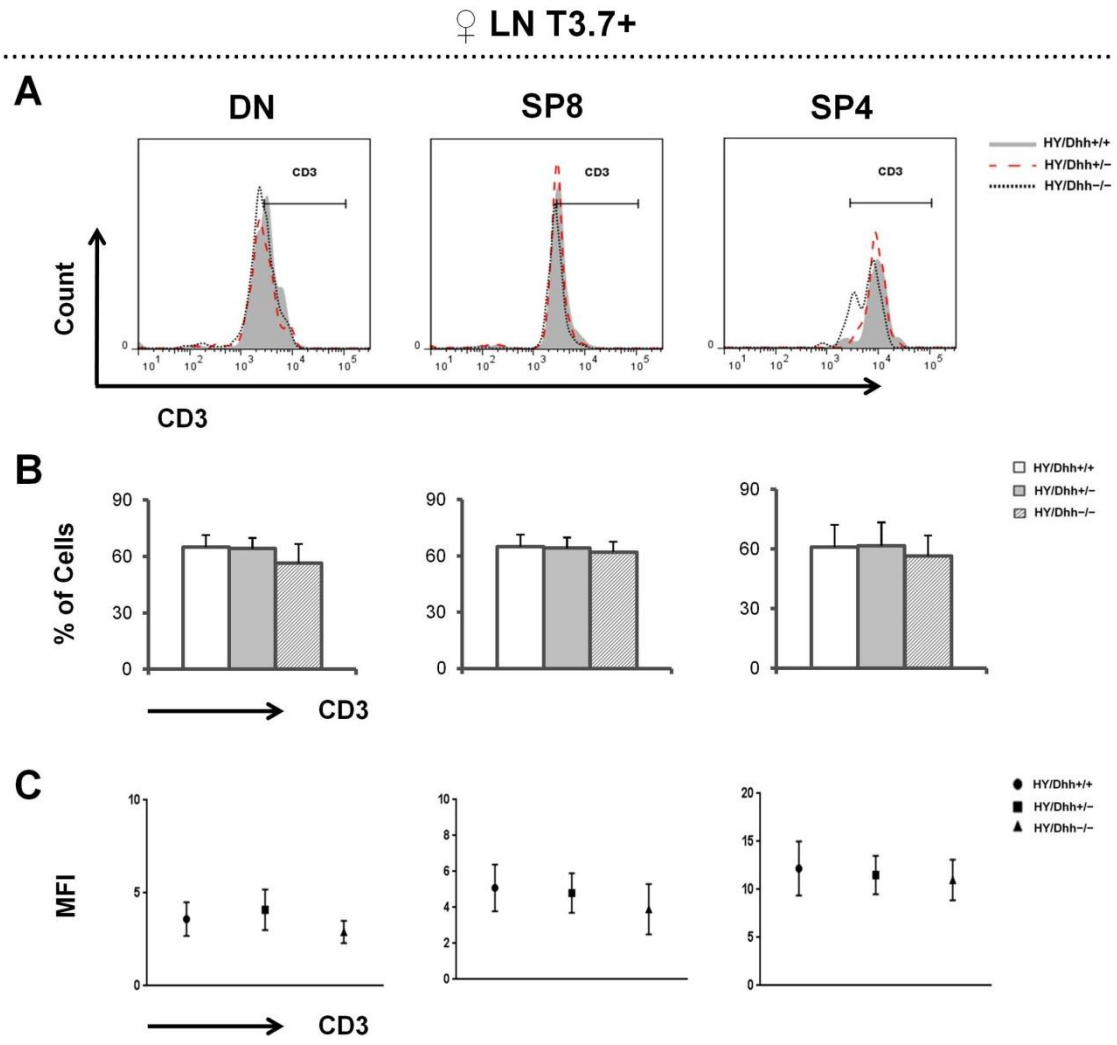

Figure 5.30

Expression of CD3 in female HY-Dhh lymph node T cells within the T3.7 positive cells. Expression of CD3 in $CD4^{-}CD8^{-}$**,** SP8 and SP4 cells from adult female HY/Dhh-WT, HY/Dhh-Het and HY/Dhh-KO littermates. Cells were stained for anti-T3.7, anti-CD3, anti-CD8 and anti-CD4, and analyzed by flow cytometry. **(A)** Representative histogram of CD3 expression in $CD4^{-}CD8^{-}$, SP8 and SP4 cells. **(B)** Representative bar graph of CD3 percentages in $CD4^{-}CD8^{-}$, SP8 and SP4 cells. **(C)** Representative scatter plot of CD3 MFI in $CD4^{-}CD8^{-}$, SP8 and SP4 cells. Figures are representative of 3 independent sets of female HY-Dhh littermates. Mean and standard deviation of each population are given. Bars represent mean ± standard deviations. **CD3 percentages; $CD4^{-}CD8^{-}$** (p= 0.8 (WT/Het), 0.3 (WT/KO), 0.3 (Het/KO), n=3). **SP8** (p= 0.8 (WT/Het), 0.5 (WT/KO), 0.6 (Het/KO), n=3). **SP4** (p= 0.9 (WT/Het), 0.6 (WT/KO), 0.5 (Het/KO), n=3). **CD3 MFI; $CD4^{-}CD8^{-}$** (p= 0.4 (WT/Het), 0.3 (WT/KO), 0.4 (Het/KO), n=3). **SP8** (p= 0.2 (WT/Het), 0.6 (WT/KO), 0.7 (Het/KO), n=3). **SP4** (p= 0.1 (WT/Het), 0.8 (WT/KO), 0.7 (Het/KO), n=3).

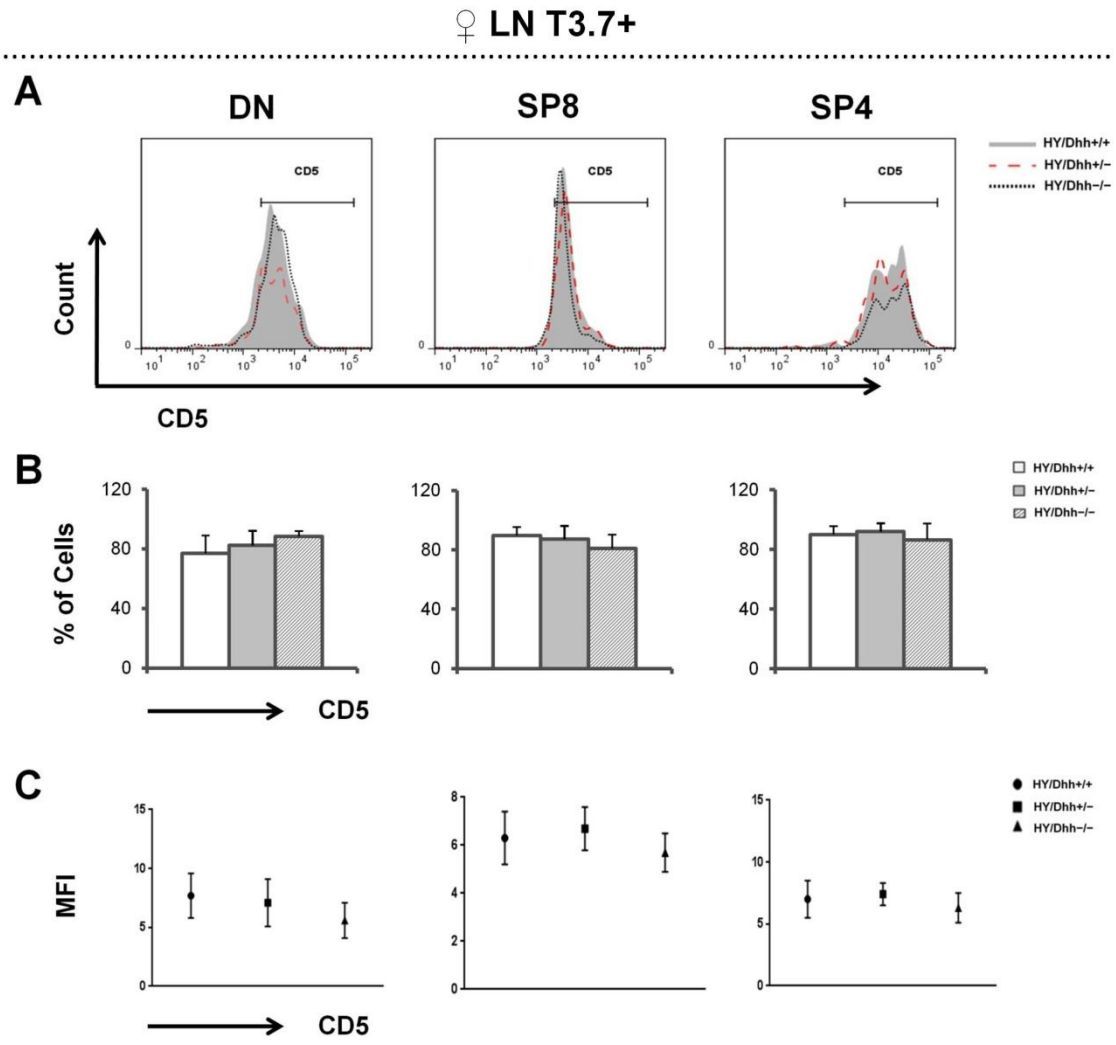

Figure 5.31

Expression of CD5 in female HY-Dhh lymph node T cells within the T3.7 positive cells. Expression of CD5 in $CD4^{-}CD8^{-}$**,** SP8 and SP4 cells from adult female HY/Dhh-WT, HY/Dhh-Het and HY/Dhh-KO littermates. Cells were stained for anti-T3.7, anti-CD5, anti-CD8 and anti-CD4, and analyzed by flow cytometry. **(A)** Representative histogram of CD5 expression in $CD4^{-}CD8^{-}$, SP8 and SP4 cells. **(B)** Representative bar graph of CD5 percentages in $CD4^{-}CD8^{-}$, SP8 and SP4 cells. **(C)** Representative scatter plot of CD5 MFI in $CD4^{-}CD8^{-}$, SP8 and SP4 cells. Figures are representative of 3 independent sets of female HY-Dhh littermates. Mean and standard deviation of each population are given. Bars represent mean ± standard deviations. **CD5 percentages; $CD4^{-}CD8^{-}$** (p= 0.5 (WT/Het), 0.1 (WT/KO), 0.3 (Het/KO), n=3). **SP8** (p= 0.6 (WT/Het), 0.1 (WT/KO), 0.3 (Het/KO), n=3). **SP4** (p= 0.6 (WT/Het), 0.6 (WT/KO), 0.4 (Het/KO), n=3). **CD5 MFI; $CD4^{-}CD8^{-}$** (p= 0.6 (WT/Het), 0.2 (WT/KO), 0.4 (Het/KO), n=3). **SP8** (p= 0.3 (WT/Het), 0.6 (WT/KO), 0.9 (Het/KO), n=3). **SP4** (p= 0.3 (WT/Het), 0.7 (WT/KO), 0.4 (Het/KO), n=3).

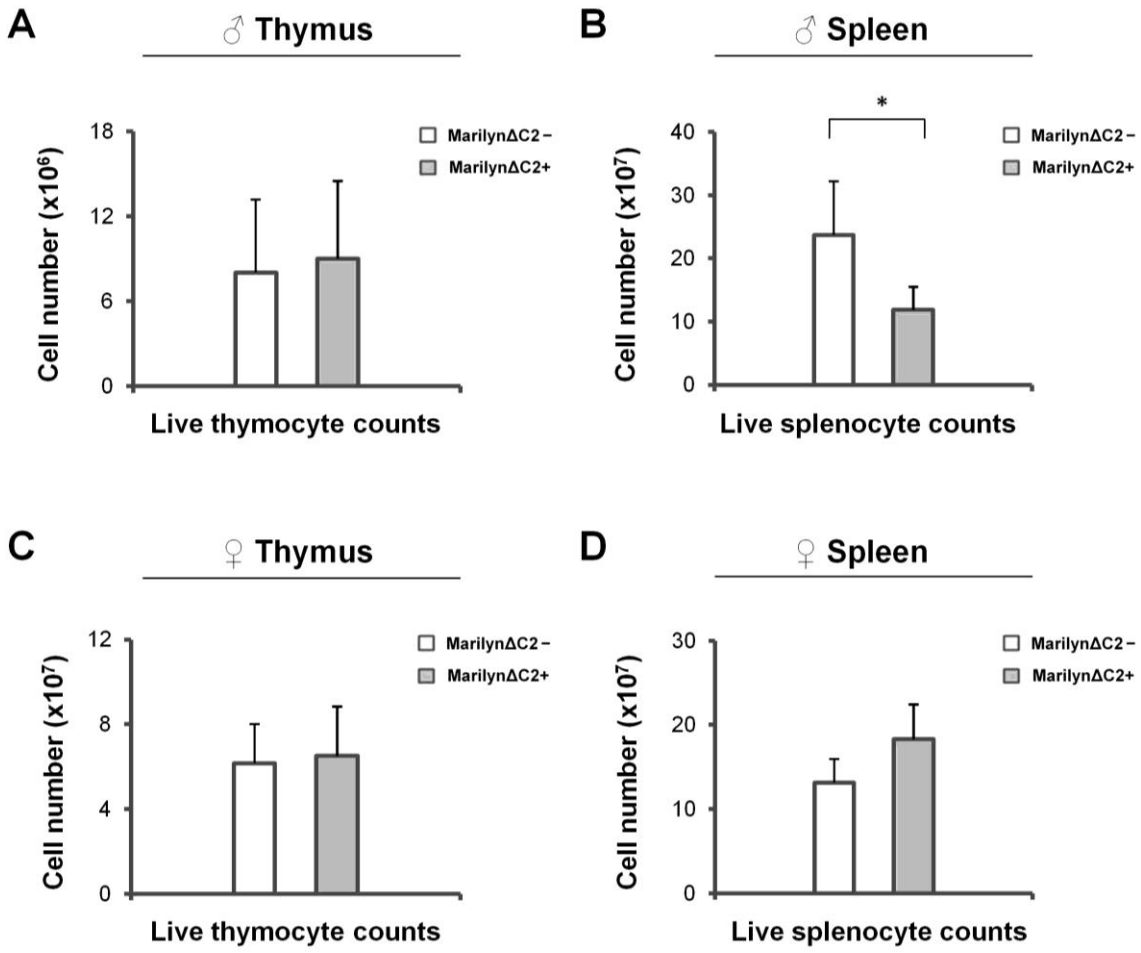

Figure 5.32

Thymus and spleen live cell counts in male and female Marilyn-Gli2ΔC2 littermates. Thymocyte and splenocyte total counts from adult male and female Marilyn-Gli2ΔC2^{-} and Marilyn-Gli2ΔC2^{+} littermates. **(A)** Live male thymocyte counts. **(B)** Live male splenocyte counts. **(C)** Live female thymocyte counts. **(D)** Live female splenocyte counts. Mean and standard deviation of each population are given. Bars represent mean ± standard deviations**. Male thymocytes;** (p=0.6, n=5). **Male splenocytes;** (p=0.03, n=4). **Female thymocytes;** (p=0.6, n=5). **Female splenocytes;** (p=0.2, n=6). *represents p≤0.05.

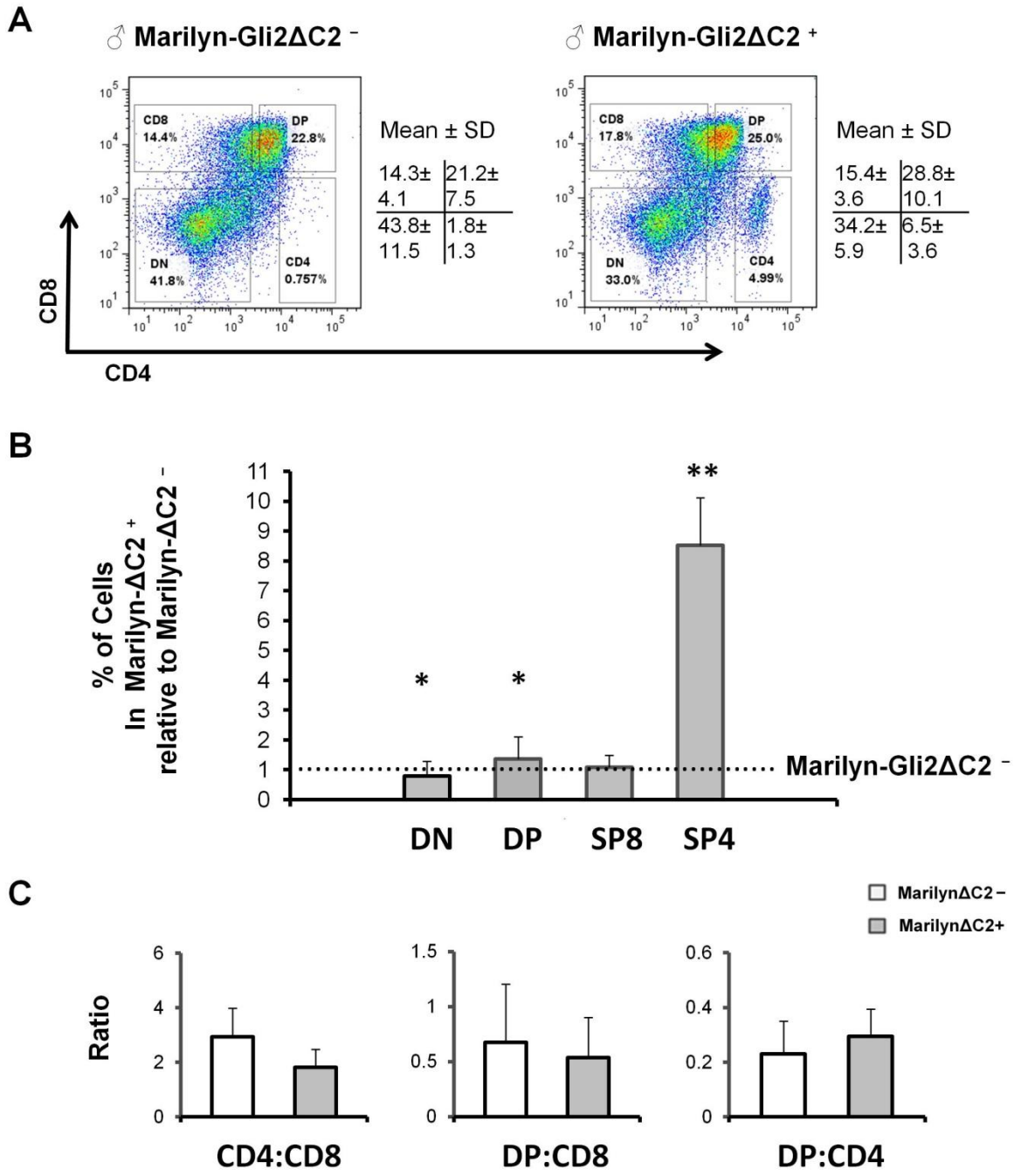

Figure 5.33

Major thymocyte populations in male Marilyn-Gli2ΔC2 mice. Percentage of thymocyte populations from adult male Marilyn-Gli2ΔC2^{-} and Marilyn-Gli2ΔC2^{+} littermates. Thymocytes were stained for anti-vβ6, anti-CD8 and anti-CD4, and analyzed by flow cytometry. **(A)** Representative dot plot of thymocyte populations. **(B)** Representative bar graph of DN, DP, SP8 and SP4 percentages. **(C)** Ratios of CD4:CD8, DP:CD8 and DP:CD4. Figures are representative of 7 independent sets of male Marilyn-Gli2ΔC2 littermates. Mean and standard deviation of each population are given. Bars represent mean ± standard deviations. **DN** (p= 0.008, n=7). **DP** (p= 0.02, n=7). **SP8** (p= 0.3, n=7). **SP4** (p=0.004, n=7). *represents p≤0.05, **represents p≤0.005.

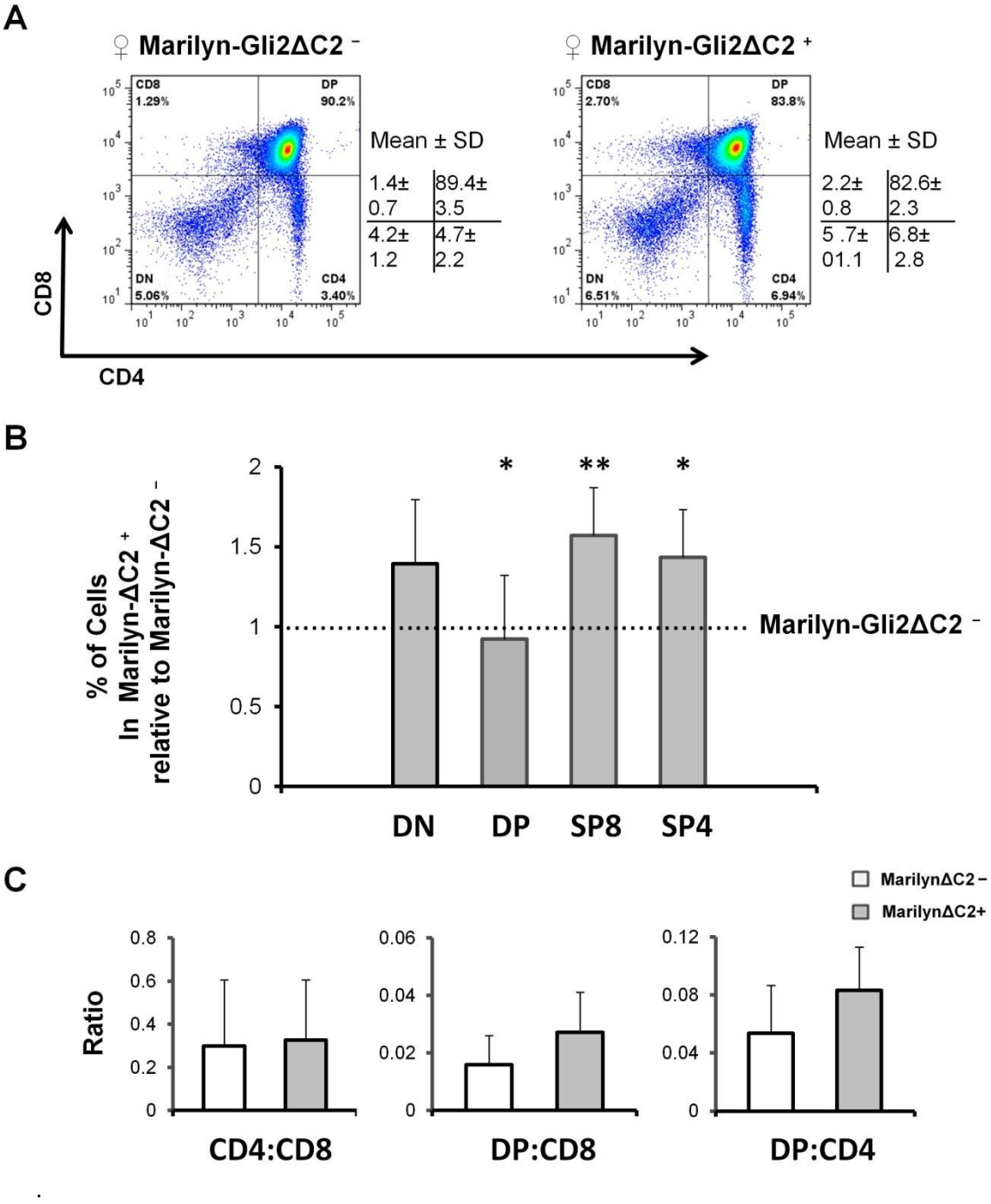

.

Figure 5.34

Major thymocyte populations in female Marilyn-Gli2ΔC2 mice. Percentage of thymocyte populations from adult female Marilyn-Gli2ΔC2^{-} and Marilyn-Gli2ΔC2^{+} littermates. Thymocytes were stained for anti-vβ6, anti-CD8 and anti-CD4, and analyzed by flow cytometry. **(A)** Representative dot plot of thymocyte populations. **(B)** Representative bar graph of DN, DP, SP8 and SP4 percentages. **(C)** Ratios of CD4:CD8, DP:CD8 and DP:CD4. Figures are representative of 6 independent sets of female Marilyn-Gli2ΔC2 littermates. Mean and standard deviation of each population are given. Bars represent mean ± standard deviations. **DN** (p= 0.06, n=6). **DP** (p= 0.007, n=6). **SP8** (p= 0.002, n=6). **SP4** (p=0.03, n=6). *represents p≤0.05. **represents p≤0.005.

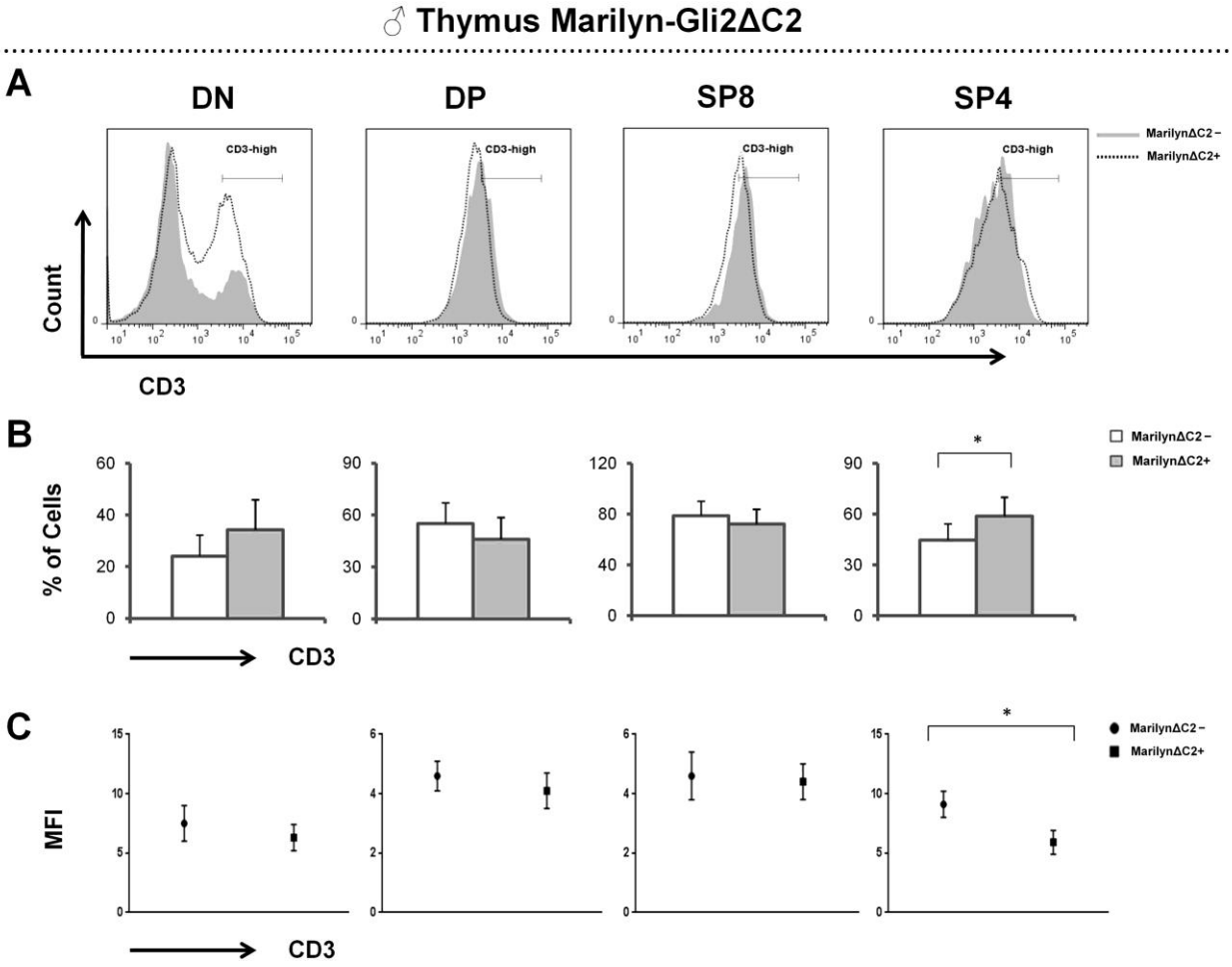

Figure 5.35

Expression of CD3 in male Marilyn-Gli2ΔC2 thymocytes. Expression of CD3 and CD5 in DN, DP, SP8 and SP4 thymocytes from adult male Marilyn-Gli2ΔC2^{-} and Marilyn-Gli2ΔC2^{+} littermates. Thymocytes were stained for anti-CD3, anti-CD8 and anti-CD4, and analyzed by flow cytometry. **(A)** Representative histogram of CD3 expression in DN, DP, SP8 and SP4 cells. **(B)** Representative bar graph of CD3 percentages in DN, DP, SP8 and SP4 cells. **(C)** Representative scatter plot of CD3 MFI in DN, DP, SP8 and SP4 cells. Figures are representative of 6 independent sets of male Marilyn-Gli2ΔC2 littermates. Mean and standard deviation of each population are given. Bars represent mean ± standard deviations. **CD3 percentages; DN** (p= 0.08, n=6). **DP** (p= 0.1, n=6). **SP8** (p= 0.3, n=6). **SP4** (p= 0.02, n=6). **CD3 MFI; DN** (p= 0.2, n=6). DP (p= 0.5, n=6). **SP8** (p= 0.7, n=6). **SP4** (p= 0.01, n=6). *represents p≤0.05.

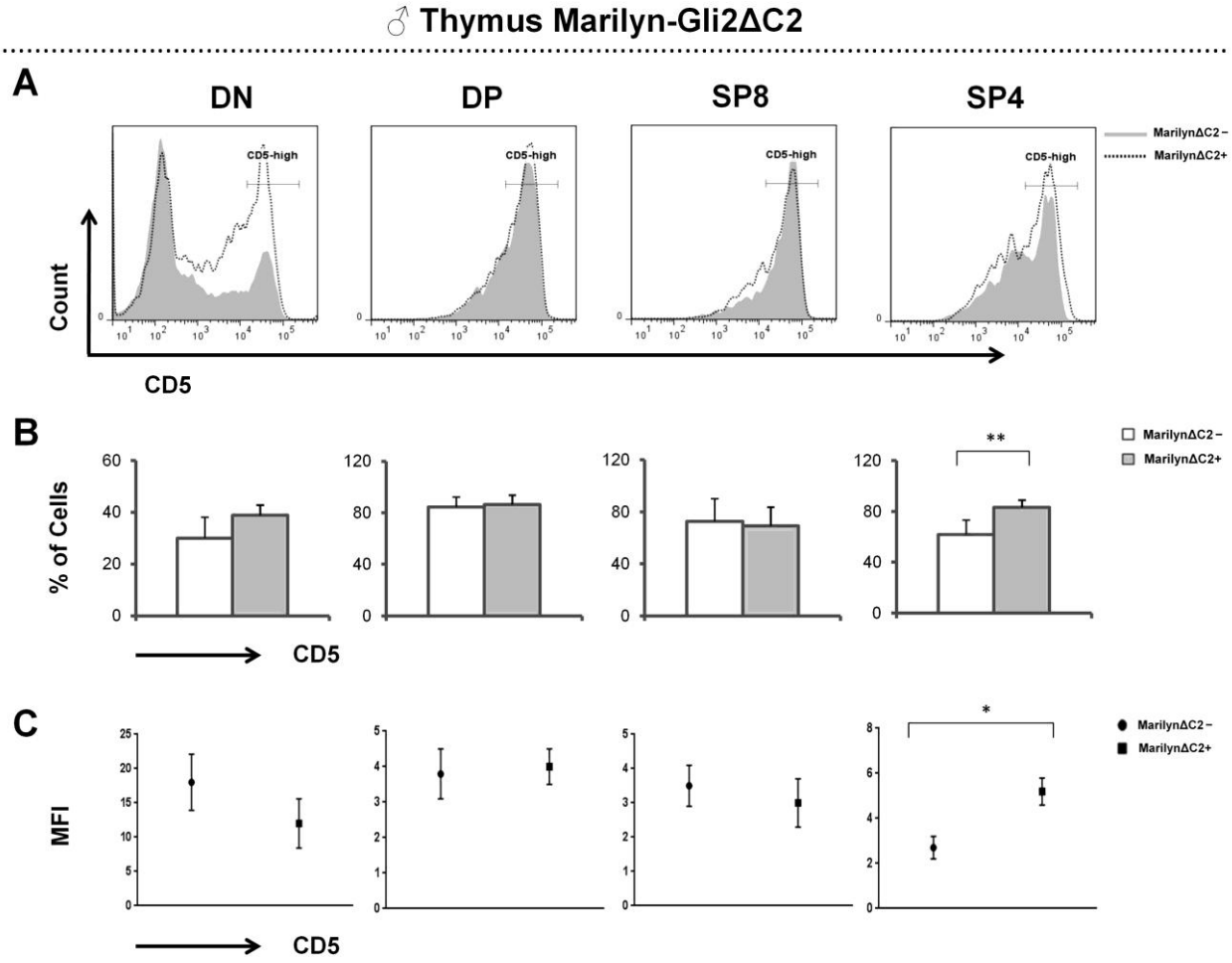

Figure 5.36

Expression of CD5 in male Marilyn-Gli2ΔC2 thymocytes. Expression of CD5 in DN, DP, SP8 and SP4 thymocytes from adult male Marilyn-Gli2ΔC2^{-} and Marilyn-Gli2ΔC2^{+} littermates. Thymocytes were stained for anti-CD5, anti-CD8 and anti-CD4, and analyzed by flow cytometry. **(A)** Representative histogram of CD5 expression in DN, DP, SP8 and SP4 cells. **(B)** Representative bar graph of CD5 percentages in DN, DP, SP8 and SP4 cells. **(C)** Representative scatter plot of CD5 MFI in DN, DP, SP8 and SP4 cells. Figures are representative of 6 independent sets of male Marilyn-Gli2ΔC2 littermates. Mean and standard deviation of each population are given. Bars represent mean ± standard deviations. **CD5 percentages; DN** (p= 0.2, n=6). DP (p= 0.5, n=6). **SP8** (p= 0.6, n=6). **SP4** (p= 0.001, n=6). **CD5 MFI; DN** (p= 0.2, n=6). **DP** (p= 0.09, n=6). **SP8** (p= 0.07, n=6). **SP4** (p= 0.03, n=6). *represents p≤0.05, **represents p≤0.005.

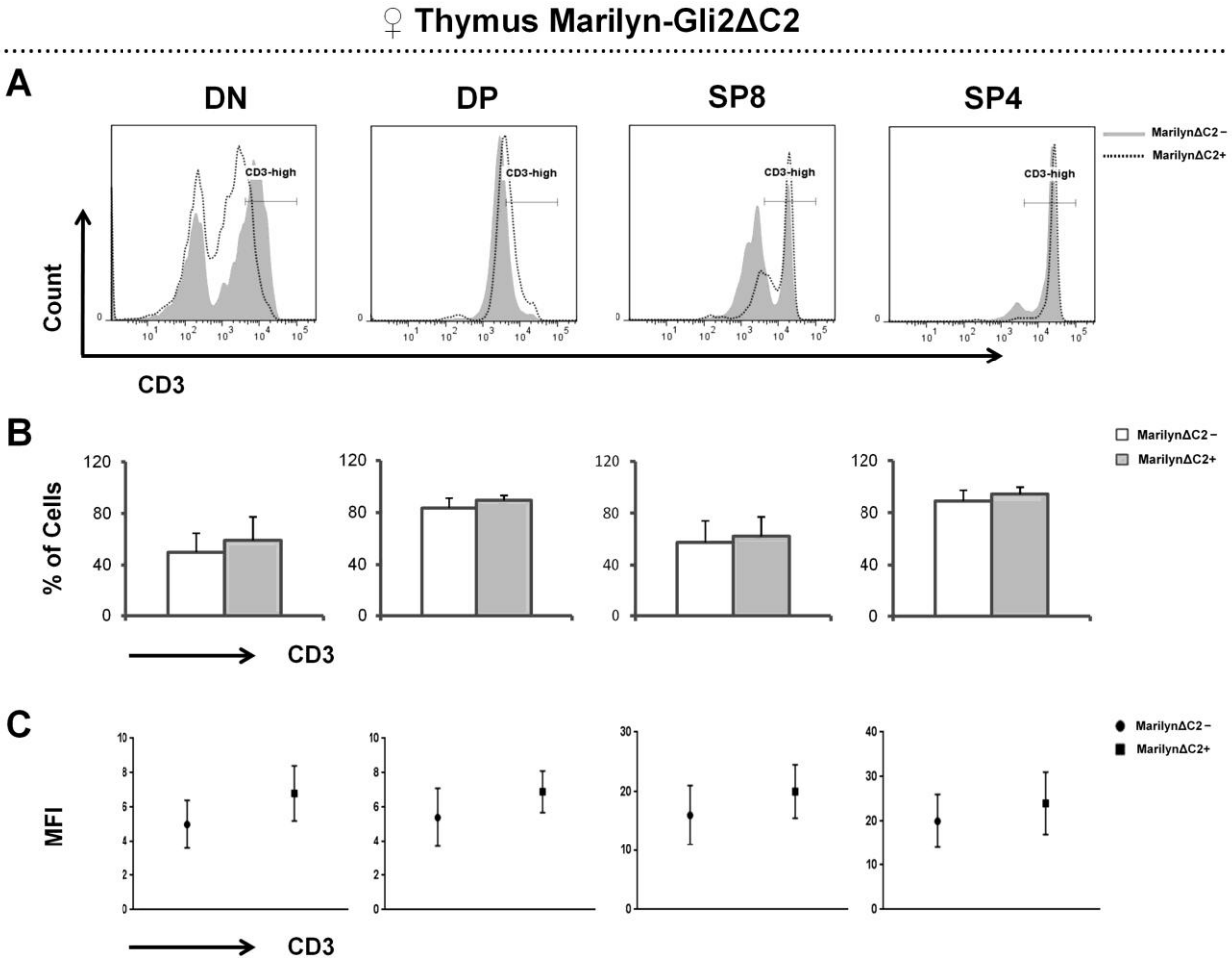

Figure 5.37

Expression of CD3 in female Marilyn-Gli2ΔC2 thymocytes. Expression of CD3 in DN, DP, SP8 and SP4 thymocytes from adult female Marilyn-Gli2ΔC2^{-} and Marilyn-Gli2ΔC2^{+} littermates. Thymocytes were stained for anti-CD3, anti-CD8 and anti-CD4, and analyzed by flow cytometry. **(A)** Representative histogram of CD3 expression in DN, DP, SP8 and SP4 cells. **(B)** Representative bar graph of CD3 percentages in DN, DP, SP8 and SP4 cells. **(C)** Representative scatter plot of CD3 MFI in DN, DP, SP8 and SP4 cells. Figures are representative of 6 independent sets of female Marilyn-Gli2ΔC2 littermates. Mean and standard deviation of each population are given. Bars represent mean ± standard deviations. **CD3 percentages; DN** (p= 0.3, n=6). **DP** (p= 0.2, n=6). **SP8** (p= 0.6, n=6). **SP4** (p= 0.3, n=6). **CD3 MFI; DN** (p= 0.06, n=6). **DP** (p= 0.07, n=6). **SP8** (p= 0.1, n=6). **SP4** (p= 0.09, n=6).

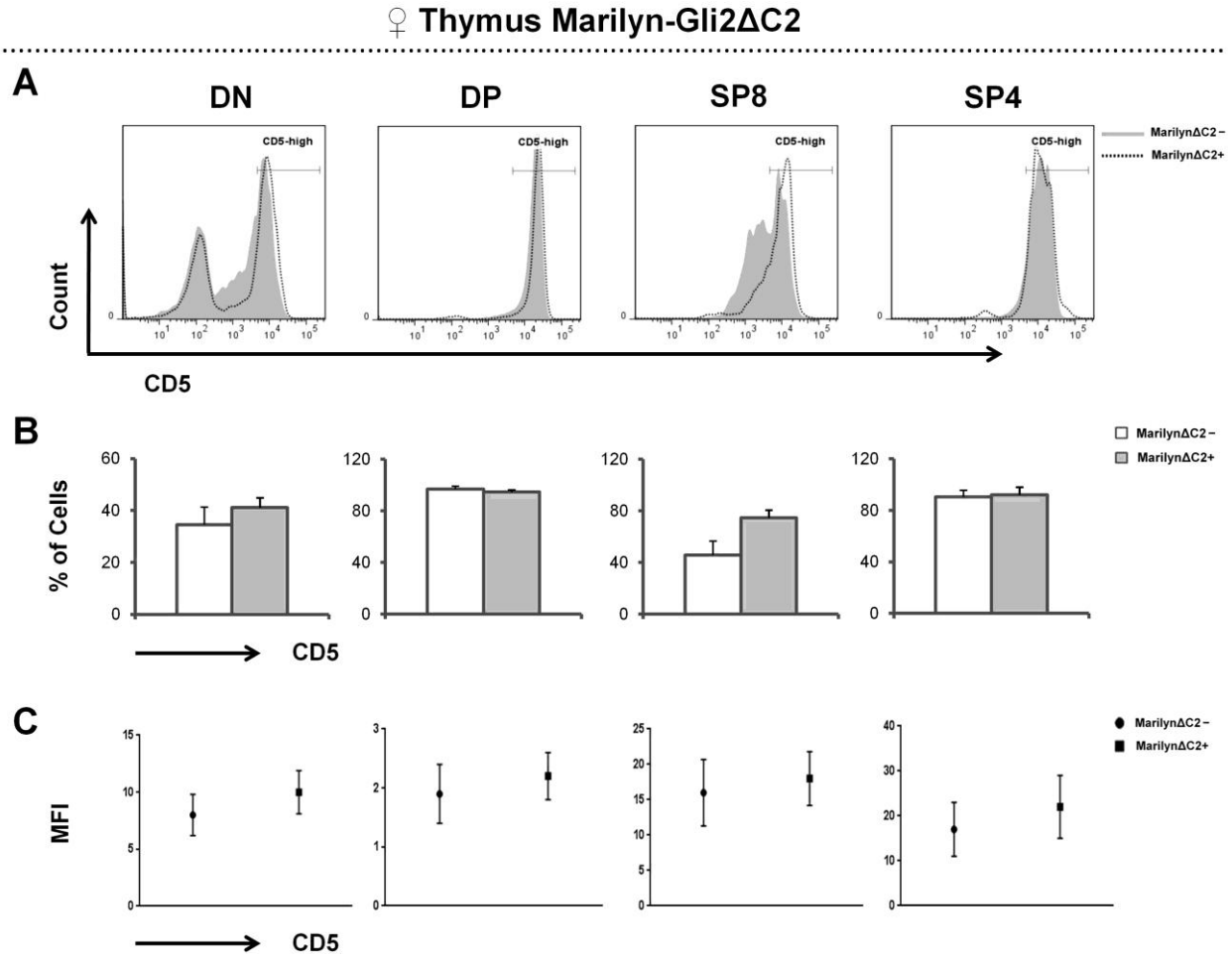

Figure 5.38

Expression of CD5 in female Marilyn-Gli2ΔC2 thymocytes. Expression of CD5 in DN, DP, SP8 and SP4 thymocytes from adult female Marilyn-Gli2ΔC2^{-} and Marilyn-Gli2ΔC2^{+} littermates. Thymocytes were stained for anti-CD5, anti-CD8 and anti-CD4, and analyzed by flow cytometry. **(A)** Representative histogram of CD5 expression in DN, DP, SP8 and SP4 cells. **(B)** Representative bar graph of CD5 percentages in DN, DP, SP8 and SP4 cells. **(C)** Representative scatter plot of CD5 MFI in DN, DP, SP8 and SP4 cells. Figures are representative of 6 independent sets of female Marilyn-Gli2ΔC2 littermates. Mean and standard deviation of each population are given. Bars represent mean ± standard deviations. **CD5 percentages; DN** (p= 0.1, n=6). **DP** (p= 0.1, n=6). **SP8** (p= 0.06, n=6). **SP4** (p= 0.7, n=6). **CD3 MFI; DN** (p= 0.07, n=6). **DP** (p= 0.08, n=6). **SP8** (p= 0.07, n=6). **SP4** (p= 0.06, n=6).

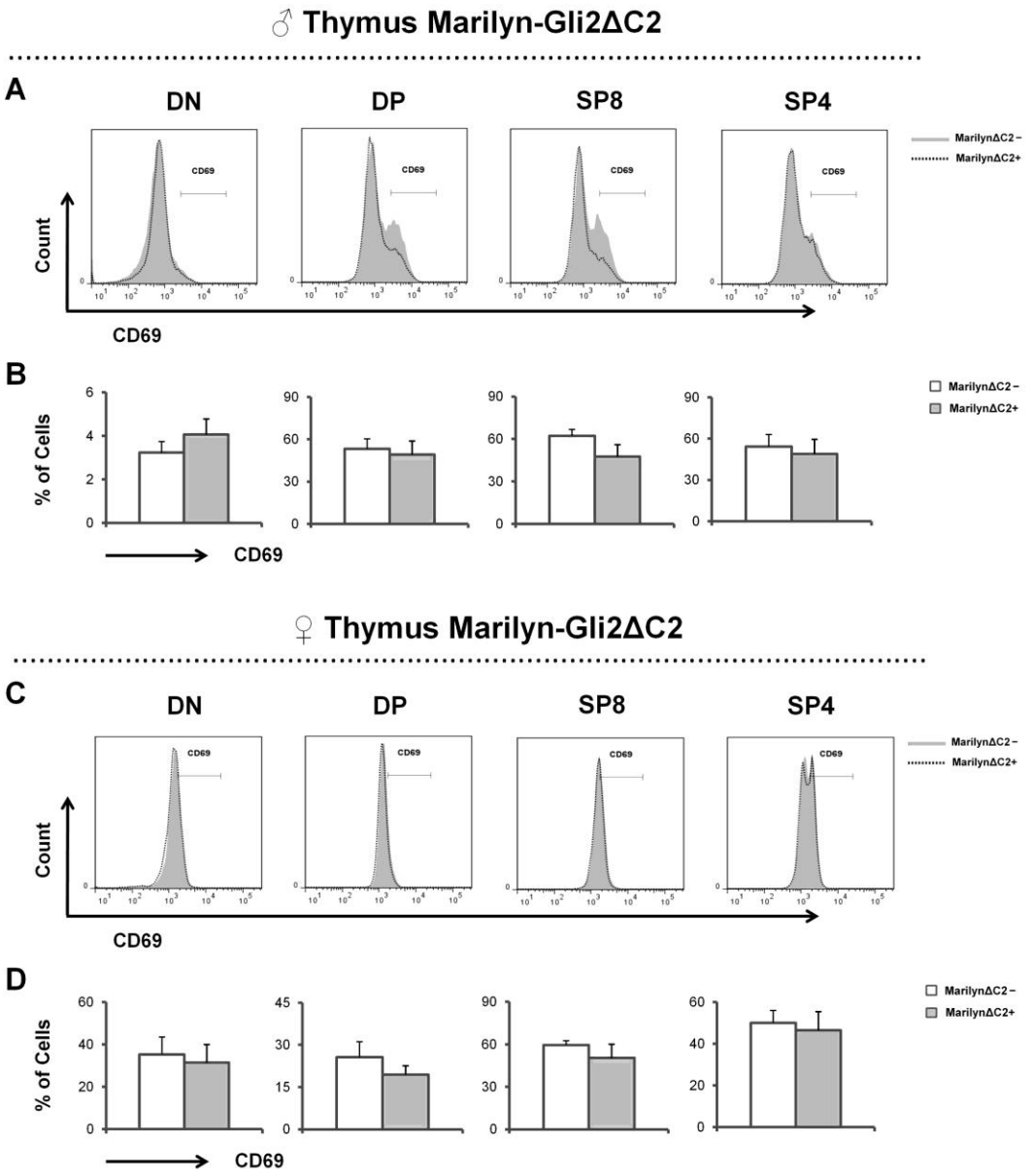

Figure 5.39

Expression of CD69 in male and female Marilyn-Gli2ΔC2 thymocytes. Expression of CD69 in DN, DP, SP8 and SP4 thymocytes from adult male and female Marilyn-Gli2ΔC2^{-} and Marilyn-Gli2ΔC2^{+} littermates. Thymocytes were stained for anti-CD69, anti-CD8 and anti-CD4, and analyzed by flow cytometry. **(A)** Representative histogram of CD69 expression in male DN, DP, SP8 and SP4 cells. **(B)** Representative bar graph of CD69 percentages in male DN, DP, SP8 and SP4 cells. **(C)** Representative histogram of CD69 expression in female DN, DP, SP8 and SP4 cells. **(D)** Representative bar graph of CD69 percentages in female DN, DP, SP8 and SP4 cells. Figures are representative of 3 independent sets of male and female Marilyn-Gli2ΔC2 littermates. Mean and standard deviation of each population are given. Bars represent mean ± standard deviations. **Male CD69 percentages; DN** (p= 0.1, n=3). **DP** (p= 0.5, n=3). **SP8** (p= 0.07, n=3). **SP4** (p= 0.5, n=3). **Female CD69 percentages; DN** (p= 0.6, n=3). **DP** (p= 0.09, n=3). **SP8** (p= 0.2, n=3). **SP4** (p= 0.3, n=3).

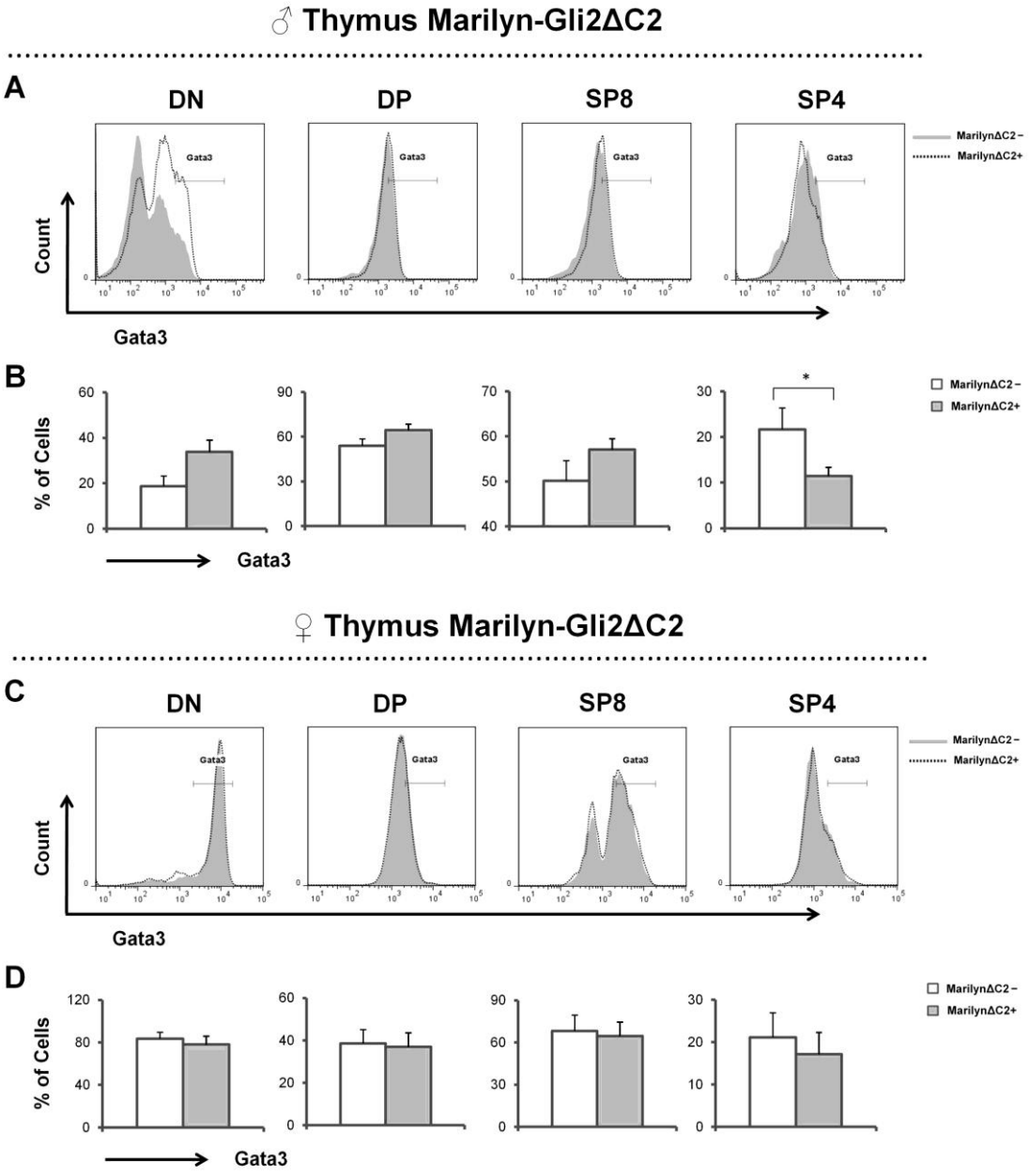

Figure 5.40

Expression of Gata-3 in male and female Marilyn-Gli2ΔC2 thymocytes. Expression of Gata-3 in DN, DP, SP8 and SP4 thymocytes from adult male and female Marilyn-Gli2ΔC2^{-} and Marilyn-Gli2ΔC2^{+} littermates. Thymocytes were stained for anti-Gata3, anti-CD8 and anti-CD4, and analyzed by flow cytometry. **(A)** Representative histogram of Gata-3 expression in male DN, DP, SP8 and SP4 cells. **(B)** Representative bar graph of Gata-3 percentages in male DN, DP, SP8 and SP4 cells. **(C)** Representative histogram of Gata-3 expression in female DN, DP, SP8 and SP4 cells. **(D)** Representative bar graph of Gata-3 percentages in female DN, DP, SP8 and SP4 cells. Figures are representative of 3 independent sets of male and female Marilyn-Gli2ΔC2 littermates. Mean and standard deviation of each population are given. Bars represent mean ± standard deviations. **Male Gata-3 percentages; DN** (p= 0.1, n=3). **DP** (p= 0.4, n=3). **SP8** (p= 0.09, n=3). **SP4** (p= 0.04, n=3). **Female Gata-3 percentages; DN** (p= 0.3, n=3). **DP** (p= 0.7, n=3). **SP8** (p= 0.7, n=3). **SP4** (p= 0.4, n=3). *represents $p \leq 0.05$.

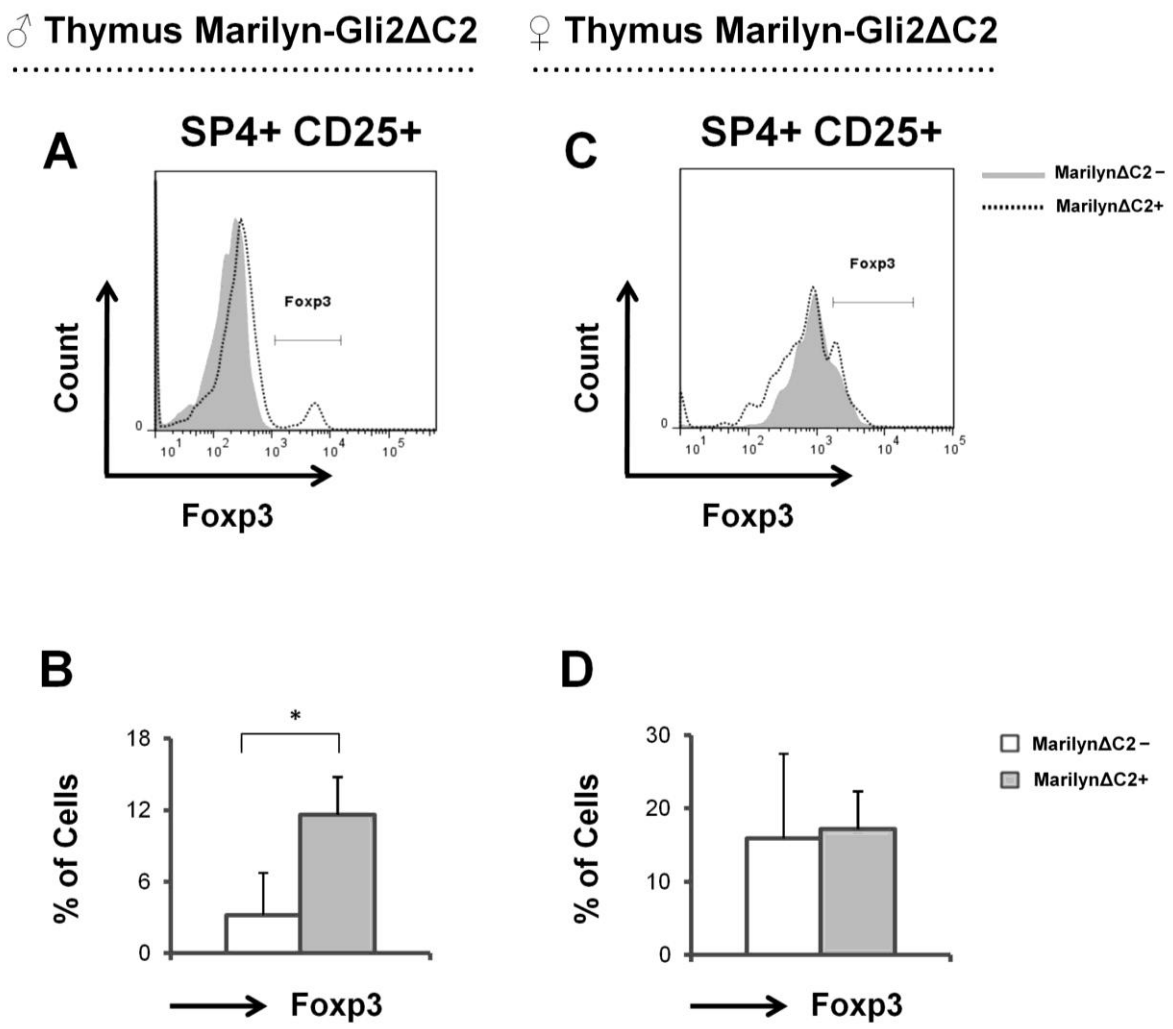

Figure 5.41

Expression of Foxp3 in male and female Marilyn-Gli2ΔC2 SP4 thymocytes. Expression of Foxp3 in SP4 cells from adult male and female Marilyn-Gli2ΔC2^{-} and Marilyn-Gli2ΔC2^{+} littermates. Thymocytes were stained for anti-Foxp3, anti-CD25, anti-CD8 and anti-CD4, and analyzed by flow cytometry. **(A)** Representative histogram of Foxp3 expression in male SP4 cells. **(B)** Representative bar graph of Foxp3 percentages in male SP4 cells. **(C)** Representative histogram of Foxp3 expression in female SP4 cells. **(D)** Representative bar graph of Foxp3 percentages in female SP4 cells. Figures are representative of 3 independent sets of male and female Marilyn-Gli2ΔC2 littermates. Mean and standard deviation of each population are given. Bars represent mean ± standard deviations. **Male Foxp3 percentage; SP4** (p= 0.05, n=3). **Female Foxp3 percentages; SP4** (p= 0.3, n=3). *represents p≤0.05.

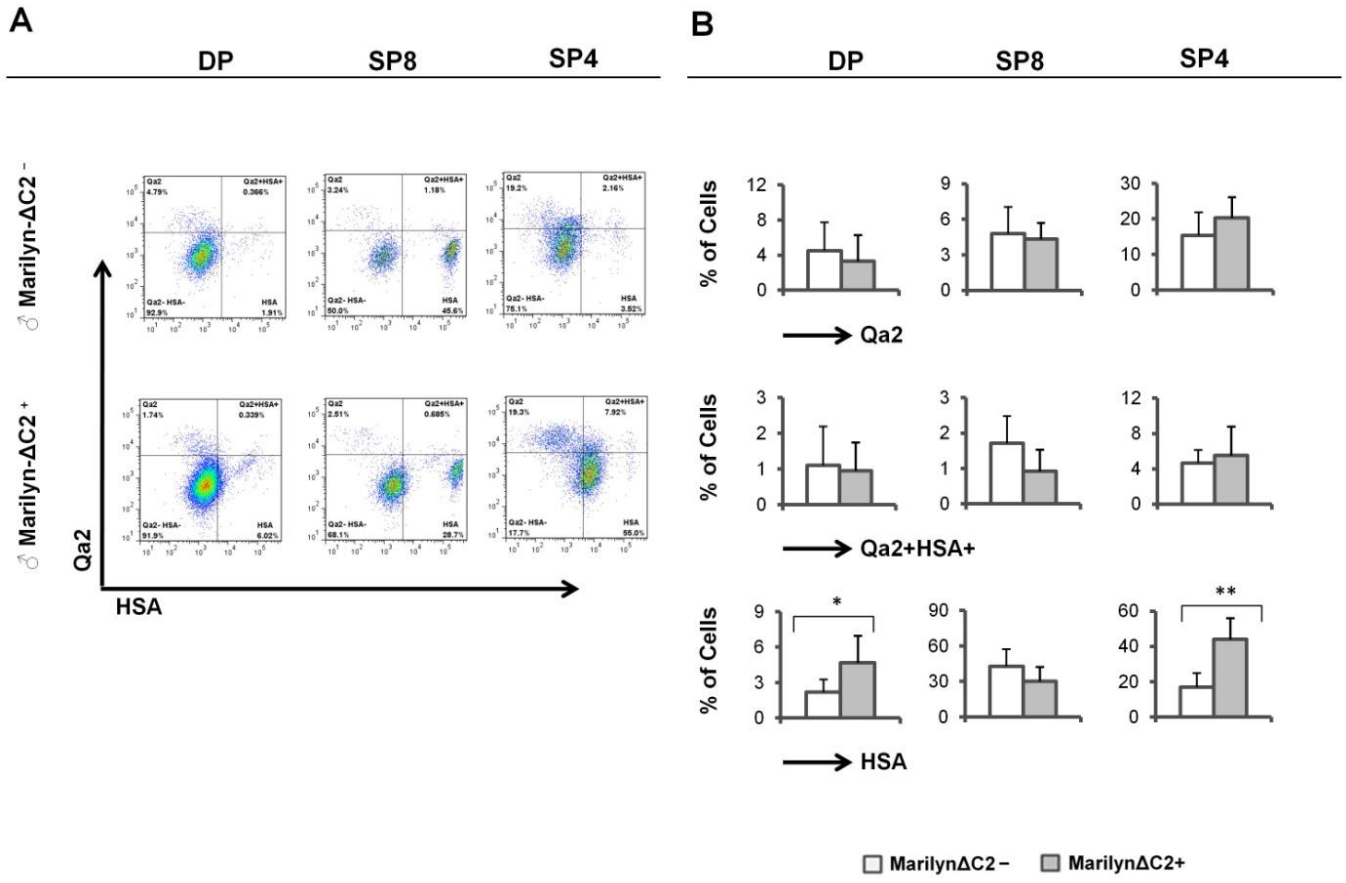

Figure 5.42

Expression of Qa2 and HSA in male Marilyn-Gli2ΔC2 thymocytes. Expression of Qa2 and HSA in DP, SP8 and SP4 cells from adult Marilyn-Gli2ΔC2^{-} and Marilyn-Gli2ΔC2^{+} littermates. Thymocytes were stained for anti-Qa2, anti-CD24, anti-CD8 and anti-CD4, and analyzed by flow cytometry. **(A)** Representative dot plot of Qa2^{+}, Qa2^{+}HSA^{+} and HSA^{+} expression in DP, SP8 and SP4 cells. **(B)** Representative bar graph of Qa2^{+}, Qa2^{+}HSA^{+} and HSA^{+} percentages in DP, SP8 and SP4 cells. Figures are representative of 3 independent sets of male Marilyn-Gli2ΔC2 littermates. Mean and standard deviation of each population are given. Bars represent mean ± standard deviations. **Qa2^{+} percentages; DP** (p= 0.5, n=3). **SP8** (p= 0.6, n=3). **SP4** (p= 0.1, n=3). **Qa2^{+}HSA^{+} percentages; DP** (p= 0.7, n=3). **SP8** (p= 0.08, n=3). **SP4** (p= 0.5, n=3). **HSA^{+} percentages; DP** (p= 0.04, n=3). **SP8** (p= 0.1, n=3). **SP4** (p= 0.001, n=3).*represents p≤0.05, **represents p≤0.005.

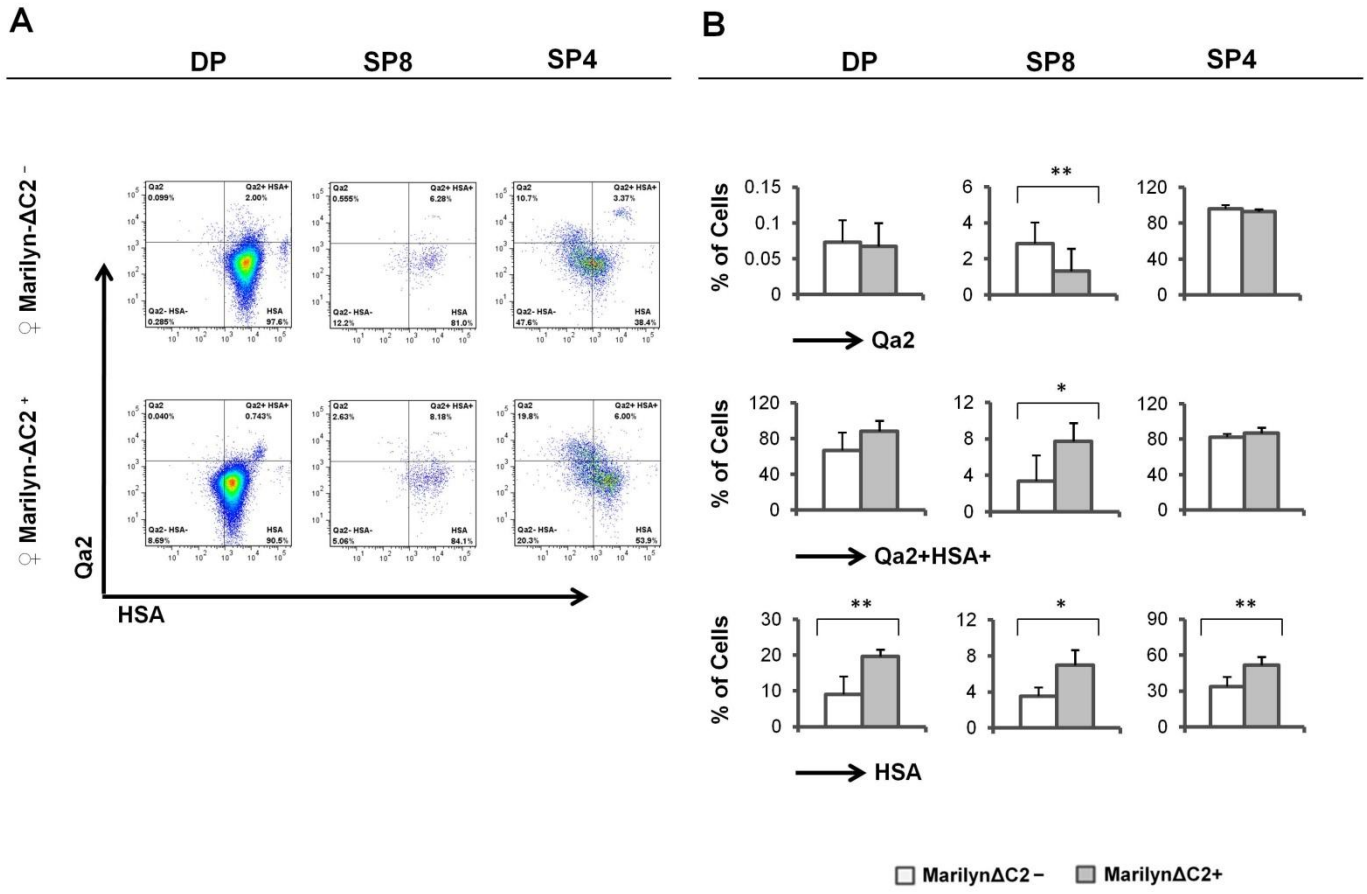

Figure 5.43

Expression of Qa2 and HSA female Marilyn-Gli2ΔC2 thymocytes. Expression of Qa2 and HSA in DP, SP8 and SP4 cells from adult Marilyn-Gli2ΔC2^{-} and Marilyn-Gli2ΔC2^{+} littermates. Thymocytes were stained for anti-Qa2, anti-CD24, anti-CD8 and anti-CD4, and analyzed by flow cytometry. **(A)** Representative dot plot of Qa2^{+}, Qa2^{+}HSA^{+} and HAS^{+} expression in DP, SP8 and SP4 cells. **(B)** Representative bar graph of Qa2^{+}, Qa2^{+}HSA^{+} and HSA^{+} percentages in DP, SP8 and SP4 cells. Figures are representative of 3 independent sets of female Marilyn-Gli2ΔC2 littermates. Mean and standard deviation of each population are given. Bars represent mean ± standard deviations. **Qa2^{+} percentages; DP** (p= 0.7, n=3). **SP8** (p= 0.002, n=3). **SP4** (p= 0.3, n=3). **Qa2^{+}HSA^{+} percentages; DP** (p= 0.1, n=3). **SP8** (p= 0.05, n=3). **SP4** (p= 0.1, n=3). **HSA^{+} percentages; DP** (p= 0.004, n=3). **SP8** (p= 0.02, n=3). **SP4** (p= 0.003, n=3).*represents p≤0.05, **represents p≤0.005.

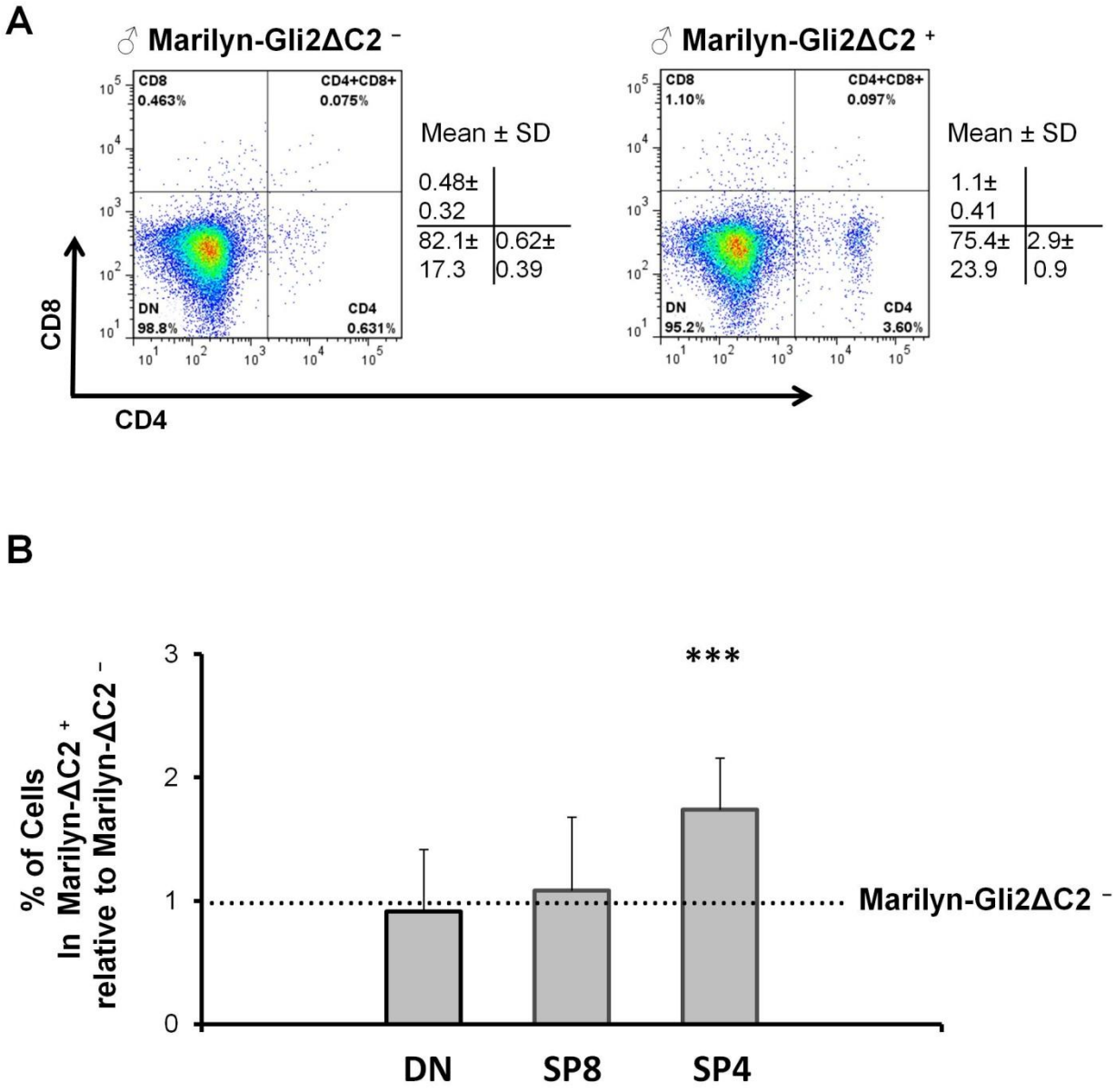

Figure 5.44

Major splenocyte populations in male Marilyn-Gli2ΔC2 mice. Percentage of splenocyte populations from adult male Marilyn-Gli2ΔC2^{-} and Marilyn-Gli2ΔC2^{+} littermates. Splenocytes were stained for anti-vβ6, anti-CD8 and anti-CD4, and analyzed by flow cytometry. **(A)** Representative dot plot of splenocyte populations. **(B)** Representative bar graph of CD4^{-}CD8^{-}, SP8 and SP4 percentages. Figures are representative of 5 independent sets of male Marilyn-Gli2ΔC2 littermates. Mean and standard deviation of each population are given. Bars represent mean ± standard deviations. **CD4^{-}CD8^{-}** (p= 0.4, n=5). **SP8** (p= 0.07, n=5). **SP4** (p= 0.0003, n=5). ***represents p≤0.0005.

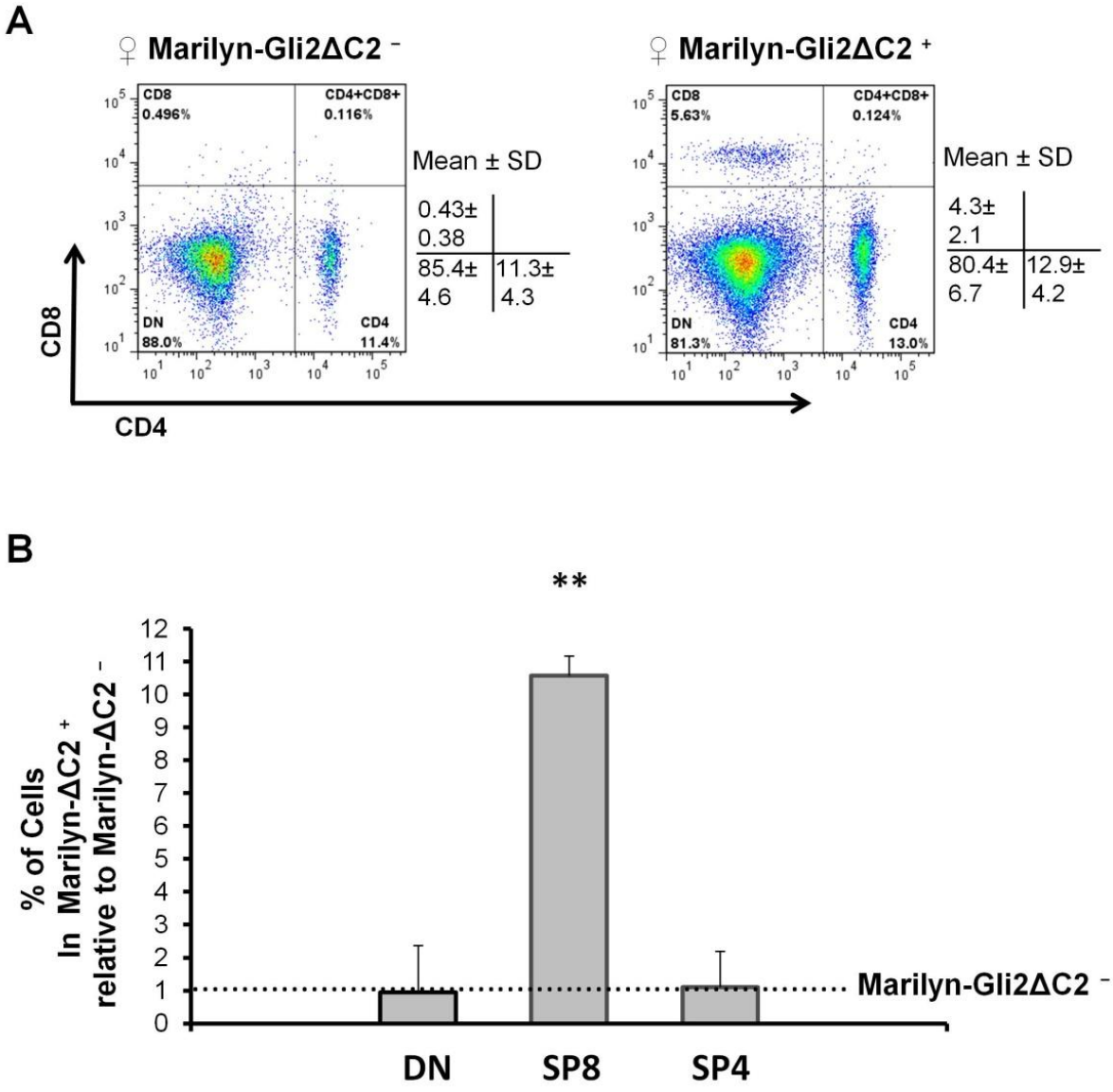

Figure 5.45

Major splenocyte populations in female Marilyn-Gli2ΔC2 mice. Percentage of splenocyte populations from adult female Marilyn-Gli2ΔC2^{-} and Marilyn-Gli2ΔC2^{+} littermates. Splenocytes were stained for anti-vβ6, anti-CD8 and anti-CD4, and analyzed by flow cytometry. **(A)** Representative dot plot of splenocyte populations. **(B)** Representative bar graph of CD4^{-}CD8^{-}, SP8 and SP4 percentages. Figures are representative of 3 independent sets of female Marilyn-Gli2ΔC2 littermates. Mean and standard deviation of each population are given. Bars represent mean ± standard deviations. **CD4^{-}CD8^{-}** (p= 0.1, n=3). **SP8** (p= 0.001, n=3). **SP4** (p= 0.5, n=3).**represents p≤0.005.

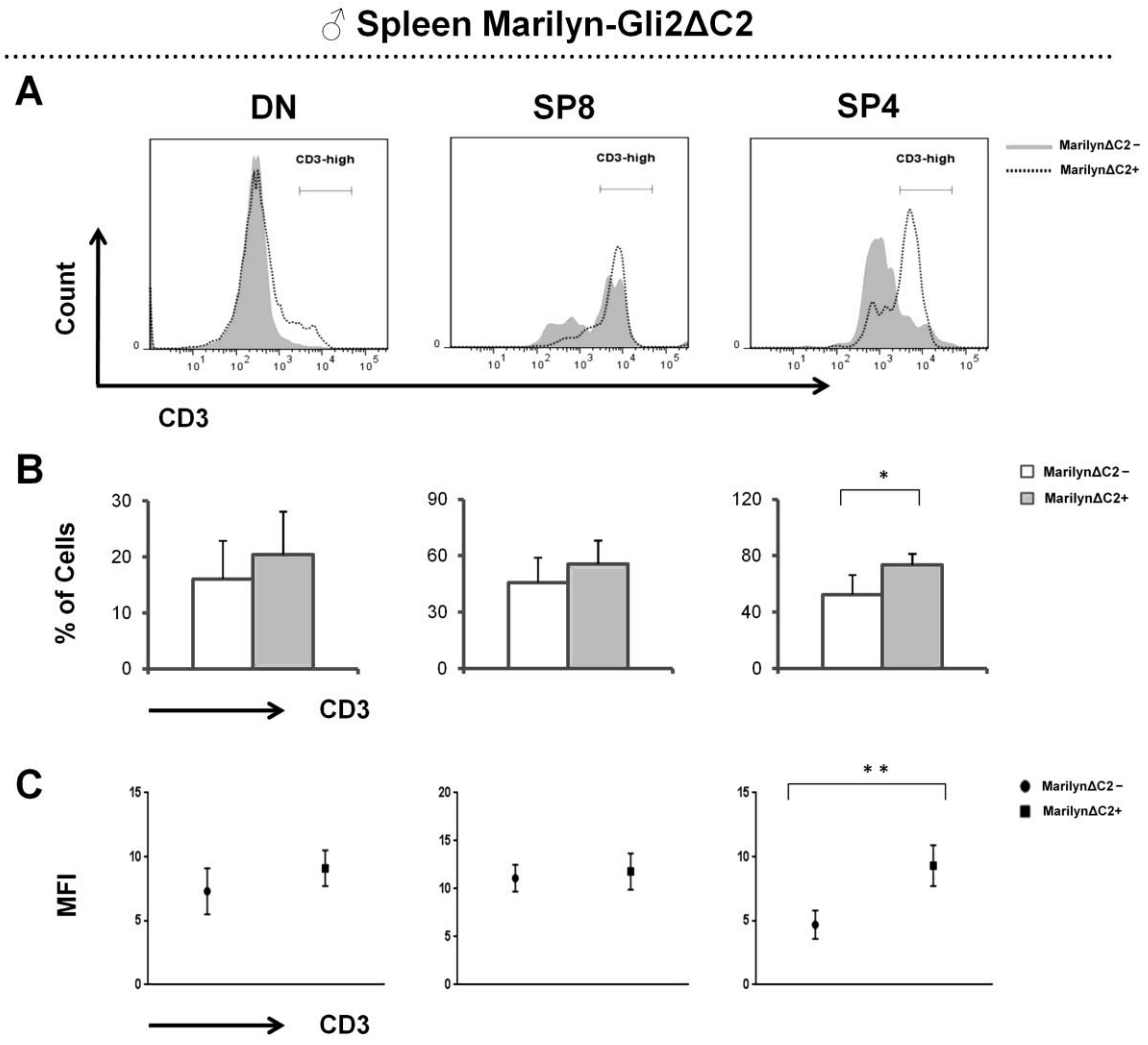

Figure 5.46

Expression of CD3 in male Marilyn-Gli2ΔC2 splenocytes. Expression of CD3 in $CD4^{-}CD8^{-}$, SP8 and SP4 cells from adult male Marilyn-Gli2ΔC2^{-} and Marilyn-Gli2ΔC2^{+} littermates. splenocytes were stained for anti-CD3, anti-CD8 and anti-CD4, and analyzed by flow cytometry. **(A)** Representative histogram of CD3 expression in $CD4^{-}CD8^{-}$, SP8 and SP4 cells. **(B)** Representative bar graph of CD3 percentages in $CD4^{-}CD8^{-}$, SP8 and SP4 cells. **(C)** Representative scatter plot of CD3 MFI in $CD4^{-}CD8^{-}$, SP8 and SP4 cells. Figures are representative of 5 independent sets of male Marilyn-Gli2ΔC2 littermates respectively. Mean and standard deviation of each population are given. Bars represent mean ± standard deviations. **CD3 percentages; $CD4^{-}CD8^{-}$** (p= 0.1, n=5). **SP8** (p= 0.08, n=5). **SP4** (p= 0.05, n=5). **CD3 MFI; $CD4^{-}CD8^{-}$** (p= 0.07, n=5). SP8 (p= 0.3, n=5). **SP4** (p= 0.002, n=5). *represents $p \leq 0.05$, **represents $p \leq 0.005$.

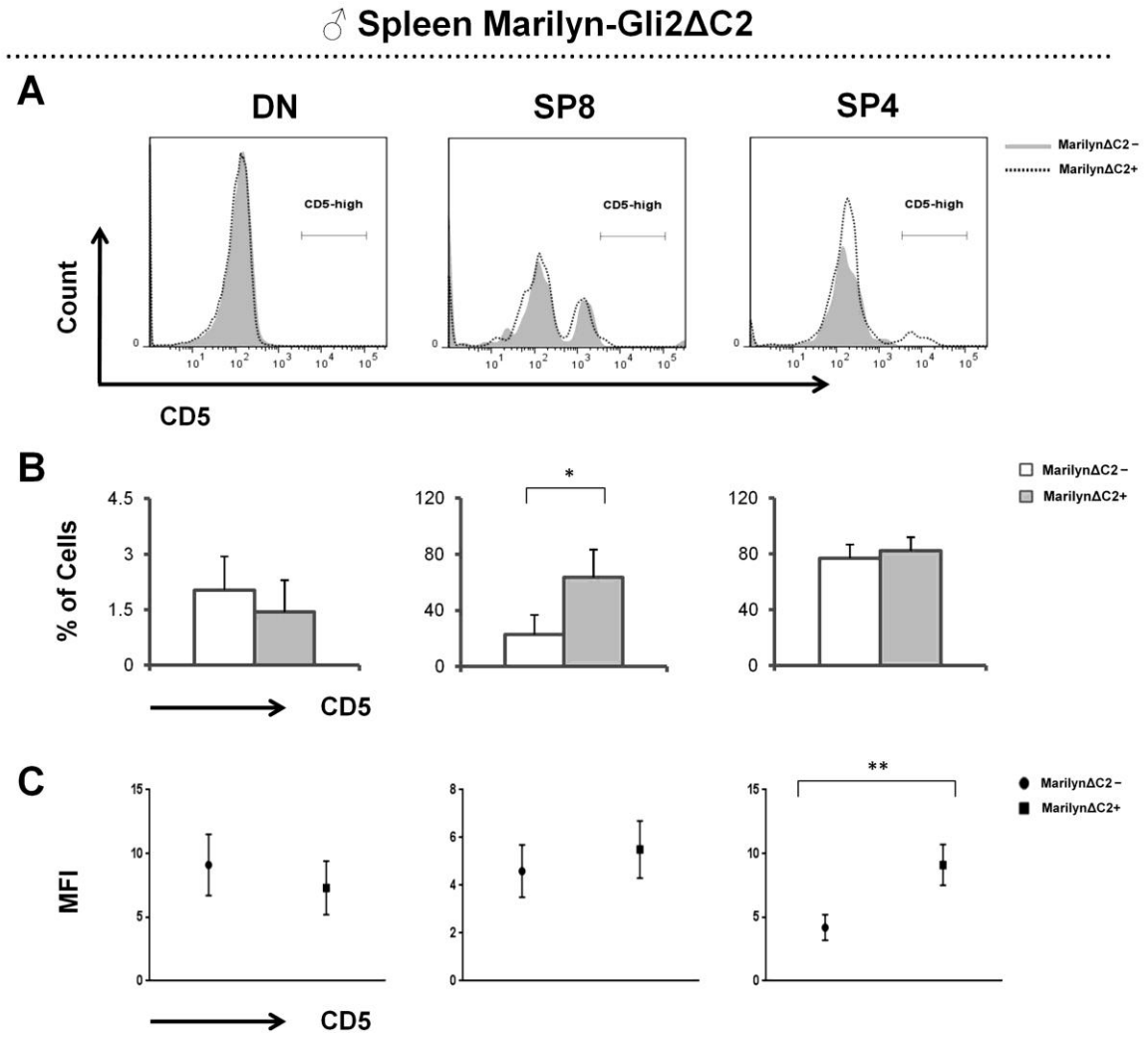

Figure 5.47

Expression of CD5 in male Marilyn-Gli2ΔC2 splenocytes. Expression of CD5 in $CD4^{-}CD8^{-}$, SP8 and SP4 cells from adult male Marilyn-Gli2ΔC2^{-} and Marilyn-Gli2ΔC2^{+} littermates. splenocytes were stained for anti-CD5, anti-CD8 and anti-CD4, and analyzed by flow cytometry. **(A)** Representative histogram of CD5 expression in $CD4^{-}CD8^{-}$, SP8 and SP4 cells. **(B)** Representative bar graph of CD5 percentages in $CD4^{-}CD8^{-}$, SP8 and SP4 cells. **(C)** Representative scatter plot of CD5 MFI in $CD4^{-}CD8^{-}$, SP8 and SP4 cells. Figures are representative of 5 independent sets of male Marilyn-Gli2ΔC2 littermates respectively. Mean and standard deviation of each population are given. Bars represent mean ± standard deviations. **CD5 percentages; $CD4^{-}CD8^{-}$** (p= 0.3, n=5). **SP8** (p= 0.02, n=5). **SP4** (p= 0.1, n=5). **CD5 MFI; $CD4^{-}CD8^{-}$** (p= 0.07, n=5). **SP8** (p= 0.4, n=5). **SP4** (p= 0.003, n=5). *represents p≤0.05, **represents p≤0.005.

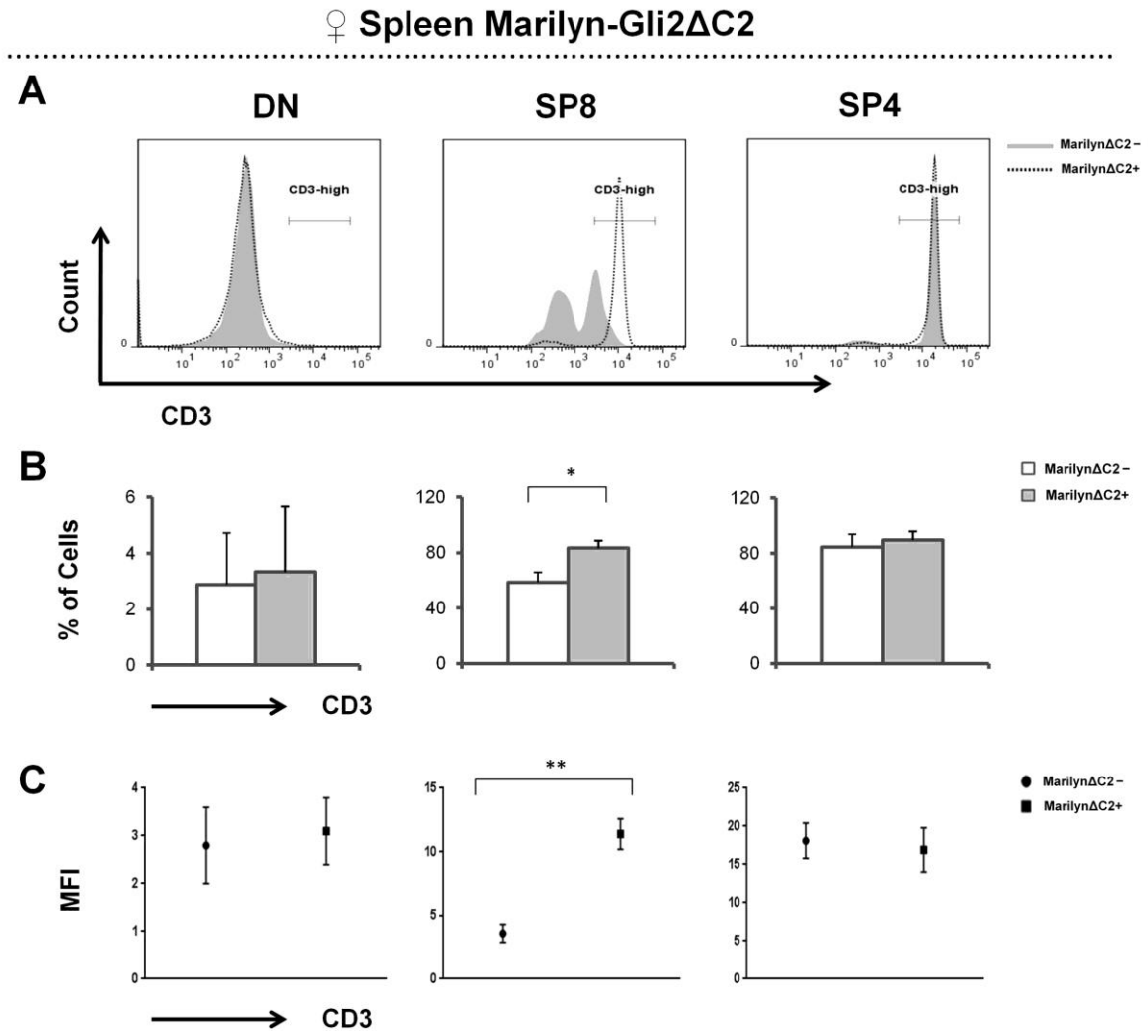

Figure 5.48

Expression of CD3 female Marilyn-Gli2ΔC2 splenocytes. Expression of CD3 in $CD4^{-}CD8^{-}$, SP8 and SP4 cells from adult female Marilyn-Gli2$\Delta C2^{-}$ and Marilyn-Gli2$\Delta C2^{+}$ littermates. splenocytes were stained for anti-CD3, anti-CD8 and anti-CD4, and analyzed by flow cytometry. **(A)** Representative histogram of CD3 expression in $CD4^{-}CD8^{-}$, SP8 and SP4 cells. **(B)** Representative bar graph of CD3 percentages in $CD4^{-}CD8^{-}$, SP8 and SP4 cells. **(C)** Representative scatter plot of CD3 MFI in $CD4^{-}CD8^{-}$, SP8 and SP4 cells. Figures are representative of 4 independent sets of female Marilyn-Gli2ΔC2 littermates respectively. Mean and standard deviation of each population are given. Bars represent mean ± standard deviations. **CD3 percentages; $CD4^{-}CD8^{-}$** (p= 0.7, n=4). **SP8** (p= 0.006, n=4). **SP4** (p= 0.3, n=4). **CD3 MFI; $CD4^{-}CD8^{-}$** (p= 0.7, n=4). **SP8** (p= 0.002, n=4). **SP4** (p= 0.06, n=4). *represents $p \leq 0.05$, **represents $p \leq 0.005$.

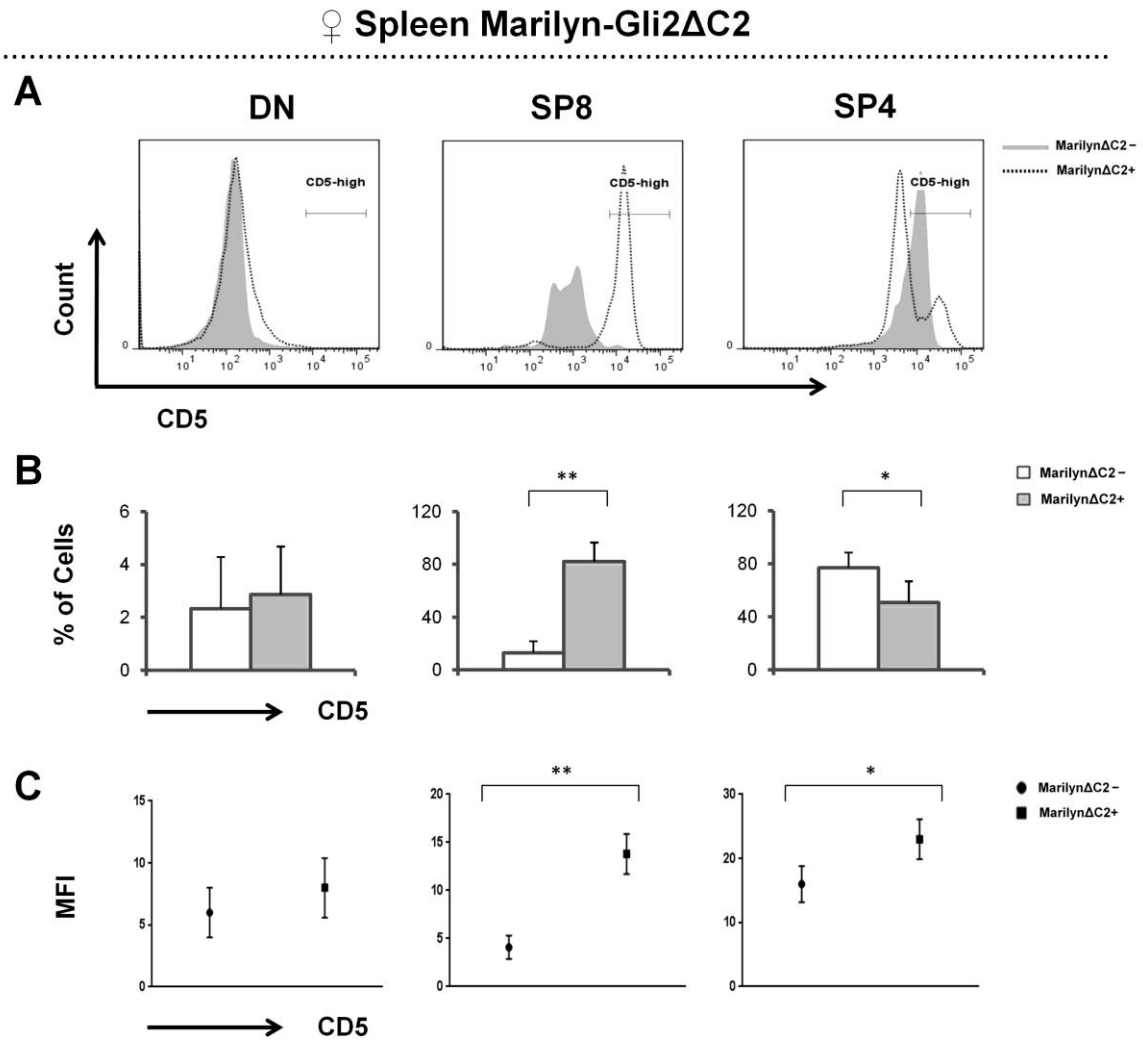

Figure 5.49

Expression of CD5 in female Marilyn-Gli2ΔC2 splenocytes. Expression of CD5 in $CD4^{-}CD8^{-}$, SP8 and SP4 cells from adult female Marilyn-Gli2ΔC2^{-} and Marilyn-Gli2ΔC2^{+} littermates. splenocytes were stained for anti-CD5, anti-CD8 and anti-CD4, and analyzed by flow cytometry. **(A)** Representative histogram of CD5 expression in $CD4^{-}CD8^{-}$, SP8 and SP4 cells. **(B)** Representative bar graph of CD5 percentages in $CD4^{-}CD8^{-}$, SP8 and SP4 cells. **(C)** Representative scatter plot of CD5 MFI in $CD4^{-}CD8^{-}$, SP8 and SP4 cells. Figures are representative of 4 independent sets of female Marilyn-Gli2ΔC2 littermates respectively. Mean and standard deviation of each population are given. Bars represent mean ± standard deviations. **CD5 percentages; $CD4^{-}CD8^{-}$** (p= 0.6, n=4). **SP8** (p= 0.003, n=4). **SP4** (p= 0.01, n=4). **CD5 MFI; $CD4^{-}CD8^{-}$** (p= 0.07, n=4). **SP8** (p= 0.002, n=4). SP4 (p= 0.05, n=4).*represents p≤0.05, **represents p≤0.005.

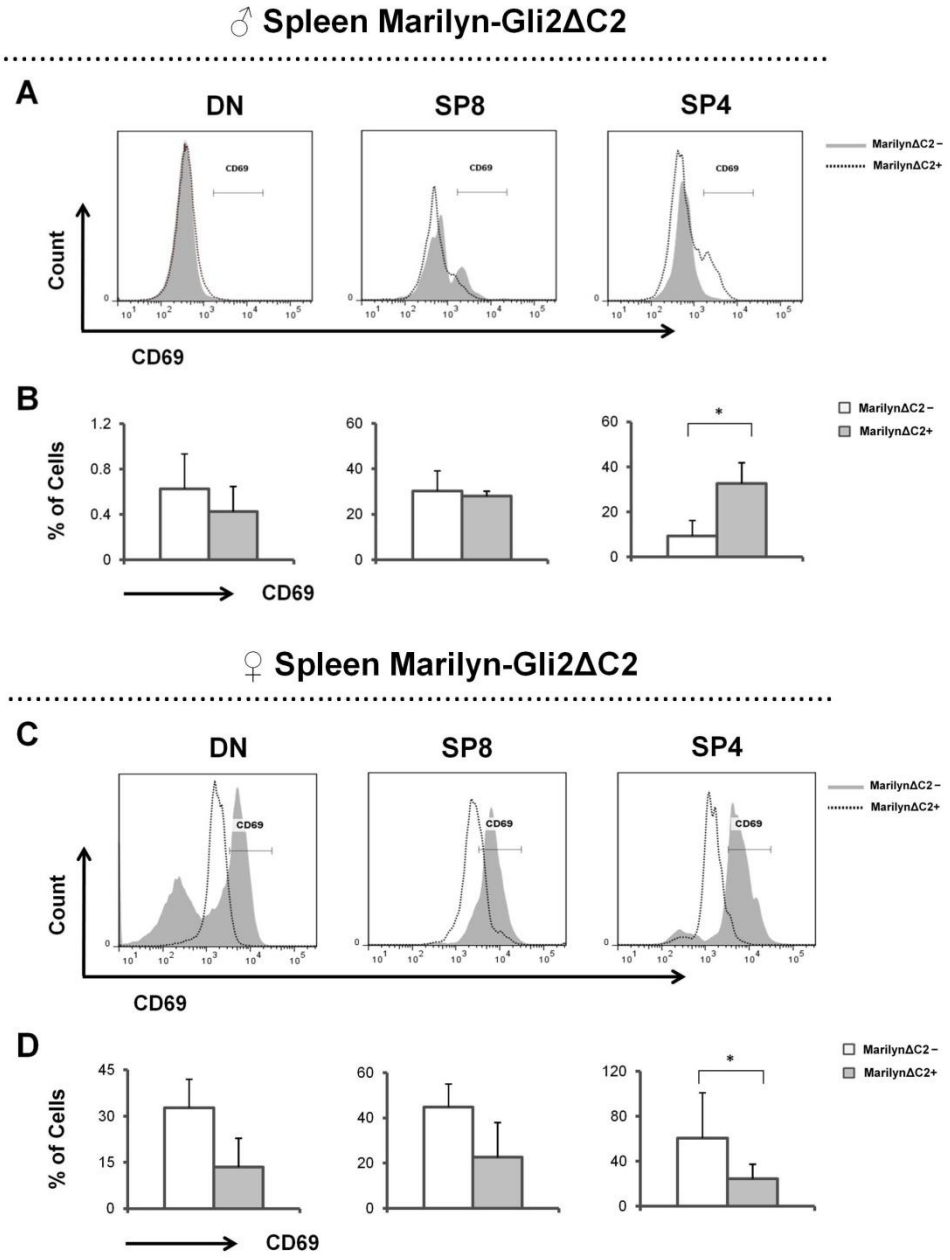

Figure 5.50

Expression of CD69 in male and female Marilyn-Gli2ΔC2 splenocytes. Expression of CD69 in $CD4^{-}CD8^{-}$, SP8 and SP4 cells from adult male and female Marilyn-$Gli2\Delta C2^{-}$ and Marilyn-$Gli2\Delta C2^{+}$ littermates. Thymocytes were stained for anti-CD69, anti-CD8 and anti-CD4 and analyzed by flow cytometry. **(A)** Representative histogram of CD69 expression in male $CD4^{-}CD8^{-}$, SP8 and SP4 cells. **(B)** Representative bar graph of CD69 percentages in male $CD4^{-}CD8^{-}$, SP8 and SP4 cells. **(C)** Representative histogram of CD69 expression in female $CD4^{-}CD8^{-}$, SP8 and SP4 cells. **(D)** Representative bar graph of CD69 percentages in female $CD4^{-}CD8^{-}$, SP8 and SP4 cells. Figures are representative of 3 independent sets of male and female Marilyn-Gli2ΔC2 littermates. Mean and standard deviation of each population are given. Bars represent mean ± standard deviations. **Male CD69 percentages; $CD4^{-}CD8^{-}$** (p= 0.3, n=3). **SP8** (p= 0.7, n=3). **SP4** (p= 0.007, n=3). **Female CD69 percentages; $CD4^{-}CD8^{-}$** (p= 0.06, n=3). **SP8** (p= 0.1, n=3). **SP4** (p= 0.01, n=3).*represents $p \leq 0.05$.

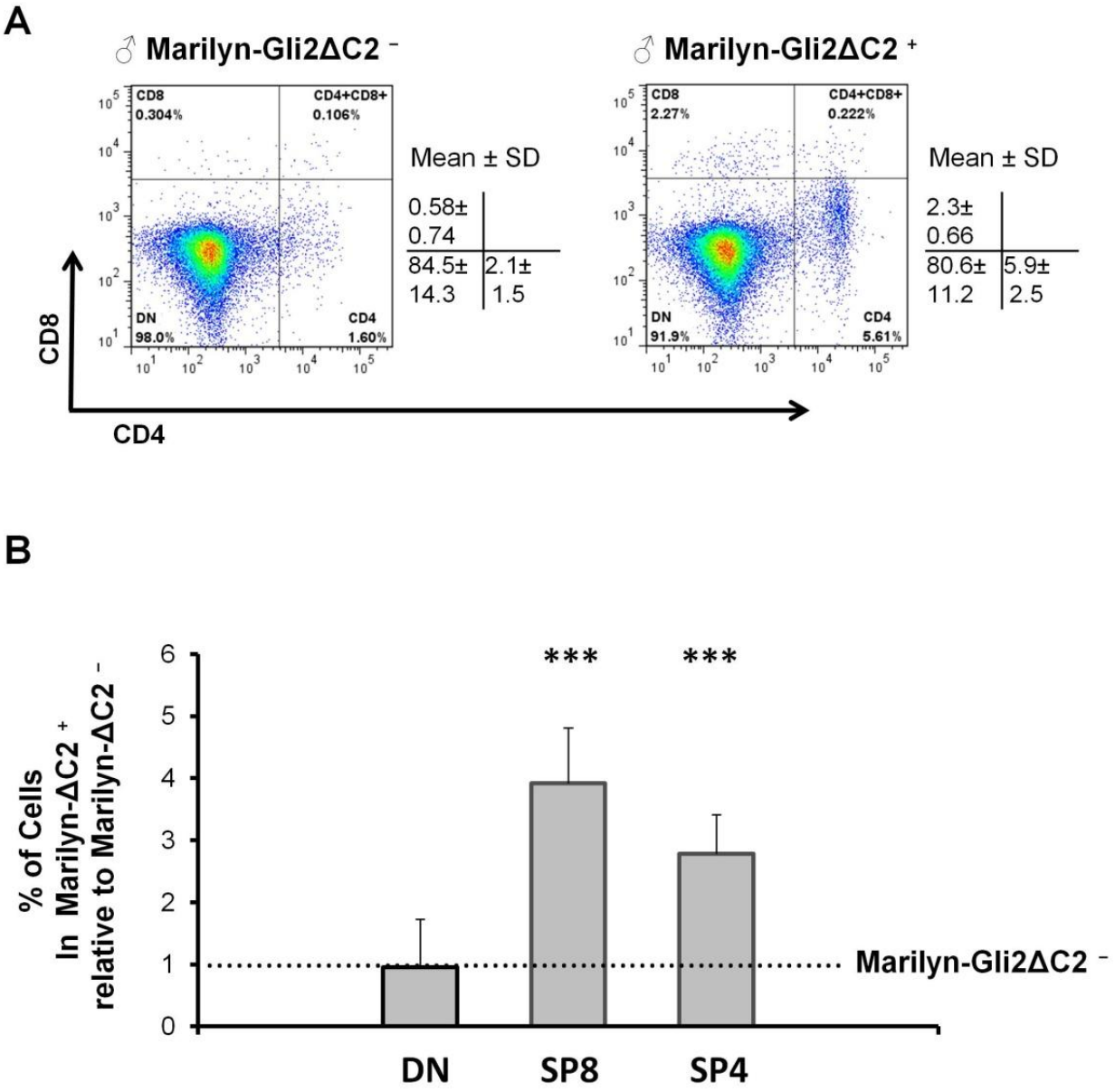

Figure 5.51

Major T cell populations in the lymph node of male Marilyn-Gli2ΔC2 mice. Percentage of T cell populations from adult male Marilyn-Gli2ΔC2^{-} and Marilyn-Gli2ΔC2^{+} littermates. Cells were stained for anti-vβ6, anti-CD8 and anti-CD4, and analyzed by flow cytometry. **(A)** Representative dot plot of T cell populations. **(B)** Representative bar graph of CD4^{-}CD8^{-}, SP8 and SP4 percentages. Figures are representative of 5 independent sets of male Marilyn-Gli2ΔC2 littermates. Mean and standard deviation of each population are given. Bars represent mean ± standard deviations. **CD4^{-}CD8^{-}** (p= 0.5, n=5). **SP8** (p= 0.0002, n=5). **SP4** (p= 0.0004, n=5).***represents p≤0.0005

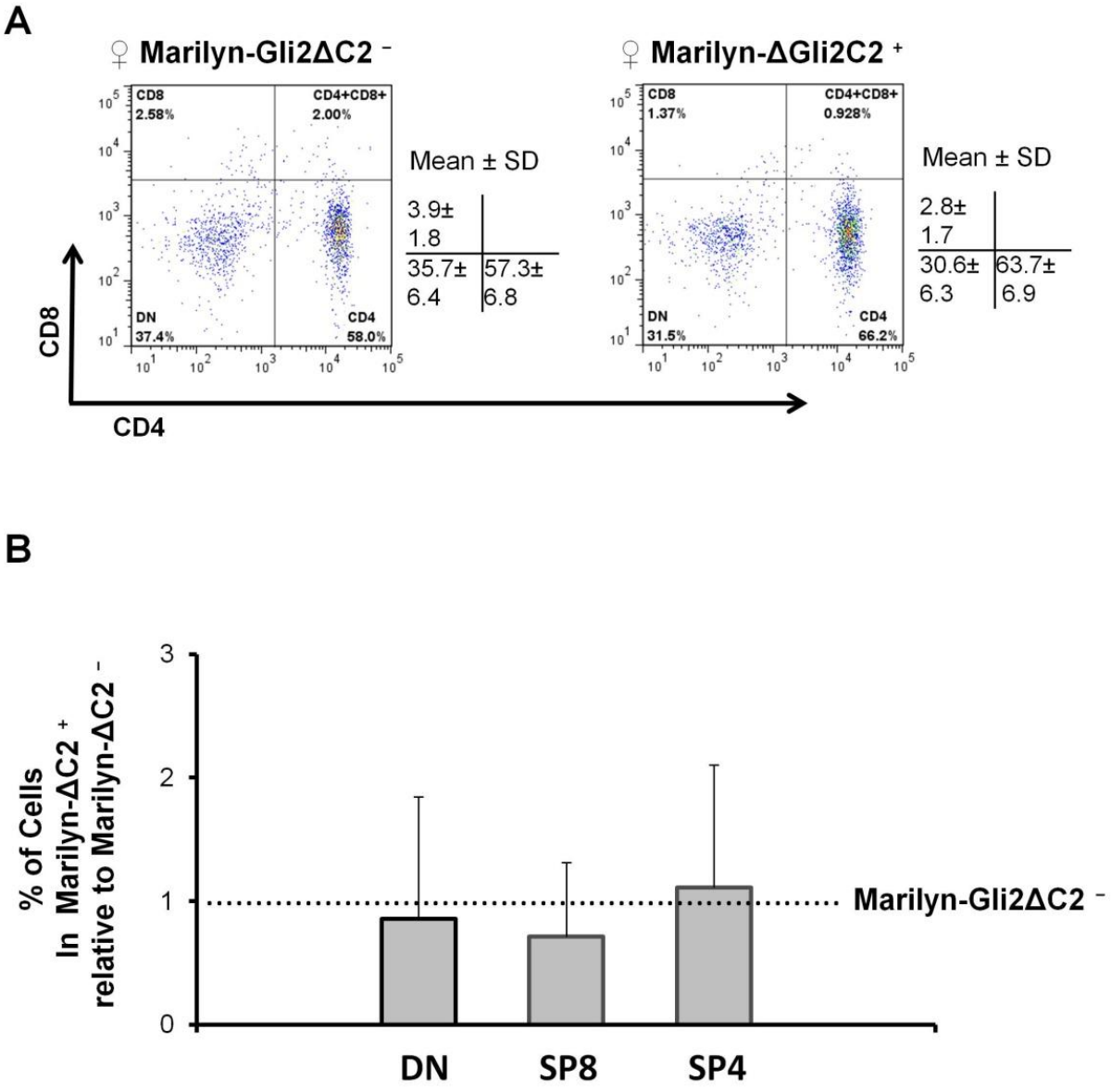

Figure 5.52

Major T cell populations in the lymph node of female Marilyn-Gli2ΔC2 mice. Percentage of T cell populations from adult female Marilyn-Gli2ΔC2^{-} and Marilyn-Gli2ΔC2^{+} littermates. Cells were stained for anti-vβ6, anti-CD8 and anti-CD4, and analyzed by flow cytometry. **(A)** Representative dot plot of T cell populations. **(B)** Representative bar graph of CD4^{-}CD8^{-}, SP8 and SP4 percentages. Figures are representative of 3 independent sets of female Marilyn-Gli2ΔC2 littermates. Mean and standard deviation of each population are given. Bars represent mean ± standard deviations. **CD4^{-}CD8^{-}** (p= 0.1, n=3). **SP8** (p= 0.2, n=3). **SP4** (p= 0.1, n=3).

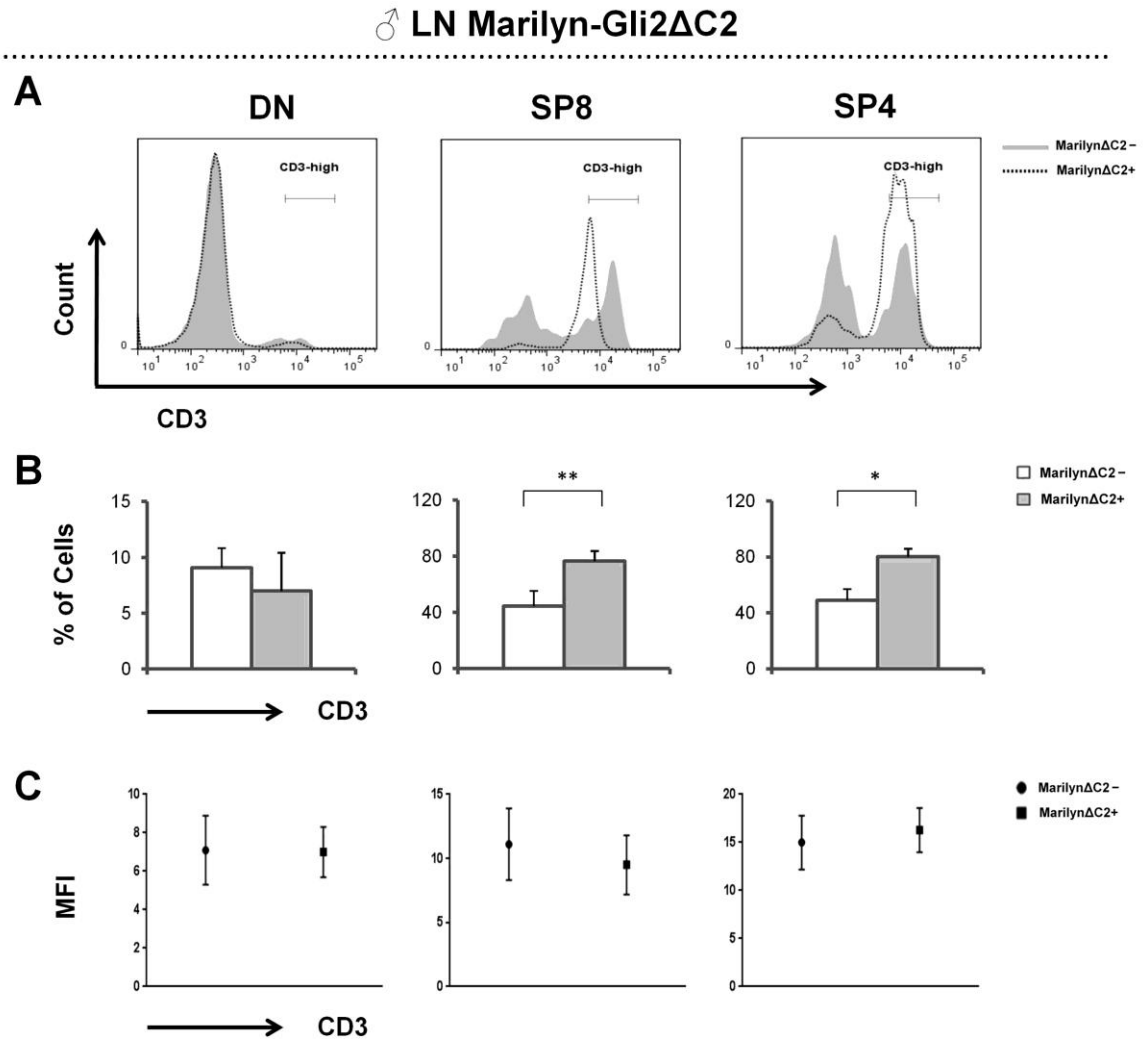

Figure 5.53

Expression of CD3 in male Marilyn-Gli2ΔC2 lymph node T cells. Expression of CD3 in $CD4^{-}CD8^{-}$, SP8 and SP4 cells from adult male Marilyn-Gli2ΔC2^{-} and Marilyn-Gli2ΔC2^{+} littermates. Cells were stained for anti-CD3, anti-CD8 and anti-CD4, and analyzed by flow cytometry. **(A)** Representative histogram of CD3 expression in $CD4^{-}CD8^{-}$, SP8 and SP4 cells. **(B)** Representative bar graph of CD3 percentages in $CD4^{-}CD8^{-}$, SP8 and SP4 cells. **(C)** Representative scatter plot of CD3 MFI in $CD4^{-}CD8^{-}$, SP8 and SP4 cells. Figures are representative of 5 independent sets of male Marilyn-Gli2ΔC2 littermates. Mean and standard deviation of each population are given. Bars represent mean ± standard deviations. **CD3 percentages; $CD4^{-}CD8^{-}$** ($p= 0.5$, $n=5$). **SP8** ($p= 0.002$, $n=5$). **SP4** ($p= 0.03$, $n=5$). **CD3 MFI; $CD4^{-}CD8^{-}$** ($p= 0.2$, $n=5$). **SP8** ($p= 0.6$, $n=5$). **SP4** ($p= 0.3$, $n=5$). *represents $p\leq0.05$, **represents $p\leq0.005$.

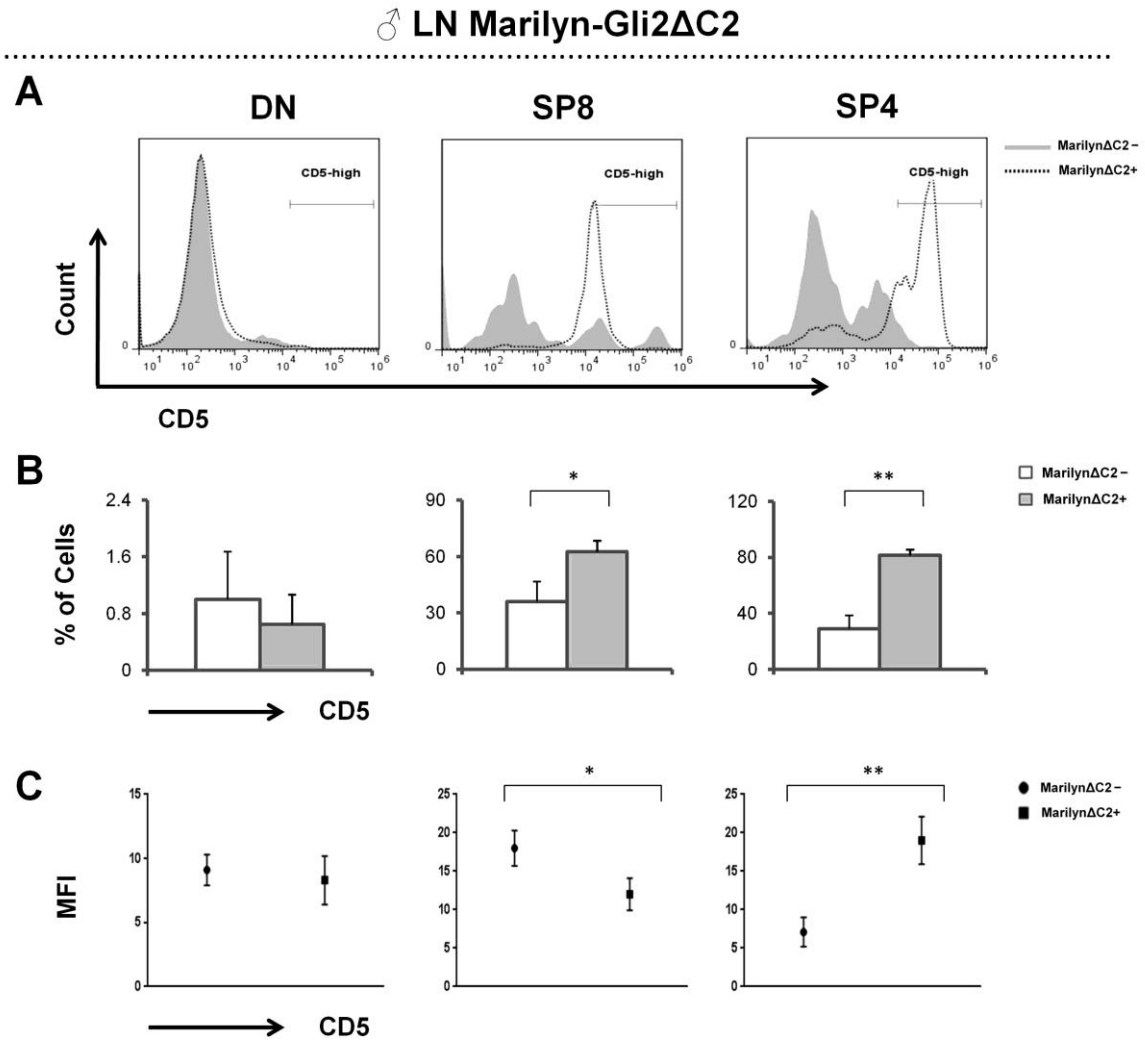

Figure 5.54

Expression of CD5 in male Marilyn-Gli2ΔC2 lymph node T cells. Expression of CD5 in $CD4^{-}CD8^{-}$, SP8 and SP4 cells from adult male Marilyn-Gli2ΔC2^{-} and Marilyn-Gli2ΔC2^{+} littermates. Cells were stained for anti-CD5, anti-CD8 and anti-CD4, and analyzed by flow cytometry. **(A)** Representative histogram of CD5 expression in $CD4^{-}CD8^{-}$, SP8 and SP4 cells. **(B)** Representative bar graph of CD5 percentages in $CD4^{-}CD8^{-}$, SP8 and SP4 cells. **(C)** Representative scatter plot of CD5 MFI in $CD4^{-}CD8^{-}$, SP8 and SP4 cells. Figures are representative of 5 independent sets of male Marilyn-Gli2ΔC2 littermates. Mean and standard deviation of each population are given. Bars represent mean ± standard deviations. **CD5 percentages; $CD4^{-}CD8^{-}$** (p= 0.1, n=5). **SP8** (p= 0.01, n=5). **SP4** (p= 0.0006, n=5). **CD5 MFI; $CD4^{-}CD8^{-}$** (p= 0.2, n=5). **SP8** (p= 0.04, n=5). **SP4** (p= 0.003, n=5). *represents $p \leq 0.05$, **represents $p \leq 0.005$.

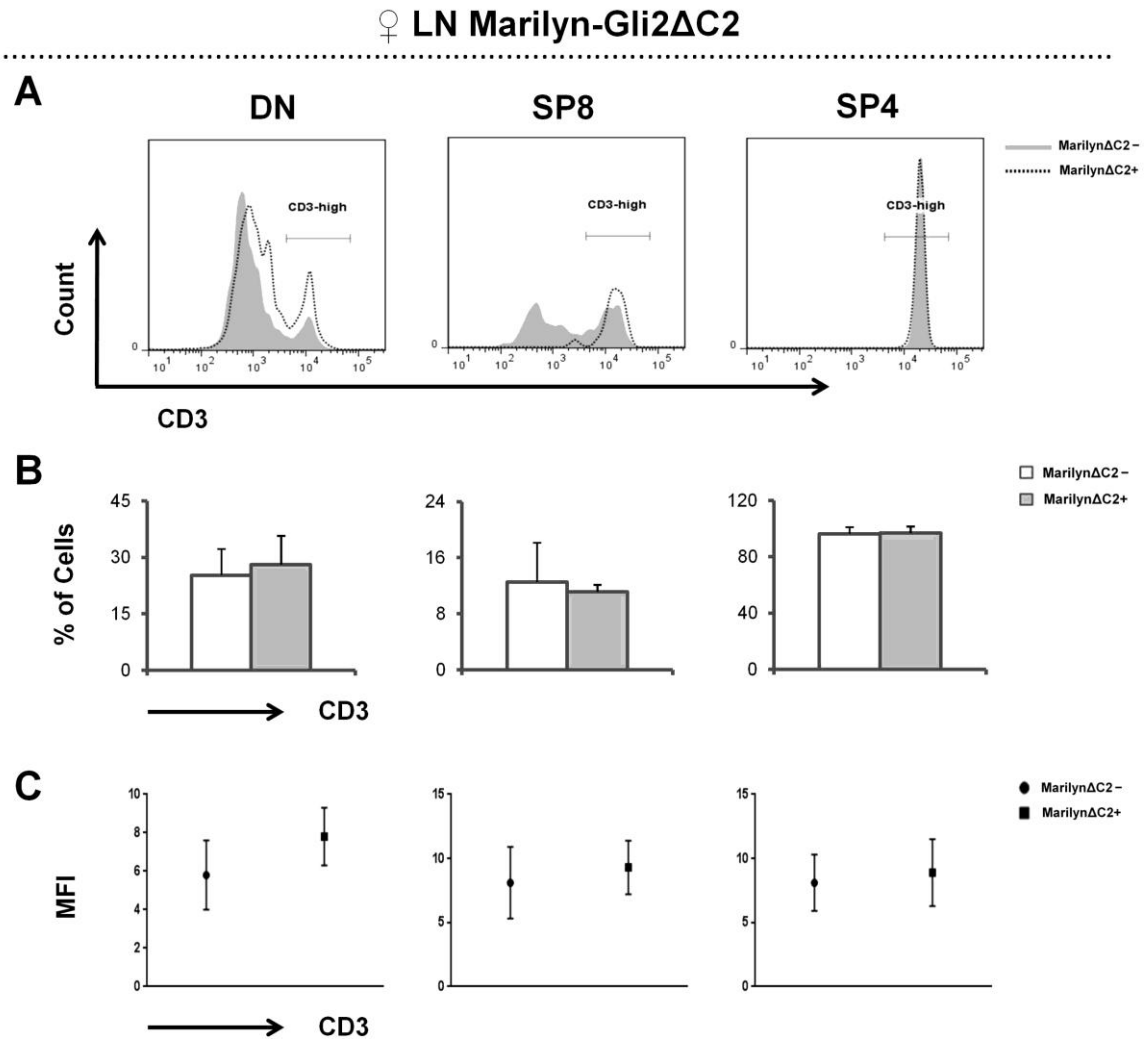

Figure 5.55

Expression of CD3 in female Marilyn-Gli2ΔC2 lymph node T cells. Expression of CD3 in $CD4^{-}CD8^{-}$, SP8 and SP4 cells from adult female Marilyn-Gli2Δ$C2^{-}$ and Marilyn-Gli2Δ$C2^{+}$ littermates. Cells were stained for anti-CD3, anti-CD8 and anti-CD4, and analyzed by flow cytometry. **(A)** Representative histogram of CD3 expression in $CD4^{-}CD8^{-}$, SP8 and SP4 cells. **(B)** Representative bar graph of CD3 percentages in $CD4^{-}CD8^{-}$, SP8 and SP4 cells. **(C)** Representative scatter plot of CD3 MFI in $CD4^{-}CD8^{-}$, SP8 and SP4 cells. Figures are representative of 5 independent sets of female Marilyn-Gli2ΔC2 littermates. Mean and standard deviation of each population are given. Bars represent mean ± standard deviations. **CD3 percentages; $CD4^{-}CD8^{-}$** (p= 0.3, n=3). **SP8** (p= 0.4, n=3). **SP4** (p= 0.7, n=3). **CD3 MFI; $CD4^{-}CD8^{-}$** (p= 0.2, n=3). **SP8** (p= 0.1, n=3). **SP4** (p= 0.4, n=3).

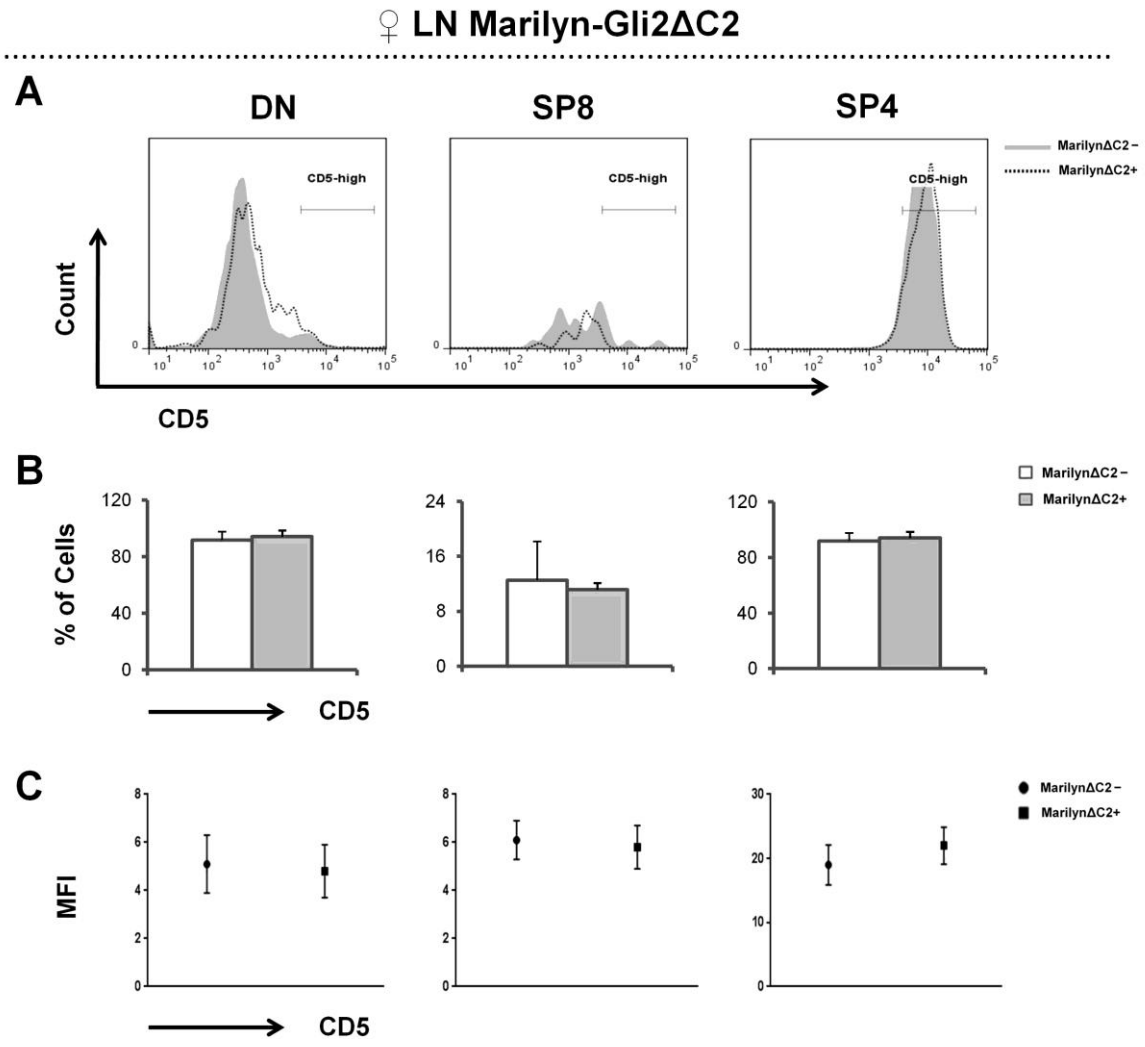

Figure 5.56

Expression of CD5 in female Marilyn-Gli2ΔC2 lymph node T cells. Expression of CD5 in $CD4^{-}CD8^{-}$, SP8 and SP4 cells from adult female Marilyn-Gli2ΔC2^{-} and Marilyn-Gli2ΔC2^{+} littermates. Cells were stained for anti-CD5, anti-CD8 and anti-CD4, and analyzed by flow cytometry. **(A)** Representative histogram of CD5 expression in $CD4^{-}CD8^{-}$, SP8 and SP4 cells. **(B)** Representative bar graph of CD5 percentages in $CD4^{-}CD8^{-}$, SP8 and SP4 cells. **(C)** Representative scatter plot of CD5 MFI in $CD4^{-}CD8^{-}$, SP8 and SP4 cells. Figures are representative of 5 independent sets of female Marilyn-Gli2ΔC2 littermates. Mean and standard deviation of each population are given. Bars represent mean ± standard deviations. **CD5 percentages; $CD4^{-}CD8^{-}$** (p= 0.2, n=3). **SP8** (p= 0.3, n=3). **SP4** (p= 0.3, n=3). **CD5 MFI; $CD4^{-}CD8^{-}$** (p= 0.4, n=3). **SP8** (p= 0.3, n=3). **SP4** (p= 0.6, n=3).

5.3 Discussion

Our data indicated that Dhh influences thymocyte selection as we observed increased escape of deletion of self-reactive T cells in the absence of Dhh in male HY-Dhh mice. We have also shown that partial expression of Dhh reduced deletion of transgenic T cells, indicating a redundant role of Dhh in TCR repertoire selection. A similar escape of deletion has been also found in the male HY-TCR^{-} cells, where endogenous TCR genes rearrangement still exists. This fnding is consistent with previously shown data that Dhh acts as a negative regulator of T cells during their development and differentiation in the thymus and lymphoid organs (chapter 4).

The female HY-TCR^{+} cells revealed a negative regulatory role of Dhh during thymocyte positive selection. The proportions of DP and SP8 cells were increased in Dhh-knockout, indicating a negative role of Dhh during SP8 positive selection. Interestingly, SP8 in Heterogeneous mice have shown a greater selection of SP8 cells, suggesting a dose dependent regulatory function of Dhh during selection of SP8 cells. Additionally, thymocyte maturation has been examined through measuring the expression of Qa2 and HSA, and our data have shown that Dhh reduce maturation of SP8 cells in male and female HY-TCR^{+} cells. In the spleen, we observed no influence on mature HY-TCR^{+} cells, however, Dhh reduced the proportions of SP4 cells expressing CD3, indicating its role in influencing splenocytes in the periphery.

Furthermore, analysis of Marilyn-TCR^{+} male mice showed a negative regulatory role of Hh signalling during thymocyte development and maturation in the thymus. These data indicate that inhibition of Hh-dependent transcription

increased positive selection of the transgenic TCR, and differentiation from DP to SP cells. Our analysis showed that the proportions of Marilyn-TCR$^+$ SP4 cells has been found to be increased in the absence of Hh signalling, suggesting a negative regulatory role of Hh during negative selection of SP4 cells. In Marilyn-TCR$^+$ female mice, the proportions of DP cells were decreased, possibly as cells undergo further development. Furthermore, examining the maturation marker Qa2 and HSA in DP and SP cells revealed that Hh signalling reduced thymocyte maturation in the DP and SP stage in male mice, and in DP and SP cells in female mice. These findings are consistent with previously shown data which indicate that inhibition of Hh-dependent transcription increased positive and negative selection in the thymus and TCR activation of peripheral T cells (Furmanski et al. 2012; Rowbotham et al. 2008; Furmanski et al. 2015).

In the spleen, we observed a reduction in the proportions of SP4 in male mice, and SP8 and SP4 cells in female mice. This observation confirms our finding in the thymus, in that the thymus allowed the escape of transgenic T cells reaching the spleen. However, the spleen size was reduced, as well as their total live cell counts. This could be due to the increase in Foxp3$^+$ cells. In the female spleen, in the absence of intrinsic Hh signalling, the proportions of SP8 and SP4 cells are increased as a result of increased positive selection.

Furthermore, the expression of TCR associated molecules CD3 and CD5 in SP cells increase during thymocyte development in the thymus, and CD5 MFI also increase in the absence of Hh signalling indicating a possible role of these molecules during selection of transgenic T cells. A similar phenotype have been also shown in the spleen and lymph node of Marilyn-TCR$^+$ mice, suggesting that

Hh signalling also regulate TCR signal transduction in mature T cells in the periphery.

5.4 Conclusion

In this chapter, our data indicated that Dhh influences thymocyte negative and positive selection as we observed increased escape of deletion of self-reactive T cells in male HY-Dhh mice, and increased proportions of DP and SP8 cells in female mice in the absence of Dhh. We have also shown that partial expression of Dhh reduced deletion of transgenic T cells, indicating a dose dependent regulatory function of Dhh during selection. Moreover, our data have shown that Dhh reduce maturation of SP8 cells promoting the inhibited clonal deletion of transgenic SP8 cells in these mice. In the spleen, Dhh reduced the proportions of SP4 cells expressing CD3, indicating its role in influencing splenocytes activation in the periphery.

Furthermore, our data from Marilyn-TCR^{+} male mice indicate that inhibition of Hh-dependent transcription increased positive selection of the transgenic TCR, and differentiation from DP to SP cells. Moreover, Hh signalling reduced thymocyte maturation through attenuating TCR signal transduction. Moreover, inhibition of Hh-dependent transcription resulted in a reduced size of the spleen and a reduced total live splenocyte counts, suggesting an autoreactive nature of T cells that escaped deletion in the thymus.

Chapter 6

Chapter Six: Role of Shh in T cell development

6.1 Introduction

6.1.1 Shh in T cell development

Shh has been found to be expressed in the thymus by epithelial cells throughout the subcapsular region, medulla and cortico-medullary region in both mice and human (Outram et al. 2000; Shah et al. 2004; Virts et al. 2006; El Andaloussi et al. 2006; Sacedón et al. 2003). Thymus stromal cells and circulating lymphoid cells has been found to be responsive to Shh signalling (Outram et al. 2000; Rowbotham, Hager-Theodorides, Cebecauer, et al. 2007; Sacedón et al. 2003; Li et al. 2002).

Our laboratory has previously established that Shh is an essential regulator of T cells during their development in the thymus. Analysis of foetal thymocyte development in Shh deficient embryos revealed that Shh is an essential regulator for thymocyte differentiation and proliferation during the transition from the DN1 to the DN2 stage (Shah et al. 2004; Hager-Theodorides et al. 2005). Shh deficient mice exhibited reduced thymocyte numbers and proliferation with partial arrest at the DN1 stage compared to WT littermates (Shah et al. 2004).

At the transition from the DN to the DP stage, our laboratory has found that Shh negatively regulates thymocyte differentiation (Outram et al. 2000; Rowbotham et al. 2009). Our lab has also shown that the DP thymocytes are Hh-responsive and that thymocyte-intrinsic Shh signalling plays a role in modulating the production of SP4 and SP8 thymocytes, whereas repression of physiological Shh signalling in

thymocytes altered the proportions of DP and SP4 thymocytes (Crompton et al. 2007; Rowbotham, Hager-Theodorides, Cebecauer, et al. 2007; Furmanski et al. 2012).

6.1.2 Chapter objectives

The purpose of this chapter is to investigate the role of Shh during T cell development and maturation in the thymus. I studied the functions of Shh in the thymus, by investigating differences in differentiation and transition from one developmental stage to the next on Shh-treatment in-vitro.

This was done using an in-vitro system of FTOC and TCR transgenic mice in which T cell repertoire selection is biased by expressing rearranged transgenic TCR αβ chains. The first model is HY transgenic mice bearing MHC class-I restricted TCR which recognizes the male antigen. The second model is Marilyn transgenic mice, bearing MHC class-II restricted TCR that recognize the male antigen on a Rag2-deficient background. These mice develop thymocytes in which lineage commitment is skewed by the specificity of their rearranged transgenic TCR, allowing us to investigate whether or not Shh will have an influence in determining lineage choice and TCR repertoire selection in these mice.

6.2 Results

6.2.1 Genotyping HY-TCR and Marilyn-TCR male and female littermates

Two mouse models were utilized in which T cell repertoire selection is biased by expression of rearranged transgenic TCR αβ chains (HY-TCR, and Marilyn-TCR transgenic mice on a Rag2-deficient background). These mice develop thymocytes in which lineage commitment is skewed by the specificity of their rearranged transgenic TCR.

HY-TCR and Marilyn-TCR transgenic mice were maintained by continuous breeding of male and female mice. Each littermate was genotyped for sex determination in embryos and neonatal mice. DNA from ear biopsies was amplified by PCR for YMT_2/B sequence, which is a member of the Ssy family present on the long arm of the Y-chromosome. Male DNA should generate a PCR product of 350bp. According to the PCR results, mice with a PCR product positive for the male gene were genotyped as male mice. Mice with a PCR product negative for the male gene were genotyped as female mice (Figure 6.1).

6.2.2 Thymus phenotype of HY-TCR mice

Embryonic (E17.5) and adult thymus of male and female HY-TCR transgenic mice were compared following anatomical dissection in order to asses thymocyte populations within the HY-TCR$^+$ (T3.7$^+$) and HY-TCR$^-$ (T3.7$^-$) compartments. within the within the T3.7$^+$ cells, embryonic male HY-TCR transgenic mice show immature thymocytes prior deletion of mature transgenic T cells, whereas adult male HY-TCR mice show severe deletion of male self-reactive T cells.

Embroynic and adult female HY-TCR mice display inverted ratio of CD4:CD8 within the $T3.7^{+}$ cells as a result of increased selection of SP8 cells (Figure 6.2).

6.2.3 Influence of Shh on thymocyte development in HY-TCR transgenic FTOCs

In order to assess the influence of Shh on thymocyte development and TCR repertoire selection, fetal thymic organ cultures (FTOCs) from male and female HY-TCR transgenic mice from embryonic day 17.5 (E17.5) were treated with recombinant mouse Shh protein (rmShh) for 7 days and compared to control/untreated cultures. Cells were analyzed for T3.7, CD8 and CD4 cell surface expression. According to T3.7 expression, cells were sub-grouped into two main populations, HY-TCR positive cells ($T3.7^{+}$) and HY-TCR negative cells ($T3.7^{-}$). Within the T3.7 positive and negative compartments, cells were sub-grouped according to the cell surface expression of CD8 and CD4 into four main populations, the $CD8^{-}CD4^{-}$ (DN), $CD8^{+}CD4^{+}$ (DP), $CD8^{+}CD4^{-}$ (SP8) and $CD8^{-}CD4^{+}$ (SP4).

To test influence of Shh in negative selection we analyzed male FTOCs. Our analysis of male FTOCs within the T3.7 positive cells revealed a significant increase in the proportions of CD8SP cells in Shh-treated cultures compared to non-treated cultures, indicating that Shh-treatment inhibited negative selection of transgenic T cells ($p \leq 0.05$, n=18). Furthermore, percentage of DP cells was significantly increased in Shh-treated cultures compared to control cultures consistent with inhibition of negative selection (Figure 6.3).

To test influence of Shh-treatment on positive selection we analyzed female FTOCs. The proportions of $T3.7^{+}$ SP8 were significantly decreased in Shh-treated culture compared to non-treated cultures ($p \leq 0.05$, n=21), indicating decreased positive selection of these cells (Figure 6.4).

Male and female FTOCs within the T3.7 negative display a positive influence of Shh on the proportions of thymocytes that did not express the self-reactive T cell deletion. In male FTOCs, the proportions of $T3.7^{-}$ DP and SP cells were significantly increased in Shh-treated cultures compared to non-treated cultures ($p \leq 0.05$, n=18) (Figure 6.5). In female FTOCs, the proportions of $T3.7^{-}$ SP cells were significantly increased in Shh-treated compared to non-treated cultures ($p \leq 0.05$, n=21) (Figure 6.6).

6.2.4 Influence of Shh on expression of CD3 and CD5 in HY-TCR thymocytes

In order to assess the potential role of Shh in regulating differentiation and TCR signal transduction of HY-TCR thymocytes during development and selection, we analyzed the cell surface expression of molecules associated with TCR signalling (CD3 and CD5) within the T3.7 positive cells for DN, DP, SP8 and SP4 cells. Furthermore we have compared the mean fluorescence intensity (MFI) of staining for these molecules, as high CD5 expression is associated with high TCR signal strength.

Our analysis of male and female FTOCs within the $T3.7^{+}$ cells show no influence of Shh on the expression of CD3 and CD5 in thymocytes from Shh-treated cultures compared to non-treated cultures (($p>0.05$, n=8) and ($p>0.05$, n=11))

respectively. Similarly, we observed no difference in CD3 and CD5 MFI in both male and female FTOCs ((p>0.05, n=8), (p>0.05, n=11)) respectively (Figure 6.7), (Figure 6.8), (Figure 6.9) and (Figure 6.10).

In addition we examined the influence of Shh on thymocyte development in male and female FTOCs within the $T3.7^{-}$ cells, and our data revealed no influence of Shh on the expression of CD3 and CD5 or their MFI in Shh-treated cultures compared to non-treated culture ((p>0.05, n=8), (p>0.05, n=11)) respectively (Figure 6.11), (Figure 6.12), (Figure 6.13) and (Figure 6.14).

6.2.5 Influence of Shh on Gata-3 expression in developing thymocytes in HY-TCR mice

In order to assess the role of Shh in the expression of Gata-3 during thymocyte development and repertoire selection of thymocytes, we analyzed Gata-3 expression in HY-TCR thymocytes.

Gata-3 is required by T cells for the execution of several developmental steps during their development in the thymus. However, our analysis of male and female FTOCs show no difference in the expression of Gata-3 in thymocytes in $T3.7^{+}$ cells in Shh-treated cultures compared to non-treated culture ((p>0.05, n=5), (p>0.05, n=7)) respectively (Figure 6.15) and (Figure 6.16).

Similarly, within the $T3.7^{-}$ cells, our data show no influence of Shh in male and female FTOCs ((p>0.05, n=5), (p>0.05, n=7)) respectively (Figure 6.15) and (Figure 6.16).

6.2.6 Thymus phenotype of Marilyn-TCR mice

Embryonic (E17.5) and adult thymus of male and female Marilyn-TCR transgenic mice were compared following anatomical dissection in order to asses thymocyte populations. Both embryonic and adult male thymus showed clonl deletion of the self-reactive DP and CD4SP populations and no $CD4^{high}$ single positive.

Interestingly, embroynic female Marilyn-TCR transgenic mice also show immature thymocytes with increased proportions of ISPCD8 cells accompanied with a severe reduction of the SP4 population, consistent with poor and delayed positive selection of this TCR. This observation led us to investigate thymocyte development at different time points. Our analysis shows that SP4 cells in female Marilyn-TCR transgenic mice start to appear around 2-weeks after birth, suggesting a delayed maturation in Marilyn-TCR transgenic mice. This is consistent with the phenotype of the male thymus, where no $CD4^{high}$ SP cells were decreased. According to this finding we decided to apply our analysis for male mice at two time points, at E17.5 and 21-days, and at 21-days for female mice (Figure 6.17) and (Figure 6.18).

6.2.7 Influence of Shh on thymocyte development in Marilyn-TCR transgenic mice

In order to assess the influence of Shh on thymocyte development and TCR repertoire selection, fetal thymic organ cultures (FTOCs) from embryonic day 17.5 (E17.5) from male Marilyn-TCR transgenic mice, and thymic organ cultures (thymic fragments) from 21-weeks old male and female Marilyn-TCR transgenic mice were used for analysis. Thymic cultures were treated with recombinant

mouse Shh protein (rmShh) for 7 days and compared to control/untreated cultures. Cells were analyzed for Vβ6 (Marilyn-TCR^{+}), CD8 and CD4 cell surface expression, and sub-grouped according to the cell surface expression of CD8 and CD4 into four main populations, the $CD8^{-}CD4^{-}$ (DN), $CD8^{+}CD4^{+}$ (DP), $CD8^{+}CD4^{-}$ (SP8) and $CD8^{-}CD4^{+}$ (SP4). Analysis of male embryos revealed no influence of Shh on thymocytes during their development in the thymus (Figure 6.19). However, analysis of male neonates revealed an increase in the SP4 population, suggesting that Shh-treatment had reduced clonal deletion.

Neonatal thymic cultures from male Marilyn-TCR transgenic mice revealed a significant increase in the proportions of SP4 cells in Shh-treated cultures compared to non-treated cultures, indicating a positive influence of Shh on T cells during selection as it inhibited deletion of transgenic T cells ($p \leq 0.05$, n=11). As a result the ratios of CD4:CD8 were decreased as well as the ratios of DP:CD8 and DP:CD4 (Figure 6.20). On the contrary, we observed no significant differences in thymocyte populations in neonatal thymic cultures from female mice ($p > 0.05$, n=7) (Figure 6.21).

6.2.8 Influence of Shh on expression of CD3 and CD5 in Marilyn-TCR thymocytes

In order to assess the potential role of Shh in regulating differentiation and TCR signal transduction of Marilyn-TCR thymocytes during development and selection, we analyzed the cell surface expression of molecules associated with TCR signalling (CD3 and CD5) for DN, DP, SP8 and SP4 cells. Furthermore we

have compared the mean fluorescence intensity (MFI) of staining for these molecules, as high CD5 expression is associated with high TCR signal strength.

Our analysis of male FTOCs show no influence of Shh on the expression of CD3 and CD5 in thymocytes from Shh-treated cultures compared to non-treated cultures (($p>0.05$, $n=8$), ($p>0.05$, $n=8$)) respectively. Similarly, we observed no difference in CD3 and CD5 MFI in these mice ($p>0.05$, $n=8$) (Figure 6.22) and (Figure 6.23).

In neonatal male cultures, the percentage of CD3 expression in DP was significantly increased in Shh-treated cultures compared to non-treated cultures ($p\leq0.05$, $n=11$). This finding indicate a possible correlation between the increased proportions of SP4 cells which escaped deletion we observed in these mice, and TCR signal strength in DP cells (Figure 6.24). Additionally, we observed no significant difference in the percentage of CD3 in male DN and SP cells, and in female thymocyte populations (($p>0.05$, $n=11$), ($p>0.05$, $n=7$)) respectively. CD3 MFI also appeared to show no difference in Shh-treated cultures compared to non-treated cultures (($p>0.05$, $n=11$), ($p>0.05$, $n=7$)) respectively (Figure 6.24) and (Figure 6.26).

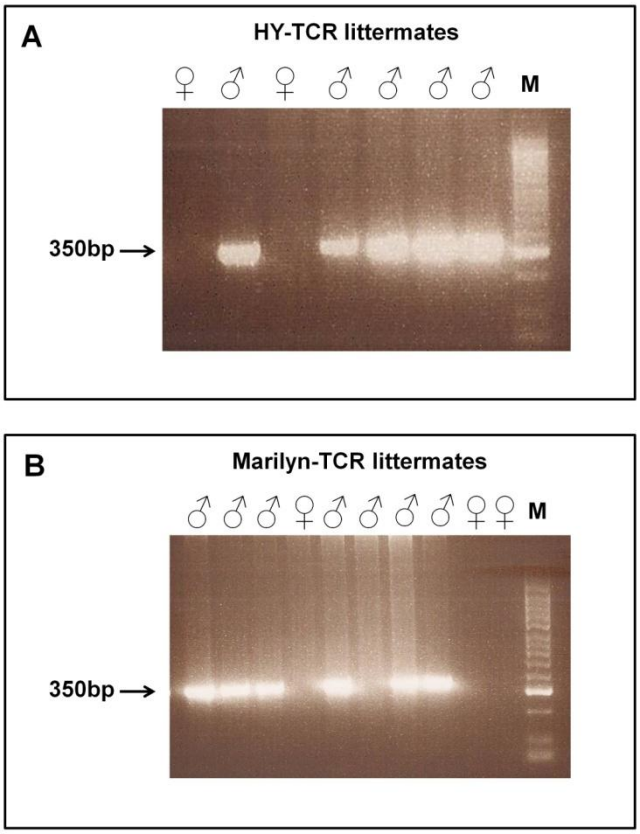

Figure 6.1

Genotyping male and female littermates. Sex determination of HY-TCR and Marilyn-TCR transgenic littermates by PCR using genomic DNA extracted from ear biopsies. **(A)** HY-TCR littermates. **(B)** Marilyn-TCR littermates. The presence of a male allele generated a PCR product of 350bp, while its absence indicates a female genotype.

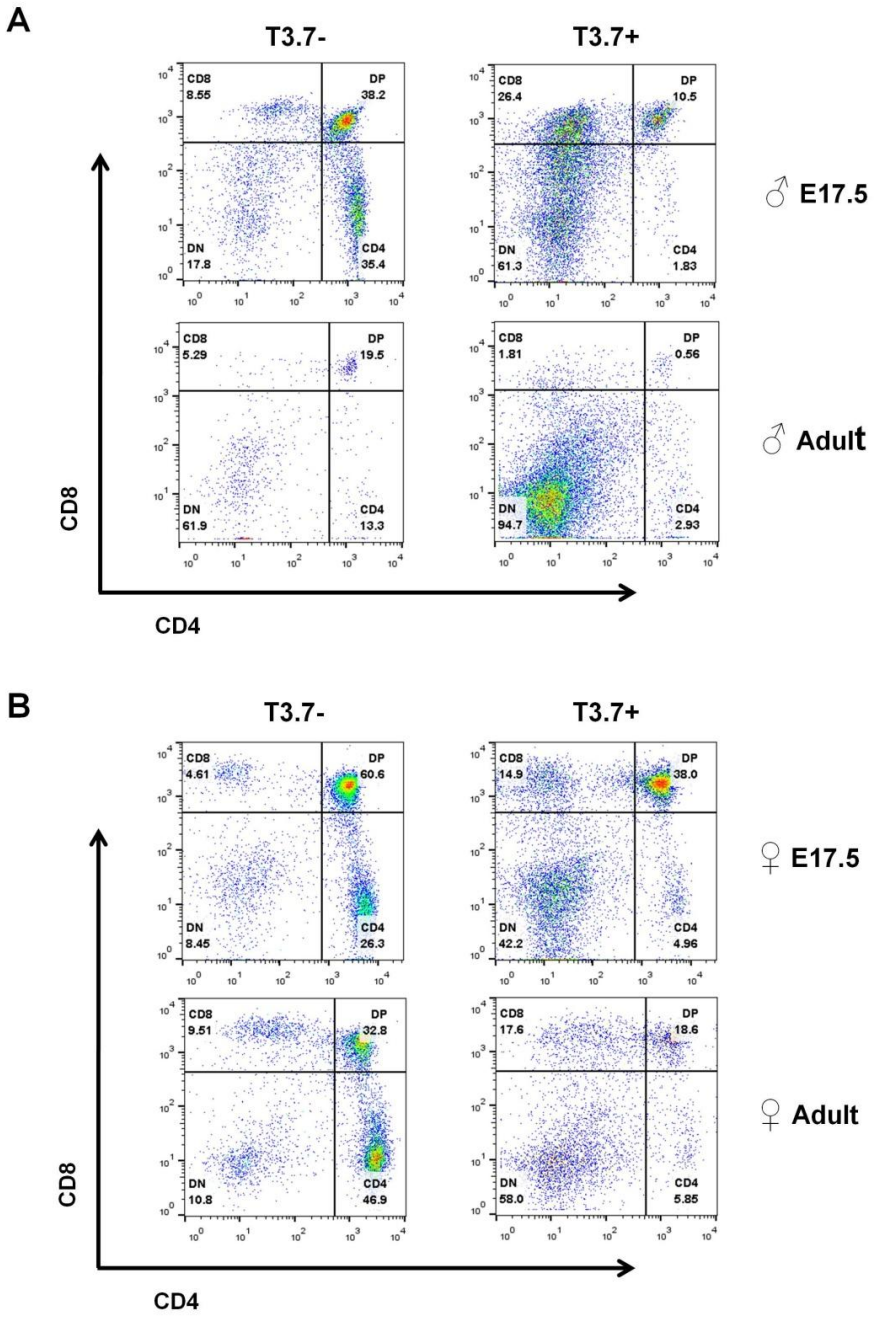

Figure 6.2

Thymus phenotype of HY-TCR mice. Thymocyte populations in adult and embryo (E17.5) of HY-TCR transgenic mice. **(A)** Thymocyte populations in male HY-TCR transgenic mice. **(B)** Thymocyte population in female HY-TCR transgenic mice. Cells were stained for anti-T3.7, anti-CD8 and anti-CD4 followed by flow cytometry analysis.

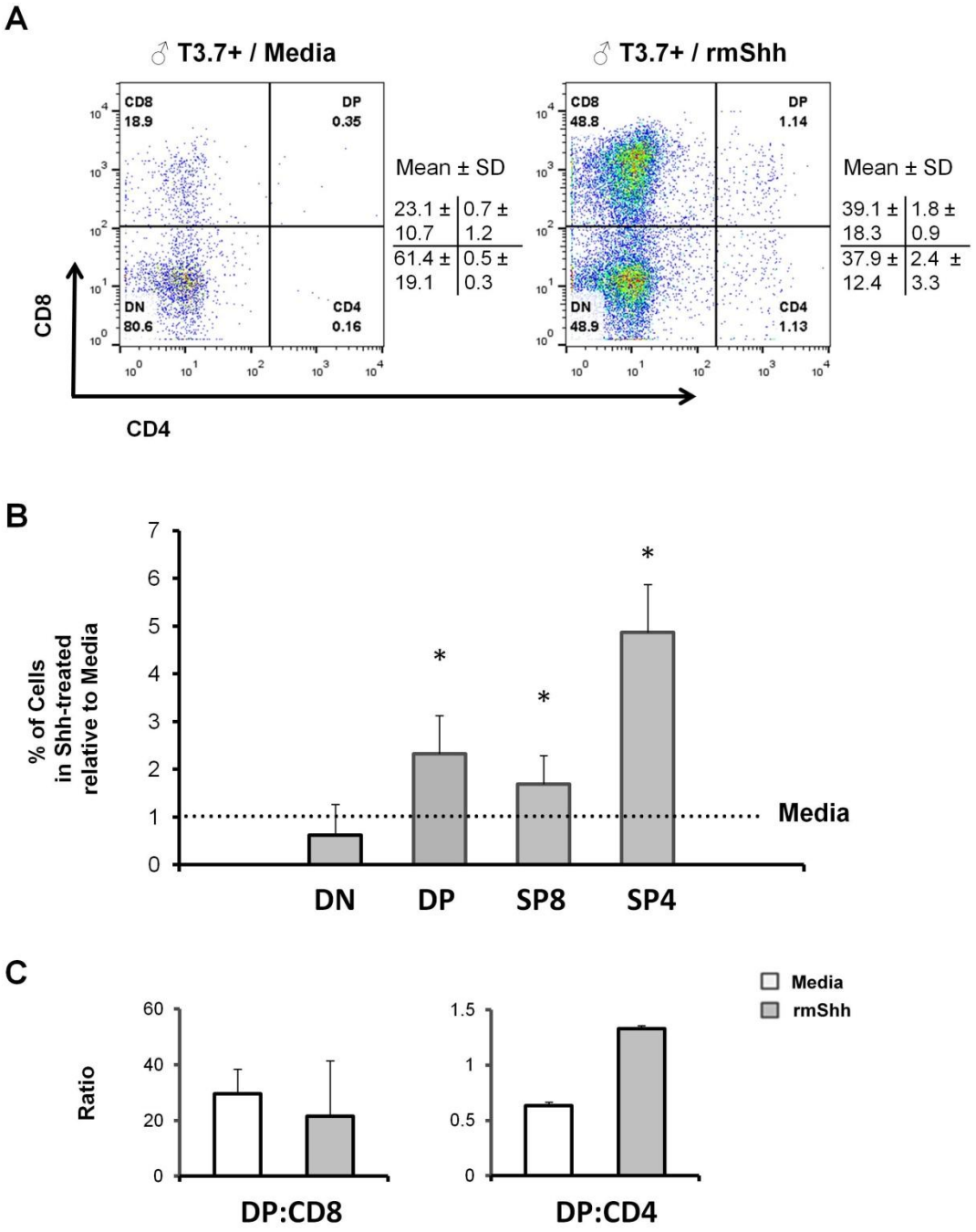

Figure 6.3

Influence of Shh on major thymocyte population in male HY-TCR transgenic mice within the T3.7 positive cells. Foetal thymic organ cultures (FTOCs) were cultured with or without rmShh for 7-days. Cells were stained for anti-T3.7, anti-CD8 and anti-CD4, and analyzed by flow cytometry. Thymocyte populations were gated within the $T3.7^{+}$ cells. **(A)** Representative dot plot of thymocyte populations. **(B)** Representative bar graph of DN, DP and SP8 percentages. **(C)** Ratio of DP:CD8 and DP:CD4. Figures are representative of 18 independent sets of E17.5 male littermates. Mean and standard deviation of each population are given. Bars represent mean ± standard deviations. **DN** (p= 0.4, n=18), **DP** (p= 0.03, n=18), **SP8** (p= 0.04, n=18), **SP4** (p= 0.01, n=18). *represents $p \leq 0.05$.

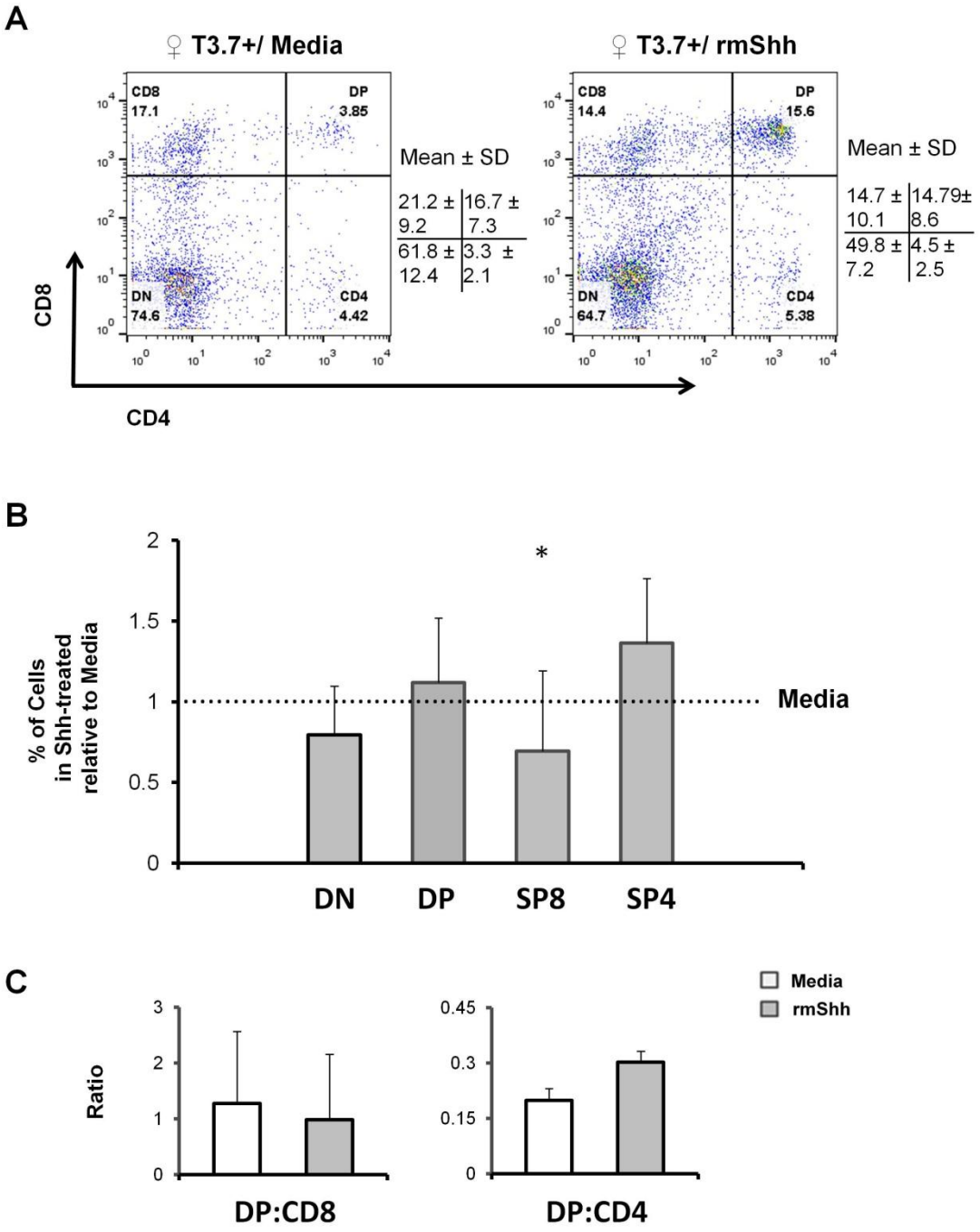

Figure 6.4

Influence of Shh on major thymocyte population in female HY-TCR transgenic mice within the T3.7 positive cells. Foetal thymic organ cultures (FTOCs) were cultured with or without rmShh for 7-days. Cells were stained for anti-T3.7, anti-CD8 and anti-CD4, and analyzed by flow cytometry. Thymocyte populations were gated within the $T3.7^{+}$ cells. **(A)** Representative dot plot of thymocyte populations. **(B)** Representative bar graph of DN, DP, SP8 and SP4 percentages. (**C)** Ratio of DP:CD8 and DP:CD4. Figures are representative of 21 independent sets of E17.5 female littermates. Mean and standard deviation of each population are given. Bars represent mean ± standard deviations. **DN** (p= 0.3, n=21), **DP** (p= 0.4, n=21), **SP8** (p= 0.03, n=21), **SP4** (p= 0.06, n=21). *represents $p \leq 0.05$.

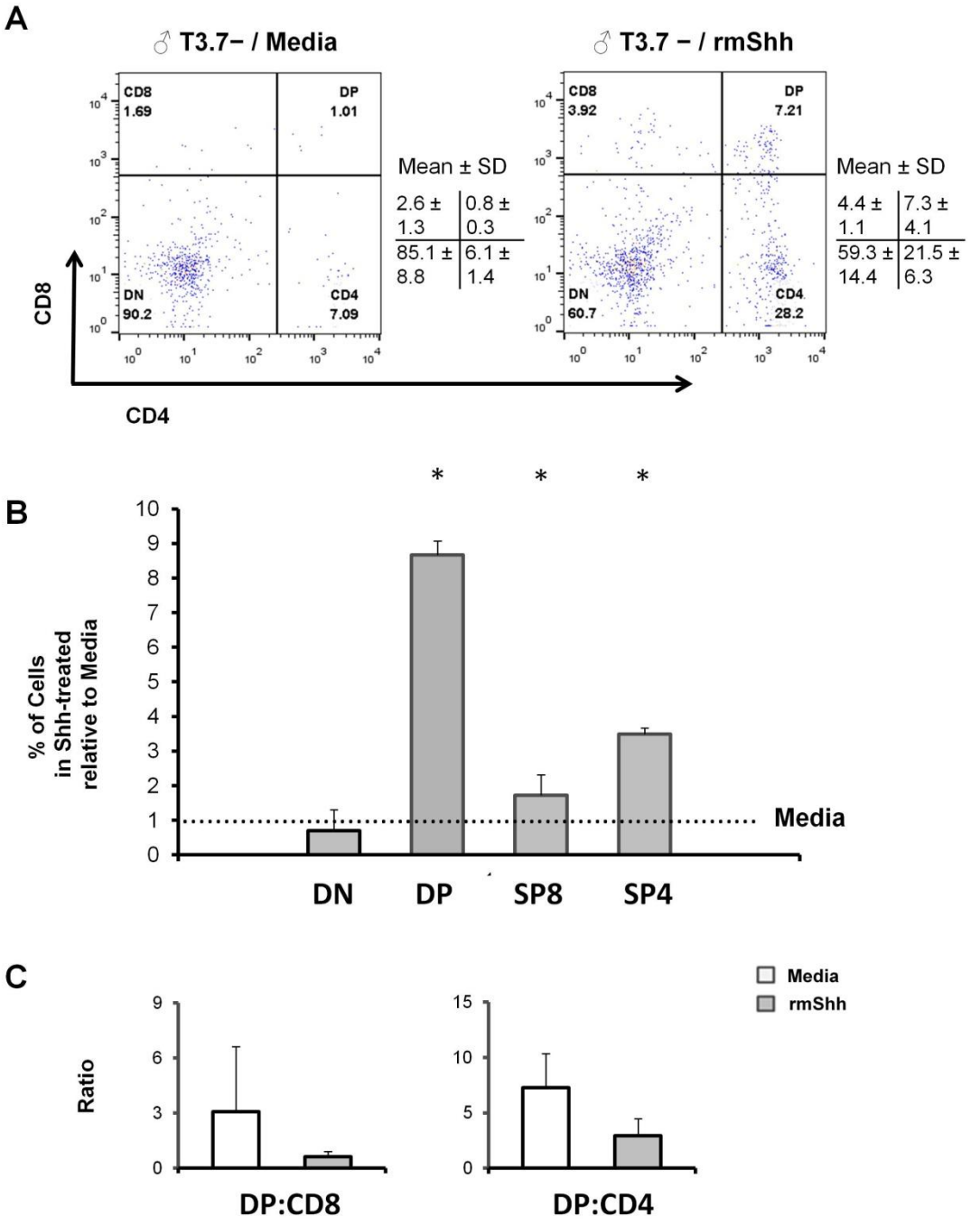

Figure 6.5

Influence of Shh on major thymocyte population in male HY-TCR transgenic mice within the T3.7 negative cells. Foetal thymic organ cultures (FTOCs) were cultured with or without rmShh for 7-days. Cells were stained for anti-T3.7, anti-CD8 and anti-CD4, and by flow cytometry. Thymocyte populations were gated within the $T3.7^{-}$ cells. **(A)** Representative dot plot of thymocyte populations. **(B)** Representative bar graph of DN, DP, SP8 and SP4 percentages. **(C)** Ratio of DP:CD8 and DP:CD4. Figures are representative of 18 independent sets of E17.5 male littermates. Mean and standard deviation of each population are given. Bars represent mean ± standard deviations. **DN** (p= 0.07, n=18), **DP** (p= 0.04, n=18), **SP8** (p= 0.03, n=18), **SP4** (p= 0.04, n=18). *represents $p \leq 0.05$.

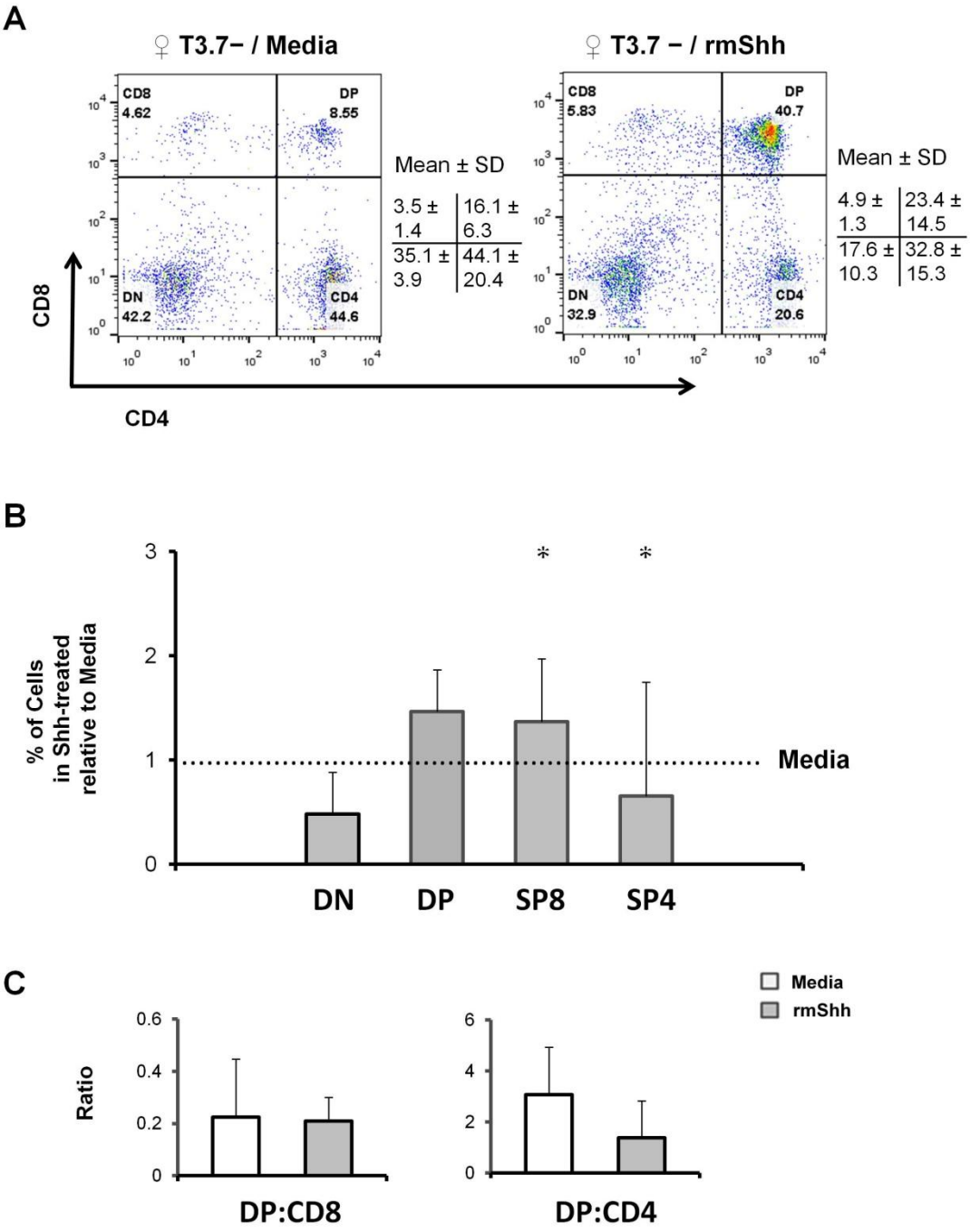

Figure 6.6

Influence of Shh on major thymocyte population in female HY-TCR transgenic mice within the T3.7 negative cells. Foetal thymic organ cultures (FTOCs) were cultured with or without rmShh for 7-days. Cells were stained for anti-T3.7, anti-CD8 and anti-CD4, and analyzed by flow cytometry. Thymocyte populations were gated within the $T3.7^{-}$ cells. **(A)** Representative dot plot of thymocyte populations. **(B)** Representative bar graph of DN, DP, SP8 and SP4 percentages. **(C)** Ratio of DP:CD8 and DP:CD4. Figures are representative of 21 independent sets of E17.5 female littermates. Mean and standard deviation of each population are given. Bars represent mean ± standard deviations. **DN** (p= 0.06, n=21), **DP** (p= 0.9, n=21), **SP8** (p= 0.01, n=21), **SP4** (p= 0.04, n=21). *represents $p \leq 0.05$.

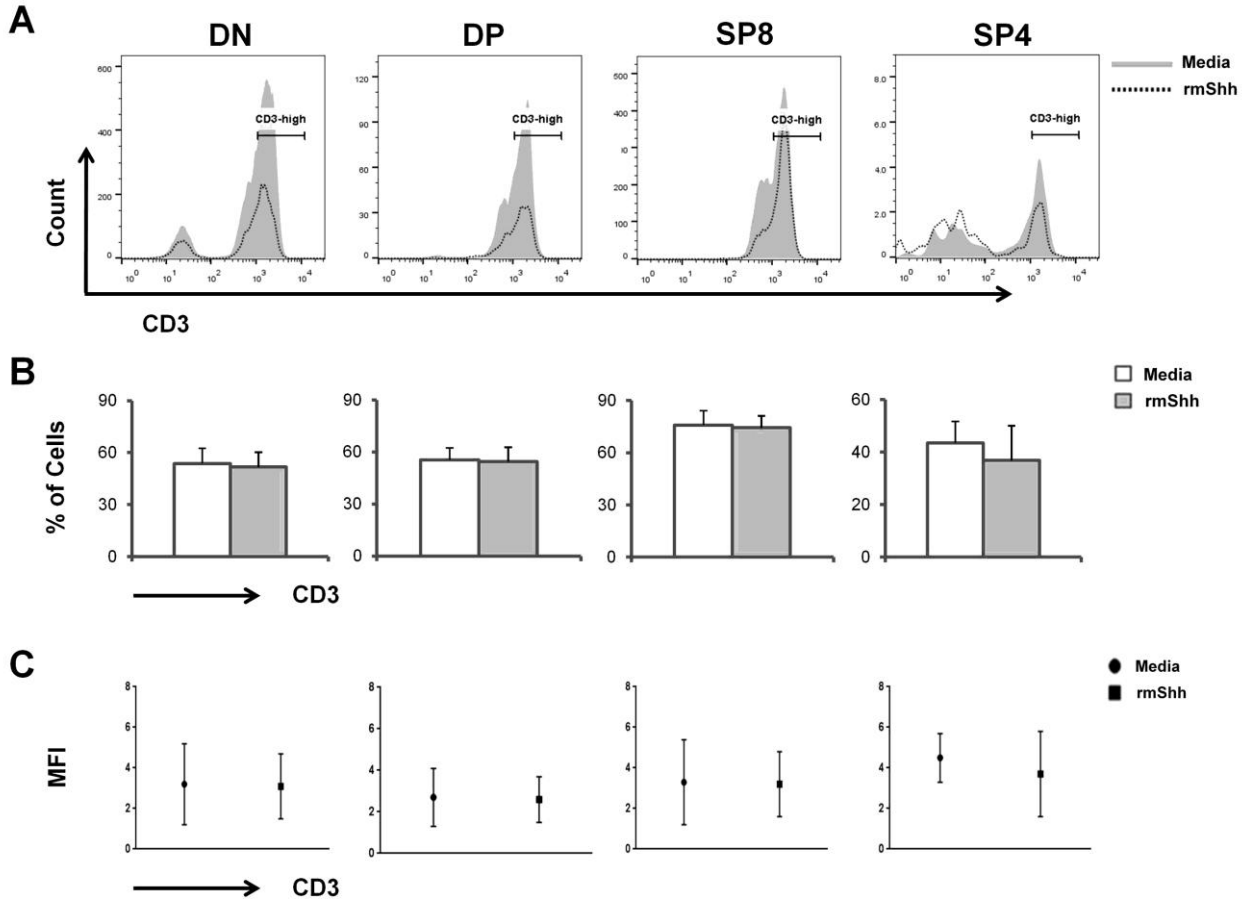

Figure 6.7

Expression of CD3 in thymocytes from male HY-TCR transgenic mice within the T3.7 positive cells. Foetal thymic organ cultures (FTOCs) were cultured with or without rmShh for 7-days. Cells were stained for anti-T3.7, anti-CD3, anti-CD8 and anti-CD4, and analyzed by flow cytometry. Thymocyte populations were gated within the $T3.7^{+}$ cells. **(A)** Representative histogram of CD3 expression in DN, DP, SP8 and SP4 cells. **(B)** Representative bar graph of CD3 percentages in DN, DP, SP8 and SP4 cells. **(C)** Representative scatter plot of CD3 MFI in DN, DP, SP8 and SP4 cells. Figures are representative of 8 independent sets of male HY-TCR transgenic littermates respectively. Mean and standard deviation of each population are given. Bars represent mean ± standard deviations. **CD3 percentages; DN** (p= 0.7, n=8), **DP** (p= 0.7, n=8), **SP8** (p= 0.8, n=8), **SP4** (p= 0.2, n=8). **CD3 MFI; DN** (p= 0.4, n=8), **DP** (p= 0.2, n=8), **SP8** (p= 0.4, n=8), **SP4** (p= 0.7, n=8).

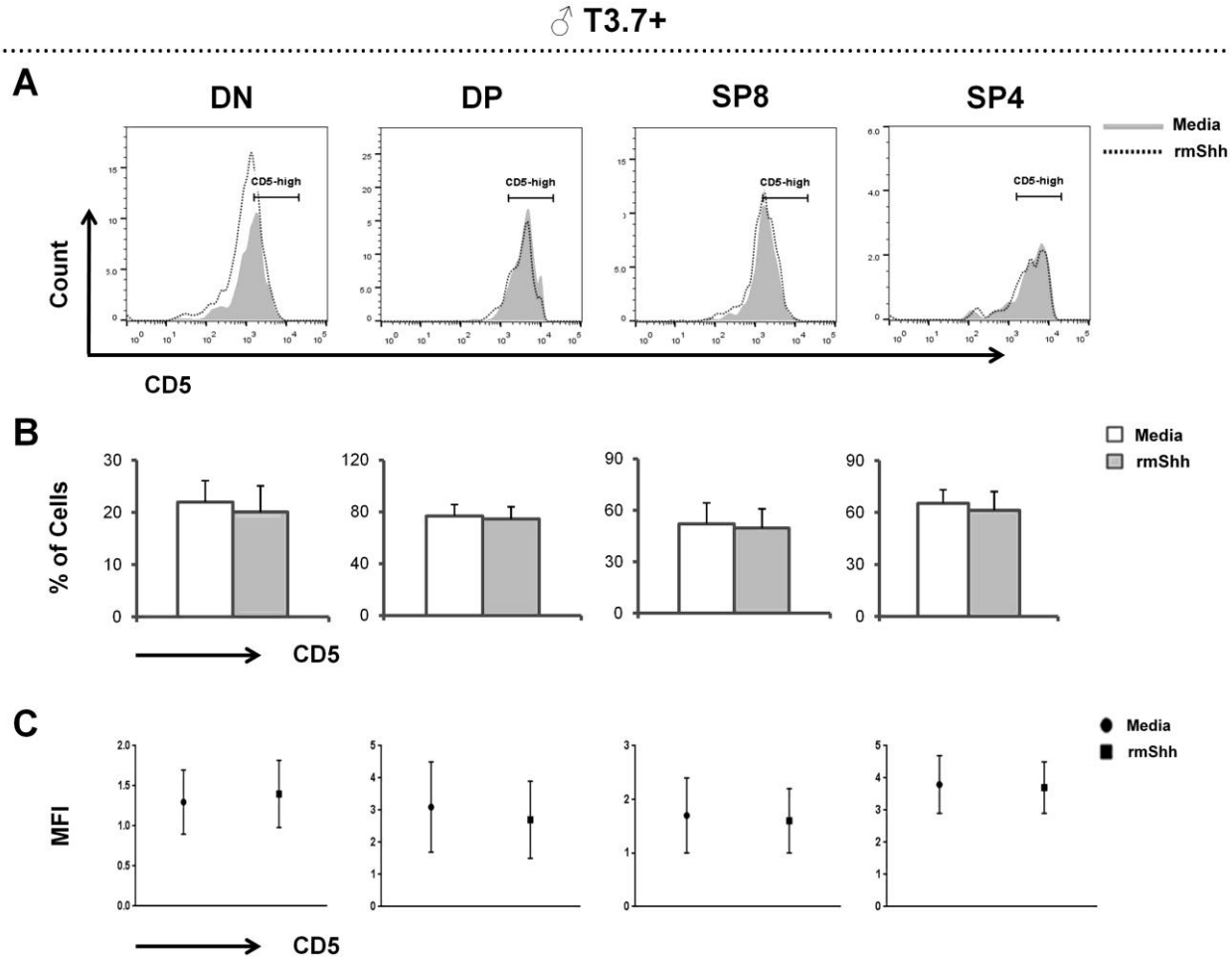

Figure 6.8

Expression of CD5 in thymocytes from male HY-TCR transgenic mice within the T3.7 positive cells. Foetal thymic organ cultures (FTOCs) were cultured with or without rmShh for 7-days. Cells were stained for anti-T3.7, anti-CD5, anti-CD8 and anti-CD4, and analyzed by flow cytometry. Thymocyte populations were gated within the $T3.7^{+}$ cells. **(A)** Representative histogram of CD5 expression in DN, DP, SP8 and SP4 cells. **(B)** Representative bar graph of CD5 percentages in DN, DP, SP8 and SP4 cells. **(C)** Representative scatter plot of CD5 MFI in DN, DP, SP8 and SP4 cells. Figures are representative of 8 independent sets of male HY-TCR transgenic littermates respectively. Mean and standard deviation of each population are given. Bars represent mean ± standard deviations. **CD5 percentages; DN** (p= 0.5, n=8), **DP** (p= 0.6, n=8), **SP8** (p= 0.7, n=8), **SP4** (p= 0.5, n=8). **CD5 MFI; DN** (p= 0.4, n=8), **DP** (p= 0.5, n=8), **SP8** (p= 0.3, n=8), **SP4** (p= 0.4, n=8).

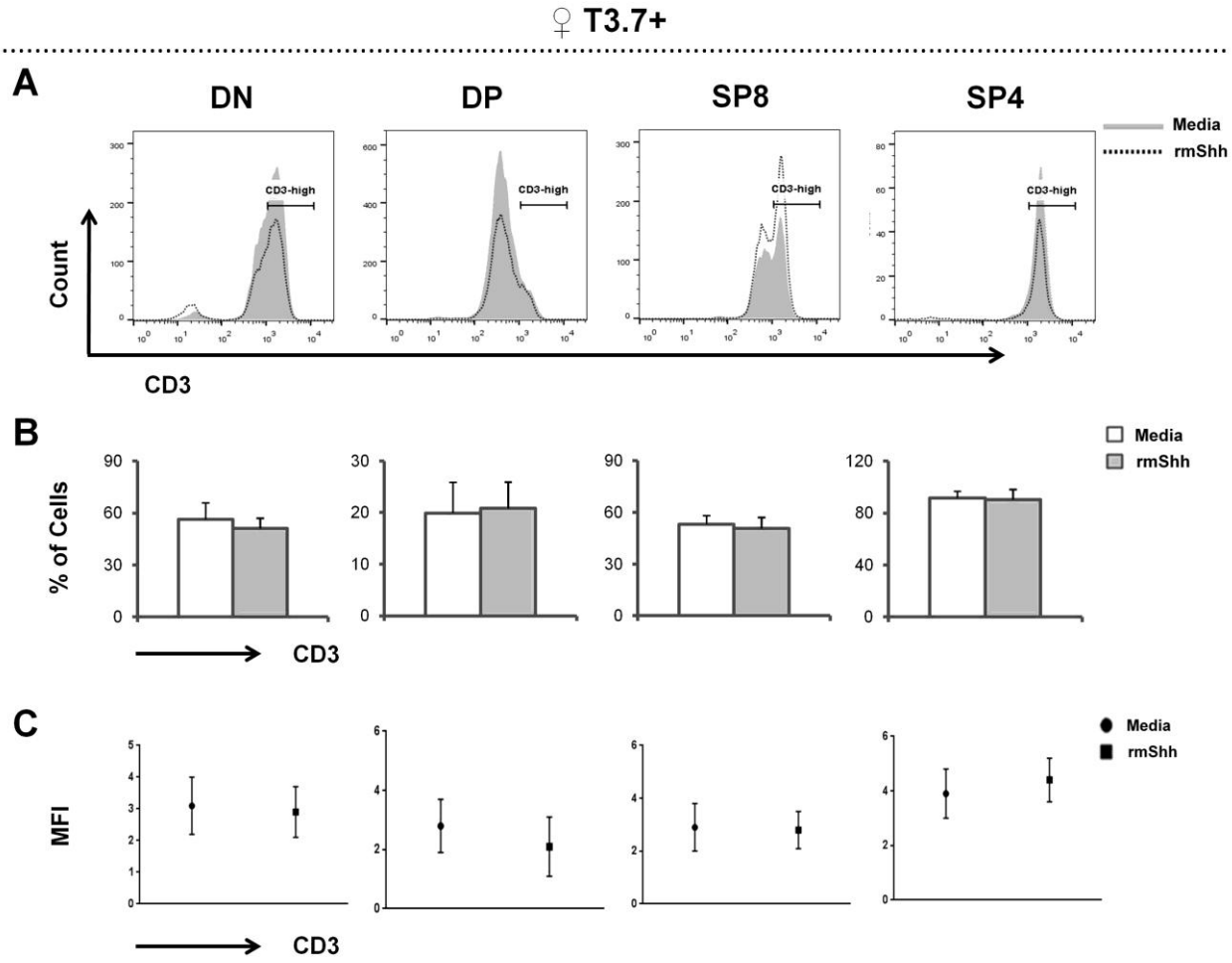

Figure 6.9

Expression of CD3 in thymocytes from female HY-TCR transgenic mice within the T3.7 positive cells. Foetal thymic organ cultures (FTOCs) were cultured with or without rmShh for 7-days. Cells were stained for anti-T3.7, anti-CD3, anti-CD8 and anti-CD4, and analyzed by flow cytometry. Thymocyte populations were gated within the $T3.7^{+}$ cells. **(A)** Representative histogram of CD3 percentages in DN, DP, SP8 and SP4 cells. **(B)** Representative scatter plot of CD3 MFI in DN, DP, SP8 and SP4 cells. **(C)** Representative dot plot of CD3 expression in DN, DP, SP8 and SP4 cells. Figures are representative of 11 independent sets of female HY-TCR transgenic littermates respectively. Mean and standard deviation of each population are given. Bars represent mean ± standard deviations. **CD3 percentages; DN** (p= 0.2, n=11), **DP** (p= 0.7, n=11), **SP8** (p= 0.4, n=11), **SP4** (p= 0.7, n=11). **CD3 MFI; DN** (p= 0.3, n=11), **DP** (p= 0.2, n=11), **SP8** (p= 0.9, n=11), **SP4** (p= 0.4, n=11).

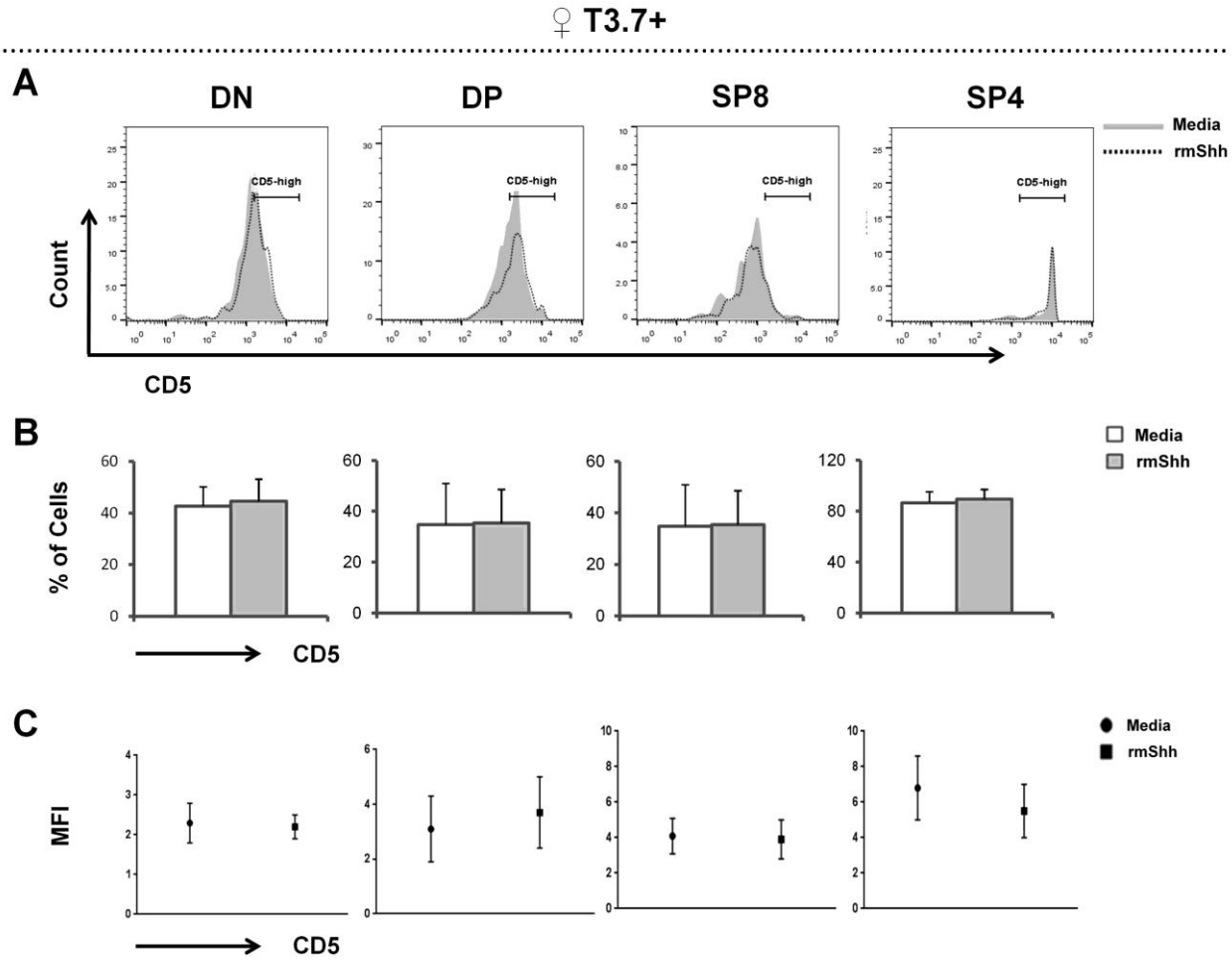

Figure 6.10

Expression of CD5 in thymocytes from female HY-TCR transgenic mice within the T3.7 positive cells. Foetal thymic organ cultures (FTOCs) were cultured with or without rmShh for 7-days. Cells were stained for anti-T3.7, anti-CD5, anti-CD8 and anti-CD4, and analyzed by flow cytometry. Thymocyte populations were gated within the $T3.7^{+}$ cells. **(A)** Representative histogram of CD5 percentages in DN, DP, SP8 and SP4 cells. **(B)** Representative scatter plot of CD5 MFI in DN, DP, SP8 and SP4 cells. **(C)** Representative scatter plot of CD5 MFI in DN, DP, SP8 and SP4 cells. Figures are representative of 11 independent sets of female HY-TCR transgenic littermates respectively. Mean and standard deviation of each population are given. Bars represent mean ± standard deviations. **CD5 percentages; DN** (p= 0.6, n=11), **DP** (p= 0.7, n=11), **SP8** (p= 0.9, n=11), **SP4** (p= 0.6, n=11). **CD5 MFI; DN** (p= 0.5, n=11), **DP** (p= 0.3, n=11), **SP8** (p= 0.7, n=11), **SP4** (p= 0.2, n=11).

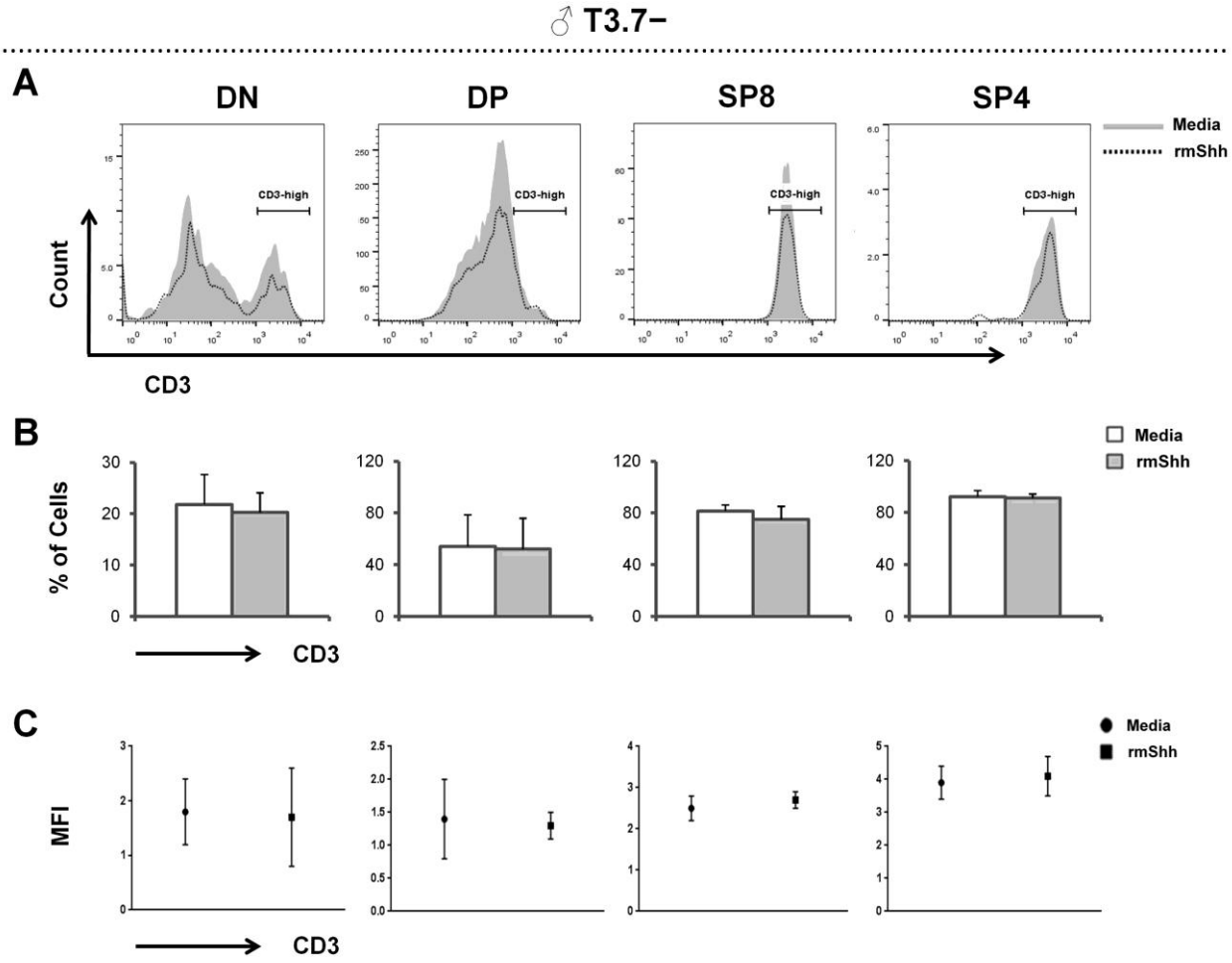

Figure 6.11

Expression of CD3 in thymocytes from male HY-TCR transgenic mice within the T3.7 negative cells. Foetal thymic organ cultures (FTOCs) were cultured with or without rmShh for 7-days. Cells were stained for anti-T3.7, anti-CD3, anti-CD8 and anti-CD4, and analyzed by flow cytometry. Thymocyte populations were gated within the $T3.7^{-}$ cells. **(A)** Representative histogram of CD3 expression in DN, DP, SP8 and SP4 cells. **(B)** Representative bar graph of CD3 percentages in DN, DP, SP8 and SP4 cells. **(C)** Representative scatter plot of CD3 MFI in DN, DP, SP8 and SP4 cells. Figures are representative of 8 independent sets of male HY-TCR transgenic littermates respectively. Mean and standard deviation of each population are given. Bars represent mean ± standard deviations. **CD3 percentages; DN** (p= 0.8, n=8), **DP** (p= 0.6, n=8), **SP8** (p= 0.8, n=8), **SP4** (p= 0.4, n=8). **CD3 MFI; DN** (p= 0.3, n=8), **DP** (p= 0.5, n=8), **SP8** (p= 0.1, n=8), **SP4** (p= 0.2, n=8).

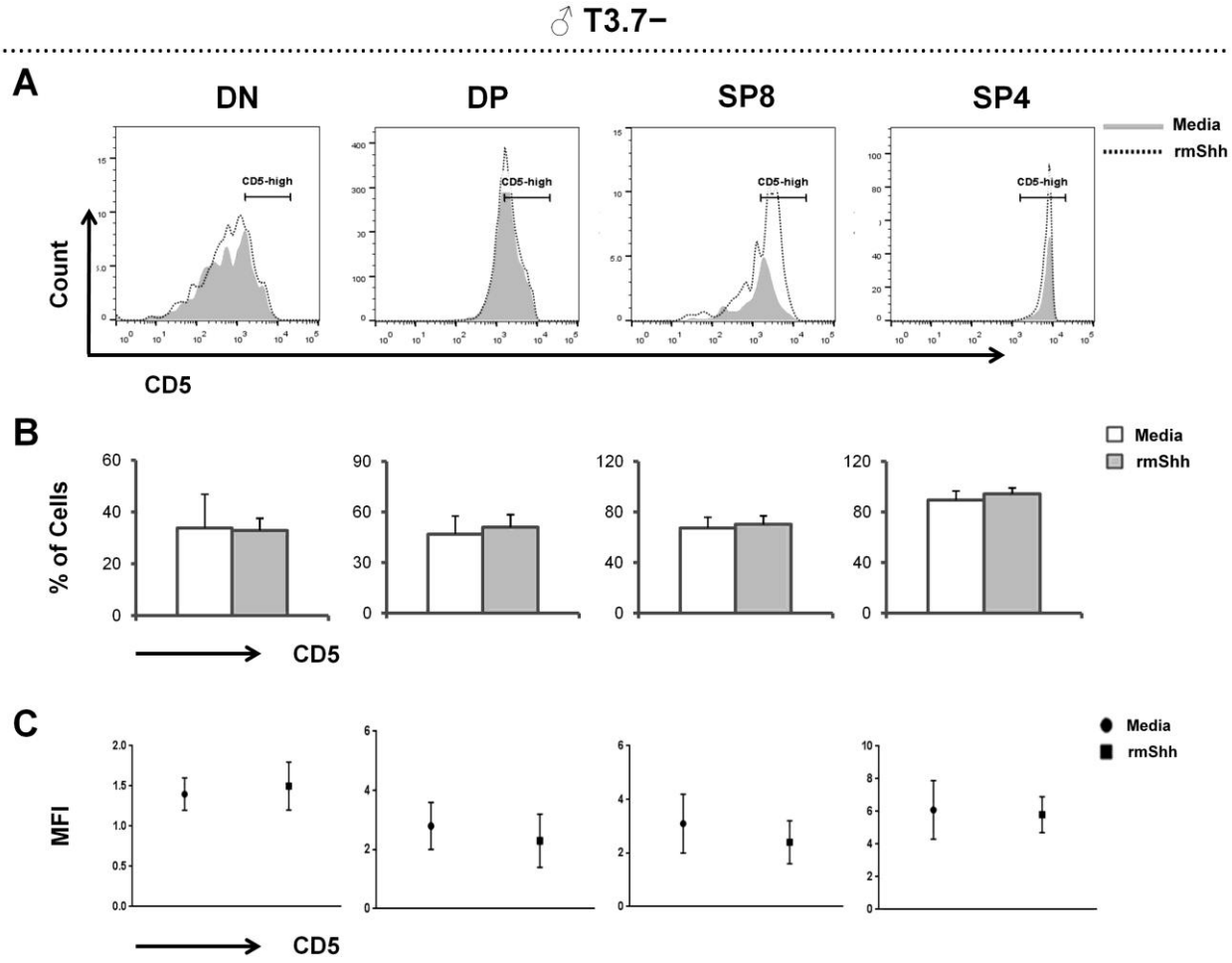

Figure 6.12

Expression of CD5 in thymocytes from male HY-TCR transgenic mice within the T3.7 negative cells. Foetal thymic organ cultures (FTOCs) were cultured with or without rmShh for 7-days. Cells were stained for anti-T3.7, anti-CD5, anti-CD8 and anti-CD4, and analyzed by flow cytometry. Thymocyte populations were gated within the $T3.7^{-}$ cells. **(A)** Representative histogram of CD5 expression in DN, DP, SP8 and SP4 cells. **(B)** Representative bar graph of CD5 percentages in DN, DP, SP8 and SP4 cells. **(C)** Representative scatter plot of CD5 MFI in DN, DP, SP8 and SP4 cells. Figures are representative of 8 independent sets of male HY-TCR transgenic littermates respectively. Mean and standard deviation of each population are given. Bars represent mean ± standard deviations. **CD5 percentages; DN** (p= 0.4, n=8), **DP** (p= 0.7, n=8), **SP8** (p= 0.9, n=8), **SP4** (p= 0.4, n=8). **CD5 MFI; DN** (p= 0.2, n=8), **DP** (p= 0.6, n=8), **SP8** (p= 0.3, n=8), SP4 (p= 0.2, n=8).

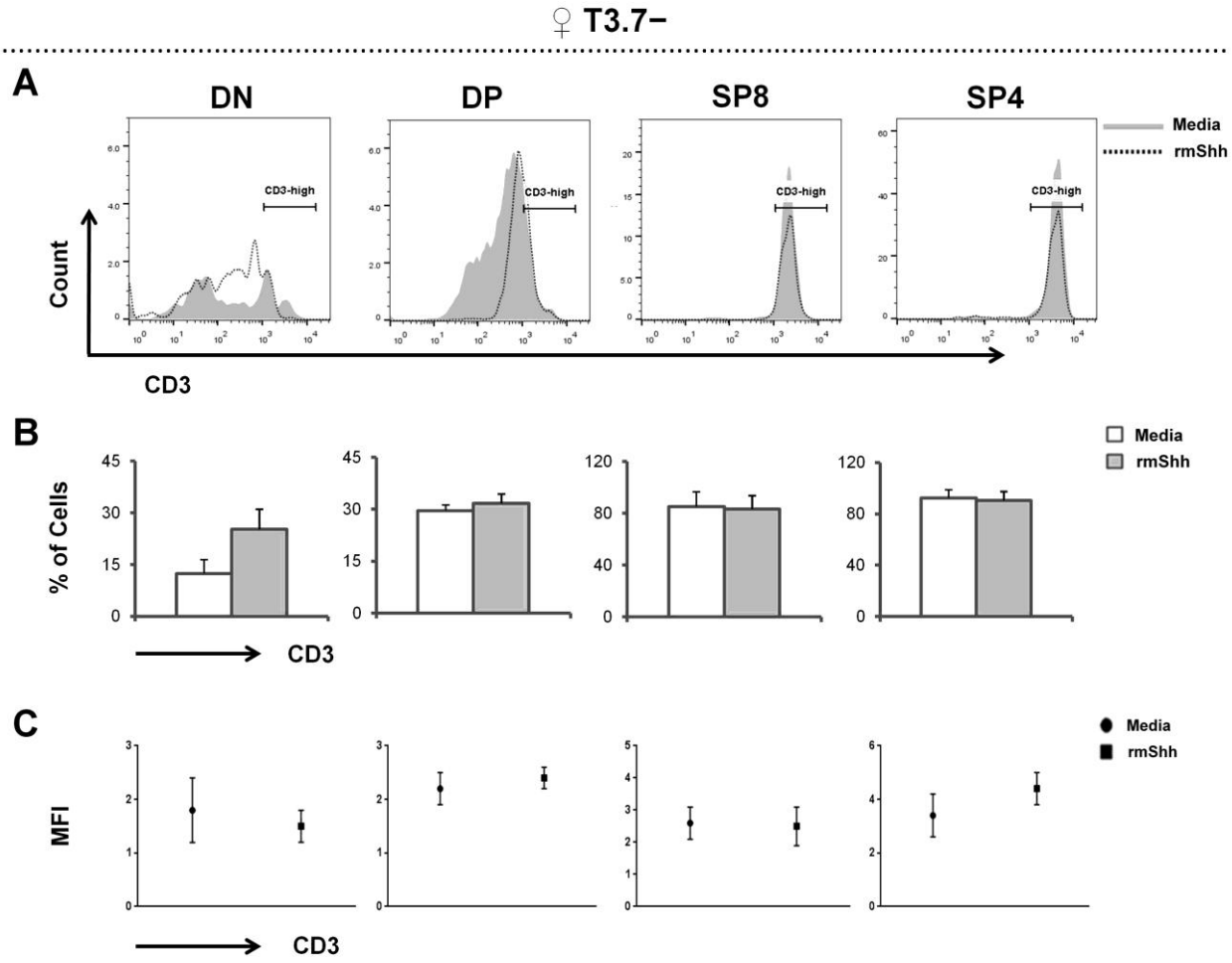

Figure 6.13

Expression of CD3 in thymocytes from female HY-TCR transgenic mice within the T3.7 negative cells. Foetal thymic organ cultures (FTOCs) were cultured with or without rmShh for 7-days. Cells were stained for anti-T3.7, anti-CD3, anti-CD8 and anti-CD4, and analyzed by flow cytometry. Thymocyte populations were gated within the $T3.7^{-}$ cells. **(A)** Representative histogram of CD3 expression in DN, DP, SP8 and SP4 cells. **(B)** Representative bar graph of CD3 percentages in DN, DP, SP8 and SP4 cells. **(C)** Representative scatter plot of CD3 MFI in DN, DP, SP8 and SP4 cells. Figures are representative of 11 independent sets of female HY-TCR transgenic littermates respectively. Mean and standard deviation of each population are given. Bars represent mean ± standard deviations. **CD3 percentages; DN** (p= 0.4, n=11), **DP** (p= 0.6, n=11), **SP8** (p= 0.3, n=11), **SP4** (p= 0.8, n=11). **CD3 MFI; DN** (p= 0.2, n=11), **DP** (p= 0.5, n=11), **SP8** (p= 0.9, n=11), **SP4** (p= 0.8, n=11).

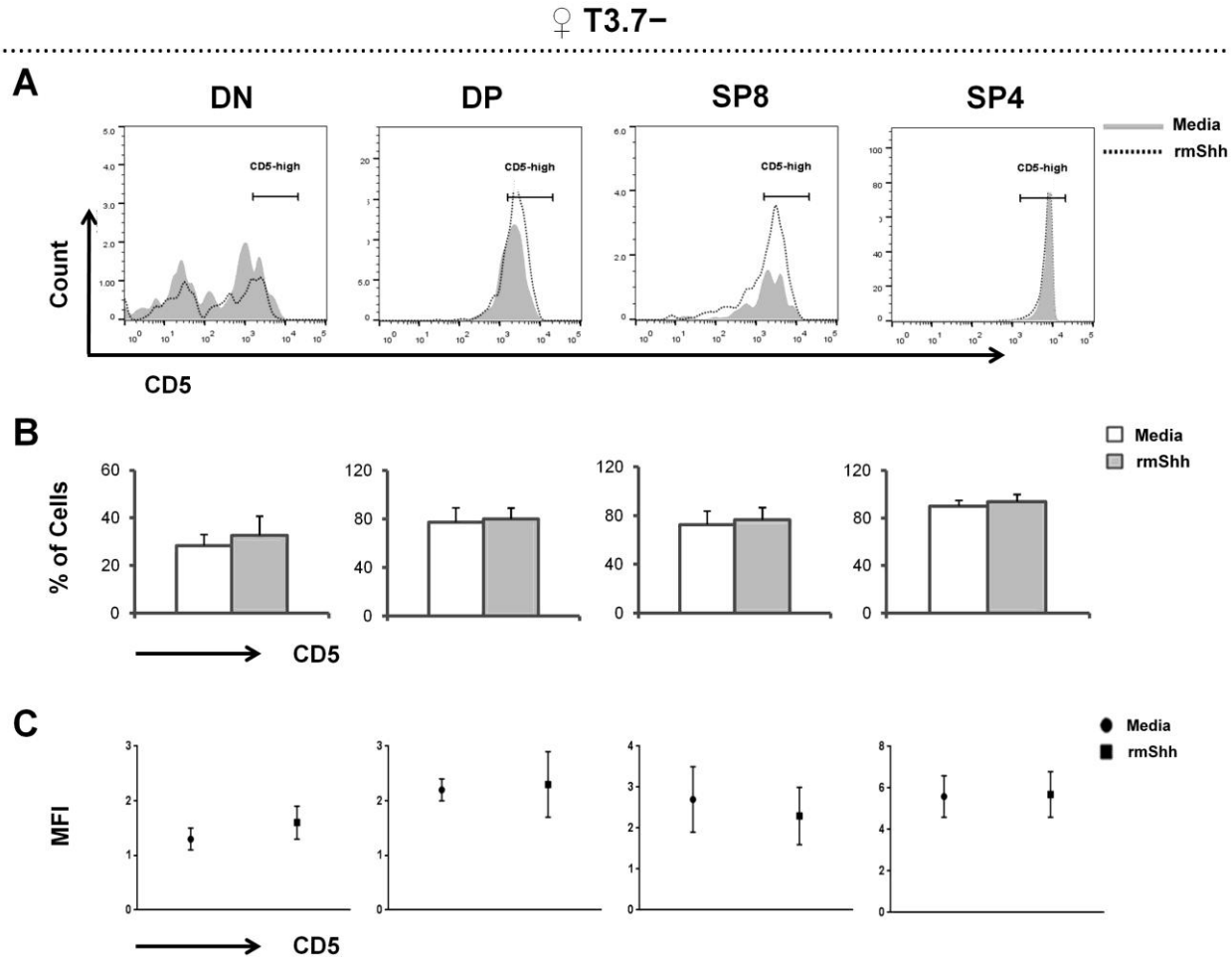

Figure 6.14

Expression of CD5 in thymocytes from female HY-TCR transgenic mice within the T3.7 negative cells. Foetal thymic organ cultures (FTOCs) were cultured with or without rmShh for 7-days. Cells were stained for anti-T3.7, anti-CD5, anti-CD8 and anti-CD4, and analyzed by flow cytometry. Thymocyte populations were gated within the $T3.7^{-}$ cells. **(A)** Representative histogram of CD5 expression in DN, DP, SP8 and SP4 cells. **(B)** Representative bar graph of CD5 percentages in DN, DP, SP8 and SP4 cells. **(C)** Representative scatter plot of CD5 MFI in DN, DP, SP8 and SP4 cells. Figures are representative of 11 independent sets of female HY-TCR transgenic littermates respectively. Mean and standard deviation of each population are given. Bars represent mean ± standard deviations. **CD5 percentages; DN** (p= 0.7, n=11), **DP** (p= 0.4, n=11), **SP8** (p= 0.6, n=11), **SP4** (p= 0.4, n=11). **CD5 MFI; DN** (p= 0.5, n=11), **DP** (p= 0.6, n=11), **SP8** (p= 0.7, n=11), **SP4** (p= 0.3, n=11).

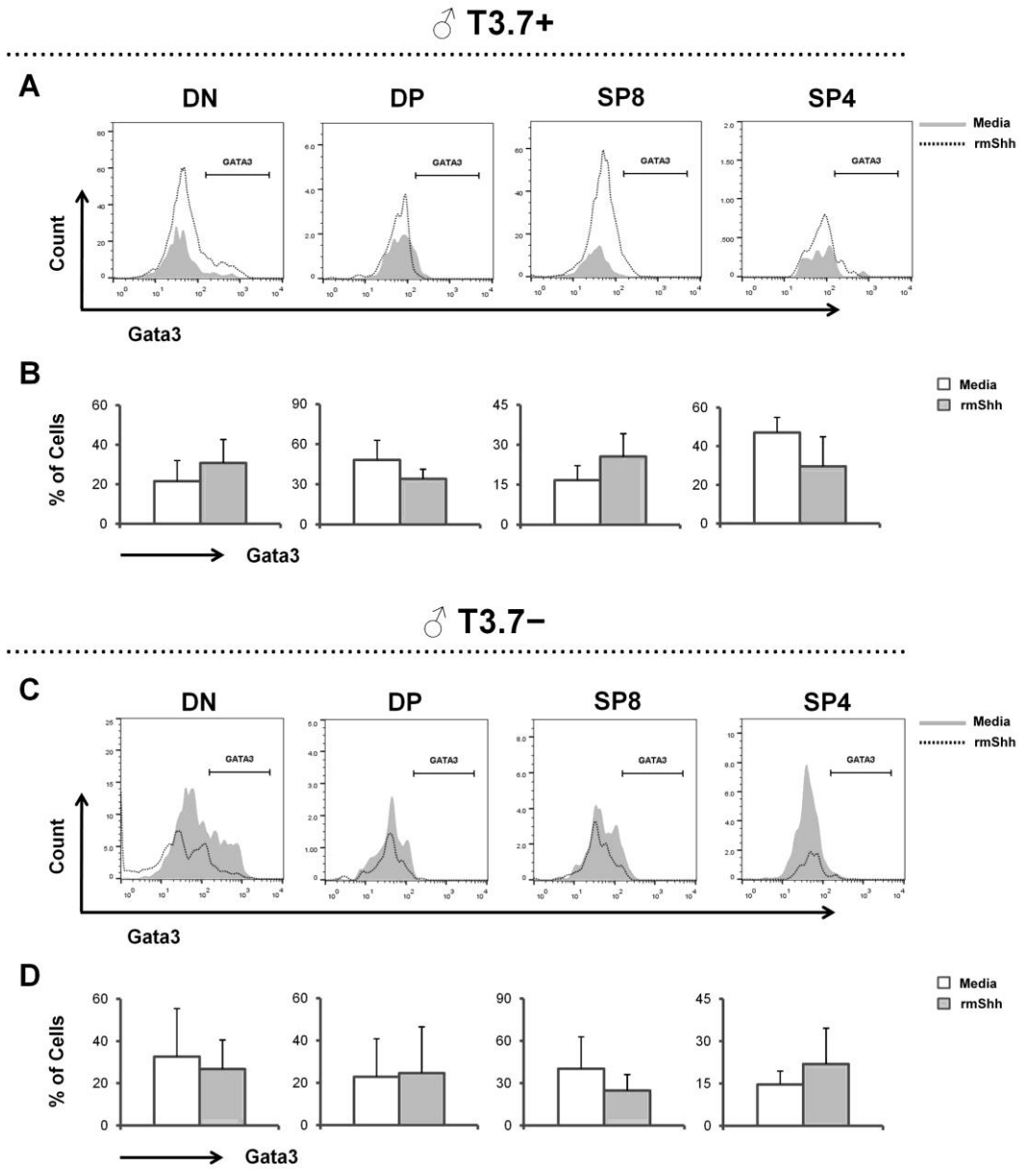

Figure 6.15

Expression of Gata-3 in thymocytes from male HY-TCR transgenic mice within the T3.7 positive and negative cells. Foetal thymic organ cultures (FTOCs) were cultured with or without rmShh for 7-days. Cells were stained for anti-T3.7, anti-Gata3, anti-CD8 and anti-CD4, and analyzed by flow cytometry. Thymocyte populations were gated within the $T3.7^+$ cells and $T3.7^-$ cells independently. **(A)** Representative histogram of Gata-3 expression in DN, DP, SP8 and SP4 within the $T3.7^+$ cells. **(B)** Representative bar graph of Gata-3 percentages in DN, DP, SP8 and SP4 within the $T3.7^+$ cells. **(C)** Representative histogram of Gata-3 expression in DN, DP, SP8 and SP4 within the $T3.7^-$ cells. **(D)** Representative bar graph of Gata-3 percentages in DN, DP, SP8 and SP4 within the $T3.7^-$ cells. Figures are representative of 5 independent sets of male HY-TCR transgenic littermates respectively. Mean and standard deviation of each population are given. Bars represent mean ± standard deviations. **Male Gata-3 percentages ($T3.7^+$); DN** (p= 0.3, n=5), **DP** (p= 0.2, n=5), **SP8** (p= 0.2, n=5), **SP4** (p= 0.1, n=5). **Male Gata-3 percentages ($T3.7^-$); DN** (p= 0.4, n=5), **DP** (p= 0.6, n=5), **SP8** (p= 0.7, n=5), **SP4** (p= 0.3, n=5).

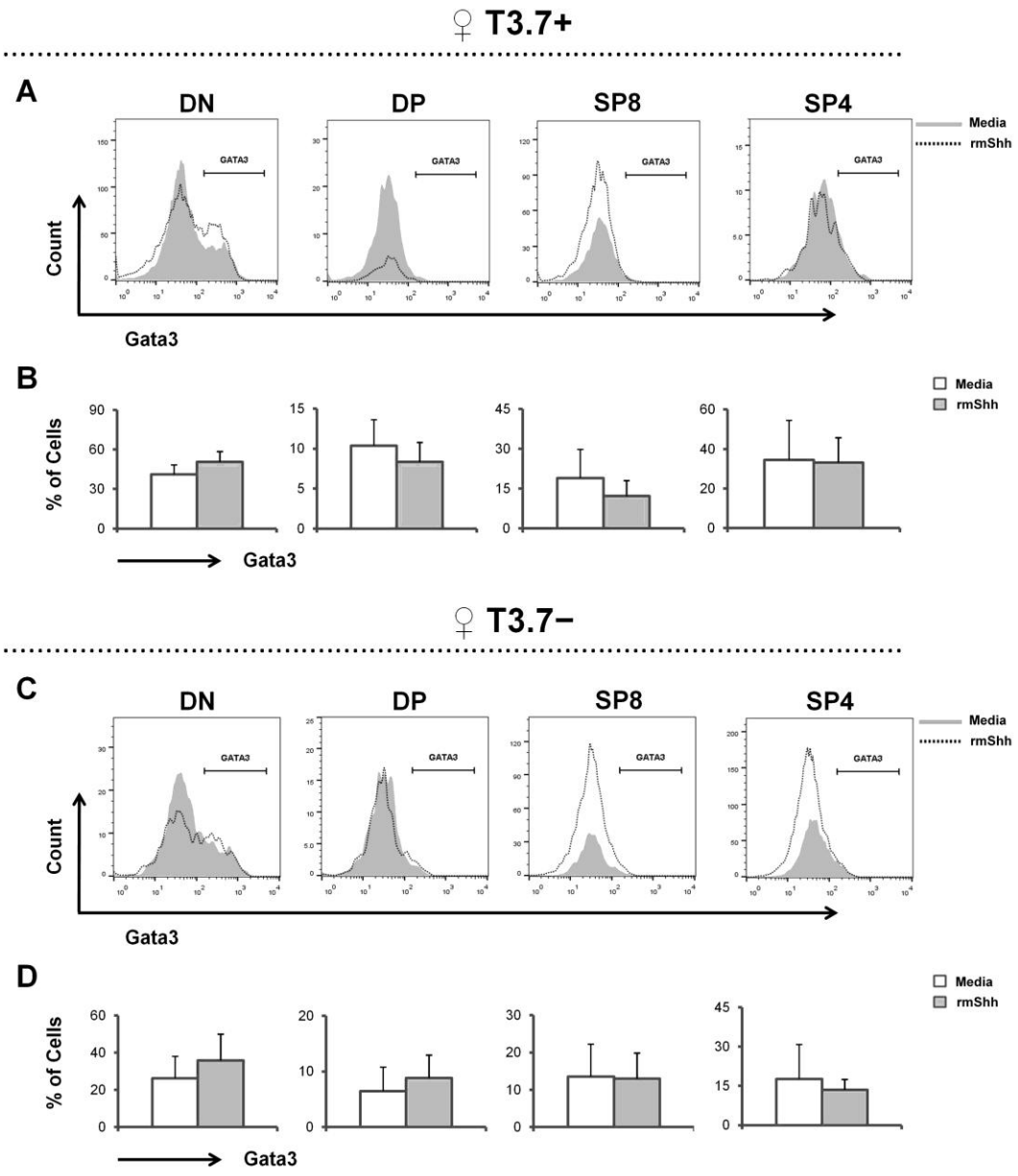

Figure 6.16

Expression of Gata-3 in thymocytes from female HY-TCR transgenic mice within the T3.7 positive and negative cells. Foetal thymic organ cultures (FTOCs) were cultured with or without rmShh for 7-days. Cells were stained for anti-T3.7, anti-Gata3, anti-CD8 and anti-CD4, and analyzed by flow cytometry. Thymocyte populations were gated within the $T3.7^+$ cells and $T3.7^-$ cells independently. **(A)** Representative histogram of Gata-3 expression in DN, DP, SP8 and SP4 within the $T3.7^+$ cells. **(B)** Representative bar graph of Gata-3 percentages in DN, DP, SP8 and SP4 within the $T3.7^+$ cells. **(C)** Representative histogram of Gata-3 expression in DN, DP, SP8 and SP4 within the $T3.7^-$ cells. **(D)** Representative bar graph of Gata-3 percentages in DN, DP, SP8 and SP4 within the $T3.7^-$ cells. Figures are representative of 7 independent sets of female HY-TCR transgenic littermates respectively. Mean and standard deviation of each population are given. Bars represent mean ± standard deviations. **Female Gata-3 percentages ($T3.7^+$); DN** (p= 0.08, n=7), **DP** (p= 0.3, n=7), **SP8** (p= 0.2, n=7), **SP4** (p= 0.8, n=7). **Female Gata-3 percentages ($T3.7^-$); DN** (p= 0.8, n=7), **DP** (p= 0.5, n=7), **SP8** (p= 0.4, n=7), **SP4** (p= 0.6, n=7).

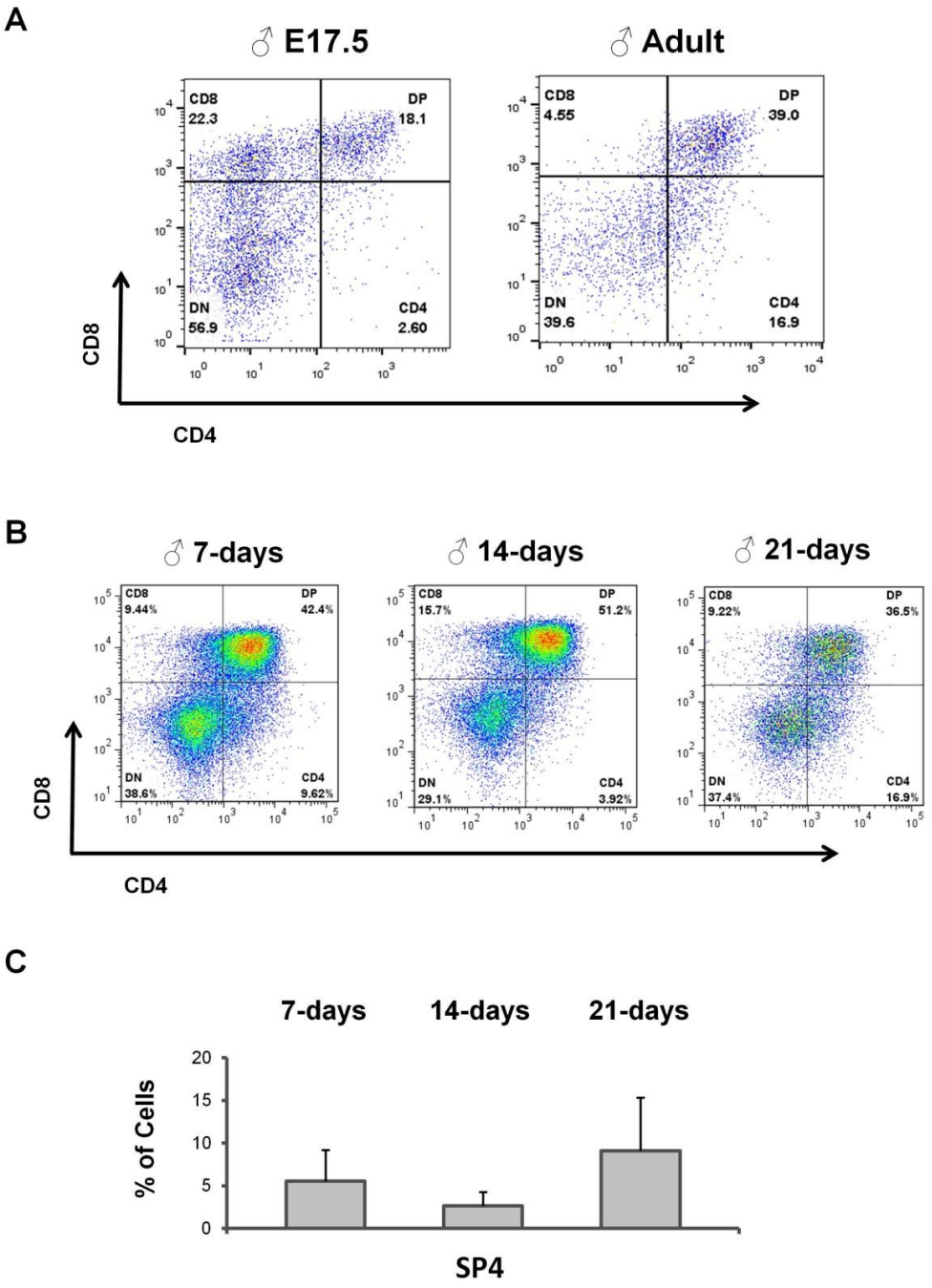

Figure 6.17

Thymus phenotype of male Marilyn-TCR transgenic mice. Thymocyte populations in male Marilyn-TCR transgenic mice. Cells were stained for anti-Vβ6, anti-CD8 and anti-CD4 and analyzed by flow cytometry. **(A)** Representative dot plot of embryonic (E17.5) and adult thymocyte populations. **(B)** Representative dot plot of thymocyte population at 3 time points; (7-days), (14-days) and (21-days). **(C)** Representative bar graph of SP4 cells percentage at 3 time-points; (7-days), (14-days) and (21-days).

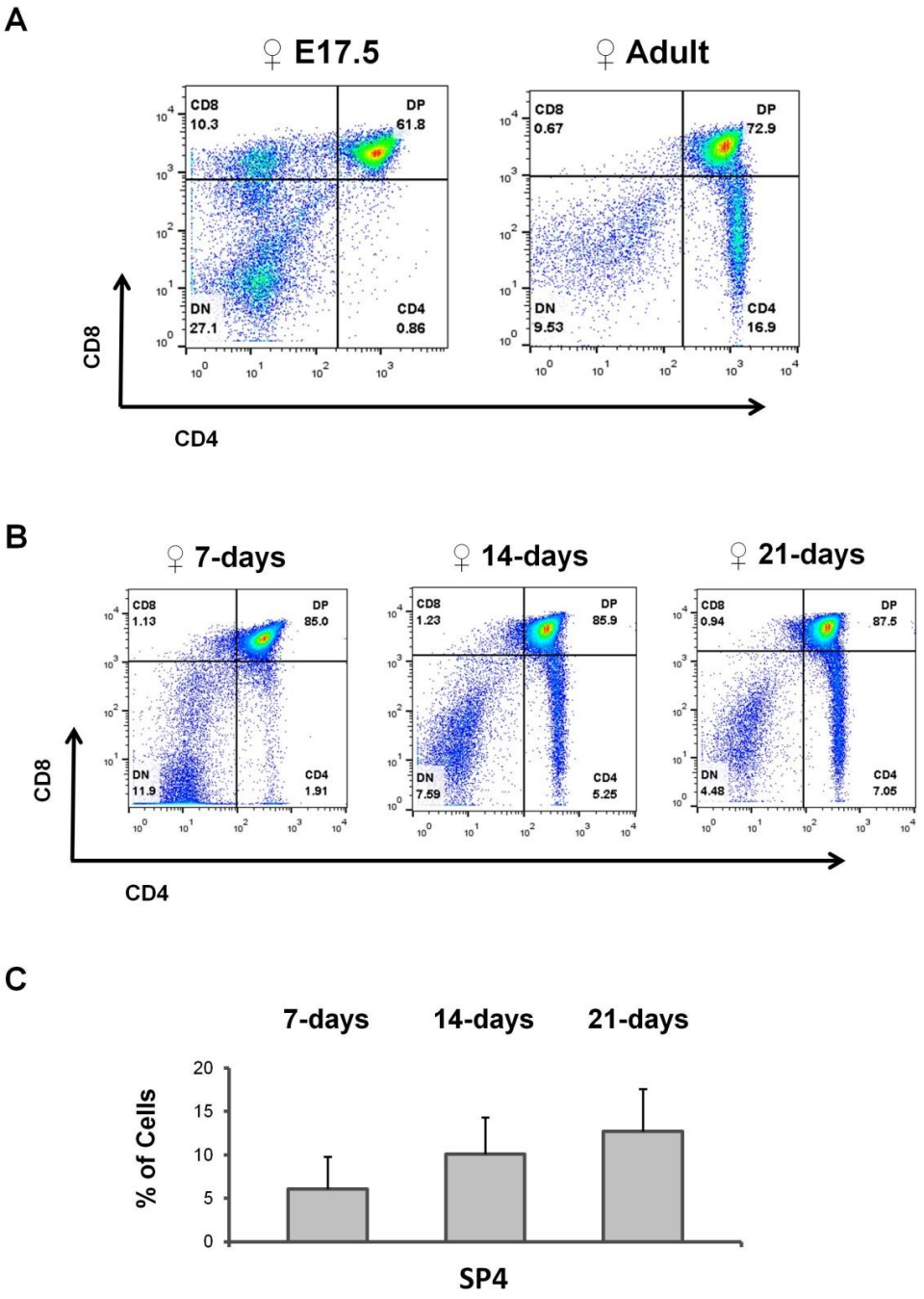

Figure 6.18

Thymus phenotype of female Marilyn-TCR transgenic mice. Thymocyte populations in female Marilyn-TCR transgenic mice. Cells were stained for anti-Vβ6, anti-CD8 and anti-CD4 and analyzed by flow cytometry. **(A)** Representative dot plot of embryonic (E17.5) and adult thymocyte populations. **(B)** Representative dot plot of thymocyte population at 3 time points; (7-days), (14-days) and (21-days). **(C)** Representative bar graph of SP4 cells percentage at 3 time-points; (7-days), (14-days) and (21-days).

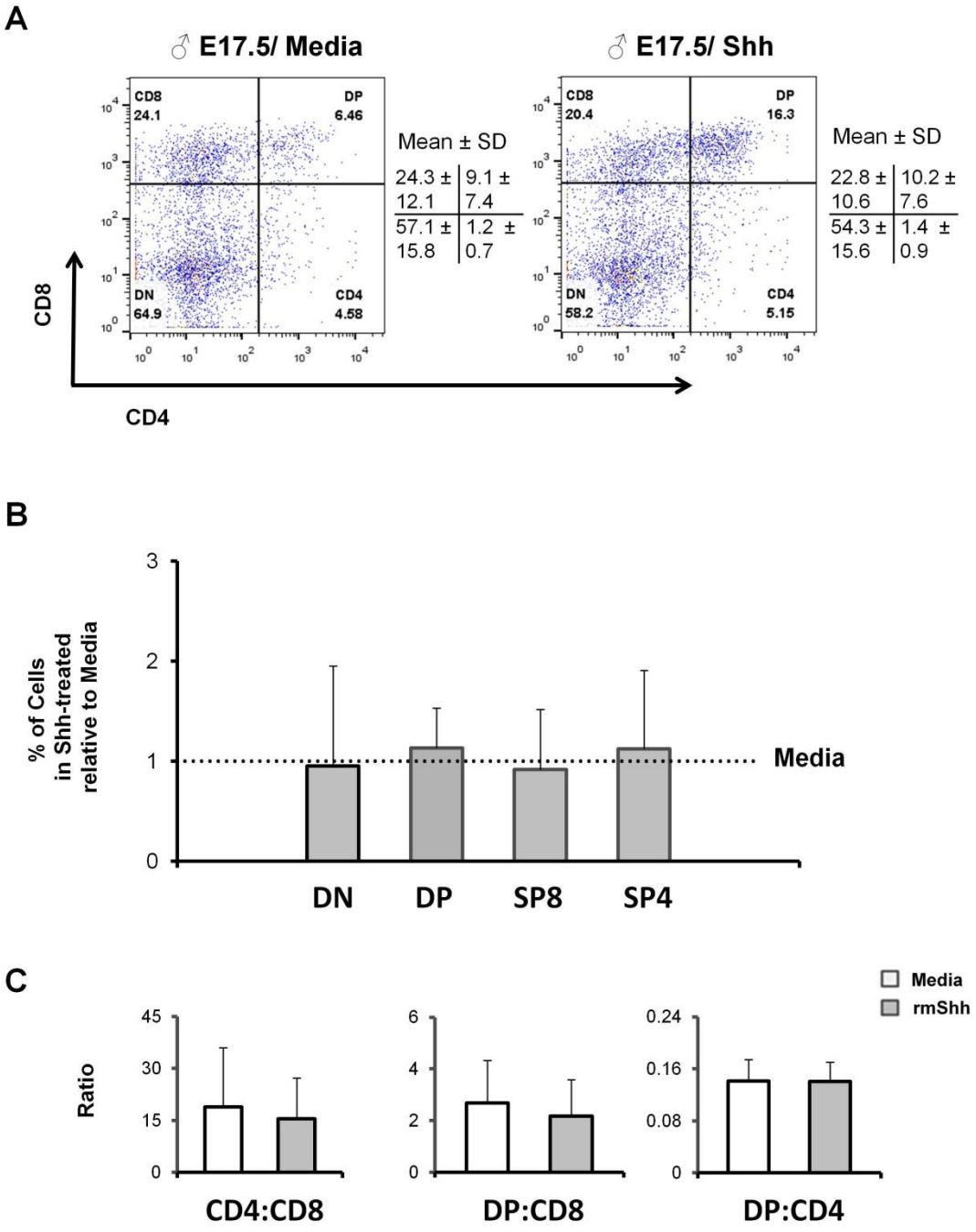

Figure 6.19

Influence of Shh on major embryonic thymocyte populations in male Marilyn-TCR transgenic mice. Fetal thymic organ cultures (FTOCs) were cultured with or without rmShh for 7-days. Cells were stained for anti-Vβ6, anti-CD8 and anti-CD4, and analyzed by flow cytometry. **(A)** Representative dot plot of thymocyte populations. **(B)** Representative bar graph of DN, DP, SP8 and SP4 percentages. **(C)** Ratios of CD4:CD8, DP:CD8 and DP:CD4. Figures are representative of 14 independent sets of E17.5 male littermates. Mean and standard deviation of each population are given. Bars represent mean ± standard deviations. **DN** (p= 0.6, n=14), **DP** (p= 0.6, n=14), **SP8** (p= 0.7, n=14), **SP4** (p= 0.9, n=14).

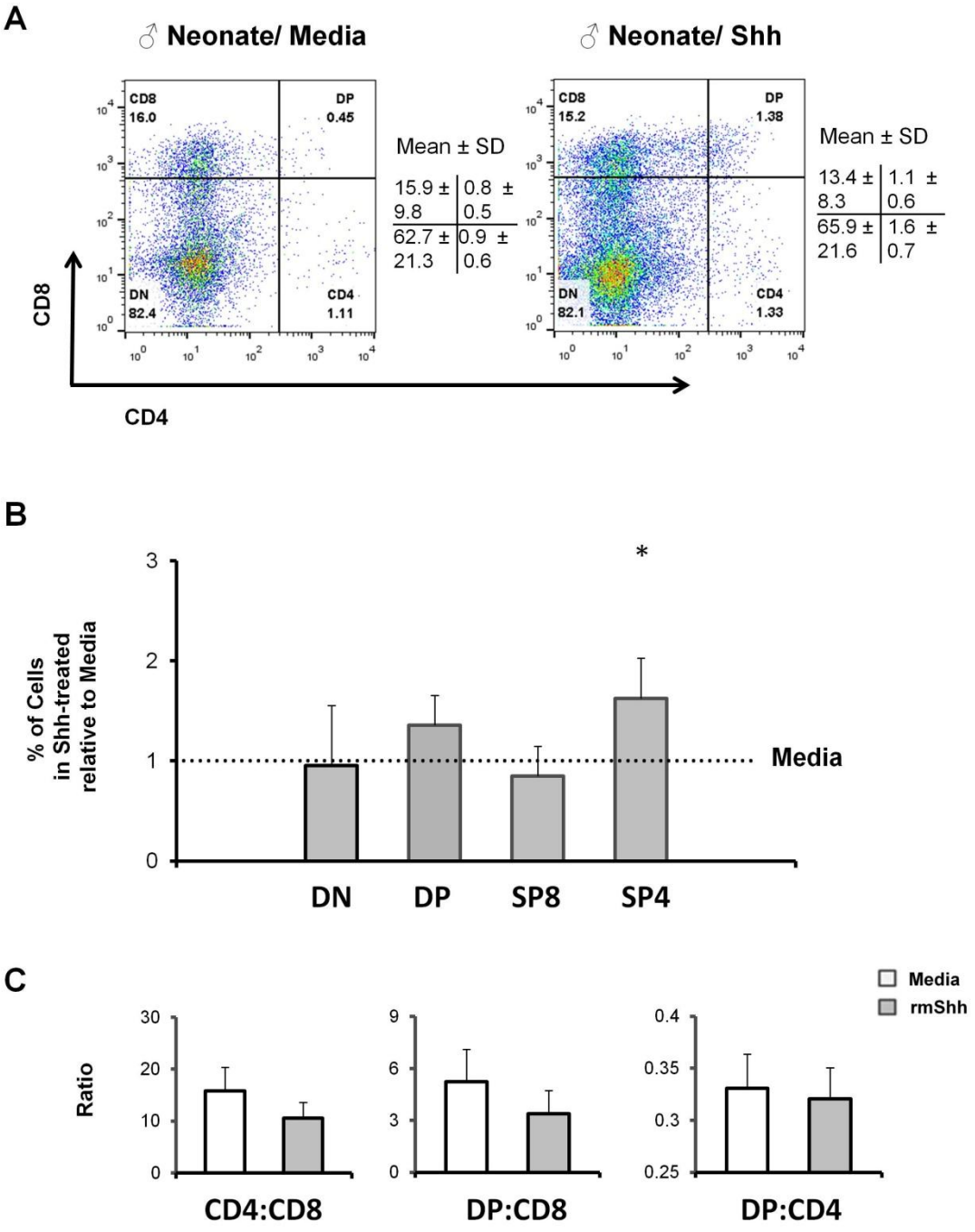

Figure 6.20

Influence of Shh on major neonatal thymocyte populations in male Marilyn-TCR transgenic mice. Thymic fragments were cultured with or without rmShh for 7-days. Cells were stained for anti-Vβ6, anti-CD8 and anti-CD4, and analyzed by flow cytometry. **(A)** Representative dot plot of thymocyte populations. **(B)** Representative bar graph of DN, DP, SP8 and SP4 percentages. **(C)** Ratios of CD4:CD8, DP:CD8 and DP:CD4. Figures are representative of 11 independent sets of 21-days old male littermates. Mean and standard deviation of each population are given. Bars represent mean ± standard deviations. **DN** (p= 0.6, n=11), **DP** (p= 0.1, n=11), **SP8** (p= 0.4, n=11), **SP4** (p= 0.03, n=11). *represents $p \leq 0.05$.

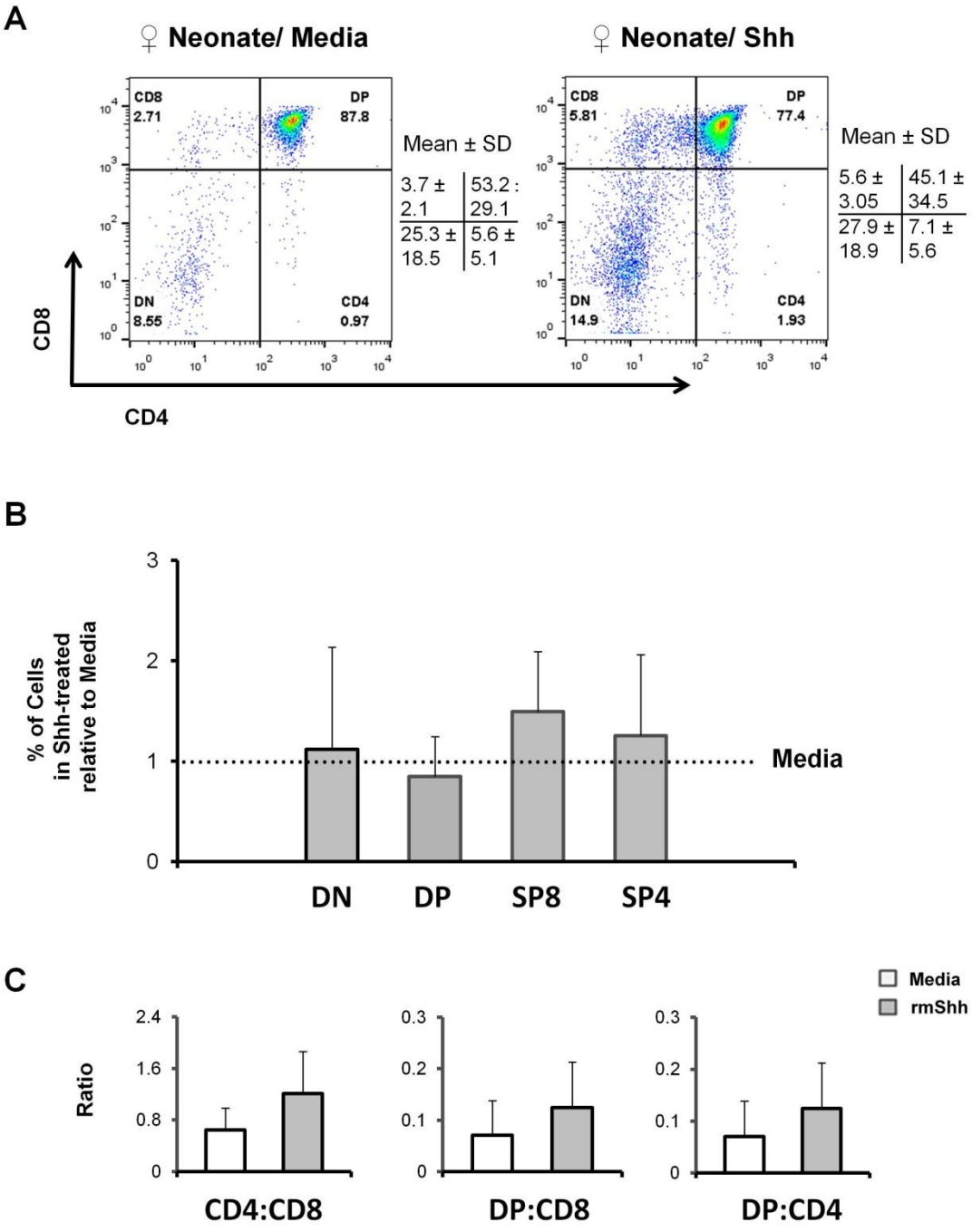

Figure 6.21

Influence of Shh on major neonatal thymocyte populations in female Marilyn-TCR transgenic mice. Thymic fragments were cultured with or without rmShh for 7-days. Cells were stained for anti-Vβ6, anti-CD8 and anti-CD4, and analyzed by flow cytometry. **(A)** Representative dot plot of thymocyte populations. **(B)** Representative bar graph of DN, DP, SP8 and SP4 percentages. **(C)** Ratios of CD4:CD8, DP:CD8 and DP:CD4. Figures are representative of 7 independent sets of 21-days old female littermates. Mean and standard deviation of each population are given. Bars represent mean ± standard deviations. **DN** (p= 0.7, n=7), **DP** (p= 0.6, n=7), **SP8** (p= 0.1, n=7), **SP4** (p= 0.6, n=7).

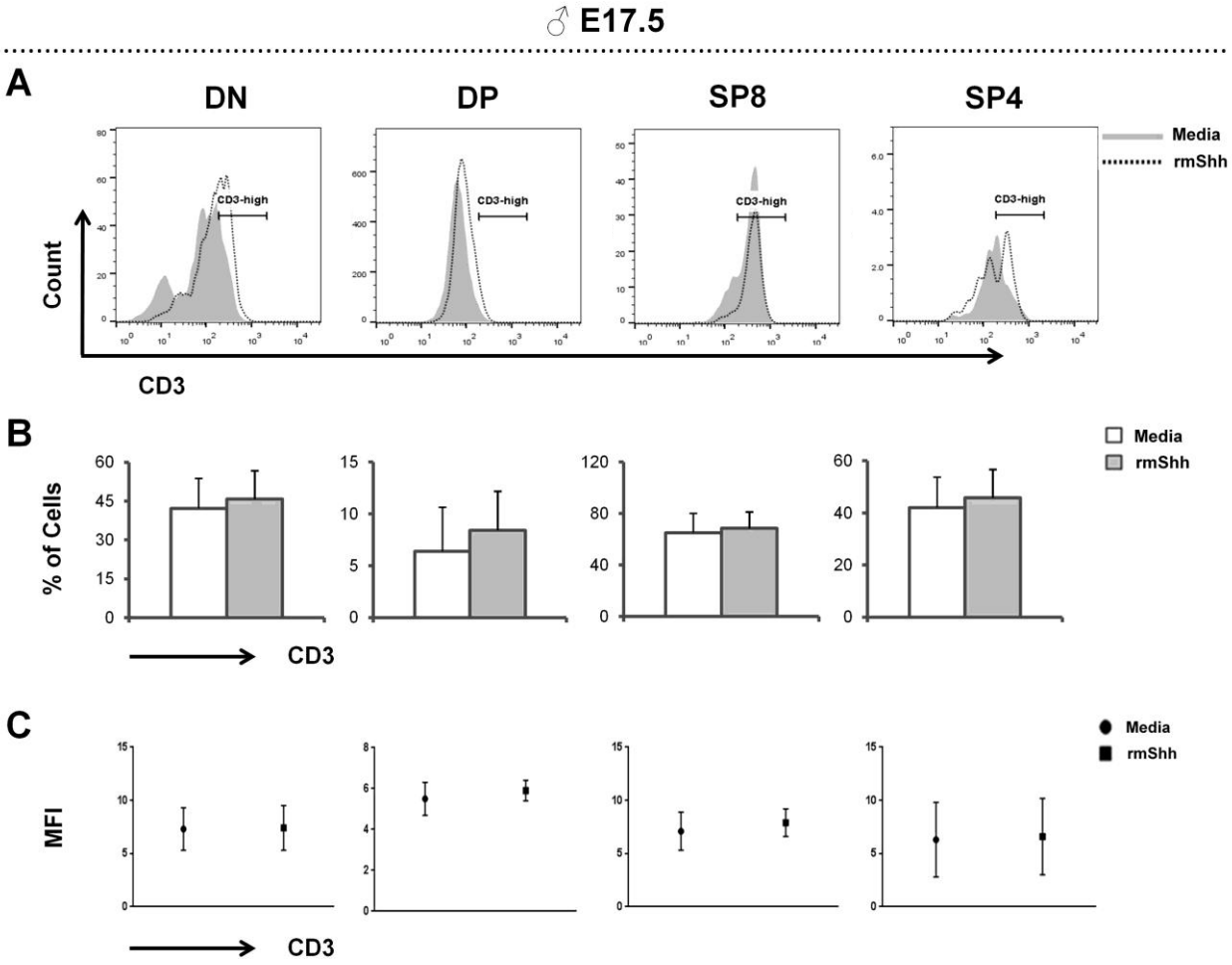

Figure 6.22

Expression of CD3 in embryonic thymocytes from male Marilyn-TCR transgenic mice. Foetal thymic organ cultures (FTOCs) were cultured with or without rmShh for 7-days. Cells were stained for anti-Vβ6, anti-CD3, anti-CD8 and anti-CD4, and analyzed by flow cytometry. **(A)** Representative histogram of CD3 expression in DN, DP, SP8 and SP4 cells. **(B)** Representative bar graph of CD3 percentages in DN, DP, SP8 and SP4 cells. **(C)** Representative scatter plot of CD3 MFI in DN, DP, SP8 and SP4 cells. Figures are representative 8 independent sets of male Marilyn-TCR transgenic littermates. Mean and standard deviation of each population are given. Bars represent mean ± standard deviations. **CD3 percentages; DN** (p= 0.8, n=8), **DP** (p= 0.3, n=8), **SP8** (p= 0.5, n=8), **SP4** (p= 0.6, n=8). **CD3 MFI; DN** (p= 0.7, n=8), **DP** (p= 0.4, n=8), **SP8** (p= 0.9, n=8), **SP4** (p= 0.5, n=8).

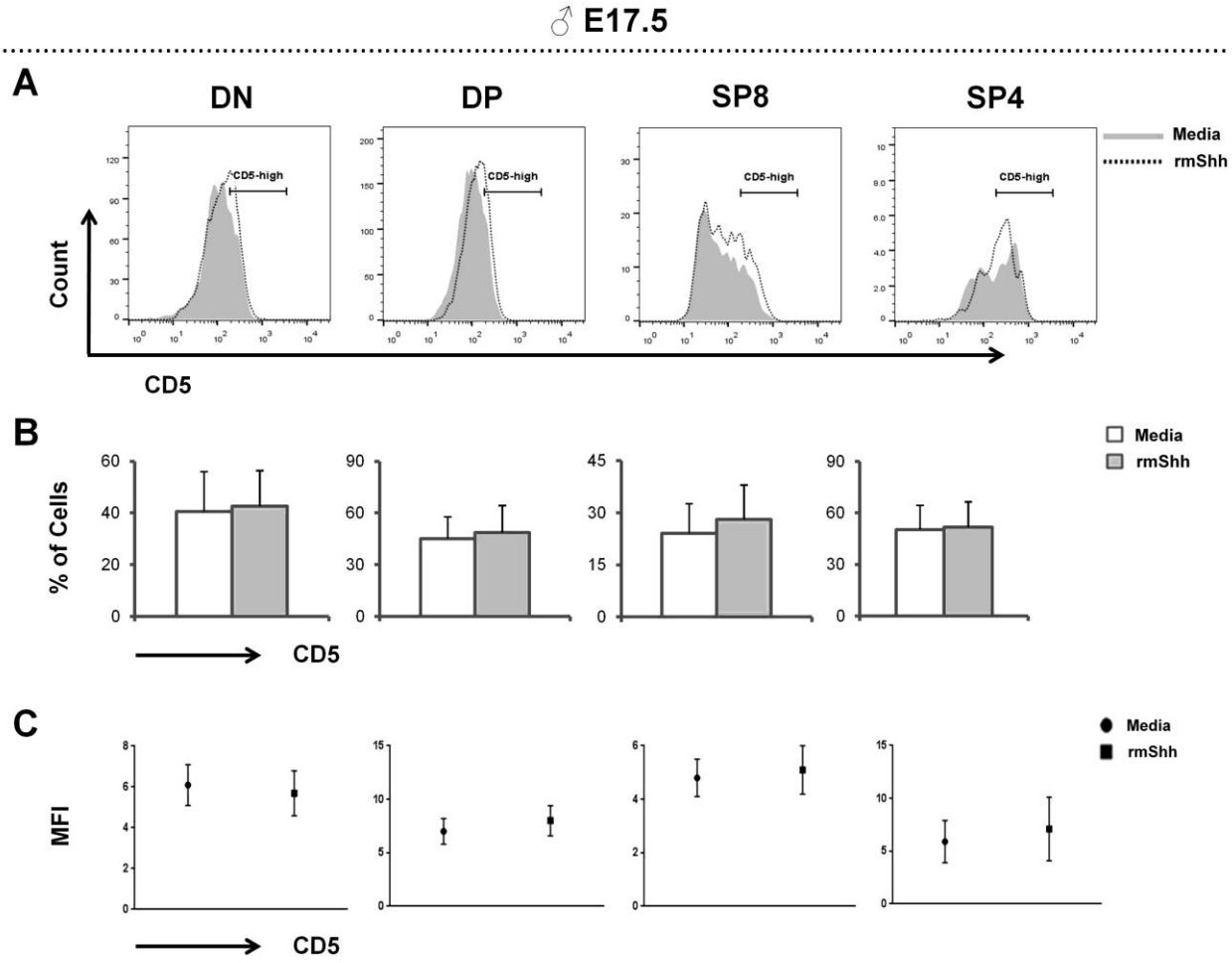

Figure 6.23

Expression of CD5 in embryonic thymocytes from male Marilyn-TCR transgenic mice. Foetal thymic organ cultures (FTOCs) were cultured with or without rmShh for 7-days. Cells were stained for anti-Vβ6, anti-CD5, anti-CD8 and anti-CD4, and analyzed by flow cytometry. **(A)** Representative histogram of CD5 expression in DN, DP, SP8 and SP4 cells. **(B)** Representative bar graph of CD5 percentages in DN, DP, SP8 and SP4 cells. **(C)** Representative scatter plot of CD5 MFI in DN, DP, SP8 and SP4 cells. Figures are representative 8 independent sets of male Marilyn-TCR transgenic littermates. Mean and standard deviation of each population are given. Bars represent mean ± standard deviations. **CD5 percentages; DN** (p= 0.7, n=8), DP (p= 0.5, n=8), **SP8** (p= 0.8, n=8), **SP4** (p= 0.5, n=8). **CD5 MFI; DN** (p= 0.3, n=8), **DP** (p= 0.7, n=8), **SP8** (p= 0.6, n=8), **SP4** (p= 0.4, n=8).

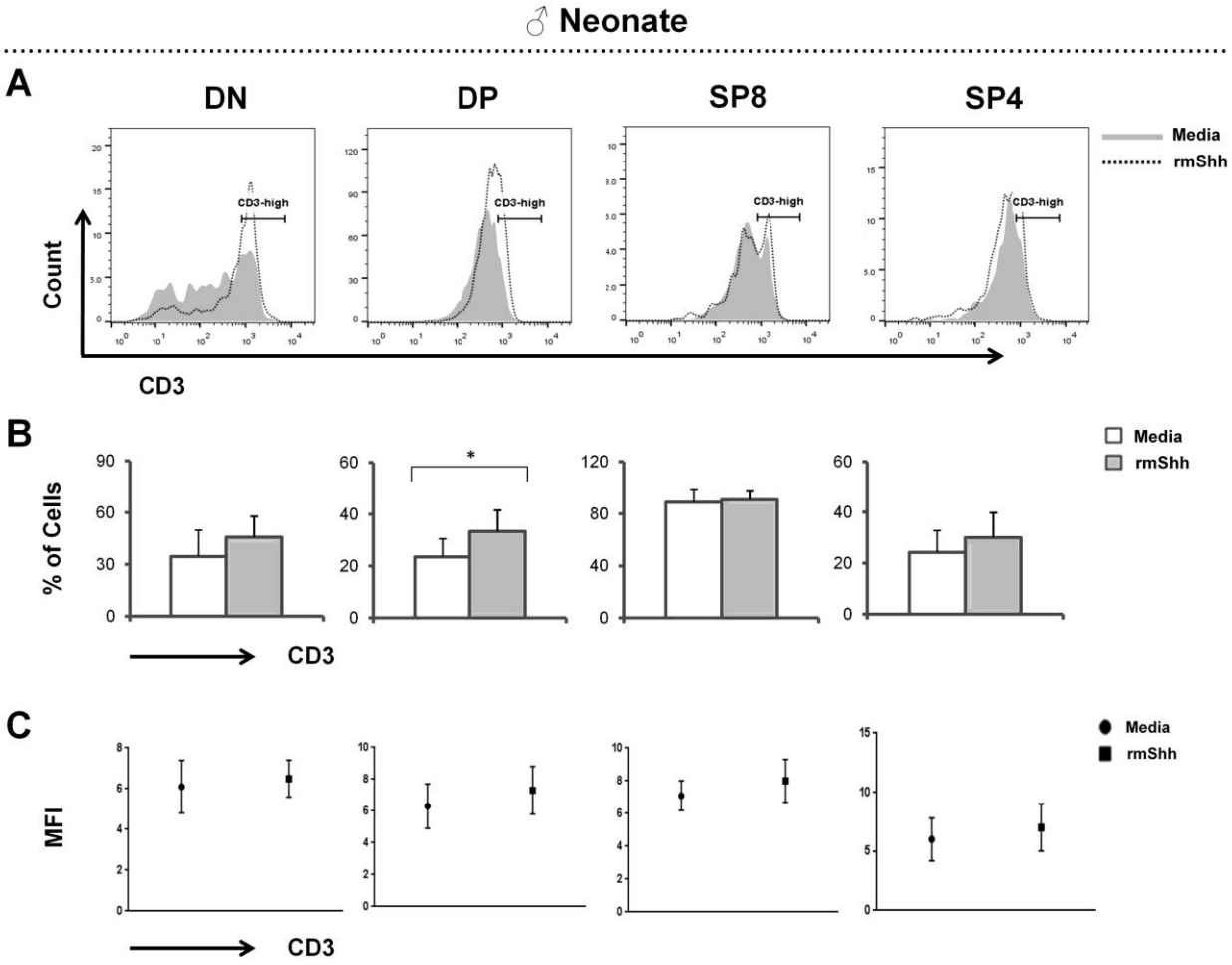

Figure 6.24

Expression of CD3 in neonatal thymocytes from male Marilyn-TCR transgenic mice. Thymic fragments were cultured with or without rmShh for 7-days. Cells were stained for anti-Vβ6, anti-CD3, anti-CD8 and anti-CD4, and analyzed by flow cytometry. **(A)** Representative histogram of CD3 expression in DN, DP, SP8 and SP4 cells. **(B)** Representative bar graph of CD3 percentages in DN, DP, SP8 and SP4 cells. **(C)** Representative scatter plot of CD3 MFI in DN, DP, SP8 and SP4 cells. Figures are representative 11 independent sets of male Marilyn-TCR transgenic littermates. Mean and standard deviation of each population are given. Bars represent mean ± standard deviations. **CD3 percentages; DN** (p= 0.08, n=11), **DP** (p= 0.01, n=11), **SP8** (p= 0.5, n=11), **SP4** (p= 0.1, n=11). **CD3 MFI; DN** (p= 0.6, n=11), **DP** (p= 0.4, n=11), **SP8** (p= 0.3, n=11), **SP4** (p= 0.9, n=11). *represents p≤0.05.

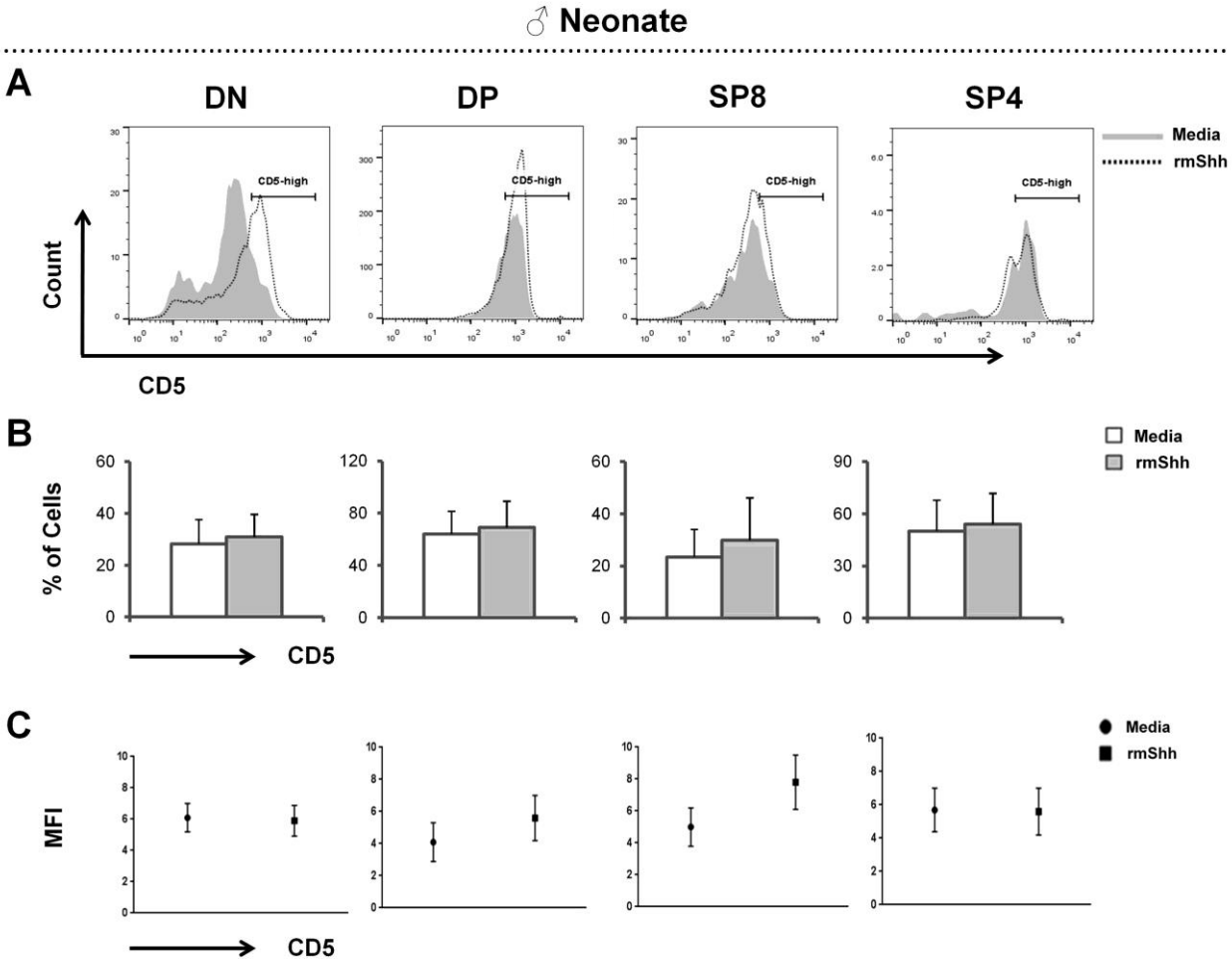

Figure 6.25

Expression of CD5 in neonatal thymocytes from male Marilyn-TCR transgenic mice. Thymic fragments were cultured with or without rmShh for 7-days. Cells were stained for anti-Vβ6, anti-CD5, anti-CD8 and anti-CD4, and analyzed by flow cytometry. **(A)** Representative histogram of CD5 expression in DN, DP, SP8 and SP4 cells. **(B)** Representative bar graph of CD5 percentages in DN, DP, SP8 and SP4 cells. **(C)** Representative scatter plot of CD5 MFI in DN, DP, SP8 and SP4 cells. Figures are representative 11 independent sets of male Marilyn-TCR transgenic littermates. Mean and standard deviation of each population are given. Bars represent mean ± standard deviations. **CD5 percentages; DN** (p= 0.5, n=11), **DP** (p= 0.5, n=11), **SP8** (p= 0.2, n=11), **SP4** (p= 0.6, n=11). **CD5 MFI; DN** (p= 0.3, n=11), **DP** (p= 0.7, n=11), **SP8** (p= 0.3, n=11), **SP4** (p= 0.8, n=11).

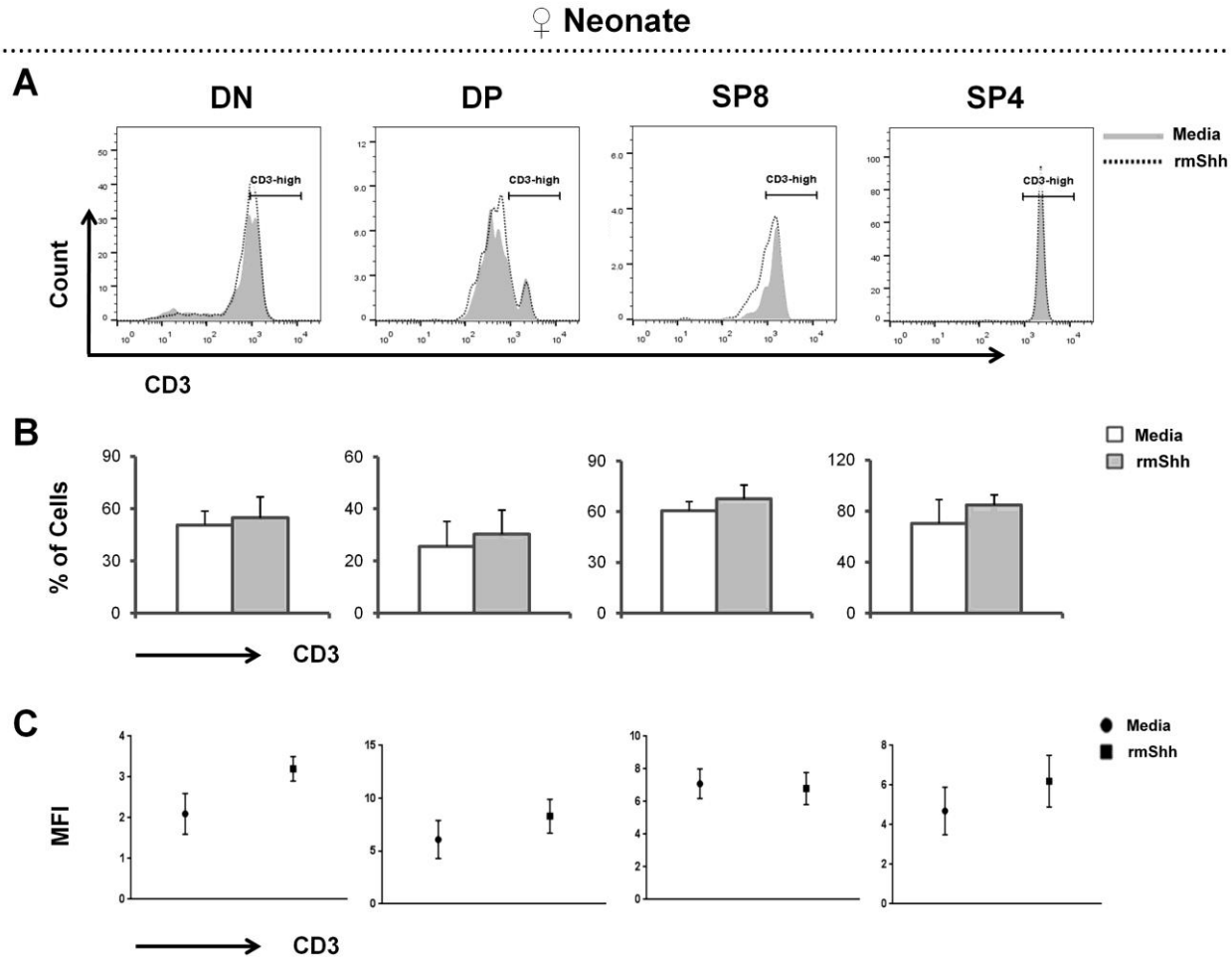

Figure 6.26

Expression of CD3 in neonatal thymocytes from female Marilyn-TCR transgenic mice. Thymic fragments were cultured with or without rmShh for 7-days. Cells were stained for anti-Vβ6, anti-CD3, anti-CD8 and anti-CD4, and analyzed by flow cytometry. **(A)** Representative histogram of CD3 expression in DN, DP, SP8 and SP4 cells. **(B)** Representative bar graph of CD3 percentages in DN, DP, SP8 and SP4 cells. **(C)** Representative scatter plot of CD3 MFI in DN, DP, SP8 and SP4 cells. Figures are representative 8 independent sets of female Marilyn-TCR transgenic littermates. Mean and standard deviation of each population are given. Bars represent mean ± standard deviations. **CD3 percentages; DN** (p= 0.5, n=7), **DP** (p= 0.5, n=7), **SP8** (p= 0.2, n=7), SP4 (p= 0.02, n=7). **CD3 MFI; DN** (p= 0.4, n=7), DP (p= 0.7, n=7), SP8 (p= 0.9, n=7), **SP4** (p= 0.6, n=7**).**

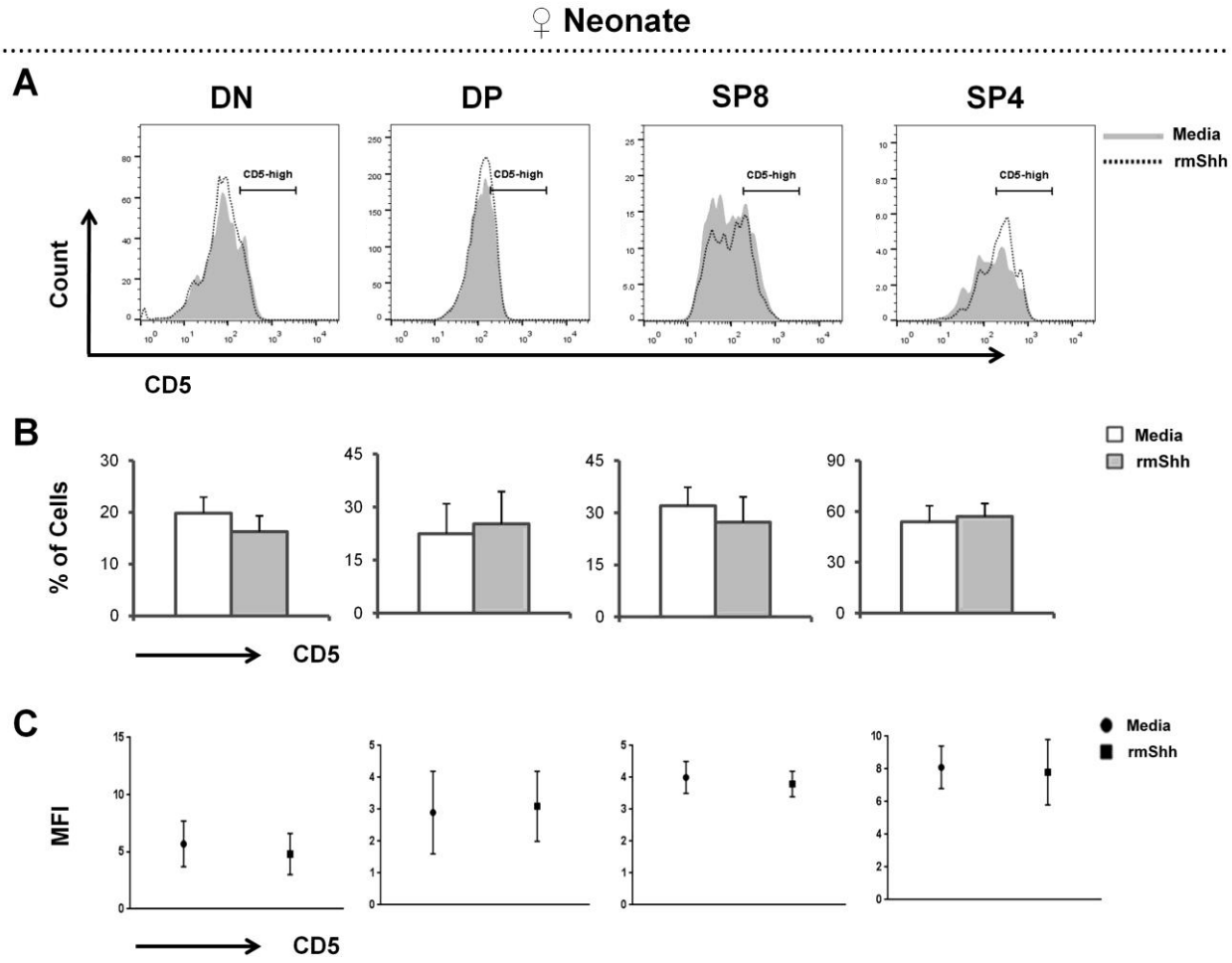

Figure 6.27

Expression of CD5 in neonatal thymocytes from female Marilyn-TCR transgenic mice. Thymic fragments were cultured with or without rmShh for 7-days. Cells were stained for anti-Vβ6, anti-CD5, anti-CD8 and anti-CD4, and analyzed by flow cytometry. **(A)** Representative histogram of CD5 expression in DN, DP, SP8 and SP4 cells. **(B)** Representative bar graph of CD5 percentages in DN, DP, SP8 and SP4 cells. **(C)** Representative scatter plot of CD5 MFI in DN, DP, SP8 and SP4 cells. Figures are representative 8 independent sets of female Marilyn-TCR transgenic littermates. Mean and standard deviation of each population are given. Bars represent mean ± standard deviations. **CD5 percentages; DN** (p= 0.1, n=7), DP (p= 0.6, n=7), **SP8** (p= 0.3, n=7), SP4 (p= 0.6, n=7). **CD5 MFI; DN** (p= 0.8, n=7), **DP** (p= 0.1, n=7), **SP8** (p= 0.3, n=7), **SP4** (p= 0.4, n=7).

6.3 Discussion

In this study we have shown that Shh is a regulator of the differentiation and selection of T cells during their development and maturation in the thymus. Our analysis of FTOCs from TCR-transgenic mice that express the male specific class-I restricted HY-TCR showed that Shh influence thymocyte development in their transition from DP to SP cell population, in both males and females.

In males, CD8SP and DP cells that express the transgenic TCR are negatively selected. We found that Shh treatment increased the proportions of HY-TCR^{+} CD8SP and DP cells indicating that Shh signalling inhibited negative selection of transgenic T cells. In female HY-TCR mice, positive selection of the transgenic TCR, in the absence of its clonal deletion, shows differentiation to the CD8 lineage. On Shh treatment, we found reduced proportions of CD8SP cells in both HY-TCR^{+} and HY-TCR^{-} thymocytes indicating decreased positive selection of these cells. This is consistent with previous reports that the CD4:CD8 ratio is increased in Shh$^{-/-}$ thymus and GliΔC2 transgenic thymus (Rowbotham, Hager-Theodorides, Cebecauer, et al. 2007; Furmanski et al. 2012). Interestingly, SP4 was also increased by Shh-treatment in both TCR^{-} and TCR^{+} thymocytes. The increase in the SP4 population might be the result of increased endogenous TCR rearrangement on Shh-treatment.

Our analysis of neonates thymic cultures from Marilyn-TCR transgenic mice model have also shown that Shh influences differentiation to SP cells in both males and females. The Marilyn-TCR recognizes a class-II restricted male antigen, and as these mice are on Rag2-deficient background, no rearrangement of endogenous TCR genes is possible, and only the Marilyn-TCR is expressed.

Therefore, in male mice there is extensive clonal deletion of DP and SP4 populations, whereas in female there is bias toward the SP4 lineage, and SP8 cells are reduced.

We carried out thymus organ culture using fragments of measured thymus. In male cultures, Shh-treatment increased SP4 cells suggesting that Shh-treatment had reduced clonal deletion. This is consistent with our finding in the male HY-TCR thymus, and shows that Shh can influence negative selection in both SP4 and SP8 lineages. In the female untreated organ cultures, treatment with Shh arrested differentiation at the fact that there was no influence of Shh-treatment on SP populations in female Marilyn mice which are also on Rag2-deficient background, supports the idea that the increase in SP4 in female HY-TCR mice was a result of increased endogenous rearrangement. Additionally, our data from Marilyn-TCR male mice have shown that Shh regulate the expression of TCR associated molecule, CD5, during thymocyte development in the DP stage.

These experiments are consistent with a previous study shown that DP thymocytes are Hh-responsive, and that thymocyte-interensic Shh signalling plays a role in modulating the production of SP4 and SP8. Whereas repression of physiological Shh signalling in thymocytes altered the proportions of DP and SP4 thymocytes (Crompton et al. 2007; Rowbotham, Hager-Theodorides, Cebecauer, et al. 2007; Furmanski et al. 2012).

6.4 Conclusion

In this chapter, we have utilized T cell receptor transgenic mice models (TCR-transgenics) to investigate the role of Shh in T cell development and repertoire selection. Our data from thymic organ cultures have shown that Shh influence T cell selection and maturation during the later stages of T cell development in their transiton from DP to SP cell population.

Chapter 7

Chapter Seven: Summary and future direction

7.1 Summary

The basis of immune tolerance and adaptive immunity is associated with the ability of the immune system to orchestrate a series of developmental steps that take the undifferentiated stem cells to finally become mature thymocytes. T cell development takes place within the unique micro-environment of the thymus. Through a complex well orchestrated network of signals within the thymus, developing thymocytes acquire all necessary cell surface ligands, cytokines and extra-cellular matrix components to develop and mature, producing a repertoire of diverse and functional non-self reactive T cells.

Development of T cells in the thymus requires the dynamic migration of developing thymocytes through the thymus. Thymus architectural stroma and travelling thymocytes have to communicate with each other both in close proximity and remotely. Such crosstalk signals come in the form of morphogens produced by thymic stromal cells and migrating thymocytes to accomplish maturation, proliferation and selection during their constant motion. The Hedgehog (Hh) family of secreted intracellular signalling molecules plays a major role in many patterning processes and organogenesis during embryonic development and are involved in the homeostasis and renewal of adult tissues.

In this thesis, our data revealed that both, intrinsic inhibition and activation of Hh signalling in thymocytes altered the proportions of SP4 cells that express GFP, suggesting a regulatory role of Gli in SP4 thymocytes. Hh signalling promotes

target gene transcription through the activation of glioblastoma-associated Gli family of transcription factors, Gli1, Gli2 and Gli3. Both Gli1 and Gli2 are transcription activators dependent on Hh signalling, however, Gli3 functions as a transcriptional regulator independent of Hh signalling (Wang et al. 2000; Pan et al. 2006; Bai et al. 2002). Gli3 has been previously shown to control thymocyte negative selection and TCR signal strength through Hh-dependent and independent mechanisms, moreover, it has been shown that defective Gli3 expression resulted in an inappropriate production of MHC class I-selected CD4 cells (Hager-Theodorides et al. 2009). This is consistent with our finding as the proportions of SP4 cells expressing GFP were increased in both Hh-suppressed and Hh-activated mouse models. Moreover, CD3 expression was reduced in SP cells when Hh-signalling was active and increased when Hh-signalling was inhibited, indicating a regulatory role of Hh in TCR signal transduction through the expression of CD3 molecule. Additionally, we have undertaken further characterization of SP4 cells through examining the expression of the master regulator of Treg lineage, Foxp3. Our data have shown that Hh-signalling influences the phenotype of SP4 cells in the thymus and spleen. In contrast, suppression of Hh-signalling in T cells reduced the expression of Foxp3 in SP4 cells suggesting a Hh-dependent regulatory role on these cells.

We investigated Hh-signalling and gene expressions by microarray analysis and our data have shown that Hh-signalling is attenuating gene transcription of various genes that may have a direct effect on T cell development and selection within the thymus. Several novel genes were found to be differentially expressed in DP thymocytes from mouse models where the physiological Hh-signalling is suppressed. Such a differential expression pattern of these genes in developing

thymocytes led us to ask if they play a role in T cell development and maturation within the thymus and the role of Hh signalling in their expression and regulation.

Our data suggested that the expression of Gli2 (glioma-asssociated oncogene-2), was upregulated when Hh-signalling was suppressed by at least 2-fold compared to WT. This increase was probably due to the very design of this mice model, where it expresses a truncated form of Gli2 which acts as a repressor of Hh-dependent transcription, so the microarray identified the transgenic transcript. The microarray data analysis also revealed that Gnb4 (Heterotrimeric guanine nucleotide binding protein β-4 subunit) was upregulated by 2.6 fold when Hh-signalling was suppressed compared to WT and its expression was validated using qRT-PCR. Gnb4 plays a key role in the signal transduction from membrane receptors to intracellular receptors. Activated G-protein coupled receptors result in the activation of many signal transduction cascades via the α-subunit and βγ-dimers. The effect of βγ-mediated signalling involves the regulation of cell growth and proliferation via Ras activation and it is now known that genetic variations in genes encoding G-protein subunit β4 are associated with cancer (Riemann et al. 2009; Schwindinger & Robishaw 2001). Furthermore, the microarray data also showed an increase in the expression of CCL19 (chemokine ligand-19) when Hh is suppressed by at least 2 fold compared to WT. CCL19 plays a role in lymphocyte recirculation and homing. It is involved in T cell trafficking in the thymus and migration to lymphoid organs. It is possible that Hh-signalling plays a role in regulating the expression of CCL19 in thymocytes during their development and selection as they constantly travel along the different compartments of the thymus.

Hh family member Dhh negatively regulates multiple stages of erythrocyte differentiation. Using Dhh-WT, Het and KO mice, we found Dhh also played a negative role in T cell production in the thymus and peripheral lymphoid organs and was critical in regulating negative and positive selection of self-reactive T cells in a dose dependent manner. In the absence of Dhh, the number of thymocytes and splenocytes increased, however, the phenotype of Dhh-Het was unusual in that, although thymocyte and splenocytes numbers increased in Dhh-KO, we observed a decrease in thymocyte numbers and yet, a greater number of splenocytes in Dhh-Het were observed, suggesting a differential role for Dhh in thymocyte and splenocyte homeostasis.

The influence of Dhh start early in the DN stages as a decrease in the DN1 and DN3 cells occurs, indicating a positive regulatory role of Dhh in thymocyte differentiation in the thymus, and during pre-TCR complex formation and β selection. Surprisingly, Dhh-Het shows an opposite effect to Dhh-KO, with an increase in the number of thymocytes during the DN1 and DN3 stages.

Dhh also influenced the later stages of thymocyte development, as the number of DP thymocytes decreased, whilst the number of SP8 thymocytes increased, suggesting that Dhh positively regulate thymocyte development during the formation of TCR complex, and negatively regulate positive selection of SP8 cells. Furthermore, Dhh influenced TCR associated CD3 molecule on SP8 cells, as partial expression of Dhh decreased the expression of CD3, whereas complete knockout showed a further decrease in CD3 expression. This finding explains the increase of SP8 thymocytes in Dhh-KO which maybe is a result of a weak TCR signal transduction defecting negative selection of SP8 thymocytes.

The expression of CD69 during thymocyte development was also examined, CD69 expression increased in both DN and SP4 cells, suggesting a negative role of Dhh on CD69 expression in the thymus. CD69 expression in immature thymocytes is believed to be associated with increased cell death on the contrary, CD69 expression in mature SP thymocytes correlated with positive selection. Our finding thus suggests that Dhh reduced positive selection of SP4 cells through attenuating the expression of CD69. The maturation marker CD62L was also been examined and we found Dhh to exert a dual function as it negatively regulated CD62L expression in DN thymocytes, and positively regulated the expression of CD62L in SP4 cells in a dose dependent manner. During the transition from DP to SP, thymocytes undergo maturation through a series of developmental stages before becoming functionally mature cells that exit the thymus. We analyzed the cell surface expression of HSA and Qa2 to measure the maturation status on DP and SP thymocytes, we found that Dhh partially arrested SP4 cell development.

Dhh also continues to regulate mature T cells in the spleen, as SP8 splenocytes were increased in Dhh-Het, suggesting a dual influence of Dhh as a negative regulator and positive regulator of mature SP8 cells. On the contrary in the lymph node, Dhh seemed to negatively regulate SP4 cells as SP4 cells were increased in Dhh-KO, suggesting a differential role of Dhh in the periphery between the spleen and lymph node. T cell characterization in the periphery has shown that Dhh positively regulated the expression of CD62L in SP8 and SP4 splenocytes. In regards to T cell activation, Dhh negatively regulated the activation of SP splenocytes. Interestingly, IL2 production in SP8 activated cells was increased in Dhh-Het.

A negative regulatory role for Dhh has been previously described (Lau et al. 2012). In this case, analysis of Dhh mutant mice showed that Dhh negatively regulates multiple stages of erythrocyte differentiation, indicating a negative role of Dhh, the study described here also suggests that Dhh is a negative regulator of T cell production. The unusual role of Hh proteins between the heterozygous and knockout has also been reported in Ihh (Outram et al. 2009). In this study, foetal $Ihh^{+/-}$ thymi had increased thymocyte numbers relative to WT, indicating that Ihh also negatively regulates thymocyte development, and our data have shown a similar finding with Dhh as a negative regulator of thymocytes and splenocytes during their development and in the periphery.

Analysis of TCR transgenic mice indicated that Dhh influences thymocyte selection as we observed increased escape of deletion of self-reactive T cells in the absence of Dhh in male HY-Dhh mice. Partial expression of Dhh reduced deletion of transgenic T cells, indicating a redundant role of Dhh in TCR repertoire selection. A similar escape of deletion has been also found in the male HY-TCR^{-} cells, where endogenous TCR genes rearrangement still exists. This finding is consistent with data that Dhh acts as a negative regulator of T cells during their development and differentiation in the thymus and lymphoid organs.

The female HY-TCR^{+} cells revealed a negative regulatory role of Dhh during thymocyte positive selection. The proportions of DP and SP8 cells were increased in Dhh-KO, indicating a negative role of Dhh during SP8 positive selection. Interestingly, SP8 in heterogeneous mice show greater selection of SP8 cells, suggesting a dose dependent regulatory function of Dhh during selection of SP8 cells. Additionally, thymocyte maturation has been examined through measuring the expression of Qa2 and HSA, and our data indicated that Dhh reduce

maturation of SP8 cells in male and female HY-TCR$^+$ cells. In the spleen, we observed no influence on mature HY-TCR$^+$ cells, however, Dhh reduced the proportions of SP4 cells expressing CD3, indicating its role in influencing splenocytes in the periphery.

Furthermore, analysis of Marilyn-TCR$^+$ male mice showed a negative regulatory role of Hh signalling during thymocyte development and maturation in the thymus. These data indicate that inhibition of Hh-dependent transcription increased positive selection of the transgenic TCR, and differentiation from DP to SP cells. Our analysis showed that the proportions of Marilyn-TCR$^+$ SP4 cells has been found to be increased in the absence of Hh signalling, suggesting a negative regulatory role of Hh during negative selection of SP4 cells. In Marilyn-TCR$^+$ female mice, the proportions of DP cells were decreased, possibly as cells undergo further development. Examining the maturation marker Qa2 and HSA in DP and SP cells revealed that Hh signalling reduced thymocyte maturation in the DP and SP stage in male mice, and in DP and SP cells in female mice. These findings are consistent with previous data which indicated that inhibition of Hh-dependent transcription increased positive and negative selection in the thymus and TCR activation of peripheral T cells (Furmanski et al. 2012; Rowbotham et al. 2008; Furmanski et al. 2015).

In the spleen, we observed a reduction in the proportions of SP4 in male mice, and SP8 and SP4 cells in female mice. This observation confirmed our finding in the thymus, in that the thymus allowed the escape of transgenic T cells reaching the spleen. However, the spleen size was reduced, as well as their total live cell counts. This could be due to the increase in Foxp3$^+$ cells. In the female spleen, in

the absence of intrinsic Hh signalling, the proportions of SP8 and SP4 cells are increased as a result of increased positive selection.

The expression of TCR associated molecules CD3 and CD5 in SP cells increased during thymocyte development in the thymus, and CD5 MFI also increased in the absence of Hh signalling indicating a possible role of these molecules during selection of transgenic T cells. A similar phenotype have been also shown in the spleen and lymph node of Marilyn-TCR^{+} mice, suggesting that Hh signalling also regulate TCR signal transduction in mature T cells in the periphery.

Our data suggested that Shh regulates the differentiation and selection of T cells during their development and maturation in the thymus. Our analysis of FTOCs from TCR-transgenic mice which express the male specific class-I restricted HY-TCR showed that Shh influences thymocyte development in their transition from DP to SP cell population. In male mice, we found that Shh treatment increased the proportions of HY-TCR^{+} CD8SP and DP cells, indicating that Shh signalling inhibited negative selection of transgenic T cells. In female mice, Shh treatment reduced the proportions of CD8SP in both HY-TCR^{+} and HY-TCR^{-} thymocytes indicating decreased positive selection of these cells. Interestingly, SP4 was also increased by Shh-treatment in both TCR^{+} and TCR^{-} thymocytes. The increase in the SP4 population might be the result of increased endogenous TCR rearrangement on Shh-treatment. Furthermore, our analysis of neonate thymic cultures from TCR-transgenic mice which express the male specific class-II restricted Marilyn-TCR also showed that Shh influences differentiation to SP cells. In male cultures, Shh-treatment increased SP4 cells suggesting that Shh reduced clonal deletion. This is consistent with our findings in the male HY-TCR thymus, that Shh can influence negative selection in both SP4 and SP8 lineages.

In female cultures, treatment with Shh arrested differentiation as there was no influence of Shh-treatment on SP populations. This observation supports the idea that the increase in SP4 in female HY-TCR mice was a result of increased endogenous rearrangement, as TCR rearrangement still exist in HY-TCR mouse model as they are not on Rag-deficient background, unlike Marilyn-TCR mouse model where TCR rearrangement still exist as these mice are on Rag2-deficient background. Additionally, our data from Marilyn-TCR male mice showed that Shh regulate the expression of CD5 during thymocyte development in the DP stage.

Lastly, our data provided both, negative and positive regulatory functions of Hh-signalling during T cell development and selection in the thymus as well as during T cell maturation and activation in the periphery. Immature T cells must undergo several developmental steps to become functionally mature T cells, and it is evident from our findings that Hh-signalling varies during these stages. A possible explanation might be that Hh signalling provides both a positive and a negative regulatory signal in order to maintain homeostatic control of developing thymocytes and T cells in the periphery. The three Hh proteins are highly conserved in vertebrates and act in the same tissues with overlapping or redundant functions (Kumar et al. 1996). Although Hh overlapping functions have not been well studied, studies on T cell development have shown that the three Hh proteins may have overlapping activities and differential functions in order to regulate T cell differentiation and homeostasis (Crompton et al. 2007; Outram et al. 2009).

7.2 Future directions

In this thesis we show for the first time the role of Dhh as a negative regulator of T cells development and maturation, and it will be of interest to further investigate the role of Dhh on the proliferation of activated T cells using the same mouse models for comparison. Furthermore, using HY-TCR or Marilyn-TCR with Hh-active or Hh-suppressed models to investigate T cells which escaped deletion through activation experiments will further characterize the nature of these autoreactive cells.

We have confirmed the role of Shh and Dhh in regulating negative a positive selection in thymocytes, however, investigating the role of Ihh in T cell repertoire selection through utilizing Ihh-TCR-transgenic mice models will provide a better understanding of the regulatory mechanism of Hh proteins and their influence during co-expression or separately.

Several novel genes have been found to be expressed differentially in Hh-supressed mouse model compared to WT, and it will be of interest to further investigate the role they play in T cell development and maturation. Using silencing RNA (siRNA) and retroviral vector techniques in HY-TCR transgenic model to investigate the impact of Hh-signalling on thymocyte repertoire selection in conjunction with the expression of CCL19 and the downstream signalling regulation of Gnb4 expression will provide more understanding of their role in T cell development and maturation.

Investigating the impact of Hh-signalling on T cells in disease will shed the light on the mechanism and role of Hh proteins during T cell development and maturation as well as their activation in the periphery. Using a mouse model

infected with a pathogen, such as Herpes simplex virus, Mycobacterium tuberculosis, or Listeria monocytogenes, will test the functions of Hh-signalling on T cells under stress. Similarly, investigating Hh-signalling components in autoimmune diseases (AIDs) as well as T cell activation and cytokine production, will provide more understanding of the aetiology behind these diseases.

Finally, it is critical in any research project conducted to validate findings using alternative methods and laboratory techniques. This is essential in providing a solid conclusion especially when the experiment yields few numbers of cells. In this thesis we have come across such difficulty in (Chapter 3), as the number of cells which expressed Gli-GFP^{+} were low in GBS-GFP/Gli2ΔN2, GBS-GFP/Gli2ΔC2 and GBS-GFP/WT. This observation makes it critical to use alternative methods to complement and verify our data, such as qPCR or immunohistochemistry (IHC). Confirming our observations by alternative methodologies will allow us to further investigate the consequence and effect of our findings. Taken together, this thesis has revealed novel aspects of Hh-signalling involved in the regulation of T cell development and function, and has provided a useful roadmap to further explore T cell biology.

References

Abele, R. & Tampé, R., 2004. The ABCs of immunology: structure and function of TAP, the transporter associated with antigen processing. *Physiology (Bethesda, Md.)*, 19, pp.216–224.

Adolfsson, J. et al., 2005. Identification of Flt3+ lympho-myeloid stem cells lacking erythro-megakaryocytic potential: A revised road map for adult blood lineage commitment. *Cell*, 121, pp.295–306.

Afkarian, M. et al., 2002. T-bet is a STAT1-induced regulator of IL-12R expression in naïve CD4+ T cells. *Nature Immunology*, 3, pp.549–557.

Agarwala, S., Sanders, T.A. & Ragsdale, C.W., 2001. Sonic hedgehog control of size and shape in midbrain pattern formation. *Science (New York, N.Y.)*, 291, pp.2147–2150.

Alcedo, J. et al., 1996. The Drosophila smoothened gene encodes a seven-pass membrane protein, a putative receptor for the hedgehog signal. *Cell*, 86, pp.221–232.

Aliahmad, P. et al., 2004. TOX provides a link between calcineurin activation and CD8 lineage commitment. *The Journal of Experimental Medicine*, 199, pp.1089–1099.

Aliahmad, P. & Kaye, J., 2008. Development of all CD4 T lineages requires nuclear factor TOX. *The Journal of Experimental Medicine*, 205, pp.245–256.

Allen, B.L. et al., 2011. Overlapping roles and collective requirement for the coreceptors GAS1, CDO, and BOC in SHH pathway function. *Developmental Cell*, 20, pp.775–787.

Allende, M.L. et al., 2004. Expression of the Sphingosine 1-Phosphate Receptor, S1P1, on T-cells Controls Thymic Emigration. *Journal of Biological Chemistry*, 279, pp.15396–15401.

Allman, D. et al., 2003. Thymopoiesis independent of common lymphoid progenitors. *Nature Immunology*, 4, pp.168–174.

El Andaloussi, A. et al., 2006. Hedgehog signaling controls thymocyte progenitor homeostasis and differentiation in the thymus. *Nature Immunology*, 7, pp.418–426.

Anderson, M.S. et al., 2002. Projection of an immunological self shadow within the thymus by the aire protein. *Science (New York, N.Y.)*, 298, pp.1395–1401.

Ara, T. et al., 2003. A role of CXC chemokine ligand 12/stromal cell-derived factor-1/pre-B cell growth stimulating factor and its receptor CXCR4 in fetal and adult T cell development in vivo. *Journal of Immunology (Baltimore, Md. : 1950)*, 170, pp.4649–4655.

Artavanis-Tsakonas, S., 1999. Notch Signaling: Cell Fate Control and Signal Integration in Development. *Science*, 284, pp.770–776.

Aza-Blanc, P. et al., 2000. Expression of the vertebrate Gli proteins in Drosophila reveals a distribution of activator and repressor activities. *Development (Cambridge, England)*, 127, pp.4293–4301.

Azuma, M. et al., 1993. B70 antigen is a second ligand for CTLA-4 and CD28. *Nature*, 366, pp.76–79.

Bai, C.B. et al., 2002. Gli2, but not Gli1, is required for initial Shh signaling and ectopic activation of the Shh pathway. *Development (Cambridge, England)*, 129(20), pp.4753–4761.

Bai, C.B. & Joyner, A.L., 2001. Gli1 can rescue the in vivo function of Gli2. *Development (Cambridge, England)*, 128, pp.5161–5172.

Bajestan, S.N. et al., 2006. Desert hedgehog-patched 2 expression in peripheral nerves during Wallerian degeneration and regeneration. *Journal of Neurobiology*, 66, pp.243–255.

Balaskas, N. et al., 2012. Gene regulatory logic for reading the sonic hedgehog signaling gradient in the vertebrate neural tube. *Cell*, 148(1-2), pp.273–284.

Barsoum, I.B. et al., 2009. Activation of the Hedgehog pathway in the mouse fetal ovary leads to ectopic appearance of fetal Leydig cells and female pseudohermaphroditism. *Developmental Biology*, 329(1), pp.96–103.

Basch, R.S. & Kadish, J.L., 1977. Hematopoietic thymocyte precursors: II. Properties of the precursors. *The Journal of Experimental Medicine*, 145, pp.405–419.

Bashir, S. et al., 2014. Role of hedgehog protein family members in autistic children. *Neurology, Psychiatry and Brain Research*, 20(3), pp.63–67.

Bassing, C.H., Swat, W. & Alt, F.W., 2002. The mechanism and regulation of chromosomal V(D)J recombination. *Cell*, 109.

Beachy, P.A. et al., 2010. Interactions between Hedgehog proteins and their binding partners come into view. *Genes and Development*, 24, pp.2001–2012.

Bell, J.J. & Bhandoola, A., 2008. The earliest thymic progenitors for T cells possess myeloid lineage potential. *Nature*, 452, pp.764–767.

Bensinger, S.J. et al., 2001. Major histocompatibility complex class II-positive cortical epithelium mediates the selection of CD4(+)25(+) immunoregulatory T cells. *The Journal of Experimental Medicine*, 194, pp.427–438.

Benz, C. et al., 2008. The stream of precursors that colonizes the thymus proceeds selectively through the early T lineage precursor stage of T cell development. *The Journal of Experimental Medicine*, 205, pp.1187–1199.

Benz, C., Heinzel, K. & Bleul, C.C., 2004. Homing of immature thymocytes to the subcapsular microenvironment within the thymus is not an absolute requirement for T cell development. *European Journal of Immunology*, 34, pp.3652–3663.

Berg, L.J. et al., 1989. Antigen/MHC-specific T cells are preferentially exported from the thymus in the presence of their MHC ligand. *Cell*, 58, pp.1035–1046.

Berman, D.M. et al., 2003. Widespread requirement for Hedgehog ligand stimulation in growth of digestive tract tumours. *Nature*, 425, pp.846–851.

Bhandoola, A. et al., 2007. Commitment and Developmental Potential of Extrathymic and Intrathymic T Cell Precursors: Plenty to Choose from. *Immunity*, 26, pp.678–689.

Bhanot, P. et al., 1996. A new member of the frizzled family from Drosophila functions as a Wingless receptor. *Nature*, 382, pp.225–230.

Bhardwaj, G. et al., 2001. Sonic hedgehog induces the proliferation of primitive human hematopoietic cells via BMP regulation. *Nature Immunology*, 2, pp.172–180.

Bigelow, R.L.H. et al., 2004. Transcriptional Regulation of bcl-2 Mediated by the Sonic Hedgehog Signaling Pathway through gli-1. *Journal of Biological Chemistry*, 279, pp.1197–1205.

Bitgood, M.J. & McMahon, A.P., 1995. Hedgehog and Bmp genes are coexpressed at many diverse sites of cell-cell interaction in the mouse embryo. *Developmental Biology*, 172, pp.126–138.

Bitgood, M.J., Shen, L. & McMahon, A.P., 1996. Sertoli cell signaling by Desert hedgehog regulates the male germline. *Current Biology : CB*, 6, pp.298–304.

Bleul, C.C. & Boehm, T., 2000. Chemokines define distinct microenvironments in the developing thymus. *European Journal of Immunology*, 30, pp.3371–3379.

Von Boehmer, H., 2005. Unique features of the pre-T-cell receptor alpha-chain: not just a surrogate. *Nature reviews. Immunology*, 5, pp.571–577.

Boehmer, V. & Fehling, H.J., 1997. Structure and function of the pre-T cell receptor. *Annual Review of Immunology*, 15, pp.433–452.

Boussiotis, V.A. et al., 1993. B7 but not intercellular adhesion molecule-1 costimulation prevents the induction of human alloantigen-specific tolerance. *The Journal of Experimental Medicine*, 178, pp.1753–1763.

Boyd, R.L. et al., 1993. Inside the thymus The thvmic microenvironment. *Immunology Today*, 14, pp.445–59.

Van den Brink, G.R., 2007. Hedgehog signaling in development and homeostasis of the gastrointestinal tract. *Physiological Reviews*, 87, pp.1343–1375.

Brooks, A.R. et al., 1996. Functional analysis of the human cyclin D2 and cyclin D3 promoters. *Journal of Biological Chemistry*, 271, pp.9090–9099.

Broussard, C. et al., 2006. Altered Development of CD8+ T Cell Lineages in Mice Deficient for the Tec Kinases Itk and Rlk. *Immunity*, 25, pp.93–104.

Brugnera, E. et al., 2000. Coreceptor Reversal in the Thymus. *Immunity*, 13, pp.59–71.

De Bruijn, M.F. et al., 2000. Definitive hematopoietic stem cells first develop within the major arterial regions of the mouse embryo. *The EMBO Journal*, 19, pp.2465–2474.

Burtrum, D.B. et al., 1996. TCR gene recombination and alpha beta-gamma delta lineage divergence: productive TCR-beta rearrangement is neither exclusive nor preclusive of gamma delta cell development. *Journal of Immunology (Baltimore, Md. : 1950)*, 157, pp.4293–4296.

Callahan, C.A. et al., 2004. MIM/BEG4, a Sonic hedgehog-responsive gene that potentiates Gli-dependent transcription. *Genes and Development*, 18, pp.2724–2729.

Canto, P. et al., 2004. Mutations in the Desert hedgehog (DHH) gene in patients with 46,XY complete pure gonadal dysgenesis. *Journal of Clinical Endocrinology and Metabolism*, 89, pp.4480–4483.

Capone, M., Hockett, R.D. & Zlotnik, A., 1998. Kinetics of T cell receptor beta, gamma, and delta rearrangements during adult thymic development: T cell receptor rearrangements are present in CD44(+)CD25(+) Pro-T thymocytes. *Proceedings of the National Academy of Sciences of the United States of America*, 95, pp.12522–12527.

Carpenter, A.C. & Bosselut, R., 2010. Decision checkpoints in the thymus. *Nature Immunology*, 11, pp.666–673.

Carstea, E.D. et al., 1997. Niemann-Pick C1 disease gene: homology to mediators of cholesterol homeostasis. *Science (New York, N.Y.)*, 277, pp.228–231.

Chaffin, K.E. & Perlmutter, R.M., 1991. A pertussis toxin-sensitive process controls thymocyte emigration. *European Journal of Immunology*, 21, pp.2565–2573.

Chan, S.H. et al., 1993. Another view of the selective model of thymocyte selection. *Cell*, 73, pp.225–236.

Chang, D.T. et al., 1994. Products, genetic linkage and limb patterning activity of a murine hedgehog gene. *Development (Cambridge, England)*, 120, pp.3339–3353.

Chen, C.-C. et al., 2005. Identification of mast cell progenitors in adult mice. *Proceedings of the National Academy of Sciences of the United States of America*, 102, pp.11408–11413.

Chen, L. & Flies, D.B., 2013. Molecular mechanisms of T cell co-stimulation and co-inhibition. *Nature reviews. Immunology*, 13, pp.227–42.

Cheshier, S.H. et al., 1999. In vivo proliferation and cell cycle kinetics of long-term self-renewing hematopoietic stem cells. *Proc Natl Acad Sci U S A*, 96, pp.3120–3125.

Chi, S. et al., 2006. Activation of the hedgehog pathway in a subset of lung cancers. *Cancer Letters*, 244, pp.53–60.

Chiang, C. et al., 1996. Cyclopia and defective axial patterning in mice lacking Sonic hedgehog gene function. *Nature*, 383, pp.407–413.

Christensen, J.L. & Weissman, I.L., 2001. Flk-2 is a marker in hematopoietic stem cell differentiation: a simple method to isolate long-term stem cells. *Proceedings of the National Academy of Sciences of the United States of America*, 98, pp.14541–14546.

Chuang, P.T., Kawcak, T.N. & McMahon, A.P., 2003. Feedback control of mammalian Hedgehog signaling by the Hedgehog-binding protein, Hip1, modulates Fgf signaling during branching morphogenesis of the lung. *Genes and Development*, 17, pp.342–347.

Ciau-Uitz, A. et al., 2014. Developmental hematopoiesis: Ontogeny, genetic programming and conservation. *Experimental Hematology*, 42, pp.669–683.

Ciau-Uitz, A., Walmsley, M. & Patient, R., 2000. Distinct origins of adult and embryonic blood in Xenopus. *Cell*, 102, pp.787–796.

Clements, W.K. & Traver, D., 2013. Signalling pathways that control vertebrate haematopoietic stem cell specification. *Nature Reviews. Immunology*, 13, pp.336–48.

Colnot, C. et al., 2005. Indian hedgehog synchronizes skeletal angiogenesis and perichondrial maturation with cartilage development. *Development (Cambridge, England)*, 132, pp.1057–1067.

Concordet, J.P. et al., 1996. Spatial regulation of a zebrafish patched homologue reflects the roles of sonic hedgehog and protein kinase A in neural tube and somite patterning. *Development (Cambridge, England)*, 122, pp.2835–2846.

Cordier, A.C. & Haumont, S.M., 1980. Development of thymus, parathyroids, and ultimobranchial bodies in NMRI and nude mice. *The American Journal of Anatomy*, 157(3), pp.227–263.

Costa, G., Kouskoff, V. & Lacaud, G., 2012. Origin of blood cells and HSC production in the embryo. *Trends in Immunology*, 33, pp.215–223.

Crompton, T., Gilmour, K.C. & Owen, M.J., 1996. The map kinase pathway controls differentiation from double-negative to double-positive thymocyte. *Cell*, 86, pp.243–251.

Crompton, T., Outram, S. V & Hager-Theodorides, A.L., 2007. Sonic hedgehog signalling in T-cell development and activation. *Nature Reviews. Immunology*, 7, pp.726–735.

Currie, P.D. & Ingham, P.W., 1996. Induction of a specific muscle cell type by a hedgehog-like protein in zebrafish. *Nature*, 382, pp.452–455.

Dahmane, N. et al., 1997. Activation of the transcription factor Gli1 and the Sonic hedgehog signalling pathway in skin tumours. *Nature*, 389, pp.876–881.

Dale, J.K. et al., 1997. Cooperation of BMP7 and SHH in the induction of forebrain ventral midline cells by prechordal mesoderm. *Cell*, 90, pp.257–269.

Davis, C.B. et al., 1993. Evidence for a stochastic mechanism in the differentiation of mature subsets of T lymphocytes. *Cell*, 73, pp.237–247.

Denef, N. et al., 2000. Hedgehog induces opposite changes in turnover and subcellular localization of patched and smoothened. *Cell*, 102, pp.521–531.

Dessaud, E. et al., 2010. Dynamic assignment and maintenance of positional identity in the ventral neural tube by the morphogen sonic hedgehog. *PLoS Biology*, 8.

Dessaud, E. et al., 2007. Interpretation of the sonic hedgehog morphogen gradient by a temporal adaptation mechanism. *Nature*, 450, pp.717–720.

Doherty, P.C. & Zinkernagel, R.M., 1975. H-2 compatibility is required for T-cell-mediated lysis of target cells infected with lymphocytic choriomeningitis virus. *The Journal of Experimental Medicine*, 141, pp.502–507.

Le Douarin, N.M. & Jotereau, F. V, 1975. Tracing of cells of the avian thymus through embryonic life in interspecific chimeras. *The Journal of Experimental Medicine*, 142, pp.17–40.

Doulatov, S. et al., 2012. Hematopoiesis: A human perspective. *Cell Stem Cell*, 10, pp.120–136.

Drakopoulou, E. et al., 2010. Non-redundant role for the transcription factor Gli1 at multiple stages of thymocyte development. *Cell Cycle*, 9(20), pp.4144–4152.

Dudley, E.C. et al., 1995. Alpha beta and gamma delta T cells can share a late common precursor. *Current Biology : CB*, 5, pp.659–669.

Duman-Scheel, M. et al., 2002. Hedgehog regulates cell growth and proliferation by inducing Cyclin D and Cyclin E. *Nature*, 417, pp.299–304.

Dyer, M.A. et al., 2001. Indian hedgehog activates hematopoiesis and vasculogenesis and can respecify prospective neurectodermal cell fate in the mouse embryo. *Development (Cambridge, England)*, 128, pp.1717–1730.

Echelard, Y. et al., 1993. Sonic hedgehog, a member of a family of putative signaling molecules, is implicated in the regulation of CNS polarity. *Cell*, 75, pp.1417–1430.

Egerton, M., Scollay, R. & Shortman, K., 1990. Kinetics of mature T-cell development in the thymus. *Proceedings of the National Academy of Sciences of the United States of America*, 87, pp.2579–2582.

Ekker, S.C. et al., 1995. Patterning activities of vertebrate hedgehog proteins in the developing eye and brain. *Current Biology : CB*, 5, pp.944–955.

Ericson, J. et al., 1997. Pax6 controls progenitor cell identity and neuronal fate in response to graded Shh signaling. *Cell*, 90, pp.169–180.

Ericson, J. et al., 1996. Two critical periods of Sonic Hedgehog signaling required for the specification of motor neuron identity. *Cell*, 87, pp.661–673.

Van Ewijk, W., 1988. Cell surface topography of thymic microenvironments. *Laboratory Investigation; a Journal of Technical Methods and Pathology*, 59, pp.579–590.

Van Ewijk, W., 1991. T-cell differentiation is influenced by thymic microenvironments. *Annual Review of Immunology*, 9, pp.591–615.

Van Ewijk, W., Shores, E.W. & Singer, A., 1994. Crosstalk in the mouse thymus. *Trends in Immunology*, 15, pp.214–217.

Fan, C. et al., 1995. Long-range sclerotome induction by sonic hedgehog: direct role of the amino-terminal cleavage product and modulation by the cyclic AMP signaling pathway. *Cell*, 81, pp.457–465.

Fan, C.M. & Tessier-Lavigne, M., 1994. Patterning of mammalian somites by surface ectoderm and notochord: evidence for sclerotome induction by a hedgehog homolog. *Cell*, 79, pp.1175–1186.

Fehling, H.J. et al., 1995. Crucial role of the pre-T-cell receptor alpha gene in development of alpha beta but not gamma delta T cells. *Nature*, 375, pp.795–798.

Felli, M.P. et al., 1999. Expression pattern of Notch1, 2 and 3 and Jagged1 and 2 in lymphoid and stromal thymus components: Distinct ligand-receptor interactions in intrathymic T cell development. *International Immunology*, 11, pp.1017–1025.

Ferkowicz, M.J. & Yoder, M.C., 2005. Blood island formation: Longstanding observations and modern interpretations. *Experimental Hematology*, 33, pp.1041–1047.

Fischer, A.M. et al., 2005. The role of Erk1 and Erk2 in multiple stages of T cell development. *Immunity*, 23, pp.431–443.

Fleischman, R.A., Custer, R.P. & Mintz, B., 1982. Totipotent hematopoietic stem cells: normal self-renewal and differentiation after transplantation between mouse fetuses. *Cell*, 30, pp.351–359.

Forbes, A.J. et al., 1993. Genetic analysis of hedgehog signalling in the Drosophila embryo. *Dev Suppl*, pp.115–124.

Foss, D.L., Donskoy, E. & Goldschneider, I., 2001. The importation of hematogenous precursors by the thymus is a gated phenomenon in normal adult mice. *The Journal of Experimental Medicine*, 193, pp.365–374.

Fugmann, S.D. et al., 2000. The RAG proteins and V(D)J recombination: complexes, ends, and transposition. *Annual Review of Immunology*, 18, pp.495–527.

Furmanski, A.L. et al., 2012. Role of Hedgehog signalling at the transition from double-positive to single-positive thymocyte. *European Journal of Immunology*, 42, pp.489–499.

Furmanski, A.L. et al., 2015. The transcriptional activator Gli2 modulates T-cell receptor signalling through attenuation of AP-1 and NFkappaB activity. *Journal of Cell Science*, 128(11), pp.2085–2095.

Furmanski, A.L. et al., 2013. Tissue-derived hedgehog proteins modulate Th differentiation and disease. *Journal of Immunology (Baltimore, Md. : 1950)*, 190, pp.2641–9.

Gao, B. et al., 2001. Mutations in IHH, encoding Indian hedgehog, cause brachydactyly type A-1. *Nature Genetics*, 28, pp.386–388.

Von Gaudecker, B., Kendall, M.D. & Ritter, M.A., 1997. Immuno-electron microscopy of the thymic epithelial microenvironment. *Microscopy Research and Technique*, 38, pp.237–249.

Gazzerro, E. & Canalis, E., 2006. Bone morphogenetic proteins and their antagonists. *Reviews in Endocrine & Metabolic Disorders*, 7, pp.51–65.

Germain, R.N., 2002. T-cell development and the CD4-CD8 lineage decision. *Nature Reviews. Immunology*, 2(5), pp.309–322.

Gil, D. et al., 2005. T cell receptor engagement by peptide-MHC ligands induces a conformational change in the CD3 complex of thymocytes. *The Journal of Experimental Medicine*, 201, pp.517–522.

Glimcher, L. & Murphy, K., 2000. Lineage commitment in the immune system: the T helper lymphocyte grows up. *Genes & Development*, 14(14), pp.1693–711.

Godfrey, D.I. et al., 1993. A developmental pathway involving four phenotypically and functionally distinct subsets of CD3-CD4-CD8- triple-negative adult mouse thymocytes defined by CD44 and CD25 expression. *Journal of Immunology (Baltimore, Md. : 1950)*, 150, pp.4244–4252.

Goetz, S.C. & Anderson, K. V, 2010. The primary cilium: a signalling centre during vertebrate development. *Nature reviews. Genetics*, 11, pp.331–344.

Goldrath, A.W. & Bevan, M.J., 1999. Selecting and maintaining a diverse T-cell repertoire. *Nature*, 402, pp.255–262.

Golub, R. & Cumano, A., 2013. Embryonic hematopoiesis. *Blood Cells, Molecules, and Diseases*, 51, pp.226–231.

Gong, Q. et al., 2001. Disruption of T cell signaling networks and development by Grb2 haploid insufficiency. *Nature Immunology*, 2, pp.29–36.

Gonzalez-Quevedo, R. et al., 2005. Receptor tyrosine phosphatase-dependent cytoskeletal remodeling by the hedgehog-responsive gene MIM/BEG4. *Journal of Cell Biology*, 168, pp.453–463.

Goodrich, L. V et al., 1997. Altered neural cell fates and medulloblastoma in mouse patched mutants. *Science (New York, N.Y.)*, 277, pp.1109–1113.

Goodrich, L. V. et al., 1996. Conservation of the hedgehog/patched signaling pathway from flies to mice: Induction of a mouse patched gene by Hedgehog. *Genes and Development*, 10, pp.301–312.

Gordon, J. & Manley, N.R., 2011. Mechanisms of thymus organogenesis and morphogenesis. *Development (Cambridge, England)*, 138(18), pp.3865–3878.

Gorlin, R.J., 1995. Nevoid basal cell carcinoma syndrome. *Dermatologic clinics*, 13, pp.113–125.

Graf, D. et al., 2002. The developmentally regulated expression of Twisted gastrulation reveals a role for bone morphogenetic proteins in the control of T cell development. *The Journal of Experimental Medicine*, 196, pp.163–171.

Green, E.K. et al., 2013. Replication of bipolar disorder susceptibility alleles and identification of two novel genome-wide significant associations in a new bipolar disorder case-control sample. *Molecular Psychiatry*, 18(12), pp.1302–1307.

Grueter, B. et al., 2005. Runx3 regulates integrin alpha E/CD103 and CD4 expression during development of CD4-/CD8+ T cells. *Journal of Immunology (Baltimore, Md. : 1950)*, 175, pp.1694–1705.

Guidos, C., 2006. Thymus and T-lymphocyte development: what is new in the 21st century? *Immunological Reviews*, 209, pp.5–9.

Gutiérrez-Frías, C. et al., 2004. Sonic hedgehog regulates early human thymocyte differentiation by counteracting the IL-7-induced development of CD34+ precursor cells. *Journal of Immunology (Baltimore, Md. : 1950)*, 173, pp.5046–5053.

Hager-Theodorides, A.L. et al., 2002. Bone morphogenetic protein 2/4 signaling regulates early thymocyte differentiation. *Journal of Immunology (Baltimore, Md. : 1950)*, 169, pp.5496–5504.

Hager-Theodorides, A.L. et al., 2014. Direct BMP2/4 signaling through BMP receptor IA regulates fetal thymocyte progenitor homeostasis and differentiation to CD4+CD8+ double-positive cell. *Cell Cycle*, 13, pp.324–333.

Hager-Theodorides, A.L. et al., 2009. The Gli3 transcription factor expressed in the thymus stroma controls thymocyte negative selection via Hedgehog-dependent and -independent mechanisms. *Journal of Immunology (Baltimore, Md. : 1950)*, 183, pp.3023–3032.

Hager-Theodorides, A.L. et al., 2005. The transcription factor Gli3 regulates differentiation of fetal CD4 -CD8- double-negative thymocytes. *Blood*, 106, pp.1296–1304.

Hahn, H. et al., 1998. Rhabdomyosarcomas and radiation hypersensitivity in a mouse model of Gorlin syndrome. *Nature Medicine*, 4, pp.619–622.

Haley, P.J., 2003. Species differences in the structure and function of the immune system. *Toxicology*, 188, pp.49–71.

Hammerschmidt, M., Brook, A. & McMahon, A.P., 1997. The world according to hedgehog. *Trends in Genetics*, 13, pp.14–21.

Hammerschmidt, M., Serbedzija, G.N. & McMahon, A.P., 1996. Genetic analysis of dorsoventral pattern formation in the zebrafish: requirement of a BMP-like ventralizing activity and its dorsal repressor. *Genes & Development*, 10(19), pp.2452–2461.

Hardcastle, Z. et al., 1998. The Shh signalling pathway in tooth development: defects in Gli2 and Gli3 mutants. *Development (Cambridge, England)*, 125, pp.2803–2811.

Hathcock, K.S. et al., 1993. Identification of an alternative CTLA-4 ligand costimulatory for T cell activation. *Science (New York, N.Y.)*, 262, pp.905–907.

Havran, W.L. & Allison, J.P., 1988. Developmentally ordered appearance of thymocytes expressing different T-cell antigen receptors. *Nature*, 335, pp.443–445.

Hayday, A.C. & Pennington, D.J., 2007. Key factors in the organized chaos of early T cell development. *Nature Immunology*, 8, pp.137–144.

Haynes, B.F. & Heinly, C.S., 1995. Early human T cell development: analysis of the human thymus at the time of initial entry of hematopoietic stem cells into the fetal thymic microenvironment. *The Journal of Experimental Medicine*, 181, pp.1445–1458.

He, X. et al., 2005. The zinc finger transcription factor Th-POK regulates CD4 versus CD8 T-cell lineage commitment. *Nature*, 433, pp.826–833.

Hebrok, M. et al., 2000. Regulation of pancreas development by hedgehog signaling. *Development (Cambridge, England)*, 127, pp.4905–4913.

Hellemans, J. et al., 2003. Homozygous mutations in IHH cause acrocapitofemoral dysplasia, an autosomal recessive disorder with cone-shaped epiphyses in hands and hips. *American Journal of Human Genetics*, 72, pp.1040–1046.

Hernández-Hoyos, G. et al., 2003. GATA-3 expression is controlled by TCR signals and regulates CD4/CD8 differentiation. *Immunity*, 19, pp.83–94.

Hernández-Hoyos, G. et al., 2000. Lck activity controls CD4/CD8 T cell lineage commitment. *Immunity*, 12, pp.313–322.

Hinck, L., Nelson, W.J. & Papkoff, J., 1994. Wnt-1 modulates cell-cell adhesion in mammalian cells by stabilizing beta-catenin binding to the cell adhesion protein cadherin. *The Journal of Cell Biology*, 124, pp.729–741.

Hogquist, K.A. et al., 1994. T cell receptor antagonist peptides induce positive selection. *Cell*, 76, pp.17–27.

Holst, J. et al., 2008. Scalable signaling mediated by T cell antigen receptor-CD3 ITAMs ensures effective negative selection and prevents autoimmunity. *Nature Immunology*, 9, pp.658–666.

Hombach, A. et al., 2001. T-cell activation by recombinant receptors: CD28 costimulation is required for interleukin 2 secretion and receptor-mediated T-cell proliferation but does not affect receptor-mediated target cell lysis. *Cancer Research*, 61, pp.1976–1982.

Hooper, J.E. & Scott, M.P., 2005. Communicating with Hedgehogs. *Nature reviews. Molecular Cell Biology*, 6, pp.306–317.

Hori, S., Nomura, T. & Sakaguchi, S., 2003. Control of regulatory T cell development by the transcription factor Foxp3. *Science (New York, N.Y.)*, 299, pp.1057–1061.

Hosoya, T., Maillard, I. & Engel, J.D., 2010. From the cradle to the grave: Activities of GATA-3 throughout T-cell development and differentiation. *Immunological Reviews*, 238, pp.110–125.

Hsu, W., Shakya, R. & Costantini, F., 2001. Impaired mammary gland and lymphoid development caused by inducible expression of Axin in transgenic mice. *Journal of Cell Biology*, 155, pp.1055–1064.

Huangfu, D. & Anderson, K. V, 2006. Signaling from Smo to Ci/Gli: conservation and divergence of Hedgehog pathways from Drosophila to vertebrates. *Development (Cambridge, England)*, 133, pp.3–14.

Hui, C.C. et al., 1994. Expression of three mouse homologs of the Drosophila segment polarity gene cubitus interruptus, Gli, Gli-2, and Gli-3, in ectoderm- and mesoderm-derived tissues suggests multiple roles during postimplantation development. *Developmental Biology*, 162, pp.402–413.

Hui, C.C. & Joyner, A.L., 1993. A mouse model of greig cephalopolysyndactyly syndrome: the extra-toesJ mutation contains an intragenic deletion of the Gli3 gene. *Nature Genetics*, 3, pp.241–246.

Ibuki, N. et al., 2013. TAK-441, a novel investigational smoothened antagonist, delays castration-resistant progression in prostate cancer by disrupting paracrine hedgehog signaling. *International Journal of Cancer*, 133, pp.1955–1966.

Igarashi, H. et al., 2002. Transcription from the RAG1 locus marks the earliest lymphocyte progenitors in bone marrow. *Immunity*, 17, pp.117–130.

Ikuta, K. & Weissman, I.L., 1992. Evidence that hematopoietic stem cells express mouse c-kit but do not depend on steel factor for their generation. *Proceedings of the National Academy of Sciences of the United States of America*, 89, pp.1502–1506.

Incardona, J.P. et al., 2000. Receptor-mediated endocytosis of soluble and membrane-tethered Sonic hedgehog by Patched-1. *Proceedings of the National Academy of Sciences of the United States of America*, 97, pp.12044–12049.

Incardona, J.P., Gruenberg, J. & Roelink, H., 2002. Sonic hedgehog induces the segregation of patched and smoothened in endosomes. *Current Biology*, 12, pp.983–995.

Ingham, P.W. & McMahon, a P., 2001. Hedgehog signaling in animal development: paradigms and principles. *Genes & Development*, 15(23), pp.3059–87.

Ingham, P.W. & McMahon, A.P., 2001. Hedgehog signaling in animal development: Paradigms and principles. *Genes and Development*, 15, pp.3059–3087.

Ingham, P.W., Nakano, Y. & Seger, C., 2011. Mechanisms and functions of Hedgehog signalling across the metazoa. *Nature reviews. Genetics*, 12, pp.393–406.

Ingham, P.W., Taylor, A.M. & Nakano, Y., 1991. Role of the Drosophila patched gene in positional signalling. *Nature*, 353, pp.184–187.

Irving, B.A., Alt, F.W. & Killeen, N., 1998. Thymocyte development in the absence of pre-T cell receptor extracellular immunoglobulin domains. *Science (New York, N.Y.)*, 280, pp.905–908.

Itano, A. et al., 1996. The cytoplasmic domain of CD4 promotes the development of CD4 lineage T cells. *The Journal of Experimental Medicine*, 183, pp.731–741.

Itano, A., Kioussis, D. & Robey, E., 1994. Stochastic component to development of class I major histocompatibility complex-specific T cells. *Proceedings of the National Academy of Sciences of the United States of America*, 91, pp.220–224.

Jenkins, M.K. et al., 1990. Inhibition of antigen-specific proliferation of type 1 murine T cell clones after stimulation with immobilized anti-CD3 monoclonal antibody. *Journal of Immunology (Baltimore, Md. : 1950)*, 144, pp.16–22.

Jenkins, M.K. & Schwartz, R.H., 1987. Antigen presentation by chemically modified splenocytes induces antigen-specific T cell unresponsiveness in vitro and in vivo. *The Journal of Experimental Medicine*, 165, pp.302–319.

Jenkinson, S.R. et al., 2007. Expression of the transcription factor cKrox in peripheral CD8 T cells reveals substantial postthymic plasticity in CD4-CD8 lineage differentiation. *The Journal of Experimental Medicine*, 204, pp.267–272.

Jessell, T.M., 2000. Neuronal specification in the spinal cord: inductive signals and transcriptional codes. *Nature Reviews. Genetics*, 1, pp.20–29.

Jia, J. et al., 2005. Phosphorylation by double-time/CKI?? and CKI?? targets Cubitus Interruptus for Slimb/??-TRCP-mediated proteolytic processing. *Developmental Cell*, 9, pp.819–830.

Jiménez, E. et al., 2001. Distinct mechanisms contribute to generate and change the CD4:CD8 cell ratio during thymus development: a role for the Notch ligand, Jagged1. *Journal of Immunology (Baltimore, Md. : 1950)*, 166, pp.5898–5908.

Johnson, R.L. et al., 1994. Ectopic expression of Sonic hedgehog alters dorsal-ventral patterning of somites. *Cell*, 79, pp.1165–1173.

Kamisago, M. et al., 1999. Assignment of human desert hedgehog gene (DHH) to chromosome band 12q13.1 by in situ hybridization. *Cytogenetics and Cell Genetics*, 87(1-2), pp.117–118.

Kang, J.-S., Zhang, W. & Krauss, R.S., 2007. Hedgehog signaling: cooking with Gas1. *Science's STKE : Signal Transduction Knowledge Environment*, 2007, p.pe50.

Kanji, S., Pompili, V.J. & Das, H., 2011. Plasticity and maintenance of hematopoietic stem cells during development. *Recent Patents on Biotechnology*, 5, pp.40–53.

Kaplan, M.H. et al., 1996. Stat6 is required for mediating responses to IL-4 and for the development of Th2 cells. *Immunity*, 4, pp.313–319.

Karhadkar, S.S. et al., 2004. Hedgehog signalling in prostate regeneration, neoplasia and metastasis. *Nature*, 431, pp.707–712.

Kawamata, S. et al., 2002. Overexpression of the Notch target genes Hes in vivo induces lymphoid and myeloid alterations. *Oncogene*, 21, pp.3855–3863.

Kawamoto, H., 2006. A close developmental relationship between the lymphoid and myeloid lineages. *Trends in Immunology*, 27, pp.169–175.

Kawamoto, H. et al., 1999. Emergence of T cell progenitors without B cell or myeloid differentiation potential at the earliest stage of hematopoiesis in the murine fetal liver. *Journal of Immunology (Baltimore, Md. : 1950)*, 162, pp.2725–2731.

Kawamoto, H., Ohmura, K. & Katsura, Y., 1997. Direct evidence for the commitment of hematopoietic stem cells to T, B and myeloid lineages in murine fetal liver. *International Immunology*, 9, pp.1011–1019.

Keefe, R. et al., 1999. Regulation of lineage commitment distinct from positive selection. *Science (New York, N.Y.)*, 286(5442), pp.1149–53.

Kiel, M.J. et al., 2005. SLAM family receptors distinguish hematopoietic stem and progenitor cells and reveal endothelial niches for stem cells. *Cell*, 121, pp.1109–1121.

Kinzler, K.W. et al., 1987. Identification of an amplified, highly expressed gene in a human glioma. *Science (New York, N.Y.)*, 236, pp.70–73.

Kinzler, K.W. et al., 1988. The GLI gene is a member of the Kruppel family of zinc finger proteins. *Nature*, 332, pp.371–374.

Kisielow, P. et al., 1988. Tolerance in T-cell-receptor transgenic mice involves deletion of nonmature CD4+8+ thymocytes. *Nature*, 333, pp.742–746.

Klein, L. et al., 2009. Antigen presentation in the thymus for positive selection and central tolerance induction. *Nature reviews. Immunology*, 9, pp.833–844.

Koch, U. et al., 2001. Subversion of the T/B lineage decision in the thymus by Lunatic Fringe-mediated inhibition of Notch-1. *Immunity*, 15, pp.225–236.

Koch, U. & Radtke, F., 2011. Mechanisms of T Cell Development and Transformation. *Annual Review of Cell and Developmental Biology*, 27, pp.539–562.

Koebernick, K. & Pieler, T., 2002. Gli-type zinc finger proteins as bipotential transducers of Hedgehog signaling. *Differentiation*, 70, pp.69–76.

Kogawa, K. et al., 2002. Expression of AIRE gene in peripheral monocyte/dendritic cell lineage. *Immunology Letters*, 80, pp.195–198.

Kondo, M. et al., 2003. Biology of hematopoietic stem cells and progenitors: implications for clinical application. *Annual Review of Immunology*, 21, pp.759–806.

Kondo, M., Weissman, I.L. & Akashi, K., 1997. Identification of clonogenic common lymphoid progenitors in mouse bone marrow. *Cell*, 91, pp.661–672.

Koudijs, M.J. et al., 2008. Genetic analysis of the two zebrafish patched homologues identifies novel roles for the hedgehog signaling pathway. *BMC Developmental Biology*, 8, p.15.

Krangel, M.S., 2009. Mechanics of T cell receptor gene rearrangement. *Current Opinion in Immunology*, 21, pp.133–139.

Krauss, S., Concordet, J.P. & Ingham, P.W., 1993. A functionally conserved homolog of the Drosophila segment polarity gene hh is expressed in tissues with polarizing activity in zebrafish embryos. *Cell*, 75, pp.1431–1444.

Kuklina, E.M., 2013. Molecular mechanisms of T-cell anergy. *Biochemistry. Biokhimiia*, 78, pp.144–56.

Kumar, S., Balczarek, K.A. & Lai, Z.-C., 1996. Evolution of the hedgehog Gene Family. *Genetics* , 142 (3), pp.965–972.

Kumaravelu, P. et al., 2002. Quantitative developmental anatomy of definitive haematopoietic stem cells/long-term repopulating units (HSC/RUs): role of the aorta-gonad-mesonephros (AGM) region and the yolk sac in colonisation of the mouse embryonic liver. *Development (Cambridge, England)*, 129, pp.4891–4899.

Ladi, E. et al., 2006. Thymic microenvironments for T cell differentiation and selection. *Nature Immunology*, 7, pp.338–343.

Lai, L.P. & Mitchell, J., 2005. Indian hedgehog: Its roles and regulation in endochondral bone development. *Journal of Cellular Biochemistry*, 96, pp.1163–1173.

Lantz, O. et al., 2000. Gamma chain required for naïve CD4+ T cell survival but not for antigen proliferation. *Nature Immunology*, 1, pp.54–58.

Lau, C.I. et al., 2012. Regulation of murine normal and stress-induced erythropoiesis by Desert Hedgehog. *Blood*, 119, pp.4741–4751.

Laufer, E. et al., 1994. Sonic hedgehog and Fgf-4 act through a signaling cascade and feedback loop to integrate growth and patterning of the developing limb bud. *Cell*, 79, pp.993–1003.

Lee, J.J. et al., 1994. Autoproteolysis in hedgehog protein biogenesis. *Science (New York, N.Y.)*, 266, pp.1528–1537.

Lee, K. et al., 2006. Indian hedgehog is a major mediator of progesterone signaling in the mouse uterus. *Nature Genetics*, 38, pp.1204–1209.

Leek, J.P. et al., 1997. Assignment of Indian hedgehog (IHH) to human chromosome bands 2q33-->q35 by in situ hybridization. *Cytogenetics and Cell Genetics*, 76(3-4), pp.187–188.

Leung, R.K. et al., 2001. Deletion of the CD4 silencer element supports a stochastic mechanism of thymocyte lineage commitment. *Nature Immunology*, 2, pp.1167–1173.

Levin, S.D. et al., 1993. A dominant-negative transgene defines a role for p56lck in thymopoiesis. *The EMBO Journal*, 12, pp.1671–1680.

Lewis, K.E. & Eisen, J.S., 2001. Hedgehog signaling is required for primary motoneuron induction in zebrafish. *Development (Cambridge, England)*, 128, pp.3485–3495.

Li, C.-L. et al., 2002. Estrogen deficiency results in enhanced expression of Smoothened of the Hedgehog signaling in the thymus and affects thymocyte development. *International Immunopharmacology*, 2, pp.823–833.

Liang, H. et al., 2007. Noncanonical Wnt signaling promotes apoptosis in thymocyte development. *The Journal of Experimental Medicine*, 204, pp.3077–3084.

Lind, E.F. et al., 2001. Mapping precursor movement through the postnatal thymus reveals specific microenvironments supporting defined stages of early lymphoid development. *The Journal of Experimental Medicine*, 194, pp.127–134.

Linsley, P.S. et al., 1991. CTLA-4 is a second receptor for the B cell activation antigen B7. *Journal of Experimental Medicine*, 174, pp.561–569.

Lipinski, R.J. et al., 2006. Unique and complimentary activities of the Gli transcription factors in Hedgehog signaling. *Experimental Cell Research*, 312, pp.1925–1938.

Liston, A. et al., 2003. Aire regulates negative selection of organ-specific T cells. *Nature Immunology*, 4, pp.350–354.

Litingtung, Y. et al., 1998. Sonic hedgehog is essential to foregut development. *Nature Genetics*, 20, pp.58–61.

Liu et al., 2005. The role of CCL21 in recruitment of T-precursor cells to fetal thymi. *Blood*, 105, pp.31–39.

Liu, X. & Bosselut, R., 2004. Duration of TCR signaling controls CD4-CD8 lineage differentiation in vivo. *Nature Immunology*, 5, pp.280–288.

Livák, F. et al., 1999. Characterization of TCR gene rearrangements during adult murine T cell development. *Journal of Immunology (Baltimore, Md. : 1950)*, 162, pp.2575–2580.

Logan, M. et al., 1998. The transcription factor pitx2 mediates situs-specific morphogenesis in response to left-right asymmetric signals. *Cell*, 94, pp.307–317.

López-Martínez, A. et al., 1995. Limb-patterning activity and restricted posterior localization of the amino-terminal product of Sonic hedgehog cleavage. *Current Biology : CB*, 5, pp.791–796.

Love, P.E. & Bhandoola, A., 2011. Signal integration and crosstalk during thymocyte migration and emigration. *Nature reviews. Immunology*, 11, pp.469–477.

Lowrey, J.A. et al., 2002. Sonic hedgehog promotes cell cycle progression in activated peripheral CD4(+) T lymphocytes. *Journal of immunology (Baltimore, Md. : 1950)*, 169, pp.1869–1875.

Luckheeram, R.V. et al., 2012. CD4+T Cells: Differentiation and Functions. *Clinical and Developmental Immunology*, 2012, pp.1–12.

Lugo-Villarino, G. et al., 2003. T-bet is required for optimal production of IFN-gamma and antigen-specific T cell activation by dendritic cells. *Proceedings of the National Academy of Sciences of the United States of America*, 100, pp.7749–7754.

Lum, L. et al., 2003. Hedgehog signal transduction via Smoothened association with a cytoplasmic complex scaffolded by the atypical kinesin, Costal-2. *Molecular Cell*, 12, pp.1261–1274.

Lum, L. & Beachy, P.A., 2004. The Hedgehog response network: sensors, switches, and routers. *Science (New York, N.Y.)*, 304, pp.1755–1759.

Lundberg, K. et al., 1995. Intermediate steps in positive selection: differentiation of CD4+8int TCRint thymocytes into CD4-8+TCRhi thymocytes. *The Journal of Experimental Medicine*, 181, pp.1643–1651.

MacDonald, H.R., Budd, R.C. & Howe, R.C., 1988. A CD3- subset of CD4-8+ thymocytes: a rapidly cycling intermediate in the generation of CD4+8+ cells. *European Journal of Immunology*, 18, pp.519–523.

MacDonald, H.R., Radtke, F. & Wilson, A., 2001. T cell fate specification and alphabeta/gammadelta lineage commitment. *Current Opinion in Immunology*, 13, pp.219–224.

Macián, F. et al., 2004. T-cell anergy. *Current Opinion in Immunology*, 16, pp.209–216.

Maggi, E. et al., 2005. Thymic regulatory T cells. In *Autoimmunity Reviews*. pp. 579–586.

Maillard, I. et al., 2004. Mastermind critically regulates Notch-mediated lymphoid cell fate decisions. *Blood*, 104, pp.1696–1702.

Mak, K.K. et al., 2008. Hedgehog Signaling in Mature Osteoblasts Regulates Bone Formation and Resorption by Controlling PTHrP and RANKL Expression. *Developmental Cell*, 14, pp.674–688.

Malissen, B. & Malissen, M., 1996. Functions of TCR and pre-TCR subunits: Lessons from gene ablation. *Current Opinion in Immunology*, 8, pp.383–393.

Mallick, C.A. et al., 1993. Rearrangement and diversity of T cell receptor beta chain genes in thymocytes: a critical role for the beta chain in development. *Cell*, 73, pp.513–519.

Mao, J. et al., 2002. Regulation of Gli1 transcriptional activity in the nucleus by Dyrk1. *Journal of Biological Chemistry*, 277, pp.35156–35161.

Marigo, V. et al., 1995. Cloning, expression, and chromosomal location of SHH and IHH: two human homologues of the Drosophila segment polarity gene hedgehog. *Genomics*, 28, pp.44–51.

Marigo, V. & Tabin, C.J., 1996. Regulation of patched by sonic hedgehog in the developing neural tube. *Proceedings of the National Academy of Sciences of the United States of America*, 93, pp.9346–9351.

Markiewicz, M.A. et al., 1998. Long-term T cell memory requires the surface expression of self-peptide/major histocompatibility complex molecules. *Proceedings of the National Academy of Sciences of the United States of America*, 95, pp.3065–3070.

Marrella, V. et al., 2012. Anti-CD3?? mAb improves thymic architecture and prevents autoimmune manifestations in a mouse model of Omenn syndrome: Therapeutic implications. *Blood*, 120, pp.1005–1014.

Martí, E., Takada, R., et al., 1995. Distribution of Sonic hedgehog peptides in the developing chick and mouse embryo. *Development (Cambridge, England)*, 121, pp.2537–2547.

Martí, E., Bumcrot, D.A., et al., 1995. Requirement of 19K form of Sonic hedgehog for induction of distinct ventral cell types in CNS explants. *Nature*, 375, pp.322–325.

Masetti, R. et al., 2013. DHH-RHEBL1 fusion transcript: a novel recurrent feature in the new landscape of pediatric CBFA2T3-GLIS2-positive acute myeloid leukemia. *Oncotarget*, 4, pp.1712–20.

Mastronardi, F.G. et al., 2000. Co-localization of patched and activated sonic hedgehog to lysosomes in neurons. *Neuroreport*, 11, pp.581–585.

Masuda, K. et al., 2005. Thymic anlage is colonized by progenitors restricted to T, NK, and dendritic cell lineages. *Journal of Immunology (Baltimore, Md. : 1950)*, 174, pp.2525–2532.

Matise, M.P. & Joyner, A.L., 1999. Gli genes in development and cancer. *Oncogene*, 18, pp.7852–7859.

Matloubian, M. et al., 2004. Lymphocyte egress from thymus and peripheral lymphoid organs is dependent on S1P receptor 1. *Nature*, 427, pp.355–360.

Matsuzaki, Y. et al., 1993. Characterization of c-kit positive intrathymic stem cells that are restricted to lymphoid differentiation. *The Journal of Experimental Medicine*, 178, pp.1283–1292.

McMahon, A.P., Ingham, P.W. & Tabin, C.J., 2003. Developmental roles and clinical significance of hedgehog signaling. *Current topics in Developmental Biology*, 53, pp.1–114.

Medvinsky, A. & Dzierzak, E., 1996. Definitive hematopoiesis is autonomously initiated by the AGM Region. *Cell*, 86, pp.897–906.

Medvinsky, A., Rybtsov, S. & Taoudi, S., 2011. Embryonic origin of the adult hematopoietic system: advances and questions. *Development (Cambridge, England)*, 138, pp.1017–1031.

Medvinsky, A.L. et al., 1993. An early pre-liver intraembryonic source of CFU-S in the developing mouse. *Nature*, 364, pp.64–67.

Meyer, N.P. & Roelink, H., 2003. The amino-terminal region of Gli3 antagonizes the Shh response and acts in dorsoventral fate specification in the developing spinal cord. *Developmental Biology*, 257, pp.343–355.

Michie, A.M. et al., 2007. Constitutive Notch signalling promotes CD4- CD8 - thymocyte differentiation in the absence of the pre-TCR complex, by mimicking pre-TCR signals. *International Immunology*, 19, pp.1421–1430.

Michie, A.M. & Zúñiga-Pflücker, J.C., 2002. Regulation of thymocyte differentiation: Pre-TCR signals and β-selection. *Seminars in Immunology*, 14, pp.311–323.

Mikkola, H.K.A. et al., 2005. Placenta as a site for hematopoietic stem cell development. *Experimental Hematology*, 33, pp.1048–1054.

Mikkola, H.K.A. & Orkin, S.H., 2006. The journey of developing hematopoietic stem cells. *Development (Cambridge, England)*, 133, pp.3733–3744.

Miller, C. & Sassoon, D.A., 1998. Wnt-7a maintains appropriate uterine patterning during the development of the mouse female reproductive tract. *Development (Cambridge, England)*, 125, pp.3201–3211.

Mirsky, R. et al., 1999. Schwann cell-derived desert hedgehog signals nerve sheath formation. *Annals of the New York Academy of Sciences*, 883, pp.196–202.

Misslitz, A. et al., 2004. Thymic T cell development and progenitor localization depend on CCR7. *The Journal of Experimental Medicine*, 200, pp.481–491.

Miyazono, K., Kusanagi, K. & Inoue, H., 2001. Divergence and convergence of TGF-beta/BMP signaling. *Journal of Cellular Physiology*, 187, pp.265–276.

Mo, R. et al., 1997. Specific and redundant functions of Gli2 and Gli3 zinc finger genes in skeletal patterning and development. *Development (Cambridge, England)*, 124, pp.113–123.

Molina, T.J. et al., 1992. Profound block in thymocyte development in mice lacking p56lck. *Nature*, 357, pp.161–164.

Mombaerts, P. et al., 1994. An activated lck transgene promotes thymocyte development in RAG-1 mutant mice. *Immunity*, 1, pp.261–267.

Mombaerts, P. et al., 1992. RAG-1-deficient mice have no mature B and T lymphocytes. *Cell*, 68, pp.869–877.

Montecino-Rodriguez, E., Leathers, H. & Dorshkind, K., 2001. Bipotential B-macrophage progenitors are present in adult bone marrow. *Nature Immunology*, 2, pp.83–88.

Moon, R.T. et al., 2002. The promise and perils of Wnt signaling through beta-catenin. *Science (New York, N.Y.)*, 296, pp.1644–1646.

Moore, M.A. & Metcalf, D., 1970. Ontogeny of the haemopoietic system: yolk sac origin of in vivo and in vitro colony forming cells in the developing mouse embryo. *British Journal of Haematology*, 18, pp.279–296.

Moran, A.E. & Hogquist, K.A., 2012. T-cell receptor affinity in thymic development. *Immunology*, 135, pp.261–267.

Morrison, S.J. & Weissman, I.L., 1994. The long-term repopulating subset of hematopoietic stem cells is deterministic and isolatable by phenotype. *Immunity*, 1, pp.661–673.

Motoyama, J. et al., 1998. Overlapping and non-overlapping Ptch2 expression with Shh during mouse embryogenesis. *Mechanisms of Development*, 78, pp.81–84.

Muller, A.M. et al., 1994. Development of hematopoietic stem cell activity in the mouse embryo. *Immunity*, 1, pp.291–301.

Mullor, J.L. & Guerrero, I., 2000. A gain-of-function mutant of patched dissects different responses to the hedgehog gradient. *Developmental Biology*, 228, pp.211–224.

Mulroy, T. et al., 2002. Wnt-1 and Wnt-4 regulate thymic cellularity. *European Journal of Immunology*, 32, pp.967–971.

Mumm, J.S. & Kopan, R., 2000. Notch signaling: from the outside in. *Developmental Biology*, 228(2), pp.151–65.

Nagamine, K. et al., 1997. Positional cloning of the APECED gene. *Nature Genetics*, 17, pp.393–398.

Nakano, Y. et al., 1989. A protein with several possible membrane-spanning domains encoded by the Drosophila segment polarity gene patched. *Nature*, 341, pp.508–513.

Nakorn, T.N. et al., 2002. Myeloerythroid-restricted progenitors are sufficient to confer radioprotection and provide the majority of day 8 CFU-S. *Journal of Clinical Investigation*, 109, pp.1579–1585.

Nam, Y. et al., 2003. Structural requirements for assembly of the CSL??intracellular Notch1??Mastermind-like 1 transcriptional activation complex. *Journal of Biological Chemistry*, 278, pp.21232–21239.

Neilson, J.R. et al., 2004. Calcineurin B1 is essential for positive but not negative selection during thymocyte development. *Immunity*, 20, pp.255–266.

Neumann, C.J. & Nuesslein-Volhard, C., 2000. Patterning of the zebrafish retina by a wave of sonic hedgehog activity. *Science (New York, N.Y.)*, 289, pp.2137–2139.

Nikolich-Zugich, J., Slifka, M.K. & Messaoudi, I., 2004. The many important facets of T-cell repertoire diversity. *Nature reviews. Immunology*, 4, pp.123–132.

Niswander, L. et al., 1994. A positive feedback loop coordinates growth and patterning in the vertebrate limb. *Nature*, 371, pp.609–612.

Nüsslein-Volhard, C. & Wieschaus, E., 1980. Mutations affecting segment number and polarity in Drosophila. *Nature*, 287, pp.795–801.

O'Hara, W.A. et al., 2011. Desert hedgehog is a mammal-specific gene expressed during testicular and ovarian development in a marsupial. *BMC Developmental Biology*, 11, p.72.

Van Oers, N.S. et al., 1996. alpha beta T cell development is abolished in mice lacking both Lck and Fyn protein tyrosine kinases. *Immunity*, 5, pp.429–436.

Oettinger, M.A. et al., 1990. RAG-1 and RAG-2, adjacent genes that synergistically activate V(D)J recombination. *Science (New York, N.Y.)*, 248, pp.1517–1523.

Okamura, R.M. et al., 1998. Redundant regulation of T cell differentiation and TCRalpha gene expression by the transcription factors LEF-1 and TCF-1. *Immunity*, 8, pp.11–20.

Orkin, S.H. & Zon, L.I., 1997. Genetics of erythropoiesis: induced mutations in mice and zebrafish. *Annual Review of Genetics*, 31, pp.33–60.

Outram, S. V et al., 2000. Hedgehog signaling regulates differentiation from double-negative to double-positive thymocyte. *Immunity*, 13, pp.187–197.

Outram, S. V. et al., 2009. Indian hedgehog (Ihh) both promotes and restricts thymocyte differentiation. *Blood*, 113, pp.2217–2228.

Owaki, T. et al., 2005. A role for IL-27 in early regulation of Th1 differentiation. *Journal of Immunology (Baltimore, Md. : 1950)*, 175, pp.2191–2200.

Owen, J.J. & Ritter, M.A., 1969. Tissue interaction in the development of thymus lymphocytes. *The Journal of Experimental Medicine*, 129, pp.431–442.

Pai, S.Y. et al., 2003. Critical Roles for Transcription Factor GATA-3 in Thymocyte Development. *Immunity*, 19, pp.863–875.

Palis, J. et al., 1999. Development of erythroid and myeloid progenitors in the yolk sac and embryo proper of the mouse. *Development (Cambridge, England)*, 126, pp.5073–5084.

Pan, Y. et al., 2006. Sonic hedgehog signaling regulates Gli2 transcriptional activity by suppressing its processing and degradation. *Molecular and Cellular Biology*, 26(9), pp.3365–3377.

Pan, Y., Wang, C. & Wang, B., 2009. Phosphorylation of Gli2 by protein kinase A is required for Gli2 processing and degradation and the Sonic Hedgehog-regulated mouse development. *Developmental Biology*, 326, pp.177–189.

Pang, S.S. et al., 2010. The structural basis for autonomous dimerization of the pre-T-cell antigen receptor. *Nature*, 467, pp.844–848.

Park, H.L. et al., 2000. Mouse Gli1 mutants are viable but have defects in SHH signaling in combination with a Gli2 mutation. *Development (Cambridge, England)*, 127, pp.1593–1605.

Park, J.-H. et al., 2007. "Coreceptor tuning": cytokine signals transcriptionally tailor CD8 coreceptor expression to the self-specificity of the TCR. *Nature Immunology*, 8, pp.1049–1059.

Parmantier, E. et al., 1999. Schwann cell-derived desert hedgehog controls the development of peripheral nerve sheaths. *Neuron*, 23, pp.713–724.

Pasca di Magliano, M. & Hebrok, M., 2003. Hedgehog signalling in cancer formation and maintenance. *Nature reviews. Cancer*, 3, pp.903–911.

Pathi, S. et al., 2001. Comparative biological responses to human Sonic, Indian, and Desert hedgehog. *Mechanisms of Development*, 106, pp.107–117.

Pearse, 2006. Normal structure, function and histology of the thymus. *Toxicologic pathology*, 34, pp.504–514.

Pearse, M. et al., 1989. A murine early thymocyte developmental sequence is marked by transient expression of the interleukin 2 receptor. *Proceedings of the National Academy of Sciences of the United States of America*, 86, pp.1614–1618.

Pepicelli, C. V, Lewis, P.M. & McMahon, A.P., 1998. Sonic hedgehog regulates branching morphogenesis in the mammalian lung. *Current biology : CB*, 8, pp.1083–1086.

Pepinsky, R.B. et al., 1998. Identification of a palmitic acid-modified form of human Sonic hedgehog. *Journal of Biological Chemistry*, 273, pp.14037–14045.

Perry, J.M. et al., 2009. Maintenance of the BMP4-dependent stress erythropoiesis pathway in the murine spleen requires hedgehog signaling. *Blood*, 113, pp.911–918.

Peters, C. et al., 2004. The cholesterol membrane anchor of the Hedgehog protein confers stable membrane association to lipid-modified proteins. *Proceedings of the National Academy of Sciences of the United States of America*, 101, pp.8531–8536.

Petrie, H.T. & Zúñiga-Pflücker, J.C., 2007. Zoned out: functional mapping of stromal signaling microenvironments in the thymus. *Annual Review of Immunology*, 25, pp.649–679.

Pivniouk, V. et al., 1998. Impaired viability and profound block in thymocyte development in mice lacking the adaptor protein SLP-76. *Cell*, 94, pp.229–238.

Plotkin, J. et al., 2003. Critical role for CXCR4 signaling in progenitor localization and T cell differentiation in the postnatal thymus. *Journal of Immunology (Baltimore, Md. : 1950)*, 171, pp.4521–4527.

Porritt, H.E. et al., 2004. Heterogeneity among DN1 prothymocytes reveals multiple progenitors with different capacities to generate T cell and non-T cell lineages. *Immunity*, 20, pp.735–745.

Porritt, H.E., Gordon, K. & Petrie, H.T., 2003. Kinetics of steady-state differentiation and mapping of intrathymic-signaling environments by stem cell transplantation in nonirradiated mice. *The Journal of Experimental Medicine*, 198, pp.957–962.

Porter, J.A., Young, K.E. & Beachy, P.A., 1996. Cholesterol modification of hedgehog signaling proteins in animal development. *Science (New York, N.Y.)*, 274, pp.255–259.

Price, M.A. & Kalderon, D., 2002. Proteolysis of the Hedgehog signaling effector Cubitus interruptus requires phosphorylation by Glycogen Synthase Kinase 3 and Casein Kinase 1. *Cell*, 108, pp.823–835.

Prockop, S. & Petrie, H.T., 2000. Cell migration and the anatomic control of thymocyte precursor differentiation. *Seminars in Immunology*, 12, pp.435–444.

Pronk, C.J.H. et al., 2007. Elucidation of the Phenotypic, Functional, and Molecular Topography of a Myeloerythroid Progenitor Cell Hierarchy. *Cell Stem Cell*, 1, pp.428–442.

Quill, H. & Schwartz, R.H., 1987. Stimulation of normal inducer T cell clones with antigen presented by purified Ia molecules in planar lipid membranes: specific induction of a long-lived state of proliferative nonresponsiveness. *Journal of Immunology (Baltimore, Md. : 1950)*, 138, pp.3704–3712.

Radtke, F. et al., 1999. Deficient T cell fate specification in mice with an induced inactivation of Notch1. *Immunity*, 10, pp.547–558.

Ramalho-Santos, M., Melton, D.A. & McMahon, A.P., 2000. Hedgehog signals regulate multiple aspects of gastrointestinal development. *Development (Cambridge, England)*, 127, pp.2763–2772.

Regl, G. et al., 2002. Human GLI2 and GLI1 are part of a positive feedback mechanism in Basal Cell Carcinoma. *Oncogene*, 21, pp.5529–5539.

Ren, Y. et al., 2012. Overactivation of Hedgehog Signaling Alters Development of the Ovarian Vasculature in Mice. *Biology of Reproduction*, 86, pp.174–174.

Riddle, R.D. et al., 1993. Sonic hedgehog mediates the polarizing activity of the ZPA. *Cell*, 75, pp.1401–1416.

Riemann, K. et al., 2009. Association of GNB4 intron-1 haplotypes with survival in patients with UICC stage III and IV colorectal carcinoma. *Anticancer Research*, 29(4), pp.1271–1274.

Robbins, D.J. et al., 1997. Hedgehog elicits signal transduction by means of a large complex containing the kinesin-related protein costal2. *Cell*, 90, pp.225–234.

Rodewald, H.R., 1995. Pathways from hematopoietic stem cells to thymocytes. *Current Opinion in Immunology*, 7, pp.176–187.

Roelink, H. et al., 1995. Floor plate and motor neuron induction by different concentrations of the amino-terminal cleavage product of sonic hedgehog autoproteolysis. *Cell*, 81, pp.445–455.

Roelink, H. et al., 1994. Floor plate and motor neuron induction by vhh-1, a vertebrate homolog of hedgehog expressed by the notochord. *Cell*, 76, pp.761–775.

Rossi et al., 2005. Recruitment of adult thymic progenitors is regulated by P-selectin and its ligand PSGL-1. *Nature Immunology*, 6, pp.626–634.

Rossi, L. et al., 2012. Less is more: Unveiling the functional core of hematopoietic stem cells through knockout mice. *Cell Stem Cell*, 11, pp.302–317.

Rowbotham, N.J., Hager-Theodorides, A.L., Furmanski, A.L., et al., 2007. A novel role for Hedgehog in T-cell receptor signaling: Implications for development and immunity. *Cell Cycle*, 6, pp.2138–2142.

Rowbotham, N.J., Hager-Theodorides, A.L., Cebecauer, M., et al., 2007. Activation of the Hedgehog signaling pathway in T-lineage cells inhibits TCR repertoire selection in the thymus and peripheral T-cell activation. *Blood*, 109, pp.3757–3766.

Rowbotham, N.J. et al., 2008. Repression of hedgehog signal transduction in T-lineage cells increases TCR-induced activation and proliferation. *Cell Cycle*, 7, pp.904–908.

Rowbotham, N.J. et al., 2009. Sonic hedgehog negatively regulates pre-TCR-induced differentiation by a Gli2-dependent mechanism. *Blood*, 113, pp.5144–5156.

Roy, S. & Ingham, P.W., 2002. Hedgehogs tryst with the cell cycle. *Journal of Cell Science*, 115, pp.4393–4397.

Ruel, L. et al., 2003. Stability and association of Smoothened, Costal2 and Fused with Cubitus interruptus are regulated by Hedgehog. *Nature Cell Biology*, 5, pp.907–913.

Sacedón, R. et al., 2003. Expression of hedgehog proteins in the human thymus. *The journal of histochemistry and cytochemistry : official journal of the Histochemistry Society*, 51, pp.1557–1566.

Saint-Ruf, C. et al., 1998. Genomic structure of the human pre-T cell receptor alpha chain and expression of two mRNA isoforms. *European Journal of Immunology*, 28, pp.3824–3831.

Sambandam, A. et al., 2005. Notch signaling controls the generation and differentiation of early T lineage progenitors. *Nature Immunology*, 6, pp.663–670.

Sarafova, S.D. et al., 2005. Modulation of coreceptor transcription during positive selection dictates lineage fate independently of TCR/coreceptor specificity. *Immunity*, 23, pp.75–87.

Sasaki, H. et al., 1999. Regulation of Gli2 and Gli3 activities by an amino-terminal repression domain: implication of Gli2 and Gli3 as primary mediators of Shh signaling. *Development (Cambridge, England)*, 126, pp.3915–3924.

Sato, T. et al., 2005. Dual functions of runx proteins for reactivating CD8 and silencing CD4 at the commitment process into CD8 thymocytes. *Immunity*, 22, pp.317–328.

Schilham, M.W. et al., 1998. Critical involvement of Tcf-1 in expansion of thymocytes. *Journal of Immunology (Baltimore, Md. : 1950)*, 161, pp.3984–3991.

Schilling, T.F., Concordet, J.P. & Ingham, P.W., 1999. Regulation of left-right asymmetries in the zebrafish by Shh and BMP4. *Developmental Biology*, 210, pp.277–287.

Schmedt, C. & Tarakhovsky, A., 2001. Autonomous maturation of alpha/beta T lineage cells in the absence of COOH-terminal Src kinase (Csk). *The Journal of Experimental Medicine*, 193, pp.815–826.

Schwarz, B.A. et al., 2007. Selective thymus settling regulated by cytokine and chemokine receptors. *Journal of Immunology (Baltimore, Md. : 1950)*, 178, pp.2008–2017.

Schwarz, B.A. & Bhandoola, A., 2004. Circulating hematopoietic progenitors with T lineage potential. *Nature Immunology*, 5, pp.953–960.

Schwindinger, W.F. & Robishaw, J.D., 2001. Heterotrimeric G-protein betagamma-dimers in growth and differentiation. *Oncogene*, 20(13), pp.1653–1660.

Scollay, R.G., Butcher, E.C. & Weissman, I.L., 1980. Thymus cell migration. Quantitative aspects of cellular traffic from the thymus to the periphery in mice. *European Journal of Immunology*, 10, pp.210–218.

Scott, C. & Ioannou, Y.A., 2004. The NPC1 protein: Structure implies function. *Biochimica et Biophysica Acta - Molecular and Cell Biology of Lipids*, 1685, pp.8–13.

Serwold, T., Ehrlich, L.I.R. & Irving, L.W., 2009. Reductive isolation from bone marrow and blood implicates common lymphoid progenitors as the major source of thymopoiesis. *Blood*, 113, pp.807–815.

Setoguchi, R. et al., 2008. Repression of the transcription factor Th-POK by Runx complexes in cytotoxic T cell development. *Science (New York, N.Y.)*, 319, pp.822–825.

Shah, D.K. et al., 2004. Reduced thymocyte development in sonic hedgehog knockout embryos. *Journal of Immunology (Baltimore, Md. : 1950)*, 172, pp.2296–2306.

Shaw, A.S. et al., 1989. The lck tyrosine protein kinase interacts with the cytoplasmic tail of the CD4 glycoprotein through its unique amino-terminal domain. *Cell*, 59, pp.627–636.

Sherman, E., Barr, V. & Samelson, L.E., 2013. Super-resolution characterization of TCR-dependent signaling clusters. *Immunological Reviews*, 251, pp.21–35.

Shimeld, S.M., 1999. The evolution of the hedgehog gene family in chordates: Insights from amphioxus hedgehog. *Development Genes and Evolution*, 209, pp.40–47.

Shinkai, Y. et al., 1992. RAG-2-deficient mice lack mature lymphocytes owing to inability to initiate V(D)J rearrangement. *Cell*, 68, pp.855–867.

Shinkai, Y. & Alt, F.W., 1994. CD3 epsilon-mediated signals rescue the development of CD4+CD8+ thymocytes in RAG-2-/- mice in the absence of TCR beta chain expression. *International Immunology*, 6, pp.995–1001.

Shortman, K., Vremec, D. & Egerton, M., 1991. The kinetics of T cell antigen receptor expression by subgroups of CD4+8+ thymocytes: delineation of CD4+8+3(2+) thymocytes as post-selection intermediates leading to mature T cells. *The Journal of experimental medicine*, 173, pp.323–332.

Shortman, K. & Wu, L., 1996. Early T lymphocyte progenitors. *Annual Review of Immunology*, 14, pp.29–47.

Sims-Mourtada, J. et al., 2007. Sonic Hedgehog promotes multiple drug resistance by regulation of drug transport. *Oncogene*, 26, pp.5674–5679.

Sinclair, C. et al., 2013. Asymmetric thymocyte death underlies the CD4:CD8 T-cell ratio in the adaptive immune system. *Proceedings of the National Academy of Sciences of the United States of America*, 110, pp.E2905–14.

Singer, A., Adoro, S. & Park, J.-H., 2008. Lineage fate and intense debate: myths, models and mechanisms of CD4- versus CD8-lineage choice. *Nature reviews. Immunology*, 8, pp.788–801.

Sisson, J.C. et al., 1997. Costal2, a novel kinesin-related protein in the Hedgehog signaling pathway. *Cell*, 90, pp.235–245.

Sohn, S.J. et al., 2001. Activated p56lck directs maturation of both CD4 and CD8 single-positive thymocytes. *Journal of Immunology (Baltimore, Md. : 1950)*, 166, pp.2209–2217.

Spangrude, G.J., Heimfeld, S. & Weissman, I.L., 1988. Purification and characterization of mouse hematopoietic stem cells. *Science (New York, N.Y.)*, 241, pp.58–62.

Spangrude, G.J. & Scollay, R., 1990. Differentiation of hematopoietic stem cells in irradiated mouse thymic lobes. Kinetics and phenotype of progeny. *Journal of Immunology (Baltimore, Md. : 1950)*, 145, pp.3661–3668.

Spicer, L.J. et al., 2009. The hedgehog-patched signaling pathway and function in the mammalian ovary: A novel role for hedgehog proteins in stimulating proliferation and steroidogenesis of theca cells. *Reproduction*, 138, pp.329–339.

Staal, F.J. et al., 2001. Wnt signaling is required for thymocyte development and activates Tcf- 1 mediated transcription. *European Journal of Immunology*, 31, pp.285–93.

Staal, F.J.T. & Clevers, H.C., 2003. Wnt signaling in the thymus. *Current Opinion in Immunology*, 15, pp.204–208.

Stamataki, D. et al., 2005. A gradient of Gli activity mediates graded Sonic Hedgehog signaling in the neural tube. *Genes and Development*, 19, pp.626–641.

Stegman, M.A. et al., 2000. Identification of a tetrameric hedgehog signaling complex. *Journal of Biological Chemistry*, 275, pp.21809–21812.

Stewart, G.A. et al., 2002. Sonic hedgehog signaling modulates activation of and cytokine production by human peripheral CD4+ T cells. *Journal of Immunology (Baltimore, Md. : 1950)*, 169, pp.5451–5457.

St-Jacques, B., Hammerschmidt, M. & McMahon, A.P., 1999. Indian hedgehog signaling regulates proliferation and differentiation of chondrocytes and is essential for bone formation. *Genes & development*, 13, pp.2072–2086.

Stone, D.M. et al., 1996. The tumour-suppressor gene patched encodes a candidate receptor for Sonic hedgehog. *Nature*, 384, pp.129–134.

Struhl, G. & Adachi, A., 1998. Nuclear access and action of Notch in vivo. *Cell*, 93, pp.649–660.

Sun, G. et al., 2005. The zinc finger protein cKrox directs CD4 lineage differentiation during intrathymic T cell positive selection. *Nature immunology*, 6, pp.373–381.

Suniara, R.K., Jenkinson, E.J. & Owen, J.J.T., 1999. Studies on the phenotype of migrant thymic stem cells. *European Journal of Immunology*, 29, pp.75–80.

Suzuki, H. et al., 1995. Asymmetric signaling requirements for thymocyte commitment to the CD4+ versus CD8+ T cell lineages: a new perspective on thymic commitment and selection. *Immunity*, 2, pp.413–425.

Szczepny, A., Hime, G.R. & Loveland, K.L., 2006. Expression of hedgehog signalling components in adult mouse testis. *Developmental Dynamics*, 235, pp.3063–3070.

Taipale, J. et al., 2002. Patched acts catalytically to suppress the activity of Smoothened. *Nature*, 418, pp.892–897.

Taipale, J. & Beachy, P.A., 2001. The Hedgehog and Wnt signalling pathways in cancer. *Nature*, 411, pp.349–54.

Takahama, Y., 2006. Journey through the thymus: stromal guides for T-cell development and selection. *Nature reviews. Immunology*, 6, pp.127–135.

Tamai, K. et al., 2000. LDL-receptor-related proteins in Wnt signal transduction. *Nature*, 407, pp.530–535.

Tan, J.B. et al., 2005. Requirement for Notch1 signals at sequential early stages of intrathymic T cell development. *Nature Immunology*, 6, pp.671–679.

Tanigaki, K. et al., 2004. Regulation of alphabeta/gammadelta T cell lineage commitment and peripheral T cell responses by Notch/RBP-J signaling. *Immunity*, 20, pp.611–622.

Tanimura, A., Dan, S. & Yoshida, M., 1998. Cloning of novel isoforms of the human Gli2 oncogene and their activities to enhance tax-dependent transcription of the human T-cell leukemia virus type 1 genome. *Journal of Virology*, 72, pp.3958–3964.

Taniuchi, I. et al., 2002. Differential requirements for Runx proteins in CD4 repression and epigenetic silencing during T lymphocyte development. *Cell*, 111, pp.621–633.

Tate, G. et al., 2000. Assignment of desert hedgehog (DHH) to human chromosome bands 12q12-->q13.1 by in situ hybridization. *Cytogenetics and Cell Genetics*, 88(1-2), pp.93–94.

Tavian, M. & Péault, B., 2005a. Analysis of hematopoietic development during human embryonic ontogenesis. *Methods in Molecular Medicine*, 105, pp.413–424.

Tavian, M. & Péault, B., 2005b. Embryonic development of the human hematopoietic system. *The International Journal of Developmental Biology*, 49, pp.243–250.

Teh, H.S. et al., 1988. Thymic major histocompatibility complex antigens and the alpha beta T-cell receptor determine the CD4/CD8 phenotype of T cells. *Nature*, 335, pp.229–233.

Tempé, D. et al., 2006. Multisite protein kinase A and glycogen synthase kinase 3beta phosphorylation leads to Gli3 ubiquitination by SCFbetaTrCP. *Molecular and Cellular Biology*, 26, pp.4316–4326.

Tenzen, T. et al., 2006. The cell surface membrane proteins Cdo and Boc are components and targets of the Hedgehog signaling pathway and feedback network in mice. *Developmental Cell*, 10(5), pp.647–56.

Thayer, S.P. et al., 2003. Hedgehog is an early and late mediator of pancreatic cancer tumorigenesis. *Nature*, 425, pp.851–856.

Thesleff, I., 2003. Epithelial-mesenchymal signalling regulating tooth morphogenesis. *Journal of Cell Science*, 116(Pt 9), pp.1647–1648.

Tinsley, K.W. et al., 2013. Ikaros is required to survive positive selection and to maintain clonal diversity during T-cell development in the thymus. *Blood*, 122, pp.2358–2368.

Tober, J. et al., 2007. The megakaryocyte lineage originates from hemangioblast precursors and is an integral component both of primitive and of definitive hematopoiesis. *Blood*, 109, pp.1433–1441.

Tomita, K. et al., 1999. The bHLH gene Hes1 is essential for expansion of early T cell precursors. *Genes and Development*, 13, pp.1203–1210.

Traver, D. & Zon, L.I., 2002. Walking the walk: Migration and other common themes in blood and vascular development. *Cell*, 108, pp.731–734.

Trinchieri, G., Pflanz, S. & Kastelein, R.A., 2003. The IL-12 family of heterodimeric cytokines: New players in the regulation of T cell responses. *Immunity*, 19, pp.641–644.

Uematsu, Y. et al., 1988. In transgenic mice the introduced functional T cell receptor beta gene prevents expression of endogenous beta genes. *Cell*, 52, pp.831–841.

Umehara, F. et al., 2006. Elevated anxiety-like and depressive behavior in Desert hedgehog knockout male mice. *Behavioural Brain Research*, 174, pp.167–173.

Umehara, F., Tate, G. & Itoh, K., 2000. A Novel Mutation of desert hedgehog in a Patient with 46, XY Partial Gonadal Dysgenesis Accompanied by Minifascicular Neuropathy. *The American Journal of …*, (Ingham 1997), pp.1302–1305.

Urban, J.A. & Winandy, S., 2004. Ikaros null mice display defects in T cell selection and CD4 versus CD8 lineage decisions. *Journal of Immunology (Baltimore, Md.: 1950)*, 173, pp.4470–4478.

Varas, A. et al., 2003. The role of morphogens in T-cell development. *Trends in Immunology*, 24, pp.197–206.

Varjosalo, M. & Taipale, J., 2008. Hedgehog: functions and mechanisms. *Genes & Development*, 22(18), pp.2454–72.

Vaziri, H. et al., 1994. Evidence for a mitotic clock in human hematopoietic stem cells: loss of telomeric DNA with age. *Proceedings of the National Academy of Sciences of the United States of America*, 91, pp.9857–9860.

Virts, E.L., Phillips, J.A. & Thoman, M.L., 2006. A novel approach to thymic rejuvenation in the aged. *Rejuvenation Research*, 9, pp.134–142.

Vortkamp, A. et al., 1996. Regulation of rate of cartilage differentiation by Indian hedgehog and PTH-related protein. *Science (New York, N.Y.)*, 273, pp.613–622.

Vortkamp, A., Gessler, M. & Grzeschik, K.H., 1991. GLI3 zinc-finger gene interrupted by translocations in Greig syndrome families. *Nature*, 352, pp.539–540.

Vortkamp, A., Gessler, M. & Grzeschik, K.H., 1995. Identification of optimized target sequences for the GLI3 zinc finger protein. *DNA and Cell Biology*, 14, pp.629–634.

Wada, H. et al., 2008. Adult T-cell progenitors retain myeloid potential. *Nature*, 452, pp.768–772.

Wall, N.A. & Hogan, B.L., 1994. TGF-beta related genes in development. *Curr Opin Genet Dev*, 4, pp.517–522.

Wang, B., Fallon, J.F. & Beachy, P.A., 2000. Hedgehog-regulated processing of Gli3 produces an anterior/posterior repressor gradient in the developing vertebrate limb. *Cell*, 100, pp.423–434.

Wang, L. et al., 2008. Distinct functions for the transcription factors GATA-3 and ThPOK during intrathymic differentiation of CD4(+) T cells. *Nature Immunology*, 9, pp.1122–1130.

Watanabe, Y. & Nakamura, H., 2000. Control of chick tectum territory along dorsoventral axis by Sonic hedgehog. *Development (Cambridge, England)*, 127, pp.1131–1140.

Watkins, D.N. et al., 2003. Hedgehog signalling within airway epithelial progenitors and in small-cell lung cancer. *Nature*, 422, pp.313–317.

Weber, B.N. et al., 2011. A critical role for TCF-1 in T-lineage specification and differentiation. *Nature*, 476, pp.63–68.

Weerkamp, F. et al., 2006. Wnt signaling in the thymus is regulated by differential expression of intracellular signaling molecules. *Proceedings of the National Academy of Sciences of the United States of America*, 103, pp.3322–3326.

Weinberg, E.S. et al., 1996. Developmental regulation of zebrafish MyoD in wild-type, no tail and spadetail embryos. *Development (Cambridge, England)*, 122, pp.271–280.

Weissman, I.L., 2000. Stem cells: units of development, units of regeneration, and units in evolution. *Cell*, 100, pp.157–168.

Wells, A.D. et al., 2000. T cell effector function and anergy avoidance are quantitatively linked to cell division. *Journal of Immunology (Baltimore, Md. : 1950)*, 165, pp.2432–2443.

Wiest, B.D.L. et al., 1993. Published November 1, 1993. , 178(November).

Wijgerde, M. et al., 2005. Hedgehog signaling in mouse ovary: Indian hedgehog and desert hedgehog from granulosa cells induce target gene expression in developing theca cells. *Endocrinology*, 146, pp.3558–3566.

Wilkinson, B. et al., 2002. TOX: an HMG box protein implicated in the regulation of thymocyte selection. *Nature Immunology*, 3, pp.272–280.

Wilkinson, B., Owen, J.J. & Jenkinson, E.J., 1999. Factors regulating stem cell recruitment to the fetal thymus. *Journal of Immunology (Baltimore, Md. : 1950)*, 162, pp.3873–3881.

Wilson, A., Held, W. & MacDonald, H.R., 1994. Two waves of recombinase gene expression in developing thymocytes. *The Journal of Experimental Medicine*, 179, pp.1355–1360.

Wilson, A., MacDonald, H.R. & Radtke, F., 2001. Notch 1-deficient common lymphoid precursors adopt a B cell fate in the thymus. *The Journal of Experimental Medicine*, 194, pp.1003–1012.

Wilson, A., de Villartay, J.P. & MacDonald, H.R., 1996. T cell receptor delta gene rearrangement and T early alpha (TEA) expression in immature alpha beta lineage thymocytes: implications for alpha beta/gamma delta lineage commitment. *Immunity*, 4, pp.37–45.

Wilson & Trumpp, 2006. Bone-marrow haematopoietic-stem-cell niches. *Nature Reviews. Immunology*, 6, pp.93–106.

Winnier, G. et al., 1995. Bone morphogenetic protein-4 is required for mesoderm formation and patterning in the mouse. *Genes and Development*, 9, pp.2105–2116.

Wojciechowski, J. et al., 2007. E2A and HEB are required to block thymocyte proliferation prior to pre-TCR expression. *Journal of Immunology (Baltimore, Md. : 1950)*, 178, pp.5717–5726.

Wolfer, A. et al., 2002. Inactivation of Notch1 impairs VDJ?? rearrangement and allows pre-TCR-independent survival of early ???? lineage thymocytes. *Immunity*, 16, pp.869–879.

Wu, L., 2006. T lineage progenitors: The earliest steps en route to T lymphocytes. *Current Opinion in Immunology*, 18, pp.121–126.

Wurbel, M.A. et al., 2001. Mice lacking the CCR9 CC-chemokine receptor show a mild impairment of early T- and B-cell development and a reduction in T-cell receptor γδ+ gut intraepithelial lymphocytes. *Blood*, 98, pp.2626–2632.

Yamada, T. et al., 1993. Control of cell pattern in the neural tube: Motor neuron induction by diffusible factors from notochord and floor plate. *Cell*, 73, pp.673–686.

Yamasaki, S. et al., 2006. Mechanistic basis of pre-T cell receptor-mediated autonomous signaling critical for thymocyte development. *Nature Immunology*, 7, pp.67–75.

Yang-Snyder, J. et al., 1996. A frizzled homolog functions in a vertebrate Wnt signaling pathway. *Current Biology : CB*, 6, pp.1302–1306.

Yao, H.H.-C., Whoriskey, W. & Capel, B., 2002. Desert Hedgehog/Patched 1 signaling specifies fetal Leydig cell fate in testis organogenesis. *Genes & Development*, 16(11), pp.1433–40.

Yashiro-Ohtani, Y. et al., 2009. Pre-TCR signaling inactivates Notch1 transcription by antagonizing E2A. *Genes and Development*, 23, pp.1665–1676.

Yasutomo, K. et al., 2000. The duration of antigen receptor signalling determines CD4+ versus CD8+ T-cell lineage fate. *Nature*, 404, pp.506–510.

Yavari, A. et al., 2010. Role of Lipid Metabolism in Smoothened Derepression in Hedgehog Signaling. *Developmental Cell*, 19, pp.54–65.

Yoder, M.C., 2004. Generation of HSCs in the embryo and assays to detect them. *Oncogene*, 23, pp.7161–7163.

Yoon, J.W. et al., 2002. Gene expression profiling leads to identification of GLI1-binding elements in target genes and a role for multiple downstream pathways in GLI1-induced cell transformation. *Journal of Biological Chemistry*, 277, pp.5548–5555.

Yu, Q. et al., 2003. In vitro evidence that cytokine receptor signals are required for differentiation of double positive thymocytes into functionally mature CD8+ T cells. *The Journal of Experimental Medicine*, 197, pp.475–487.

Yücel, R. et al., 2003. The transcriptional repressor Gfi1 affects development of early, uncommitted c-Kit+ T cell progenitors and CD4/CD8 lineage decision in the thymus. *The Journal of Experimental Medicine*, 197, pp.831–844.

Zeng, X. et al., 2001. A freely diffusible form of Sonic hedgehog mediates long-range signalling. *Nature*, 411, pp.716–720.

Zhang, C. & Evans, T., 1996. BMP-like signals are required after the midblastula transition for blood cell development. *Developmental Genetics*, 18, pp.267–278.

Zhang, N. & Bevan, M.J., 2011. CD8+ T Cells: Foot Soldiers of the Immune System. *Immunity*, 35, pp.161–168.

Zhang, X.M., Ramalho-Santos, M. & McMahon, A.P., 2001. Smoothened mutants reveal redundant roles for Shh and Ihh signaling including regulation of L/R asymmetry by the mouse node. *Cell*, 105, pp.781–792.

Zinkernagel, R.M. et al., 1978. On the thymus in the differentiation of "H-2 self-recognition" by T cells: evidence for dual recognition? *The Journal of Experimental Medicine*, 147, pp.882–896.